Vincenzo Naddeo · Malini Balakrishnan ·
Kwang-Ho Choo   *Editors*

Frontiers in Water-Energy-Nexus

Nature-Based Solutions, Advanced Technologies and Best Practices for Environmental Sustainability

Proceedings of the 2nd WaterEnergyNEXUS Conference, November 2018, Salerno, Italy

IEREK
RESEARCH & KNOWLEDGE ENRICHMENT

Springer

Advances in Science, Technology & Innovation

IEREK Interdisciplinary Series for Sustainable Development

Advances in Science, Technology & Innovation (ASTI) is a series of peer-reviewed books based on the best studies on emerging research that redefines existing disciplinary boundaries in science, technology and innovation (STI) in order to develop integrated concepts for sustainable development. The series is mainly based on the best research papers from various IEREK and other international conferences, and is intended to promote the creation and development of viable solutions for a sustainable future and a positive societal transformation with the help of integrated and innovative science-based approaches. Offering interdisciplinary coverage, the series presents innovative approaches and highlights how they can best support both the economic and sustainable development for the welfare of all societies. In particular, the series includes conceptual and empirical contributions from different interrelated fields of science, technology and innovation that focus on providing practical solutions to ensure food, water and energy security. It also presents new case studies offering concrete examples of how to resolve sustainable urbanization and environmental issues. The series is addressed to professionals in research and teaching, consultancies and industry, and government and international organizations. Published in collaboration with IEREK, the ASTI series will acquaint readers with essential new studies in STI for sustainable development.

More information about this series at http://www.springer.com/series/15883

Vincenzo Naddeo · Malini Balakrishnan ·
Kwang-Ho Choo
Editors

Frontiers in Water-Energy-Nexus—Nature-Based Solutions, Advanced Technologies and Best Practices for Environmental Sustainability

Proceedings of the 2nd WaterEnergyNEXUS Conference, November 2018, Salerno, Italy

Springer

Editors
Vincenzo Naddeo
Department of Civil Engineering
University of Salerno
Fisciano, Salerno, Italy

Malini Balakrishnan
The Energy and Resources Institute (TERI)
New Delhi, India

Kwang-Ho Choo
Department of Environmental Engineering
Kyungpook National University
Daegu, Korea (Republic of)

About the Conference Steering Committee

Honorary Chair

Vincenzo Belgiorno, University of Salerno, Italy

Symposium Chairpersons

Malini Balakrishnan, The Energy and Resources Institute (TERI), India

Vincenzo Naddeo, University of Salerno, Italy

Kwang-Ho Choo, Kyungpook National University, Korea

Conference Organization Committee

Salvatore Barba, University of Salerno, Italy
Laura Borea, University of Salerno, Italy
Fabiano Castrogiovanni, University of Salerno, Italy
Alessandra Cesaro, University of Salerno, Italy
Lucia D'Elia, Sponge s.r.l
Angela Fraiese, University of Salerno, Italy
Simona Iannizzaro, University of Salerno, Italy
Alessandra Marra, University of Salerno, Italy
Giusy Oliva, University of Salerno, Italy
Domenico Russo, University of Salerno, Italy
Francesco Villecco, University of Salerno, Italy
Tiziano Zarra, University of Salerno, Italy

Scientific Committees

Topic 1: Nexus Framework and Governance

Prof. Damià Barceló, Consejo Superior de Investigaciones Científicas (CSIC), Spain
Dr. Malini Balakrishnan, The Energy and Resources Institute (TERI), India
Dr. Robert Brears, Urban Water Security, New Zealand
Prof. Kwang-Ho Choo, Kyungpook National University, Korea
Prof. Ola M. Gomaa, Egyptian Atomic Energy Authority, Egypt
Dr. Nabil Khélifi, Springer, a part of Springer Nature, Germany
Prof. Mohamed Ksibi, University of Sfax, Tunisia

Topic 2: Advanced Technologies or Nature-Based Solutions for the Environmental Sustainability of the Water Sector

Dr. Massimo Spadoni, Embassy of Italy in New Delhi, India
Dr. Daniele Di Trapani, University of Palermo, Italy
Prof. Jeonghwan Kim, INHA University, Korea
Prof. Gregory Korshin, University of Washington, USA
Prof. Changha Lee, Seoul National University, Korea
Dr. Jeong-ik Oh, Korea Land & Housing Corporation, Korea
Prof. Gaspare Viviani, University of Palermo, Italy
Prof. Jannis Wenk, University of Bath, UK
Prof. Maria Chiara Zanetti, Politecnico di Torino, Italy

Topic 3: Control of Hazardous Substances in Water and Recovery of Renewable/Valuable Resources from Wastewater

Prof. Kangwoo Cho, Pohang University of Science and Technology, Korea
Prof. Shadi Wajih Hasan, Khalifa University of Science and Technology, UAE
Prof. Haizhou Liu, University of California Riversides, USA
Prof. Vincenzo Naddeo, University of Salerno, Italy
Dr. Stefano Papiro, University of Napoli Federico II, Italy
Prof. Francesco Pirozzi, University of Napoli Federico II, Italy
Prof. Alberto Tiraferri, Politecnico di Torino, Italy
Prof. Ngai Yin Yip, Columbia University, USA

Topic 4: Energy Saving Technologies and Future Clean Energy Solutions Under Water Constraints

Prof. Marc A. Anderson, University of Wisconsin–Madison, USA
Prof. Vincenzo Belgiorno, University of Salerno, Italy
Prof. Massimiliano Fabbricino, University of Napoli Federico II, Italy
Prof. Claudio Lubello, University of Firenze, Italy
Prof. Raul Munoz, Valladolid University, Spain
Dr. Jesus Palma, IMDEA Energy, Spain
Prof. Sebastià Puig, Universitat de Girona, Spain
Prof. Mohammad Taherzadeh, University of Borås, Sweden

Topic 5: Implementation and Best Practices

Prof. Florencio C. Ballesteros, University of the Philippines Diliman, Philippines
Dr. Alessandra Cesaro, University of Salerno, Italy
Prof. Mark Daniel G. De Luna, University of the Philippines Diliman, Philippines
Prof. Takaya Higuchi, Yamaguchi University, Japan

Prof. Predrag Miranovic, University of Montenegro, Montenegro
Dr. Marwa S. Shalaby, National Research Center, Egypt
Dr. Giacomo Viccione, University of Salerno, Italy
Dr. Tiziano Zarra, University of Salerno, Italy

Contents

About the Editors

Dr. Vincenzo Naddeo is Associate Professor at Department of Civil Engineering of the University of Salerno, Italy, where he drives research activities at the Sanitary Environmental Engineering Division (SEED). His research focuses on water/wastewater treatment, characterization and control of environmental odours and environmental impact assessment (EIA). He developed advanced biological processes for wastewater treatment and control of emerging contaminants, novel ultrasound-based technological processes for the treatment of environmental matrices (solid, liquid and gaseous) and biotechnologies for wastewater reuse with simultaneous energy production. He is Associate Editor of the Euro-Mediterranean Journal for Environmental Integration (Springer) and Co-founding Chair of the conference series WaterEnergyNEXUS. He presently serves on the editorial board of several ISI journals including Scientific Reports (Nature Research), Heliyon (Elsevier), PeerJ (Life, Bio, Environment and Health Sciences), and he is actively involved in a variety of scientific organizations, funding agencies and European networks. He has (co-)authored over 190 refereed publications in ISI journals, congress proceedings and book volumes, and he holds 5 patents. From January 2018, he is CEO and Co-founder of Sponge s.r.l., a spin-off of the University of Salerno working in environmental technology field.

Dr. Malini Balakrishnan is Senior Fellow in the Environment and Waste Management Division at The Energy and Resources Institute (TERI), New Delhi, India. She has been closely involved with different industry sectors working on a range of issues including resource use particularly energy and water. The work on enhancing resource efficiency in small and medium enterprises (SMEs) (covering sectors such as metal fabrication/finishing, chemicals and intermediates' manufacture) in India and select South Asian countries has achieved significant savings in energy, water and raw materials. In addition, she works on process upgradation in sugar manufacturing, value-added utilization of waste bagasse ash from sugar factories and efficient water use and advanced wastewater

treatment in alcohol distilleries. These efforts are primarily targeted at evolving affordable solutions to specific local problems. She has experience in execution and coordination of pilot demonstrations of technologies such as membrane filtration for upgrading the juice clarification process in the Indian sugar industry, diffusion dialysis, acid retardation and nanofiltration-based recovery systems for waste acid/rinse water in Indian metal finishing SMEs. She is also leading TERIs efforts in field testing of membrane bioreactors using indigenously prepared membranes from industrial waste. These demonstrations have provided a deeper understanding of challenges in technology adaptation and possible approaches that would encourage the uptake of such technologies. She has directed over 20 projects including several European-Commission-supported multi-partner projects where TERI was the lead partner. She is a nominated expert in Department of Science and Technology (DST), Government of India, in Water Technology Initiative programme advisory committee and in the Chemical Division Council of Bureau of Indian Standards (BIS).

She has a doctorate in biochemical engineering, with master's and bachelor's degrees in chemical engineering. She has over 80 publications in journals and books, over 100 presentations in conferences/workshops and 3 patent applications to her credit and is a reviewer for several peer-reviewed international journals.

Prof. Kwang-Ho Choo received his Ph.D. from Seoul National University, Korea, in 1996, and since then has been working on membrane science and technology for water and wastewater, pursuing innovative solutions for sustainable water production and reuse. His recent research interests include membrane electro-oxidizers and quorum quenching membrane bioreactors. He is currently keen to find synergistic options for water–energy nexus issues, using membranes in conjunction with physicochemical/biological strategies, such as iron oxide adsorption, photocatalysis, electrocatalysis and microbial quorum quenching. He has been actively involved in academic societies, such as International Water Association, Korean Society of Environmental Engineers and Membrane Society of Korea, and Korean Institute of Chemical Engineers, as an active board/editorial member.

About the Invited Speakers

Prof. Marc A. Anderson has been, for more than 24 years, Full Professor at University of Wisconsin–Madison; Professor of Civil and Environmental Engineering, Materials Science Program and Professor and Chair of Environmental Chemistry and Technology Program. Since June 2008, he is acting as advisor and principal researcher of the Electrochemical Processes Unit at IMDEA Energy with special emphasis on energy storage for renewable energy systems and applications to energy-efficient water desalination.

He graduated with distinction (cum laude) from UW-Whitewater and got his Ph.D. at Johns Hopkins University in 1974. He has completed research stages at CIEMAT, Spain, besides sabbatical leaves as Visiting Professor at the Institute of Ceramics and Glass CSIC—Madrid, Spain (1988–1989) and Université Catholique—Louvain, Belgium (1980–1981). His current research interests are: ceramic membranes; microporous ceramic materials; colloidal thin-film ceramics; colloid chemistry; catalysis, gas and liquid ceramic membrane separation processes; adsorption in aqueous systems; photocatalysis; photoelectrochemistry; batteries; ultra-capacitors and fuel cells.

At the Electrochemical Unit of IMDEA Energy Institute, he is in charge of the development of nanoporous materials from sol-gel chemistry as well as collecting the necessary know-how concerning the transport of both electrons and ions that dictate the performance of battery and ultracapacitor systems. He is also developing energy-efficient materials and devices and novel methods of regeneration for water desalination processes based on nanostructured materials applied to capacitive deionization (CD) or electrosorption. In his career in academia, his research projects have been funded by National Science Foundation, Environmental Protection Agency, Sea Grant, NASA, Department of Energy, Department of Defence and the Office of Naval Research. Private funding has come from both large corporations such as Air Products, Kimberly Clark and RayOVac and smaller companies. Currently, he has projects that include support from Annheuser Bush, Gusmer Industries, Cardinal Glass, Regal Ware and WCR.

He has published around 180 papers in peer-reviewed journals, with a historical Hirsch index of 48, and is author of 27 patents. He has presented more than 100 communications in national and international conferences, about 40 of them being invited talks or keynotes. He has been honoured with the Byron Bird "Best Paper in Engineering Award" by UW-Madison; Fulbright Fellow; Alumni of the Year by UW-Whitewater; Outstanding Paper Award by AICHE; Phoebe Apperson Hearst Distinguished Lecturer by UC Berkeley.

Prof. Damià Barceló born in Menàrguens (Lleida) in 1954, obtained a B.Sc. in chemistry from the University of Barcelona (UB) in 1977 and a Ph.D. in analytical chemistry from the same university in 1984. He is currently working as a research professor and deputy director of the Institute of Environmental Diagnosis and Water Studies (IDAEA) in Barcelona, which is run by the Spanish National Research Council (CSIC). He was appointed Director of the Catalan Institute for Water Research (ICRA) in Girona in 2008. During 2010 and 2011, he was a visiting professor at the King Saud University, Riyadh, Saudi Arabia.

His research career has been focused on the area of water quality, particularly in the development of methods for controlling organic pollution by the so-called emerging pollutants (polar pesticides, surfactants, detergents, endocrine disruptors and pharmaceutical products) in waste and natural water.

Since 2010, he is listed among the most internationally cited scientists (ISI highly cited), by the number and the exceptional quality of his publications. According to Scopus, he has the Hirsch index of 104 and total number of citations over 50,000. According to Google Scholar, his h-index is 132 and the total number of citations is almost 80,000.

Since the 1990s, he has been editor of various journals (TRAC, Talanta, ABC, Environment International) and book series (Comprehensive Analytical Chemistry and The Handbook of Environmental Chemistry). Since 2012, he is Co-Editor-in-chief of the Science of the Total Environment. In 2007, he received the King James I Prize for Environmental Protection, Spain, in 2012 the Prince Sultan Bin Abdulaziz International Prize for Water of Saudi Arabia, and in 2012 the Recipharm International Environmental Prize, from a Swedish company that is a leading pharmaceutical manufacturer in Europe. In 2011, he was appointed as Chairman of the Scientific and Technical Board (STB) in the frame of the European Union-Joint Programming Initiative on "Water Challenges for a Changing World". In 2014, he was awarded Doctor Honoris Causa by the University of Ioannina, Greece. As of March 2018, he has been supervisor of 53 PhDs, short and continuous education courses in universities from Spain, South Korea, Brazil, Greece, Saudi Arabia and among others, at PITTCON, SETAC and ExTech international conferences.

Dr. Shadi Wajih Hasan is working at Department of Chemical and Environmental Engineering at Khalifa University of Science and Technology, Abu Dhabi. He holds B.Sc., M.A.Sc. and Ph.D. in chemical, mechanical and environmental engineering, respectively. His field of expertise includes water purification, wastewater treatment and reuse, water desalination and nanotechnology. He has been leading several projects in water desalination using forward osmosis, reverse osmosis, membrane distillation and capacitive deionization technologies in Abu Dhabi, and has also led a wastewater treatment project with Massachusetts Institute of Technology (MIT), Cambridge, USA. Throughout his academic career, he has been recognized as an excellent designer (first to design the novel submerged membrane electro-bioreactor for municipal wastewater treatment at a pilot scale in Montreal, Canada) and has obtained a number of prestigious awards including FQRNT. He has authored and co-authored over 50 articles in peer-reviewed journals such as Desalination, Scientific Reports Nature, Bioresource Technology and RSC Advances; and conference proceedings including IWA, IDW, EREM and WEFTEC; and generated significant research interest abroad in the USA and overseas. His research has significant impacts and led to several funding opportunities both internally and externally. He is an active reviewer for more than 30 scientific journals and has supervised more than 25 M.Sc. and Ph.D. students and research fellows.

Prof. Arun Kansal is Dean (research and relationships) and Head of Department of Regional Water Studies at TERI School of Advanced Studies, India. He received his Ph.D. in environmental engineering from Indian Institute of Technology, Delhi, after completing his M.Tech. and B.Tech. in civil engineering. He has over 20 years of research/consultancy/ teaching experience in the areas of water resource management, waste management with a focus on resource recovery and recycling, urban environment and energy–environment– climate linkages. He is a recipient of Best Teacher Award from GGS Indraprastha University, India; Best Research Paper Award from Indian Water Works Association, and has received the Roll of Honour by TERI. In his academic career, he has been a visiting professor (as ICCR Chair Professor from Government of India) to Freie University, Berlin, Germany, during 2010–2011, an Honorary Senior Research Fellow at the University of Birmingham, UK (2011–2014), a visiting professor at the University of Derby in Natural Sciences (2015–2018) and Key Technology Partner Visiting Fellow at the University of Technology Sydney (UTS), Australia. He also served as a lead author for IPCC 5th Assessment Report WGIII.

He has also coordinated an e-learning programme at TERI School of Advanced Studies on Sustainable Development Practices in Public Policy for mid-career professionals. The programme was under the aegis of UNU-IAS, Japan, and was

in collaboration with Tongji University, China; Universiti Sains Malaysia; University of South Pacific, Fiji; and AIT, Thailand. He also served as a core team member of the project for development of Alternative University Appraisal for Education on Sustainable Development led by Hokkaido University, Japan, along with Yonsei University, Republic of Korea; AIT, Thailand; and Universiti Sains Malaysia. He also developed two full courses (e-content generation) for postgraduate students in environmental science, which was funded by MHRD, Government of India. He has served as a member of expert committee constituted by Ministry of Environment, Forest and Climate Change (MoEF&CC), Government of India, for review of "common effluent treatment scheme". He has also served as a member of project review committee constituted by MoEF&CC for the project entitled "Environmental friendly technology in the highly polluting small-scale glass industry at Firozabad" and has been the expert member for evaluating Ford Foundation fellowship applications.

His research and consultancy experience is evident from the list of peer-reviewed publications and success in winning grants from Government of India, multilateral and bilateral organizations and industrially funded research and consultancy. Recently, he has successfully completed three research projects as Principal Investigator in the area of metabolism approach for water planning of megacities, funded by Enel Foundation; Understanding and quantifying water–energy nexus for low-carbon development in Asian cities, funded by Asia-Pacific Network in collaboration with Hiroshima University, Japan, and AIT, Thailand; and strengthening water and sanitation in urban settings, funded by USAID.

Prof. Gregory Korshin has been working at the University of Washington since 1991. He has also held invited appointments at the University of Paris VII Diderot, Australian Water Quality Centre and University of South Australia in Adelaide, University of Catania in Italy and Peking University, China. He is an editor and a member of the editorial board of Water Research, which is one of the highest-ranked journals in the area of water treatment. His research interests include characterization of natural organic matter (NOM), disinfection and formation of disinfection by-products, online methods to monitor drinking water quality, electrochemical processes in environmental systems, environmental chemistry of heavy metals, advanced oxidation processes and degradation of trace-level organic contaminants in wastewater. He has published >160 refereed publications, most of them in leading journals such as Water Research and Environmental Science and Technology. He has participated in numerous projects funded by Water Research Foundation, Water ReUse Foundation, National Science Foundation, U.S. Environmental Protection Agency and other organizations.

Dr. Changha Lee obtained both B.S. and Ph.D. in chemical engineering (environmental engineering major) at Seoul National University in 2001 and 2007, respectively. During his Ph.D. studies, he worked as a visiting scientist at Swiss Federal Institute of Aquatic Science and Technology (EAWAG) from 2005 to 2006. After graduation, he worked as a postdoctoral fellow at the Department of Civil and Environmental Engineering, University of California, Berkeley, from 2007 to 2009. Then he joined the Faculty of Urban and Environmental Engineering at Ulsan National Institute of Science and Technology (UNIST). He is interested in various subjects related to water chemistry and chemical processes for water and wastewater treatment. He has published 88 papers in international peer-reviewed journals to date.

Dr. Raúl Muñoz is Associate Professor at the Department of Chemical Engineering and Environmental Technology, University of Valladolid, Spain. He holds a Ph.D. in environmental biotechnology from Lund University (2005). His main fields of expertise are biological gas treatment, biogas upgrading and wastewater treatment in algal–bacterial photobioreactors. Over the last 10 years, he has published more than 164 ISI papers (h-index = 40), 30 chapters, more of 115 International Conference proceedings (72 oral platforms + 46 posters) + 14 invited keynotes/plenary lectures and supervised 14 Ph.D. theses and 22 master theses.

Dr. Sebastià Puig is a senior lecturer at the Laboratory of Chemical and Environmental Engineering (LEQUIA), University of Girona (UdG), Spain.

His main research interests are: bioelectrochemical systems (BES) for (1) biofuels and value-added production from wastes (liquid and gas phases); (2) bioenergy production during wastewater treatment, and (3) bioremediation of contaminated waters; bio-leading edge technologies for the treatment and nutrient (nitrogen, phosphorus, magnesium and potassium) recovery (struvite) of wastewaters.

He has participated in 20 research projects and R&D contracts, and has supervised 2 postdoctoral researchers, 5 doctoral theses and 8 master theses. As a result of his outstanding scientific career, he received the accreditation as a tenure-track lecturer and the accreditation of having merits in his research from the Quality Assurance Agency for the University System in Catalonia, Spain. He has published 59 peer-reviewed papers in international journals (including top A1 journals)—24 as corresponding author, h-index 21–64 congress publications and two European patents on METs. In 2014, he received the award "Young talented researcher in Sustainable Water Management" from Fundación Botin, Spain.

Prof. Mohammad Taherzadeh is Professor in bioprocess technology since 2004 at University of Borås in Sweden and Director of Research School at Swedish Centre for Resource Recovery (www.scrr.se). He has Ph.D. in bioscience from Sweden, and M.Sc. and B.Sc. in chemical engineering from Iran. He is developing processes to convert wastes and residuals to value-added products such as ethanol, biogas, human food, animal feed and biopolymers by fermentation. He has published more than 220 papers in scientific peer-reviewed journals, 18 chapters, 5 patents and 3 books. More information about him is available at www.taherzadeh.se.

Prof. Stefan Uhlenbrook is Coordinator of the UN World Water Assessment Programme (WWAP, UNESCO programme) and Director of the Programme Office on Global Water Assessment in Perugia, Italy, since November 2015. Before that he worked at UNESCO-IHE as Professor of hydrology (since 2005), Deputy Director (Vice-Rector) for Academic and Student Affairs (2000–2014) and Director a.i. (Acting Rector; 2014–2015). He did his Ph.D. (1999) and habilitation (2003) at the University of Freiburg, Germany. He is also a professor for experimental hydrology at Delft University of Technology, The Netherlands (since 2009).

His main expertise includes water assessments, hydrological process research, river basin modelling and water resources management. Many of his research and development projects have demonstrated the impact of global changes on water cycle dynamics in different hydroclimate regions in Africa and Asia. He is keen on translating science-based water knowledge to effective policies and strategies that contribute to environmental, economic and societal sustainability. Therefore, he is involved in supporting Member States in achieving the Sustainable Development Goals (SDGs), particularly SDG 6 on Water and Sanitation.

Prof. Kala Vairavamoorthy is an internationally recognized water resource management expert, with particular expertise in urban water issues. He combines a strong engineering background with practical international experience. He has published extensively and has a strong international profile working closely with the World Bank, UN-Habitat, UNESCO, GWP, SIWI and the EU. This includes leading several urban water management projects for the World Bank, African Development Bank, Asian Development Bank and DFID.

Prior to joining the International Water Association (IWA) as its Executive Director, he was the Deputy Director General for Research at the International Water Management Institute (IWMI). In this position, he was responsible for research strategy and science quality, and driving research to address global development challenges for water security and natural resource management. This included leading the

identification of innovative research areas, ensuring relevance of thematic content for the development agenda that contributes to the United Nations Sustainable Development Goals, global climate agenda and other regional and national imperatives.

He was Founding Dean of the Patel College of Global Sustainability and a tenured professor in the Department of Civil and Environmental Engineering, University of South Florida, USA. Prior to that, he was Full Professor and Chair of Water Engineering at the University of Birmingham, UK, and Professor and Head of Core of Sustainable Urban Water Infrastructure Systems at UNESCO-IHE, Netherlands. He still holds professorial appointments at the University of South Florida and UNESCO-IHE.

He has been a member of many International Scientific Committees. Currently, he serves on the Stockholm's World Water Week's Scientific Program Committee and the Global Water Partnership's Technical Committee. He was Co-chair of IWA's Cities of the Future Program and also a member of Singapore International Water Week's Program Committee. He has a Ph.D. and M.Sc. in environmental engineering from Imperial College, University of London, UK, and a B.Sc. (Hons) from King's College, London.

Dr. Jannis Wenk studied environmental engineering at the Technical University Berlin, Germany, including a one-year stay at POSTECH, Korea, followed by Ph.D. studies at EAWAG and ETH Zurich, Switzerland, from where he graduated in 2012. Subsequently, he worked as a postdoctoral fellow at UC Berkeley, USA. He joined the Department of Chemical Engineering at the University of Bath as a lecturer (assistant professor) in January 2015.

His research has been in the areas of aquatic oxidation processes, transformation pathways of trace organic water contaminants, chemistry of humic substances and environmental photochemistry. More recently, he has also become interested on the fate of pathogens during water treatment and nature-oriented, low-energy water treatment systems.

At the University of Bath and the recently formed Water Innovation and Research Centre (WIRC), he would like to utilize his knowledge in aquatic oxidation chemistry and build up his initial research programme on oxidation and advanced oxidation processes for water treatment. Key aspects will be the combination of oxidative processes with other treatment processes, integration of oxidative processes into existing water treatment schemes and process design for oxidative waste water treatment applications for both chemical contaminant and pathogen removal. He is also interested in understanding and improving the performance of natural water treatment systems such as constructed wetlands, reed beds and riverbanks.

Approaching Bioelectrochemical Systems to Real Facilities Within the Framework of CO$_2$ Valorization and Biogas Upgrading

Laura Rovira, Pau Batlle-Vilanova, Sebastià Puig,
Maria Dolors Balaguer, Pilar Icaran, Victor M. Monsalvo,
Frank Rogalla, and Jesús Colprim

Abstract

Biogas production within wastewater treatment plants plays a decisive role in the water–energy nexus. Biogas obtained from sewage sludge digestion can be converted into biomethane as CO$_2$ emissions are reduced. Techno-economic assessment of the process is presented. Anodic valorization through chlorine production is performed. Potential impacts of this technology in a wastewater treatment plant are discussed.

Keywords

Microbial electrosynthesis • Biomethane • Carbon capture and utilization • Circular economy • Anodic valorization

1 Introduction

Carbon dioxide (CO$_2$) concentration in the atmosphere is rising as energy demand also does (EPA 2018; Hamiche et al. 2016). Meanwhile, it may suppose some effects to other interconnected critical resources such as water. In this sense, wastewater treatment plants (WWTPs) are an example of water–energy–CO$_2$ nexus as these facilities use energy-intensive processes and produce CO$_2$-saturated effluents to deal with water treatment. Biogas is the main product obtained from the anaerobic digestion (AD) of organic residues, which typically contains about 65% of methane (CH$_4$) and 35% of CO$_2$. Valorization of biogas in WWTP is carried out in cogeneration engines to obtain heat and electricity simultaneously (Appels et al. 2011). In order to

increment biomethane content as a sustainable and affordable biofuel, nowadays biogas upgrading technologies are getting more interest (European Biogas Association 2013). However, some of them such as water scrubbing release high amounts of CO$_2$ to the atmosphere (Rotunno et al. 2017), increasing the global warming potential (GWP). Recently, the exploitation of CO$_2$ using bioelectrochemical system (BES) has been presented as an alternative to increase biomethane production and reduce CO$_2$ emissions from biogas upgrading (Batlle-Vilanova et al. 2015). This system was tested in treating both synthetic and real effluents to demonstrate the technical feasibility. Here, a techno-economic assessment, valorization alternatives through the production of chlorine compounds, and foreseen impacts that the application of both technologies would have in a case scenario are also analyzed and discussed.

2 Materials and Methods

A two-chamber tubular BES separated by a cation exchange membrane (CMI-1875T) was constructed at 25 ± 1 ℃. Graphite granules were used as the cathode (working electrode), while Ti-MMO was used as anode (counter electrode) and Ag/AgCl electrode was placed in the cathode chamber (−0.8 V vs. SHE) and used as a reference electrode. The system was operated in continuous flow (60 mL h^{-1}), and as the net liquid volume of the cathode and the anode was 0.3 and 0.5 L, the resulting hydraulic retention time (HRT) was 4.9 and 8.3 h, respectively. The cathode was inoculated with an enriched mixed microbial culture dominated by *Methanobacterium spp.*, first fed by the synthetic medium based on a modified ATCC1754 PETC and after 60 days with treated wastewater from a WWTP located in Lleida (Spain). In both cases, CO$_2$ gas (99.9%, Praxair, Spain) was used as the only carbon source to simulate the scrubber absorbent effluent after treating biogas.

On the other hand, an abiotic two-chamber H-shape BES separated by a cation exchange membrane (standard CMX

L. Rovira (✉) · S. Puig · M. D. Balaguer · J. Colprim
LEQUiA, University of Girona, Campus Montilivi, C/Maria Aurèlia Capmany, 69, Girona, 17003, Catalonia, Spain
e-mail: laura.roviraalsina@udg.edu

P. Batlle-Vilanova · P. Icaran · V. M. Monsalvo · F. Rogalla
Department of Innovation and Technology, FCC Aqualia,
Avda. Del Camino de Santiago, 40, Madrid, Spain

Neosepta, Tokuyama Corp., Japan) was constructed focused on chlorine production in the anodic chamber. It consisted of a Ti-MMO electrode operated at +1.4 V versus SHE (Du et al. 2015), while graphite granules were used as a cathode electrode and Ag/AgCl electrode was used as a reference in the anodic chamber. The net liquid volume of the anode and the cathode was in both cases 0.12 L. The compartments were operated with a continuous flow of 15 mL h^{-1}, resulting in an HRT of 8 h. In this case, NaCl was added to the anode medium in different concentrations to assess chlorine formation. An overview of the whole process is exposed in Fig. 1.

Gas and liquid samples were periodically taken to measure pH, electric conductivity, and the production of organic compounds; free chlorine; and quantify gas production. Coulombic efficiency (CE) was also calculated to perform a techno-economic assessment and evaluate the impact of this technology in a real WWTP.

3   Results and Discussion

The proposed BES configuration was able to convert the CO_2 from biogas to biomethane. The CE was around 80% when the synthetic medium was used and diminished to 70% and when it was changed to real wastewater. This can be related to the low electric conductivity of the treated wastewater, which could have caused an osmotic stress period for the microorganisms and an increase of the overpotential of the system. These conditions led to a decrease of the intensity demand of the system. Moreover, CH_4 production rate also dropped to 38 mmol L^{-1} d^{-1} using real wastewater, but the process was still feasible. In addition, the gas composition was maintained at approximately 78% of

CH_4 and the CO_2 transformation efficiency of 30% remained unaltered, showing the potential of BES to use real effluents for the transformation of CO_2 into CH_4.

The techno-economic assessment revealed the need to valorize also the anodic process of the BES, so the abiotic chlorine production was studied to be included in the process flow diagram of WWTPs. It determined a CE threshold minimum value of 13% to make the process economically viable, which was achieved when reaching a chlorine concentration of 60 mg L^{-1}. However, the utilization of more specific electrodes for chlorine production would lead to an increase of CE values with lower NaCl input. This product entails an added economic value of the process and rises the application potential of this technology in the current circular economy framework.

4   Conclusion

The feasibility of using water scrubbing-like effluents obtained during biogas upgrading as a CO_2 source in BES was demonstrated. In the real case scenario approach exposed in this study, this system may produce an extra 41 Nm^3/d of biomethane, which supposes an increase of 17.5% of CH_4 and a decrease up to 42.8% of CO_2 content in the biogas composition. Moreover, chlorine produced may be used as a disinfection agent in the tertiary treatment of WWTPs, reinforcing the industrial application of this technology. Further efforts must be focused on coupling both reactions in the same system with high product formation rates and enough CE to make the technology a viable and competitive option. Otherwise, the use of renewable energy is also an attractive option to reduce the operation costs of the system.

Fig. 1 BES implementation proposal within WWTP for biogas upgrading and chlorine production
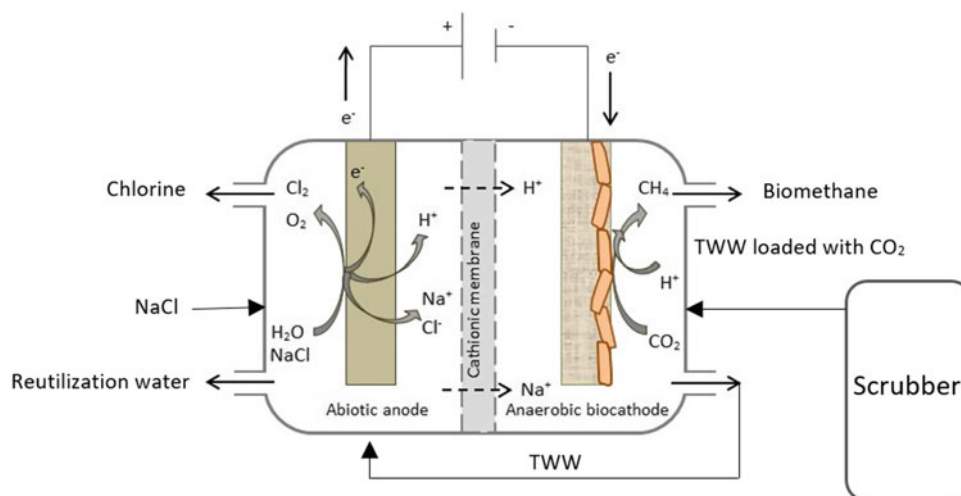
References

Appels, L., Lauwers, J., Degrève, J., Helsen, L., Lievens, B., Willems, K. … Dewil, R. (2011). Anaerobic digestion in global bio-energy production: Potential and research challenges. *Renewable and Sustainable Energy Reviews*, 15(9), 4295–4301. https://doi.org/10.1016/j.rser.2011.07.121.

Batlle-Vilanova, P., Puig, S., Gonzalez-Olmos, R., Vilajeliu-Pons, A., Balaguer, M. D., & Colprim, J. (2015). Deciphering the electron transfer mechanisms for biogas upgrading to biomethane within a mixed culture biocathode. *RSC Advances, 5*(64), 52243–52251. https://doi.org/10.1039/C5RA09039C.

Du, J., Chen, Z., Chen, C., & Meyer, T. J. (2015). A half-reaction alternative to water oxidation: Chloride oxidation to chlorine catalyzed by silver ion. *Journal of the American Chemical Society, 137*(9), 3193–3196. https://doi.org/10.1021/jacs.5b00037.

EPA. (2018). *Inventory of U.S. greenhouse gas emissions and sinks: 1990–2016*.

European Biogas Association. (2013). *Green gas grid. Proposal for a European biomethane roadmap*. Brussels, Belgium.

Hamiche, A. M., Stambouli, A. B., & Flazi, S. (2016). A review of the water-energy nexus. *Renewable and Sustainable Energy Reviews, 65,* 319–331. https://doi.org/10.1016/j.rser.2016.07.020.

Rotunno, P., Lanzini, A., & Leone, P. (2017). Energy and economic analysis of a water scrubbing based biogas upgrading process for biomethane injection into the gas grid or use as transportation fuel. *Renewable Energy, 102,* 417–432. https://doi.org/10.1016/j.renene.2016.10.062.

Water-Energy Nexus in the Gulf: A Complex Network of Multi-level Interdependencies

Ghena Alhanaee and Najmedin Meshkati

Abstract

The Persian/Arabian Gulf plays a critical role in the sustenance of its surrounding countries, home to over two-thirds of the world's proven oil reserves. With minimal rainfall and natural water sources, these countries rely heavily on desalination of the Gulf for potable water. A new industry is now emerging in the region: nuclear power. This adds another layer of complexity to the preservation of the already stressed Gulf water.

1 Introduction

The Arabian/Persian Gulf has quickly become a global hub for trade, tourism and transport. With oil at the root of this economic success, the countries surrounding the Gulf have evidently become highly dependent on this commodity. However, when taking a deeper look, another dependency arises, perhaps a much more stark, critical and vital one: water. The surrounding countries do not only rely on the Gulf for oil production and transportation of oil tankers, but in fact, a considerable amount of their drinking water as well. Eight countries surround the Gulf as depicted in Fig. 1: Iran, Iraq, Kuwait, Bahrain, Saudi Arabia, Qatar, UAE and Oman. This body of water is only 615 miles long with an average depth of 164 ft. The single opening to the wider ocean is the Strait of Hormuz and is only 35 miles wide (Meshkati et al. 2015). In terms of area, this enclosure is roughly half the size of the State of California. Yet, it holds nearly **half the world's desalination capacity**, at 45%.

This dependency is even more apparent when considering the percent of drinking water that is supplied by the Gulf for the surrounding countries. 99% of Qatar's drinking water is from desalination of Gulf water, while UAE and Kuwait are at 95%, according to statistics from 2010 (Meshkati et al. 2015). With the limited supply of groundwater being depleted and rainfall in the region scarce at only 7 in. of average rainfall per year, this dependency is only expected to climb. Even more alarming is that these countries do not have a reliable back-up source of water in the case of an emergency. Current storage capacity in these countries ranges from 48 to 72 h. This is being addressed by some of the countries, with Abu Dhabi city in UAE pioneering the way by building a large underground storage reservoir that can hold a 90-day supply of water for the residents of Abu Dhabi city, which was completed in early 2018 (Meshkati et al. 2015).

2 Materials and Methods

The interconnection of these two industries (oil and desalination) is clear. The success of each of them depends on the other. Without the availability of cost-effective energy provided by the oil industry, the energy-intensive desalination plants would not be practicable. UAE alone used more than 13 million tonnes of oil equivalent in 2016 to power their desalination plants (Energy Efficient Desalination 2018). Moreover, without the resources desalination plants are providing, a community would not be able to thrive in the region and support the oil industry. The two industries are critical for its people and for each other, but now a third industry has entered the scene and is growing: nuclear power.

G. Alhanaee (✉) · N. Meshkati
University of Southern California, Los Angeles, USA
e-mail: alhanaee@usc.edu

N. Meshkati
e-mail: meshkati@usc.edu

Fig. 1 Map of the Persian Gulf (Persian Gulf Map 2018)

There is currently only one operating nuclear reactor in the region, located in Bushehr, Iran. This status, however, is rapidly changing. Due to an acceleration in population growth and increasing demand for energy, the surrounding countries have turned to alternative sources of energy and several have identified nuclear power to be the most viable option for the future. UAE has 4 nuclear reactors under construction on the Gulf expected to go live in 2020, while Saudi Arabia has 16 nuclear reactors being planned. Site selection has not been concluded yet for Saudi Arabia; therefore, it is unclear whether all or only a portion of the reactors will be located on the Gulf, as Saudi Arabia also borders the Red Sea. This small body of water could potentially go from having only one nuclear reactor to **over 20 nuclear reactors** by the year 2030.

This emerging industry adds another complex layer to the already critical interdependency of the two large existing industries (oil and desalination). Nuclear reactors need extensive amounts of highly treated water for cooling. This means pumping water from the Gulf, and after specialized treatment, into the reactors to cool, and subsequently dumping out much warmer water into the Gulf. The Gulf is already expecting to see an increase in water temperature due to climate change, and this will only exacerbate the effect (Pal and Eltahir 2016). This change in temperature will not only impact the oil and desalination industries by reducing fuel conversion efficiencies, but will also impact the nuclear reactors. The warmer the water gets, the less efficient it is in cooling, resulting in larger amounts of water needed to cool, and in turn larger amounts of warmer water dumped back out into the Gulf. It develops a vicious cycle of temperature change. These industries become very highly interdependent on each other as they all inherently share the same lifeline of the Gulf water, as is summarized in Fig. 2.

3 Results and Discussion

It is imperative that these industries have some form of linkage that allows them to work interdependently with each other rather than independently, through a coordinated policy-making initiative that regulates their practices collectively and allows the sharing of data and information. Moreover, there is another crucial layer to the network. Not only is it necessary for these industries to collaborate and work collectively to protect and preserve their water source, but the surrounding countries must do so as well. A board that unites all countries collectively to share practices, information and make informed decisions on regulations is critical to sustain this water source for generations to come.
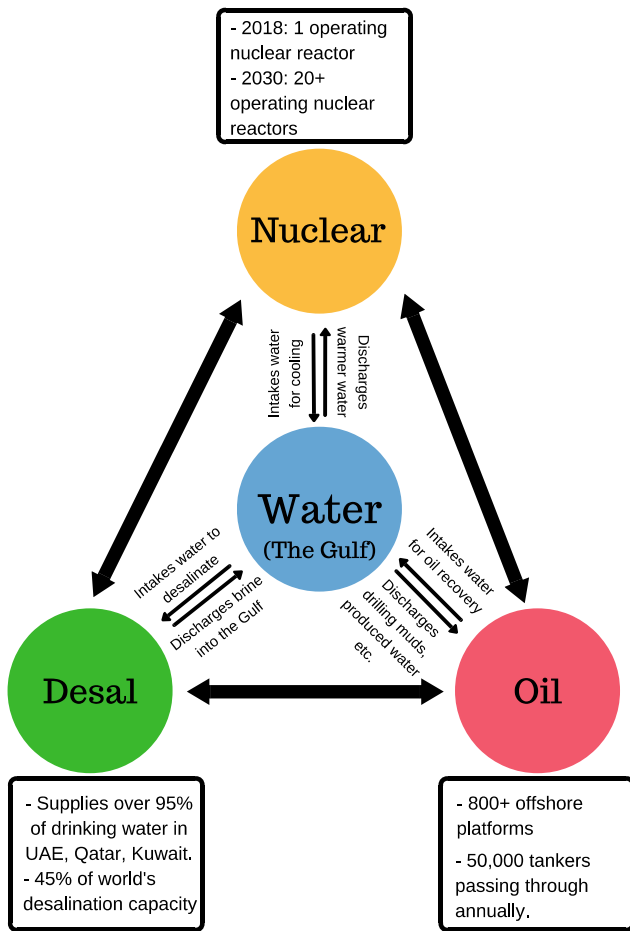
Fig. 2 Interdependent network of oil, desalination and nuclear industries in the Gulf

Figure 3 depicts a summary of what this layered network could look like. The top layer consists of a board in charge of establishing policies, regulating and monitoring practices by the surrounding countries. The second layer consists of transparent communication between countries and engagement and collaboration in sharing of data and resources. The final layer is the interdependent industries working together within each country to effectively and efficiently use the Gulf as a resource for their respective industries.

4 Conclusion

The Gulf is not just a lifeline for the countries directly surrounding it, but in fact, its safety and sustainability have serious global implications. At the end of 2017, the proven crude oil reserves collectively located in the surrounding eight countries was **over two-thirds** of the world's share (OPEC share of world crude oil reserves 2018). The success and preservation of the Gulf should be in *all* our shared interest.
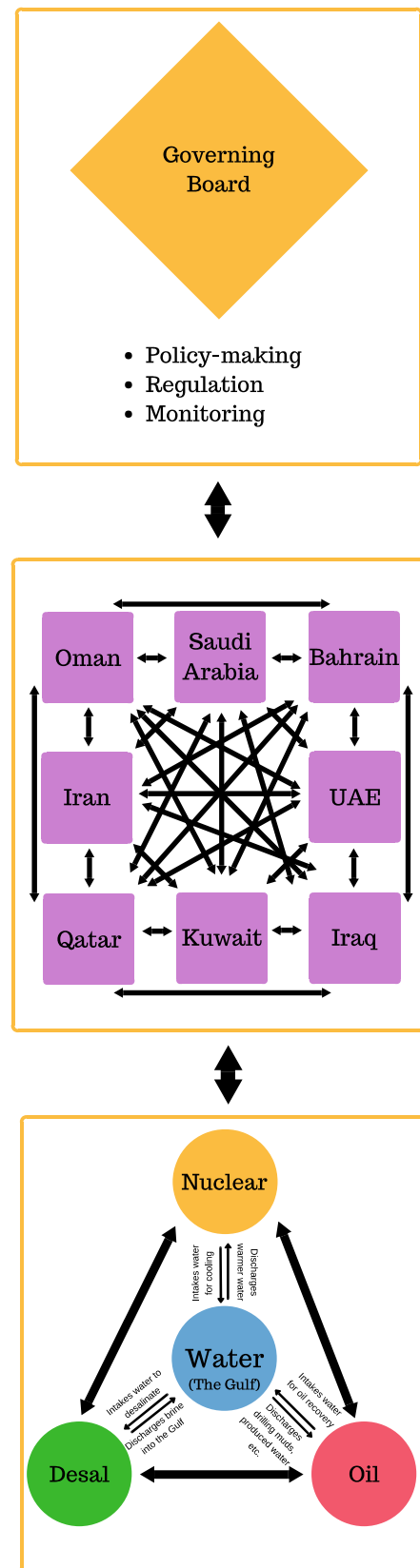
Fig. 3 Integrated network of co-ordination and collaboration among countries on the Gulf

References

Energy Efficient Desalination. International water summit. [Online] www.internationalwatersummit.com. Accessed June 27, 2018.

Meshkati, N., Tabibzadeh, M., Farshid, A., Rahimi, M., & Alhanaee, G. (2015). People-technology-ecosystem integration: A framework to ensure regional interoperability for safety, sustainability and resilience of interdependent energy, water and seafood in the Gulf. *Human Factors, 58,* 43.

OPEC share of world crude oil reserves. [Online] http://www.opec.org. Accessed June 27, 2018.

Pal, J. S., & Eltahir, E. A. (2016). Future temperature in southwest Asia to exceed human adaptability. *Nature Climate Change, 6,* 197–200.

Persian Gulf Map. On The World Map. [Online] www.ontheworldmap.com. Accessed June 27, 2018.

A Risk Assessment Approach for Water-Energy Systems

Antonio Nesticò, Gianluigi De Mare, and Gabriella Maselli

Abstract

Projects aimed at reducing water and/or energy consumption present technical and economic complexity profiles that require the analysis of the many components of investment risk. Risk analysis is essential to express judgements on the economic convenience of projects in the water-energy sectors. It is important to study actions for the mitigation of investment risk, so as to report the residual risk within tolerability limits. The integration of the as low as reasonably practicable (ALARP) logic with the cost-benefit analysis allows to define a protocol for the acceptance of the residual investment risk.

1 Introduction

Water and energy are the basis of economic and social development. Strictly interrelated, water is used in all processes for energy production. It considers, for example, extraction, transport and processing of fossil fuels or even irrigation for producing biofuels. In the same way, energy is required in all phases of water abstraction, transport and treatment. Suffice it to consider the pumping from underground or surface sources for the extraction of water resources; the supply through pipelines, also for household use, as regards the transport, desalination and treatment processes for water reuse (Mehzabeen et al. 2018; Zaman et al. 2017; Al-Saidi and Elagib 2017; Uen et al. 2018). From this, we understand that water-energy inter-linkages have significant implications for both water and energy security. With the increase in demand for water and energy, due to both rapid population growth and continuous climatic changes, it has become ever more important to understand the interconnections between the water and energy sectors (Chang et al. 2016; Shah et al. 2018; Khalkhali et al. 2018; Langergraber and Masi 2018). This is because the analysis of the possible stress-points related to the integrated use of water and energy is a necessary condition for adopting those policies, technologies and practices useful for mitigating the associated risks (International Energy Agency 2016).

Therefore, in order to a correct and transparent allocation process of resources to be allocated to the sectors of interest, i.e. water and energy, it is necessary to assess all the risks that may affect the overall performance of the single project. In fact, investments for the reduction of water and/or energy consumption—think, for example, of the technologies to decrease the consumption of energy required by a wastewater treatment plant—inevitably lead to environmental impacts to evaluate. Similarly, it is necessary to assess the financial risk of the investment to establish whether the costs incurred are disproportionate to the benefits obtained (Nesticò and Sica 2017; Guarini et al. 2019; Nesticò and Maselli 2019).

The purpose of the study is to propose a model for the economic evaluation of the mentioned initiatives, which allows to express a judgement on the acceptability of the risk, including not only financial rates but also those that affect the environment and the community. This integrates into the evaluation protocols, and therefore in the Cost-Benefit Analysis (CBA), the ALARP logic, able to define a risk tolerable only if as low as reasonably practicable and therefore to establish the disproportion of the mitigation costs with respect to the benefits achieved. Defined by the Health and Safety

A. Nesticò · G. De Mare · G. Maselli (✉)
Department of Civil Engineering, University of Salerno,
Fisciano, SA, Italy
e-mail: gmaselli@unisa.it

A. Nesticò
e-mail: anestico@unisa.it

G. De Mare
e-mail: gdemare@unisa.it

Executive (HSE), and generally applied to high-risk sectors for health and safety issues, the ALARP principle provides a guide for the acceptance of the residual risk associated with an investment (HSE 2001, 2014a, b, c).

The paper is structured in three paragraphs. In the first one, the ALARP logic is analysed in order to understand in which phase of the risk analysis process it can intervene. In the second part, it is shown how the ALARP approach can become an integral part of the decision-making if applied together with the cost-benefit analysis (CBA); therefore, a model for the acceptance of residual risk, useful for guiding the analyst towards a correct selection of possible alternatives in ex ante economic evaluations, is synthetically outlined. In the third part, the potentialities of the model and the possibility of applying it to evaluate the "extended" risk are displayed. The "extended" risk that is what includes also the components of non-financial risk. This becomes crucial with regard to projects involving an integrated use of water and energy.

2 ALARP Principle and CBA in the Decision-Making Process

It has been said that the projects in the water and energy sectors are characterized by multiple risk profiles that must be considered in the economic evaluations, since they significantly influence the final result of the CBA. To this end, we intend to outline an innovative risk assessment approach where the traditional evaluation techniques are integrated with the ALARP logic. This allows to express a judgement on the acceptability of the residual risk related to the investment, i.e. the risk that remains even after the adoption of the proposed mitigation measures. In light of the above, it is necessary to summarize the essential principles of both the ALARP and the CBA.

The ALARP principle assumes that «there is a level of risk which is tolerable and requires that the risk be at least below that level. (…) So ALARP assumes that there is a risk level which is so low that "it is not worth the cost" to reduce
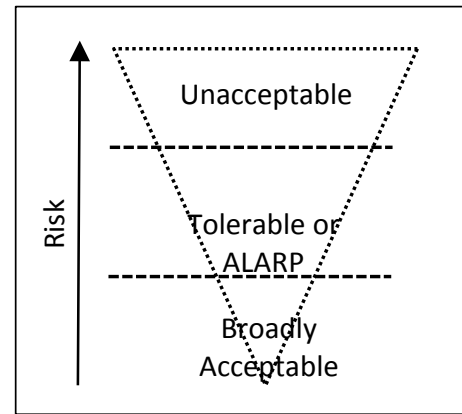
Fig. 2 ALARP principle

it further. In essence this means that risk reduction measures should be implemented until no further risk reduction is possible without very significant capital investment, or other resources expenditure that would be grossly disproportionate to the amount of risk reduction achieved» [Ale 2005, p. 1]. In Fig. 1, the downward slope shows the decrease in risk as the mitigation cost increases, while the upward slope shows that the clean-up costs in the event of damage are proportional to the level of risk. This means that a risk is tolerable if it falls in the ALARP area, i.e. if the costs for its minimization are greater than the expected costs in the event that damage occurs (Aven and Abrahamsen 2007; Jones-Lee and Aven 2011; Ale et al. 2015; Aven 2016). In this regard, in a triangular graph (Fig. 2), HSE identifies three risk regions separated by two thresholds: the tolerability threshold, which distinguishes the ALARP region from the "unacceptable" one in which the risk must necessarily be mitigated; the acceptability threshold, which separates the ALARP region, where the risk is tolerable if the costs to mitigate it are disproportionate, from the region in which the risk is widely accepted without requiring any reduction.

Therefore, in the risk analysis process, which in short consists in the identifying the risks related to the project initiative, in the characterization and assessment of risk and

Fig. 1 Risks and mitigation costs according to the ALARP principle
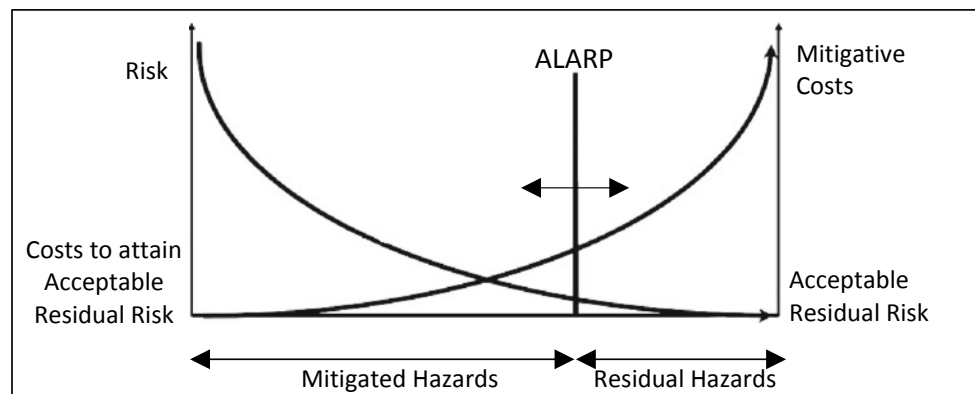
in the consequent detection of risk mitigation measures, the ALARP logic is useful to express a judgement on the acceptability of the residual risk, i.e. the one that remains despite the treatment strategy undertaken.
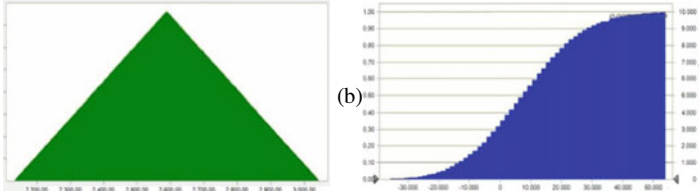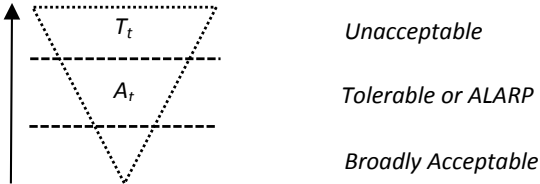
It should be noted that in the ALARP context the disproportion between costs and benefits obtained is reflected in the estimate of the Implied Cost of Averting one Fatality (ICAF). This indicator, which represents the cost or investment made to save an additional life, represents the investment divided by the decrease in expected number of fatalities due to the action:

$$\text{ICAF} = \frac{\text{Cost of mitigation measure}}{\text{Reduction in Potential Loss of Life}} \quad (1)$$

Comparing the estimated ICAF for the proposed option with reference ICAF values, specific according to the sectors considered, it is verified whether there is a disproportionate between the costs for risk mitigation and the advantages obtained. The risk is tolerable if it falls in the ALARP area, as additional costs to bring the risk to the acceptability threshold would be excessive.

In this sense, ALARP logic can be useful in the application of the ACB, which allows to evaluate the economic performance of a project or to identify, among different intervention alternatives, the most economically advantageous one. The careful forecast of the costs and benefits that the project generates in the analysis period, the timing and the subsequent discounting of the cash flows (CFs) makes it

Table 1 The phases of the analysis protocol

Activity 1	Definition of goals to be pursued through the risk analysis process	Verification of economic performance of the project for the investor. In terms of NPV: $$\text{NPV} = \sum_{t=0}^{n} \frac{B_t - C_t}{(1+r)^t} > 0$$ with B_t e C_t respectively benefits and costs of the project; r discount rate
Activity 2	Risk analysis	(a) Identification of project risk (b) Estimate of the probability distribution of the risk variables (c) Generation of the cumulative frequency distribution of the performance indicator, to verify the feasibility of the project. The probability to have NPV = 0 expresses the risk of failure R_f for the investor (a) (b)
Activity 3	Risk assessment	Comparison between R_f and the acceptability and tolerability thresholds (respectively A_t and T_t)
Activity 4	Selection of interventions for risk mitigation	- Estimate of the costs and benefits for the identified mitigation measures - Cost-benefit analysis in probabilistic terms - Probabilistic estimation of economic performance indicators following mitigation actions
Activity 5	Evaluation of residual risk	Estimation of the C coefficient: $C = \frac{C_m}{R_{f2} - R_{f1}}$ C_m = costs for mitigation intervention; R_{f1} = risk of failure before mitigation; R_{f2} = risk of failure after mitigation. Comparison between C and D_F, where D_F expresses the maximum cost that you are willing to support to bring the risk from the tolerability threshold T_t to the threshold of acceptability A_t: - if $C < D_F$, then the mitigation intervention is acceptable; - if $C > D_F$, then the mitigation intervention is acceptable only if $A_t < R_{f1} < T_t$, that is only if R_{f1} is ALARP

possible to estimate a synthetic indicator of profitability: the net present value (NPV), the internal rate of return (IRR), the benefits/costs ratio and the payback period.

3   Acceptance of Residual Risk for Projects in the Energy and Water Sectors

The ALARP logic, used in the evaluation schemes of cost-benefit analysis, is useful in decision-making concerning investments (Aven and Abrahamsen 2007; Jones-Lee and Aven 2011; Ale et al. 2015; Aven 2016). This is because ALARP makes it possible to consider the qualitative and holistic components of the project within the operational framework of the ACB, which is based on well-defined quantitative principles: «ALARP being on the qualitative, holistic, principles-based side does not necessarily lead to uniformly predictable outcomes, whereas CBA is on the quantitative, limited, precisely defined side. These characteristics expose both principles to criticism. Application of the ALARP process may to lead to different decisions in similar contexts resulting in uncertainty and unpredictability in decision-making. CBA leads to decisions in which only money counts and all that cannot be expressed in money or is perceived of no monetary value is neglected» [Ale et al. 2015, p. 91].

Precisely, the elements characterizing the ALARP logic and the ACB guide in the characterization of a protocol for the risk analysis related to the project initiatives. This protocol is briefly described in Table 1.

4   Conclusion

Investments aimed at the sustainable development of the water and energy sectors reveal multiple risk components, both financial and non-financial. These strongly influence the concrete feasibility of the interventions. Consequently, the assessment of risk becomes essential in the related judgements of economic convenience (Guarini et al. 2019; Nesticò and Maselli 2019; De Mare et al. 2017). Thus, the aim of the paper is to propose a protocol for the management of project risk. This can be done by integrating the ALARP logic into the procedural scheme of the ACB, providing a methodology for the acceptance of a residual risk that can guide the evaluator in choosing the most appropriate initiatives in relation to financial performance but also according to the environmental implications that the investment determines on the territory.

According to the structure of the economic investigation protocol, using the ICAF principles, it is possible to estimate a C coefficient useful to express an opinion on the acceptability of the residual investment risk in relation to

the cost of the interventions for the mitigation of the risk itself. The study highlights the potential of the model, which can be applied for the assessment of the "extended" risk also to the externalities deriving from the execution of the project. This is through the definition of coefficients able to express the disproportion between mitigation costs and benefits, but also through the characterization of the acceptability and tolerability thresholds of the individual residual risk rates attributable to non-financial effects, which are certainly relevant for the investments in question. Insights into the measurement of risk acceptance thresholds according to the nature of the project and concrete applications of the model to real cases outline prospects for future research.

References

Ale, B. J. M. (2005). Tolerable or acceptable, a comparison of risk regulation in the UK and in the Netherlands. *Risk Analysis, 25*(2), 231–241.

Ale, B. J. M., Hartford, D. N. D., & Slater, D. (2015). ALARP and CBA all in the same game. *Safety Science, 76,* 90–100.

Al-Saidi, M., & Elagib, N. A. (2017). Towards understanding the integrative approach of the water, energy and food nexus. *Science of the Total Environment, 574,* 1131–1139.

Aven, T. (2016). Risk assessment and risk management: Review of recent advances on their foundation. *European Journal of Operational Research, 253,* 1–13.

Aven, T., & Abrahamsen, E. B. (2007). On the use of cost-benefit analysis in ALARP processes. *International Journal of Performability Engineering, 3,* 345–353.

Chang, Y., Li, G., Yao, Y., Zhang, L., & Yu, C. (2016). Quantifying the water-energy-food nexus: Current status and trends. *Energies, 9*(2), 65.

Danish., Shah, S., Muhammad, AB., Lodhi, RN. (2018). The nexus between energy consumption and financial development: Estimating the role of globalization in next-11 countries. *Environmental Science and Pollution Research*, 1–11.

De Mare, G., Nesticò, A., & Macchiaroli, M. (2017). Significant appraisal issues in value estimate of quarries for the public expropriation. *Valori e Valutazioni, 18,* 17–23.

Guarini, M. R., Nesticò, A., Morano, P., & Sica, F. (2019). A multicriteria economic analysis model for urban forestry projects. *Smart Innovation, Systems and Technologies, 100,* 564–571. https://doi.org/10.1007/978-3-319-92099-3_63.

HSE. (2001). Reducing risks, protecting people: HSE's decision-making. HSE Books, London.

HSE. (2014a). http://www.hse.gov.uk/risk/theory/alarpglance.htm.

HSE. (2014b). Principles and guidelines to assist HSE in its judgements that dutyholders have reduced risk as low as reasonably practicable. http://www.hse.gov.uk/risk/theory/alarp1.htm.

HSE. (2014c). http://www.hse.gov.uk/risk/theory/alarpcba.htm.

International Energy Agency. (2016). Water energy nexus. Excerpt from the World Energy Outlook 2016.

Jones-Lee, M., & Aven, T. (2011). ALARP—What does it really mean? *Reliability Engineering and System Safety, 96,* 877–882.

Khalkhali, M., Westphal, K., & Mo, W. (2018). The water-energy nexus at water supply and its implications on the integrated water and energy management. *Science of the Total Environment, 636,* 1257–1267.

Langergraber, G., & Masi, F. (2018). Treatment wetlands in decentralised approaches for linking sanitation to energy and food security. *Water Science and Technology, 77*(4), 859–860.

Mehzabeen, M., Al-Ansari, T., Mackey, H. R., & Al-Ghamdi, G. (2018). Quantifying the energy, water and food nexus: A review of the latest developments based on life-cycle assessment. *Journal of Cleaner Production, 193,* 300–314.

Nesticò, A., & Maselli, G. (2019). Intergenerational discounting in the economic evaluation of projects. *Smart Innovation, Systems and Technologies, 101,* 260–268. https://doi.org/10.1007/978-3-319-92102-0_28.

Nesticò, A., & Sica, F. (2017). The sustainability of urban renewal projects: A model for economic multi-criteria analysis. *Journal of Property Investment and Finance, 35*(4), 397–409. https://doi.org/10.1108/JPIF-01-2017-0003.

Uen, T. S., Changh, F. J., Yanlai, C., & Tsai, W. P. (2018). Exploring synergistic benefits of water-food-energy nexus through multi-objective reservoir optimization schemes. *Science of the Total Environment, 633,* 341–351.

Zaman, K., Shamsuddin, S., & Ahmad, M. (2017). Energy-water-food nexus under financial constraint environment: Good, the bad, and the ugly sustainability reforms in sub-Saharan African countries. *Environmental Science and Pollution Research, 24*(15), 13358–13372.

Estimating the Declining Discount Rate for the Economic Evaluation of Projects in the Energy and Water Sectors

Antonio Nesticò and Gabriella Maselli

Abstract

In the cost-benefit analysis (CBA), the declining discount rate (DDR) certainly allows to assign the right weight for the long-term effects of investment projects. The DDR gives the opportunity to properly evaluate projects for sustainable development in the water and energy sectors. The estimation model of the DDR based on probabilistic logic solves the problem of the excessive contraction of the project cash flows that occur in temporal instants that are distant from the evaluation one.

1 Introduction

In the cost-benefit analysis (CBA) of an investment project, the parameter that most influences the economic performance is the social discount rate (SDR), which allows to make financially comparable the cash flows (CFs) that occur in different time periods (Arrow et al. 2013). Generally, the social discounting conducted for public projects takes place through a constant rate. In this way, we tend to attribute a progressively lower weight to the more distant costs and benefits in time. This problem, crucial for investments with long-term effects and therefore for those with environmental implications, is extremely topical. In fact, both the selection of sustainable projects and the use of energy and environmental resources, according to an integrated approach, are among the most urgent and complex issues that governments today wish. The rapid economic and demographic growth of the last decades, together with the increase in living standards and the unplanned urbanization, have caused an inefficient use of resources as well as sources of energy supply (Al-Saidi and Elagib 2017; Zaman et al. 2017; Khalkhali et al. 2018; Mehzabeen et al. 2018). This led us to consider the water, energy and food sectors as a unique system of scarce resources, even if characterized by intrinsic antagonisms. It follows that any intervention related to one of these three sectors inevitably affects its effects in the other two (Chang et al. 2016; Shah et al. 2018; Langergraber and Masi 2018; Uen et al. 2018). In other words, the use of the so-called nexus approach is necessary first to understand the energy–water interconnections and then to encourage the implementation investment initiatives that are more sustainable from both the environmental and the economic perspectives (Nesticò and Sica 2017; Guarini et al. 2019). The selection of these investment initiatives requires an *ex-ante* economic evaluation able to consider all the possible effects, even in the long term, that the initiatives will be able to generate (Nesticò and Maselli 2019). This applies precisely to those investments that require substantial consumption of water and energy and that inevitably entail environmental impacts. For instance, just think of the construction of thermal power stations, of water projects and of industrial plants, and of interventions to protect the soil or to reduce greenhouse gas emissions. These are all projects whose benefits are realized for many decades, while the mitigation costs are concentrated essentially in the first years of life of the works or in the immediate future (Arrow et al. 2013; Newell and Pizer 2003). A concrete possibility to consider in the economic analyses both the net benefits that the investment generates from the beginning and those concerning the future generations consists in resorting to time-declining discount rates. In this way, using namely discount rate progressively decreasing over time to be

A. Nesticò (✉) · G. Maselli
Department of Civil Engineering, University of Salerno, Fisciano, SA, Italy
e-mail: anestico@unisa.it

G. Maselli
e-mail: gmaselli@unisa.it

applied to cash flows according to the *consumption-based approach* or based on the *expected net present value approach* (ENPV), it is possible to reduce the contraction effect that the financial discounting causes on the most distant monetary terms in time. Such terms would become very small, even negligible, if a constant discount rate was used.

The first part of the paper deals with the theoretical issues concerning the estimation of the declining discount rate (DDR), whose use is crucial for the correct evaluation of projects with strong energy–water interconnections. An innovative evaluation model of the DDR is therefore outlined. This model is based on a probabilistic logic for estimation of the parameters on which the measurement of the rate depends. In the third part, the conclusions of the study are made and therefore prospects for future research are proposed.

2 Theoretical Approaches for Estimating the Declining Discount Rate

The use of declining discount rates makes it possible to solve the problem of the excessive contraction of CFs in discounting concerning investments that have a long "life", i.e. those that generate benefits, costs and risks over a period of time that goes beyond of the generations that evaluate them (Arrow et al. 2013; Newell and Pizer 2003). There are essentially two approaches recognized in the literature for estimating the declining discount rate:

1. The *consumption-based approach*;
2. The *expected net present value approach* (ENPV).

Following the first approach, the costs and benefits of the project are discounted to the consumption discount rate, i.e. the rate r_t at which «the society would be willing to exchange a unit of consumption in year t for a unit of consumption today» (Zhuang et al. 2007; Dasgupta 2008; Goulder and Williams 2012). It is a function of the discount rate of utility ρ, of the elasticity of the marginal utility with respect to consumption η and of the growth rate of consumption g_t:

$$r_t = \rho + h \cdot g_t \tag{1}$$

The greatest difficulty in the implementation of Formula (1) is linked to the estimate of the growth rate of consumption, because «any evaluation of g_t for the next century or millennium is subject to a potentially enormous error» (Gollier 2008). And it is precisely the uncertainty about this

parameter that determines declining functions of the discount rate. For example, Gollier (Gollier 2008) shows that when the consumption register follows a random trend and the relative average growth rate μ depends on an uncertain parameter θ, then g_t can be modelled as a sequence of random variables that are normally, independently and identically distributed (iid) with mean μ and variance σ^2. The function of g_t that is obtained is declining over time according to (2):

$$g_t = E_\theta \exp\left[-\eta \cdot t \left(\mu(\theta) - 0.5\eta \cdot \sigma^2\right)\right] \tag{2}$$

Using progressively more complex econometric models according to the starting hypothesis, a prediction of the trend of g_t is carried out, which conditions the term structure of r_t (Gollier 2011).

According to the *expected net present value* approach, precisely the uncertainty on the measurement of the discount rate r_t justifies the decreasing term structure of this parameter (Weitzman 1994, 1998, 2001). In fact, Weitzman (2001) demonstrates «that computing the expected net present value of a project (ENPV) with an uncertain but constant discount rate is equivalent to computing the NPV with a certain but decreasing "certainty-equivalent" discount rate» until reaching the minimum t value at the time $t = \infty$. On the basis of this corollary, the discounting of costs and benefits occurring at the future t is carried out using the discount factor P_t defined as:

$$P_t = \exp\left(-\sum_{i=1}^{t} r_i\right) \tag{3}$$

In particular, when r is a stochastic variable, it is necessary to introduce an uncertainty factor E which defines the declining structure of the discount rate. Then, the discount factor $E(P_t)$, called "certainty-equivalent", is written:

$$E(P_t) = E\left(\exp\left(-\sum_{i=1}^{t} r_i\right)\right) \tag{4}$$

It follows that the corresponding "certainty-equivalent" discount rate, intended as the exchange rate of the expected discount factor, applies:

$$\frac{E(P_t)}{E(P_t + 1)} - 1 = \widetilde{r_t} \tag{5}$$

In this circumstance, through specific econometric models, the goal is to forecast the long-term trend of the discount rate based on past trends of the interest rate (Nesticò and Maselli 2019; Groom et al. 2005; Hepburn et al. 2009).

3 The Economic Evaluation of Projects for the Sustainable Development of the Water and Energy Sectors—A Model for Estimating the DDR

The search for an innovative model for the DDR estimation, which is decisive for the cost-benefit analysis of projects with strong energy–water links, is derived from criticalities that connote each of the two approaches briefly described in the previous paragraph.

As regards the *consumption-based approach*, it should first be noted that the forecast of the growth rate of the consumption g_t that appears in (1) is based on econometric models that are not always simple to implement. For example, estimating the correlation parameters of the shocks relative to the growth rate of consumption is conditioned by preliminary hypotheses capable of significantly affecting the final result.

The *expected net present value approach*, on the other hand, is criticizable both for the nature of the data to be used, since the interest rates of the government bonds cannot be representative of the socio-economic structure of a country, and for the already highlighted difficulties of econometric models to predict the values of r_i that appear in (4).

The model that is outlined has two objectives. The first is to use data easily available from national and international databases. Hence the use of the formula of Ramsey (1), moreover able to reflect the socio-demographic structure of a country. This is a condition that does not occur by resorting to the interest rates of the Government Bonds. The second objective is to avoid the use of econometric models that require stringent preliminary hypotheses.

Thus, according to the steps in Fig. 1, we propose an approach based on the forecast of the r_t of the Ramsey formula according to probabilistic laws. In essence, the growth rate of consumption g_t can be modelled as a random variable, to which is associated the probability function that best approximates the historical starting data (steps 1 and 2 in Fig. 1). Starting from this probability function, through the Monte Carlo method, we estimate a series of probable values to be associated with the rate g_t and, consequently, to the unknown r_t (steps 3a and 3b). In this way, we arrive at the estimate of the discount factor and the "certainty-equivalent" discount rate (steps 4a and 4b). Models that are more sophisticated can also include more than one uncertain variable, associating probabilistic laws also with the ρ and η parameters.

4 Conclusion

«Water and electricity are fundamentally linked. At a basic level electricity generation requires water, and water treatment and transportation use electricity. Historically, there has been little reason to understand the nature of these links, due largely to the presumption that water was not a threat to energy security, nor electricity a threat to water security» [Hamiche et al. 2016, p. 319]. Today, however, it is commonly accepted that energy and water systems depend heavily on each other and «contribute significantly to several environmental impacts such as GHG emission, resource depletion and eutrophication, among others» [Al-Saidi and Elagib 2017, p. 312]. Therefore, it is essential to optimize the use of resources to minimize the impact on the environment. To this end, it is important to provide the decision-makers with a complete cognitive framework on the effects, both financial and non-financial, that the projects produce. This information framework can be obtained by implementing the economic evaluations that adequately consider the total costs and benefits that investments generate also in the long term (Guarini et al. 2019; De Mare et al. 2013).
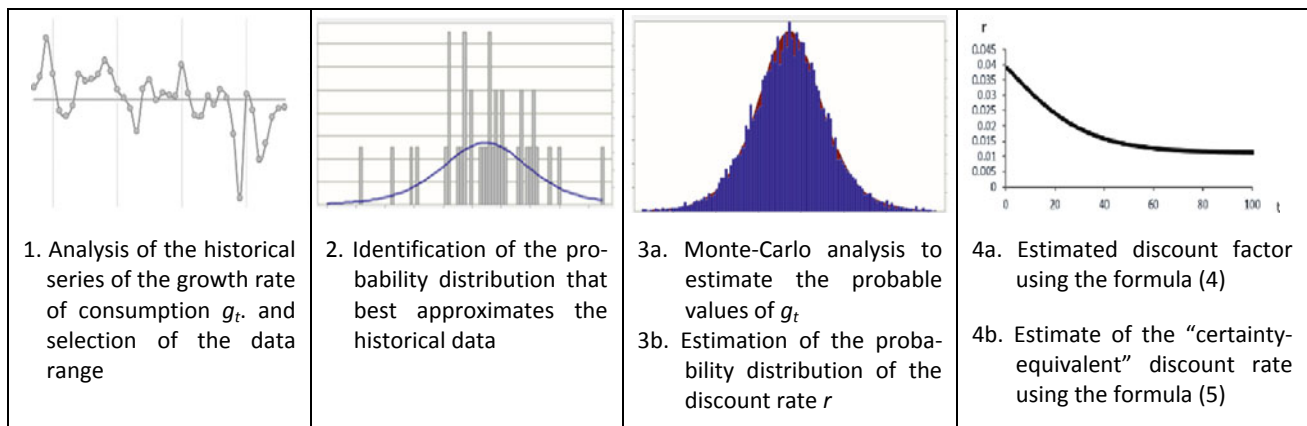
Fig. 1 Main steps of the model

In the CBA, the recourse to a declining discount rate makes it possible to attribute the right weight to the long-term positive externalities that the interventions propose for sustainable development. On the contrary, if a constant discount rate was applied, for example for the evaluation of projects whose purpose is to contain the greenhouse gas emissions, the marginal benefits expected from the mitigation of climate change would be underestimated, ignoring the uncertainty on the discount rate same (Arrow et al. 2013). In consideration of the centrality of the theme with respect to the objectives of the economic policy, the work outlines a model for the estimation of the declining discount rate, able to overcome the limits of the theoretical approaches recognized in the literature. The use of a probabilistic analysis approach allows to increase the reliability on the estimates of the economic performance of the projects with inter-generational effects whose extent is to be determined in the light of future research developments.

References

Al-Saidi, M., & Elagib, N. A. (2017). Towards understanding the integrative approach of the water, energy and food nexus. *Science of the Total Environment, 574,* 1131–1139.

Arrow, K. J., Maureen, L., Cropper, C. G., Groom, B., Heal, G. M., Newell, R.G., Nordhaus, W. D. (2013). *How should benefits and costs be discounted in an intergenerational context? The views of an expert panel.* Resources for the Future Discussion Paper, 12–53.

Chang, Y., Li, G., Yao, Y., Zhang, L., & Yu, C. (2016). Quantifying the water-energy-food nexus: Current status and trends. *Energies, 9*(2), 65.

Danish., Shah, S., Muhammad, AB., Lodhi, RN. (2018). The nexus between energy consumption and financial development: Estimating the role of globalization in next-11 countries. *Environmental Science and Pollution Research*, 1–11.

Dasgupta, P. (2008). Discounting climate change. *Journal of Risk and Uncertainty, 37*(2), 141–169.

De Mare, G., Manganelli, B., Nesticò, A. (2013). Dynamic analysis of the property market in the city of Avellino (Italy): The wheaton-di pasquale model applied to the residential segment. Lecture Notes in Computer Science, 7973 LNCS (PART 3), pp. 509–523. https://doi.org/10.1007/978-3-642-39646-5_37.

Gollier, C. (2008). Discounting with fat-tailed economic growth. *Journal of Risk and Uncertainty, 37,* 171–186.

Gollier, C. (2011). *Pricing the future: The economics of discounting and sustainable development.* NJ: Princeton University Press.

Goulder, L. H., & Williams, R. (2012). The choice of discount rate for climate change policy evaluation. *Climate Change Economics, 3*(4), 1–18.

Groom, B., Hepburn, C., Koundouri, P., & Pearce, D. (2005). Declining discount rates: The long and the short of it. *Environmental & Resource Economics, 32,* 445–493.

Guarini, M. R., Nesticò, A., Morano, P., & Sica, F. (2019). A multicriteria economic analysis model for urban forestry projects. *Smart Innovation, Systems and Technologies, 100,* 564–571. https://doi.org/10.1007/978-3-319-92099-3_63.

Hamiche, A. M., Stambouli, A. B., & Flazi, S. (2016). A review of the water-energy nexus. *Renewable and Sustainable Energy Reviews, 65,* 319–331. https://doi.org/10.1016/j.rser.2016.07.020.

Hepburn, C., Koundouri, P., & Pasnopoulou, E. (2009). Pantelidis T: Social discounting under uncertainty: A cross-country comparison. *Journal of Environmental Economics and Management, 57,* 140–150.

Khalkhali, M., Westphal, K., & Mo, W. (2018). The water-energy nexus at water supply and its implications on the integrated water and energy management. *Science of the Total Environment, 636,* 1257–1267.

Langergraber, G., & Masi, F. (2018). Treatment wetlands in decentralised approaches for linking sanitation to energy and food security. *Water Science and Technology, 77*(4), 859–860.

Mehzabeen, M., Al-Ansari, T., Mackey, H. R., & Al-Ghamdi, G. (2018). Quantifying the energy, water and food nexus: A review of the latest developments based on life-cycle assessment. *Journal of Cleaner Production, 193,* 300–314.

Nesticò, A., & Maselli, G. (2019). Intergenerational discounting in the economic evaluation of projects. *Smart Innovation, Systems and Technologies, 101,* 260–268. https://doi.org/10.1007/978-3-319-92102-0_28.

Nesticò, A., & Sica, F. (2017). The sustainability of urban renewal projects: A model for economic multi-criteria analysis. *Journal of Property Investment and Finance, 35*(4), 397–409. https://doi.org/10.1108/JPIF-01-2017-0003.

Newell, R. G., & Pizer, W. A. (2003). Discounting the distant future: How much do uncertain rates increase valuations? *Journal of Environmental Economics and Management, 46*(1), 52–71.

Uen, T. S., Changh, F. J., Yanlai, C., & Tsai, W. P. (2018). Exploring synergistic benefits of water-food-energy nexus through multi-objective reservoir optimization schemes. *Science of the Total Environment, 633,* 341–351.

Weitzman, M. (1994). On the environmental discount rate. *Journal of Environmental Economics and Management, 26*(2), 200–209.

Weitzman, M. (1998). Why the far-distant future should be discounted at its lowest possible rate. *Journal of Environmental Economics and Management, 36*(3), 201–208.

Weitzman, M. (2001). Gamma discounting. *American Economic Review, 91*(1), 261–271.

Zaman, K., Shamsuddin, S., & Ahmad, M. (2017). Energy-water-food nexus under financial constraint environment: Good, the bad, and the ugly sustainability reforms in sub-Saharan African countries. *Environmental Science and Pollution Research, 24*(15), 13358–13372.

Zhuang, J., Liang, Z., Lin, T., De Guzman, F. (2007). *Theory and practice in the choice of social discount rate for cost–benefit analysis: A survey.* ERD, Working Paper No. 94, Asia Development Bank.

Towards Resilience-Informed Decision-Making in Critical Infrastructure Networks

Maryam Imani, Donya Hajializadeh, and Vasos Christodoulides

Abstract

Resilience-informed decision-making is crucial for infrastructure interdependencies management; infrastructure interdependencies management requires shared interventions; resilience-informed interdependency management will support investments' prioritization for infrastructure improvement.

1 Introduction

Critical infrastructures (CI)s, including water network, energy network and transport network, provide essential services to the society. The centralized nature of these CIs and the interdependencies amongst services implies that damage at a point in the system can have knock-on effects on the system itself and other infrastructure systems (Guthrie and Konaris 2012). CI's criticality means it is vital that these systems to be resilient to any type of disturbances in the sense that they have an ability to resist failures and/or quickly resume their functionality when events occur (Mattioli and Levy-Bencheton 2014). Therefore, the pursuit

for infrastructure resilience requires a pursuit for the reduction of failure probabilities, reduction of negative consequences when failure does occur and reduction in recovery time (Walker et al. 2004; Chang 2009). Hence, the importance of protecting the infrastructure from threats lies not only in its critical role of sustaining societies, but also in its role of helping communities and the economy to rebuild themselves post-disruptions (shocks and stresses).

The common challenge currently faced by asset owners and managers is the lack of a robust resilience-informed business planning and management strategies in response to interdependent assets' failures due to low-probability/high-impact hazards. Currently, the available decision support systems (DSS) (e.g. iRoad and Neptune) rely on risk/vulnerability measures while interdependencies and their resilience in response to extreme hazards are overlooked. Therefore, better understanding of these interdependency relations can support enhancing planning, maintenance, emergency decision-making and CI's overall performance. This paper approaches water-energy nexus from resilience-informed CI's interdependency management point of view. Resilience-informed decision-making can provide greater scope than risk analysis and can account for a wider range of threats, particularly in response to low-probability/high-impact hazards.

2 Materials and Methods

The methodology of this study consists of four steps:

Step 1: **Benchmark development**

Network theory has been used to generate and characterize the topology of the hypothetical benchmark network comprising of three key infrastructures of water, energy and transport (Fig. 1a), utilized for resilience evaluation of the interconnected infrastructure network. Mathematically, a topological network can be represented as a graph with

M. Imani (✉) · V. Christodoulides
School of Engineering and the Built Environment (EBE), Anglia Ruskin University, Chelmsford, Essex, CM1 1SQ, UK
e-mail: Maryam.Imani@anglia.ac.uk

V. Christodoulides
e-mail: Vasos.Christodoulides@anglia.ac.uk

D. Hajializadeh
Lecturer in Structure and Bridge Engineering, Department of Civil and Environmental Engineering, University of Surrey, Guildford, Surrey, GU2 7XH, UK
e-mail: d.hajializadeh@surrey.ac.uk

Fig. 1 **a** Numerical benchmark network; **b** Failure propagation map
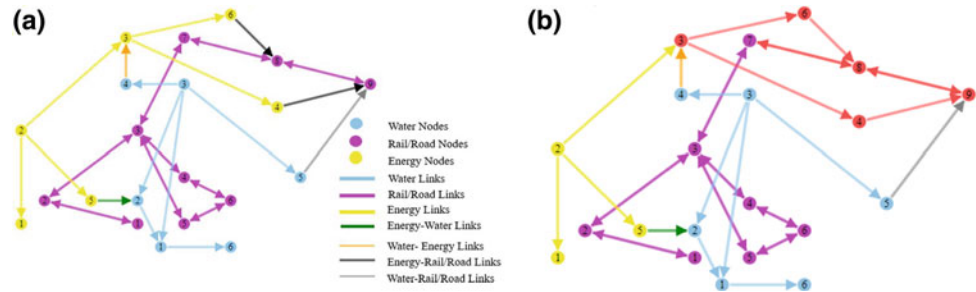
Fig. 2 **a** Resilience evaluation curve; **b** Resilience thresholds and zones
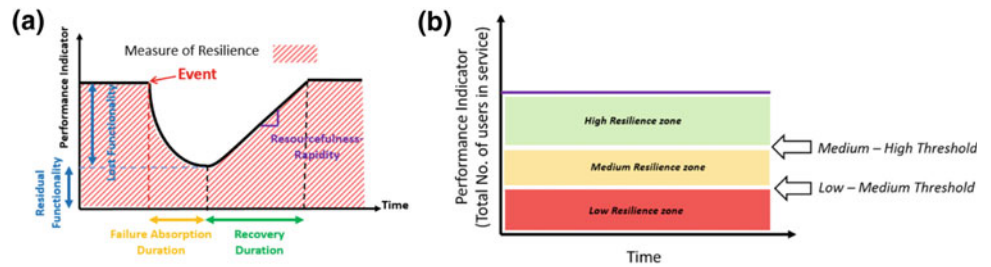
nodes and links representing their connectivity nature (in total, 21 nodes, 20 links and 5 interdependent links in Fig. 1a). These nodes and links represent different assets in each network, for example generators, transmission lines, switches and breakers in energy network; reservoirs, water mains, pumping stations in water network and bridges, junctions, roads and rail lines in transport network. Additionally, an asset register records network properties such as the present value of each asset, maintenance history (e.g. recovery cost, recovery time), dependencies type and flow. In this study, a *number of users per asset* were used as the network performance indicator.

Step 2: **Failure scenarios and failure propagation**

Failure at asset level and overall network depends upon network attribute assignment, topological characteristics and their mapping to special scales. The failure scenarios are defined regardless of the origin, type and severity of the initiating hazardous event (e.g. extreme rainfall and earthquake), so-called failure state. Failure state represents the condition (operational condition and/or physical condition) of a network, causing a negative impact on network performance (partially or fully), regardless of the initiating source. The impacts of these failure scenarios are reflected on the number of users remain in service. Figure 1b illustrates an example of a single failure scenario with its impact on the total network performance assuming 3 h of failure propagation time.

Step 3: **Resilience evaluation**

To measure resilience, a two-dimensional metric has been used to reflect on time and performance indicator (network functionality) at the same time (Fig. 2a). As can be seen from Fig. 2a, resilience is defined as the area covered by the performance indicator diagram. This area reflects network robustness, recoverability, rapidity and resourcefulness in one single metric. To calculate resilience, this study uses the recovery initiation time and average recovery duration, to calculate the full recovery time since failure time and produces the area of the performance indicator diagram as a measure of resilience.

Step 4: **Interventions assessment**

In this study, intervention is a function of recovery cost and recovery time (initiation time/lag and duration). The impacts of the interventions are assessed through resilience improvement in the network. For this purpose, *£100 cost per one user in service × one unit of time (i.e. unit of resilience)* has been assumed and used to measure the effectiveness of the intervention strategies.

The concept of 'level of resilience' has been introduced in this study to demonstrate the resilience level in a network pre and post interventions. These values can be interpreted as acceptable risk zones in resilience context. These values are generated by default; however, the user has the possibility of varying these thresholds (low-medium threshold and medium-high threshold) depending on the acceptable 'level of resilience' for each network. The unit for these thresholds is 'number of user in service × time'. Hence, three resilience zones of low resilience zone (in red), medium resilience zone (in amber) and high resilience zone (in green) are created (Fig. 2b). The improvement in recovery strategies can include increase in redundancy, robustness or resourcefulness in different part of the interdependent network.

3 Results and Discussion

Figure 3a demonstrates a single failure scenario and its propagation across the whole system. The failure of node 2E results in full failure of energy network. Assuming the recovery initiation time and recovery duration of 1 and 4 h, respectively, the performance indicators will demonstrate the bouncebackability of the network. As can be seen from Fig. 3b, the failure is not fully propagated to water and transport network as the initiating failed asset has recovered prior to the full propagation, leaving transport network without any failure and water network with maximum of 20% loss in functionality. To investigate the impact of change in recovery measure, the recovery duration has changed from 4 to 3 h. Figure 3c shows the change in performance indicator. It can be seen from this figure, the resilience of energy network changes from 1650 (no. users × time) to 1750. Assuming unit cost of £100/(no. users × time), this change represents £10,000 saving in resilience. This value then can represent the benefit in recovery measure against the cost of the recovery.

It is crucial for infrastructure asset owners to have a better understanding of the dynamics of their networks' 'interdependency zones', their resilience levels and the impacts of the resilience changes across the integrated network. This will enable them to track the failure propagation at times of failure to make resilience-informed decisions for shared interventions. Drawing on this, an 'impact matrix' has been produced (see Fig. 4) to map the resilience of interdependent zones vs a user-defined maximum failure allowed (e.g. 50 users without service in this study) to identify the most critical zones in each CI network. The 'impact matrix' will particularly support decision-makers to prioritize their decisions for interventions. Figure 4 maps all the interdependency zones in Benchmark network in Fig. 1a (total of 8) presented as grey dots in Figs. 4a–c (each grey dot represent one interdependency-induced failure). The exemplary interdependency-induced failure scenario shown in Fig. 3a (i.e. failure of node 2E) has been highlighted in red for each network in Fig. 4a–c in comparison with other scenarios.

As can be seen, this interdependency-induced scenario doesn't have much impact on water and road networks as it falls in green area, but it is quite concerning in energy network as the maximum failure is high while resilience level is low (according to the user-defined thresholds). This was expected as failure of node 2E technically fails all the assets in the energy network due to its high level of dependency on this node and vulnerability of the system to its failure. Similar scenarios could be investigated and mapped by the 'impact matrix' to assist CI asset owners to prioritize the interdependency-induced scenarios based on their resilience levels.
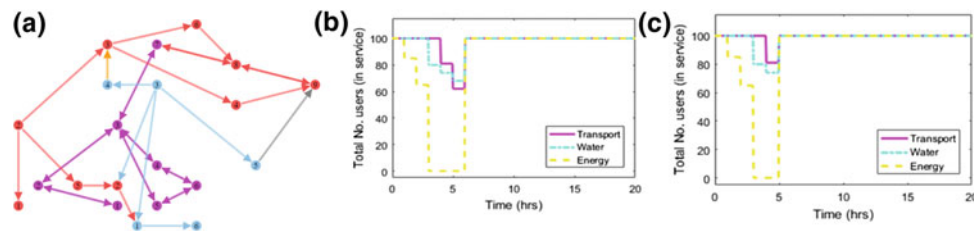
Fig. 3 **a** Failure propagation map of the node 2E; Change in performance indicator considering the recovery of the failed asset (2E); **b** Recovery duration of 2 h (default); **c** Recovery duration of 1 h (amended)

Fig. 4 Resilience impact matrix; **a** Water network; **b** Energy network; **c** Transport network
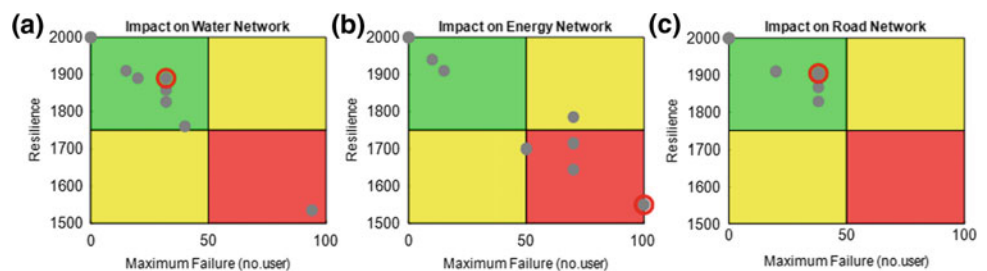
4 Conclusion

This paper presents some outcomes of the resilience-vulnerability–informed decision-making framework tool feasibility study and its application to a numerical case study. In chaotic environments such as emergency response to catastrophic events, CI decision-makers should understand the dynamics underlying the infrastructures. Failure to understand these dynamics will result in ineffective response and poor coordination between decision-makers and agencies responsible for rescue, recovery and restoration. The results show that resilience-informed decision-making can complement the conventional risk-informed decision-making for infrastructure management particularly in dealing with low-probability high-impact events. Also, enhanced CI interdependencies management requires collaboration and shared intervention amongst all the role players. Resilience-informed interdependency management can transform the investment strategies in CI sectors.

References

Chang, S.E. (2009). Infrastructure resilience to disasters. In *2009 Frontiers of Engineering Symposium* (pp. 1–4).

Guthrie, P., & Konaris, T. (2012). *Infrastructure and resilience, government office of science, foresight project 'reducing risks of future disasters: Priorities for decision makers'*, London, UK.

Mattioli, R., & Levy-Bencheton, C. (2014). Methodologies for the identification of critical information infrastructure assets and services, European Union Agency for Network and Information Security (ENISA). ISBN 978-92-9204-106-9. https://doi.org/10.2824/38100.

Walker, B., Holling, C. S., Carpenter, S., & Kinzig, A. (2004). Resilience, adaptability and transformability in social—ecological systems. *Ecology and Society*, *9*(2).

Short-Term Forecasting of Tank Water Levels Serving Urban Water Distribution Networks with ARIMA Models

Claudio Guarnaccia, Carmine Tepedino, Giacomo Viccione, and Joseph Quartieri

Abstract

Urban water demand forecasting is a powerful supporting tool for specific water utility decision making problems. Among the others, ARIMA is one of the possible approaches to achieve an efficient short-term forecasting.

Keywords

Short-term forecasting • Urban water demand • Time series • ARIMA models

1 Introduction

Accurate urban water demand forecasting (Gardiner and Herrington 1990) provides the basis for making operational and strategic decisions for drinking water utilities, e.g., to control the production, storage and water delivery, either in the short (Bougadis et al. 2005) and long period (Xu et al. 2015). Most of the papers dealing with forecasting urban water demand consider annual or monthly data. Few address daily water use. For instance, Maidment and co-workers (1985) developed a short-term forecasting model based on Box–Jenkins time series analysis. Chen and Boccelli (2014) proposed an integrated Time Series Forecasting Framework (TSFF) to statistically predict hourly/quarter-hourly demands. The problem is not trivial as many variables are considered of influence in determining drinking water demand, e.g., trend, seasonality, climatic correlation and autocorrelation. In contrast to time-distant observations, close ones are expected to be highly correlated.

C. Guarnaccia · C. Tepedino · G. Viccione (✉) · J. Quartieri
Department of Civil Engineering, University of Salerno, Fisciano, Italy
e-mail: gviccion@unisa.it

C. Guarnaccia
e-mail: cguarnaccia@unisa.it

J. Quartieri
e-mail: quartieri@unisa.it

In the following, the authors prove that water levels of urban tanks serving water distribution networks are properly forecasted by a stochastic model with moving average and autoregressive approaches, namely the AutoRegressive Integrated Moving Average (ARIMA) model (Box et al. 2015). The proposed models will be calibrated on a dataset of tank water levels recorded in the tank of Cesine (Avellino, Italy).

2 Materials and Methods

In this section, the two models chosen for analyzing the available dataset are presented. Let us underline that the coefficients of the models have been evaluated in the framework of "R" statistical software, using part of the available dataset for calibration purposes. Adopting the maximization of the likelihood, the software provides the estimation of the model parameters.

2.1 Model 1, ARIMA(2,0,2)

This model does not present a differentiation in the data. The model forecasting, given by Eq. (1), furnishes the estimation of the quantity Y at the time t. In our case, Y is the tank level, and μ is the intercept of the model, while φ_1, φ_2, ϑ_1, ϑ_2 are, respectively, the autoregressive (AR1 and AR2) and moving average (MA1 and MA2) parameters:

$$\hat{Y}_t = \mu + \varphi_1(Y_{t-1} - \mu) + \varphi_2(Y_{t-2} - \mu) + \vartheta_1(e_{t-1}) + \vartheta_2(e_{t-2}) \tag{1}$$

e_{t-i} is the residual at time t-i (the difference between observed and estimated tank level). The need of knowing e_{t-1} for giving the forecast forces this model to furnish prediction only "one step ahead". Values of the model parameters, estimated using the calibration dataset, are reported in Table 1. An intercept of about 2.7 m can be considered the mean value of the tank level during the calibration period.

Table 1 Estimated coefficients of the ARIMA (2,0,2) model and related standard errors

ARIMA (2,0,2)	Intercept	AR1	AR2	MA1	MA2
Estimated value	2.7314	1.8491	−0.8926	−0.4743	−0.1794

2.2 Model 2, ARIMA (3,1,3)

This model presents an order one differentiation and includes one more term, both on the autoregressive and on the moving average parts. The model forecasting formula is reported below and, again, furnishes the estimation of the quantity Y at the time t. Y, φ_i, ϑ_i and e_{t-i} have the same meaning of above:

$$\hat{Y}_t = Y_{t-1} + \varphi_1(Y_{t-1} - Y_{t-2}) + \varphi_2(Y_{t-2} - Y_{t-3}) \\ + \varphi_3(Y_{t-3} - Y_{t-4}) + \vartheta_1(e_{t-1}) + \vartheta_2(e_{t-2}) + \vartheta_3(e_{t-3}) \quad (2)$$

Again, in order to give the prediction, this model needs e_{t-1}, thus only "one step ahead" forecasts can be produced. Table 2 reports the estimation of the model parameters, estimated using the calibration dataset.

3 Case Study and Dataset Description

The models presented above have been calibrated on a time series of water tank levels measured in the Cesine tank. This tank belongs to the network that provides drinking water to the city of Avellino, Italy. The chosen time series refers to 2014 and reports the daily level measurements, in meter. The first 333 data (from January 2 to November 30, 2014) have

been used for calibrating the models and to estimate the parameters in the "R" software (see Sect. 2). The last month, December 2014, has been used to validate the models, i.e., comparing the results of models with data that have not been used in the estimation of the parameters. The results of the validation will be presented in a further work.

Since some data were missing and since the models need to work on a continuous dataset, the missing data have been imputed with the mean of the previous and successive measured data. This simple approach usually works in non-seasonal time series, such as the one considered here, since the linear interpolation takes care of the temporal location of the missing data, with respect to closest points (Moritz et al. 2015). Other possible imputation techniques can be found in literature, for example, in (Guarnaccia et al. 2015), in which a deterministic time series model and a regression method are compared.

4 Results and Discussion

The results of the models are plotted in Figs. 1 and 2, overlapped with the observed data. The statistics of the residuals (i.e., observed minus predicted tank level in each time period) are reported in Table 3.

Table 2 Estimated coefficients and standard error of the ARIMA (3,1,3) model

ARIMA (3,1,3)	AR1	AR2	AR3	MA1	MA2	MA3
Estimated value	1.2350	0.2090	−0.5201	−0.8703	−0.5839	0.4542

Fig. 1 Observed and forecasted water levels of the Cesine tank in the calibration time range. The black line is the observed series, and the red line is the forecast of the ARIMA (2,0,2) model
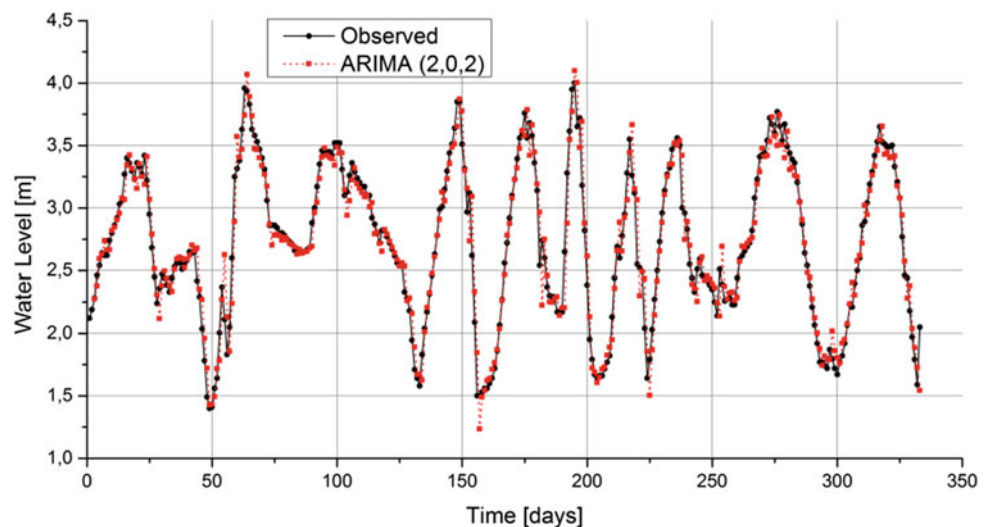
Fig. 2 Observed and forecasted water levels of the Cesine tank in the calibration time range. The black line is the observed series, and the blue line is the forecast of the ARIMA (3,1,3) model
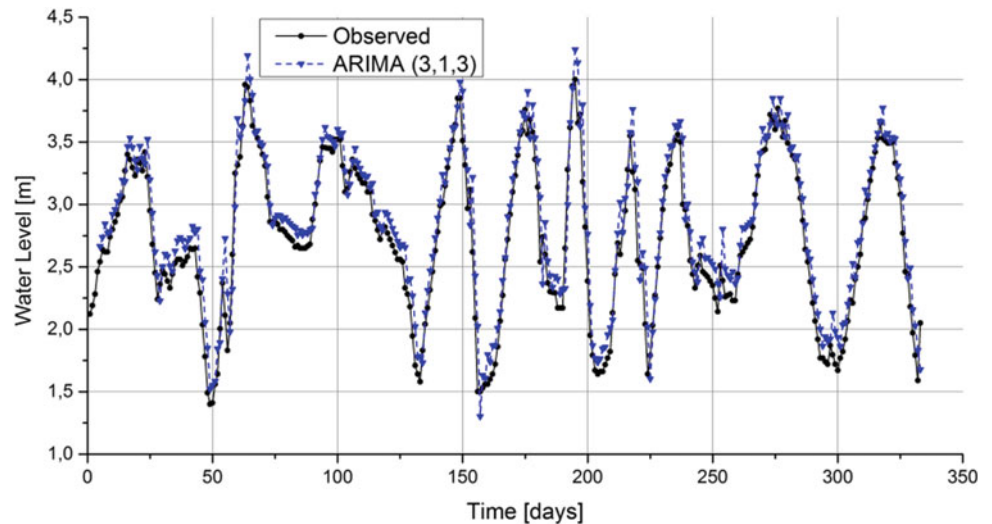
Table 3 Summary statistics of the residuals during the calibration phase

ARIMA model	Mean (m)	Std. Dev. (m)	Median (m)	Min (m)	Max (m)	Skewness	Kurtosis
#1, (2,0,2)	0.00	0.15	0.00	−0.52	0.52	−0.22	2.18
#2, (3,1,3)	−0.12	0.15	−0.12	−0.63	0.38	−0.15	2.03

Let us underline that both models provide "one step ahead" prediction, adopting the data of the previous day to produce the forecast (see formulas 1 and 2).

It can be noticed from Fig. 1 that model 1 (red line), i.e., ARIMA (2,0,2), follows quite precisely the observed data (black line). The sudden and steep fluctuations of the tank level are not exactly captured by the model. This is due to the fact that the model needs at least one period of time (in this case one day) to get the sudden variations of the series.

Looking at Fig. 2, the plot of model 2 (blue line), i.e., ARIMA (3,1,3), can be compared with the observed data (black line). It can be deduced that the implementation of a more complex model, with first order differentiation and with two terms more, does not provide strong benefits in the prediction. There is a quite general overestimation by the model, and this is confirmed by the mean of the residuals, as can be seen in Table 3. Model 1 performs better than model 2 and should be preferred in this case study of "one step ahead" prediction of daily water tank levels.

5 Final Remarks

In this paper, the modeling of water tank daily level behavior has been faced by means of ARIMA approach. The case study of Cesine tank, that provides drinking water to Avellino, Italy, has been used for calibration of the parameters and comparison between observed and forecasted data. The proposed models provide predictions for the following day, giving quite good results. Model 1, i.e., ARIMA (2,0,2), gives, on average, better results of model 2, i.e., ARIMA (3,1,3), even though it has a lower number of parameters. The mean of the residuals, that are the differences between observed and predicted tank levels, is very close to zero, for both models, suggesting that this approach can be successfully used in these kinds of problems.

References

Bougadis, J., Adamowski, K., & Diduch, R. (2005). Short-term municipal water demand forecasting. *Hydrological Processes, 19* (1), 137–148. https://doi.org/10.1002/hyp.5763.

Box, G. E. P., Jenkins, G. M., Reinsel, G. C., & Ljung, G. M. (2015). *Time series analysis: forecasting and control*, (5th ed.). Wiley Series in Probability and Statistics, ISBN 978-1-118-67502-1.

Chen, J., Boccelli, D. L. (2014). Demand forecasting for water distribution systems. In *12th International Conference on Computing and Control for the Water Industry*, CCWI2013, Procedia Engineering (Vol. 70, pp. 339–342).

Gardiner, V., & Herrington, P. (1990). *Water demand forecasting* (1st ed.). London: Spon Press.

Guarnaccia, C., Quartieri, J., Tepedino, C., & Petrovic, L. (2015). A comparison of imputation techniques in acoustic level datasets. *International Journal of Mechanics, 9*, 272–278.

Maidment, D. R., Miaou, S. P., & Crawford, M. M. (1985). Transfer function models of daily urban water use. *Water Resources Research, 21*(4), 425–432.

Moritz, S., Sardá, A., Bartz-Beielstein, T., Zaefferer, M., & Stork, J. (2015). Comparison of different methods for univariate time series imputation in R. arXiv preprint, arXiv:1510.03924.

Xu, W., Zhao, J., Zhao, T., & Wang, Z. (2015). Adaptive reservoir operation model incorporating nonstationary inflow prediction. *Journal of Water Resources Planning and Management, 141*(8), 04014099.

Energy Balance in the Water Cycle in Italy: State of the Art and Perspectives

Giorgio Bertanza, Sabrina Sorlini, and Mentore Vaccari

Abstract

Energy consumption for water withdrawal is the main contribution to energy consumption in drinking water supply systems. Energy consumption in large Italian WWTPs should be lower than about 25 kWh PE^{-1} y^{-1}. Energy recovery in Italian WWTPs takes place mostly by the exploitation of biogas from anaerobic digestion of sewage sludge.

1 Introduction

There is an increasing interest towards energy efficiency in the water cycle due to the increasing cost for energy supply and the consequent emission of greenhouse gases and air pollution. In drinking water supply systems (DWSSs), the predominant electrical energy consumption (EEC) is due to pumping: in groundwater-based DWSSs, raw water extraction accounts for about 30% of the overall EE consumption, 69% being the contribution of water distribution. As regards surface water-based DWSSs, raw water extraction accounts for 10%, clean water distribution for 80% and treatment for 10% of the total EEC.

Energy consumption in a wastewater treatment plant (WWTP) is affected by several factors, such as design capacity, population served, plant configuration, type of sewer system, inlet and outlet wastewater quality, electrical efficiency of electro-mechanical devices and age of the plant; as a consequence, the EEC of a WWTP can vary from 1.5 to 40 kWh kg BOD$_{removed}^{-1}$. Wastewater pumping and bioreactor aeration are responsible for the major contribution to the overall EEC; sludge recirculation and aerobic stabilisation can be comparably relevant in small WWTPs (Foladori et al. 2015).

The energy potential of wastewater is quite interesting (about 500 kWh PE^{-1} y^{-1} of thermal energy and about 150 kWh PE^{-1} y^{-1} of chemical energy). Actually, renewable energy recovery (through biogas production and utilisation, hydropower or heat from wastewater) is quite practicable. Consolidated sludge pre-treatment options (e.g. hydrolysis) are available for boosting the anaerobic stage. Another interesting solution is the sludge co-digestion with other organic substrates with high methane yield. Moreover, biogas cleaning for producing bio-methane to be used in higher efficiency machineries is being practised in large plants. In addition, research is focusing on Microbial Fuel Cells (MFCs), hydrogen and methanol production. In the field of sludge combustion, pyrolysis-gasification is being proposed, together with Organic Rankine Cycle (ORC) systems for recovering energy from low-temperature streams. Finally, wind and solar energy exploitation is another practicable option.

The workgroup "Water treatment plant management" (WG), which has been active at the University of Brescia since 1998, has focused on the water-energy nexus for about 10 years. As regards the DWSSs, the WG conducted a research aimed at analysing EEC in seven full-scale Italian DWSSs. Italian companies usually have data concerning a global EEC in DWSSs, resulting from the electricity bill, and they do not carry on any analytical monitoring of EEC. This prevents them from having any control of EEC in each single stage of the DWSS and from identifying opportunities

G. Bertanza (✉) · S. Sorlini · M. Vaccari
University of Brescia, Brescia, Italy
e-mail: giorgio.bertanza@unibs.it

S. Sorlini
e-mail: sabrina.sorlini@unibs.it

M. Vaccari
e-mail: mentore.vaccari@unibs.it

for reducing energy consumption in DWSS. The first aim of the research was to divide this all-inclusive EEC data into three main parts, respectively, related to water withdrawal, treatment and distribution. Moreover, the objective was to focus on the drinking water treatment plant (DWTP) to detect EEC related to each drinking water treatment process, in order to quantify the incidence of each treatment phase in the whole DWTP.

The WG carried out also one of the largest surveys in Europe about energy consumption of WWTPs, based on a total population equivalent of more than 9,000,000 PE, with the aim of adding a new benchmark to the international framework of energy consumption in WWTPs. Moreover, a survey on about 600 Italian WWTPs (corresponding to approximately a quarter of the national load of treated sewage) was carried out to understand the current status of implementation of energy recovery options (Papa et al. 2017).

In case a new (water or wastewater) treatment plant has to be built, the entire design-to-construction process can focus on optimising the interactions among the different treatment units. Thus, original solutions including energy saving and recovery can be properly addressed. On the contrary, retrofitting existing plants is indeed a challenge. The choice either or not to implement new solutions is quite a difficult task: consequences at various levels (environmental, economic, social, technical and administrative) must be carefully evaluated. An example of such a kind of analysis is shortly reported here for the case of wastewater treatment.

2 Materials and Methods

The investigation on the EEC in DWSSs was carried out on seven different DWSSs, managed by two drinking water companies. The DWSS water flow ranges from 78,000 to 634,682 m^3 y^{-1}, supplying between 1000 and 6223 inhabitants. Raw water is taken from groundwater in all the plants and the main contaminants are iron, manganese, ammonia and arsenic. Only two DWTPs apply non-conventional treatments (ozone oxidation and reverse osmosis filtration, respectively), whereas the remaining plants adopt conventional schemes (such as air oxidation, sand filtration, disinfection by sodium hypochlorite or chlorine dioxide). The monitoring activity was carried out using two different methodologies depending on factors as the availability of remote data, the type of data recording, of installed equipment, the availability of skilled personnel, etc. A detailed description of the methods applied is reported in Collivignarelli and Sorlini (2014).

A number of 289 plants located in Italy were included in the WWTP survey. Data were obtained from a questionnaire compiled by the treatment plant managers of 19 large multi-utility bodies. In total, 45 variables were considered in the survey. Three energy consumption indicators (ECIs) were calculated for each WWTP: ECI_{m3} (=daily energy consumption/daily treated volume); ECI_{COD} (=daily energy consumption/daily COD load removed); ECI_{PE} (annual energy consumption/PE served). Details are in Vaccari et al. (2018).

As for the investigation on the extent of implementation of resource recovery options in Italian WWTPs, an easy-to-fill-out questionnaire was elaborated and sent out to several water management companies. The survey outcomes were parameterised according to WWTP size. For details, the reader may refer to Papa et al. (2017).

Finally, for discussing the implications of improving the energy production in existing WWTPs, commercially available systems were supposed to be used for retrofitting two plants of different size (50,000 and 500,000 PE): a detailed evaluation of technical, social, economic, administrative and environmental aspects was carried out, following the procedure described in Bertanza et al. (2018).

3 Results and Discussion

The survey on DWSS showed that the EEC for water withdrawal and distribution represented from 76 to 96% of the total: the specific consumption for water withdrawal increased from 0.184 to 0.433 kWh m^{-3} with increasing the aquifer depth, while the specific consumption related to the distribution system was a little lower (from 0.146 to 0.325 kWh m^{-3}). On average, as regards the conventional DWTPs monitored, treatments accounted for 8% of the total DWSS energy consumption. In both DWTPs using more energy-consuming unconventional technologies, the impact on total DWSS energy consumption was greater, ranging from 18% in case of ozone oxidation to 24% in case of reverse osmosis. When ozone was used as oxidant, the oxidation phase covered about 92% of the DWTP energy consumption, due to EEC of the ozone generator (responsible for 47% of the ozone oxidation consumption), the booster pump (24%) and the air compressor (18%). When oxygen was used instead of ozone, the specific EEC was reduced to 0.019 kWh m^{-3}. Among the conventional treatments, sand filtration had a specific consumption of 0.007 kWh m^{-3}, due to sludge extraction pumps, backwashing pumps and blowers. Finally, EEC of disinfection

was negligible when sodium hypochlorite was used while it increased with chlorine dioxide due to in situ generation.

As concerns EEC in WWTPs, the median value of ECI_{m3} for all the plants was 0.45 kWh m^{-3}. Observing the single classes, the higher median (0.60 kWh m^{-3}) was for small plants in the class <2000 PE. The classes from 2000 to over 100,000 PE had medians in the range 0.28–0.42 kWh m^{-3}, not significantly different among the classes. The median of ECI_{PE} was 70 kWh PE^{-1} y^{-1} for the entire data sample, but it decreased significantly for increasing capacity of the plants, passing from 120 kWh PE^{-1} y^{-1} for plants <2000 PE, to 68.3 for plants with 2000–10,000 PE, to 53.3 for plants with 10,000–100,000 PE and to 35 for plants >100,000 PE. The indicator ECI_{COD} had the same trend, passing from 3.2 kWh kg$_{COD}^{-1}$ for plants <2000 PE, to 1.76 for plants with 2000–10,000 PE, to 1.45 for plants with 10,000–100,000 PE and to 0.85 for plants >100,000 PE. The statistical analysis confirmed that ECI_{COD} and ECI_{PE} had a high positive correlation, which means that the two indicators provided the same information.

Energy recovery in the Italian WWTPs takes place mostly by the exploitation of biogas from anaerobic digestion of sewage sludge. This option is common only in large WWTPs (almost half). Heat is the main product, but there is also room for electricity production through co-generation systems. Interestingly, 80% of WWTPs exploiting biogas also implement some actions for increasing its production (mechanical or chemical sludge pre-treatment, co-digestion with other organic substrates and enhanced primary sedimentation). On the other hand, hydropower and heat recovery from wastewater streams were indicated in 3 and 1 WWTPs, respectively. Finally, 17 WWTPs produce energy by means of photovoltaic systems.

By simulating the effect of WWTPs retrofitting scenarios, it was shown that, actually, both small (50kPE) and large plants (500kPE) may substantially achieve the power self-sufficiency. Nevertheless, for small plants, potential criticalities should be accounted for, such as the increased complexity of the upgraded plant, the lower reliability of the whole system, the requirement of skilled personnel, new permissions, licences and administrative constraints, a greater use of reagents and a considerably higher overall cost (personnel and depreciation of new equipment being the most relevant items). On the contrary, the large plant case study received a positive overall score: the impact of potential critical aspects, in fact, is less relevant if compared to the small plant, because the large plant was supposed to be already equipped with anaerobic digestion and primary sedimentation.

4 Conclusion

In DWTPs using unconventional technologies, the impact of treatment on the total DWSS energy consumption is greater compared to conventional plants, ranging from 18% in case of ozonation to 24% in case of membrane filtration by reverse osmosis. On average, for the monitored conventional DWTPs, treatments account for 8% of the total DWSS energy consumption. Although the main EEC in the DWSSs is for water pumping, the EEC in the treatment plant should not be neglected, especially if advanced technologies (e.g. membrane systems) or in situ generated oxidants (e.g. ozone or chlorine dioxide) are required. Therefore, it is important to adopt high energy demanding technologies only in case of highly contaminated water and to use appropriate pre-treatments to improve water quality before energy-consuming treatments (such as membrane filtration).

About EEC in WWTPs, the survey allowed to identify the following benchmark values: 23 kWh PE^{-1} y^{-1} for large plants (more than 100,000 PE served), 42–48 kWh PE^{-1} y^{-1} for intermediate size plants (2000–100,000 PE) and 76 kWh PE^{-1} y^{-1} for small plants. Those targets can be reached by changing old electrical devices with high efficiency ones, installing inverters and adequate automation in the pumping stations, adopting controls based on DO in aeration tanks, optimising the air distribution in aerobic stabilisation basins (Campanelli et al. 2013).

In addition, the Italian survey revealed that there is room for improving energy production, the exploitation of biogas being the most common action, but diffused only in large WWTPs. Nevertheless, moving in this direction means that the plant configuration must be modified and the operation strategies adjusted consequently, so that retrofitting existing plants may pose a challenge. Hence, since energy saving and recovery represent surely a task to be encouraged, a very detailed (holistic) investigation has to be performed, case by case, in order to highlight all those aspects that can result in critical situations, so as to guide, eventually, to the definition of the best upgrading option.

References

Bertanza, G., Canato, M., & Laera, G. (2018). Towards energy self-sufficiency and integral material recovery in waste water treatment plants: assessment of upgrading options. *Journal of Cleaner Production, 170,* 1206–1218.

Campanelli, M., Foladori, P., & Vaccari, M. (2013). *Consumi elettrici ed efficienza energetica nel trattamento delle acque reflue.* Bologna, Italy: Maggioli Editore. ISBN 978-88-387-8368-5.

Collivignarelli, C., & Sorlini, S. (2014). *Il consumo energetico nei sistemi di approvvigionamento* (idropotabile ed.). Bologna, Italy: Maggioli Editore. ISBN 978-88-916-0586-3.

Foladori, P., Vaccari, M., & Vitali, F. (2015). Energy audit in small wastewater treatment plants—Methodology, energy consumption indicators and lessons learned. *Water Science and Technology, 72,* 1007–1015.

Papa, M., Foladori, P., Guglielmi, L., & Bertanza, G. (2017). How far are we from closing the loop of sewage resource recovery? A real picture of municipal wastewater treatment plants in Italy. *Journal of Environmental Management, 198,* 9–15.

Vaccari, M., Foladori, P., Nembrini, S., & Vitali, F. (2018). Benchmarking of energy consumption in municipal wastewater treatment plants—a survey of over 200 plants in Italy. *Water Science and Technology, 77,* 2242–2252.

Water–Energy Nexus: Evaluation of the Environmental Impact on the National and International Scenarios

Alessia Murena, Laura Borea, Tiziano Zarra,
Joanna Boguniewicz-Zablocka, Vincenzo Belgiorno,
and Vincenzo Naddeo

Abstract

Water and energy are two essential resources for our future since these two resources are strongly interconnected. The identification of the future scenarios and the evaluation of the possible impact on the water sector due the production of electricity are essential actions to be performed in order to obtain a picture of possible developments that could affect the national and the international energy scenarios.

Keywords

Water–energy nexus • Electricity • Impact • World • Environment

1 Introduction

Nowadays, water and energy are interdependent. Water is used in all the processes of energy production and, in order to be used, water itself requires energy consumption in the phases of collection, treatment, disposal, transport and potabilization.

Over time, the importance of this interdependence, called "water–energy nexus," is continuously increased, and in 2012, the International Energy Agency (IEA) recognized the importance of this link, calculating that the production of electricity requires 15% of the global water withdrawals and that, in the next 20 years, this share is destined to increase by 20%.

According to the estimates provided by the IEA, in 2014 the withdrawals of water for the production of electricity were estimated to be around 398 billion m^3, whereas the water consumption, or the water quantities not returned to the source, was around 48 billion m^3.

In the coming years, the electricity demand and, accordingly, the relative consumption of water are destined to grow. This phenomenon will have an impact on the water sector that should not be underestimated, since only 3% of global water reserves are composed by freshwater and the two-thirds of this quantity is trapped in polar ice caps and glaciers.

Predicting the evolution of the electricity demand and the relative water consumption appears to be the right action to put in place in order to be able to manage the future impacts, particularly in those countries located in the areas affected by water stress.

2 Materials and Methods

In this context, it is important to define the "water intensity," an indicator needed to determine and quantify the impact deriving by the use of water resources in the production of electricity, for the main energy sources.

These sources are distinguished between non-renewable sources, such as fossil fuels and uranium, and renewable sources, such as hydropower, biomass, geothermal, solar and wind energy. After having identified their main plants, their process diagrams have been analyzed in order to determine the functions performed by water during both the operating phase and within its life cycle.

In order to estimate the water resource consumed in the electricity generation processes, the environmental declarations of some Italian plants were analyzed, for all the main energy sources. For the nuclear power plants, some plants in Spain and in UK were studied. The estimation of the water quantities consumed has been done analyzing the data of water consumed for the electricity generation, both during the operating phase and during the life cycle of the plants,

A. Murena · L. Borea · T. Zarra · V. Belgiorno · V. Naddeo (✉)
Sanitary Environmental Engineering Division, Department of Civil Engineering, University of Salerno, Fisciano, Italy
e-mail: vnaddeo@unisa.it

J. Boguniewicz-Zablocka
Department of Thermal Engineering and Industrial Facilities, Opole University of Technology, Opole, Poland

and even the data related to the electricity produced in Italy and in Europe provided by the "Terna" database.

Indeed, water is also present in the life cycle of the plants. In fact, it is present in the phases needed to start up the plant and, at the end of its lifetime, even during the disposal phases. The data used in this analysis are taken from the scientific literature and, in particular, from the "World Energy Outlook 2016."

By using the data provided by the "World Energy Council" on the evolution of the electricity demand in the national and in the international scenarios, an estimation of the evolution of water resource utilization for electricity generation up to 2060 has been done.

3 Results and Discussion

The values related to the water quantities used in the electricity generation processes are summarized in Table 1.

Using these values for the calculation of the "water intensity," it was possible to estimate the water consumed for the production of electricity in Italy, in Europe and in the world.

In 2016, in Italy 289,768 GWh of electricity was produced with a consequent water consumption of 452 million m^3. The largest contribution of electricity, amounting to 199,430 GWh, is derived from thermoelectric sources which corresponds to the consumption of water equal to 90.5 million m^3.

In Europe, the country that consumes the highest quantity of water for electricity production, equal to 1074 million m^3, is France, where the generation of electricity from nuclear and hydroelectric power reaches the highest values. In the world, on the other hand, the largest producer of electricity and, at the same time, the largest consumer of water is Asia, where the water consumed is around 16 billion m^3.

In order to predict the evolution of the future water consumption, three different scenarios presented in the "World Energy Council 2016" were analyzed. By 2060, the world will be characterized by some predetermined factors such as the constant increase in population, which will increase by 0.7%, and the increasingly widespread digitization, whereas other factors, the critical uncertainties, determine three scenarios, whose particular names compare the style of the musical genre with the future scenario.

In the "modern jazz" scenario, the world will be characterized by the improvement of the life quality, associated with a rapid technological and economic development, which will lead to produce more electricity in order to meet the ever-increasing energy needs.

In the "unfinished symphony" scenario, there will be strong global cooperations that will aim, in particular, to protect the environment. All this will lead to a decisive increase in the use of renewable sources, which will cover over 60% of the global electricity production in 2060.

In the "hard rock" scenario, the world will be fragmented, where the interests of individual nations will prevent global cooperation. This will lead each state to implement its own electricity production, avoiding the creation of import–export trade relations.

Starting from the data related to the evolution of electricity production from the main energy sources, the estimates on the relative consumption of water in the world have been identified, and they are reported in Fig. 1.

Although the higher energy production will be recorded in the first scenario, with a value of 48.491 TWh in 2060, in the second scenario is forecasted a higher water consumption, equal to 80 billion m^3. In the European and in the Italian panorama, the greatest water consumption is forecasted in the first scenario, since the "unfinished symphony" scenario is characterized by a strong development of solar and wind technologies.

Table 1 Water quantities used in the electricity generation processes (Flury and Frischknecht 2012; Fthenakis and Kim 2010; IEA 2016; Meldrum et al. 2013; Terna 2016)

	Water intensity: Total water consumed per unit electrical energy produced (l/kWh)	Water intensity: Total water consumed in the installation and disposal phases of the plants (l/kWh)
Coal	1.06	$3.78 \times 10^{-3} < x < 0.09$
Oil	1.19	$3.78 \times 10^{-3} < x < 0.02$
Natural gas	0.26	$3.78 \times 10^{-3} < x < 0.01$
Nuclear energy	1.59	$3.78 \times 10^{-3} < x < 0.02$
Hydroelectric energy	5.71	0.10
Biomass	0.21	3.78×10^{-3}
Geothermal energy	16.16	7.58×10^{-3}
Solar energy	Negligible	$0.12 < x < 0.60$
Wind energy	Negligible	$3.78 \times 10^{-3} < x < 0.03$
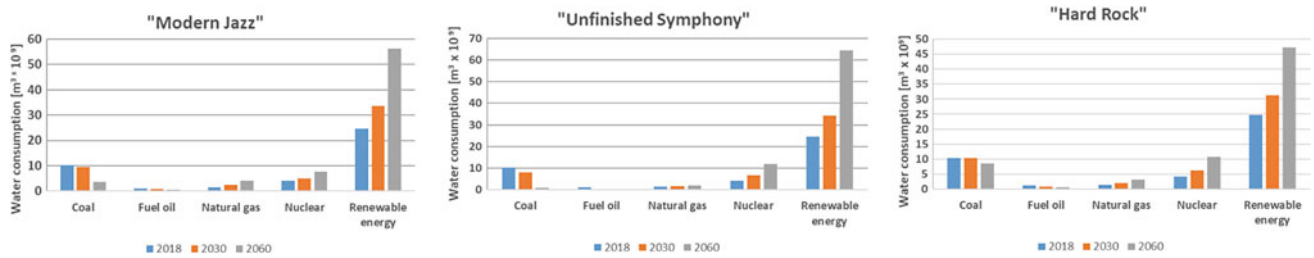
Fig. 1 Water consumption for the main energy sources

4 Conclusion

In the assessment of the impacts on water in the electricity production sector, it appears that it will be necessary:

- To reduce the use of fossil fuels for the production of electricity. Even if the specific consumption of water is not excessive, the thermoelectric plants are very widespread: They consume large quantities of water, and they use non-renewable sources, destined to run out;
- To develop solar and wind technologies as clean energy forms that consume very low quantities of water;
- To adopt strategic technologies to find a compromise to limit all possible impacts, ensuring that the use of water does not limit access to electricity and vice versa;
- The Italian index that identifies the ratio of water consumed and electricity produced is one of the highest among the main European countries and slightly higher than the European one;
- The least impacting scenario on a global level is "hard rock." In 2060, the energy needs will be covered by 40% from renewable sources, where 20% arises by solar and wind plants. The total estimated water consumption is

about 70 billion m^3, for an energy production electricity equal to 44.914 TWh.

- The most impacting scenario is "unfinished symphony" with a global water consumption estimated to be about 80 billion m^3, relative to an electricity production of 44.474 TWh.

References

Flury, K., Frischknecht, R. (2012). Life cycles inventories of hydroelectric power generation. *ESU—services fair consulting in sustainability*, 1–15.

Fthenakis, V., & Kim, H. C. (2010). Life-cicle uses of water in U.S. electricity generation. *Renewable and Sustainable Energy Reviews, 14*, 2039–2248.

IEA. (2016). *Water energy nexus—excerpt from the world energy outlook 2016*. Parigi: IEA.

Meldrum, J., Nettles-Anderson, S., Heath, G., & Macknick, J. (2013). Life cycle water use for electricity generation: a review and harmonization of literature estimates. *Enviromental Research Letters, 8*, 1–18.

Terna (2016). *Analisi sinteticadei dati elettrici più rappresentativi dell'anno 2016*. Roma: Terna S.p.A.

World Energy Council (2016). *World Energy Scenarios 2016 – The Great Transition*. Londra.

Water Scarcity and Shale Gas Prospects in Tunisia—Potential Impacts of Hydraulic Fracturing on Regional Water Stress

Lisa Murken

Abstract

Hydraulic fracturing of shale plays requires large quantities of water and could pollute water resources, which is especially problematic in the water-scarce North African context. This study investigates the potential impacts of fracking on regional water stress in Tunisia by forecasting shale development and water stress for two key regions. To also understand the political economy of shale gas in Tunisia, experts from different backgrounds were interviewed. The results show that fracking could add important volumes to regional water demand, especially in peak drilling years. However, water concerns are of secondary importance to decision-makers, and the promise of economic benefits weighs heavier, increasing the likelihood of shale gas development.

1 Introduction

In 2011, the US Energy Information Administration (US EIA) published a report estimating the world shale resources. This brought a lot of attention to North African shale gas; Tunisia is estimated to have 651 billion m^2 in technically recoverable shale gas (US EIA 2013). For the relatively small country, which has long reached its peak in conventional oil and gas production, this marks a very interesting development—especially since Tunisia imports much of its energy and mainly uses natural gas for electricity production (ANME 2012). To extract oil and gas trapped in low-permeability

formations, a technique called hydraulic fracturing—often referred to as "fracking"—has been developed, stimulating low-permeability formations to enable gas production (Stuart 2011). However, environmentalists have voiced concerns over the environmental impacts of fracking—particularly on water resources: the technique can pollute water and is very water-intensive. This study assesses the implications of fracking for water-scarce areas and places the debate on water and shale gas in a wider environment and development context. Concentrating on deterministic volumetric effects, it seeks to quantify the impact of potential shale gas extraction scenarios in Tunisia on regional water supply, attempting to answer the following question:

(1) How could shale gas exploitation in Tunisia affect regional water stress?

Local water environments are keys to informing energy policy, as water is more difficult to transport. Water stress is therefore mostly localised, whereas energy offers more scope for an adjustment (Scott et al. 2011). Consequently, next to the main research question, the paper aims to address two sub-research questions to better understand local implications and the role of water in this process:

(2) How is the shale gas development process governed and influenced by political considerations?
(3) How are shale gas and the environmental risk for Tunisia perceived amongst Tunisian experts and decision-makers?

2 Materials and Methods

A mixed-methods approach with semi-structured interviews for questions (2) and (3) and a forecasting exercise to answer the main research question (1) is employed. The sub-research questions are treated before the main research question, as the

L. Murken (✉)
Potsdam Institute for Climate Impact Research, Telegrafenberg A31, Potsdam 14473, Germany
e-mail: Lisa.Murken@pik-potsdam.de

interview responses informed the water impact projections. To assess the context and perception of the issue in Tunisia and gather local opinions, in a first step semi-structured expert interviews were conducted, with a question catalogue being adapted for each specific expertise, to allow for flexible interviews. This also complemented only scarcely available public information and data on fracking operations in Tunisia and enabled a better tailoring of the quantitative approach. Between June and July 2017, twelve interviews were conducted in person in Tunisia, of which two were group interviews, with two additional interviews taking place via Skype. Additionally, several informal meetings and written communications informed this work. Purposive sampling was employed to select the interviewees, as only a very limited amount of people appeared qualified to contribute to answering the research questions. The interviewees can be broadly categorised into (former) government employees, employees of oil and gas companies, environmental activists and researchers. As a method of data analysis, thematic analysis was employed, following the Attride-Stirling model (Attride-Stirling 2001). The second part of the paper answers the main research question, quantifying the impact of shale gas development in Tunisia on regional water stress under different scenarios. Similar modelling studies have been conducted for Poland (Vandecasteele et al. 2015) and the Chinese Sichuan Basin (Yu et al. 2016). In a first step, water volumes for shale gas production under different scenarios were projected, with different well drilling rates and water usages for hydraulic fracturing, as well as different production targets. Three shale gas development scenarios were adapted from Oxford Economics (2013). A fourth scenario was added to model full exploitation of the estimated reserves in the Ghadames Basin. To then evaluate the potential future impact of water withdrawals for fracking on regional water stress, an index of water stress for the concerned governorates was defined under a baseline scenario and projected for a timeline of 27 years. Data from DGRE (2009) was combined with the size of the affected governorates to determine the average regional water supply. Regional water demand per capita was calculated using data on drinking water supply by the national water supplier SONEDE (SONEDE 2016). Per capita water demand and regional population figures were then projected using the Holt-Winters smoothing method in R, and accounting for the additional agricultural water share the projected total water demand for the next 27 years was computed. Finally, the water volumes used for the different fracking scenarios were put in relation to local water demand and water stress.

3   Results and Discussion

As the quantitative analysis has shown, shale gas development could put considerable additional strain on water supplies in Tataouine and Kairouan during peak drilling years, with adding as much as 4–8% of additional water demand in Kairouan and 13–49% in Tataouine. Higher scenarios need more water, but with economies of scale and infrastructure requirements also offer better economic and energy prospects. When comparing the results to the outcomes of similar studies for the USA (Nicot and Scanlon 2012) and China (Yu et al. 2016), it becomes clear that the water conditions in Tunisia would be under even higher relative pressure than those in other water-strained areas. Clearly, in areas as water-scarce as the Tunisian South and Centre, even relatively low volumes of water in off-peak years can have devastating consequences, especially since the effects will be much more localised than simulated here and yearly variability of available water is high. The water source is also important, the Tunisian South and Centre are primarily supplied via groundwater, which notably in the South largely stems from profound aquifers and is mostly non-renewable (FAO 2016). It is also highly saline, in the South only 3% of water resources are considered good quality (ibid.), and good quality is, however, necessary for fracking use. In line with the literature on shale gas and water and the interviews conducted, in Tunisia quality may in fact be an even bigger problem than the quantity of water. Water transfers could be a technical solution, but in Tunisia transfers from the North to the Southern regions are already at a maximum possible level (Burak and Margat 2016). In fact, transfers from Southern to coastal areas might increase. Kairouan already today supplies Sousse, Monastir and Mahdia with important water volumes (HBS 2015). The often promoted solution of desalination could free up important amounts of water, but may make fracking too costly, not to speak of overall energy life-cycle analysis. Using wastewater would require better treatment capacities. As the qualitative analysis has shown, the main local trade-off when it comes to water will be between shale gas and agriculture. Agriculture with 80% of total water demand is by far the biggest water consumer in Tunisia. There is a scope to improve irrigation efficiency to free up water, but in the future those amounts may be needed to ensure drinking water supply. With increasing exploitation, the costs of additional water mobilisation also rise. To understand why shale gas is interesting for the Tunisian government despite those challenges, the interviews provided important insights into the political economy of shale gas, highlighting the role of jobs and energy security in this process. Tunisian decision-makers prioritise job prospects over water concerns, in that their assessment differs much from that of researchers and environmentalists. Economic impacts of fracking, however, are often overestimated, as Kinnaman (2011) finds in a review of non-peer-reviewed reports, and jobs might mainly go to foreign workers, as Paredes et al. (2015) conclude for Texas. Kairouan is Tunisia's main agricultural region, with the largest irrigated area in the country (FAO 2016). If shale gas is indeed exploited, this region may be the biggest loser, with water being diverted from agriculture, which could cost farmers their yields and jobs. For Tataouine, new employment prospects are tempting, as it

has by far the highest unemployment rate in Tunisia (INS 2015), but activists and researchers doubt the marginalised will benefit. Since the shale gas process is governed and controlled by well-connected government and gas company elites, the dominant strategy is likely to be the creation of short-term gas jobs to the detriment of long-term sustainability and the Tunisian South. This direction can be explained with the greater context of energy security, competition with Algeria and existing oil and gas infrastructure. The intransparent and highly politicised governance of shale gas development so far hinders a better integration of water concerns and largely neglects local effects. A number of uncertainties and limitations of this study have to be considered: firstly, there is great uncertainty surrounding the future production of shale gas, the connected well development and the resulting water consumption. Future shale gas production may be overestimated as a result of too simplistic forecasting methods; however, future technology could render other shale resources technically recoverable and resources in the Pelagian Basin have not yet been estimated, potentially increasing total shale production. Wells may also have to be repeatedly fractured in order to enhance productivity (Berman 2009), which would lead to greater water consumption. Secondly, future water availability was highly simplified, not considering likely water quality deterioration and climate change effects. Generally, water demand is likely to have been slightly underestimated, while water availability may have been severely overestimated, especially for Tataouine. Thirdly, the scope of this study could be expanded. So far, only shale gas but not shale oil was considered. Wastewater from fracking was not modelled and discussed, which may however pose important difficulties in treatment and storage. Most interviewees mentioned renewable energy as an alternative to fracking. Future research could contrast the water impact of shale gas with that of renewable energy.

4 Conclusion

The main objective of this study was to assess the potential impact of shale gas development on regional water stress in a particularly water-scarce country, Tunisia. The results of a forecasting exercise showed that shale gas development in two key regions of Tunisia could substantially increase water demand and therefore stress, especially in peak drilling years. In Kairouan, fracking may add as much as 4–8% in additional water demand in peak years, in Tataouine, up to 13–49%. Despite acute water stress, Tunisian decision-makers may opt for shale gas development nonetheless, prioritising quick success in employment and revenue creation over sustainable water management, as interviews revealed. Environmental risk perception differs considerably across relevant actors;

with the governance of shale gas development in Tunisia characterised by a lack of information, coordination and communication, the likely dominating assessment will be that of government officials, leaving only a secondary role to water concerns. This may leave the affected populations unprotected and marginalised, which highlights the urgent need to reframe the water–shale gas debate in evaluating fracking impacts on people's water resources, instead of assessing water limitations to shale gas development. Local water impacts of fracking deserve greater attention and inclusive evaluation, not only in Tunisia.

References

ANME (Agence Nationale pour la Maitrise de l'Energie). (2012). Maîtrise de l'Energie en Tunisie - Chiffres Clés, p. 19.

Attride-Stirling, J. (2001). Thematic networks: an analytic tool for qualitative research. *Qualitative Research, 1*(3), 385–405.

Berman, A. (2009). *Lessons from the Barnett Shale suggest caution in other shale plays*. USA: Association for the Study of Peak Oil and Gas.

Burak, S., & Margat, J. (2016). Water management in the mediterranean region: Concepts and policies. *Water Resources Management*, 5779–5797. Available at: https://doi.org/10.1007/s11269-016-1389-4.

DGRE (Direction Général des Ressources en Eau Tunisie). (2009). *Les ressources en eau en Tunisie Introduction Potentiel en Eau.*

FAO. (2016). *AQUASTAT website*. Food and Agriculture Organization of the United Nations (FAO). Website Accessed on July 25 2017.

HBS (Heinrich Böll Stiftung). (2015). Gaz de schiste en Tunisie: entre mythes et réalités, HBS Afrique du Nord Tunis.

INS (Institut National de la Statistique). (2015). Annuaire Statistique de la Tunisie 2010–2014, Tunis.

Kinnaman, T. C. (2011). The economic impact of shale gas extraction: A review of existing studies. *Ecological Economics, 70*(7), 1243–1249.

Nicot, J., & Scanlon, B. R. (2012). *Water use for shale-gas production in Texas, U.S.*

Oxford Economics. (2013). The economic impact of liquid rich shale and shale gas exploration in Tunisia.

Paredes, D., Komarek, T., & Loveridge, S. (2015). Income and employment effects of shale gas extraction windfalls: Evidence from the Marcellus region. *Energy Economics, 47,* 112–120.

Scott, C. A., et al. (2011). Policy and institutional dimensions of the water—Energy nexus. *Energy Policy, 39*(10), 6622–6630.

SONEDE (Société nationale d'exploitation et de distribution des eaux). (2016). Rapport des Statistiques Année 2015.

Stuart, M. E. (2011). *Potential groundwater impact from exploitation of shale gas in the UK*, Open Report OR/12/001, British Geological Survey.

US EIA (U.S. Energy Information Administration). (2013). *Shale gas resources: An assessment of 137 shale formations in 41 countries outside the United States*. U.S. Energy Information Administration, Washington, DC.

Vandecasteele, I., et al. (2015). Impact of shale gas development on water resources: A case study in northern Poland. *Environmental Management, 55,* 1285–1299.

Yu, M. et al. (2016). Water availability for shale gas development in Sichuan Basin, China. *Environmental Science & Technology.*

Energy Performance of Italian Urban Water Systems

L. Mancusi, M. Volonterio, and E. Garofalo

Abstract

Relationships between energy consumption and characteristic data of the urban water system in Italy have been researched.

Keywords

Energy efficiency • Water supply • Wastewater treatment system

1 Introduction

The urban water system is a highly energy-consuming sector. According to the national figures published by Terna (the Italian TSO), the Italian water service yearly electric consumption represents around 2% of the total national electric demand.

This paper deals with the need to evaluate to which extent measures to improve the overall efficiency of the urban water service can be a viable option to reduce energy consumption and contribute to the national transition towards decarbonization.

Up to now, data made available publicly have been hardly suitable to this goal, since they are mostly aggregated at the national level, and few and scattered information has been made available on energy intensity at local/system level. If evaluated as national average, unit consumption is not suitable for efficiency analysis because energy intensity is site-specific and depends on many factors, such as the topography of the land that extends between the water

L. Mancusi (✉) · M. Volonterio · E. Garofalo
R.S.E. SpA, Milan, Italy
e-mail: Leonardo.Mancusi@rse-web.it

M. Volonterio
e-mail: Volonterio.Michela@rse-web.it

E. Garofalo
e-mail: Garofalo.Elisabetta@rse-web.it

source and its destination, the distance from the bulk water supply, water consumption and pressure levels.

However, in the last years, the Italian Regulatory Authority for Energy, Networks and Environment (ARERA, former AEEGSI) has started a specific survey to gather information about the efficiency of the Italian water utilities. The survey gathers information about water withdrawal from the environment, electricity consumption for the aqueduct, sewage and wastewater treatment phases and other information useful to characterize the systems, such as the average head pressure of water supply booster pump stations. Starting from these data, we have carried out an analysis at a scale of greater detail, in order to define the reference unitary consumption that takes into account specific site conditions of the urban water system. Subsequently, by comparison between actual and expected consumption, an energy efficiency estimate was made for the whole national system.

2 Materials and Methods

Activities have been focused on the analysis of the integrated water service (aqueduct, sewage and wastewater treatment) with the objective of obtaining an overall classification of the energetic performances either of the Italian aqueducts and wastewater treatment systems. The analysis was carried out on the basis of data aggregated at the level of Optimal Territorial Areas (ATOs), representing the territorial units within which the water utilities are organized in order to assure an optimal water supply. After the publication of Law No. 36 of 1994, usually known as the Galli Law, 91 ATOs were defined all over Italy.

Data provided by ARERA concern a significant sample of the Italian urban water service (representing 78% of the population) and are related to the year 2014. The main analyses were focused on water supply which is the most energy-consuming phase of the whole water service (4000 GWh out of 6400 GWh). Specifically, statistical

analyses were carried out for determining significant relationships between service performance indicators—unit water consumption (litres/day/person) and unit electric consumption (kWh/m^3)—with respect to a number of characteristic parameters of the ATOs.

The identification of parameters or characteristic factors that may explain the differences in consumption between different ATOs can be used for the definition of local specific standards. Furthermore, through the comparison between real values and estimated parameters, it is possible to provide general indications about efficiency.

With regard to the unit water consumption (computed considering annual water withdrawal), a significant correlation has been identified with users' density: a similar correlation is highlighted in other literature studies (Renaud et al. 2007), and the result can be explained by the fact that the higher the density of users, especially in rural areas, the higher the physiological loss and therefore the higher the withdrawal from the environment. As regards the specific electrical consumption analysing the altitude distribution of served population, a significant correlation has been observed with the percentage of served population located in the hills, highlighting that water supply in hilly areas needs on average more energy consumption due to water pumping requirements.

In order to have a more complete analysis, especially for the wastewater treatment system, the available data have been further integrated with information from the Italian Statistical Institute (ISTAT) regarding the 2014 population survey and drinking water use for the years 2012 and 2015 (altitude location of the population and volumes of drinking water supplied and distributed to the population). In regard to the wastewater treatment system plants, data from the European database have been as well considered, updated to 2014. This database, developed in the framework of the Urban Waste Water Treatment Directive (UWWTD), gathers information from all European countries regarding water pollution loads generated and collected from urban agglomeration, pollution loads collected by wastewater treatment systems, organic design capacity of the treatment plants and type of treatments.

After a congruence analysis among the different data sets, statistical analyses were performed on the resulting data set in order to identify correlations between unit electricity consumption and territorial characteristics that are able to statistically explain the variability of unit consumption and therefore to define the expected consumption standard values on the basis of local characteristics. Student's t-test was applied for testing the data correlation coefficient to conclude if there is a linear relationship in the data between the predictor x and response y.

3 Results and Discussion

As regards the evaluation of the expected unit consumption for the aqueducts, the analysis led to the identification of the following linear relationship with the altitude distribution of the population:

$$kWh\_cm\_supply = 0.301 + 0.095 \cdot RateLowland \\ + 0.494 \cdot RateHill \tag{1}$$

where kWh_cm_supply is the expected unit consumption in kWh/m^3, $RateLowland$ is the rate of ATOs' resident population living on the flat land, and $RateHill$ is the rate of resident population on the hill, according to the ISTAT altitude classification. Figure 1 shows the graph of the correlation: being a multiple correlation between two predictive variables and one response variable, the graph is represented

Fig. 1 Graph of correlation from unit energy use for water supply services and distribution of the population by elevation
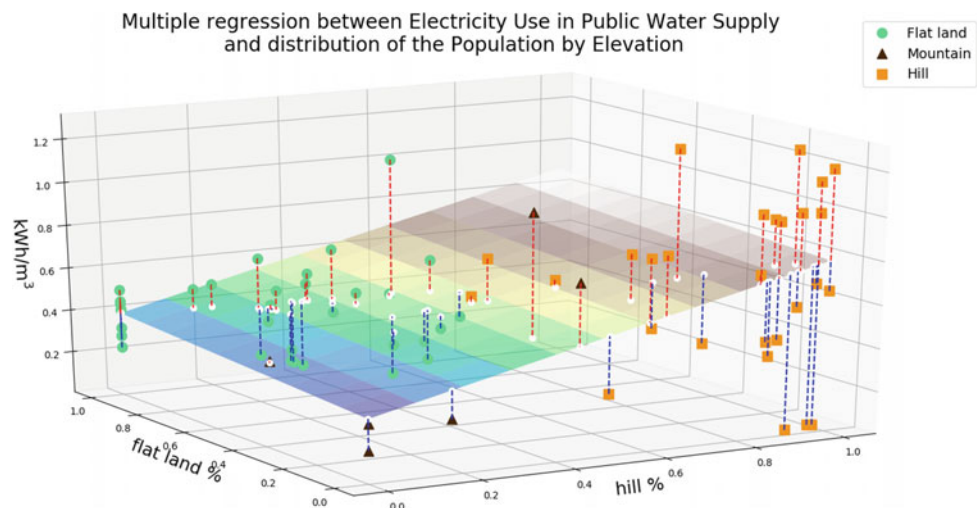
Table 1 Percentage of ATOs for different ratio range between observed and expected energy

Range actual/expected	Water supply (% ATOs)	Sewers (% ATOs)	Wastewater treatm. (% ATOs)	Notes
0.00÷0.50	8.8	16.7	7.6	Percentage of ATOs with better performance
0.50÷0.90	33.8	33.3	25.3	
0.90÷1.10	17.6	8.3	34.2	Percentage of ATOs with expected consumption
1.10÷1.50	30.9	23.3	25.3	Percentage of ATOs with worse performance
>1.50	8.8	18.3	7.6	

in a Cartesian coordinate system for a three-dimensional space in which the relationship consists of a plane and input data of scattered points.

In the graph, the dashed red lines show the distances from the correlation plane of the points with consumption higher than expected, while the blue ones those with lower consumption.

With regard to the energy consumption for the sewers of the collecting system, a similar correlation with the number of pump stations in the ATOs has been found: this is justified by the fact that the electricity consumed in this phase is mainly used for pumping. This correlation is summarized in the following formula:

$$kWh\_cm\_sewer = 0.06145 + 1.209 \cdot 10^{-4} \\ \cdot NumPumpingStation \qquad (2)$$

where kWh_cm_sewer is the expected unit consumption in kWh/m^3 and $NumPumpingStation$ is the number of pumping stations in the ATOs.

Among the three phases of the integrated water service, the collecting system is the least energy-consuming, since a great number of sewers still work by gravity. In fact, the average value of the unit consumption based on the survey is 0.094 kWh/m^3, smaller by one order of magnitude than the aqueduct service (0.57 kWh/m^3) and wastewater treatment (0.53 kWh/m^3).

With regard to the consumption analysis of the wastewater treatment phase, a significant correlation was found between the unit consumption and the weighted average organic design capacity of the treatment plants in each ATO, weighted by the load entering the plants:

$$kWh\_pe = 35.354 - 6.085 \cdot 10^{-6} \\ * UwwtpCapacity + 0.0458 * RateTreatment$$
$$(3)$$

where kWh_pe is the electrical energy consumption per equivalent population, $UwwtpCapacity$ is the weighted arithmetic mean capacity of wastewater treatment plants in the ATO, weighted by the load entering into the Urban Waste Water Treatment Plants (UWWTPs), and the $RateTreatment$ is the rate of intensity of treatment of UWWTPs in the ATO compared to a hypothetical situation in which they all have UWWTPs with tertiary treatments.

The energy performances of the processes in the ATOs have been evaluated from the comparison between the values from the survey and the calculated energy unit consumption based on Eqs. 1, 2 and 3 (Table 1).

4 Conclusion

Relationships between energy consumption and characteristic parameters of the urban water system in Italy have been investigated. The analysis has revealed (1) a multiple correlation between the electrical consumption of the water supply service and the distribution of the population by topography (hill and lowland); (2) a correlation between the electricity consumption of the wastewater treatment system service with the weighted average organic design capacity of the treatment plants. The correlations have been used for a classification of the ATOs' energy performances. The result shows that 33–40% of the ATOs have large potential for significant energy savings.

Reference

Renaud, E., Bremond, B., Poulton, M. (2007). Studies of reference values for the linear losses index in the case of rural water distribution systems. In *Water Loss 2007 Conference Proceedings, Vol. 3*, Bucharest.

Analysis of the Economic Net Benefit of Green Infrastructure by Comparing the Water-Retentive Block and the Normal Block

Kyeonjae Woo, Bae Woo Bin, Ko Jong Hwan, Kim Sang Rae, and Kim Yong Gil

Abstract

Evaluation of water-retentive block and normal block to derive the net benefit of green infrastructure.

Keywords

Green infrastructure • Water-retentive block • Climatic chamber • Net benefit • Rainwater runoff

1 Introduction

Due to climate change, the heat-wave phenomenon is showing an increasing tendency recently in Korea. In order to mitigate urban heat wave, domestic municipalities are promoting urban greening, securing urban open water, securing urban winds, expanding the proportion of renewable energy, and cool roofs. The increase in outside temperature occurs with the decrease of microclimate because the rainwater in the city flows out to the river and the occurrence of urban microclimate is suppressed. Urban heat is an important factor promoting the use of cooling power by building users. Therefore, to promote the prevention of an increase in cooling energy and rainfall runoff, the economic effect of GI product such as water-retentive blocks capable of promoting microclimate must form a social consensus. It is urgent to study the application of GI for heat reduction in order to advance related policy as well as rainwater runoff mitigation. This study evaluates the temperature reduction effect and the rainwater storage capacity of the water-retentive blocks and normal blocks and finally estimates their net benefits.

2 Theory Review

The performance of normal blocks and water-retentive blocks, which is a GI product that constitutes the sidewalk, penetrates the storm drainage layer, and absorbs rainwater and evaporates it into the air, was evaluated in the range of humid temperate climate. The experimental preparation was as follows.

K. Woo (✉) · B. W. Bin · K. J. Hwan · K. S. Rae · K. Y. Gil
Korea Conformity Laboratories, Seoul, South Korea
e-mail: kjwoo84@kcl.re.kr

Performance evaluation target	– Amount of evapotranspiration, infiltration (storage capacity), runoff, and soil moisture content – Surface and air temperature of normal and water-retentive blocks
Climate environmental condition and the equipments	– 10 m (width) × 10 m (depth) × 4.5 m (height) climatic chamber with humid temperate climate controlled by temp/humidity (with HVAC), rainfall (50 ± 10 mm/h) device, solar radiation (800 ± 40) lamp, sensors in the sand, sensors in the air and surface of blocks, runoff and infiltration reservoir at the bottom
Block performance evaluation device	– Device that can infiltrate and leak out the rainwater in size 1 m × 1 m × 0.5 m (WLH) – Install each from the bottom: permeable sheet, infiltrate layer (150 mm), support layer (30–50 mm), blocks (60–80 mm)

Assuming that the durability of GI is 20 years and the maintenance cost has 5-year interval, the discount rate is 10%, and the net benefit of GI is calculated according to the following formula.

$$\text{GI net benefit} = \text{GI construction cost} + \text{annual GI maintenance cost}$$
$$- \text{GI water saving profit} + \text{cooling energy reduction}$$
$$\text{profit due to the decrease of outside temperature}$$

The maintenance cost of GI for 20 years is determined according to the following formula. This formula is also applied to the cost of rainwater storage capacity, which is assumed to be the private benefit of the water utility cost, and the energy cost benefits associated with reduced cooling energy for 20 years.

$$\text{PV} = \sum_{k=0}^{n-1} \left(\frac{C}{(1+r)^k} \right)$$

PV: Present value of total maintenance cost for 20 years, k: 0, 1, …, k, 19, C: Annual maintenance cost, r: Discount rate, n: Duration years

3 Evaluation of the Water-Retentive Block and the Normal Block

The experimental results show that the water-retentive blocks evaporate about 2.6 times and infiltrate 3.12 times more than the normal blocks, and the surface runoff is about ten times lower. The amount of rainfall absorbed into the soil and the water-retentive blocks for 1 h are 0.187 t, which resulted in 54% infiltration effect, and the reservoir amount is 0.0218 t, which resulted in 6% reservoir effect (Table 1).

The water content of the soil changes for about 2 h. In the case of the normal blocks, the water content did not change significantly during 2 h, but the water-retentive blocks showed a higher value by about 4% more than the normal blocks at the start time and 3% higher after 2 h. Through a thermal camera, it was found that the normal blocks have the 72 °C max surface temperature (min temp. 51.6 °C) and water-retentive blocks have the 60.1 °C max surface temperature (min temp. 44.2 °C). As a result of comparing the surface temperature through the thermal camera, it was found that the temperature was lowered by about 10 °C due

Table 1 Water-retentive block evaluation result

Rainfall	Time	Area (m²)	Amount of rainfall (L)	Rainfall (t) or soil moisture content	Reservoir amount	Evapotranspiration amount	Runoff amount	Reservoir effect	Infiltration effect
55 mm	1 h	6.25	343.75	0.187	0.0218	0.008	0.00003	6% of rainwater	54% of rainwater
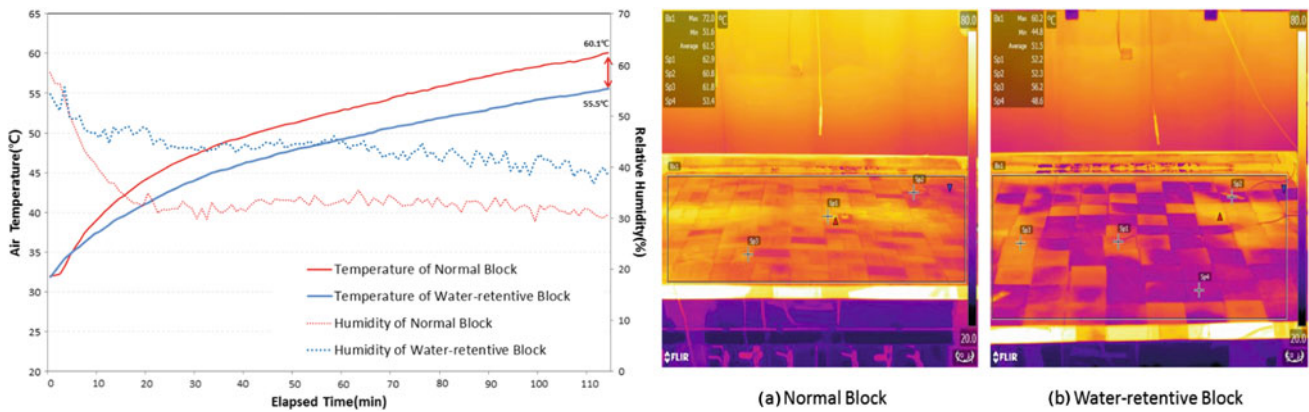
Fig. 1 Comparison of air and surface temperatures of normal block and water-retentive block

to the evaporation of the moisture which the water-retentive blocks were functioning. After about 2 h, the air temperature was about 4.6 °C reduced. The experimental results show that the water-retentive blocks can achieve sufficient evaporation performance and contribute to air temperature reduction (Fig. 1).

4 Analysis of Economic Effects

The installation cost of the blocks is composed of land excavate, sand delivery, soil removal processing, blocks, broken stones, sand, permeable sheets, compactor, forklift, and excavator. This shows that the initial cost of 578.41 USD requires for the experiment area of 6.25 m^2 (Table 2).

The maintenance cost is 623.17 USD, calculated by applying the present value method (10% applied) to the cost of only blocks, broken stones, sand, permeable sheet, compactor, and forklift, assuming 5-year cycle of replacement work due to block wear.

The benefit of GI in preparation for maintenance cost is the cost of rainwater storage due to the increase in groundwater resources and the decrease in the use of tap water. Among local governments in Korea, Seoul Metropolitan City has set water rates based on the following criteria. Based on the rate table, it can be assumed that the actual base rate of water usage was about 1.18 USD per h if only the amount of 0.187 m^3 infiltrated.

$$\text{Experimental Rainfall Rate} : \text{Base Rate} \ (1 \ \text{USD}) + \text{Usage Charge}$$
$$(\text{Rainfall } 0.187 \ \text{m}^3 \times 0.36 \ \text{USD})$$
$$+ \text{Water use charge}$$
$$\times (0.187 \ \text{m}^3 \times 0.17 \ \text{USD})$$
$$= 1.18 \ \text{USD}$$

The benefits of GI in comparison to the maintenance costs of GI will be the profit of rainwater storage due to increased groundwater resources and reduced water utility use. When we look at the precipitation data released by the Korea Meteorological Agency, it shows rainfall of 251 mm in spring, 653 mm in summer, 255 mm in autumn, 94 mm in winter and 1,125 mm in average rainfall. This is applied to the average rainfall of the actual Korean season (an average rainfall is 251 mm in spring, 653 mm in summer, 255 mm in autumn and 94 mm in winter from 2008 to 2016) by the area of the rainfall in the experiment, the following benefits of rainwater storage appears and based on the total cost of reservoir cost (24.62 USD) of 6.25 m^2 for 20 years is USD 448 with a discount rate 10% (Table 3).

The experimental results show that the water-retentive blocks have the effect of reducing the external temperature by about 5 °C compared with the normal blocks. This can be regarded as a reduction effect due to the evapotranspiration after the rain stops. However, it is estimated that there will be a reduction effect of about 1 °C in area 6.25 m^2 by subtracting 90% or more of actual external factors (automobile heat, shadow generation, various climatic factors).

Table 2 Initial cost of green infrastructure (water-retentive block) cost

Area (m^2)	Dig	Sand delivery	Soil processing	Blocks	Broken stone	Sand	Permeable sheet	Compactor	Forklift	Excavator	Total initial cost (USD)
6.25	1.6	1.2	1.2	3.2	0.972	0.638	9.6	80	80	400	578.41

Table 3 Water-retentive block rainwater storage benefit

Season	Average rainfall	Hour	Rainfall day	Area (m²)	Rainwater amount (t)	Storage amount (t)	Storage cost (USD)	Infiltration amount (t)	Infiltration cost (USD)	Subtotal (USD)
Spring	251.98	1	24.3	6.25	38.269	2.29614	3.69	20.66526	33.27	36.96
Summer	653.31	1	40.8	6.25	166.594	9.99564	16.09	89.96076	144.83	160.92
Fall	255.78	1	24.1	6.25	38.526	2.31156	3.72	20.80404	33.49	37.21
Winter	94.05	1	19.7	6.25	11.579	0.69474	1.11	6.25266	10.06	11.18
Total cost							24.62		221.66	246.29

Table 4 Cooling energy benefit of water-retentive block

Product	Temp. reduction (°C)	Area	Cooling capability (kW)	Power consume (kW)	Hours use	Days use	Monthly cost (USD)	Total years	Total present value (USD)
Normal block	0	18	7.2–2	1.82	4	30	26.87	20	489.73
GI block	1	18	7.2–2	1.82	2	30	8.04	20	146.57
Benefit of GI									343.19

The AC with Korea's energy efficiency level 1 has a cooling capability of 2.0–7.25 kW and power consumption of 0.3–1.82 kW. In this study, the power consumption of residential AC is 1.82 kW, the average daily use time is 30 days, and the average daily use time is 4 h based on the cooling day data (2008–2017). In the case of normal blocks, the average maximum temperature is from 3 to 5 PM by the heat wave and from 0 to 2 AM after sunset by the heat island in August, and an average of 4 h. As a result, it was estimated that a monthly fee of about 26.87 USD would be generated by the Korean standard. In the case of water-retentive blocks, it is assumed that the average 2 h is used in the afternoon when the cooling rate is reduced by 1 °C by the evapotranspiration effect of GI and the cooling degree occurs. As a result, a monthly fee of about 8.04 USD was generated, resulting in a charge difference of three times that of the normal blocks. If the 20-year usage fee is calculated by applying the present value of 10%, the following benefits of GI, 343.19 USD, will be generated as follows (Table 4).

In result, subtracting 20 years the water-saving benefit of 448.90 USD and 20 years the cooling energy benefit of 343.19 USD from GI water-retentive blocks (6.25 m²)

initial construction cost of 578.41 USD and their 20 years (5-year cycle) maintenance cost of 623.17 USD makes net benefit of 616.31 USD. It is an economic effect, which is 51% cost advantage compared to the normal blocks that reduce initial construction cost and maintenance cost.

5 Conclusion

In this study, the actual performance of the water-retentive blocks and normal blocks was analyzed through the performance evaluation of using the climatic chamber and block performance evaluation device. Based on the analysis results, the economic effect of the water-retentive blocks against the normal blocks was calculated based on the cost of construction and maintenance and benefit from the reduction of cooling energy and increase in rainwater storage capacity. However, this study is limited to the experimental area, and it did not consider the possibility of energy reduction in the areas where the options of various housing units, the office, and industrial buildings exist. As a result, it is expected that the simulation results based on the actual

urban area with climate data and experimental data from the climatic chamber would become necessary in the future to evaluate the green infrastructure.

References

Korea Energy Efficiency Level Regulation and Electric Cost Calculation Standard, Korean Electric Power Co., Inc., S. Korea.

Water Utility Standard and Summer Heat Island Report, Seoul Metropolitan City, S. Korea. 2008–2016 Rainfall Data and 2008∼-2017 Seoul City Cooling Day Data, Korea Meteorological Agency. https://data.kma.go.kr/climate/degreeDay/selectDegreeDay Chart.do. Accessed July 2018.

Levering Industry and Professional Qualifications Over Water Efficiency and Water–Energy Nexus in Buildings

Ana Poças, Pedro Cardoso, Filipa Newton, Diogo Beirão,
Charalampos Malamatenios, Georgia Veziryiani, Esther Rodriguez,
Javier González, Rossella Martino, and Diego De Gisi

Abstract

Skills for water efficiency and water–energy nexus in building construction and retrofit; skill upgrading of construction and green professionals on water efficiency and water–energy nexus.

A. Poças · P. Cardoso · F. Newton (✉) · D. Beirão
ADENE—Agência para a energia, Lisbon, Portugal
e-mail: filipa.newton@adene.pt

A. Poças
e-mail: ana.pocas@adene.pt

P. Cardoso
e-mail: pedro.cardoso@adene.pt

D. Beirão
e-mail: diogo.beirao@adene.pt

C. Malamatenios · G. Veziryiani
Centre for Renewable Energy Sources
and Saving, Pikermi, Greece
e-mail: malam@cres.gr

G. Veziryiani
e-mail: gvezir@cres.gr

E. Rodriguez · J. González
Fundacion Laboral de la Construccion, Madrid, Spain
e-mail: esrodriguez@fundacionlaboral.org

J. González
e-mail: jgonzalez@fundacionlaboral.org

R. Martino · D. De Gisi
Formedil ente Nazionale per la Formazione e l' Addestramento,
Rome, Italy
e-mail: rossella.martino@formedil.it

D. De Gisi
e-mail: diegodegisi@formedil.it

51

1 Introduction

Water scarcity is a serious problem for many European regions, with ca. 45% of the territory expected to face water restraints while damage caused by floods may increase fivefold by 2050. Meanwhile, there has been intense debate in Europe, with ongoing process for setting standards for water-efficient products in buildings (COM 2012, 2015). Efforts have also been made to move towards a European framework of core indicators for assessing environmental performance in buildings, including water efficiency, towards the progressive transformation of markets, with growing introduction of water-efficient devices, systems and labelled products. These changes will require new harmonized skills within the water professionals and within both the construction sector and "green" professionals (including water and energy efficiency, as well as water–energy nexus consultants), together with market and consumer trust for the adoption of water efficiency solutions for buildings. On the other hand, national and European legislation need to be prepared to disclose any risks of potential negative effects on the quality of the provided services, particularly regarding water quality, and guarantee consumer safety, well-being and confidence, as well as energy efficiency of the newly water-efficient solutions, systems and technologies.

The development of new water efficiency approaches may include water demand-side management strategies (WWAP (United Nations World Water Assessment Programme) 2014), such as labelling or certification of products and buildings, in line with the path taken on the energy efficiency side. Although effective, the energy efficiency approaches were mostly triggered by law and strongly connected with the price per kilowatt-hour, thus limiting full consumer engagement or preference on sustainable choices for best and long-term resource efficiency performance. For this reason, and because the instruments taken on the energy side may differ from that of water, there should be strong consumer engagement at the same time of market

preparation. Likewise, to enable consumer capacitation and successful engagement on the choice of water-efficient products, there is a need for adequate training, capacity building and qualification of construction professionals (including plumbers, technical agents or designers), as well as "green" professionals (including water and energy efficiency, as well as water–energy nexus consultants) (Cardoso et al. 2018). Conversely, sustained and reliable independent schemes, certifying the technical knowledge and skills/capacities of such professionals towards market recognition and confidence, need to be developed. With WATTer Skills project (*Water Efficiency and Water-Energy Nexus in Building Construction and Retrofit*, http://watterskills.eu/), new and upskilled professionals—water efficiency technicians and water efficiency experts—will support consumers and help them to apply strategies seeking both water and water–energy efficiency measures (for instance, in some cases, water bills may be reduced by 30% (Silva Afonso and Pimentel Rodrigues 2017), plus another 23% corresponding to the water–energy nexus [hot water], with replacement of old water devices), together with societal revenues of adopting water conservation behaviour.

Under the water–energy nexus, WATTer Skills is a European project, co-funded by the ERASMUS+ programme that recognizes the strong interrelation and interdependence between energy and water consumption. The goal of WATTer Skills is to maximize water and energy efficiency opportunities in buildings, rather than focusing in any of the terms solely. It is therefore important to assure that the new solutions, equipment and technologies for water efficiency will not increase the demand for energy in buildings, which may happen if there is not both integrated approach and skills on the new energy uses associated with water efficiency systems and technologies. The same shall be considered when addressing energy-efficient solutions, equipment and technologies for energy efficiency. A common example of isolated approaches is to have energy-friendly equipment (e.g. dishwashers) implying high water usages. Also, in countries where energy efficiency has already been maximized, new approaches to higher efficiency towards other resources such as water may need to be applied, and since only by improving water efficiency, or through wastewater heat recovery, the total energy use may decay (e.g. Sweden). Simply put, the key message over the water–energy nexus is that the resources should be conserved as a whole, rather than separately, because, in a broader sense, water is critical for energy production while energy is critical for water production and use.

2 WATTer Skills Objectives, Approach and Methodology

With more detail, the goals of the WATTer Skills project (2017–2020) are to develop, implement and propose common curricula, qualification framework and certification schemes at the European level, for water efficiency training and skills upgrading of construction professionals (technicians and experts). In this context, a framework where the main skills for the professionals in the field are identified has been developed, considering the necessary competences over the implementation of water efficiency and water–energy nexus measures (Cardoso et al. 2018). Involving Portugal (ADENE), Spain (FLC), Italy (Formedil) and Greece (CRES), WATTer Skills will deliver a tool to promote transparent curricula and training for the development of sustainable and sound practices for water efficiency and water–energy nexus by its related professionals.

The WATTer Skills approach is to build upon the best practices drawn from previous projects on water efficiency and energy efficiency training, such as the AquaVET Project (*Strategic Partnership for the Development of a Vocational Education Training course on water efficiency technologies for water technicians*, www.aquavet.eu), the BUILD UP Skills initiative Pillar II projects funded within the IEE (Intelligent Energy for Europe Programme, www.buildup.eu) and the ENACT Project (*Strategic Partnerships for ENergy Auditors Competences, Training and profiles, enactplus.eu*), and go further, by moving towards a European common qualification and accreditation system for professionals on water efficiency and water–energy nexus in buildings. With this purpose, the methodology used followed three main steps: (1) setting the perimeter and the WATTer Skills map at a European level; (2) developing a common qualification framework and certification schemes, based on the learning outcomes designed for water efficiency skills under the water–energy nexus; and (3) developing and proposing a common certification of qualifications system.

Setting the perimeter was the starting point for the definition of the WATTer Skills map in terms of learning outcomes (definition of expected knowledge, skills and autonomy-responsibility for water efficiency technicians and water efficiency experts), at a European level. This was accompanied by a definition and collection of monitoring metrics and indicators, to compare water and water–energy efficiency practices and consumptions in buildings, before and after the implementation of the training and qualification schemes. In the ongoing development of a common

qualification framework, the training courses as well as the qualification and accreditation requirements are based on the previously defined learning outcomes and need to be in line with the European Qualifications Framework (EQF) provisions, while they must be able to adopt and adapt (nationally), to the training and qualification of the different types of targeted professionals. Last but not least, the common accreditation system for water efficiency technicians and water efficiency experts is based on the European Credit system for Vocational Education and Training (ECVET) training credits, capable of being used in all European Union countries, fostering mobility and recognition of professionals in the European market.

3 WATTer Skills Framework: Results and Main Expected Outcomes

Targeted at the main professionals involved in water facilities design and installation in buildings, the training curricula, qualification framework and certification schemes will directly involve the water installation technicians and high-skilled professionals, addressed and upskilled in WATTer Skills, as water efficiency technicians (WET) and water efficiency experts (WEE), respectively. In this context, WATTer Skills introduces new definitions and professionals, including:

- Water efficiency technician (WET)—the person certified to install, maintain and repair water-efficient systems, including rainwater harvesting and greywater reuse, also addressing the water–energy nexus-related measures in buildings, considering site conditions, the building type and the most adequate systems and installation principles, water- and energy-efficient home appliances, equipment and devices, and water efficiency in green areas and the outdoor environment
- Water efficiency expert (WEE)—the person certified to design, select, propose and inspect water-efficient

systems, including rainwater harvesting and greywater reuse, also addressing the water–energy nexus-related issues in buildings, considering site conditions and the building type and the most adequate systems and design principles, water- and energy-efficient home appliances, equipment and devices, and water efficiency in green areas and site-based passive measure design.

In comparison to mentioned previous projects, like AquaVET, where "water technician" included the skilled tradesperson, responsible for the management aspects of systems used for the circulation of potable (drinking) and hot water from the point of source until its end-use, including sewage, and drainage in residential and non-residential applications, in the WATTer Skills approach, the water-related professions focus on efficiency, requiring increased water- and energy-saving skills. Naturally, the two new definitions are similar since the WEE is a more qualified version of the WET.

The skills maps were then defined in terms of the learning outcomes for the WET and WEE, based on two main steps: (1) description of the job positions and their functions/tasks related to water efficiency, allowing the skills identification for the WET and WEE qualifications or expertise, and (2) description of competence units on water efficiency, for the identified skills to be completed with knowledge on what it is necessary to achieve water and energy savings, also under the water–energy nexus. In Table 1, an example for each of the professionals, with reference to two areas of competence and the corresponding generated skills, is provided. Overall, the WET shows 21 skills divided by 7 areas of competence, whereas the WEE shows 18 skills divided by 4 areas of competence.

Each skill will be further complemented with the full set of the learning outcomes (i.e. knowledge, skills and autonomy-responsibility) that will form the basis for the development of the training contents for the future courses. These need to be related to ECVET credits in terms of recognition and transferability.

Table 1 Examples of areas of competence and the corresponding skills for the WET and the WEE

Category	Areas of competence	Example of a necessary skill to achieve water efficiency, including the water–energy nexus
WET	Hydraulic installations and water losses	Effective implementation and renovation of the thermo-hydraulic installations design aiming at the improvement of their performance
	Domestic hot water supply	Recognition of the new efficient technologies and/or equipment for domestic hot water production
WEE	Design of water-efficient buildings	Considering the site conditions to propose an efficient composition and distribution of spatial elements, thermal and hydraulic installations
	Water measurements and water–energy nexus	Quantify water and energy consumption to establish baselines for water and/or energy use or demand

4 Preliminary Results and Conclusions

During WATTer Skills execution, the data collected for each country showed dissimilarities amongst the existing qualification and certification systems, particularly in the number and duration of national qualifications, vocational education and vocational training, showing the importance of consistency and harmonization in such a water professional's framework, at least within European countries with similar needs. Considering not only the share of context with respect to water stress in countries from the Mediterranean area, which is also increasing in northern European Countries, but also the need to tackle a more efficient use of resources, WATTer Skills provides the framework and tools to training and qualifying new water efficiency technicians (WET) and water efficiency experts (WEE) to achieve increased water and energy savings in buildings.

References

Cardoso, P., Newton, F., Poças, A., Beirão, D., Malamatenios, C., Veziryianni, G., González, J., Carapella, G., Martino, R. (2018). Skills for water efficiency and water-energy nexus in building construction and retrofit. In *Water Efficiency Conference 2018* (accepted for oral communication).

COM. (2012). *673 final*. A blueprint to safeguard Europe's water resources. Brussels: European Comission.

COM. (2015). *614 final*. Closing the loop—an EU action plan for the Circular Economy European Comission, Brussels.

Silva Afonso, A., Pimentel Rodrigues, C. (2017). *Manual de Eficiência Hídrica em Edifícios*, 1st edn. ANQIP—Associação Nacional para a Qualidade nas Instalações Prediais.

WWAP (United Nations World Water Assessment Programme). (2014). *The United Nations World Water Development Report: Water and Energy*. Paris: UNESCO.

WEFSiM: A Model for Water–Energy–Food Nexus Simulation and Optimization

Albert Wicaksono, Gimoon Jeong, and Doosun Kang

Abstract

A Water-Energy-Food Nexus Simulation Model (WEFSiM) is proposed to quantify the nation-wide resources sustainability. WEFSiM considers the feedback connections between water, energy, and food sectors in a single framework. The optimization module provides more alternatives for resource management planning. The effect of a new energy plan in South Korea (Energy 2030) is simulated in a nexus perspective.

1 Introduction

Water-Energy-Food nexus (WEF nexus) is a novel concept for resource management that considers the feedback connections among sectors in a single framework (Hoff 2011). Recently, several computer models have been developed and applied to simulate this concept. In this study, a Water-Energy-Food Nexus Simulation Model (WEFSiM) is introduced to simulate the feedback analysis and calculate the demand and supply of WEF resources on a nation-wide scale based on a system dynamics approach. Being different with other simulation models, the feedback analysis in WEFSiM is also utilized to identify the critical factors that affecting the availability of specific resources (e.g., food production can be affected by either land, water, or energy

availability). Various types of water resources, power plants, and foods are implemented in the model to provide a detail simulation. Moreover, the optimization module is implemented to provide optimal decisions of resource allocation to maximize supplying reliability. The optimization scheme is expected to assist stakeholders to decide the suitable policy and management plan.

As one of the most energy-consuming countries, South Korea relies on the thermal (64%) and nuclear (34%) plants to fulfill the energy demand, while only 2% is supplied from the renewable energy (U.S. Energy Information and Administration 2015). The thermal and nuclear power plants produce greenhouse gases and consume a significant amount of water to generate electricity. South Korea government is planning to increase the usage of renewable energy up to 20% of total electricity production by 2030 while reducing the thermal and nuclear plants (Lee 2017). Here, this new energy plan is simulated using WEFSiM to evaluate the effect of this plan to other sectors.

The simulation results revealed that the implementation of the new energy plan (Energy 2030) in South Korea reduces the water consumption overall. The results showed that the reserved water could be supplied to the food sector to enhance food production. Furthermore, the optimization analysis provides several combinations of user priority and water allocation strategies to improve overall resource sustainability.

2 Materials and Methods

WEFSiM is developed based on a conceptual scheme in Fig. 1 that represents the possible connection between water, energy, and food sectors. In general, the water is calculated as a direct demand to municipal and industrial users, while calculated as indirect demand when it becomes irrigation water or cooling water in a power plant. Energy is used for pumping, processing (treating), and distributing water to municipal and industrial users, and it is needed to produce fertilizers and pesticides, and pump irrigation water into

A. Wicaksono · G. Jeong · D. Kang (✉)
Kyung Hee University, Seoul, Republic of Korea
e-mail: doosunkang@khu.ac.kr

A. Wicaksono
e-mail: albert.wcso@gmail.com

G. Jeong
e-mail: gimoon1118@gmail.com
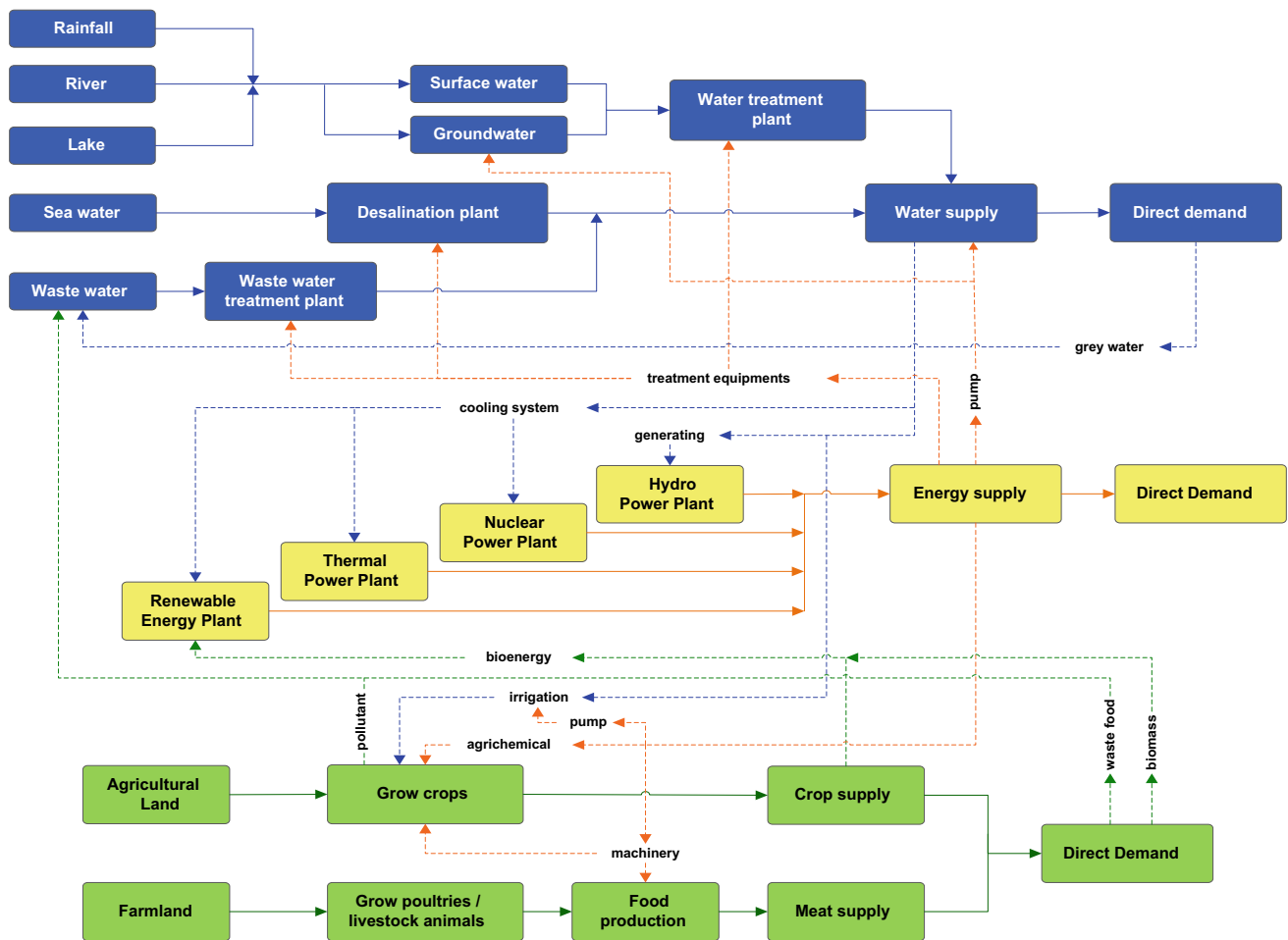
Fig. 1 Conceptual scheme of WEFSiM

agricultural areas. On the other hand, agricultural products can be transformed into bioenergy.

In this study, the interconnections among elements are represented/quantified by an intensity value that determines the indirect amount of a resource required to produce a particular resource. The interlinkage among the resources is simulated using a system dynamics approach, so-called feedback analysis. In addition, an optimization module is implemented in WEFSiM using a genetic algorithm (GA). The optimization is executed to maximize the resources reliability index by optimizing 21 decision variables.

A database that is composed of various information of the water, energy, and food sectors, as well as population, socioeconomic, and climate-related data was also developed to supply input data for the simulation model. Data was collected from open-access references and summarized in a spreadsheet format to be linked directly to WEFSiM. The collected data was also used as a reference in model calibration and projection of future condition.

In this study, three scenarios are developed to predict the conditions in the next 20 years. The first scenario is the base condition assuming the projection of current trends. The second scenario represents the new energy plan in South Korea (Energy 2030). In this plan, renewable energy production is assumed to increase linearly, while the nuclear power generation is decreasing and finally closed without further construction (see Fig. 2). The third scenario is an
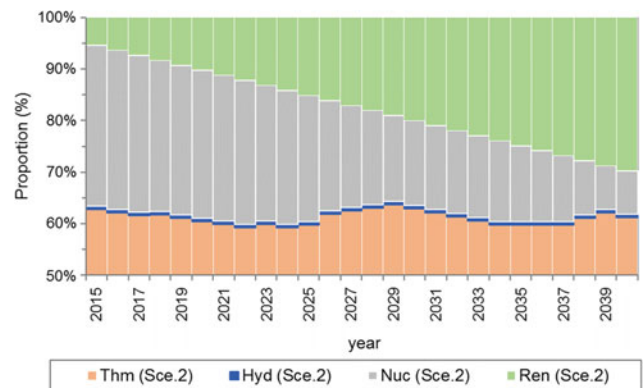
Fig. 2 New energy plan in South Korea

optimization of scenario 2 with the objective to find better-supplying reliability. In the first and second scenarios, the priority order of water and energy users has been pre-defined, i.e., municipal–industry–energy–food, and municipal–water–industry–food, respectively. Meanwhile, the priority order in the third scenario will be determined based on the optimization results.

3 Results and Discussion

For the base scenario, South Korea is predicted not to experience any energy shortage (Fig. 3b), but some significant droughts might occur in the future, and subsequently affect food availability (Fig. 3a, c). It can be seen that water availability consequently affects food production, especially the crop-based food sector since they depend on irrigation. The limitation of the available agricultural area also limits the self-sufficiency of food, so it is unable to fulfill the food demands and requires importation from outside.

The implementation of a new energy plan can reduce the consumption of water for energy sector by 4.7% (Fig. 4). The reduction is not significant because the thermal power (another water-intensive power plant) still dominates the energy supply. However, the reserved water can be used to supply additional water for food sector although it only slightly increases food production since the excess water is only 0.3% of the total indirect demand water for food. Hence, the reliability index between scenario 1 and scenario 2 is not significantly different (Fig. 5). Here, the optimization is performed to improve system reliability by optimizing the resources allocation.

The optimization results showed enhanced resource reliability by optimizing the combination of priority index and water allocation. The optimization results placed the water and energy users at the same priority level, which means they should be considered simultaneously and equally in the resources allocation process. The results show a slight decrement in the water supply for municipal and energy sectors but increases for food production. Hence, the food
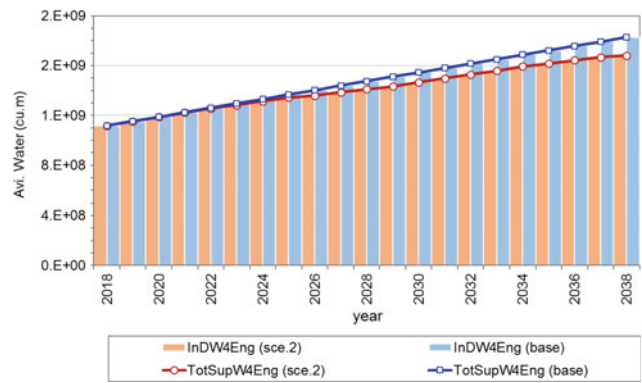
Fig. 4 Water consumption for the energy sector
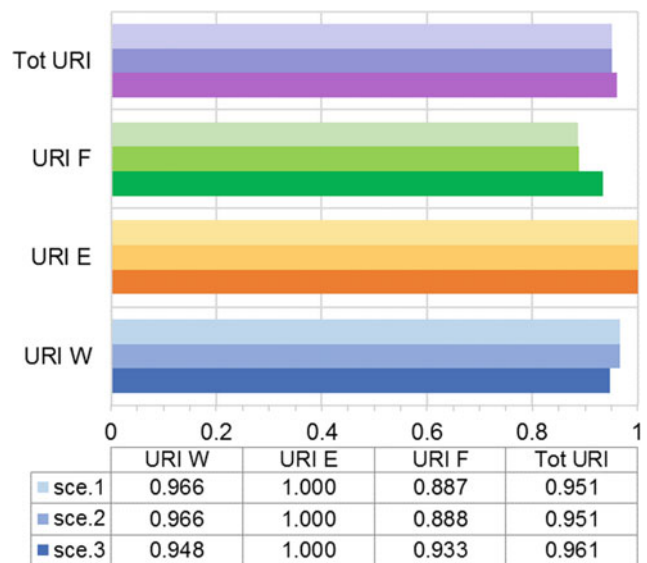
Fig. 5 Reliability index

reliability index is increasing, but the water reliability index is slightly decreasing. However, the reduction of water supply for energy does not affect the energy reliability index because of the implementation of a renewable energy plan that consumes less water.
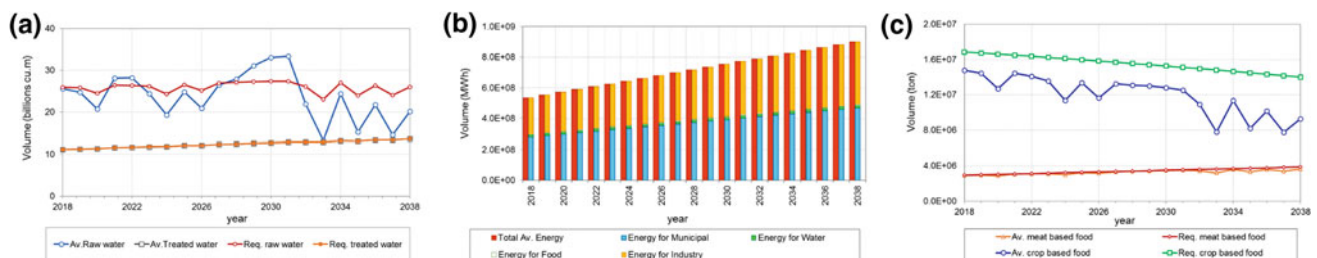
Fig. 3 Projection of **a** water, **b** energy, and **c** food demand and availability in the base condition

4　Conclusion

This study proposes a new simulation model that simulates the interconnections between water, energy, and food sectors using a nexus concept. Based on the analysis of the simulation results, WEFSiM is able to simulate the interconnections and quantify the resources supply, demand, and reliability. The results can be used to identify the critical factors affecting certain element and evaluate the effect of a change of an element on other elements. Here, this concept is used to evaluate the implementation of a new energy plan in South Korea to other sectors. In this scenario, the new energy plan has a beneficial impact on reducing water consumption in the energy sector and used it to increase food production. The optimization module could provide some alternatives to increase resources sustainability. In this study, the best result is obtained by slightly decreasing the water supply for municipal and energy, and allocating it for food production. By implementing this alternative, the food and total reliability index can be increased without sacrificing other resources significantly. The optimization module is a helpful tool to provide optimal strategies in creating resource management plan.

References

Hoff, H. (2011). *Understanding the Nexus*. Stockholm: Stockholm Environment Institute.

Lee, W. (2017). *2030 Energy Masterplan of South Korea*. Chuncheon, Republic of Korea: Research Institute for Gangwon.

U.S. Energy Information and Administration. (2015, July 15). *International energy statistics: Total primary energy production 2013*. Retrieved from U.S. Energy Information and Administration: http://www.eia.gov/beta/international/data/browser/.

Assessment of Rain Harvesting and RES Desalination for Meeting Water Needs in an Island in Greece

Konstantinos Kotsifakis, Ioannis Kourtis, Elissavet Feloni, and Evangelos Baltas

Abstract

Three different scenarios for meeting domestic water demand in a small island in Greece were examined and compared. Life-cycle cost analysis was performed in order to evaluate each scenario from an economic point of view.

1 Introduction

The use of decentralized water supply technologies has increased worldwide over the last decades, as policy makers and water professionals have sought to find solutions to the water scarcity—and the associated economic development—problems over remote areas. In this frame, rainwater harvesting (RH), a water management practice followed for over 4000 years, today gains more and more ground as a modern, relatively inexpensive and simple water-saving technology (e.g., Londra et al. 2015). Several studies have been conducted in order to determine the optimal size of rainwater tanks (e.g., Londra et al. 2018; Tsihrintzis and Baltas 2014; Campisano and Modica 2012; Fewkes and Butler 2000), while others have focused on the economic aspects of RH systems (e.g., Morales-Pinzón et al. 2015; Tam et al. 2010; Rahman et al. 2012). Another method which is becoming increasingly attractive and may be an economic solution to the water scarcity problem of remote areas and islands, in particular, is desalination plants for freshwater production integrated with renewable energy resources (e.g., Alkaisi et al. 2017; Espino et al. 2003; Garcia-Rodriguez et al. 2001).

The purpose of this research work is to perform a techno-economic analysis on three different approaches, i.e., (i) domestic RH, (ii) wind-powered reverse osmosis (WPRO) desalination plant operation, and (iii) a combined scenario (RH-WPRO), for meeting domestic water demand in Lipsi Island, a complex of 30 small islands located in south-east Aegean Sea, Greece. The total area of the complex is approximately 17.4 km^2, with the main island, which is the only inhabited, covering an area of 15.8 km^2. According to the last census conducted in 2011, the population is 790 people, while tourism results in an increase of about five times during the period from April to September. Regarding water needs, they are primarily met by water hauling via ship, with a mean cost of 10.8 €/m^3, combined with the exploitation of the existing infrastructure of limited capacity, mainly consisting of water supply boreholes, with an average cost of 0.83 €/m^3 (RBMP-GR14 2015). The water supply system consists of four water tanks with a total capacity of 4000 m^3 (1000 m^3 each) and a reservoir of 32000 m^3 capacity, which is not connected to the water supply system, as it is only used for irrigation purposes.

K. Kotsifakis (✉) · E. Feloni · E. Baltas
Department of Water Resources and Environmental Engineering, School of Civil Engineering, National Technical University of Athens, Heroon Polytechniou 9, Zografou, 15780 Athens, Greece
e-mail: kkotsifakis@chi.civil.ntua.gr

E. Feloni
e-mail: feloni@chi.civil.ntua.gr

E. Baltas
e-mail: baltas@chi.civil.ntua.gr

I. Kourtis
Department of Infrastructure and Rural Development, Laboratory of Reclamation Works and Water Resources Management, School of Rural and Surveying Engineering, Centre for the Assessment of Natural Hazards and Proactive Planning, National Technical University of Athens, Zografou, Greece
e-mail: gkourtis@mail.ntua.gr

2 Materials and Methods

Three scenarios for meeting domestic water requirements were developed, implemented, and evaluated regarding their overall life-cycle cost over an examined lifetime cycle of 30 years. Given the unavailability of detailed data, an average daily consumption of 0.18 m^3/capita was assumed based on Tsihrintzis and Baltas (2014). In addition, the number of the permanent residents, visitors, and tourists during summer months was considered to increase, with an annual rate equal to 1.5%, taking into account the historical population growth at the island.

2.1 Scenario I: Rainwater Harvesting (RH)

The evaluation of water saving obtained by RH was carried out by simulating water balances with a behavioral model based on the yield-after-spillage (YAS) algorithm as tank release rule (Fewkes and Butler 2000), using a daily rainfall time series. Initially, the model was applied for various combinations of: (i) residents per household, only single-family houses were examined since they are the majority in the island, (ii) rainfall collection areas and, (iii) water tank volumes. Fixed values of 15 and 30% of the daily water consumption, which correspond to laundry and toilet-flushing demand, respectively, as well as, non-fixed values for garden demand (Domènech and Saurí 2011) were examined as non-potable water needs. From these, the toilet-flushing demand scenario was adopted for the entire analysis. For selecting an efficient tank size, the following criterion was introduced: the mean annual toilet water demand met should be at least 95%, and at the same time, tank volume should not exceed a capacity of 40 m^3, for spatial planning reasons. For the life-cycle cost analysis (LCCA) of the RH scenario, data were collected from different sources, including personal contact with local technicians. In all cases, above-ground water storage tanks were selected. For the typical household of two residents with a rainfall collection roof area of 80 m^2, and for a 95% demand for toilet-flushing water, the costs used in calculations were: tank and water pump purchase (3800 €), pump replacement after 15 years of operation (250 €), plumbing installation (500 €), ongoing operating and maintenance cost (0.05 €/m^3), and additional maintenance cost (20 €/year). A discount rate of 3% and a government rebate equal to 70% of the overall initial cost—necessary so as the investment to be profitable for the end user, as proved through a separate analysis that was performed—were introduced.

2.1.1 Scenario II: Wind-Powered Reverse Osmosis (WPRO) Desalination Plant

For the model development and, finally, for determining the WPRO plant capacity (m^3/day), data regarding existing infrastructure in the study area (e.g., water tanks capacity, position and altitudes, pipes drainage capacity), as well as, the daily needs of the permanent population and tourists were taken into account. The required energy for the operation was calculated using a standard energy consumption of 5 kWh/m^3 (Alkaisi et al. 2017), and the WPRO system was assumed to be interconnected with the electricity grid of the study area. In this way, any deficit of energy should be met by the grid. After determining the required capacity, using available climate data of wind speed from the neighboring island of Leros and assuming a Vestas V126-3.45 wind turbine, the produced energy was calculated. The costs used for performing the LCCA were (Alkaisi et al. 2017; Bertsiou et al. 2017): (i) investment cost of 2250 €/m^3 for the WPRO plant, (ii) investment cost of 750000 € for the wind turbine, (iii) operation and maintenance cost of 1 €/m^3/day for the WPRO plant, (iv) operation and maintenance cost of 20000 € for the wind turbine. Finally, a VAT equal to 24% for all costs and a discount rate of 3% were assumed.

2.1.2 Scenario III: (RH-WPRO)

The third scenario involved the operation of a RH system in each household in Lipsi for meeting the toilet-flushing water demand. The remaining (i.e., not supplied by the RH) amount of toilet water, as well as, the fresh water requirements were met by a WPRO for a reliability level of 99%. Correspondingly, a LCCA for this scenario was performed and the results were compared with the other three scenarios examined (i.e., zero, I, II).

3 Results and Discussion

The aforementioned approaches were developed and analyzed on a daily basis for a period of 30 years, taking into account a population growth scenario. The designed desalination plant resulting from the model implementation under the WPRO and RH-WPRO scenarios was of 460 and 400 m^3/day capacity, respectively. In all cases, a system reliability level of 99% was achieved and the alternatives were compared on the basis of the life-cycle cost. The results are presented in Fig. 1.

It is obvious that the zero scenario, which includes a combination of water hauling by ship and existing infrastructure contribution, is the most expensive over time.

Fig. 1 Life-cycle cost analysis for all examined scenarios (i.e., existing: zero: RH: I, WPRO: II, RHS-WRPO: III scenario)
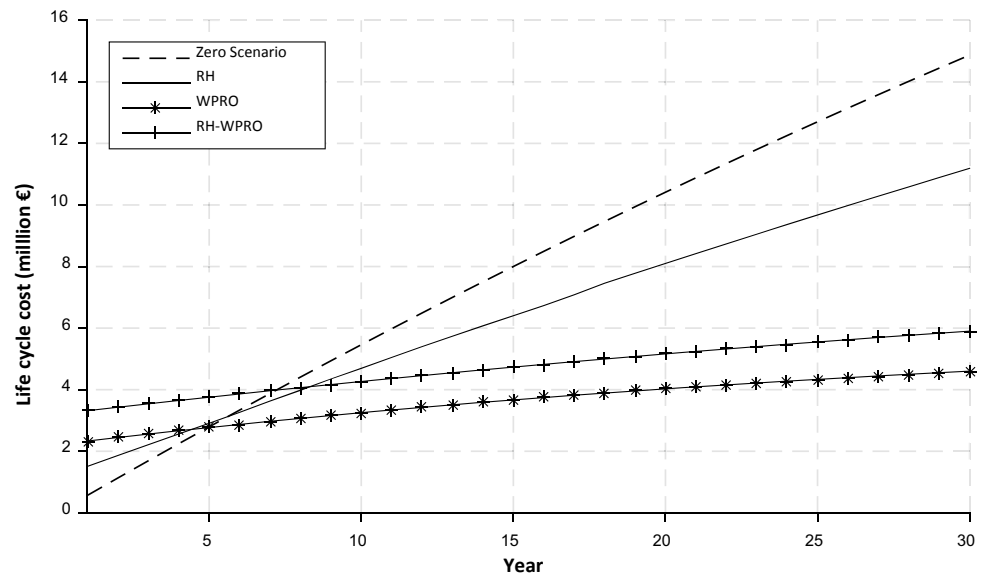
On the other hand, the WPRO scenario is the most efficient, from an economic perspective, achieving a capital return after less than 5 years. Almost the same capital return period is achieved under the RH scenario as well, although the cumulative cost over the 30-year analysis is significantly higher, as the deficit of water (i.e., water not supplied by the RH tanks) still needs to be transported to the island under the high present cost. While the combined solution (RH-WPRO) is advantageous in comparison to the zero scenario, the initial investment required—at which the rebate offered by the state to the island residents is integrated—makes it more expensive than the WPRO desalination plant operation alone.

4 Conclusions

In this research work, three different alternatives for achieving water security in the island of Lipsi in Greece were examined and compared, based on their economic feasibility, for a typical life cycle of 30 years. The RH scenario targeted in reducing the amount of water that is currently transported to the island and, thus, the overall cost of water supply, while the WPRO and the combined RH-WPRO scenarios aimed at eliminating this amount by meeting the total water needs for 99% reliability. Findings suggested that all examined scenarios result in significantly reduced costs, compared to the water management practices that are currently followed, while the WPRO solution was found to be the most cost-effective for the study area. Nevertheless, when it comes to decision making, other parameters which were not examined in the present study— such as environmental costs and impacts—are also of great

importance and should be carefully assessed before any solution is characterized as optimal.

References

Alkaisi, A., Mossad, R., & Sharifian-Barforoush, A. (2017). A review of the water desalination systems integrated with renewable energy. *Energy Procedia, 110,* 268–274.

Bertsiou, M, Feloni, E.G., & Baltas, E. (2017). Cost-benefit analysis for a hybrid renewable energy system in Fournoi island. In: *Proceeding of the Sixth International Conference on Environmental Management, Engineering, Planning and Economics (CEMEPE) and to the SECOTOX Conference*, June 25–30, Thessaloniki, Greece.

Campisano, A., & Modica, C. (2012). Optimal sizing of storage tanks for domestic rainwater harvesting in Sicily. *Resources, Conservation and Recycling, 63,* 9–16.

Domènech, L., & Saurí, D. (2011). A comparative appraisal of the use of rainwater harvesting in single and multi-family buildings of the Metropolitan Area of Barcelona (Spain): social experience, drinking water savings and economic costs. *Journal of Cleaner Production, 19*(6–7), 598–608.

Espino, T., Penate, B., Piernavieja, G., Herold, D., & Neskakis, A. (2003). Optimised desalination of seawater by a PV powered reverse osmosis plant for a decentralised coastal water supply. *Desalination, 156*(1–3), 349–350.

Fewkes, A., & Butler, D. (2000). Simulating the performance of rainwater collection and reuse systems using behavioural models. *Building Services Engineering Research and Technology, 21*(2), 99–106.

Garcia-Rodriguez, L., Romero-Ternero, V., & Gómez-Camacho, C. (2001). Economic analysis of wind-powered desalination. *Desalination, 137*(1–3), 259–265.

Londra, P. A., Theocharis, A. T., Baltas, E., & Tsihrintzis, V. A. (2015). Optimal sizing of rainwater harvesting tanks for domestic use in Greece. *Water Resources Management, 29*(12), 4357–4377.

Londra, P. A., Theocharis, A. T., Baltas, E., & Tsihrintzis, V. A. (2018). Assessment of rainwater harvesting tank size for livestock use. *Water Science and Technology: Water Supply, 18*(2), 555–566.

Morales-Pinzón, T., Rieradevall, J., Gasol, C. M., & Gabarrell, X. (2015). Modelling for economic cost and environmental analysis of rainwater harvesting systems. *Journal of Cleaner Production, 87,* 613–626.

Rahman, A., Keane, J., & Imteaz, M. A. (2012). Rainwater harvesting in Greater Sydney: Water savings, reliability and economic benefits. *Resources, Conservation and Recycling, 61,* 16–21.

RBMP-GR14. (2015). River basin management plan for River Basin District 'GR14—Aegean Islands, Greece'. Approved in 2015 according to the requirements of the Framework Directive 2000/60/EC. http://wfdver.ypeka.gr/el/project/gr14–00-approved-legislation-fek-gr/ (In Greek, last visited on 28/07/2018).

Tam, V. W., Tam, L., & Zeng, S. X. (2010). Cost effectiveness and tradeoff on the use of rainwater tank: An empirical study in Australian residential decision-making. *Resources, Conservation and Recycling, 54*(3), 178–186.

Tsihrintzis, V. A., & Baltas, E. (2014). Determination of rainwater harvesting tank size. *Global NEST Journal, 16*(5), 822–831.

Grounding Nexus Governance: De-Nexused Developments in Nepal

Dipak Gyawali and Jeremy Allouche

Abstract

There appears to be little agreement on the precise meaning of the nexus, whether it only complements existing environmental governance approaches or how it can be enhanced in national contexts. Technical solutions for improving coherence and governance within the nexus may have unintended and negative impacts in other policy areas, such as poverty alleviation. The nexus is yet to be extensively grounded, into national policies and practices, and broad-based local demand for nexus-framed policies is currently limited. Through a mini-case study in Nepal, this article seeks to analyse what is the local understanding and practice around the relationship between food, energy and water to inform nexus thinking and practice. These mini-case studies will inform us on the interaction between formal and informal institutional arrangement and how these interactions form the basis of a nexus system.

Keywords

Nexus • Governance • Nepal • Informality

1 Introduction

The idea of "the nexus" between water, food and energy is institutively compelling. It promises better integration of multiple sectoral elements, a better transition to greener economies and sustainable development. Addressing this challenge requires innovation in all policy dimensions (Larcom and van Gevelt 2017). Many related discussions are emerging about what integration is, what it means and what it achieves. Numerous analytical frameworks are being developed for identifying leverage points to break path dependencies, adapt to unknown change and enable robust decision making in the face of uncertainty (Allouche et al. 2014; Leck et al. 2015). However, there appears to be little agreement on its precise meaning, whether it only complements existing environmental governance approaches or how it can be enhanced in national contexts.

There are divergent framings of the nexus between its various proponents, on risk and security, or economic rationality, which mask different types of politics: politics of difference, politics of knowledge, international political economy and geopolitics (Allouche et al. 2015). Our perspective acknowledges it as a fundamentally political process requiring negotiation amongst different actors with distinct perceptions, interests and practices (Rees 2013; Allouche et al. 2014; Stein et al. 2014). This perspective, concerned with equity and social progress, highlights the fact that technical solutions for improving formal governance within the nexus may have unintended and negative impacts in other policy areas, such as poverty alleviation.

This article challenges the managerial–technical conceptions definitions of the nexus by bringing to the forefront the politics of the nexus, around two key dimensions—a dynamic understanding of water–food–energy systems and a normative positioning around nexus debates, in particular around social justice. The author argues that a shift in nexus governance is required towards approaches where limits to control are acknowledged, and more reflexive/plural strategies adopted.

2 Materials and Methods

Methodologically, we develop a mini-case study analysis of the nexus in Nepal, examining case studies that exemplify nexused-dilemmas and where divergent, plural perspectives and contestations have emerged in response. The article is

D. Gyawali
Nepal Academy of Science and Technology, Patan, Nepal
e-mail: dipakgyawali@ntc.net.np

J. Allouche (✉)
Institute for Development Studies, STEPS Centre, Brighton, UK
e-mail: j.allouche@ids.ac.uk

based on a series of semi-structured interviews conducted between January and April 2014.

3 Results and Discussion

Nexus and integrated management are ongoing, unresolved problems of complex development and its governance. The opposite of a more holistic or interdisciplinary water–food–energy nexus approach is silo-fication which is the natural consequence of hierarchic organizing and specializing at levels of social organization above the primary one of the farming family. With funding from high-income country donors, it is found to have diffused from a global policy arena into a regional one that includes international and regional organisations, academic networks, and civil society, and national politicians and government officials (Middleton et al. 2015). The nexus is yet to be extensively grounded, however, into national policies and practices, and broad-based local demand for nexus-framed policies is currently limited. This article will not focus on the official nexus policy and its impact on the ground but rather look at how nexus issues are being constructed under hybrid governance systems involving local institutions and individuals. Through a mini-case study in Nepal, this article seeks to analyse what is the local understanding and practice around the relationship between food, energy and water to inform nexus thinking and practice. This case study will inform us on the interaction between formal and informal institutional arrangement and how these interactions form the basis of a nexus system.

The case of Nepal's only large reservoir, the Kulekhani Hydroelectric Power Stations, is instructive in understanding how, despite the multiple benefits of a nexus approach, the ground imperatives of government agency practices promote de-nexusing the water–food–energy sectors that converge around the reservoir into silo approaches. Conceived purely as a peaking hydroelectric plant, considerations of using the stored water either within the reservoir for fisheries or downstream for irrigation and drinking water were never part of the official project design by the various actors involved in the project design, whether government agencies, multilateral development banks (i.e. the World Bank) or bilateral donors (in this case, Japanese aid agency JICA). There have been writings by activists and academics in the local media suggesting nexus activities. They range from: using the higher water level in the reservoir to supply gravity flow drinking water to the chronically water-scarce capital city of Kathmandu located at a lower altitude; promoting tourism and fisheries in the lake; increasing dry season irrigation in the downstream reaches from the stored releases; providing more municipal water supply to the town of Hetauda; and enhancing eFlows to the national wildlife

parks in the downstream reaches (Gyawali 2015). The interesting point in terms of nexus governance is that some of these initiatives were taken forward informally, as small livelihood activities by the communities living around the dam. A nexus governance approach was being developed at the local level, while being unrecognised and unacknowledged for.

The population surrounding the Kulekhani Watershed, and most of rural Nepal, has a deep and integrated relationship with the geography and land where livelihoods and culture depend on this relationship with the environment. Resilience and adaptability is a constant trend living in the middle hills of Nepal. With their susceptibility to the effects of climate change and major developments like the Kulekhani HEP, villagers have continued to live and make use of the land despite the changes to the ecosystems as a result of the construction of the dams, creation of the reservoir and the socio-economic effects of the process of major infrastructural development. The creation of the reservoir also brought about (as an afterthought) the potential for new livelihood options, including aquaculture and improved fishing opportunities, and the use of dry season regulated/stored water for downstream municipal uses (Gyawali 2015).

The real conflicts with the project began long after its completion with the restoration of multiparty democracy and the ability of the populace to voice public grievances. In July 1993, a major disaster struck the project when an intense cloudburst, lasting 30 h with intensity of up to 60 mm/h, dumped as much as 540 mm of rain in just 24 h. There was much mass wasting and landslides in the catchment area that practically filled up KL-1's entire dead storage volume that was planned to last 100 years. Bridges and sections of the national highways were washed off as were 67 small and large irrigation projects, and some two thousand people lost their lives. Subsequent bathymetric surveys indicated that actual sedimentation was orders of magnitude higher than designed for. The torrential rains dislodged hill slopes and washed away the penstock of KL-1 shutting down its operation completely (equivalent to 40% of the total grid power) and necessitating serious and expensive countermeasure constructions. An innovative "sloping intake" was constructed that allows the intake point of the headrace tunnel to move up as the lower part of the reservoir fills up with sediment. It is during this phase of rehabilitation/reconstruction that conflicts came to the fore highlighting the nexused nature of the reservoir.

The people who lived within the catchment around the reservoir area but who lost their lands at the valley bottom when the river was dammed began cage fish farming with encouragement by activists and some Japanese volunteers. There were no official agreements with the national utility that managed the dam, and the officials were not bothered

either since it did not affect their power generation. When the 1993 disaster struck and the sloping intake had to be constructed to make the plant functional again, the utility resorted to sudden and quick dewatering of the reservoir killing all the fish that the villagers had been farming. A massive conflict issued at the local level.

The initial official utility position was that it was their pond and they could do what they liked that the people fishing there had no official right to do so. Due to political pressure, a compromise of sorts was worked out. The fisher folks would be paid a one-time compensation of almost a million rupees, and they would be free to continue with their fish farming in an informal way. However, if anything untoward happened due to reservoir operations by the utility, they could not claim any compensation in the future.

The fish farming continues de-nexused in the informal economy engaging some 307 families around the reservoir area. They are now self-organizing into a self-help cooperative with members having fixed shares so as to prevent overfishing through self-regulation.

4 Conclusion

For many rural farmers, fishers and community groups, food, water and energy resources are not considered as separate pillars but are part of the system they live and work in and need to be managed accordingly. Therefore, at the local level, the nexus is a practical everyday reality. In terms of governance, a de-nexused food–water–energy nexus exists in the largest and only big reservoir in Nepal, and the nexusing is happening only with local and informal initiatives, but not at the official national Nepal government or international aid agency levels. This case study highlights the disjuncture between the official and the unofficial, the formal versus the informal and the national versus the local. The second point is that about the nature of nexus governance itself. Governance should not be about control, but recognizing and encouraging diverse forms of initiatives and leadership in plural forms. This is why a shift in nexus governance is required towards approaches where limits to control are acknowledged, and more reflexive/plural strategies adopted.

References

Allouche, J., Middleton, C., & Gyawali, D. (2015). Technical veil, hidden politics: Interrogating the power linkages behind the nexus. *Water Alternatives*, 8(1).

Allouche, J., Middleton, C., & Gyawali, D. (2014). Nexus Nirvana or Nexus Nullity? A dynamic approach to security and sustainability in the water-energy-food nexus. In *STEPS Working Paper* no. 63, STEPS Centre, Institute of Development Studies. University of Sussex Brington.

Gyawali, D. (2015). Nexus Governance: Harnessing contending forces at work. *Nexus Dialogue Synthesis Papers*. Gland, Switzerland: IUCN.

Larcom, S., & van Gevelt, T. (2017). Regulating the water-energy-food nexus: Interdependencies, transaction costs and procedural justice. *Environmental Science & Policy, 72,* 55–64.

Leck, H., Conway, D., Bradshaw, M., & Rees, J. (2015). Tracing the water–energy–food nexus: description, theory and practice. *Geography Compass, 9*(8), 445–460.

Middleton, C., Allouche, J., Gyawali, D., & Allen, S. (2015). The rise and implications of the water-energy-food nexus in Southeast Asia through an environmental justice lens. *Water Alternatives, 8*(1).

Rees, J. (2013). Geography and the nexus: Presidential Address and record of the Royal Geographical Society (with IBG) AGM 2013. *Geographical Journal, 179*(3), 279–282.

Stein, C., Barron, J., & Moss, T. (2014). *Governance of the nexus: From buzz words to a strategic action perspective. Thinkpiece Series*. London, UK: The Nexus Network.

Maximizing Water–Food–Energy Nexus Synergies at Basin Scale

Rogier E. A. Burger and Edo Abraham

Abstract

In this short paper, we show how solutions for mitigating resource security in one sector can be found in another. We demonstrate—by means of a case study in Burkina Faso and Ghana—how investing in the electricity grid in the south leads to increase food security in the north. A new nexus framework was developed ('MAXUS') which was built to understand, simulate and optimize intersectoral (and international) development strategies in the water, food and energy sectors. We believe this new type of geospatial integral resource management, supported by the exponential increase of data availability of the twenty-first century, could finally turn nexus models into decision support tools.

Keywords

Nexus optimization framework • Bottom-up approach • Integrated resource management • Remote sensing

1 Introduction

Population growth, meat-focused diets and emerging industries are increasing stress on water, energy and food (hereafter, WEF) supply around the globe. As stress on the resources rises, the interdependencies between the sectors become more apparent and often lead to unforeseen chain reactions. An example of which is a drought leads to reduced hydropower generation that leaves groundwater pumps inoperable, which in turn leads to disappointing harvests (CERC 2012).

Because of these and many non-trivial/hidden interdependencies, synergizing water, food and energy policy is no easy task. Millions are spent to build reservoirs, food storage facilities, roads, canals, irrigated fields, electricity grids, energy production facilities, etc. These infrastructures are key to improve WEF security around the globe. With the strong connection of the WEF resources, infrastructure built in one sector impacts the others. With an unclear idea of this impact, newly built infrastructure may turn out to be ineffective and sometimes even harmful to other sectors. Especially, when the infrastructure of multiple sectors is developed in parallel, it is difficult to have a good understanding of the final outcome without an integrated analysis.

The need to obtain an integrated framework for policies and infrastructure design is now globally advocated (Asian Development Bank 2013; FAO 2014; Hoff 2011; UN 2014). As a result, several nexus models were developed but they have several uncertainties. The main critique of these models so far has been that many cannot serve as a decision support tool because they lack the ability to investigate specific governance actions or the implementation of technical interventions. These models generally have intensive data requirements and not flexible enough to perform for nexus studies at different scales with the same model framework (Bazilian et al. 2011; Kaddoura and El Khatib 2017; Dai et al. 2018).

In this paper, we propose a new optimization model framework for nexus studies titled 'MAXUS' (Burger 2018). It was built to fill the gap where current models fall short. It was built to customize a model for a specific nexus study. To test the methodology of MAXUS, it was applied to a case study for Ghana and Burkina Faso. Allocation of water and

R. E. A. Burger (✉) · E. Abraham
Faculty of Civil Engineering and Geosciences, Delft University of Technology, Stevinweg 1, 2628 CN Delft, Netherlands
e-mail: rogier.burger@gmail.com

E. Abraham
e-mail: e.abraham@tudelft.nl

land resources for the final supply of WEF was optimized over space and time.

2 Materials and Methods

Considering the wide range of nexus issues, which may have different scales in space and time and have different data availability, flexibility of a nexus model framework, is indispensable. The challenge with nexus issues is succinctly captured by Bazilian et al. (2011, p. 5): "to draw system boundaries wide enough to encompass the enormity of the interacting vectors, while maintaining it small enough to be able to conduct useful analysis."

To make sure that important interactions are captured for the nexus study at stake, a systematic methodology is required. In MAXUS, we used a bottom-up approach to define the objective, balances, interactions, constraints, dimensions and decision variables for a given nexus study.

A case study was developed for Burkina Faso and Ghana in which the approach was applied. Economic cost minimization was set as an objective while satisfying given water, food and energy demands of both countries. First, the nexus optimization was performed to explore the benefits of a multipurpose dam proposed in Ghana, then, to explore possible locations for additional irrigation and reservoir capacity. Both these cases highlight how a nexus analysis can be used for infrastructure development.

3 Results and Discussion

In Ghana, plans have been made for the construction of a multipurpose dam, near Pwalugu (Volta River Authority 2014), of which the location is shown by the red arrow. It will be developed to serve for hydropower, as well as irrigation. To investigate the benefits of such construction, the proposed extra water storage and irrigation capacities are added (by changing constraints) to the region in the MAXUS model. An optimization is solved for this new infrastructure. In this optimization, the water, food and energy demand is to be satisfied under minimal costs. Decision variables are food production, transport and storage, import and export; water transport, storage and irrigation; electricity transport, import and thermal power production.

In the figure, we show how the new dam is used to store water coming from the northern regions in the wet season and to discharge in the dry season. Part of the discharged water is used for irrigation in the region itself. With land being cropped, water is also being evaporated. Because of a significant change in crop evaporation, the total hydropower production has decreased, even though additional hydropower capacity was installed. Still, which is remarkable, less thermal power was required to be generated. Because of the relocation of hydropower generation, from south to north, transmission losses could be reduced, and consequently, more net energy is left. The power now produced is closer to the demand.
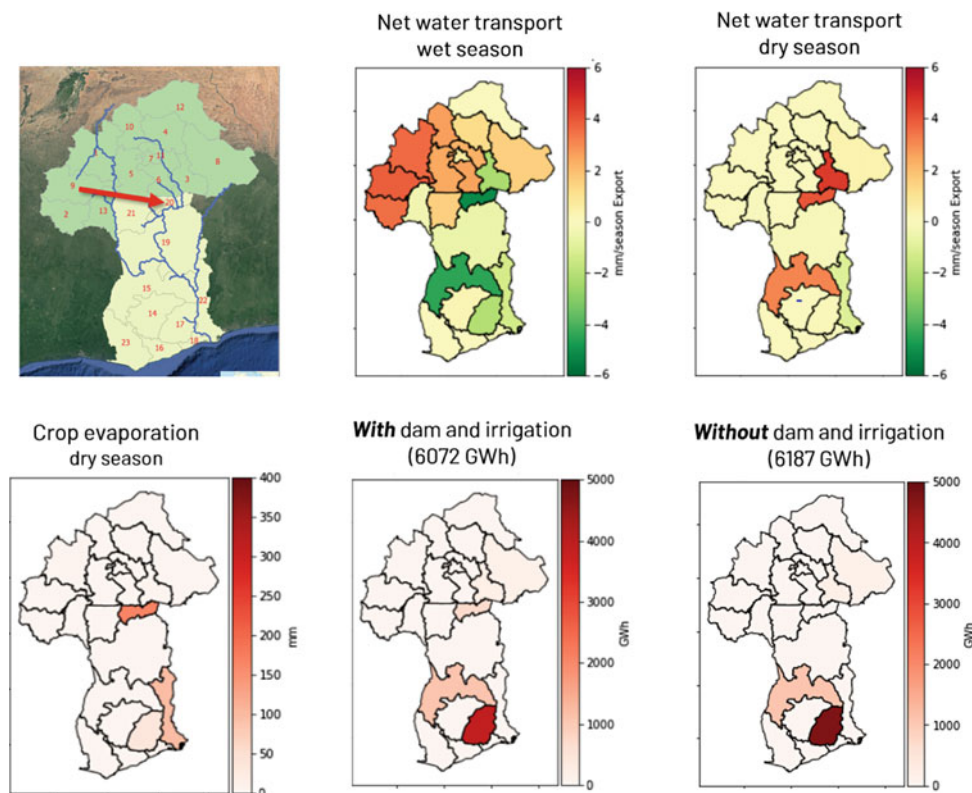
If the impact of infrastructure expansion can be determined for the optimization by the model, a new question arises: where (and when) is infrastructure worth the investment? To answer that, a new strategy is adopted. By making infrastructure expansion part of the optimization problem, MAXUS determines where infrastructure is beneficial against a certain cost.

The results show that two regions become for the larger part equipped with irrigation capacity. The region of the capital of Ghana and the region for new plans are proposed. This is no coincidence. Both regions are just downstream of a hydropower dam and therefore water storage. In the capital region, water has benefitted from all possible hydropower production before it is used for irrigation purposes and in addition is close to a large centre of food consumption—the capital Accra. The region where the dam is proposed is home to a large river junction, located relatively close to Ouagadougou the capital of Burkina Faso, another node of large demand. This region becomes key in supplying the north. Storage is built mostly in the northern areas. Here, there is relatively little storage capacity and building it provides essential water resources for irrigation. Besides storing water here means that it can always be used for hydropower on a later stage. IWMI (2012) reports that this is actually the place where a large number of reservoirs have been constructed in the last decades.

4 Conclusion

By using a newly developed optimization framework, we have shown how dependencies of WEF infrastructure can be found and taken into account for infrastructure planning. In an example, we showed that MAXUS is able to find non-trivial, multisectoral spatial (and temporal) trade-offs for the construction of a dam. We demonstrated in another example how strategic locations for irrigation capacity and water storage can be derived even though they would affect one another and the WEF sectors. The MAXUS model framework can be applied to a wide range of nexus studies; allowing adaptation objective functions, balances, decision variables, constraints and dimensions. It is scalable in time and space and therefore also has a flexible data input structure as to respond to different data availabilities worldwide. With the potential growth of geospatial and material flow data availability in the coming years, with the aid of remote sensing and new data management tools like block chain (Kshetri 2017), we believe that integrated nexus optimization models could be the foundation to provide decision support at basin/country level.
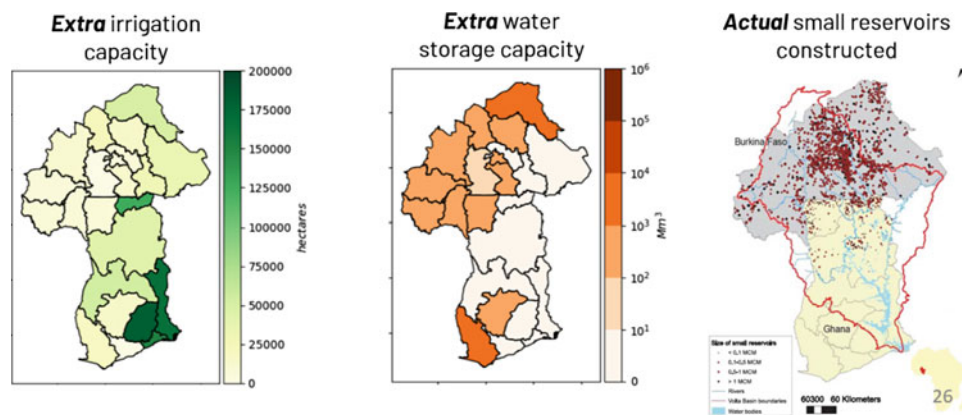
References

Asian Development Bank. (2013). *Thinking about water differently: Managing the water–food–energy nexus*.

Bazilian, M., et al. (2011). Considering the energy, water and food nexus: Towards an integrated modelling approach. *Energy Policy, 39*(12), 7896–7906.

Burger, R. E. A. (2018). *MAXUS: Synergizing water, food and energy policy*. TU Delft Repository.

CERC. (2012). *Report on the grid disturbance on 30th July and grid disturbance on 31st July* (No. 167).

Dai, J., et al. (2018). Water-energy nexus: A review of methods and tools for macro-assessment. *Applied Energy, 210,* 393–408.

FAO. (2014). *Walking the nexus talk: Assessing the water-energy-food nexus in the context of the sustainable energy for all initiative*.

Hoff, H. (2011). Understanding the nexus. Background paper for the Bonn2011. In *Conference: The Water, Energy and Food Security Nexus*, Stockholm.

IMWI. (2012). *Revisiting dominant notions: A review of costs, performance and institutions of small reservoirs in sub-Saharan Africa*.

Kaddoura, S., & El Khatib, S. (2017). Review of water-energy-food nexus tools to improve the nexus modelling approach for integrated policy making. *Environmental Science and Policy, 77,* 114–121. (Elsevier Ltd.).

Kshetri, N. (2017). Will blockchain emerge as a tool to break the poverty chain in the Global South? *Third World Quarterly, 38*(8), 1710–1732.

UN. (2014). *The United Nations world water development report 2014: Water and energy* (Vol. 1).

Volta River Authority. (2014, June). *Pwalugu multipurpose dam environmental and social impact assessment*.

Visualizing CO$_2$ to Account for Emission Obligation in Power Systems

Mahdi Rouholamini, Carol Miller, Caisheng Wang,
Mohsen Mohammadian, and Mohammadamin Moghbeli

Abstract

The electricity use is a significant part of human's environmental footprint. Fossil energy is still used as the major energy resource for power generation. Policy makers seek a remedy to mitigate carbon emissions of fossil fuels. A virtual carbon emission tracing method is discussed in this paper. This paper facilitates allotting carbon obligation in power systems.

Keywords

Carbon emission flow • Power systems • Power tracing • Proportional sharing principle

1 Introduction

A dramatic rise in human population and productions starting from the Industrial Revolution has resulted in great demand for energy, subsequently releasing into the atmosphere a large-scale quantity of carbon and causing climate change globally (Jung and Koo 2012; Kang et al. 2012). Therefore, a considerable number of research studies have been conducted in recent years on low-carbon technologies. However, aside from the technical aspects, the methodology for evaluating the emitted amount of emission is also of vital importance in low-carbon development and for setting up appropriate emission-related policies (Kang et al. 2012). Power systems, connecting various fossil fuel-based power plants, play a key role in environmental issues. The concerns coming from electricity usage occur in the form of pollution of air and water and consequently the climate change (Munksgaard and Pedersen 2001). With regard to what has been conducted in literature, two principles regarding who is responsible for the CO$_2$ emitted emerge—the producer or the consumer (Marriott and Matthews 2005). The first one assumes that a significant part of the CO$_2$ emissions is linked to the energy production sector, mostly the power generators, and therefore, the producer is responsible for the CO$_2$ emissions. More recently, an increasing number of studies have asked for attention to the fact that "consumers" should also be responsible when it comes to CO$_2$ that is emitted at the time of the production, rather than "producers" alone (Marriott and Matthews 2005; Kang et al. 2015). Thus, this paper focuses on the relationship between carbon emissions and power consumers. The way carbon emissions are dealt with in this paper differs from the way in which they are usually treated. We consider them as a sort of carbon flow in power systems and not as a sort of greenhouse gas (GHG) emissions. The paper provides policy makers with a more tangible understanding of emission, and the results can help power utilities improve the system design and operation for the purpose of carbon emission mitigation.

M. Rouholamini (✉) · C. Wang
Electrical and Computer Engineering Department,
Wayne State University, Detroit, MI, USA
e-mail: gj9598@wayne.edu

C. Wang
e-mail: cwang@wayne.edu

C. Miller
Department of Civil and Environmental Engineering,
Wayne State University, Detroit, MI, USA
e-mail: ab1421@wayne.edu

M. Mohammadian
Notashan Sanat Co., Tehran, Iran
e-mail: mohammadian@notashan.com

M. Moghbeli
University of Politecnico di Milano, Milan, Italy
e-mail: m.moqbeli@gmail.com

2 Virtual Emission Tracing in Power Systems

In power systems, a virtual carbon emission flow can be assumed tightly integrated with the power flow (Kang et al. 2012), however, in this paper in a direction opposed to that of power, but with the same pathway as power flow (Kang et al. 2012). For example, consider a single customer–single producer system as shown in Fig. 1. The power producer is a
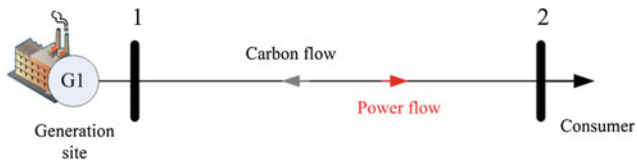
Fig. 1 A single customer–single producer system

thermal unit. He causes or "emits" a certain amount of emission. As mentioned earlier, we are to get the consumer involved in emission responsibility or at least specify how the emitted emission is affected by her behaviour. The carbon emission physically emits at generation site, leading us to assuming the direction of the virtual carbon flow opposed to that of power flow. This means that she receives some service or product in the form of electricity whose waste (or the useless part of the product) in the form of carbon emission is then sent back upstream to where the electricity was originally imported from. This virtual carbon emission travels as fast as electricity does. However, in a real-life power network, performing the above-mentioned virtual carbon emission tracing is much more complicated than Fig. 1. Therefore, we need to do power tracing first. By performing energy (or power) tracing, one can compute how much power flows from a given generator to a given load as well as determining to what degree a load or generator contributes to the power flow in a line (or branch) of the network (Kirschen and Strbac 1999; Abdelkader 2008). It is worth noting that the quality of electricity is identical throughout the system and that is why power tracing arises.

Methods to implement power tracing can be categorized as numerical and graphical (Davidson et al. 2013). Numerical methods benefit from matrix computation and are of simple algorithms. There are different methods given in the literature to perform power tracing (Kirschen and Strbac 1999; Abdelkader 2008; Wei et al. 2000; Ming et al. 2004; Achayuthakan et al. 2010; Kirschen 1997; Kuo et al. 2018; Zimmerman et al. 2011). We utilize the numerical one given in (Achayuthakan et al. 2010) as it not only accounts for the influence of transmission losses, but also can be used for systems with and without power circulating flows, and more importantly, it is quite transparent. It should be mentioned that steady-state analysis of power systems including economic dispatch and power flow equations (optimal power flow) as well as the utilized power tracing method (Achayuthakan et al. 2010) is not discussed in this paper for the sake of brevity. As an example, assume that the system under study is the IEEE 5-bus test system whose optimal power flow results are shown in Fig. 2. The system data can be obtained from MATPOWER (Zimmerman et al. 2011).
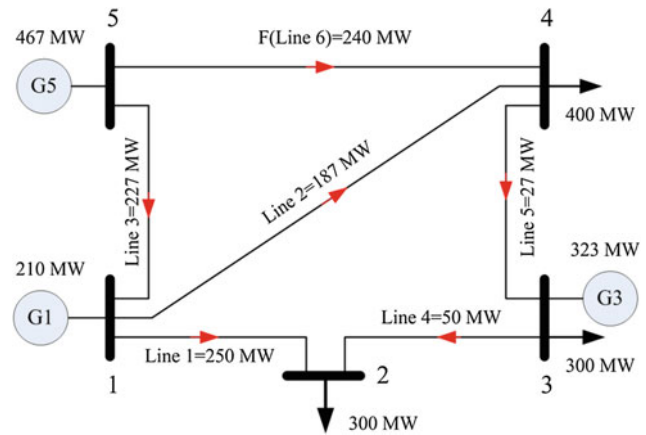
Fig. 2 IEEE 5-bus test system with optimal power flow results

Like the assumption of (Kang et al. 2015), each of the generators in the test system is considered as one of the three types given in Table 1. In case the power tracing method introduced in (Achayuthakan et al. 2010) as well as the CO_2/kWh rates presented in Table 1 is applied to the power grid benchmark shown in Fig. 2, the results will be as Fig. 3 indicates. As both the power flow (Fig. 2) and the virtual carbon emission flows (Fig. 3) in all the branches are now given, we may calculate the carbon intensity of branches and nodes. The branch carbon intensity can be defined as the ratio of the amount of carbon emission flow to the corresponding power flow. Similarly, the nodal carbon intensity is defined as the sum of all the branch carbon emissions entering a given node divided by the nodal power of the same node. These two criteria facilitate sorting the branches and nodes of the network, indicating to what degree a line or bus is clean.

3 Discussion and Conclusions

A virtual carbon emission tracing model was introduced in this paper, starting with the power tracing and then transforming electricity circulates to carbon emission flows. Although the carbon emission flows are hypothetical, meaning that they do not actually travel physically between the loads and generators, they are clearly visualized and quantified in a systematic way. The method outstandingly helps us improve our comprehension of both the emission levels of a region and how to encourage demand-side measures to prompt emission reduction. It also clearly shows to what extent the electricity being consumed at different locations is clean. Having known this spatial distribution of emissions, policy makers can set up the appropriate strategy

Table 1 Carbon emission rates of the generators (Kang et al. 2015)

Unit type	Capacity (MW)	Emission rate (kgCO$_2$/kWh)
Coal-fired	$C > 330$	0.875
Gas-turbine	$100 < C < 330$	0.500
Zero-emission	$C < 100$	0.000

Fig. 3 The results of virtual emission tracing
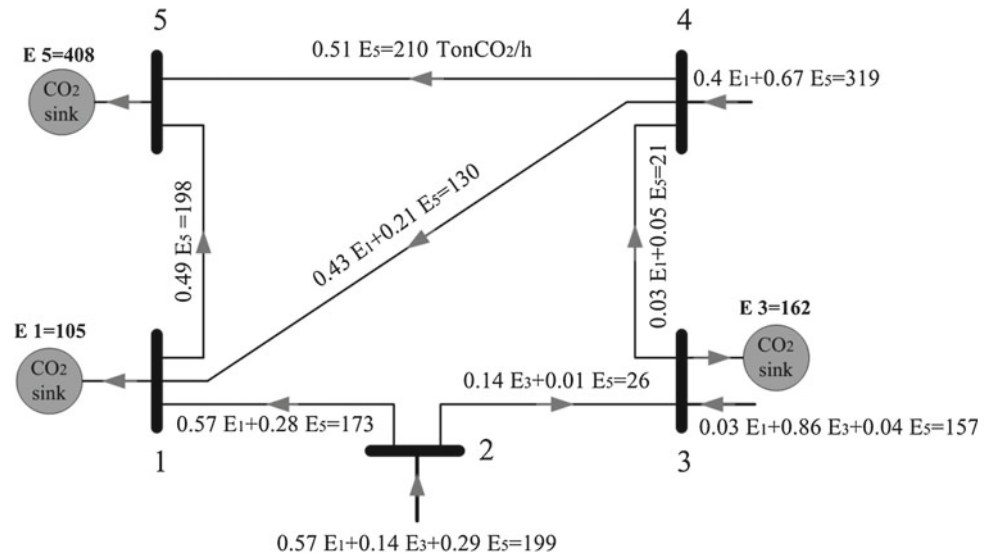
to have large-scale consumers move towards load nodes with less environmental responsibility leading to the development of renewable energies. The method can also be promising for environmentally friendly and therefore sustainable network expansion planning. For example, in a power system, a transmission line that most of the time carries electricity of low-carbon intensity should be expertly taken care of when power network upgrading. In addition, by relying on the proposed method, price signals of carbon emission can be well integrated with nodal electricity prices, thereby guiding customers to best optimize their consumptions to spare money, and consequently mitigating carbon emissions. One more important advantage of the proposed method is being capable of identifying how much carbon emission has been embodied in goods and services which are not usually included in traditional methods of carbon footprints accounting. This is useful to effectively found our future carbon-trading framework, which is an emerging research topic (Lin et al. 2015; Wiedmann et al. 2016; Chen et al. 2016). The authors would like to name it "Energy-Emission Nexus" meaning how much carbon is hidden in one watt-hour at different buses of a power grid. This aspect of dialogue between producer and consumer clarifies how electricity-importing countries may covertly impose their carbon reduction obligation to the exporter ones without being charged.

References

Abdelkader, S. (2008). Determining generators' contribution to loads and line flows & losses considering loop flows. *International Journal of Electrical Power & Energy Systems, 30*(6–7), 368–375.

Achayuthakan, C., Dent, C. J., Bialek, J. W., & Ongsakul, W. (2010). Electricity tracing in systems with and without circulating flows: Physical insights and mathematical proofs. *IEEE Transactions on Power Systems, 25*(2).

Chen, G., Wiedmann, T., Hadjikakou, M., & Rowley, H. (2016). City carbon footprint networks. *Energies, 9,* 602. https://doi.org/10.3390/en9080602.

Davidson, E., Currie, R., Kwon, Y., Martínez, J., Mcneill, N., & Hey, R. (2013). Tracing the carbon intensity of active power flows in distribution networks. In *22nd International Conference on Electricity Distribution*, Stockholm, June 10–13, 2013.

Jung, T. W., & Koo, J. H. (2012). A study on U-city carbon footprint calculation method to prepare for carbon emission trading system. In *8th International Conference on Computing Technology and Information Management (ICCM)*, Seoul, South Korea.

Kang, C., Zhou, T., Chen, Q., Wang, J., & Xia, Q. (2015). Carbon emission flow from generation to demand: A network-based model. *IEEE Transactions on Smart Grid, 6*(5).

Kang, C., Zhou, T., Chen, Q., Xu, Q., Xia, Q., & Ji, Z. (2012). Carbon emission flow in networks. *Journal of Scientific Reports*. https://doi.org/10.1038/srep00479.

Kirschen, D. (1997). Contributions of individual generators to loads and flows. *IEEE Transactions on Power Systems, 12*(1).

Kirschen, D., & Strbac, G. (1999, November). Tracing active and reactive power between generators and loads using real and imaginary currents. *IEEE Transactions on Power Systems, 14*(4).

Kuo, M.-T., Lu, S., & Tsou, M. (2018). Considering carbon emissions in economic dispatch planning for isolated power systems: A case study of the Taiwan power system. *IEEE Transactions on Industry Applications, 54*(2).

Lin, J., Hu, Y., Cui, S., Kang, J., & Ramaswami, A. (2015). Tracking urban carbon footprints from production and consumption perspectives. *Environmental Research Letters, 10*.

Marriott, J., & Matthews, H. S. (2005). Environmental effects of interstate power trading on electricity consumption mixes. *Environmental Science and Technology, 39,* 8584–8590.

Ming, Z., Liying, S., Gengyin, L., & Ni, Y. (2004, April). A novel power flow tracing approach considering power losses. In *IEEE International Conference on Electric Utility Deregulation, Restructuring and Power Technologies (DRPT2004)*, Hong Kong.

Munksgaard, J., & Pedersen, K. A. (2001). CO_2 accounts for open economies: Producer or consumer responsibility? *Energy Policy, 29,* 327–334.

Wei, P., Yuan, B., Ni, Y., & Wu, F. F. (2000). Power flow tracing for transmission open access. In *International Conference on Electric Utility Deregulation and Restructuring and Power Technologies*, London, UK.

Wiedmann, T. O., Chen, G., & Barrett, J. (2016, August). The concept of city carbon maps: A case study of Melbourne, Australia. *Journal of Industrial Ecology, 20*(4), 676–691.

Zimmerman, R. D., Murillo-Saìnchez, C. E., & Thomas, R. J. (2011). MATPOWER: Steady-state operations, planning, and analysis tools for power systems research and education. *IEEE Transactions on Power Systems, 26*(1), 12–19.

Selection of Key Characteristics for Crops to Deal with Climate Change Through Quality Function Deployment

A. Robayo Avendaño and D. Prato Garcia

Abstract

The use of genetically modified (GM) varieties represents the best strategy to adapt to climate change. The use of quality function deployment (QFD) provides a simple tool for decision taking. The characteristics of water, soil, chemical fertilizers, pesticides, and herbicides are indispensable criteria in the selection of adaptation alternatives.

Keywords

Quality function deployment • Conservation agriculture • Organic agriculture • Genetically modified varieties • Climate change

1 Introduction

Although in the last years, the productivity of crops has increased notoriously, their yield and stability are affected by the particular impact exerted by climate change in the geographical zone where they are developed. In low latitudes (tropical regions), the climate change effect could be more adverse as a consequence of the temperature increase and the development of extreme events like droughts and floods. This phenomenon also impacts biodiversity, the soil, water availability; likewise, it affects how pests are dispersed and determines the use of agrochemicals (Mall et al. 2017). As can be inferred, this will have a dramatic impact on the use and distribution of resources such as soil and water, the cost of food, and on the productivity and rentability of crops meant for energy production.

Currently, climate change adaptation alternatives are available, such as inclusion of improved agricultural practices (also called conservation agriculture), organic agriculture, and use of genetically modified (GM) varieties (Camarotto et al. 2018; Hole et al. 2005; Adenle et al. 2015). Conservation agriculture (CA) aims at reducing CO_2 emissions and the impact of crops on soil erosion through crops rotation, protecting the soil with vegetal cover generated by the same crop, and the optimized use of both fertilizers and herbicides (Camarotto et al. 2018). On the other hand, organic agriculture (OA) develops crops without the use of artificial chemical products. This alternative reduces notoriously soil erosion and emission of greenhouse gases (GHG); however, it is limited by the low capacity to supply nitrogen to the plants (Hole et al. 2005). The GM varieties are developed by inserting genes of a donor organism to a receptor one using biotechnological techniques; this genetic transfer provides the receiving organism with a new characteristic that can include resistance to insects, tolerance to herbicides, and tolerance to varying climate conditions, among others (Adenle et al. 2015).

Although there are different tools to assess the impact of climate change on crops, the methodology known as quality function deployment (QFD) is more simple and efficient because it translates the needs or requirements of the interested parties in technical characteristics or alternatives that will respond to a necessity. Based on the relevance of the topic, this work is aimed at applying the QFD methodology for the selection of the best adaptation alternative to climate change in crops (food or bioenergetics) analyzing three adaptation strategies (conservation agriculture, organic agriculture, and sowing of GM varieties). For this, we took as reference five key requirements for a crop (water, soil use, herbicides, pesticides, and fertilizers).

A. Robayo Avendaño
Facultad de Ingeniería, Universidad Santiago de Cali, Campus Pampalinda, Calle 5 No. 62-00, Cali, Valle del Cauca, Colombia

D. Prato Garcia (✉)
Facultad de Ingeniería y Administración, Universidad Nacional de Colombia—Sede Palmira, Carrera 32 No. 12-00, Chapinero, Vía Candelaria, Palmira, Valle del Cauca, Colombia
e-mail: dpratog@unal.edu.co

2 Materials and Methods

Review of the literature and the confirmation of a focal group of experts were indispensable to establish the scores for each variable integrating the QFD. Initially, we *identified the needs* and translated in our study as the requirements of crops under changing climate conditions (water, soil, herbicides, pesticides, and fertilizers). Crop requirements with a weight closer to one (1) were considered more important, whereas those close to zero (0) were irrelevant or less important (Table 1). By means of group discussions, the adaptation strategies to climate change were filtered and those that could be incorporated to the productive practices in emerging economies were *selected* (conservation agriculture, organic agriculture, and GM varieties). The next step was to establish a *matrix of relations*; for this reason, the experts were asked to perform an evaluation granting a score (one, two, or three) to each relation (Table 1). If the variable affected highly the performance of the crop, a score of 1 was granted, if, in contrast, the use of the variable resulted not relevant for the crop's performance, the score was of 3. Finally, if the variable affected in a limiting fashion the performance of the crop, the assigned score was of 2 (Table 1). To select the most convenient adaptation alternative, we calculated the absolute weight (AW) (Eq. 1); in this equation, *I* represents the importance of the requirement and *S* the assigned score by the group of experts to each alternative. Taking as reference the AW, the relative weight (RW) was calculated (Eq. 2). Priority (PRY) was defined consecutively, granting the first option to the RW of highest value and the last option to the RW of lowest value.

$$PA_i = \sum_{i=1}^{n} I_i P_i \qquad (1)$$

$$PR_i = \frac{PA_i}{\sum PA_i} \qquad (2)$$

3 Results and Discussion

In this study, *CA* obtained the lowest absolute and relative weights, 1.7 and 0.26, respectively. For *CA*, the water factor resulted in critical for the development of the crop because crops do not present tolerance to water stress. Regarding use of soil and agrochemicals, *CA* incorporates strategies like crop rotation, use of the residues generated by the productive process to minimize both consumption of agrochemicals (pesticides, herbicides, and fertilizers) and mechanical procedures like cutting with rotating blades to control undergrowth; notwithstanding, the use of agrochemical products is still needed for the adequate development of the crop. For this reason, *CA* presents a disadvantage regarding the reduction of GHG emissions as compared to other alternatives (Camarotto et al. 2018). The *OA* is an attractive alternative (AW = 2.2 and RW = 0.34) as it uses organic fertilizers and pesticides, which affect less the biological activity and soil fertility; additionally, it promotes the use of good management practices for the soil and water (crop rotation, use of mixed crops, and farming techniques), which influence notably the environmental sustainability of the crops (Hole et al. 2005).

The use of *GM varieties* resulted in the most outstanding alternative (AW = 2.55 and RW = 0.40) as these include features of tolerance to drought and pesticides, which could make the growth of plants feasible under certain conditions (water stress and poor soils). Besides, it grants resistance to pest insects, leading to minimal applications of pesticides and reducing the impact on the environment. Our findings agree with those reported in (Adenle et al. 2015), as they recognize the potential shown by GM varieties addressed at specific characteristics for the adaptation to climate change, contributing to the reduction of GHG emissions by diminishing the applications of fertilizers and pesticides. The *CA* is assumed as a useful production system in the development of small-scale crops; however, its performance depends on

Table 1 Matrix of relations between crop requirements and climate change adaptation alternatives

Requirement	Importance (*I*)	Score assigned to the adaptation alternative (*S*)		
		Conservation agriculture	Organic agriculture	GM varieties
Water	0.40	1	1	2
Soil	0.30	1	1	2
Chemical fertilizers	0.20	2	3	2
Chemical pesticides	0.15	2	3	3
Herbicides	0.15	2	3	2
Absolute weight, (AW)		1.7	2.2	2.55
Relative weight, (RW)		0.26	0.34	0.40
Priority, (PRY)		3	2	1

its capacity to adapt to the conditions of the zone where the crop is sown (Camarotto et al. 2018). The *OA* is recognized as an environmentally friendly alternative, notwithstanding its benefits are limited by the location, climate, type of crop, and the applied management practices (Hole et al. 2005).

4 Conclusion

The QFD analysis reveals that according to the characteristics needed for a crop to be able to support changing climate conditions, the use of GM varieties could be the most convenient option. However, it must be recognized that the economic variables could also play a notable role in the selection of alternatives. Application of the QFD methodology together with the participation of a focal group of experts represents a valuable tool for decision taking in agriculture.

References

Adenle, A., Azadi, H., & Arbiol, J. (2015). Global assessment of technological innovation for climate change adaptation and mitigation in developing world. *Journal of Environmental Management, 161,* 261–275.

Camarotto, C., Dal Ferro, N., Piccoli, I., Polese, R., Furlan, L., Chiarini, F., et al. (2018). Conservation agriculture and cover crop practices to regulate water, carbon and nitrogen cycles in the low-lying Venetian plain. *Catena, 167,* 236–249.

Hole, D., Perkins, A., Wilson, J., Alexander, I., Grice, P., & Evans, A. (2005). Does organic farming benefit biodiversity? *Biological Conservation, 122,* 113–130.

Mall, R., Gupta, A., & Sonkar, G. (2017). Effect of climate change on agricultural crops. In C. Larroche, M. Á. Sanroman, G. Du, & A. Pandey (Eds.), *Current developments in biotechnology and bioengineering* (p. 850). Amsterdam: Elsevier.

Combined Electrodialysis and Photo-Electro-Chlorination for Energy Efficient Control of Brine Water

Hyeonjeong Kim, Wonyong Choi, and Kangwoo Cho

Abstract

A combined electrodialysis and photo-electro-chlorination process was evaluated. The current efficiency of the chlorine evolution reaction increased with the $[Cl^-]$. UV/Chlorine boost the oxidation rate of recalcitrant organic compounds.

1 Introduction

In recent decades, stringent water treatment regulation and growing demands on water reuse allowed the wide implementation of membrane-based processes, such as reverse osmosis (RO), for tertiary polishing of domestic and industrial wastewater effluent (Drioli and Fontananova 2004; IWA 2018). However, these separation methods inevitably generate brine water which is most often returned and combined with wastewater influent. The substantial concentrations of refractory organic compounds could deteriorate the operation efficiency of the existing wastewater treatment plants (WWTPs). On the other hand, distillation-based zero liquid discharge processes or advanced oxidation processes for handling the concentrates are too energy expensive for practical application (Malaeb and Ayoub 2011; Mike Mickley 2011). Therefore, a secondary volume reduction of brine water would be necessary to reduce either the burden to the WWTPs or overall energy consumption.

The electrodialysis (ED) is an electric-field assisted membrane separation method, where the ion transport through the anion/cation exchange membranes can be accelerated by external potential bias. Previous experiences suggest that ED is more energy efficient than distillation and even RO when the total dissolved solids concentration is lower than 3 g/L, as in the case of brine water from domestic wastewater reuse facilities (Greenlee et al. 2009). Nevertheless, control of non-ionic organic species is infeasible, whereas the anodes/cathodes of the ED catalyze oxygen and hydrogen evolution reactions that are actually useless for water treatment. In this study, we propose a combined ED and photo-electro-chlorination simultaneously, as shown in Fig. 1. When a small fraction of secondary brine water was introduced onto the anode, an efficient chlorine evolution reaction could occur owing to a high concentration of chloride ion. The resulting free chlorine species could be utilized for organic compounds destruction in the presence of UV irradiation for generation of reactive oxygen and chlorine radical species. The present study evaluated the operational parameters for deionization, free chlorine generation, and UV-chlorine reactions.

2 Materials and Methods

2.1 Composition of the Target Brine Water

The target brine water in this study was from capacitive deionization (CDI) facility for reuse of cooling water blow-down (CWBD) in a chemical manufacturing company. The composition of brine water could be summarized as 3.5 mS/cm of conductivity, 800 mg/L of Cl^-, 210 mg/L of SO_4^{2-}, 560 mg/L of Ca^{2+}, 230 mg/L of Mg^{2+}, 420 mg/L of Na^+, 21 mg/L COD_{Cr}, and 9.4 mg/L of TOC.

H. Kim · W. Choi · K. Cho (✉)
Division of Environmental Science and Engineering, Pohang University of Science and Technology (POSTECH), Pohang, 790-784, Korea
e-mail: kwcho1982@postech.ac.kr
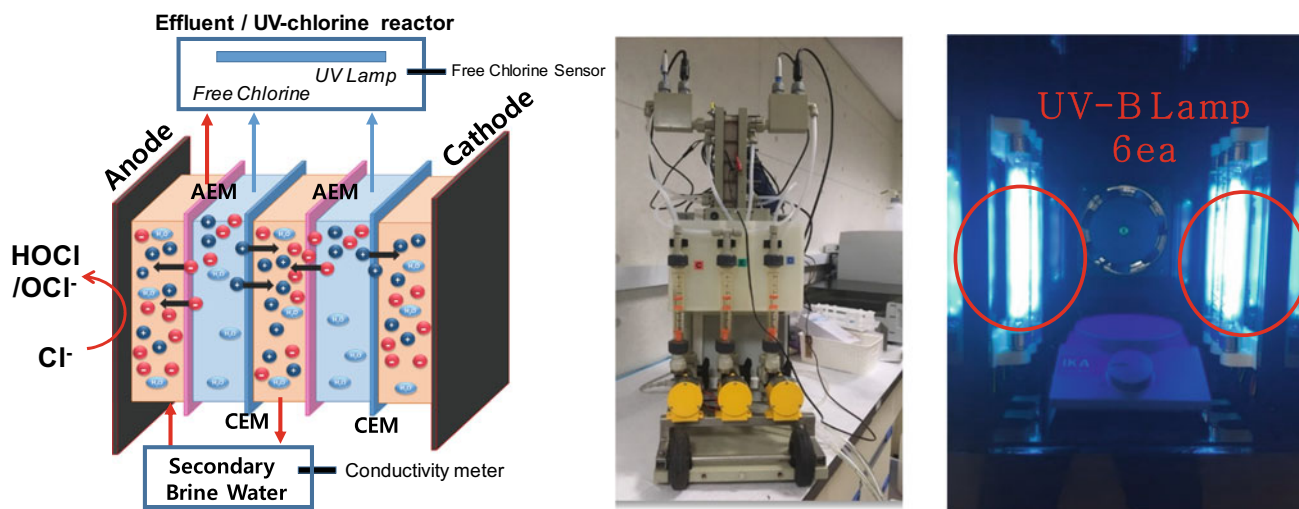
Fig. 1 A schematic diagram and pictures of combined electrodialysis and photo-electro-chlorination

2.2 Electrodialysis of Model Brine Water

Laboratory ED experiments employed a commercial unit P EDR-Z (MEGA, Czech Republic), ordinarily equipped with a module with RALEX® membranes and electrodes. 10 pieces of anion exchange membranes (AEM) and 11 pieces of cation exchange membranes (CEM) were installed in turn with the spacer of 0.8 mm. The effective cross-sectional membrane area was 64 cm² (16 cm by 4 cm). The bulk of the monovalent selective RALEX® membrane consisted of polyester fitting fabrics and polyethylene binder on base. The outer CEMs of the membrane module were paralleled with Ti/IrO_2 anode and Ti/Pt cathode. Parametric study was performed with adjusting the constant cell voltage from 8 to 24 V, the flow rate through the module from 45 to 65 L/h, and recovery ratio from 70 to 90%. The volume of effluent was typically 0.25 L and the volume of the secondary brine water was controlled for recovery ratio adjustment. Waterproof multimeters (Multi 340i and pH/Cond 340i Handheld Multimeters, WTW) were used to collect pH and conductivity data. Small aliquot of samples were collected periodically for ion concentration measurement by ion chromatography (Dionex, USA).

2.3 Free Chlorine Generation from Secondary Brine Water

In order to assess the effects of chloride ion concentration to the free chlorine generation rate, batch chlorine generation experiments were performed in a batch reactor (120 mL) with Ti/IrO_2 anode and Ti/Pt cathodes (10 cm² each). The concentration of chloride ion was adjusted from 20 to 400 mM, in order to simulate the recovery ratio of 0–95% in

the ED module. Under a galvanostatic regime at the current density of 40 mA/cm² (in compatible with the condition in ED), the free chlorine generation rate was estimated by measuring (free chlorine) by DPD (N,N-diethyl-p-phenylenediamine) reagent.

2.4 UV-Chlorine Experiments for a Model Organic Compound

For photo-electro-chlorination or electrochemical UV/chlorine experiments, methylene blue (MB) was employed as a model organic compound. 30 μM of MB (60 mL) in quartz reactor was subjected to the addition of free chlorine from 12 to 36 $mgCl_2$/L, to determine the injection ratio of the secondary brine water to the ED module. In order to demonstrate the effectiveness of UV irradiation, photoelectrochemical reaction was carried out inside of a black box installed with six UV-B lamps. Aliquots were collected periodically, and absorbance was measured at 664 nm using UV-Vis spectrophotometer (model S-3100, Scinco).

3 Results and Discussion

3.1 Secondary Volume Reduction of Brine Water by ED

Figure 2 shows the conductivity in effluent and the secondary brine water during ED treatment of CWBD, as a surrogate of total dissolved solids concentration. Overall results interestingly indicated insignificant effects of operational condition for effluent conductivity. On the contrary,

Fig. 2 Changes in conductivity in effluent and secondary brine water during ED treatment
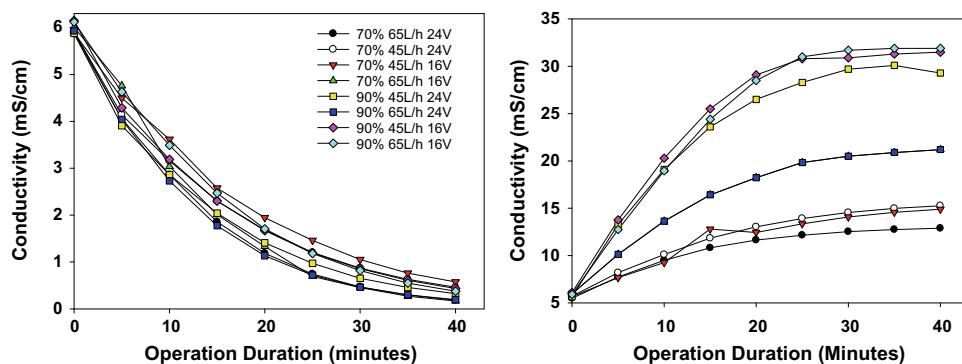
the corresponding influences were definitely much more substantial for the conductivity of the secondary brine water. In particular, a low flow rate (45 L/h) coupled with higher voltage (24 V) would bring about higher conductivity in the secondary brine water. Meanwhile, in our experimental conditions, the impact of flow rate was found to be less significant than the voltage or recovery ratio for the secondary brine water conductivity. Our results concluded that 12 V of cell voltage, 65 L/h of flow rate, and 90% of recovery rate would be the optimal condition for the target CWBD. On the other hand, the pH change in the effluent was more remarkable than that in the secondary brine water, while the variations were more significant under greater cell voltage.

The removal efficiency of Cl^- and SO_4^{2-}, the primary anions, showed similar evolutions with the conductivity for the effluent. Nevertheless, sulfate ion removals were greater than those of chloride ion; removal efficiency for SO_4^{2-} were near 100% in most of the test conditions. Taking into account that $[Cl^-] = 5.8$ mM and $[SO_4^{2-}] = 0.57$ mM, the greater concentration gradient and electrostatic attraction (valency) would account for the high removal of sulfate ions. As a consequence, the sulfate ions were found to be more susceptible to the operational parameters in our experimental conditions.

3.2 Free Chlorine Generation from Secondary Brine Water

Figure 3 (left) shows the free chlorine generation rate on the Ti/IrO_2 anode under the varying concentration of chloride ions. It was more than evident that an increase of $[Cl^-]$ led to the elevation in free chlorine generation. In contrast to the charge limited oxygen evolution reaction, the chlorine evolution reaction has been known to be limited by the diffusion of chloride ion toward the anode surface. The results in this study indicated that $[Cl^-]$ greater than 200 mM, corresponding to the recovery ratio of 90%, was sufficient for a maximal generation of free chlorine.

3.3 UV-Chlorine Experiments for a Model Organic Compound

Figure 3 (middle) shows the rate of MB degradation under UV-B irradiation and free chlorine injection. When compared to the cases without the UV irradiation (Fig. 3 right), the rates increased more than an order of magnitude, corroborating the effectiveness of the photo-electrochemical-chlorination. In our experimental conditions employing UV-B lamps, the rate of MB degradation was enhanced in circum-neutral pH.
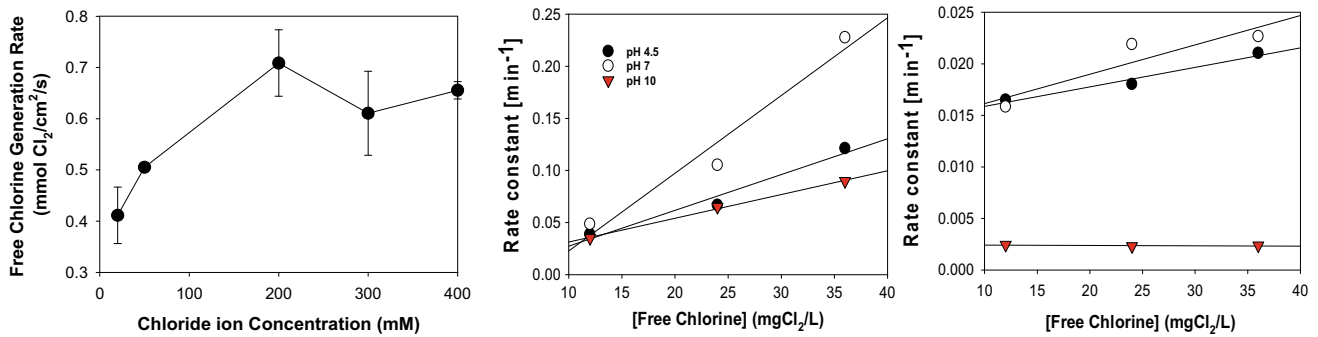
Fig. 3 The effects of [Cl⁻] on free chlorine generation (left), effects of [free chlorine] on MB degradation with (middle) and without (right) UV-B irradiation

4 Conclusion

A combined ED and photo-electro-chlorination process was evaluated in this study. The current efficiency of the chlorine evolution reaction increased with the [Cl⁻], corroborating the effectiveness of our process. In addition, the resulting free chlorine could boost the oxidation potential by combination with UV irradiation.

References

Drioli, E., & Fontananova, E. (2004). Membrane technology and sustainable growth. *Chemical Engineering Research and Design, 82*(12), 1557–1562. https://doi.org/10.1205/cerd.82.12.1557.58031.

Greenlee, L. F., Lawler, D. F., Freeman, B. D., Marrot, B., & Moulin, P. (2009). Reverse osmosis desalination: Water sources, technology, and today's challenges. *Water Research, 43*(9), 2317–2348. https://doi.org/10.1016/j.watres.2009.03.010.

IWA. (2018). *The reuse opportunity. Wastewater report* (pp. 1–26). https://doi.org/10.5194/acp-2016-176.

Malaeb, L., & Ayoub, G. M. (2011). Reverse osmosis technology for water treatment: State of the art review. *Desalination, 267*(1), 1–8. https://doi.org/10.1016/j.desal.2010.09.001.

Mike Mickley, J. J. (2011). *Development of a knowledge base on desalination concentrate and salt management* (Revised Draft Final Report). Water Reuse Research Foundation.

Advanced Technologies or Nature-Based Solutions for the Environmental Sustainability of the Water Sector

Hydrogen Production in Electro Membrane Bioreactors

Laura Borea, Fabiano Castrogiovanni, Giovanna Ferro,
Shadi Wajih Hasan, Vincenzo Belgiorno, and Vincenzo Naddeo

Abstract

Reduction of organic and nutrient compounds. Membrane fouling control through the decrease of membrane fouling precursors and quorum sensing. Energy production in terms of hydrogen.

This paper shows the combination of electro membrane bioreactor (eMBR) with microbial electrolysis cell (MEC) in one hybrid system at the laboratory scale and under anaerobic conditions. The study aimed at evaluating the performance of eMBR-MEC in terms of water quality and energy production in the form of hydrogen.

L. Borea · F. Castrogiovanni · G. Ferro · V. Belgiorno · V. Naddeo (✉)
Sanitary Environmental Engineering Division, Department of Civil Engineering, University of Salerno, Fisciano, Italy
e-mail: vnaddeo@unisa.it

L. Borea
e-mail: lborea@unisa.it

F. Castrogiovanni
e-mail: fcastrogiovanni@unisa.it

G. Ferro
e-mail: gferro@unisa.it

V. Belgiorno
e-mail: v.belgiorno@unisa.it

S. W. Hasan
Center for Membrane and Advanced Water Technology, Department of Chemical Engineering, Khalifa University of Science and Technology, Masdar City Campus, P.O. Box 127788 Abu Dhabi, UAE
e-mail: shadi.hasan@ku.ac.ae

1 Introduction

Membrane bioreactor (MBR) is a reliable and established technology for wastewater treatment and reuse applications (Aslam et al. 2017) due to its notable advantages such as excellent effluent quality, good disinfection capability, higher volumetric loading, reduced footprint, and sludge production. The selection made by the membrane, in fact, makes obsolete the secondary sedimentation generating a positive impact on project costs. Considering the increasing demand for water, as a result of demographic change and climate change, the MBR appears to be a good solution for water reuse. However, membrane fouling is the major hindrance for the application of this technology since it reduces system productivity, increases energy requirement for air scouring, and also increases the frequency of chemical cleaning of membranes (Lin et al. 2014; Meng et al. 2017). Fouling is the phenomena that cause obstruction of pores and the coating of the membrane's surface. Many scientific studies have identified the major cause of fouling, the microbial secretions caused by bacterial metabolism: soluble microbial products (SMP), extracellular polymeric substances (EPS), and just recently, in many studies about the desalination, transparent exopolymer particles (TEP). Scientific research has been focused on the identification of different strategies for the control of fouling as, recently, the integration of electrochemical processes into MBR (i.e., electro MBR or eMBR) in order to reduce membrane fouling and enhance the quality of treated effluents (Borea et al. 2017a, b; Ensano et al. 2017; Ho et al. 2017; Jiang et al. 2017). Although these studies have proven the improved performance of the treatment in terms of conventional and emerging compound removal and the reduction of membrane fouling rate through the decrease of membrane fouling precursors' concentration, the potential of eMBR for energy production was never investigated.

Consequently, this research study aimed at assessing the performance of eMBR under anaerobic conditions exploiting

the mechanisms that occur in a microbial electrolysis cell (MEC) (Das and Veziroğlu 2001; Logan 2004) in order to obtain a high-quality effluent and, at the same time, produce energy in the form of hydrogen. The interest in assessing the amount of hydrogen produced by electrochemical processes, with reference to the amount of wastewater treated, is very important since hydrogen is a source of energy with many possible uses. Indeed, hydrogen, having a high calorific value, it is a clean energy source and present in many compounds. The difficulty lies in the extraction of hydrogen from these compounds. Therefore, the use of microbial electrolysis cells is a very attractive solution that links performance improvement in energy yield resulted from hydrogen production through the oxidation of organic matters by the bacteria.

2   Materials and Methods

A laboratory-scale eMBR-MEC plant operated with a working volume of 13 L. It was continuously fed with synthetic wastewater prepared in the laboratory and having characteristics similar to a real wastewater (Borea et al. 2017a, b).

The removal efficiencies obtained from the integrated eMBR-MEC system in terms of emerging and conventional contaminants were assessed using standard methods (APAT and CNR-IRSA 2003). Membrane fouling was evaluated in terms of fouling rate, membrane fouling precursors such as EPS, soluble microbial products (SMPs) and transparent exopolymeric particles (TEP) (Borea et al. 2017a, b) and

quorum sensing (Iqbal et al. 2018) through quorum sensing signaling molecule C8-HSL. Estimation of hydrogen production in the integrated reactor was made through the colorimetric tubes whose change of color is in direct correlation to the concentration of gas present.

In Fig. 1 the experimental setup of the hybrid system is shown.

3   Results and Discussion

The combination of eMBR with the MEC process resulted in an increase of the treatment performance with high removals of organic and nutrient compounds. With reference to membrane fouling, this study confirmed that the application of an intermittent electric field minimizes membrane fouling with a decrease in TMP over time. The electric field applied also acted on the particles responsible for membrane fouling. Indeed, a reduction of membrane fouling precursors' concentrations (EPSc, SMPc, EPSp, and TEP) was observed. Electrocoagulation and electrophoresis mechanisms enhanced the removal and degradation of these membrane fouling precursors and so, membrane fouling reduction.

The application of an electric field influenced the concentration of quorum sensing signaling molecule C8-HSL. Electrochemical processes caused a decrease of this molecule since it regulates quorum sensing-mediated membrane biofouling. This was corroborated by the decrease of membrane fouling precursors inside the bioreactor.

Hydrogen production at anaerobic conditions was detected due to the establishment of MEC mechanisms in the

Fig. 1 Scheme of experimental setup

LEGEND:
1.   Influent;
2.   Influent pump;
3.   Wastewater inlet valve;
4.   Anaerobic eMBR-MEC reactor;
5.   Valve for wastewater sample;
6.   Membrane module;
7.   Mixer;
8.   Diffusers;
9.   Cathode;
10. Anode;
11. Fixing electrodes by means of bolts and electrodes connection to the potentiostat;
12. Permeate pump;
13. Permeate tank;
14. Membrane backwashing pump;
15. Backwashing pump;
16. Potentiostat;
17. Valve for biogas sample;
18. Biogas tank;
19. Biogas recirculation;
20. Data logger.

DIAMETRO 30 CM

hybrid process. It was found that, by applying the electro-chemical processes in anaerobic conditions, the production of hydrogen is much greater than in a simple anaerobic reactor and is closely linked to the concentration of microorganisms. Indeed, the microorganisms catalyzed the oxidation of the organic substance producing hydrogen ions and using the anode as external the electron acceptor. These electrons, reducing hydrogen ions at the cathode, produce hydrogen gas. Therefore, it is possible to produce hydrogen by applying such processes even within an eMBR reactor in anaerobic conditions.

4 Conclusion

The study showed the potential applicability of the eMBR-MEC process not only for improving the performance of the conventional MBR process and reducing membrane fouling rate but also for the production of energy.

References

APAT and CNR-IRSA. (2003). *Metodi analitici per le acque*. Manuali e Linee Guida 29/2003.

Aslam, M., Charfi, A., Lesage, G., Heran, M., & Kim, J. (2017). Membrane bioreactors for wastewater treatment: A review of mechanical cleaning by scouring agents to control membrane fouling. *Chemical Engineering Journal, 307,* 897–913. https://doi.org/10.1016/j.cej.2016.08.144.

Borea, L., Naddeo, V., & Belgiorno, V. (2017a). Application of electrochemical processes to membrane bioreactors for improving nutrient removal and fouling control. *Environmental Science and Pollution Research, 24*, 321–333. https://doi.org/10.1007/s11356-016-7786-7.

Borea, L., Naddeo, V., & Belgiorno, V. (2017b). An electro moving bed membrane bioreactor (eMB-MBR) as a novel technology for wastewater treatment and reuse. In *Frontiers in wastewater treatment and modelling* (pp. 159–164). Presented at the Frontiers International Conference on Wastewater Treatment and Modelling. Cham: Springer. https://doi.org/10.1007/978-3-319-58421-8_24.

Das, D., & Veziroğlu, T. N. (2001). Hydrogen production by biological processes: A survey of literature. *International Journal of Hydrogen Energy, 26,* 13–28. https://doi.org/10.1016/S0360-3199(00)00058-6.

Ensano, B. M. B., Borea, L., Naddeo, V., De Luna, M. D. G., & Belgiorno, V. (2017). Control of emerging contaminants by the combination of electrochemical processes and membrane bioreactors. *Environmental Science and Pollution Research*, 1–10. https://doi.org/10.1007/s11356-017-9097-z.

Ho, K. C., Teow, Y. H., Ang, W. L., & Mohammad, A. W. (2017). An overview of electrically-enhanced membrane bioreactor (EMBR) for fouling suppression. *Journal of Engineering Science and Technology Review, 10*, 128–138. https://doi.org/10.25103/jestr.103.18.

Iqbal, T., Lee, K., Lee, C.-H., & Choo, K.-H. (2018). Effective quorum quenching bacteria dose for anti-fouling strategy in membrane bioreactors utilizing fixed-sheet media. *Journal of Membrane Science, 562,* 18–25. https://doi.org/10.1016/j.memsci.2018.05.031.

Jiang, B., Du, C., Shi, S., Tan, L., Li, M., Liu, J., et al. (2017). Enhanced treatment performance of coking wastewater and reduced membrane fouling using a novel EMBR. *Bioresource technology, 229,* 39–45. https://doi.org/10.1016/j.biortech.2016.12.116.

Lin, H., Zhang, M., Wang, F., Meng, F., Liao, B.-Q., Hong, H., et al. (2014). A critical review of extracellular polymeric substances (EPSs) in membrane bioreactors: Characteristics, roles in membrane fouling and control strategies. *Journal of Membrane Science, 460*, 110–125. https://doi.org/10.1016/j.memsci.2014.02.034.

Logan, B. E. (2004). Extracting hydrogen and electricity from renewable resources. *Environmental Science and Technology, 38*, 160A–167A.

Meng, F., Zhang, S., Oh, Y., Zhou, Z., Shin, H. S., & Chae, S. R. (2017). Fouling in membrane bioreactors: An updated review. *Water Research, 114,* 151–180. https://doi.org/10.1016/j.watres.2017.02.006.

Use of High-Valent Metal Species Produced by the Fenton (-like) Reactions in Water Treatment

Changha Lee

Abstract

The iron- and copper-based Fenton (-like) reactions produce high-valent metal species (ferryl and cupryl ions). Ferryl and cupryl ions as reactive oxidants are capable of oxidizing refractory organic compounds in water. Ferryl and cupryl ions can be used for the inactivation of microorganisms in both planktonic and biofilm states.

Keywords

High-valent metal species • Ferryl ion • Cupryl ion • Fenton reaction • Water treatment

The iron- and copper-based activation of oxygen and hydrogen peroxide via the Fenton (-like) reactions produce high-valent metal species such as ferryl and cupryl ions (i.e., Fe(IV) and Cu(III)). The high-valent metal species are less reactive than hydroxyl radical, but still, they are strong oxidants ($E^o[M^{(v+1)+}/M^{v+}]$ = ca. 1.5–2.5 V_{NHE}) capable of oxidizing refractory organic compounds in water. These reactive oxidants can be used in the oxidative degradation of organic contaminants as well as in the inactivation of harmful microorganisms. In spite of recent advances in the chemistry of high-valent metal species, limited information is available about the reactivity of these oxidants with organic compounds and the mechanisms through which organic compounds are oxidized in the reactions. In addition, the studies on the microbial inactivation using high-valent metal species are rare.

Our recent studies investigated the nature and reactivity of Fe(IV) and Cu(III) produced by different iron- and copper-based Fenton (-like) reactions, and assessed the potential of these oxidants for the degradation of organic contaminants and the inactivation of microorganisms (Kim et al. 2015a, b; Lee et al. 2016, 2017). It was found that the reactivity of Fe(IV) and Cu(III) vary with their forms; Fe(IV) and Cu(III) usually exist as coordination complexes, and the coordinating ligand affects the reactivity of these complexes. Fe(IV) and Cu(III) degraded different organic contaminants via selective and non-selective reactions, depending on the reactivity of Fe(IV) and Cu(III). In addition, Fe(IV) and Cu(III) effectively inactivated microorganisms in both planktonic and biofilm states.

References

Kim, H.-H., Lee, H., Kim, H.-E., Seo, J., Hong, S. W., Lee, J.-Y., et al. (2015a). Polyphosphate-enhanced production of reactive oxidants by nanoparticulate zero-valent iron and ferrous ion in the presence of oxygen: Yield and nature of oxidants. *Water Research, 86,* 66–73.

Kim, H.-E., Nguyen, T. T. M., Lee, H., & Lee, C. (2015b). Enhanced inactivation of *Escherichia coli* and MS2 coliphage by cupric ion in the presence of hydroxylamine: Dual microbicidal effects. *Environmental Science and Technology, 49,* 14416–14423.

Lee, H., Lee, H.-J., Seo, J., Kim, H.-E., Shin, Y. K., Kim, J.-H., et al. (2016). Activation of oxygen and hydrogen peroxide by copper(II) coupled with hydroxylamine for oxidation of organic contaminants. *Environmental Science and Technology, 50,* 8231–8238.

Lee, H.-J., Kim, H.-E., & Lee, C. (2017). Combination of cupric ion with hydroxylamine and hydrogen peroxide for the control of bacterial biofilms on RO membranes. *Water Research, 110,* 83–90.

C. Lee (✉)
School of Chemical and Biological Engineering, Institute of Chemical Process (ICP), Seoul National University, 1 Gwanak-ro, Gwanak-gu, Seoul, 08826, Republic of Korea
e-mail: leechangha@snu.ac.kr

Photocatalytic Oxidation of Organic Compounds by Visible Light-Illuminated g-C$_3$N$_4$-AQ in Combination with Fe(III)

Jiwon Seo, Soo Yeon Park, Hak-Hyeon Kim, and Changha Lee

Abstract

A visible light-responsive photocatalyst (g-C$_3$N$_4$-AQ) has been synthesized. g-C$_3$N$_4$-AQ produces hydrogen peroxide with the response to visible light. g-C$_3$N$_4$-AQ in combination with Fe(III) produces hydroxyl radical by Fenton-like reaction. Fe(III) accelerates the hole oxidation reaction at the valence band (VB) by capturing electrons at the conduction band (CB).

1 Introduction

Photocatalytic water treatment systems have been extensively studied. However, the fast hole–electron recombination and weak oxidizing power of holes often limit oxidation of recalcitrant organic compounds. A variety of approaches have been performed and the combination of the photocatalytic system with Fenton-like's reagents (Fe(III) and H$_2$O$_2$) could be the solution to delay hole–electron recombination and oxidize recalcitrant organic compounds. Some of the previous studies have reported that the combination of photocatalysts (TiO$_2$ or WO$_3$) with Fenton-like reagents enhances oxidation efficacy of organic compounds (Durán and Monteagudo [2007]; Kim et al. [2012]; Lee et al. [2013]). However, these combination systems require continuous injection of H$_2$O$_2$ to maintain a Fenton-like reaction.

Meanwhile, photochemical production of H$_2$O$_2$ has raised attention recently in the environmentally friendly liquid fuel production, and graphitic carbon nitride (g-C$_3$N$_4$) has been considered as a proper photocatalyst for in situ H$_2$O$_2$ production. Several modifications of g-C$_3$N$_4$ have been attempted to increase photochemical productivity of H$_2$O$_2$, and Kim et al. ([2018]) suggested a new approach of g-C$_3$N$_4$ modification (anthraquinone-augmented graphitic carbon nitride) and the modified g-C$_3$N$_4$ could generate H$_2$O$_2$ effectively under visible light illumination.

In this study, g-C$_3$N$_4$-AQ/Fe(III) system was evaluated for the oxidation of various organic compounds under visible light illumination. The in situ H$_2$O$_2$ generating photocatalyst (g-C$_3$N$_4$-AQ) was synthesized by simple two steps: thermal polymerization and augmentation of anthraquinone. Photochemical activity of the combined system (g-C$_3$N$_4$-AQ/Fe(III)) was evaluated by the oxidation of various organic compounds, and the photochemical mechanism is discussed.

J. Seo · S. Y. Park · H.-H. Kim
School of Urban and Environmental Engineering, Ulsan National Institute of Science and Technology (UNIST), 50 UNIST-gil, Ulju-gun, Ulsan, 44919, Republic of Korea
e-mail: jwseo@unist.ac.kr

S. Y. Park
e-mail: psy95mj@unist.ac.kr

H.-H. Kim
e-mail: hakci123@unist.ac.kr

C. Lee (✉)
School of Chemical and Biological Engineering, Institute of Chemical Process (ICP), Seoul National University, 1 Gwanak-ro, Gwanak-gu, Seoul, 08826, Republic of Korea
e-mail: leechangha@snu.ac.kr

2 Materials and Methods

Reagents All chemicals were reagent grade and used without further purification. Chemicals used in this study included the following: dicyandiamide, anthraquinone-2-carboxylic acid (AQ-COOH), perchloric acid, sodium hydroxide, phenol, 4-chlorophenol (4-CP), benzoic acid (BA), carbamazepine (CBZ), methanol, phosphoric acid, ferric perchlorate, 1,10-phenanthroline (all from Sigma-Aldrich Co.), and acetonitrile (J.T. Baker Co.). All solutions were prepared in deionized water (18 MΩ cm

Milli-Q water, Millipore Co.). Stock solutions of phenol (10 mM), 4-CP (10 mM), BA (10 mM), and CBZ (0.1 mM) were prepared and stored at 4 °C until use. A Fe(III) stock solution (10 mM) was prepared by dissolving ferric perchlorate in a 0.1 M perchloric acid solution.

Synthesis of g-C$_3$N$_4$-AQ Synthesis of g-C$_3$N$_4$-AQ was divided into two steps: synthesis of graphitic carbon nitride (g-C$_3$N$_4$) and augmentation of AQ to g-C$_3$N$_4$. First, g-C$_3$N$_4$ was synthesized through thermal polymerization of dicyandiamide. In detail, 5 g of dicyandiamide was heated at the rate of 2.3 °C/min to 520 °C for 4 h. The collected solid was ground to powder in an alumina mortar. Next, prepared g-C$_3$N$_4$ (0.4 g) powder and AQ-COOH (0.04 g) were added into acetonitrile (36 mL). The suspension was sonicated for 30 min, and augmentation process was performed with stirring for 12 h at 50 °C. g-C$_3$N$_4$-AQ was collected by filtration and subsequently washed with DI water.

Photochemical experiments All experiments were performed in a quartz batch reactor at room temperature (22 ± 2 °C). The light illumination was performed by xenon arc lamp (LS 150, Abet Technologies, Inc.) equipped with an AM 1.5 G filter and a 400 nm longpass filter. The experimental solution (50 mL) was prepared by addition of g-C$_3$N$_4$-AQ powder (0.5 g/L), ferric ion (0.1 mM), and target organic compound (10 μM). Initial pH of the solution was adjusted at 3.0. The photochemical experiments were initiated by the illumination of visible light. Samples were withdrawn at a predetermined time and immediately filtered using a 0.45 μM PTFE syringe filter (Advantech Co.).

3 Results and Discussion

Figure 1a shows the oxidation of benzoic acid by g-C$_3$N$_4$-AQ/Fe(III) system and its respective control systems (AQ-COOH/Fe(III), g-C$_3$N$_4$/Fe(III), and g-C$_3$N$_4$/AQ-COOH/Fe(III)) under visible light illumination. AQ-COOH/Fe(III) and g-C$_3$N$_4$/Fe(III) demonstrated weak photochemical activities for the oxidation of BA: 17% and 27% for 2 h, respectively. g-C$_3$N$_4$/AQ-COOH/Fe(III) could degrade 53% of BA for 2 h, whereas, the synthesized g-C$_3$N$_4$-AQ could degrade 88% of BA with Fe(III) for 2 h. Comparing with the respective controls, g-C$_3$N$_4$-AQ could generate H$_2$O$_2$ effectively by the photochemical reduction of dissolved oxygen. The in situ generated H$_2$O$_2$ triggered Fenton-like reaction, which concluded with the enhancement of BA oxidation. Figure 1b shows the effect of dissolved oxygen for the photochemical oxidation of various organic compounds in g-C$_3$N$_4$-AQ/Fe(III) system. The photochemical oxidation of 4-CP was the fastest in the presence of dissolved oxygen (k_{4-CP} = 3.28 h^{-1}) followed by phenol, CBZ, and BA (k_{phenol} = 2.46 h^{-1}, k_{CBZ} = 2.04 h^{-1}, and k_{BA} = 0.97 h^{-1}). In deaerated condition, 4-CP and phenol could be degraded by g-C$_3$N$_4$-AQ/Fe(III) under visible light illumination (k_{4-CP} = 1.24 h^{-1} and k_{phenol} = 1.34 h^{-1}), however, CBZ and BA were hardly degraded (k_{CBZ} = 0.24 h^{-1} and k_{BA} = 0.0008 h^{-1}). In deaerated condition, g-C$_3$N$_4$-AQ could not generate H$_2$O$_2$ from the reduction of dissolved oxygen and hole at the surface of g-C$_3$N$_4$-AQ oxidized organic compounds selectively.

4 Conclusion

In this study, the combined system of photochemical H_2O_2 production and Fenton-like reaction examined oxidation efficacy of various organic compounds. g-C_3N_4-AQ/Fe(III) exhibited effective photochemical activity for oxidation of various organic compounds in the presence of dissolved oxygen because the photochemically generated H_2O_2 leads to Fenton-like reaction (Fe(III)/H_2O_2) which enhanced oxidation of organic compounds. In the absence of dissolved oxygen, the hole at the surface of g-C_3N_4-AQ affected the oxidation of target organic compounds selectively. The roles of g-C_3N_4-AQ and Fe(III) will be elucidated by further studies (effect of radical scavengers, measurement of oxidation products, and reduction of Fe(III)) and the physical/chemical properties of g-C_3N_4-AQ also characterized by various analysis tools (XRD, XPS, DRS, and FT-IR etc.).

References

Durán, A., & Monteagudo, J. M. (2007). Solar photocatalytic degradation of reactive blue 4 using a Fresnel lens. *Water Research, 41,* 690–698.

Kim, H.-E., Lee, J., Lee, H., & Lee, C. (2012). Synergistic effects of TiO$_2$ photocatalysis in combination with Fenton-like reactions on oxidation of organic compounds at circumneutral pH. *Applied Catalysis B: Environmental, 115–116,* 219–224.

Kim, H.-I., Choi, Y., Hu, S., Choi, W., & Kim, J.-H. (2018). Photocatalytic hydrogen peroxide production by anthraquinone-augmented polymeric carbon nitride. *Applied Catalysis B: Environmental, 229,* 121–129.

Lee, H., Choi, J., Lee, S., Yun, S.-T., Lee, C., & Lee, J. (2013). Kinetic enhancement in photocatalytic oxidation of organic compounds by WO$_3$ in the presence of Fenton-like reagent. *Applied Catalysis B: Environmental, 138–139,* 311–317.

Microalgae-Based Processes as an Energy Efficient Platform for Water Reclamation and Resource Recovery

María del Rosario Rodero, Roxana Ángeles, Victor Pérez, Juan Gancedo, Silvia Bolado, Raquel Lebrero, and Raúl Muñoz

Abstract

Microalgae provide a low-cost and environmentally friendly oxygenation. Enhanced nutrient recovery as a result of the dual photoautotrophic and heterotrophic metabolism. Microalgae can turn the energy balance of conventional wastewater treatment into positive. Microalgae-based processes can be engineered into multiple configurations. Wastewater treatment and biogas upgrading can be combined in algal-bacterial photobioreactors.

Keywords

Nutrient recovery • Microalgae • Photobioreactors • Wastewater treatment

M. del Rosario Rodero · R. Ángeles · V. Pérez · J. Gancedo · S. Bolado · R. Lebrero · R. Muñoz (✉)
Department of Chemical Engineering and Environmental Technology, School of Industrial Engineering, Venue Dr. Mergelina, University of Valladolid, C/Dr. Mergelina, s/n, 47011 Valladolid, Spain
e-mail: mutora@iq.uva.es

M. del Rosario Rodero
e-mail: mrrodero@iq.uva.es

R. Ángeles
e-mail: roxana@iq.uva.es

V. Pérez
e-mail: victor.perez@iq.uva.es

J. Gancedo
e-mail: jgancedoverdejo@hotmail.es

R. Lebrero
e-mail: raquel.lebrero@iq.uva.es

M. del Rosario Rodero ·
R. Ángeles · V. Pérez · S. Bolado · R. Lebrero · R. Muñoz
Institute of Sustainable Processes, University of Valladolid, 47011 Valladolid, Spain

1 Introduction to Microalgae-Based Wastewater Treatment

The treatment of urban wastewater is nowadays carried out using activated sludge processes due to their high robustness, efficient removal of carbon, nitrogen and phosphorus at low-moderate temperatures and extensive experience in their design and operation. However, activated sludge processes still exhibit a negative energy balance, low nutrient recovery and a high carbon footprint. These processes are particularly inefficient from an energy point of view in wastewater treatment plants with population sizes of 1000–20,000 inhabitants equivalent. On the other hand, the treatment of wastewater in algal-bacterial photobioreactors based on solar-driven photosynthetic oxygenation of the process results in a cost-efficient elimination of contaminants, a high recovery of nutrients and a positive energy balance. Figure 1 shows the energy balance for the treatment of 100 g of chemical oxygen demand (COD) using activated sludge processes and a microalgae-based wastewater treatment process (Alcántara et al. 2015).

Wastewater treatment with microalgae is based on the bacterial oxidation of organic matter and ammonium using the O_2 photosynthetically produced by microalgae. In return, the bacteria release the CO_2 necessary for the algal photosynthesis that sustains the process. Apart from this symbiotic exchange of CO_2 and O_2, bacteria can release substances that promote algal growth (e.g. vitamin B 12, phytohormones, etc.). On the other hand, microalgae are capable of generating in the cultivation broth of the photobioreactor high concentrations of oxygen, pH and high temperatures, which favor the elimination of pathogens and emerging contaminants. Traditionally, this symbiosis between microalgae and bacteria has supported the treatment of domestic, livestock and industrial wastewater, although the photoautotrophic metabolism of microalgae makes them the best candidates for the recovery of nitrogen and phosphorus from anaerobic digestates (Posadas et al. 2017). Recent studies in the field of algal

Fig. 1 Energy balance for the treatment of 100 g of COD in an activated sludge process (left) and microalgae (right)

microbiology have revealed the large metabolic versatility of microalgae, which is able to degrade heterotrophically from aromatic compounds such as cresol, phenol and phenanthrene to azo dyes. The operation of open raceway photobioreactors (namely HRAP) at hydraulic retention times of three–four days allows achieving removals of organic matter of 70–80%, of total nitrogen of 60–70%, of ammonium of 98–100% and of 40–60% of phosphate. Recent studies carried out within the ALL-GAS project have estimated that this technology would reduce wastewater treatment costs from 0.2 to 0.15 € m^{-3} and would result in a reduction in electricity consumption of 400% compared to conventional activated sludge processes (Acién et al. 2017). This reduction in treatment cost and energy consumption has been achieved with a R&D of less than ten years, compared to the more than 100 years of development of its counterpart, the activated sludge process. Despite the progress made in such a short period of time, microalgae-based wastewater treatment still suffers today from several limitations, which need to be overcome to lead to even greater reductions in operating costs and electricity consumption. The main limitations of microalgae-based wastewater treatment are:

- Poor sedimentation of the algal biomass.
- Limited treatment efficiency in wastewaters with a low C/N ratio (when no residual CO_2 source is available).

- Limited number of process configurations, which hinders the application potential of this technology.

In this context, the Environmental Technology Group at University of Valladolid has focused its research activity on the design of innovative process configurations based on microalgae to overcome the limitations above mentioned. Two technologies that are currently in a demonstration phase after a promising experimentation on a pilot scale at the University of Valladolid are denitrification–nitrification processes and photosynthetic biogas upgrading coupled to centrate treatment.

2 Denitrification-Nitrification Processes

This process configuration is based on the classic denitrification–nitrification activated sludge process but with photosynthetic oxygenation of the nitrification stage (Fig. 2). This configuration also includes a stage of sedimentation and recirculation of the algal biomass, which allows process operation at 2–3 g biomass L^{-1} (this prevents the process from photoinhibition in the peak hours of solar radiation), the enrichment of algae-bacteria consortia with high sedimentation velocities (1.5–2 m h^{-1}) and with low sludge volumetric indexes (<100 mL g^{-1}). This process configuration

Fig. 2 Scheme of the denitrification–nitrification configuration in algal-bacterial photobioreactors
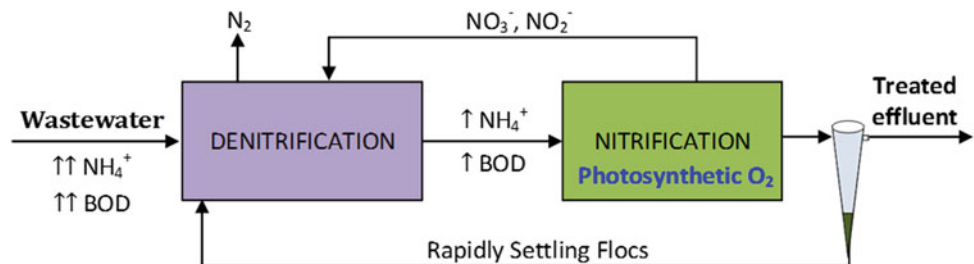
Fig. 3 Process configuration engineered at the University of Valladolid for photosynthetic biogas upgrading
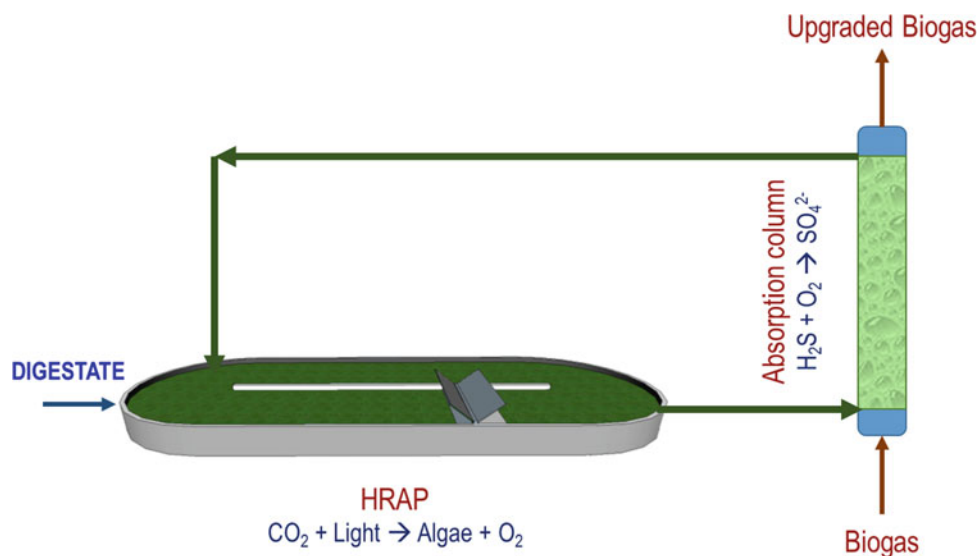
supports removals of organic matter >90%, total nitrogen >80%, ammonium >98% and phosphate >60% (García et al. 2017).

3 Photosynthetic Biogas Upgrading Coupled to Centrate Treatment

Photosynthetic biogas upgrading coupled to nutrient recovery from digestates is based on the photosynthetic fixation of the CO_2 present in biogas and the oxidation of H_2S to sulfate (NH_3 to nitrate, BTX to CO_2 and H_2O) using the oxygen photosynthetically generated during microalgae growth. The biogas produced in the anaerobic digestion of sewage sludge in wastewater treatment plants is introduced into an absorption column where CO_2 and H_2S are transferred to an algal broth stream recirculated from the photobioreactor. This absorption is favored by the high pH (pH = 9–10) and alkalinity of the algal cultivation broth. The H_2S absorbed is oxidized in the biogas absorption column using the photosynthetic O_2 dissolved in the cultivation broth recirculated from the photobioreactor, while the CO_2 absorbed is photosynthetically fixed in the photobioreactor (Fig. 3) (Muñoz et al. 2015). This technology allows to use the digestate produced in the plant as a source of N and P for algal growth. Removals of nitrogen greater than 90% and phosphate between 60 and 80% are common for centrates. The optimization of the ratio [Liquid flow rate: Biogas flow rate] mediates the production of a biomethane with a CH_4 content >96%, N_2 <3%, CO_2 <1%, O_2 <0.1% and with 100% H_2S removal efficiencies. A comparison of this technology with a classic activated carbon filter (for H_2S removal) + water absorption unit (for CO_2 removal) revealed that photosynthetic upgrading presents a reduction in the energy demand of 400% (Toledo-cervantes et al. 2017).

References

Acién, F. G., Molina, E., Fernández-Sevilla, J. M., Barbosa, M., Gouveia, L., Sepúlveda, C., et al. (2017). Economics of microalgae production. In R. Muñoz & C. Gonzalez (Eds.), *Microalgae-based biofuels and bioproducts* (pp. 485–503). Elsevier. ISBN: 978-0-08-101023-5.

Alcántara, C., Posadas, E., Guieysse, B., & Muñoz, R. (2015). Microalgae-based waste water treatment. In K. Se-Kwon (Ed.), *Handbook of microalgae: Biotechnology advances* (pp. 439–455). Elsevier. ISBN: 978-0-12-800776-1.

García, D., Alcántara, C., Blanco, S., Pérez, R., Bolado, S., & Muñoz, R. (2017). Enhanced carbon, nitrogen and phosphorus removal from domestic wastewater in a novel anoxic-aerobic photobioreactor coupled with biogas upgrading. *Chemical Engineering Journal, 313,* 424–434.

Muñoz, R., Meier, L., Diaz, I., & Jeison, D. (2015). A critical review on the state-of-the-art of physical/chemical and biological technologies for an integral biogas upgrading. *Reviews in Environmental Science and Bio/Technology, 14,* 727–759.

Posadas, E., Alcántara, C., García-Encina, P. A., Gouveia, L., Guieysse, B., Norvill, Z., et al. (2017). Microalgae cultivation in wastewater. In C. Gonzalez & R. Muñoz (Eds.), *Microalgae-based biofuels and bioproducts* (pp. 67–92). Elsevier. ISBN: 978-0-08-101023-5.

Toledo-Cervantes, A., Estrada, J. M., Lebrero, R., & Muñoz, R. (2017). A comparative analysis of biogas upgrading technologies: Photosynthetic vs physical/chemical processes. *Algal Research, 25,* 237–243.

Ozonation in the Framework of Sustainable Future Water Management

Jannis Wenk, Garyfalia A. Zoumpouli, and John Y. M. Chew

Abstract

A resourceful and continuously operating ozonation-biofiltration column experimental set-up was built and tested. The set-up is useful for predictions on the fate of ozonation products under different conditions and process configurations. Computational fluid dynamics (CFD) modelling helps to better understand and quantify the membrane-facilitated mass transfer of ozone into water. Modelling and experimental approaches provide the basis for establishing more efficient membrane ozonation processes.

Keywords

Sand filtration • Transformation products • Wastewater • Drinking water • Ozone • Membranes • Computational modelling

1 Introduction

Ozone is a chemical oxidant that has been used for water treatment for many years. Ozone applications have been mainly in drinking water treatment for disinfection, as an alternative to chlorine, and for aesthetical improvements of the water quality. More recently, ozone has become also important for advanced wastewater treatment and water recycling for the removal of trace contaminants. Given the wide range of ozone applications, the installed ozonation treatment capacity has been steadily increasing (Loeb et al. 2012). Nevertheless, water treatment with ozone can be energy-intensive since ozone needs to be produced on site from oxygen via electrical methods (Mundy et al. 2018).

In our research groups, we address these sustainability issues for ozone by two different approaches.

(a) We are investigating how to improve the linkage of chemical oxidation processes such as ozonation with natural engineered water treatment more effective. Full oxidative water treatment by ozone is effective for contaminant removal but energy-intensive and therefore expensive, while natural engineering treatment using soil aquifers or wetlands is cost-efficient but not effective in removing trace contaminants. Our hypothesis is that supplying relatively small ozone doses or using minimal ozone doses in intermittent water treatment steps may reduce energy costs significantly but will still make recalcitrant trace contaminants more accessible to subsequent biodegradation processes. To test our hypothesis and shed light on complex combined oxidation and biotransformation processes of trace contaminants, we have developed a small footprint continuously operating ozonation device based on an electrochemical ozone generation method and combined to biofiltration columns (Zoumpouli et al. 2018a).

(b) Conventional ozonation at full-scale treatment facilities is usually being performed with bubble reactors, where a mixture of ozone and oxygen is bubbled into the water using different types of gas spargers, such as porous diffusers or venturi-type injectors. Using such approaches, a significant amount of ozone is not utilized in the reactor but is released in the off-gas (Zhou and Smith 2000), where it needs to be converted back to oxygen for disposal or sometimes reused (Oneby et al. 2010). An alternative approach for the transfer of ozone into

J. Wenk (✉) · J. Y. M. Chew
Department of Chemical Engineering, Water Innovation and Research Centre (WIRC), University of Bath, Bath, UK
e-mail: j.h.wenk@bath.ac.uk

J. Y. M. Chew
e-mail: Y.M.Chew@bath.ac.uk

G. A. Zoumpouli
Centre for Doctoral Training, Centre for Sustainable Chemical Technologies, University of Bath, Bath, UK
e-mail: G.Zoumpouli@bath.ac.uk

water is the use of membrane contactors, leading to bubble-less ozonation. In this case, the gas phase and the liquid phase are separated by a membrane, which allows for better control of mass transfer and also offers the potential for recycling of the off-gas. We used computational fluid dynamics (CFD) modelling and fundamental convection-diffusion theory to better understand and quantify of the membrane-facilitated mass transfer of ozone into water (Berry et al. 2017) and built a flexible-use membrane contactor system for experimental investigations (Zoumpouli et al. 2018b).

The objective of this lecture is to provide an overview of our recent research activity on ozonation for water treatment with an emphasis on how our results can be embedded into sustainable water management scenarios of the future.

2 Materials and Methods

(a) The small-scale column set-up for continuous ozonation consisted of an ozonation column and three post-ozonation filtration columns, two storage tanks for the influent and the effluent, a pump and an ozone generation vessel. The columns were all made of glass. Ozone was produced electrochemically from small amounts of deionized water with an ozone microcell (Ozon-Micro-Zelle OMZ, Innovatec GmbH, Rheinbach, Germany). A schematic of the experimental set-up is shown in Fig. 1. The set-up operated continuously for three months and was fed with different types of water that were spiked with trace contaminants. The analysis of contaminants was conducted with high-performance liquid chromatography coupled to mass spectrometry (HPLC-MS). For details, refer to Zoumpouli et al. (2018a).

(b) The membrane contactor set-up is shown in Fig. 2. A glass shell was used to accommodate an ozone permeable tubular polydimethylsiloxane membrane of 20 cm length. Ozone was generated with a BMT 803N device, BMT Messtechnik, Berlin, Germany. Experiments were performed at different gas-phase ozone concentrations and in various types of water, including buffered ultrapure water, river water and secondary wastewater effluent, at different flow rates. For details, refer to reference Zoumpouli et al. (2018b). The fluid dynamics modelling package COMSOL 5.2 was used to simulate the mass transfer of ozone and oxygen through a capillary-sized non-porous membrane into water. For details on modelling, refer to reference Berry et al. (2017).
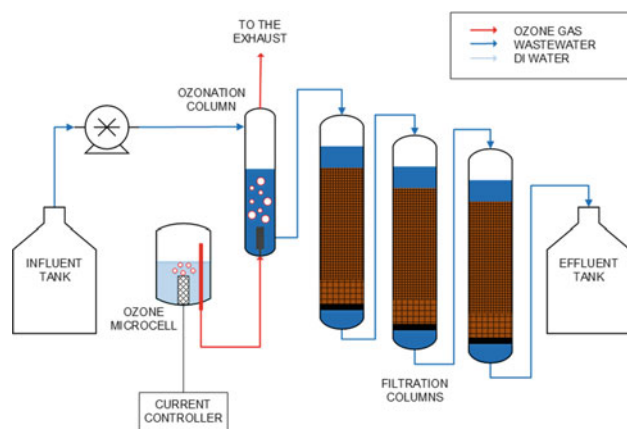
Fig. 1 Experimental setup for continuous ozonation and sand filtration
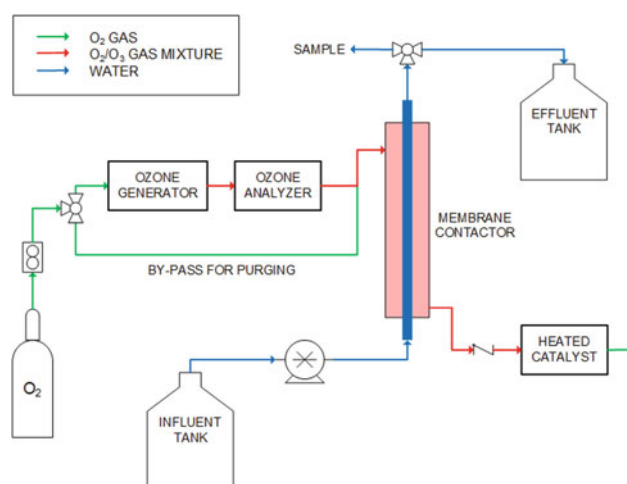
Fig. 2 Membrane contactor ozonation experimental setup

3 Results and Discussion

(a) The fate of the pharmaceutical carbamazepine (CBZ) at a concentration of 2.5 μM in synthetic wastewater during combined ozonation biofiltration is shown in Fig. 3 as an example. At ozone doses of 1–2 mg/L, which is a typical value for water treatment more than 99% of CBZ was removed. Two main transformation products were formed: BQM and BaQD. During the column passage, these ozonation products are further transformed. Overall removal of BQM during column passage was more than 50%. It shows that BQM biodegrades, while its parent compound CBZ is usually recalcitrant towards microbial degradation. Increased BQM removal at later dates indicated adaptation of the microbial community in the columns. Result indicates that biotransformation of ozonation
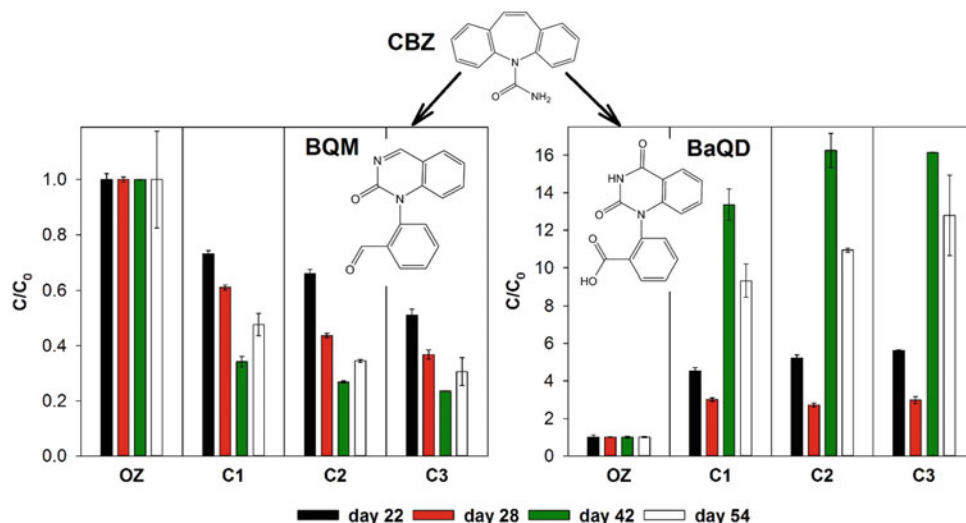
Fig. 3 Fate of two ozonation of CBZ products during column passage (Zoumpouli et al. 2018a)
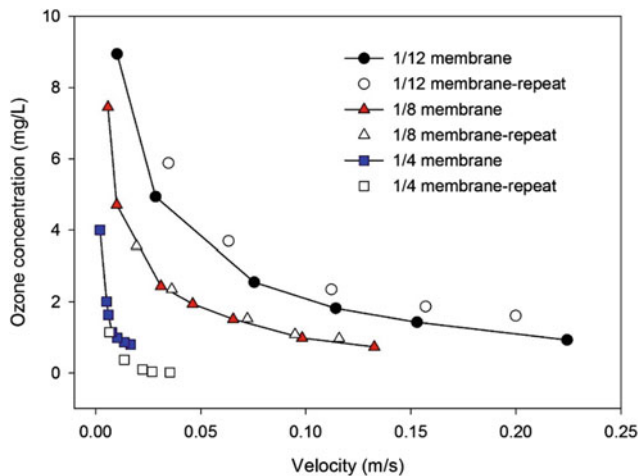
Fig. 4 Dissolved ozone concentration versus liquid velocity for different membranes sizes: 1/12, 1/8 and 1/4 in.
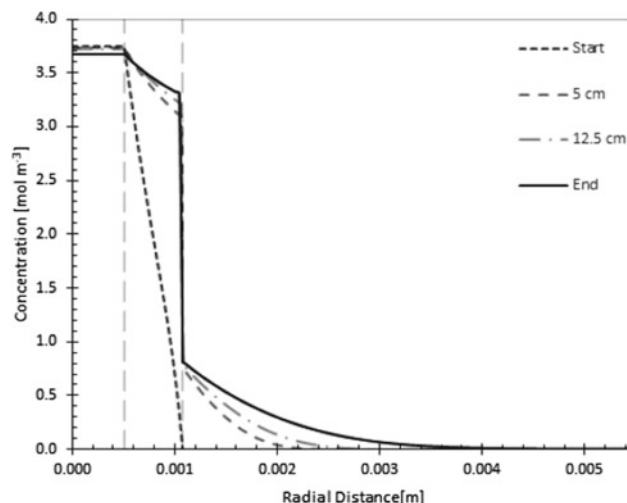
Fig. 5 Ozone concentration along length for a 1/12 in. tubular membrane

products of CBZ is an important degradation pathway that should be monitored in addition to the fate of CBZ itself.

(b) Figure 4 shows results on mass transfer experiments for ozone given as final ozone concentration at the end of a membrane section, through differently sized model membranes made of polydimethylsiloxane (PDMS), at different water velocities through the membrane. The ozone concentration was found to increase with decreasing velocity and increasing residence time. Computational fluid dynamic (CFD) modelling has shown that for a single PDMS tube with internal gas flow and external liquid flow the main resistance for ozone transfer is in the liquid side (Berry et al. 2017).

This means that the liquid flow rate is a critical parameter. In practice, multiple membranes operating in parallel, or multiple passes through the same reactor would be required to maintain low flow rates and a large throughput of water for treatment. Similarly, the ozone transfer decreases with increasing membrane thickness. Thin membranes would be most efficient; however, mechanical properties and membrane stability need to be considered. By using a refined modelling approach, it was also calculated how ozone concentration profiles establish with progression along the membrane. An exemplary result is shown in Fig. 5. Ozone moves quickly into the membrane but does not

enter the liquid due to the mass transfer resistance caused by the solubility of ozone and the diffusivity into the water. As distance progresses along the tube, the ozone concentration increases.

Energy-efficient ozonation water treatment systems will be an important building block for sustainable water treatment schemes.

4 Conclusion

(a) Ozonation combined with natural engineering low-energy treatment approaches involving microbiological degradation is a promising hybrid technology to remove organic trace contaminants during advanced water treatment schemes and water recycling. To further elucidate the fate of trace organic contaminants after ozonation and to assess the efficiency of the treatment process, more research is needed. The practical obstacle to enable extensive studies has been the difficulty to combine ozonation with continuous biofiltration at laboratory-scale.

(b) Ozone mass transfer for PDMS membranes was experimentally measured. In addition, ozonation concentration profiles across a capillary membrane tube and further parameters including single mass transfer resistances and overall mass transfer coefficients for ozone for varying membrane lengths, thicknesses and laminar flow liquid side velocities, by considering both the influence of diffusivity and solubility of gases in the membrane. Our studies provide an important basis for more advanced modelling of membrane ozonation contactors and ultimately for dimensioning and optimizing full-scale contactor systems for water treatment.

References

Berry, M., Taylor, C. M., King, W., Chew, Y. M. J., & Wenk, J. (2017). Modelling of ozone mass-transfer through non-porous membranes for water treatment. *Water, 9*, 452.

Loeb, B. L., Thompson, C. M., Drago, J., Takahara, H., & Baig, S. (2012). Worldwide ozone capacity for treatment of drinking water and wastewater: A review. *Ozone: Science & Engineering, 34*, 64–77.

Mundy, B., Kuhnel, B., Hunter, G., Jarnis, R., Funk, D., Walker, S., et al. (2018). A review of ozone systems costs for municipal applications. Report by the Municipal Committee—IOA Pan American Group. *Ozone: Science & Engineering, 40*, 266–274.

Oneby, M. A., Bromley, C. O., Borchardt, J. H., & Harrison, D. S. (2010). Ozone treatment of secondary effluent at U.S. municipal wastewater treatment plants. *Ozone: Science & Engineering, 32*, 43–55.

Zhou, H., & Smith, D. W. (2000). Ozonation dynamics and its implication for off-gas ozone control in treating pulp mill wastewaters. *Ozone: Science & Engineering, 22*, 31–51.

Zoumpouli, G. A., Scheurer, M., Brauch, H.-J., Kasprzyk-Hordern, B., Wenk, J., & Happel, O. (2018a). COMBI, continuous ozonation merged with biofiltration to study oxidative and microbial transformation of trace organic contaminants. Submitted to *Water Research*.

Zoumpouli, G. A., Baker, R., Taylor, C. M., Chippendale, J. C., Smithers, C., Xian, S. H. S., et al. (2018b). A single tube contactor for experimental and computational fluid dynamics (CFD) modelling testing of the performance of membrane ozonation for water. Treatment submitted to *Water*.

Pilot Study for Spiral Wound-PVDF Supported UF Membranes for Brackish Water Desalination System

M. S. Shalaby, H. Abdallah, and Ahmed M. H. Shaban

Abstract

Groundwater availability in Egypt and its quality. RO pretreatment of groundwater to secure drinking water. Large-scale production of flat sheet UF membranes and its evaluation. Spiral wound 4040 modules preparation and its application in the real continuous system.

Keywords

UF membranes • Polluted brackish water • Spiral wound module

1 Introduction

The availability of fresh water depends on the quality of groundwater and mainly influenced by rainfall, which is very rare in Egypt now. The quality of groundwater is not the same all time due to intrusion especially in areas as Upper Egypt - villages where the efficiency of traditional sewage treatment plants may be improper (Singh et al. 2013; Fan et al. 2013; Zhang et al. 2013). Groundwater as the main source of water in many remote areas that has been intruded by sea water or contaminated by waste, has led to the performance of the existing conventional water treatment unit is not able to meet a drinking water quality and high cost of operation because of high chloride salt content and other pollutants in the raw water. Therefore, advanced treatment is required to produce drinking water quality. In this pilot study, suitability

membrane process to treat raw water source or brackish water was done by applying the ultrafiltration (UF) membrane as pretreatment of reverse osmosis (RO) membrane. The system employs a UF membrane completed air lift system to separate colloidal and suspended solid in brackish water, therefore, reducing the concentration of fouling constituent in UF or RO membranes (Goncharuk et al. 2011). In this work, humic acid synthetic solution saline water (2000 ppm) was used to evaluate the prepared flat sheet supported UF membranes, followed by rolling of these sheets and formation of UF industrial modules 4040 for a pilot UF evaluation compared with filmtech commercial membranes.

2 Materials and Methods

2.1 Materials

Polyvinylidene difluoride (PVDF) was used as the main polymer; polyethylene glycol was purchased from Sigma Aldrich. N-methyl-2-pyrrolidine (NMP) was used as a solvent and also purchased from Sigma Aldrich. Two types of nonwoven support polyester compressed nonwoven purchased from Holykem company, China and spunbond polypropylene was purchased from Egypt local market.

2.2 Preparation of PVDF Membranes, Characterization and Spiral Wound Modules

PVDF membranes were prepared using a phase inversion process. The polymer dope solutions of 18% PVDF were dissolved in NMP with 2% of polyethylene glycol. The mixing process was carried out for 8 h. The polymeric solution was cast onto two types of nonwoven supports fixed on a glass plate, and the casting process was carried out using fabricated large-scale casting machine. The membranes were characterized by SEM, mechanical properties and membrane performance lab test. The prepared

M. S. Shalaby (✉) · H. Abdallah
Chemical Engineering and Pilot Plant Department, National Research Centre, El Buhouth St., Dokki, Giza, Egypt
e-mail: marwashalaby_4@yahoo.com

H. Abdallah
e-mail: drhebaabdallah3@gmail.com

A. M. H. Shaban
Water Pollution Department, National Research Centre, El Buhouth St., Dokki, Giza, Egypt
e-mail: ashaban12311@gmail.com

membranes were rolled and formed as spiral wound modules for the pilot test.

2.3 Spiral Wound Evaluation

A spiral wound UF membrane module formed with a flat sheet casted continuously by flat sheet group in the National Research Centre, which then was rolled (4040), side cut and fully finished for pilot scale testing experiments. The above 4040 UF membrane was tested in a pilot testing unit shown in Fig. 1.

A feed tank (250 L) was attached with the membrane housing module. Rotameter was fitted with the permeate line to estimate the flow rates together with the feed pressure through a pressure gauge. Spiral wound UF commercial membrane module was obtained from AQUA SERVICE Co., Egypt. A high-pressure (up to 2894 kPa) plunger pump was attached with the pilot plant to circulate the feed in the UF membrane module. PVDF UF membrane module 4040 with an effective membrane cross-sectional area of 8.1 m^2 was kept in a fibre housing cylindrical shell. Prior to the experiment, UF commercial membrane module was compacted with de-ionized water at 758 kPa for 1 h. While for the UF module locally produced in our labs, the module was washed with de-ionized water for 3 h under normal operation. The ability to simulate polluted brackish water which will be fed to RO desalination units to produce drinking water in far away villages from River Nile was not as easy

and so was taken as humic acid as maximum proposed pollution load in low salinity brackish water (1100 ppm). Synthetic polluted brackish water was made by dissolving different concentration of humic acid (3–10 g/l) in saline water (1100 ppm) which will be used in evaluating the spiral wound.

The produced spiral wound membranes will be tested in a pilot testing unit designed and located in a flat sheet membrane group—National Research Centre.

3 Results and Discussion

3.1 Membrane Characterization

Figure 2a and b indicate the PVDF membrane with different support during membrane preparation. Figure 2a indicates finger like on the sub-layer, and the bottom layer was the compacted structure of nonwoven support (China); while Fig. 2b indicates the large finger like in the sub-layer and bottom porous layer due to woven support (Satin), where the polymeric solution impregnation is through the textile of woven support.

3.2 Flat Sheet Results

Figures 3 and 4 show the performance of prepared membranes in terms of humic acid rejection percentage and
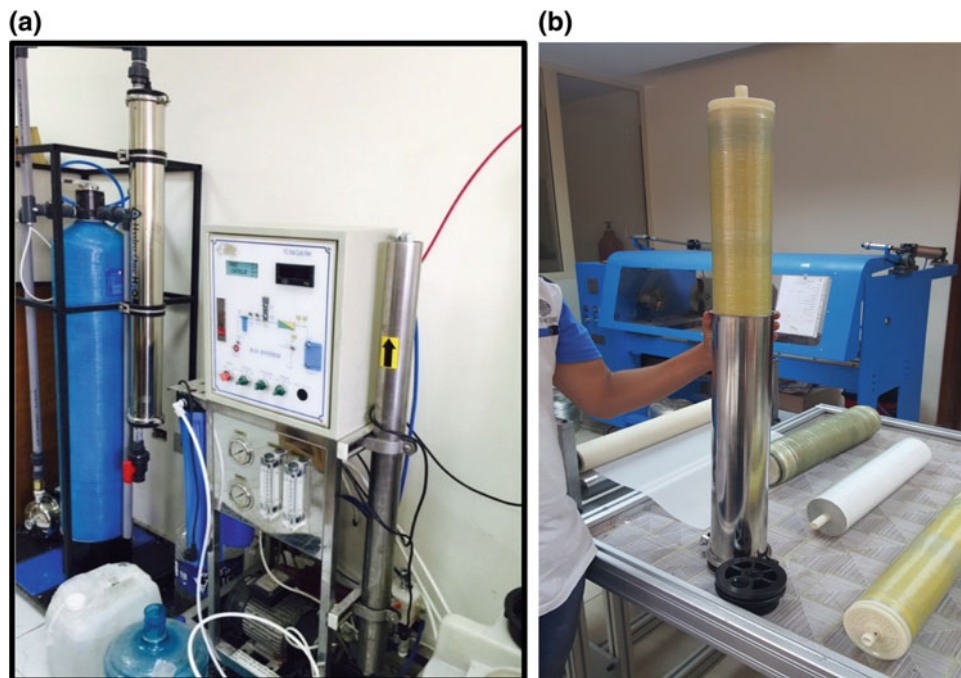
Fig. 1 UF spiral wound module and UF-RO pilot testing unit (**a**) Spiral wound module (**b**) Pilot testing unit

Fig. 2 SEM of prepared PVDF membrane with nonwoven support (**a**) and woven support (**b**)
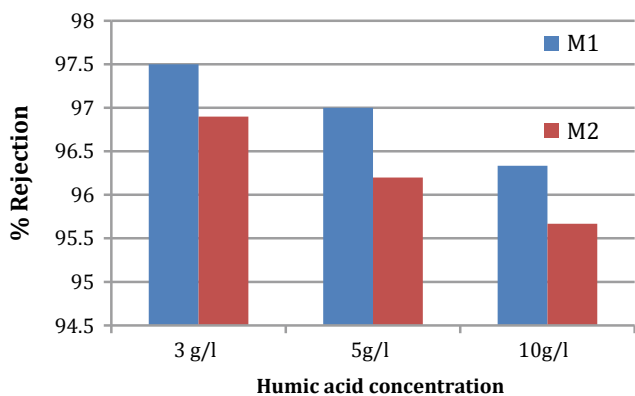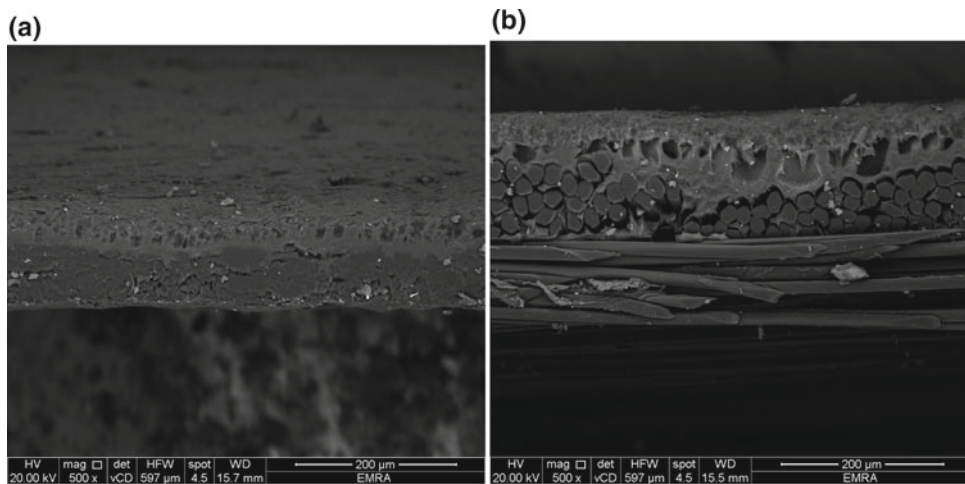
Fig. 3 Rejection % of prepared PVDF supported membranes with increased humic acid saline water

Fig. 5 Flux of spiral wound module for humic acid saline water

Fig. 4 Flux of prepared PVDF supported with different supported membranes

permeate flux, respectively. The experiments were performed under operating pressure of 8 bar using different humic acid saline water concentration to determine the applicability of these membranes in the ultrafiltration process as pretreatment of RO desalination units. It is clearly from

Fig. 3 that M1 provides the best membrane performance depending on rejection percentage but not so high and this can be attributed to the effect of woven (Satin) support structure. While for permeate flux presented in Fig. 4, M1 shows a higher increase in flux when compared with M2 (nonwoven china) support with the increase in humic acid concentration which shows a good antifouling behaviour as the flux is showing a sharp decrease with the increase in humic acid concentration from 3 to 10 g/l.

The pilot scale testing for prepared flat sheet converted to spiral wound modules was presented in Figs. 5 and 6, where a comparison between prepared modules with the commercial nonwoven module was fulfilled. It was clear from Fig. 6 that for prepared module tested with humic acid of concentration 5 g/l and of TDS 1100 ppm of satin support the flux was about 80 l/m^2 h, which shows a decrease when compared with M1 in Fig. 4 as it gives about 105 l/m^2 h, and this can be attributed to higher fouling ability with spiral wound module when compared with flat sheet. The higher flux of commercial module was a point where further research can be done to increase the reached flux of satin PVDF supported modules to reach commercial one.
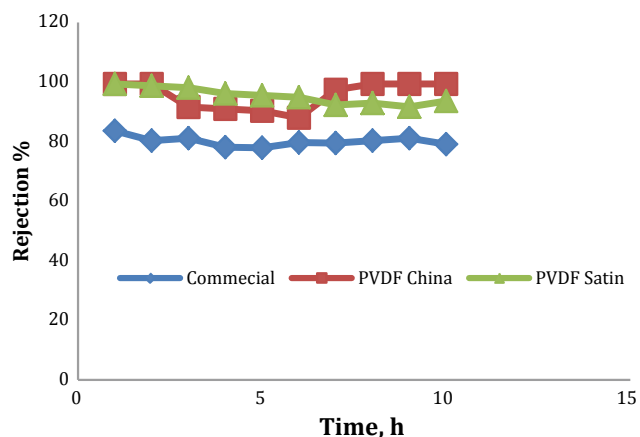
Fig. 6 Rejection % of spiral PVDF supported module for humic acid saline water

Figure 6 shows the effect of different support materials on PVDF membrane behaviour as UF membrane for humic acid (5 g/l) saline water as a model for polluted brackish water. The rejection % of prepared membranes on woven and nonwoven support was nearly the same of about 97–99%, but the commercial was about 80% which shows a decrease and highlights the superiority of our prepared membranes.

4   Conclusion

The effect of different support materials (woven and nonwoven support) on prepared PVDF flat sheet membranes was studied with a complete characterization of such UF membranes. The effectiveness of the woven supported UF membranes was shown by results of different characterization techniques especially SEM, but this was not enough to govern without continuous evaluation experiments on flat sheet which gives about 97% rejection decreased to reach 96.25% humic acid rejection per cent by increasing its concentration from 3 to 10 g/l after repeated operation for ten hours. The flux value was dramatically decreased when tested for ten hours continuously as a spiral wound module to reach a maximum value of about 80%, and this can be attributed to fouling behaviour. The application of prepared PVDF UF membranes in a real pilot plant of continuous operation shows an acceptable good behaviour compared with the commercial applied modules.

References

Fan, H., Peng, Y., Li, Z., Chen, P., Jiang, Q., & Wang, S. (2013). Preparation and characterization of hydrophobic PVDF membranes by vapor-induced phase separation and application in vacuum membrane distillation. *Journal of Polymer Research, 20,* 1–15.

Goncharuk, V. V., Kavitskaya, A. A., & Skil'skaya, M. D. (2011). Nanofiltration in drinking water supply. *Journal of Water Chemistry and Technology, 33,* 37–54.

Singh, V., Jain, P. K., & Das, C. (2013). Performance of spiral wound UF membrane module for with and without permeate recycle: Experimental and theoretical consideration. *Desalination, 322,* 94–103.

Zhang, J., Xu, Z., Mai, W., Min, C., Zhou, B., Shan, M., et al. (2013). Improved hydrophilicity, permeability, antifouling and mechanical performance of PVDF composite ultrafiltration membranes tailored by oxidized low dimensional carbon nanomaterials. *Journal of Materials Chemistry A, 1,* 3101–3111.

Energy Monitoring of a Wastewater Treatment Plant in Salerno, Campania Region (Southern Italy)

Maria Rosa di Cicco, Antonio Spagnuolo, Antonio Masiello, Carmela Vetromile, Carmine Lubritto, Mariano Nappa, and Gaetano Corbo

Abstract

Results of an energy audit on a large wastewater treatment plant (wwtp) are shown; critical issues related to the use of energy resources in this plant are identified; parasitic inflows negatively affect the plant performances and a distinction between organic and hydraulic load is a useful tool in describing this problem.

Keywords

Wastewater • wwtp • Parasitic inflows • KPI • Energy audit

1 Introduction

Wastewater treatment accounts for 25% of the total energy spent in the water sector on a global scale, and this electricity consumption may than increase by more 60% by 2040, due to the strong increasing of polluted water requiring treatments (WERF and EPRI 2013; IEA 2016). There are several possibilities to reduce these energy consumptions: (i) increasing performances of machinery through the adoption of frequency variators (Freni and Sambito 2017); (ii) improving aeration effectiveness in the biological sector (Ferrentino et al. 2018); (iii) reusing the biogas recovered from the sludge digestion (Mema et al. 2017); reducing the amount of parasite water inflows (Weiß et al. 2002). Also, by using system dynamic monitoring, it is possible to track in real-time system parameters trend and actively check the operating conditions of the facility compartments (Campanelli et al. 2013).

In this paper, the results of an energy audit performed on a large plant located in the city of Salerno (Campania region, southern Italy) are showed, and critical issues related to the use of energy resources in this plant are identified.

2 Materials and Methods

S.I.I.S. wastewater treatment plant (below *wwtp*) started working in 1988 with the aim of treating mixed civil and industrial sewage from the city of Salerno and a number of neighbouring municipalities.

With a maximum capacity of 700,000 PE and designed to treat an average flow rate of about 1.815 m^3/s, the plant performs its treatments with a CAS process scheme (Metcalf & Eddy 2006; Masotti 2011), and it only uses electricity as an energy vector for the technological services of the facility. The plant collects wastewaters from a 85 km network of collectors, and ten sewage lifting stations are included in the network. In recent years, it has been observed a significant increase in parasite inflows, particularly amplified in the years between 2013 and 2015.

The present energy audit covers a period of four years, from January 2014 to December 2017; data used for the study were obtained through field inspections and documentation provided by the company (e.g. energy consumption billing, environmental waste analysis reports, etc.). Data were collected on a monthly basis and include: (i) the total electricity consumption of the system, with the corresponding tonnes of oil equivalent and CO_2 equivalent emissions; (ii) the total volume of wastewater treated by the facility; the average daily concentration of polluting loads entering and leaving the system, namely (*COD*) chemical oxygen demand, (*BOD5*) biochemical oxygen demand and (*TSS*) total suspended solids.

M. R. di Cicco (✉) · A. Spagnuolo · A. Masiello · C. Vetromile · C. Lubritto
Department of Environmental, Biological and Pharmaceutical Sciences and Technologies, University of Campania "Luigi Vanvitelli", Via Vivaldi 43, 81100 Caserta, Italy
e-mail: mariarosa.dicicco@hotmail.it

C. Vetromile
Energreenup s.r.l, Via Parata 3, 81051 Pietramelara, Italy

M. Nappa · G. Corbo
Servizi Idrici Integrati Salernitani S.p.A, Viale A. De Luca 8, 84131 Salerno, Italy

With the aim of evaluating the plant performances, operational indicators and key performance indexes (*KPIs*) found in the literature were used. As operational indicators, it was decided to use the *population equivalent* effectively served by the plant (PE_{served}), the *dilution factor* (DF) and the *load factor* (LF) (Longo et al. 2016); also, in order to get more information about the impact of parasite inflows, it introduced a distinction between *organic* load and *hydraulic* load. As regards, instead, the KPIs, it was decided to use the specific energy consumption evaluated with respect to *treated flow rate* (KPI_1), *population equivalent served* (KPI_2) and *removed amount of COD* (KPI_3) (Benedetti et al. 2008; Quadros et al. 2010; Silva & Rosa 2015). The following table summarizes the indicators described above.

Comparing the amount of pollutants entering and leaving the system, the plant shows a high pollutant removal level, thus demonstrating the proper functioning of the depuration process, which complies with all legal limits imposed by the current legislation regarding both output values and removal rates (D.Lgs 152/2006 e s.m.i.).

Results coming from the evaluation of KPIs (values for the year 2014 are reported in Fig. 4) and operational indicators show that the plant is energy efficient compared to similar case studies found in the literature (Campanelli et al. 2013).

The amount of parasitic inflows is remarkable so that the plant works in a condition close to the maximum hydraulic capacity, while it looks oversized with respect to the amount

Indicator	Relation	Used for
$PE_{served}^{organic}$	$\dfrac{[n\,gBOD5_{in}*day^{-1}]}{[60\,gO_2*PE^{-1}*day^{-1}]}$	Population equivalent actually served by the wwtp, calculated with respect to the amount of biodegradable pollutants (BOD5) to be removed
$PE_{served}^{hydraulic}$	$\dfrac{\text{Daily wastewater flow rate } [L*day^{-1}]}{\text{Water supply } [L*PE^{-1}*day^{-1}] \times \text{Return Coefficient}}$	Population equivalent actually served by the wwtp, calculated with respect to the wastewater flow rate entering the plant
$LF_{organic}$	$\dfrac{\text{equivalent people served } [PE_{served}^{oric}]}{\text{project equivalent people } [PE_{design}]} \times 100$	It expresses how much the plant is working close to the maximum capacity, from a organic point of view
$LF_{hydrauic}$	$\dfrac{\text{equivalent people served } [PE_{served}^{hydrauic}]}{\text{project equivalent people } [PE_{design}]} \times 100$	It expresses how much the plant is working close to the maximum capacity, from an hydraulic point of view
DF	$\dfrac{\text{Daily flow of wastewater } [L*day^{-1}]}{\text{equivalent people served } [PE_{served}^{organic}]}$	It expresses the amount of wastewater related to a single inhabitant, thus giving further information about the wastewater dilution due to infiltrations and parasitic inflows
KPI_1	$\dfrac{\text{energy consumption } [kWh]}{\text{unit of volume treated } [m^3]}$	The indexes can be compared with values of the same index reported in the literature for similar plants, thus giving information about the energy performances
KPI_2	$\dfrac{\text{energy consumption } [kWh]}{\text{equivalent people served} \times \text{year } [PE_{served}^{organic}*year]}$	
KPI_3	$\dfrac{\text{energy consumption } [kWh]}{\text{unit quantity of removed COD } [kgCOD_{removed}]}$	

3   Results and Discussion

The energy consumptions of the whole system (wwtp and ten sewage lifting stations) are about 10 GWh year^{-1}, corresponding to an emission of 4800 tons of CO_{2eq} and a consumption of over 1800 tons of oil equivalent (Fig. 1).

The time plot of the wastewaters entering the plant shows a reduction in the average monthly flow rate of about 39%, over the entire period of four years (Fig. 2).

The ratio between COD and BOD5 remains almost constant over the entire survey period around a mean value of 2.5, as shown in Fig. 3, consequently pointing up the high dilution of sewage by waters with a strong inorganic component (parasite water inflows) (Samudro and Mangkoedihardjo 2010).

of pollutants to be removed. The evidence is clearly shown in Fig. 5, where the presence of the parasitic inflows is highlighted by the difference between the organic and hydraulic population equivalent served.

Another evidence of the negative effects of excessive dilution, on the energy performance of the plant, can be noticed in the KPI_3 trend. As it can be seen in Fig. 6, there is a positive correlation between the KPI_3 index and the wastewater dilution degree: the presence of parasitic waters induces an increase in the energy required for removal treatments of a unit quantity of COD. On the other hand, as the organic load factor increases, the specific consumption of the depuration process rapidly decreases (Fig. 7), proving that the system works efficiently when the biodegradable pollutant load (BOD5) is present in a more concentrated form and when the plant sizing is efficient. The trend shown
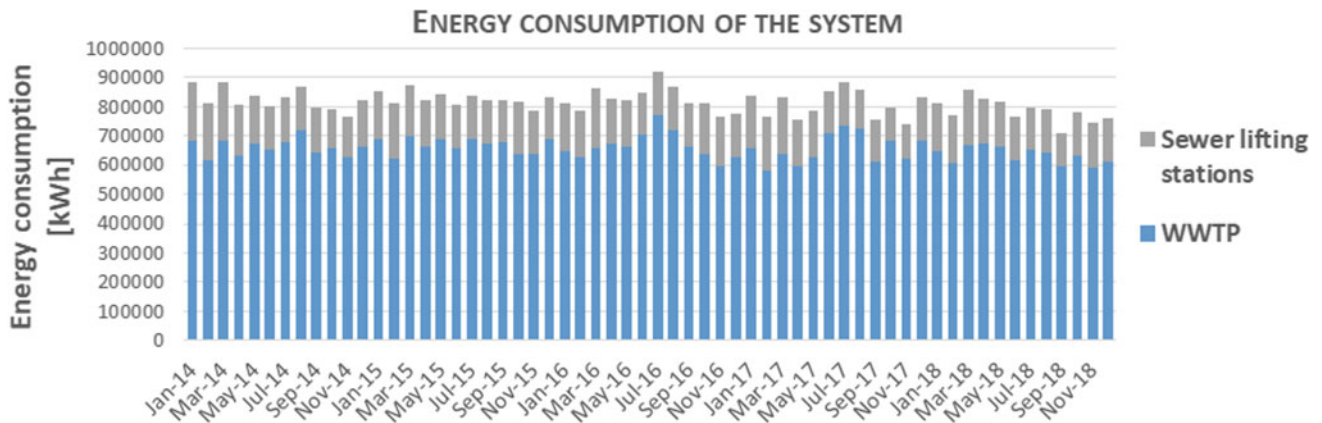
Fig. 1 Energy consumptions of the wwtp and the ten sewer lifting stations

Fig. 2 Time trend of wastewater flow rate entering the plant, on a monthly basis
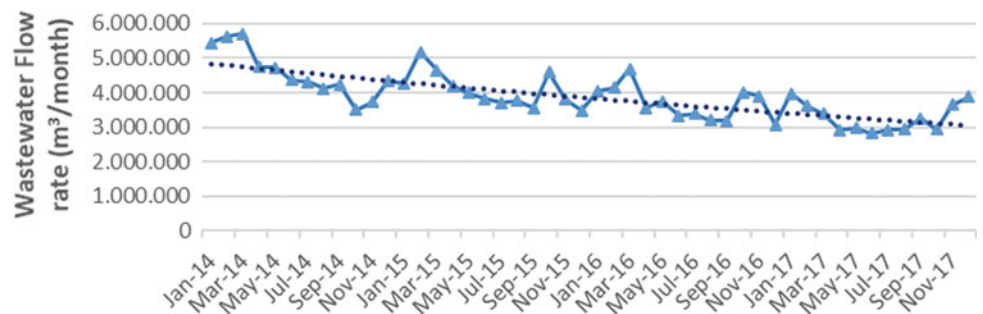
Fig. 3 Time trend of Biodegradability Index
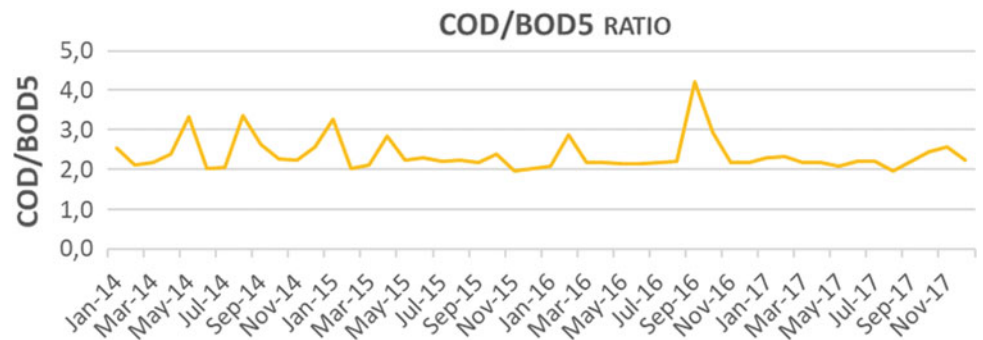
S.I.I.S. wwtp KPIs and Operational Indicators	2014
KPI1 ($kWh\ m^{-3}$)	0,1
KPI2 ($kWh\ PE_{served}^{organic\ -1}\ year^{-1}$)	28
KPI3 ($kWh\ kgCOD_{removed}^{-1}$)	0,6
DF ($L\ PE_{served}^{organic\ -1}\ day^{-1}$)	537
LF$_{organic}$ (%)	42%
LF$_{hydraulic}$ (%)	84%

Fig. 4 Average values of KPIs and operational indicators for 2014

in the two graphs is consistent with the one reported in the literature for similar plants (Longo et al. 2016).

4 Conclusion

The study has the principal goal to identify critical issues related to the use of energy resources within the wastewater plant.

The conclusions that can be drawn from the data analysis are listed below.

(i) The plant shows similar performances with respect to other case studies, with particular regard to the energy efficiency for the COD removal (KPI$_3$) and its relation to operational indicators (Dilution Factor and Organic Load Factor).

Fig. 5 Time trend of the population equivalent served by the wwtp
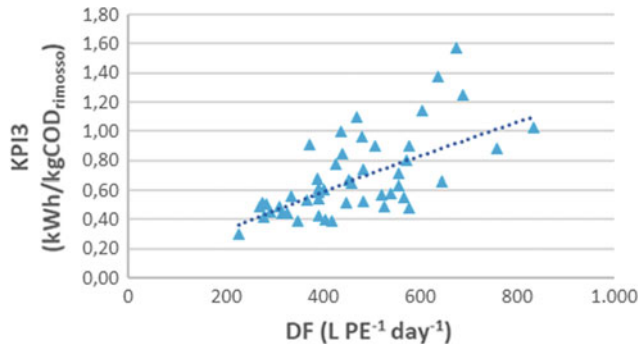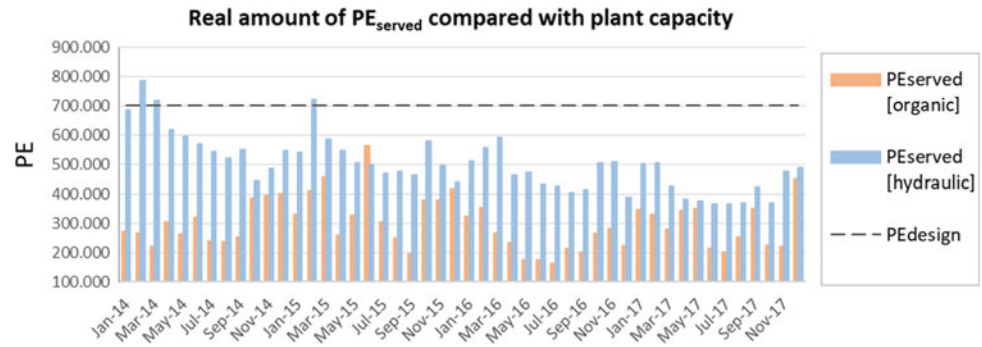
Fig. 6 KPI3 vs dilution factor
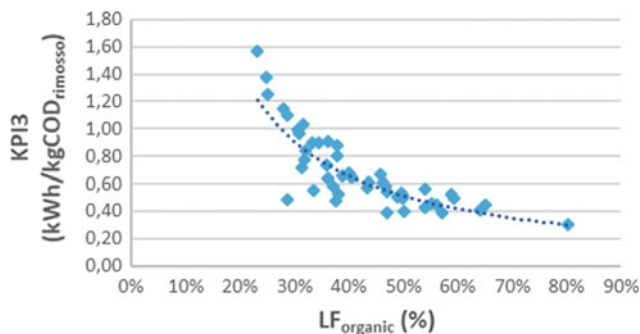
Fig. 7 KPI3 vs organic load factor

(ii) The system collects a large percentage of parasite water inflows (rainwater and groundwater infiltrations), which dilute the wastewater; the distinction between organic load and hydraulic load for the evaluation of the population equivalent served, and the load factor is a valuable tool in finding evidence of the problem.

(iii) The high percentage of infiltration affects the energy performances, forcing the plant to work in conditions close to the maximum hydraulic capacity.

(iv) The wastewater dilution affects the specific consumption calculated with respect to the COD removed (KPI_3), thus constraining the plant to use a greater amount of energy to remove the same pollutants load.

References

Benedetti, L., Dirckx, G., Bixio, D., Thoeye, C., & Vanrolleghem, P. A. (2008). Environmental and economic performance assessment of the integrated urban wastewater system. *Journal of Environmental Management, 88*(4), 1262–1272.

Campanelli, M., Foladori, P., & Vaccari, M. (2013). *Consumi elettrici ed efficienza energetica nel trattaento delle acque reflue*. Maggioli Editore.

D.Lgs 152/2006 e s.m.i. Decreto Legislativo n.152 del 3 aprile 2006. Norme in materia ambientale. In *Gazzetta Ufficiale*.

Ferrentino, R., Langone, M., Vian, M., & Andreottola, G. (2018). Application of real-time nitrogen measurement for intermittent aeration implementation in a biological nitrogen removal system: Performances and efficiencies. *Environmental Technology,* 1–14.

Freni, G., & Sambito, M. (2017). *Energy saving and recovery measures in integrated urban water systems.*

IEA. (2016). *Water energy nexus. Excerpt from the world energy outlook 2016*. Organisation for Economic Co-operation and Development/International Energy Agency, OECD/IEA.

Longo, S., d'Antoni, B. M., Bongards, M., Chaparro, A., Cronrath, A., Fatone, F., et al. (2016). Monitoring and diagnosis of energy consumption in wastewater treatment plants. A state of the art and proposals for improvement. *Applied Energy, 179,* 1251–1268.

Masotti, L. (2011). *Depurazione delle acque. Tecniche ed impianti per il trattamento delle acque di rifiuto*. Milano: Edagricole-New Business Media.

Mema, V., Hlabela, P., & Marx, S. (2017). Assessing electric power potential of municipal wastewater sludge. *Journal of Clean Energy Technologies, 5*(1), 60–63.

Metcalf & Eddy. (2006). *Ingegneria delle acque reflue. Trattamento e riuso*. McGraw Hill.

Quadros, S., Joao Rosa, M., Alegre, H., & Silva, C. (2010). A performance indicators system for urban wastewater treatment plants. *Water Science and Technology, 62*(10), 2398–2407.

Samudro, G., & Mangkoedihardjo, S. (2010). Review on BOD, COD, and BOD/COD ratio: A triangle zone for toxic, biodegradable and stable levels. *Internation Journal of Academic Research, 2*(4), 235–239.

Silva, C., & Rosa, M. J. (2015). Energy performance indicators of wastewater treatment: A field study with 17 Portuguese plants. *Water Science and Technology, 72*(4), 510–519.

Weiß, G., Brombach, H., & Haller, B. (2002). Infiltration and inflow in combined sewer systems: Long-term analysis. *Water Science and Technology, 45*(7), 11–19.

WRF and EPRI. (2013). *Electricity use and management in the municipal water supply and wastewater industries*. Palo Alto, California.

Sulfate Radicals-Based Technology as a Promising Strategy for Wastewater Management

María Arellano, M. Ángeles Sanromán, and Marta Pazos

Abstract

Successful persulfate activation by iron was achieved. Amberlite was demonstrated to be a suitable support for obtaining an efficient iron catalyst. Electro-activation of peroxymonosulfate in the presence of iron-based minerals as catalyst was developed. Reusability of heterogeneous catalysts was demonstrated. Lissamine Green B and 1-butyl-1-methylpyrrolidinium chloride removal through sulfate radicals was accomplished.

Keywords

Sulfate radicals • Persulfate • Peroxymonosulfate • Ionic liquid • Dye • Heterogeneous catalyst

1 Introduction

The world population is constantly growing and the climate change with several episodes of floods and droughts, together with the pollution of surface water and aquifers, decreases the resources of drinking water around the world. The pollution is a problem that can spread between different areas, from surface water to groundwater, affecting either fluvial and seawaters. In this vein, the deleterious alteration of water quality is usually the result of the different activities of the industries such as textile, paper, iron and steel, food,

and solvents. This problem is obvious because all of them entail high water consumption and the resulting generation of wastewater contains mainly organic matter, heavy metals, solvents, detergent, or industrial oil.

The development of strategies for removing pollutants in industrial wastewater allowing its recycling could be a safe bet on saving water and decreasing wastes generation. Moreover, the selection of specific remediation technologies should not be exclusively based on the efficiency and must integrate environmental and economic aspects for achieving its implementation at real scale. Therefore, a constant search for new processes and technologies, more efficient and respectful with the environments, is required. In recent years, the population is becoming more aware that it is vitally important to preserve and protect the environment. In this context, it is fundamental to develop new technologies more friendly to the environment.

Advanced oxidation processes (AOPs) are known to be powerful processes for the removal of recalcitrant organic pollutants that the traditional treatments are not able to eliminate. These methods are based on the in situ generation of mighty oxidants, such as hydroxyl radical (HO·), which attack the pollutants until its mineralization (Brillas and Martínez-Huitle 2015). Lately, sulfate radicals-based technology has attracted the interest of scientific community. This fact is because the sulfate radicals ($SO_4^{·-}$) have higher selectivity and longer half-life than hydroxyl radicals (Wang and Wang 2017). Sulfate radicals can be produced through the activation of persulfate ($S_2O_8^{2-}$) or peroxymonosulfate (HSO_5^-). Up to date, several methods of activation have been reported in the literature, including the presence of transition metals, UV irradiation, ultrasound, conduction electron, and so on (Ghanbari and Moradi 2017). In Fig. 1 are presented some of these processes.

The aim of this study was to evaluate the potential use of persulfate or peroxymonosulfate as active oxidants which generate sulfate radicals in the treatment of several

M. Arellano · M. Á. Sanromán · M. Pazos (✉)
BIOSUV Research Group, Centro de Investigación Tecnolóxico Industrial—MTI, University of Vigo, Campus As Lagoas-Marcosende, 36310 Vigo, Spain
e-mail: mcurras@uvigo.es

M. Arellano
e-mail: marellano@uvigo.es

M. Á. Sanromán
e-mail: sanroman@uvigo.es

Fig. 1 Activation methods of persulfate and peroxymonosulfate
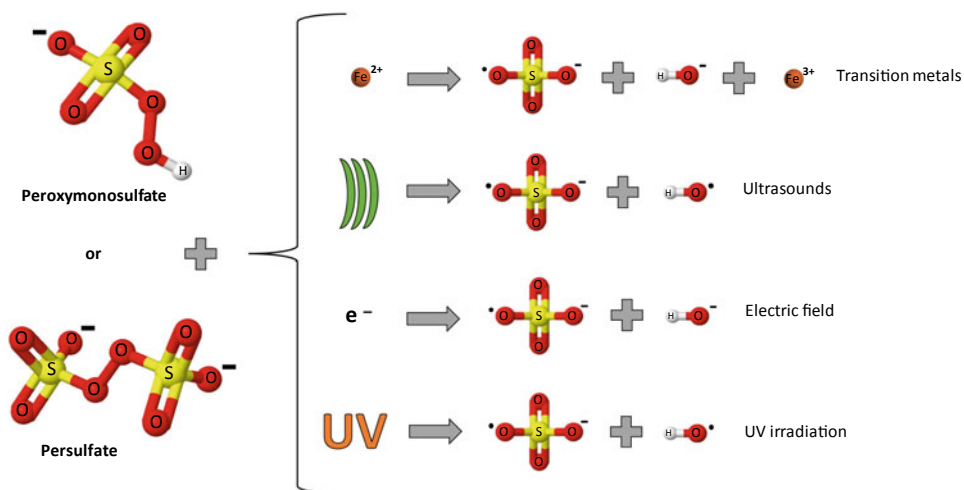
pollutants. For the pollutant selection, we focused on a classical industry such as textile, known as one of the oldest industrial procedures with a great economic relevance around the world, and the use of new solvents as ionic liquid, considered as contaminant on horizon. Thus, the selected pollutants were the dye, Lissamine Green B, and the ionic liquid 1-butyl-1-methylpyrrolidinium chloride ([bmpyr]Cl).

2 Materials and Methods

2.1 Chemicals

Persulfate (PS, $Na_2S_2O_8$), peroxymonosulfate (PMS, Oxone® $2KHSO_5 \cdot KHSO_4 \cdot K_2SO_4$), and iron (II) sulfate heptahydrate ($FeSO_4 \cdot 7H_2O$) were purchased from Sigma-Aldrich in analytical grade. H_2SO_4 or NaOH was used to adjust the pH and purchased from Prolabo. All of them were used without further purification. The solutions were prepared using purified water obtained by reverse osmosis technology (AquaMax-Basic 360).

2.2 Experimental Procedures

On the one hand, the homogeneous degradation of Lissamine Green B was evaluated through the activation of PS with iron. The experiments were carried out in a 0.25 L cylindrical glass reactor with 0.15 L of Lissamine Green B solution (7.5 mg/L) and PS concentration was 1 mM. Heterogeneous experiments were accomplished similar to previous experiments, and the catalyst was prepared by fixing the iron by adsorption on a cationic resin as Amberlite IR120 Na^+ form.

On the other hand, the removal of [bmpyr]Cl was assessed through the activation of PMS with the combination of iron catalyst (pyrite, goethite and magnetite) and

electric field. The [bmpyr]Cl concentration was 1.82 mM and different concentration ratios of PMS and iron were studied. The electrochemical experiments were accomplished in a cylindrical reactor with an operational volume of 150 mL. The assays were performed using a double-sided boron-doped diamond (BDD) as anode and carbon felt as cathode. Both electrodes were connected to a direct current power supply, using 10 mM Na_2SO_4 as supporting electrolyte.

2.3 Analytical Methods

The dye removal was followed by a spectrophotometer Jasco V-360, whereas the [bmpyr]Cl degradation was monitored by ionic chromatography with a conductivity detector (Metrohm 733 IC) equipped with a column Dionex™ Ion-Pac™ CS12 (CACTI, University of Vigo). The mineralization of pollutants was monitored from TOC decay, measured via TOC cuvette test Lange kit in a Hach DR 3900 spectrophotometer. It was determined as the difference between the total and the inorganic carbon.

3 Results and Discussion

3.1 Dye Lissamine Green B

The PS activation was evaluated through the efficiency of the dye degradation using iron as activator. Homogeneous and heterogeneous catalysts were carried out with an initial concentration of Lissamine Green B 7.5 mg/L and PS 1 mM. The dye removal was monitored by the absorbance measurement (Fig. 2).

In the case of the homogeneous catalyst, different concentrations of iron were added to the solution (0.1–0.4 mM)
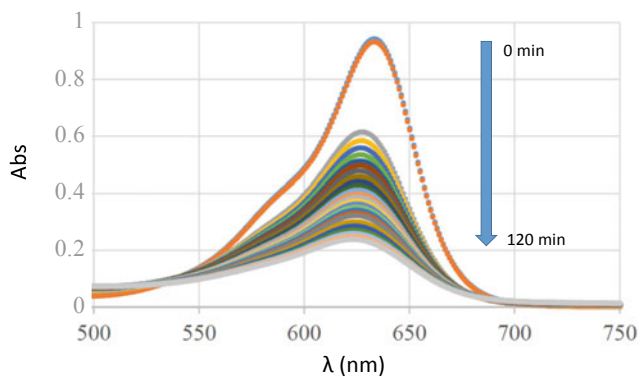
Fig. 2 Absorbance versus wavelength over time (Lissamine Green B = 7.5 mg/L, PS = 1 mM, Fe^{2+} = 0.1 mM)
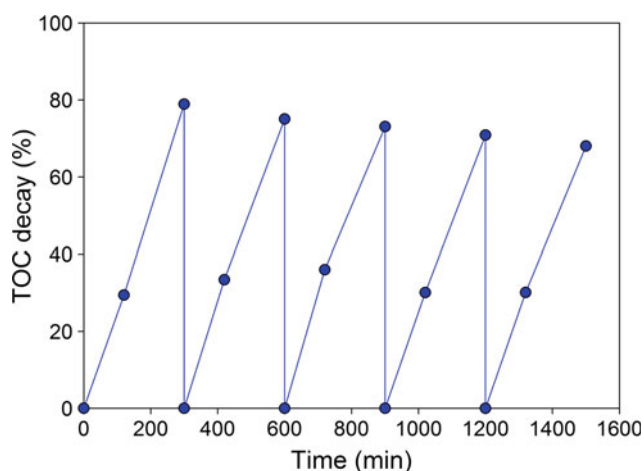
Fig. 3 Reusability of pyrite in order of TOC decay ([bmpyr] Cl = 1.82 mM, PMS = 10 mM, pyrite = 1 mM, I = 150 mA)

and it was demonstrated that the optimal concentration of iron was 0.3 mM. On the other hand, in the heterogeneous catalyst, the iron was adsorbed in amberlite. Several assays vary in the catalyst dosage (0.5–5 g), and when the concentration increases, highest degradation levels were achieved with dye removal of 93%, by adding 5 g of catalyst.

3.2 Ionic Liquid [bmpyr]Cl

The PMS activation was activated by the combination of electric field and iron. Various assays were carried out in order to set the optimal parameters, such as PMS concentration, source of iron, and current applied. Among the sources of iron used (pyrite, goethite, and magnetite), the best results were achieved with pyrite (1 mM) and PMS 10 mM under 150 mA. The use of solid catalyst eased its separation from the solution, and it was demonstrated that it can be reused at least 5 cycles (Fig. 3).

4 Conclusion

In this study, a sulfate radicals-based technology was proposed to the degradation of two different pollutants. Sulfate radicals were generated through the activation of PS and PMS, and their potential as powerful oxidants capable of degrading complex organic pollutants was demonstrated. Thus, the application of these processes for the management of effluents contaminated is a promising technology.

References

Brillas, E., & Martínez-Huitle, C. A. (2015). Decontamination of wastewaters containing synthetic organic dyes by electrochemical methods. An updated review. *Applied Catalysis B: Environmental, 166–167.* https://doi.org/10.1016/j.apcatb.2014.11.016.

Ghanbari, F., & Moradi, M. (2017). Application of peroxymonosulfate and its activation methods for degradation of environmental organic pollutants: Review. *Chemical Engineering Journal, 310,* 41–62. https://doi.org/10.1016/j.cej.2016.10.064.

Wang, J., & Wang, S. (2017). Activation of persulfate (PS) and peroxymonosulfate (PMS) and application for the degradation of emerging contaminants. *Chemical Engineering Journal, 334,* 1502–1517. https://doi.org/10.1016/j.cej.2017.11.059.

Fluoxetine and Pirimicarb Abatement by Ecofriendly Electro-Fenton Process

Emílio Rosales, António Soares, G. Buftia, Marta Pazos, G. Lazar,
Cristina Delerue-Matos, and M. Ángeles Sanromán

Abstract

Electro-Fenton generation of ·OH is more efficient and significant than the ·OH produced in the anode surface by anodic oxidation. Electro-Fenton process was optimised determining the relationship among key variables as electrodes surface and stirring rate. At optimal conditions, the combination of fluoxetine and pirimicarb was easily degraded with high mineralisation level.

Keywords

Fluoxetine • Pirimicarb • Electro-Fenton • Optimisation • Environmental treatment

E. Rosales · M. Pazos · M. Á. Sanromán (✉)
Centro de Investigación Tecnolóxico Industrial-MTI, University of Vigo, Campus As Lagoas-Marcosende, 36310 Vigo, Spain
e-mail: sanroman@uvigo.es

E. Rosales
e-mail: emiliorv@uvigo.es

M. Pazos
e-mail: mcurras@uvigo.es

A. Soares · C. Delerue-Matos
REQUIMTE-LAQV, Instituto Superior de Engenheria de Porto, Instituto Politécnico do Porto, Porto, Portugal
e-mail: tucasalves@hotmail.com

C. Delerue-Matos
e-mail: cmm@isep.ipp.pt

G. Buftia · G. Lazar
Faculty of Engineering, "Vasile Alecsandri" University of Bacau, Calea Marasesti 157, 600115 Bacau, Romania
e-mail: gabrielbuftia@gmail.com

G. Lazar
e-mail: glazar@ub.ro

1 Introduction

Emerging organic pollutants and persistent organic pollutants comprise a group of man-made compounds including pharmaceuticals and personal care products, pesticides, plasticisers whose consumption has increased in the last years due to the widespread use of these compounds. The presence of pharmaceuticals and pesticides has been confirmed in different water bodies, and one of the main sources of these pollutants is the effluents discharged from wastewater treatment plants (WWTPs). Traditional WWTPs are not able to remove efficiently these pollutants, and thus, the development of clean alternative technologies is a social requirement.

Advanced oxidation processes have arisen as sustainable alternatives for green remediation of wastewater. Among them, anodic oxidation (AO) and electro-Fenton (EF) processes are efficient and environmentally friendly technologies to remove organic compounds. Both processes are based on the *in situ* generation of a powerful oxidant, hydroxyl radical (·OH), which is able to degrade a wide variety of organic compounds. AO process is based on the direct reaction of the pollutants with the adsorbed ·OH formed at the anode surface (Rosales et al. 2019). The EF process is based on the Fenton reaction that is the catalytic decomposition of hydrogen peroxide in the presence of iron. One of the main advantages of the electrochemical process is the *in situ* generation of the hydrogen peroxide in the cathode surface by oxygen reduction reaction through a two-electron mechanism and also the regeneration of the catalyst in the cathode surface. As it was aforementioned, the cathode has an important role in the process and the most commonly used electrode materials include graphite, boron-doped diamond electrodes, carbon felt, ruthenium, etc.

In this work, the degradation of an emerging pollutant (fluoxetine) and a persistent organic pollutant (pirimicarb) by electro-Fenton was probed. Initially, a comparison

between two alternative techniques AO and EF was carried out. After that, several EF variables were studied and the optimisation of electrode sizes (anode and cathode) and agitation rate was carried out based on a response surface methodology for the degradation of fluoxetine. Then, operating at the optimal conditions, the simultaneous degradation of both pollutants was evaluated.

2 Materials and Methods

2.1 Reagents

Fluoxetine, pirimicarb, sodium sulphate and iron sulphate were purchased from Sigma-Aldrich. Sulphuric acid and acetonitrile were obtained from Panreac and Fisher Scientific. All the reagents were analytical grade. Electrode materials were purchased from Mersen and Neocoat S.A for graphite felt (GF) and boron-doped diamond (BDD), respectively.

2.2 Experimental Set-up

AO and EF assays were performed in a cylindrical reactor with an operational volume of 150 mL. AO assays were performed using a double-sided BDD (active area of 16 cm^2) as anode and GF as cathode, and EF assays were performed using GF of different sizes as anode and cathode electrodes. Both electrodes were connected to a direct current power supply by using 10 mM Na_2SO_4 as supporting electrolyte. The solution was acidified to pH 3 with H_2SO_4 and magnetic stirring was used to avoid concentration gradients. In the EF assays, iron sulphate (0.01 M) was added as catalyst for the generation of the Fenton reagent, and in order to assure the presence of enough oxygen in the treatment cell, air was continuously pumped close to the cathode at a flow of 1 L/min.

2.3 Response Surface Methodology (RSM)

It is an important tool for the improvement of treatment processes. RSM allows to study different design parameters and their influences in the behaviour of the degradation system determining those that have a significant effect on the treatment performance. In this work, the study was based on a central composite design face centred (CCDFC), and the selected factors for the study were: anode (6–41.40 cm^2) and cathode surface (6–41.40 cm^2) and cell stirring rate (200–800 rpm). The removal of pollutant was selected as response.

2.4 Fluoxetine and Pirimicarb Determination

Both pollutants were determined by HPLC-DAD (Agilent 1260 Infinity) using a column Agilent XDB8 5 μm, 150 mm × 4.6 mm (i.d.). An isocratic programme was used with 50% of acetonitrile (organic phase) and 50% of 10 mM KH_2PO_4 at pH 3.0 (aqueous phase) with a flow rate of 1 mL/min and a injection volume of 10 μL. The separation was carried out at room temperature, and the quantification of fluoxetine and pirimicarb was monitored spectrophotometrically at $\lambda = 227$ nm and $\lambda = 246$ nm, respectively.

2.5 Total Organic Carbon (TOC) Measurement

The mineralisation of pollutants was monitored from TOC decay, measured via TOC cuvette test Lange kit in a Hach DR 3900 spectrophotometer. It was determined as the difference between the total and the inorganic carbon.

3 Results and Discussion

3.1 AO Versus EF Degradation

Initially, two alternative treatments (AO and EF) were evaluated for the removal of the pharmaceutical compound. The obtained results showed that almost 90% of fluoxetine was removed after only 60 min with a higher degradation rate. On the other hand, AO achieved a degradation of 77% at the same time. The comparison of both techniques leads to conclude that the EF generation of ·OH is more efficient and significant than that produced in the anode surface by AO achieving higher removal efficiencies.

The removal of a pollutant not always implies the complete degradation of the compound, and therefore, the generation of intermediate compounds is feasible. For this reason, the mineralisation of the target pollutant was evaluated by following the TOC reduction. Similar behaviour to the previously exposed for the removal was observed. EF attained a higher TOC reduction around 50% after 60 min which was reduced close to 40% when the AO treatment was considered. A significant mineralisation is achieved after the treatment, but more time is required for attaining the complete mineralisation.

EF resulted in the most efficient technique for the elimination of fluoxetine from removal and mineralisation point of view, and as a consequence, the following experiments were carried out only using this technique.

3.2 EF Degradation Enhancement

Once the best performance of the EF system was confirmed, the treatment process was studied using a response surface methodology. Three operational variables affecting the performance of the treatment were selected, and their individual as well as combined effects were studied using a CCDFC. The experimental design resulted in 20 runs with 5 replicates at the central point.

The ANOVA using a second-order quadratic regression showed that the model was significant (*F value* 21.87 and *p-value* <0.001). The goodness of the fitting to the model and the description of the relation between the variables and the response were evaluated by the determination coefficient (R^2) with a value of 0.9516. It was also observed that the terms anode surface, cathode surface, stirring rate, the combination of anode–cathode surface, anode surface–stirring and the quadratic term of cathode surface resulted in significant model terms and showed an important effect in the pollutant abatement.

The combined effects of the independent variables in the degradation of fluoxetine are depicted in Fig. 1. As can be seen, the degradation increases with the anode surface and stirring. It is clear that both variables have a positive effect on the degradation. The cathode surface also influences the degradation, but operating at the maximum surface values presented a negative effect for the fluoxetine abatement.

3.3 Optimisation of the Degradation Process

Once it was demonstrated that the developed model can be applied to the design space, the optimisation of the process was performed under the premise of the maximisation of the pollutant abatement. Based on the desirability function, the optimal obtained conditions were: anode surface 28.96 cm^2, cathode surface 33.26 cm^2 and stirring 730 rpm. The determined conditions were validated experimentally, and the results showed differences lower than 2% between the theoretical and experimental degradation values proving the adequacy of the model for the prediction of the optimal conditions.

3.4 Simultaneous Degradation of Fluoxetine and Pirimicarb

Finally, the degradation of the combination of fluoxetine and pirimicarb was carried out operating at the optimal conditions determined previously and the mineralisation degree was also evaluated.

When the mixture of pollutants was treated, it was observed that a complete abatement for both of them was achieved after 60 min. The pesticide concentration profile showed a faster degradation rate attaining the total elimination of the pirimicarb after 10 min of treatment. In the
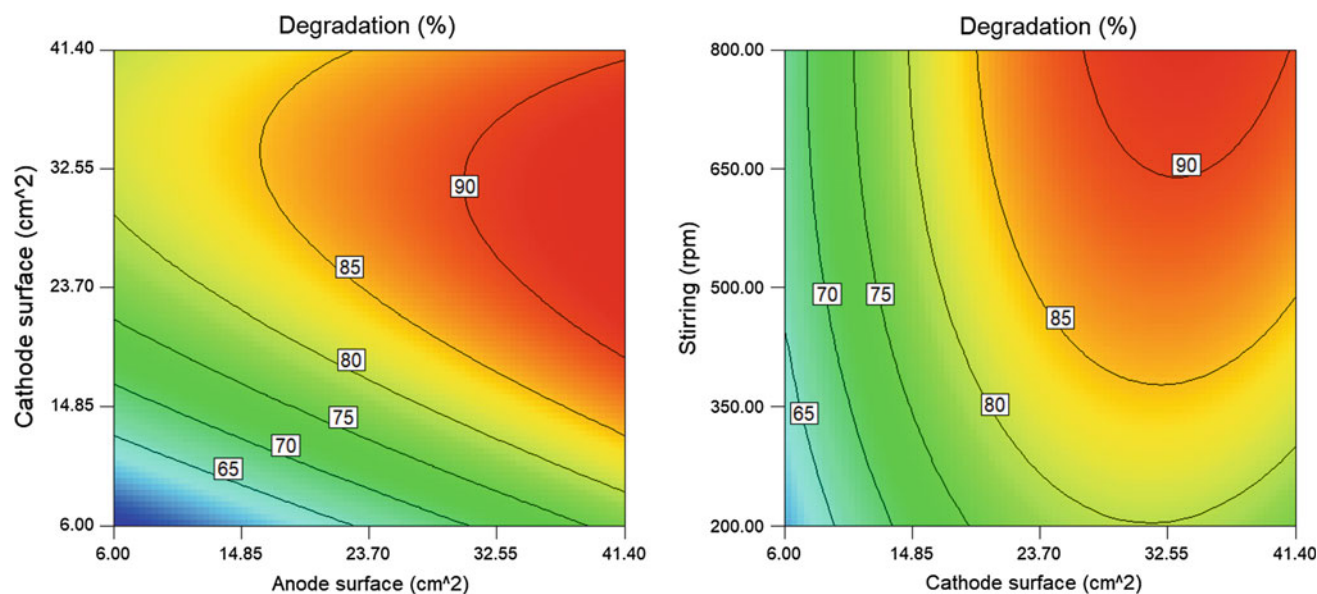
Fig. 1 Response surface plots for the evaluated variables

meantime, fluoxetine reached a degradation value around 55%, and 60 min was required for its abatement. Those data were compared with the obtained for the individual degradation of each compound separately. According to the individual degradation data, pirimicarb was not affected by the presence of another contaminant in the solution decreasing slightly its degradation rate. However, fluoxetine degradation was influenced by the presence of the pesticide showing differences between 10 and 20% on the removal levels along the time. The mineralisation data showed a different behaviour of the system after 60 min, however, the level reached confirms that EF process is an interesting alternative to the conventional treatment processes.

4 Conclusion

The abatement of the combination of a pesticide (pirimicarb) and the pharmaceutical (fluoxetine) was successfully performed by EF attaining high degradation and mineralisation levels. RSM resulted in an efficient tool for the determination of the selected optimal operational conditions. The developed treatment proved to be a viable solution for the removal of both pesticide and pharmaceutical products from effluents in a short period.

Reference

Rosales, E., Díaz, S., Pazos, M., & Sanromán, M. A. (2019). Comprehensive strategy for the degradation of anti-inflammatory drug diclofenac by different advanced oxidation processes. *Separation and Purification Technology* 208, 130–141.

Diversity and Performance of Sulphate-Reducing Bacteria in Acid Mine Drainage Remediation Systems

Enoch A. Akinpelu, Elvis Fosso-Kankeu, Frans Waanders, Justine O. Angadam, and Seteno K. O. Ntwampe

Abstract

Microbial diversity in acid mine drainage from eMalahleni, Mpumalanga, South Africa. Enrichment of SRB improves its performance in sulphate reduction. Microbial community shows synergy between SRB *Proteobacteria* and facultative *Bacilli*. Sulphate reduction of 85% and cadmium reduction of 98% were observed within 7 days of continuous operational mode. The microbial community showed wider substrates utilisation.

Keywords

Acid mine drainage • Sulphate-reducing bacteria • Heavy metal removal • Microbial diversity

1 Introduction

One of the perils of increasing industrial activity is the current increase in wastewater generation, which poses a threat to both human and aquatic environments. Mining is an example of such activities that has been on the rise, especially in developing nations due to its contribution to the economy of those countries. Mining activities do not utilise a considerable quantity of potable water compared to other industries, yet it is the largest producer of toxic wastewater (Corcoran 2010). Over a century, mining has contributed to the well-being of South Africans; hence, the country has many abandoned mine sites that are the primary source of several environmental and health problems (Mhlongo and Amponsah-Dacosta 2016). There are about 5906 abandoned mine sites in South Africa, due to the fact that mining operations cannot be relocated, generating approximately 6 billion tons of mine wastewater (Auditor-General 2009). The extraction of pyrite (sulphide bearing minerals) during mining activities exposes them to the atmosphere which leads to a chain of complex geochemical reactions that produce metal-laden acid mine drainage (AMD) and residual sulphate. Biological treatment with sulphate-reducing bacteria (SRB) is a recognised technology for the treatment of AMD. The ability of the SRB to remediate AMD and thus produce sulphide and bicarbonate in the presence of a suitable electron donor and carbon source aids the treatment of AMD. Culture-dependent and culture-independent approaches have been used to study the microbial diversity of air, soil, water and wastewater (Kamika and Momba 2014). The culture-independent technique has the advantage of direct analysis and classification of microbial populations in a specific environmental sample (Handelsman 2004; Riesenfeld et al. 2004). This study aims at, firstly, profiling the microbial community of SRB in AMD collected from coal mine in Mpumalanga, South Africa, and secondly, to determine the performance of the SRB consortium in a continuously stirred tank reactor (CSTR) containing AMD.

2 Materials and Methods

Acid mine drainage (AMD) samples were collected as wastewater from a coal mining site in Mpumalanga Province, South Africa, using standard sampling procedure (EPA 2007). The samples were filtered using 45-µm cellulose acetate filters and stored in a polyethylene bottle

E. A. Akinpelu (✉) · E. Fosso-Kankeu · F. Waanders
Water Pollution Monitoring and Remediation Initiatives Research Group, School of Chemical and Minerals Engineering, North-West University, P. Bag X60001, Potchefstroom, 2520, South Africa
e-mail: biyipelu@gmail.com

J. O. Angadam · S. K. O. Ntwampe
Bioresource Engineering Research Group (BioERG), Department of Chemical Engineering, Cape Peninsula University of Technology, Bellville Campus, Symphony Way, P.O. Box 1906 Cape Town, 7535, South Africa

at 4 °C. The physicochemical characteristics of AMD sample at a temperature of 20 °C had high redox potential (Eh = 229.5 mV) and low pH (2.98) including turbidity of 145 NTU and electrical conductivity of 7.84 mS/cm. A volume (100 mL) of AMD was inoculated in a sterile 500-mL bioreactor containing sterilised 400 mL modified Postgate medium B (Postgate 1984). The constituents of Postgate medium B were (g/L): KH_2PO_4 0.5; NH_4Cl 1.0; Na_2SO_4 1.0; $CaCl_2 \cdot 2H_2O$ 0.1; $MgSO_4$ 2.0; yeast extract 1.0; ascorbic acid 0.1; thioglycolic acid 0.1; $FeSO_4 \cdot 7H_2O$ 0.5; NaCl 26; sodium lactate 5 mL; and pH 7–7.5. The bioreactor was incubated anaerobically at 35 °C for 7 days until the colour of the medium changed to black-grey, which indicated a positive growth of the SRB (Ghazy et al. 2011). After 7 days of anaerobic incubation, 100 mL of inoculum containing numerous isolates was transferred into 400 mL sterile Postgate medium B in a new sterilised 500-mL bioreactor. The procedure was repeated thrice. All reagents were analytical grade.

The genomic DNA of the SRB sample was extracted and sequencing was done using 341F (5′—CCTACGG GNGGCWGCAG—3′) and 785R (5′—GACTACHVGGG-TATCTAATCC—3′) targeting V3—V4 of the 16S rRNA genes. The culturable SRB were cultured on nutrient agar supplemented with cycloheximide for bacteria growth, and rose bengal and potato dextrose agar supplemented with chloramphenicol and penicillin-streptomycin, respectively, for fungi growth. The identities of the pure strains and SRB consortium, together with the associated enzymes, were further confirmed in a series of biochemical reactions carried out on a VITEK® 2 Compact 30 system (BioMérieux, France) using the colorimetric reagent cards: BCL (Gram-positive spore-forming Bacilli), GN (Gram-negative), GP (Gram-positive) and YST (yeast and yeast-like organisms) as described previously (Akinpelu et al. 2017).

The anaerobic experiments were conducted in a 1-L working volume glass reactor equipped with an overhead stirrer fitted with a two-blade propeller for continuous mixing at 250 rpm. The bioreactors containing 800 mL Postgate medium B were initiated with 10% inoculum at 35 °C and pH around 7 for 21 days with 70% of the medium being drawn weekly and replaced with fresh Postgate medium B. Sodium bromoethanesulphonate (3.2 g/L) was added to the culture during enrichment (21 days) to avoid methanogenic activity. After establishing viable microbial population, fresh wastewater—AMD (10% v/v)—was introduced to the reactors operated in continuous mode. The reactors were kept in the continuous mode for 7 days and sampled at predetermined intervals. The reactors were left in a static batch mode for the next 14 days and then sampled.

3 Results and Discussion

According to the Illumina MiSeq analysis, a total read count of 133, 191 sequences of high quality was obtained from the AMD sample and assigned to different phyla. Overall, 11 phyla with 16 classes were identified, of which phyla *Firmicutes* (75.11%) and unknown microorganisms (24.61%) were the most abundant followed by *Proteobacteria* (0.25%), *Actinobacteria* (0.02%) and other low-abundance phyla. This study confirmed the dominance of *Firmicutes* and *Proteobacteria* in the microbial community of the AMD as was previously reported (Teng et al. 2017; Méndez-García et al. 2015; Kamika and Momba 2014). The biochemical results concurred with the metagenomics analyses, showing dominance of *Bacilli* in the microbial community; however, most of the species identified in VITEK® are facultative organisms such as *Bacillus smithii*, *B. cereus* and *B. thuringiensis*, as well as *B. subtilis* which grows strictly under anaerobic condition using nitrate as electron acceptor (Nakano and Zuber 1998; Hoffmann et al. 1995). The microbial community showed a wider range of substrate utilisation as expected. Notable amongst the substrates utilised were pyruvate, D-glucose, urea, acetate, and DL-lactate, amongst others.

In this study, the bioreactor was operated at temperature 35 ± 2 °C for 42 days, which included an enrichment stage and start-up pH of 7–7.5. On the 22nd day, raw heavy metal-laden AMD containing 8080 mg/L was supplied to the system. There was a gradual increase in sulphate reduction up to 1195 mg/L on the 7th day in continuous mode which was accompanied by microbial proliferation. This was indicative of a high performance by the SRB consortium, considering the initial sulphate concentration used in the system. The high residual sulphate concentration could be attributed to the low rate of reduction as well as higher concentrations of heavy metals in the raw AMD used. Earlier, Jong and Parry (2003) had shown that higher metal concentration inhibits SRB activities in sulphate reduction due to their toxicity and thus reduces SRB metabolism. In addition, a 50% reduction in SRB removal efficiency was caused by high copper concentration (Song et al. 1998). A drop in pH and an increase in redox potential (Eh) were observed at commencement of the continuous operational mode probably due to the introduction of highly acidic with high Eh of the raw AMD. After day 2 of operating in a continuous mode, there were a steady increase in the pH and a decrease in Eh, an indication of the SRB' adaptation to the new conditions. A similar increase in pH and a reduction in Eh were observed when AMD was treated in an up-flow anaerobic sludge blanket bioreactor and a packed bed bioreactor (Najib et al. 2017; Dev et al. 2016; Jong and Parry 2003).

Heavy metals were removed in the form of metal sulphide precipitates. Except Mg^{2+}, Zn^{2+}, As^{3+} and Cr^{3+} which showed removal percentages of 55, 58, 66 and 69%, respectively, all other metals being removed above 70%. It was reported that Al^{3+}, Cu^{2+}, Ni^{2+}, Fe^{2+} and Pb^{2+} are precipitated at pH below 7 but are completely precipitated at pH above 9.5 (Kurniawan et al. 2006; Aubé and Zinck 2003). Cd^{2+} showed the highest removal efficiency (98%) followed by Al^{3+} (97%). The high metal removal was due to the pH being below 7 and the presence of facultative heavy metal tolerant *B. cereus* which was identified in the SRB consortium. Some research has reported a complete removal of heavy metals in the range 80–90% of sulphate reduction operation (Chang et al. 2000; Drury 1999). Therefore, the high sulphate reduction (85%) and incomplete heavy metal removal in this study can be improved by optimising the process parameters such as pH, initial sulphate concentration and hydraulic retention time (HRT) while maintaining kinetically favourable conditions for the growth of the SRB.

4 Conclusion

The microbial profile showed that the phylum *Proteobacteria* was the predominant phylum constituting the SRB consortium with facultative members of phylum *Firmicutes*, being determined to be helpful in the removal of heavy metal in the form of precipitation. It was evident that enrichment time (21 days) of the SRB played a major role in the high sulphate reduction and heavy metal precipitation, including the ability of the SRB being able to utilise a wider substrate range as energy sources with the production of several aminopeptidases which act as biocatalyst in raw AMD treatment. This study can thus be helpful in the design of an effective bioprocess for the treatment of sulphate and heavy metal-laden AMD.

References

Akinpelu, E. A., Adetunji, A. T., Ntwampe, S. K. O., Nchu, F., & Mekuto, L. (2017). Biochemical characteristics of a free cyanide and total nitrogen assimilating *Fusarium oxysporum* EKT01/02 isolate from cyanide contaminated soil. *Data in Brief, 14,* 84–87.

Aubé, B., & Zinck, J. (2003). *Lime treatment of acid mine drainage in Canada* (pp. 1–12). Brazil-Canada Seminar on Mine Rehabilitation: Florianópolis.

Auditor-General, S. A. (2009). *Report of the Auditor-General to Parliament on a performance audit of the rehabilitation of abandoned mines at the Department of Minerals and Energy.* Pretoria.

Chang, I. S., Shin, P. K., & Kim, B. H. (2000). Biological treatment of acid mine drainage under sulfate-reducing conditions with solid waste materials as substrate. *Water Research, 34.*

Corcoran, E. (2010). *Sick water? The central role of wastewater management in sustainable development: A rapid response assessment.* UNEP/Earthprint.

Dev, S., Roy, S., & Bhattacharya, J. (2016). Understanding the performance of sulfate reducing bacteria based packed bed reactor by growth kinetics study and microbial profiling. *Journal of Environmental Management, 177,* 101–110.

Drury, W. J. (1999). Treatment of acid mine drainage with anaerobic solid-substrate reactors. *Water Environment Research, 71,* 1244–1250.

EPA. (2007). *EPA guidelines: Regulatory monitoring and testing water and wastewater sampling* (E. P. Authority, Ed.). South Australia.

Ghazy, E., Mahmoud, M., Asker, M., Mahmoud, M., Abo Elsoud, M., & Abdel Sami, M. (2011). Cultivation and detection of sulfate reducing bacteria (SRB) in sea water. *Journal of American Science, 7,* 604–608.

Handelsman, J. (2004). Metagenomics: Application of genomics to uncultured microorganisms. *Microbiology and Molecular Biology Reviews, 68,* 669–685.

Hoffmann, T., Troup, B., Szabo, A., Hungerer, C., & Jahn, D. (1995). The anaerobic life of *Bacillus subtilis*: Cloning of the genes encoding the respiratory nitrate reductase system. *FEMS Microbiology Letters, 131,* 219–225.

Jong, T., & Parry, D. L. (2003). Removal of sulfate and heavy metals by sulfate reducing bacteria in short-term bench scale upflow anaerobic packed bed reactor runs. *Water Research, 37,* 3379–3389.

Kamika, I., & Momba, M. N. (2014). Microbial diversity of Emalahleni mine water in South Africa and tolerance ability of the predominant organism to vanadium and nickel. *PLoS ONE, 9,* e86189.

Kurniawan, T. A., Chan, G. Y. S., Lo, W.-H., & Babel, S. (2006). Physico–chemical treatment techniques for wastewater laden with heavy metals. *Chemical Engineering Journal, 118,* 83–98.

Méndez-García, C., Peláez, A. I., Mesa, V., Sánchez, J., Golyshina, O. V., & Ferrer, M. (2015). Microbial diversity and metabolic networks in acid mine drainage habitats. *Frontiers in Microbiology, 6.*

Mhlongo, S. E., & Amponsah-Dacosta, F. (2016). A review of problems and solutions of abandoned mines in South Africa. *International Journal of Mining, Reclamation and Environment, 30,* 279–294.

Najib, T., Solgi, M., Farazmand, A., Heydarian, S. M., & Nasernejad, B. (2017). Optimization of sulfate removal by sulfate reducing bacteria using response surface methodology and heavy metal removal in a sulfidogenic UASB reactor. *Journal of Environmental Chemical Engineering.*

Nakano, M. M., & Zuber, P. (1998). Anaerobic growth of a "strict aerobe" (*Bacillus subtilis*). *Annual Review of Microbiology, 52,* 165–190.

Postgate, J. (1984). *The sulphate-reducing bacteria.* Cambridge: Cambridge University Press.

Riesenfeld, C. S., Schloss, P. D., & Handelsman, J. (2004). Metagenomics: Genomic analysis of microbial communities. *Annual Review of Genetics, 38,* 525–552.

Song, Y.-C., Piak, B.-C., Shin, H.-S., & La, S.-J. (1998). Influence of electron donor and toxic materials on the activity of sulfate reducing bacteria for the treatment of electroplating wastewater. *Water Science and Technology, 38,* 187–194.

Teng, W., Kuang, J., Luo, Z., & Shu, W. (2017). Microbial diversity and community assembly across environmental gradients in acid mine drainage. *Minerals, 7,* 106.

Sustainable Materials for Affordable Point-of-Use Water Purification

Sritama Mukherjee, Ligy Philip, and Thalappil Pradeep

Abstract

Nanoscale ferrihydrite incorporated biopolymeric composites prepared for arsenic removal from water. Composite shows excellent adsorption capacities for both arsenite and arsenate (overall >100 mg/g). Low dosage of the composite shows very fast kinetics over a wide pH range of water sample. The green synthesis yields a thermally stable composite with very high mechanical strength. This robust nanocomposite is industrially viable and offers an affordable and sustainable solution to arsenic contamination.

Keywords

Arsenic contamination • Nanomaterials • Remediation • Biopolymers • Ferrihydrite • Sustainability

1 Introduction

The United Nations considers universal access to clean water a basic human right and an essential step towards improving living standards worldwide. Based on the sources, water can have contaminants like microorganisms (pathogens), radionuclides such as uranium, nitrates and nitrites, fluoride and other heavy metal pollutants like lead, cadmium, chromium, mercury and arsenic, leading to poor-quality drinking water (Edition 2011). The World Health Organization (WHO) and leading environmental monitoring agencies have declared arsenic (As) contamination as a serious concern. Several countries across the world, like Bangladesh, India, Chile, China, Nigeria, etc., have higher levels of inorganic arsenic [As(III) and As(V)] levels reaching up to 3.05 ppm in groundwater, where 10 ppb is the permissible limit set by WHO (Edition 2011; Mandal and Suzuki 2002). Arsenic is an element, which is colourless, odourless and tasteless when dissolved in water, and is extremely toxic to human health (Bagla and Kaiser 1996). Arsenic poisoning or arsenicosis occurs when someone is exposed to high levels of arsenic, typically by unknowingly ingesting it, or occurs by inhalation or through dermal absorption (Bagla and Kaiser 1996).

The fundamental requirements for water purification are appropriate materials with high removal capacity, low cost, porosity and easy regeneration. Conventional remediation techniques like coagulation and various membrane-based filtration techniques have become obsolete due to their high cost, tedious handling or ineffectiveness in removal performance. In this regard, nanomaterials having very high surface area show large scope in the application of water purification, but its agglomeration restricts its use, which can be solved by converting nanomaterials to nanocomposites (Habuda-Stanić and Nujić 2015). In this context, biopolymers which have the characteristics like non-toxicity, biocompatibility, biodegradability, multifunctionalities and adsorption properties are important to be used as reinforcement agents for the nanoparticles which would provide higher mechanical strength to the composite and offer stability against agglomeration or disintegration, giving birth to efficient nanoadsorbents (Mohan and Pittman 2007). Various metallic/bimetallic nanoparticles based on Ti, Cu, Zr, Mn, Ce etc., have been studied for arsenic removal, but their expensive synthesis and environmental toxicity have restricted their transformation to technologies. While alumina, zero-valent iron and iron oxides-based magnetic

S. Mukherjee · T. Pradeep (✉)
DST-UNS, Department of Chemistry, Indian Institute of Technology Madras, Chennai 600036, India
e-mail: pradeep@iitm.ac.in

S. Mukherjee
e-mail: sritama.pu13@gmail.com

L. Philip
EWRE Division, Department of Civil Engineering, Indian Institute of Technology Madras, Chennai 600036, India
e-mail: ligy@iitm.ac.in

nanoparticles have been widely tested and were found to give a ray of hope, incorporation of such nanoparticles in biopolymeric cages has given rise to a new generation of nanocomposites (nanoadsorbents) which not only show superior adsorption capacities, but also prove to be sustainable and affordable for arsenic-affected communities. Biopolymers like chitosan, cellulose, alginate, lignin, etc., play an important role in the formation of templates in which relevant nanoparticles can be embedded. These polymers exhibit a range of hetero-atoms in their chemical structure which makes them very easily modifiable by insertion of different functional groups as per requirement, and they also impart good strength to the composite due to their ease of crosslinking. Chitosan (derived from chitin) has been deeply explored which shows great utility towards decontamination of water or wastewater from various pollutants like organic (dyes, etc.) and inorganic (metal ions, etc.), with the help of suitable modifications. Nanocrystalline metal oxyhydroxide-chitosan granular composite materials with silver nanoparticles embedded in it were investigated by Sankar et al., to achieve antimicrobial activity along with scavenging toxic species like arsenic, lead, etc., from water (Sankar et al. 2013). Similarly, Anil Kumar et al. have shown confined metastable 2-line iron oxyhydroxide-chitosan composite for effective removal of As(III) and As(V) from water, resulting in a technology called AMRIT (Arsenic and Metal Removal by Indian Technology), which has been implemented in the arsenic- and iron-affected regions of West Bengal and currently serving 30,000 people (Kumar et al. 2017).

Cellulose is another class of biopolymer emerging as a cost-effective, efficient, environment-friendly and an alternative technique to conventional technologies. Abundance, ease of availability and relatively less-complicated extraction process make cellulose a cheaper and greener option for making nanoadsorbents, as compared to other biopolymers. In this work, we exhibit microcrystalline cellulose (MCC) templated 2-line ferrihydrite nanocomposite used for arsenic removal from water which has high affinity towards both As(III) and As(V), showing large adsorption capacities for both species.

2 Materials and Methods

Synthesis: Microcrystalline cellulose (MCC) templated 2-line ferrihydrite nanocomposite was synthesized at room temperature by one-pot procedure involving mixing cellulose and iron precursor in water, followed by precipitation, by simple mechanical stirring throughout, for 24 h. This water-based green synthesis finally resulted in the formation of a slurry which was then filtered, washed and subsequently dried to get granular composite.

Batch studies: 25 mg of the composite was added to 100 ml of As(III)/As(V) spiked water, shaken for 2 h at pH 7. The treated water was then acid digested to prepare samples for inductively coupled plasma mass spectrometry (ICPMS) measurements.

3 Results and Discussion

The granular composite was subjected to various characterization techniques like scanning electron microscope (SEM), high-resolution tunneling electron microscope (HRTEM) and elemental mapping, energy-dispersive spectroscopy (EDS), X-ray diffraction (XRD) etc., to confirm its structural and functional properties. Figure 1a and b shows the optical images of native microcrystalline cellulose powder used as raw material and the final form of granular composite to be used for the adsorption experiments, respectively. Upon the formation of composite, metastable ferrihydrite nanoparticles get entrapped in cellulosic fibre cages, and the overall composite exhibits amorphous behaviour which is shown in Fig. 1c. Upon illuminating the composite with electron beam of regulated energy for sometime, we can see polycrystalline features of ferrihydrite and hematite (more stable form) appear. Appearance of 110 and 115 planes in XRD features shown in Fig. 1c[(i) and (ii)] further confirmed the formation of 2-line ferrihydrite (FeOOH), which also shows that the composite lost the crystalline nature shown by parent MCC fibres. Elemental mapping of adsorbed As(III) and As(V) on the composite is shown in inset of Fig. 1c, which reveals homogeneous distribution of arsenic species over the surface of the composite. EDS of the saturated As(III)/As(V) composites revealed that more amount of As(III) was adsorbed on the surface than As(V) at pH 7. To probe the surface morphology, SEM was done, as shown in Fig. 1d and e, where MCC shows flaky structure, and the composite shows completely different granular and dense morphology, respectively. No change in surface characteristics was observed after the composite was exposed to As(III)/As(V), suggesting high mechanical strength of the composite. To analyse the strength in details, direct shear tests in dry and wet conditions were conducted which gave decent values for angle of internal friction (Φ), comparable to that of sand. Mechanical strength is an important parameter to be considered in this regard because it not only suggests about the durability of the granular material but also indicates the tendency to leach adsorbate molecules in water again. TGA of the composites showed that a total of only 23% weight loss occurred when heated from room temperature to 900 °C, suggesting good thermal stability of the material. Batch studies have shown that about 25 mg of the composite dosage is enough for lowering the As value from 1000 ppb
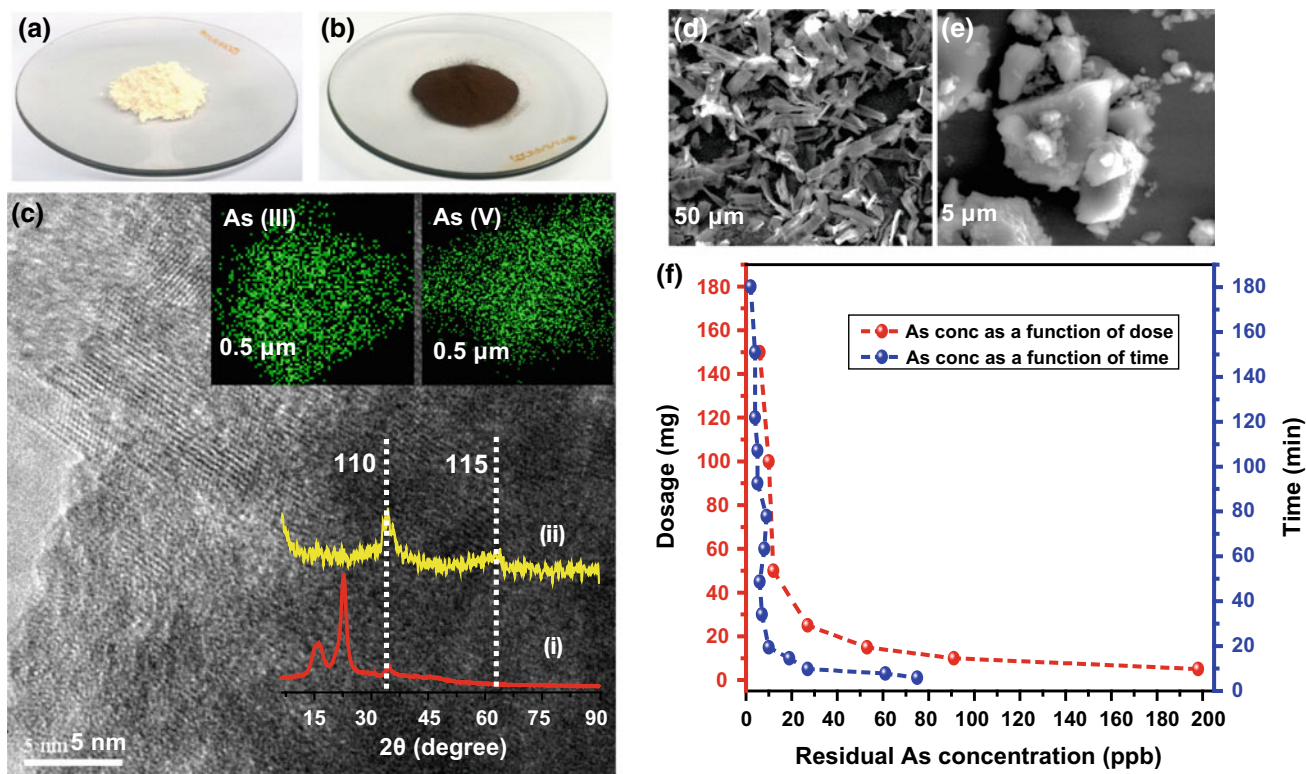
Fig. 1 Characterization of the composite and batch studies. Optical images of **a** native MCC; **b** composite; **c** HRTEM of composite, elemental mapping of As(III) and As(V) (inset), XRD pattern of (i) native MCC, (ii) composite, SEM images; **d** native MCC; **e** composite; **f** batch studies showing dosage and kinetics of adsorption

to less than 10 ppb for 100 mL of water sample. The composite shows very fast kinetics of adsorption; that is, exposure of 15 min is enough for bringing down the As concentration to safe level, as shown in Fig. 1f.

Also, the performance of the composite was studied in a wide range of pH 4–10. It was observed that the adsorption performance remained unaffected by the pH environment. Applying the Langmuir isotherm equation, high adsorption capacities of the composite for As(III) as 140 mg/g and As(V) as 50 mg/g were obtained, which prove to be much higher as compared to other commercial adsorbents currently available. Moreover, to check the factor of sustainability, the composite does not leach out As or Fe in water with time, even at its saturated state, as indicated by toxicity characteristic leaching protocol (TCLP) studies, along with easy regeneration possibility.

4 Conclusion

To summarize this work, MCC templated 2-line ferrihydrite composite was prepared by green synthesis at room temperature, water as solvent and the synthesis did not generate any harmful by-products. The nanocomposite has high affinity towards both As(III) and As(V) with an average removal capacity of >100 mg/g. The developed nanoadsorbent is composed of the active FeOOH nanoparticles tightly confined in a cellulose matrix to prevent contaminant leaching and exhibit excellent removal performance with fast kinetics. The composite is robust and can be used in a gravity-fed water purifier in which arsenic and iron-containing water is passed through the composite filter unit to obtain water, conforming to international standards. This nanotechnology will result in an energy-efficient prototype, making it a sustainable solution and capable of delivering affordable As-free drinking water at an estimated cost of US $ 1.5 per year per person in resource-limited settings. (The full work has been published as Sritama Mukherjee et al., ACS Sustainable Chem. Eng. 2019, 7, 3, 3222–3233).

References

Bagla, P., & Kaiser, J. (1996). India's spreading health crisis draws global arsenic experts. *Science, 274,* 174–175.

Edition, F. (2011). Guidelines for drinking-water quality. *WHO Chronicle, 38,* 104–108.

Habuda-Stanić, M., & Nujić, M. (2015). Arsenic removal by nanoparticles: A review. *Environmental Science and Pollution Research, 22,* 8094–8123.

Kumar, A. A., Som, A., Longo, P., Sudhakar, C., Bhuin, R. G., Gupta, S. S., et al. (2017). Confined metastable 2-line ferrihydrite for affordable point-of-use arsenic-free drinking water. *Advanced Materials, 29.*

Mandal, B. K., & Suzuki, K. T. (2002). Arsenic round the world: A review. *Talanta, 58,* 201–235.

Mohan, D., & Pittman, C. U., Jr. (2007). Arsenic removal from water/wastewater using adsorbents—A critical review. *Journal of Hazardous Materials, 142,* 1–53.

Sankar, M. U., Aigal, S., Maliyekkal, S. M., Chaudhary, A., Kumar, A. A., Chaudhari, K., et al. (2013). Biopolymer-reinforced synthetic granular nanocomposites for affordable point-of-use water purification. *Proceedings of the National Academy of Sciences, 110,* 8459–8464.

Self-Forming Dynamic Membrane: A Review

J. M. J. Millanar-Marfa, Laura Borea, Mark Daniel G. De Luna,
Vincenzo Belgiorno, and Vincenzo Naddeo

Abstract

This paper presents self-forming dynamic membrane (SFDM) process as a promising alternative to membrane technology. A stable dynamic membrane (DM) is mainly composed of gel layer and cake layer which are responsible for filtration and biodegradation. An understanding of the formation mechanism and impact of operating conditions, support mesh, sludge properties and configuration on the formation, and characteristics of the dynamic membrane is essential to optimize the efficiency and reduce fouling propensity of this technology. The paper thus aims to promote its applicability on wastewater treatment. Review of the influence of mesh support properties, different operating conditions and sludge properties on SFDM performance, and cost comparison between MBR and SFDMBR technologies.

J. M. J.Millanar-Marfa · M. D. G. De Luna
Environmental Engineering Program, National Graduate School of Engineering, University of the Philippines, Quezon City, Philippines

L. Borea · V. Belgiorno · V. Naddeo (✉)
Sanitary Environmental Engineering Division, Department of Civil Engineering, University of Salerno, Fisciano, Italy
e-mail: vnaddeo@unisa.it

M. D. G. De Luna
Department of Chemical Engineering, University of the Philippines, Quezon City, Philippines

1 Introduction

Conventional activated sludge (CAS) process has been widely used due to its efficiency in removing organic matter and suspended solids from wastewater since the 1930s. As population increased with industrialization in the 1940s, water use increased twice as much. Large volume of wastewater, high effluent quality requirements, and limitation in space for sedimentation led to new methods for wastewater treatment (Pellegrin et al. 2009; Visvanathan et al. 2017).

The advantages of membrane bioreactors (MBR) over CAS such as small footprint, high effluent quality, low sludge production, (Saleem et al. 2016), high nutrients, and persistent organic micropollutants removal (Meng et al. 2017) led to their application on wastewater treatment. However, low flux, fouling, high energy demand, and high cost of membrane modules have been the major drawbacks of this process.

As an alternative to membrane filtration, mesh filtration coupled with dynamic membrane (DM) has been explored (Alibardi et al. 2016). This process has lower operational and capital cost, easier membrane fouling control, and higher membrane flux (Xiong et al. 2016). This method utilizes the deposited layer of suspended solids (SS), colloids, and microbial cells on the mesh support commonly referred to as DM.

Several studies have been made to explore the applicability of DM to wastewater treatment. Due to the complexity of DM formation, a thorough study is needed to understand the effects of various factors on its formation, efficiency, and fouling propensity. It is also worthwhile to check the cost-effectiveness of SFDMBR compared to MBRs.

2 Dynamic Membrane: Parts, Function, and Formation

The DM is comprised of cake layer and gel layer (Ersahin et al. 2014). Some studies noted that the cake layer removes COD by biodegradation and the gel layer removes total suspended solids (TSS) (Fan and Huang 2002; Zhang et al. 2014) while other studies (Xiong et al. 2016; Zhou et al. 2008) cited that the role of cake layer is crucial in the filtration process and membrane filtration resistance.

DM formation is a vital key in the self-forming dynamic membrane (SFDM) technology. Liu et al. (2009) proposed that DM formation occurs in four stages including substrate formation, separation layer formation, fouling layer formation, and filtration cake formation. Studies on submerged DM noted the formation of an effective DM within 10–20 days (Ersahin et al. 2014, 2017) while (Xiong et al. 2016) noted that the cake layer which protects the inner gel layer can be formed within an hour of operation whereas the gel layer takes more time to form. Once formed, the gel layer tightly binds on the surface and makes the surface more hydrophilic (Fan and Huang 2002).

3 Support Material, Operating Conditions, and Sludge Properties: Impact on Dynamic Membrane

SFDM efficiency is highly dependent on the formation and characteristics of the DM (Alibardi et al. 2016) that may be affected by support material, operating conditions, and sludge properties. Several materials from woven and non-woven fabric to stainless steel were used as support material for SFDM. Studies noted that flux and effluent turbidity decrease with decreasing pore size (Cai et al. 2018;

Wu 2003). The same result was obtained by Salerno et al. (2017) where smaller pore size and low air scouring intensity in aerobic SFDMBR gave higher effluent quality. Furthermore, support material hydrophobicity was noted to affect DM formation (Liang et al. 2013).

Moreover, Saleem et al. (2016), found that high filtration flux resulted in faster DM deposition but caused high effluent TSS due to DM deterioration. Mixed liquor suspended solids (MLSS) had less significance compared to filtration flux. Furthermore, increasing organic loading rate (OLR) by low hydraulic retention time (HRT) caused a significant transmembrane pressure (TMP) to increase. It was also noted that high SRT and low F/M ratio led to lower biodegradation due to endogenous growth (Alibardi et al. 2016; Ersahin et al. 2014; Zhang et al. 2014).

The impact of aeration rate and dissolved oxygen (DO) concentration is essential in SFDMBR technology. Aeration increases DO concentration for biodegradation process in the reactor (Rezvani et al. 2014). Wu et al. (2005) and Zhou et al. (2008) noted that higher biodegradation happened on the DM surface where DO concentration was higher. Nonetheless, high aeration rate was observed to increase effluent TSS, finer flocs, and higher resistance (Ersahin et al. 2014; Salerno et al. 2017).

Sludge properties such as particle size distribution, viscosity, hydrophobicity, and EPS content strongly affect the DM. Contrary to MF/UF systems, DM formation was observed faster for sludge with large particle size. Faster DM formation was also noted with high sludge relative hydrophobicity. Furthermore, sludge viscosity was correlated to EPS concentration and was concluded to cause SFDM fouling (Liang et al. 2013; Yu et al. 2015, 2016, 2018). In order to enhance SFDM applicability, Liang et al. (2012), found that intermittent effluent production is important to reduce irreversible fouling of SFDM.
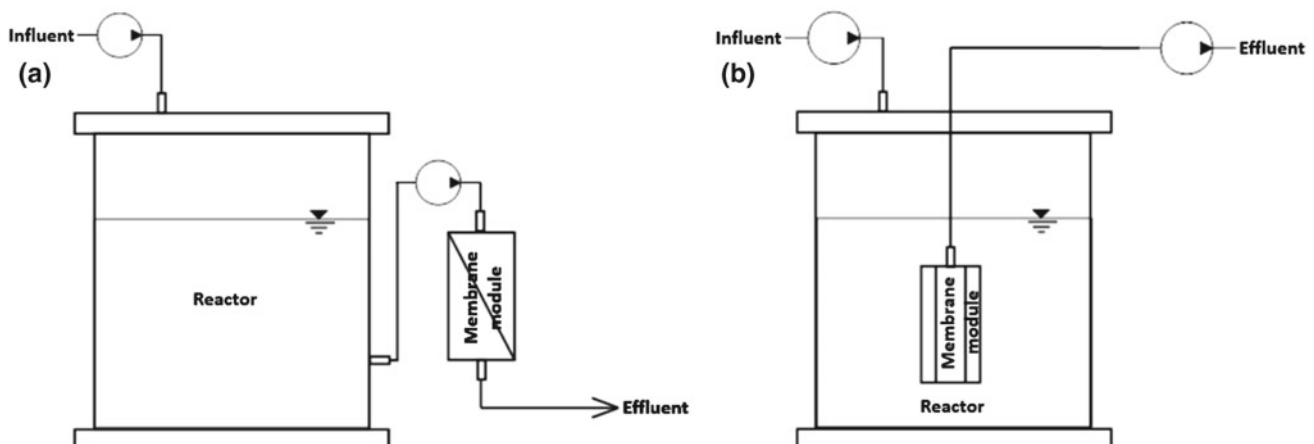
Fig. 1 SFDMBR configurations **a** external, **b** submerged

4 Self-Forming Dynamic Membrane Bioreactor (SFDMBR) Configuration

Generally, SFDMBR configuration is classified into two types, namely external and submerged configurations. However, submerged type is widely explored since this configuration requires less energy for cleaning the module. Figure 1 shows the basic diagrams of SFDMBR configurations.

5 SFDMBR and MBR: Cost Comparison

SFDMBR has recently been gaining attention due to its relatively lower capital and operational cost compared to MBR. Firstly, the support material in SFDMBR can be cheap materials with large pore size such as woven or non-woven fabric and mesh whereas MBR requires polymers with intricately small pores. Additionally, due to smaller pore size, MBR operation needs more frequent cleaning that can be energy intensive and can lead to shorter membrane longevity (Zhang et al. 2014).

References

Alibardi, L., Bernava, N., Cossu, R., & Spagni, A. (2016). Anaerobic dynamic membrane bioreactor for wastewater treatment at ambient temperature. *Chemical Engineering Journal, 284,* 130–138. https://doi.org/10.1016/j.cej.2015.08.111.

Cai, D., Huang, J., Liu, G., Li, M., Yu, Y., & Meng, F. (2018). Effect of support material pore size on the filtration behavior of dynamic membrane bioreactor. *Bioresource Technology, 255,* 359–363. https://doi.org/10.1016/j.biortech.2018.02.007.

Ersahin, M. E., Ozgun, H., Tao, Y., & van Lier, J. B. (2014). Applicability of dynamic membrane technology in anaerobic membrane bioreactors. *Water Research, 48*(1), 420–429. https://doi.org/10.1016/j.watres.2013.09.054.

Ersahin, M. E., Tao, Y., Ozgun, H., Gimenez, J. B., Spanjers, H., & van Lier, J. B. (2017). Impact of anaerobic dynamic membrane bioreactor configuration on treatment and filterability performance. *Journal of Membrane Science*, *526*, 387–394. https://doi.org/10.1016/j.memsci.2016.12.057.

Fan, B., & Huang, X. (2002). Characteristics of a self-forming dynamic membrane coupled with a bioreactor for municipal wastewater treatment. *Environmental Science and Technology, 36*(23), 5245–5251. https://doi.org/10.1021/es025789n.

Liang, S., Qu, L., Meng, F., Han, X., & Zhang, J. (2013). Effect of sludge properties on the filtration characteristics of self-forming dynamic membranes (SFDMs) in aerobic bioreactors: Formation time, filtration resistance, and fouling propensity. *Journal of Membrane Science, 436,* 186–194. https://doi.org/10.1016/j.memsci.2013.02.021.

Liang, S., Zhao, T., Zhang, J., Sun, F., Liu, C., & Song, L. (2012). Determination of fouling-related critical flux in self-forming dynamic membrane bioreactors: Interference of membrane compressibility. *Journal of Membrane Science, 390–391,* 113–120. https://doi.org/10.1016/j.memsci.2011.11.026.

Liu, H., Yang, C., Pu, W., & Zhang, J. (2009). Formation mechanism and structure of dynamic membrane in the dynamic membrane bioreactor. *Chemical Engineering Journal, 148*(2–3), 290–295. https://doi.org/10.1016/j.cej.2008.08.043.

Meng, F., Zhang, S., Oh, Y., Zhou, Z., Shin, H. S., & Chae, S. R. (2017). Fouling in membrane bioreactors: An updated review. *Water Research, 114,* 151–180. https://doi.org/10.1016/j.watres.2017.02.006.

Pellegrin, M.-L., Menniti, A., Zhang, K., McCandless, R., Law, K., Gluck, S. … Deniz, T. (2009). *Membrane processes*. *Water environment research* (Vol. 81). https://doi.org/10.2175/106143009X12445568399578.

Rezvani, F., Mehrnia, M. R., & Poostchi, A. A. (2014). Optimal operating strategies of SFDM formation for MBR application. *Separation and Purification Technology, 124,* 124–133. https://doi.org/10.1016/j.seppur.2014.01.028.

Saleem, M., Alibardi, L., Lavagnolo, M. C., Cossu, R., & Spagni, A. (2016). Effect of filtration flux on the development and operation of a dynamic membrane for anaerobic wastewater treatment. *Journal of Environmental Management, 180,* 459–465. https://doi.org/10.1016/j.jenvman.2016.05.054.

Salerno, C., Vergine, P., Berardi, G., & Pollice, A. (2017). Influence of air scouring on the performance of a Self Forming Dynamic Membrane BioReactor (SFD MBR) for municipal wastewater treatment. *Bioresource Technology, 223,* 301–306. https://doi.org/10.1016/j.biortech.2016.10.054.

Visvanathan, C., Aim, R. B., & Parameshwaran, K. (2017). Technology membrane separation bioreactors for wastewater treatment, *3389*. https://doi.org/10.1080/10643380091184165.

Wu, Y. (2003). Effect of mesh pore size on performance of a self-forming dynamic membrane coupled bioreactor for domestic wastewater treatment. In *5th International Membrane Science and Technology Conference*, November (pp. 1–6). Retrieved from http://www.membrane.unsw.edu.au/imstec03/content/papers/WWT/imstec183.pdf.

Wu, Y., Huang, X., Wen, X., & Chen, F. (2005). Function of dynamic membrane in self-forming dynamic membrane coupled bioreactor. *Water Science and Technology, 51*(6–7), 107–114.

Xiong, J., Fu, D., Singh, R. P., & Ducoste, J. J. (2016). Structural characteristics and development of the cake layer in a dynamic membrane bioreactor. *Separation and Purification Technology, 167,* 88–96. https://doi.org/10.1016/j.seppur.2016.04.040.

Yu, H., Wang, Z., Wu, Z., & Zhu, C. (2015). Dynamic membrane formation in anaerobic dynamic membrane bioreactors: Role of extracellular polymeric substances. *PLoS ONE, 10*(10). https://doi.org/10.1371/journal.pone.0139703.

Yu, H., Wang, Z., Wu, Z., & Zhu, C. (2016). Enhanced waste activated sludge digestion using a submerged anaerobic dynamic membrane bioreactor: Performance, sludge characteristics and microbial community. *Scientific Reports, 6*(1), 20111. https://doi.org/10.1038/srep20111.

Yu, Z., Hu, Y., Dzakpasu, M., & Wang, X. C. (2018). Thermodynamic prediction and experimental investigation of short-term dynamic membrane formation in dynamic membrane bioreactors: Effects of sludge properties. *Journal of Environmental Sciences (China)*, 1–12. https://doi.org/10.1016/j.jes.2018.06.017.

Zhang, Y., Zhao, Y., Chu, H., Dong, B., & Zhou, X. (2014). Characteristics of dynamic membrane filtration: Structure, operation mechanisms, and cost analysis. *Chinese Science Bulletin, 59*(3), 247–260. https://doi.org/10.1007/s11434-013-0048-x.

Zhou, X. H., Shi, H. C., Cai, Q., He, M., & Wu, Y. X. (2008). Function of self-forming dynamic membrane and biokinetic parameters' determination by microelectrode. *Water Research, 42*(10–11), 2369–2376. https://doi.org/10.1016/j.watres.2008.01.004.

Influence of Membrane Flux, Ultrasonic Frequency and Recycle Ratio in the Hybrid Process USAMe

Laura Borea, Vincenzo Naddeo, and Vincenzo Belgiorno

Abstract

This paper focused on the combination of membrane ultrafiltration, adsorption and ultrasound processes in one hybrid process called USAMe for improving membrane wastewater treatment performance and membrane fouling control. Different tests were conducted at different ultrasound frequencies and recycle ratio. Improved permeate quality in the USAMe process. Membrane fouling reduction with the combined application of ultrasound and activated carbon. Influence of ultrasound frequency, membrane flux and recycle ratio on treatment performance.

1 Introduction

The water resources scarcity and its increasing demand have put the attention on water quality protection and the implementation of wastewater reuse practices.

Therefore, the need of high effluent quality in wastewater treatment plant, even related to the more stringent regulation standard, has led to the development of tertiary treatment in order to increase the removal efficiencies of conventional and emerging contaminants.

The tertiary treatments include membrane filtration processes, adsorption, advanced oxidation processes such as the ultrasonic process, ion exchange and other chemical and physical processes (Ahmad et al. 2012; Gogate et al. 2003; Naddeo et al. 2013). The choice of tertiary treatment to be applied is influenced by different factors such as the end use of the effluent, the nature of the wastewater, the compatibility of the various units of the process and the construction and management costs.

Advanced oxidation processes are able to degrade recalcitrant organic substances that are transformed into simpler compounds by hydroxyl radical formations.

Membrane filtration process, using different porosity, allows colloidal and particulate separation through a physical separation. This technology is characterized by reduced dimensions of the treatment units and high removal efficiencies. The main disadvantage, however, is related to membrane fouling formation which results in an increase in the operating costs. Conventional fouling control methods are physical, such as the flushing and backwashing, or chemical methods.

In the last decades, the research studies have been focused on the identification of innovative strategies for membrane fouling reduction. To this end, the combination of membrane filtration with different processes such as ultrasound or adsorption has been investigated (Borea et al. 2018; Naddeo et al. 2015; Secondes et al. 2014). These processes allow simultaneously, unlike conventional techniques, the fouling formation control and the filtration activity, without their interruption. The adsorption on activated carbons increases, indeed, the performance of membrane filtration process since it removes the substances responsible for membrane fouling formation which deposit on the membrane surface and, at the same time, increases permeate water quality. The ultrasonic process causes the detachment of fouling layer on the surface of the membrane created by the cavitation bubbles collapse while hydroxyl radicals,

L. Borea · V. Naddeo (✉) · V. Belgiorno
Sanitary Environmental Engineering Division, Department of Civil Engineering, University of Salerno, Fisciano, Italy
e-mail: vnaddeo@unisa.it

L. Borea
e-mail: lborea@unisa.it

V. Belgiorno
e-mail: v.belgiorno@unisa.it

formed by sonolysis, degrade the organic substance increasing the quality of the effluent (Hashemi Shahraki et al. 2014).

The present study regards the application of the USAMe process, which involves the combined use of membrane filtration, ultrasound and activated carbon adsorption, for real municipal wastewater treatment in order to investigate its efficiencies at different ultrasonic frequencies and recycle ratios.

The results showed that ultrafiltration treatment is much more effective when combined with adsorption and/or ultrasound, both to reduce fouling and the improvement of the characteristics permeate.

The tests combined with adsorption, ultrafiltration and ultrasounds have shown regardless of stream used, speed training of minor fouling, especially at low frequencies, and an improvement of the characteristics of the permeate. In the ultrasonic process with lower frequencies, the cavitation bubbles are larger and collapse more vigorously causing over the posting of fouling and improving the effluent turbidity. While the high frequencies produce a greater number of cavitation bubbles, that smaller, but collapsing favour an increased formation of hydroxyl radicals with high oxidizing power which allow a high reduction of the organic substance. The permeate quality, however, is independent of the flow conditions.

USAMe® tests, which include combining all processes, have shown a decrease in the rate of formation of fouling as transmembrane pressures increase less rapidly than the individual processes and characteristics of the permeate will be improved.

The tests USAMe®, involving the combination of all the processes, have demonstrated a decrease of fouling rate since the transmembrane pressures increase rapidly less than the individual processes, and the quality permeate is improved.

This technology has, therefore, proved to be an effective upgrading of ultrafiltration membrane as well as a valid alternative to conventional commercial processes.

Further studies will be needed to pilot scale by assessing the applicability of the treatment in terms of efficiency and cost estimation.

2 Materials and Methods

Different tests were run by ultrafiltration and its combination with ultrasound and/or adsorption on wastewater effluent of secondary sedimentation from a municipal wastewater treatment plant. The experimental set-up, utilized in this study, was reported in Fig. 1. An ultrasonic bath (Elma® TI-H-10 MF3 230 V) with a volume of about 8.6 L was used as an ultrasonic source.

The US bath was characterized by an electrical nominal power varying from 200 to 800 W and an average ultrasonic power intensity from 0.3 to 1.1 W/cm^2. Laboratory tests were conducted changing three streams for the feed flow rate (75, 150 and 225 l/m^2 h), two ultrasonic frequencies (35 and 130 kHz) and three different ratios of recirculation.

The membrane unit was made of a single hollow fibre polysulfone ultrafiltration membrane (A/G Technology Corporation, USA) enclosed in a glass tube in order to collect the permeate with an inside-outside flow in a cross-flow configuration. The membrane, characterized by a filtration area of 6.6 cm^2 and a nominal pore size of 0.1 μm, was immersed at the centre of bath, filled with 5 L of DI water, and at a distance of 2.5 cm.

3 Results and Discussion

The results showed that ultrafiltration treatment is much more effective when combined with adsorption and/or ultrasound, both to reduce fouling and to improve the effluent quality.

The tests combined with adsorption, ultrafiltration and ultrasounds have shown lower fouling rates, especially at low frequencies, and an improvement of the characteristics of the permeate. In the ultrasonic process with lower frequencies, the cavitation bubbles are larger and collapse more vigorously. While the high frequencies increased the formation of hydroxyl radicals with high oxidizing power which allowed a high reduction of the organic substances.
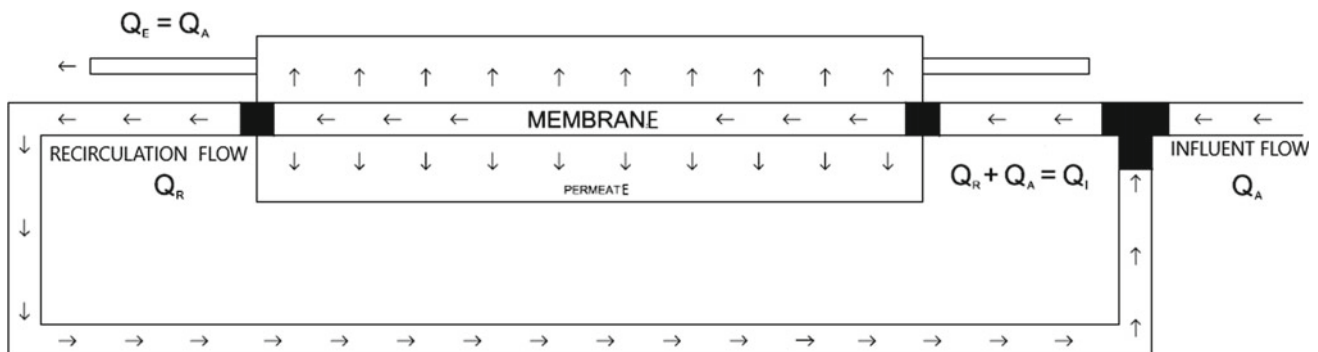
Fig. 1 Experimental set-up

USAMe tests, in particular with the double recycle ratio, have shown a decrease in the fouling rate since transmembrane pressures increased less rapidly than the individual processes and improved effluent quality.

4   Conclusion

This technology has, therefore, proved to be an effective upgrading of the ultrafiltration membrane process. Further studies will be needed to pilot scale by assessing the applicability of the treatment in terms of efficiency and cost estimation.

References

Ahmad, A. L., Che Lah, N. F., Ismail, S., & Ooi, B. S. (2012). Membrane antifouling methods and alternatives: Ultrasound approach. *Separation and Purification Reviews, 41,* 318–346. https://doi.org/10.1080/15422119.2011.617804.

Borea, L., Naddeo, V., Shalaby, M. S., Zarra, T., Belgiorno, V., Abdalla, H., et al. (2018). Wastewater treatment by membrane ultrafiltration enhanced with ultrasound: Effect of membrane flux and ultrasonic frequency. *Ultrasonics, Ultrasonic Advances Applied to Materials Science, 83,* 42–47. https://doi.org/10.1016/j.ultras.2017.06.013.

Gogate, P. R., Mujumdar, S., & Pandit, A. B. (2003). Large-scale sonochemical reactors for process intensification: Design and experimental validation. *Journal of Chemical Technology and Biotechnology, 78,* 685–693. https://doi.org/10.1002/jctb.697.

Hashemi Shahraki, M., Maskooki, A., & Faezian, A. (2014). Effect of various sonication modes on permeation flux in cross flow ultrafiltration membrane. *Journal of Environmental Chemical Engineering, 2,* 2289–2294. https://doi.org/10.1016/j.jece.2014.10.005.

Naddeo, V., Belgiorno, V., Borea, L., Secondes, M. F. N., & Ballesteros, F. (2015). Control of fouling formation in membrane ultrafiltration by ultrasound irradiation. *Environmental Technology, 36,* 1299–1307. https://doi.org/10.1080/09593330.2014.985731.

Naddeo, V., Landi, M., Scannapieco, D., & Belgiorno, V. (2013). Sonochemical degradation of twenty-three emerging contaminants in urban wastewater. *Desalination Water Treat, 51,* 6601–6608. https://doi.org/10.1080/19443994.2013.769696.

Secondes, M. F. N., Naddeo, V., Belgiorno, V., & Ballesteros, F. (2014). Removal of emerging contaminants by simultaneous application of membrane ultrafiltration, activated carbon adsorption, and ultrasound irradiation. *Journal of Hazardous Materials, 264,* 342–349. https://doi.org/10.1016/j.jhazmat.2013.11.039.

Using Water–Energy Nexus as Greenhouse Gas Emissions Mitigation Tool in Wastewater Treatment Plants

B. Del Río-Gamero, A. Ramos-Martín, N. Melián-Martel, and S. O. Pérez-Baez

Abstract

Climate change mitigation in the integral water cycle. WWTPs as energy producers. Use of the plant intrinsic energy. Integration of renewable energies in WWTPs. Water–energy nexus as greenhouse gas emissions reduction tool.

1 Introduction

Water and energy, throughout history, have been determining factors in the development of humanity (Hamiche et al. 2016). Even being conceptually different, water needs energy for the diverse stages that make up the cycle (Hardy et al. 2010). Likewise, energy needs water (Siddiqi and Anadon 2011) since the discovery of the steam engine (year 1712). Despite this union, water and energy have been two sectors studied and managed independently until Peter H. Gleick (Pacific Institute, 1994) demonstrates an intrinsic relationship between both resources in the nineties, arising from this merger, the concept known as "water–energy nexus" (Gleick 1994). Development of science and technology has confirmed the interrelation between both concepts (Tan and Zhi 2016).

The interdependence between water and energy—as well as in an isolation—leads to the world's main problems. According to the forecasts of the United Nations, the population will increase to 9600 million inhabitants by 2050, which will lead to a raise in energy and water consumption (WWAP 2014). Moreover, in 2040 it is estimated that the amount of energy used in the water sector will double that of today (International Energy Agency 2016).

Itself being a complex problem, water–energy nexus should be added the contribution to global warming due to the emission of greenhouse gases in the management of both resources. The above is supported in the different conclusions of the Kyoto Protocol, the Climate Change Summit, as well as in different international actions (FCCC, CDM, OECD…) like the 2020 European Union's Strategy, which marks challenge of a 20% reduction in primary energy, 20% reduction in GHG, and 20% penetration of renewable energies, among others.

This document aims to tackle the problem by optimizing the interdependencies between these sectors. Wastewater treatment plants were the selected scenario for this study since this stage of the integrated water cycle is one of the greatest GHGs emitter and they have an intensive energy consumption within local city and community loads (Helal et al. 2013). The main objective is to present a new concept of a wastewater treatment plant known as a green factory, which will use the intrinsic energy of the plant in all its aspects: chemical, potential, and kinetic and renewable technologies external to it, to guarantee climate change mitigation through clean energy consumption.

B. Del Río-Gamero (✉) · A. Ramos-Martín · N. Melián-Martel · S. O. Pérez-Baez
Department of Process Engineering, University of Las Palmas de Gran Canaria, Las Palmas de Gran Canaria, Spain
e-mail: Beatriz.delrio@ulpgc.es

A. Ramos-Martín
e-mail: Alejandro.ramos@ulpgc.es

N. Melián-Martel
e-mail: Noemi.melian@ulpgc.es

S. O. Pérez-Baez
e-mail: sebastianovidio.perez@ulpgc.es

2   Materials and Methods

Methodology is based on the study of different technologies that allow WWTP to be less dependent on fossil energy, creating a clean energy mix with the purpose of reducing the carbon footprint. This was achieved by analyzing the feasibility of introducing alternative technologies—anaerobic digestion, hydraulic power, micro-turbines, wind power, and solar power—that were later sized to ensure an energy production that meets the plant's own demand.

2.1   Selection of Green Energy Plant

Jinamar WWTP, with a design capacity of 10,000 m^3/d, was selected as the test-bed site after the previous feasibility analysis in the integration of clean energies (wind regime, solar radiation, sludge production, plant location) within the Canarian archipelago WWTPs (Spain). Plant loads, according to its design, were grouped and distributed throughout their working hours to form its load profile (Fig. 1).

2.2   Design and Estimation of Green Energy Production Technologies

To carry out the mitigation of climate change, alternative technologies have been classified according to their implementation in plants—external or internal. The range of priorities in the installation begins with the use of the intrinsic energy that the purification plant can develop internally.

2.2.1   Internal Energy Recovery Technologies to the Plant

Chemical energy obtained through the sludge treatment solves a dual problem unilaterally. The main waste becomes a second-generation product that facilitates the circular economy development. Anaerobic digestion has been the technology selected for its industrial maturity and simple operation. For sizing, the plant sludge was previously analyzed, resulting in a two-stage digestion system that works in a range of mesophilic temperature at high speed. The amount of biogas obtained is 190,800 m^3/year, which is pre-treated and introduced in a steam reformer to obtain hydrogen that is later transformed into electricity through the use of fuel cells (31.95 kWh).

The other intrinsic energy resource in plant is based on the use of kinetic energy that occurs with the passage of an effluent through a pipe moving the blades of a micro-turbine implanted in it. Due to its diameter and height jump, the secondary reactor outlet pipe has been selected. The micro-turbine model is the S3 of the Hydro-eKIDs (4 kWh).

2.2.2   Energy Production Technologies External to the Plant

Solar photovoltaic technology, installed on the south facade of the two WWTP roofs, will provide an energy production of 1,620,578 kWh/year, which corresponds to a power of 100 kW obtained from 440 solar panels. 220 panels will be placed on each roof with one inverter in each. The distribution will correspond with 22 modules in series and 10 rows in parallel.

Wind technology will provide 1,620,578.1 kWh/year after the study of wind speed at the plant location, developing a histogram of it, and showing the probability distribution of Weibull that ends with the sizing calculations.
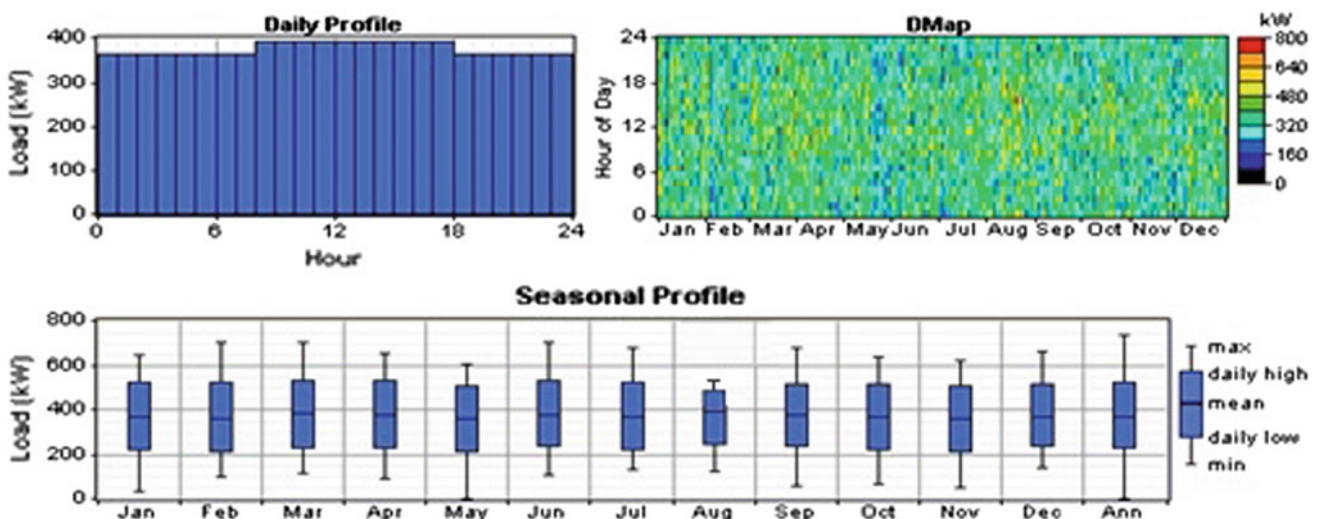
Fig. 1 Jinamar WWTP energy consumption analysis
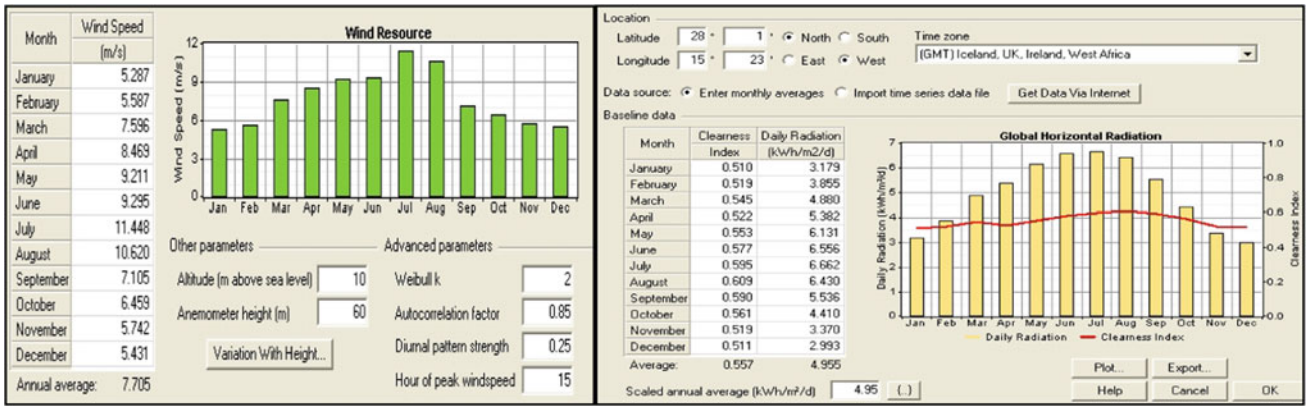
Fig. 2 Renewable technologies. Data treatment
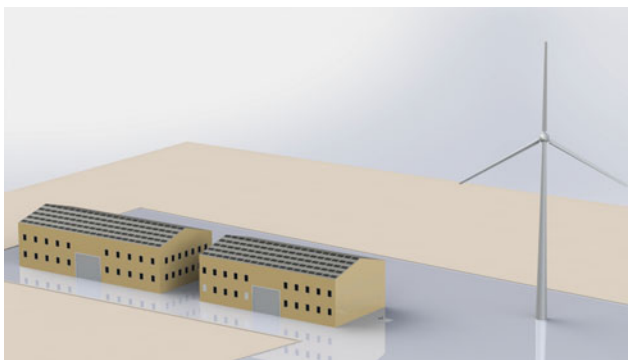
Fig. 3 Sketch of the renewable energy penetration in the plant

Finally, two pico-turbines are installed in the largest water jump found in the plant, obtaining with them an energy production of 8526.4 kWh/year (08:00–24:00 h) and 2832.4 kWh/year (24:00–08:00 h) (Fig. 2).

3 Results and Discussion

Results are represented by simulations using MATLAB tool. Four scenarios are created that differ in the configuration of the dimensioned technologies with the aim of completely covering the plant energy consumption (Fig. 3).

Fig. 4 Simulation of renewable energies integration in the plant example. Scenario 4
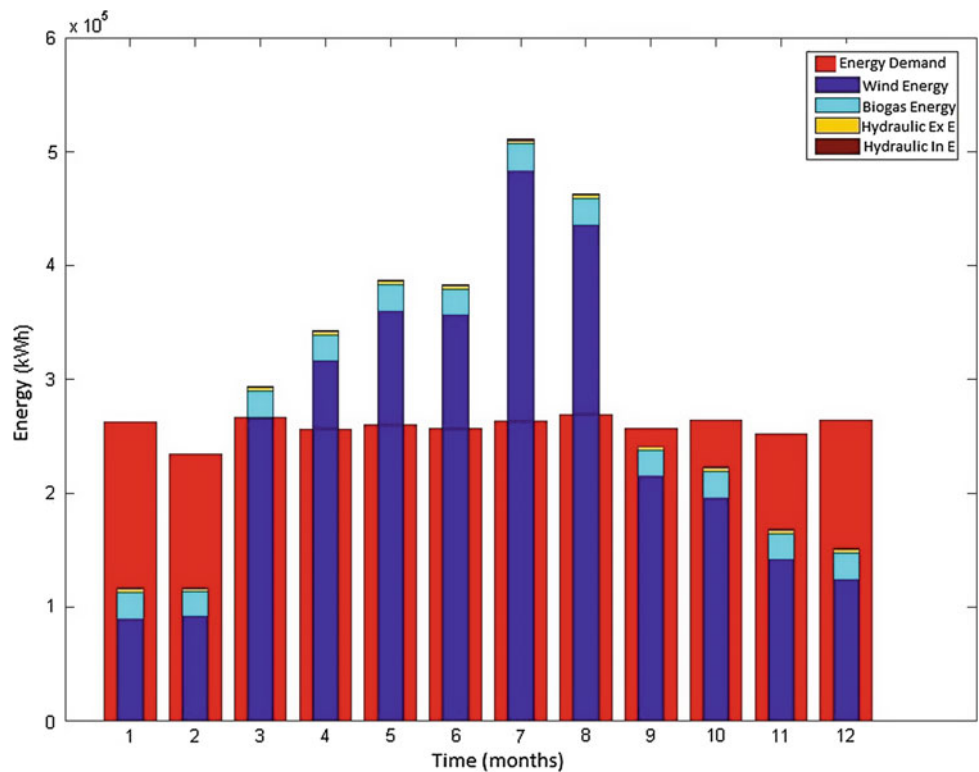
Graphs show that both the third and the fourth scenarios are the most appropriate and viable techno-economically. Scenario 4 stands out for being able to surpass the demand of the plant (3,396,326.39 kWh) (Fig. 4).

4 Conclusion

The interdependence of water–energy and its consequent contribution to climate change in all stages of the integral water cycle has been analyzed.

At the end of the research work, it has been possible to eliminate the traditional concept of wastewater treatment plants as mere energy consumers and establish a new treatment plant concept known as "green factory."

Scenario 4 confirmed the technical and economic possibility of reducing power consumption from the grid by 100%, thus eliminating the annual emission of 2754 tons of GHGs with a production of 3,396,326.39 kWh/year.

References

Gleick, P. H. (1994). Water and energy. *Annual Review of Energy and the Environment, 19*(1), 267–299.

Hamiche, A. M., Stambouli, A. B., & Flazi, S. (2016). A review of the water-energy nexus. *Renewable and Sustainable Energy Reviews, 65,* 319–331.

Hardy, L., Garrido, A., & Sirgado, L. J. (2010). *Análisis y evaluación de las relaciones entre el agua y la energía en España.* Santander, Spain: Fundación Marcelino Botín.

Helal, A., Ghoneim, W., & Halaby, A. (2013). Feasibility study for self-sustained wastewater treatment plants—Using biogas CHP fuel cell, micro-turbine, PV and wind turbine systems. *Smart Grid and Renewable Energy, 4*(02), 227.

International Energy Agency. (2016). World Energy Outlook, 2016. Executive Summary.

Siddiqi, A., & Anadon, L. D. (2011). The water–energy nexus in Middle East and North Africa. *Energy Policy, 39*(8), 4529–4540.

Tan, C., & Zhi, Q. (2016). The energy-water nexus: A literature review of the dependence of energy on water. *Energy Procedia, 88,* 277–284.

WWAP (United Nations World Water Assessment Programme). (2014). *The United Nations world water development report 2014: Water and energy.* Paris: UNESCO.

Corrosion Behavior of Carbon Steel in the Presence of *Escherichia coli* and *Pseudomonas fluorescens* Biofilm in Reclaimed Water

Ping Xu, Yumin Ou, and Zhigang Wei

Abstract

The results show that compared with *Escherichia coli* promoting corrosion and *Pseudomonas fluorescens* inhibiting corrosion, in mixed bacteria, the average corrosion rate of carbon steel is reduced by 25.66%. Corrosion current density (Icorr) decreases and the diameter of Nyquist plots increases with time. Meanwhile, the dominant bacteria in mixed condition is verified with different phases. Extracellular polymeric substances (EPS) of *E. coli* promote the growth of *P. fluorescens*, and EPS of *P. fluorescens* can inhibit the growth of *E. coli* at 400 mg L^{-1}. Scanning electron microscope (SEM) and X-ray diffraction (XRD) demonstrate that the transformation of corrosion products makes the biofilm-corrosion products film formed on the surface of carbon steel more compact in mixed bacteria.

Keywords

Microbiologically influenced corrosion • *Escherichia coli* • *Pseudomonas fluorescens* • Carbon steel • Reclaimed water

P. Xu (✉) · Y. Ou
Key Laboratory of Urban Stormwater System and Water Environment, Ministry of Education, National Demonstration Center for Experimental Water Environment Education, Beijing University of Civil, Engineering and Architecture, 100044 Beijing, China
e-mail: xuping@bucea.edu.cn

Y. Ou
e-mail: Ouyumin19960925@163.com

Z. Wei
China Railway 16th Bureau Group Co., LTD, 100018 Beijing, China
e-mail: 13391517514@163.com

1 Introduction

It is well known that microorganisms and metabolic activities will promote or inhibit metal corrosion process when microorganisms are on the metal surface (Videla 1996; Basheer et al. 2013; Moreno et al. 2014; Castaneda and Benetton 2008; Beese et al. 2013; Xu et al. 2016). Studying microbiologically influenced corrosion (MIC) will help reduce the losses caused by metal corrosion. Previous laboratory studies have mainly focused on the corrosion of single culture. The research mechanism of corrosion mainly focuses on functional bacteria, such as sulfate-reducing bacteria (SRB) (Booth and Tiller 1960, 1968), iron-reducing bacteria (IRB) (Obuekwe et al. 1981; Little et al. 1997; Borenstein 1994), and iron-oxidizing bacteria(IOB) (Xu et al. 2008; Liu et al. 2015, 2014). The influence of two or more microorganisms on the corrosion behavior of metals is closer to the actual corrosive environment. The majority of microbes live as multispecies biofilms in natural environments. However, many mixed systems are also studied around functional bacteria. Meanwhile, in aquatic environments including pipe systems, microorganism species are different, and the mechanism of interaction may change. There is a cooperative relationship between microbes in the same environment, and there is also a competitive relationship. Few studies have reported on the effect of similar growth characteristics of mixed bacteria on the corrosion of metals.

Escherichia coli (*E. coli*) and *Pseudomonas fluorescens* (*P. fluorescens*) are common in reclaimed water. Carbon steel is a common metal material used in water systems. The aim of this work is to research the influence of the interaction process of *E. coli* and *P. fluorescens* on the corrosion behavior of carbon steel and provide base knowledge for metal corrosion control in reclaimed water.

2 Materials and Methods

E. coli and *P. fluorescens* are bought from the China Center of Industrial Culture Collection (CICC). The bacteria were cultured in nutrient agar medium for 48 h, and the EPS was extracted by NaOH method. Different concentrations of *P. fluorescens* and *E. coli* EPS solution (100, 200, 300, 400 mg L^{-1}) were prepared, respectively. The numbers of bacteria were tested by DR6000 ultraviolet–visible spectrophotometer (Hach, USA).

Corrosion products morphology was observed by Hitachi S4330 SEM and its energy spectrum (EDS, Brook). The crystal structure of the corrosion products was characterized by X-ray diffraction technique (XRD, X`PERT PRO, CuK radiation, 40 kV, 40 mA).

The calculation of corrosion weight loss and corrosion rate should be calculated according to the ordinary methods. Chenhua electrochemical workstation (Chenhua, China) was used for electrochemical experiments. The Larsen index of artificially experimental water was 1.93 according to the water quality of circulating cooling water.

The size of corrosion coupon was $50 \times 25 \times 2$ mm in corrosion weight loss experiment. Cylinder coupons with a diameter of 10 mm and thickness of 20 mm were used for electrochemical measurements.

During the corrosion experiments, the coupons were taken out of 1d, 3d, 6d, 9d, 12d, and 14d, respectively, which were used for corrosion weight loss, microbial number, scanning electron microscope (SEM), and energy spectrum analysis (EDS). The composition of corrosion products on the coupon was analyzed by X-ray diffraction (XRD). At the same time, the electrochemical experiments were carried out in the same conditions.

3 Results and Discussion

3.1 Weight Loss

The corrosion rates of mixed bacteria are smaller than that of sterile condition except for the 1 day, indicating that the corrosion behavior of carbon steel is inhibited, and the average corrosion inhibition rate is 25.66%. The average corrosion inhibition rate of *P. fluorescens* is 48.14%. The corrosion rates of *E. coli* increase gradually and remain stable after 1 day, and the average promotion rate is 29.22%.

3.2 Electrochemical Analysis

According to the results, in the sterile condition, the Nyquist plot diameter increases from 1d to 6d, then decreases with time gradually afterward. In the presence of *E. coli* alone, the Nyquist plot diameter decreases gradually. In the presence of *P. fluorescens* alone, the Nyquist plot diameter becomes significantly higher compared to the sterile and *E. coli* condition, indicating inhibition corrosion caused by *P. fluorescens*. In the mixed bacteria, the change of impedance indicates that the corrosion process of carbon steel is affected by the competition of *E. coli* and *P. fluorescens*. The change of EIS in different conditions is basically the same as that of corrosion rates, which is probably due to the interaction of *E. coli* and *P. fluorescens*.

The corrosion potential of 14 days between each condition varies greatly with the change of time. Fluctuation range of corrosion potential of mixed bacteria is small. There is an increasing trend of corrosion, which leads to poor stability of *E. coli* and *P. fluorescens* in the interaction of the metal surface. However, the corrosion current density of mixed bacteria decreases from 0.1305 to 0.0930 μA cm^{-2} on the 14th day.

According to the experimental results of EIS, polarization curve and corrosion rate, the corrosion behavior of the mixed bacterial is between that of *E. coli* and *P. fluorescens* due to above bacteria competition in the biofilm. *P. fluorescens* ultimately promotes the formation of corrosion product film and inhibit corrosion. Changes in the number of bacteria in the mixed bacteria have an effect on the change of EIS. The changes in the corrosion potential of the mixed bacteria also indicate that there is competition between the two bacteria.

3.3 Biofilm Analysis

In the mixed bacteria, the number of *E. coli* is 1.1×10^6 cfu mL^{-1}, and the number of *P. fluorescens* is 3.7×10^5 cfu mL^{-1} at 1 day. The number of *E. coli* is more than that in the pure culture, while the number of *P. fluorescens* is less than that in the single culture. *E. coli* is the dominant bacteria in the early stage, and the corrosion rate is accelerated to 0.4271 mm a^{-1}. On the 3rd day, the number of *E. coli* and *P. fluorescens* is the same as 1.4×10^6 cfu mL^{-1}, and the corrosion rate is still relatively high at 0.2538 mm a^{-1}. With the development of the experiment, the number of *P. fluorescens* increased rapidly and exceeded the number of *E. coli*, and the corrosion rate gradually decreased at the same time. Finally, the corrosion is inhibited.

Under *P. fluorescens* condition and the mixed bacteria condition, surface morphology of corrosion products is Fe_2O_3 or Fe_3O_4. Meanwhile, there is relatively high content of the *P* element. The surface morphology analysis of sterile and *E. coli* showed that the structure of corrosion product appeared loose and porous.

Some previous studies have shown that EPS secreted by certain microorganisms can inhibit the corrosion behavior of metal surfaces (Xu et al. 2016; Badr et al. 2005; Finnie and Mcfadden 1978; Zhang et al. 2007; Chongdar et al. 2005; Stadler et al. 2015; Dong et al. 2011). This work shows that in the 400 mg L^{-1} under *P. fluorescens* EPS, the number of *E. coli* is far less than the number of bacteria under 300 mg L^{-1} of *P. fluorescens* EPS. This indicates that the addition of *P. fluorescens* EPS slows the growth and reproduction of *E. coli*. Under different EPS concentrations of *E. coli*, the absorbance of *P. fluorescens* rapidly increases at the first stage and then reduces gradually.

3.4 Analysis of Corrosion Products

The corrosion products on the coupons were analyzed by XRD. According to the results, the main components of corrosion products of the coupon are α-FeOOH, γ-FeOOH, Fe_2O_3, Fe_3O_4, and $FeCO_3$ in mixed bacteria and *P. fluorescens* condition. However, the main components of corrosion products of the coupon are α-FeOOH, γ-FeOOH, Fe_2O_3, and Fe_3O_4 in sterile and *E. coli* condition. Previous studies have shown that when the corrosion product contains $FeCO_3$, the corrosion product film is denser and has a protective effect on the carbon steel substrate (Lin et al. 2013; Ueda and Takabe 2001; Nyborg and Dugstad 1998). FeOOH is a looser structure (Liu et al. 2016), and Fe_2O_3 and Fe_3O_4 are stable iron oxides (Welbourn et al. 2016).

4 Conclusion

In the artificial water environment, the interaction of *E. coli* and *P. fluorescens* on the corrosion behavior of carbon steel is studied. In the mixture of *E. coli* and *P. fluorescens*, the corrosion rates decreased and the corrosion current density decreased, which are between the single bacteria condition, and the corrosion is inhibited. On the surface of carbon steel, forming a biofilm-corrosion products film composed of bacteria, EPS, and corrosion products. The composition and content of corrosion products change with time, which was different from that of the *E. coli*. The corrosion products of the mixed bacteria were more similar to that of the *P. fluorescens*. But the content was slightly less than that of *P. fluorescens*, indicating that the presence of *E. coli* slowed the transformation of corrosion products. The interaction between the two bacteria is mainly biological competition. *P. fluorescens* inhibits the adhesion of *E. coli* and promotes the formation of surface protective film of carbon steel.

References

Badr, H. M., Habib, M. A., Ben-Mansour, R., et al. (2005). Numerical investigation of erosion threshold velocity in a pipe with sudden contraction [J]. *Computers & Fluids, 34*(6), 721–742.

Basheer, R., Ganga, G., Chandran, R. K., Nair, G. M., Nair, M. B., & Shibli, S. M. A. (2013). Effect of W-TiO2 composite to control microbiologically influenced corrosion on galvanized steel [J]. *Applied Microbiology and Biotechnology, 97* (12), 5615.

Beese, P., Venzlaff, H., Srinivasan, J., et al. (2013). Monitoring of anaerobic microbially influenced corrosion via electrochemical frequency modulation [J]. *Electrochimica Acta, 105,* 239.

Booth, G. H., & Tiller, A. K. (1960). Polarization studies of mild steel in cultures of sulphate-reducing bacteria [J]. *Transactions of the Faraday Society, 56,* 1689–1696.

Booth, G. H., & Tiller, A. K. (1968). Cathodic characteristics of mild steel in suspensions of sulphate-reducing bacteria [J]. *Corrosion Science, 8*(8), 583–600.

Borenstein, S. W. (1994). *Microbiologically influenced corrosion handbook* (p. 12). Cambridge, London: Woodhead.

Castaneda, H., & Benetton, X. D. (2008). SRB-biofilm influence in active corrosion sites formed at the steel-electrolyte interface when exposed to artificial seawater conditions [J]. *Corrosion Science, 50* (4), 1169.

Chongdar, S., Gunasekaran, G., & Kumar, P. (2005). Corrosion inhibition of mild steel by aerobic biofilm [J]. *Electrochimica Acta, 50*(24), 4655–4665.

Dong, Z., Liu, T., & Liu, H. (2011). Influence of EPS isolated from thermophilic sulphate-reducing bacteria on carbon steel corrosion [J]. *Biofouling, 27*(5), 9.

Finnie, I., & Mcfadden, D. H. (1978). On the velocity dependence of the erosion of ductile metals by solid particles at low angles of incidence [J]. *Wear, 48*(1), 181–190.

Lin, X., Liu, W., Zhang, J., et al. (2013). Characteristics of corrosion scale of 3Cr steel at high temperature and pressure in an O2 and CO2 environment [J]. *Acta Physico-Chimica Sinica*.

Little, B., Wagner, P., Hart, K., et al. (1997). *The role of metal-reducing bacteria in microbiologically influenced corrosion [R]*. Houston, TX (United States): NACE International.

Liu, H., Zheng, B., Xu, D., et al. (2014). Effect of sulfate-reducing bacteria and iron-oxidizing bacteria on the rate of corrosion of an aluminum alloy in a central air-conditioning cooling water system [J]. *Industrial and Engineering Chemistry Research, 53*(19), 7840–7846.

Liu, H., Fu, C., Gu, T., et al. (2015). Corrosion behavior of carbon steel in the presence of sulfate reducing bacteria and iron oxidizing bacteria cultured in oilfield produced water [J]. *Corrosion Science, 100,* 484–495.

Liu, H., Gu, T., Zhang, G., et al. (2016). The effect of magneticfield on biomineralization and corrosion behavior of carbon steel induced by iron-oxidizing bacteria [J]. *Corrosion Science, 102,* 93–102.

Moreno, D. A., Ibars, J. R., Polo, J. L., et al. (2014). EIS monitoring study of the early microbiologically influenced corrosion of AISI 304L stainless steel condenser tubes in freshwater [J]. *Journal of Solid State Electrochemistry, 18*(2), 377.

Nyborg, R., Dugstad, A. (1998). Mesa corrosion attack in carbon steel and 0.5% chromium steel [A]. *NACE International,* Houston, USA.

Obuekwe, C. O., Westlake, D. W. S., Plambeck, J. A., et al. (1981). Corrosion of mild-Steel in cultures of ferric iron reducing bacterium isolated from crude-oil, mechanism of anodic depolarization [J]. *Corrosion, 37*(11), 632–637.

Stadler, R., Wei, L., Fürbeth, W., et al. (2015). Influence of bacterial exopolymers on cell adhesion of Desulfovibrio vulgaris on high alloyed steel: Corrosion inhibition by extracellular polymeric substances (EPS) [J]. *Materials & Corrosion, 61*(12), 1008–1016.

Ueda, M., & Takabe, H. (2001). The formation behavior of corrosion protective films of low cr bearing steels in CO2 environments [J]. *Annals of Surgery, 244*(5), 700–705.

Videla, H. A. (1996). *Manual of biocorrosion* [M]. CRC Press.

Welbourn, R. J. L., Truscott, C. L., Skoda, M., et al. (2016). Corrosion and inhibition of copper in hydrocarbon solution on a molecular level investigated using neutron reflectometry and XPS [J]. *Corrosion Science*, S0010938X16311787.

Xu, C., Zhang, Y., Cheng, G., et al. (2008). Pitting corrosion behavior of 316L stainless steel in the media of sulphate-reducing and iron-oxidizing bacteria [J]. *Materials Characterization, 59*(3), 245–255.

Xu, P., Wei, Z., Wang, J., et al. (2016). Inhibition of carbon steel corrosion behavior by extracellular polymeric substances of *Lactobacillus reuteri* [J]. *Surface Technology*.

Zhang, Y., Reuterfors, E. P., Mclaury, B. S., et al. (2007). Comparison of computed and measured particle velocities and erosion in water and air flows [J]. *Wear, 263*(1–6), 330–338.

Development of Pilot-Scale Photocatalytic Reactor Employing Novel TiO₂ Epoxy Grains for Wastewater Treatment

Yasmine Abdel-Maksoud, Emad Imam, and Adham Ramadan

Abstract

High-density TiO₂ epoxy grains for easy gravitational separation after treatment ends. Passive aeration for maintaining high DO levels. Degradation rate constant and reactor throughput as benchmarks for reactor performance. Water turbidity indicator for photocatalyst resistance to abrasion. Promising for scale-up: modular design, integrated storage, no UV transmitting parts.

1 Introduction

TiO₂ photocatalysis is one of the promising routes for sustainable wastewater treatment due to five distinctive features: (1) it can be used at ambient temperature and atmospheric pressure, (2) pollutants are mineralized into CO_2, water and mineral acids, (3) TiO₂ is abundant, cheap and non-toxic, (4) oxygen required for the process can be obtained from the atmosphere, (5) sunlight can be used for catalyst activation.

Y. Abdel-Maksoud (✉)
Environmental Engineering, The American University in Cairo, Cairo 11835, Egypt
e-mail: ymaksoud@aucegypt.edu

E. Imam
Department of Construction Engineering, The American University in Cairo, Cairo 11835, Egypt
e-mail: eimam@aucegypt.edu

A. Ramadan
Department of Chemistry, The American University in Cairo, Cairo 11835, Egypt
e-mail: aramadan@aucegypt.edu

Research on the use of TiO₂ photocatalysis for water/wastewater treatment for the removal of persistent non-biodegradable emerging water pollutant is active worldwide (Byrne et al. 2018; Zangeneh et al. 2015).

A thorough review of the literature revealed that commonly tested reactor configurations for TiO₂ photocatalysis suffer from limitations that hamper their scale-up and commercialization (Abdel-Maksoud et al. 2016; Dong et al. 2015). These limitations might be attributed to high capital cost of use of UV transmissive walls or pipes. Use of UV transmissive components also poses a limitation on photoreactor size and the associated risk of breakage. Other limitations might be related to high operating cost related to continuous supply of oxygen to reaction solution or consumption of oxidants that act as electron scavengers. There are also technical limitations associated with the use of immobilized catalysts. These technical limitations are either due to prevalence of laminar flow conditions resulting in slow degradation rates or due to difficulty of immobilization of photocatalyst on large surfaces efficiently and at a low cost.

Widespread use of photocatalytic wastewater treatment requires the development of an innovative photocatalytic reactor that is efficient, simple to construct, easy to maintain, has low energy consumption, low capital and operating cost and provides easy separation of catalyst after treatment ends. In an attempt to develop this desired photocatalytic reactor, the immobilized water-bell photocatalytic reactor (IWBPR) using TiO₂ immobilized on high-density grains was designed and constructed. The photocatalyst grains are fully dispersed in the wastewater matrix and can be easily recovered after treatment ends. Taking into account all the attributes for an efficient TiO₂ photocatalytic process, a pilot model was developed. This was followed by fabrication of the immobilized TiO₂ photocatalyst and its characterization. The prototype employing the immobilized TiO₂ was tested using phenol as a model contaminant to evaluate the photodegradation efficiency, effluent water turbidity was used as an indicator of the stability of supported TiO₂ and its

resistance to abrasion. Finally, the system performance was evaluated using benchmarks.

2 Materials and Methods

2.1 Pilot-Scale Photocatalytic Reactor

The IWBPR is based on dispersing immobilized TiO_2 in a thin water film. The unsupported thin water film guarantees photocatalyst activation and water oxygenation. TiO_2 is immobilized on high-density grains for easy gravitational separation after the treatment ends. A schematic section of the pilot-scale photocatalytic reactor is shown in Fig. 1. A detailed description of the photocatalytic reactor has been detailed in our work reporting the results of testing the reactor in the slurry mode using commercial TiO_2 (Abdel-Maksoud et al. 2018).

2.2 Supported Photocatalyst Preparation

Studies have shown that epoxy TiO_2 coatings have promising photocatalytic and photodisinfection properties (Santhosh and Natarajan 2015; Sangermano et al. 2009). In our previous work, TiO_2 was immobilized on sand grains using epoxy coating. The epoxy TiO_2 sand composite achieved phenol degradation and was resistant to abrasion for multiple treatment runs (Abdel-Maksoud et al. 2018). In this work, two photocatalysts were developed: (i) TiO_2 epoxy sand particles (TESP) and (ii) TiO_2 epoxy grains (TEG). TiO_2, incorporated in the epoxy matrix for preparation of the immobilized photocatalysts, was lab-synthesized using a simple sol-gel technique. TiO_2 nanoparticles crystallite phase and size were determined uing X-ray diffraction.

For the preparation of TESP, sand fraction having particle size ranging from 63 to 88 μm (passing sieve 170 and retained on sieve 230) was used as a support for TiO_2. TiO_2 dispersed in the epoxy matrix was added to the sieved sand and thoroughly mixed. The amount of epoxy used was just enough to wet the sand particles such that after drying the formed agglomerates are easy to break into free-flowing particles. TESP was characterized using scanning electron microscope (SEM) and energy dispersive X-ray (EDX). TESP was gold sputtered for 120 s at a current of 10 mA using Hummer 8 sputtering system prior to SEM analysis. For the preparation of TEG, TiO_2 was dispersed in the epoxy matrix. After drying, the TiO_2 epoxy film was crushed and ground. The fraction having particle size ranging from 420 to 841 μm (passing sieve 20 and retained on sieve 40) was used.

2.3 Photocatalytic Degradation Tests

Photocatalytic degradation tests were conducted in a recirculating batch mode. Phenol used as received was added to tap water. The 4-Aminoantipyrine method adapted from EPA method # 420.1 (EPA, March 1983), and Hach method # 8047 (Hach, 3/2014, Edition 8) was used for phenol

Fig. 1 Pilot-scale immobilized water-bell photocatalytic reactor
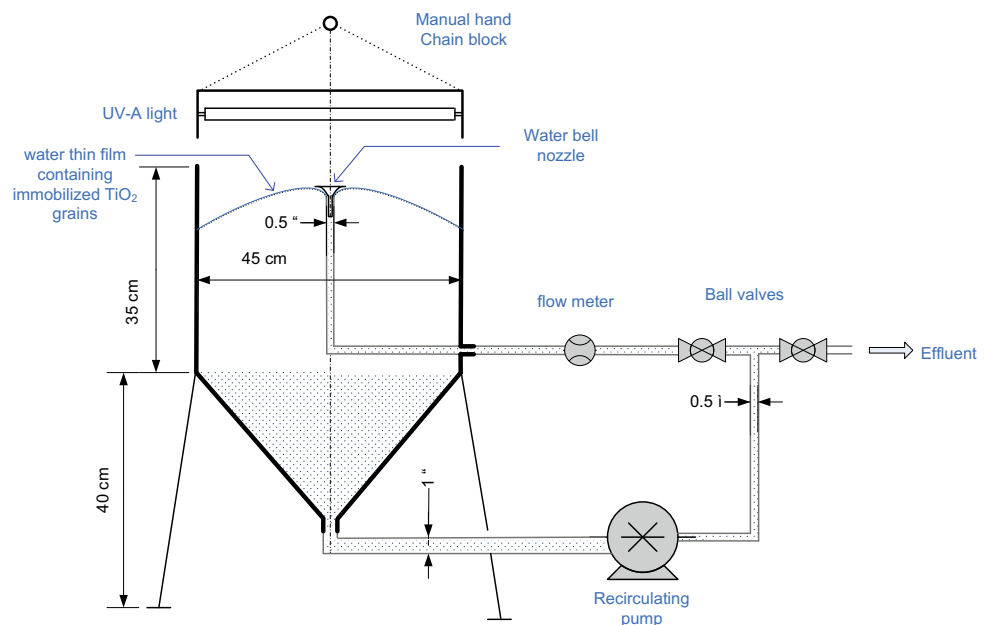
concentration determination. Dissolved oxygen levels, temperature and pH were monitored through all the conducted tests. The water turbidity was measured as an indicator for photocatalyst stability and resistance to abrasion.

3 Results and Discussion

The crystal size of the lab-synthesized TiO_2 nanoparticles was calculated using the Scherrer equation. The crystal size was found to be 11.5 nm. The phase content was calculated using the Spurr-Myers equation. The TiO_2 nanoparticles composed of 77% anatase and 23% rutile. N2 sorption analysis revealed that BET specific surface area was 142.5 m^2/g. The TESP SEM demonstrated discrete sand particles. The TiO_2/epoxy coating was free of any cracks. However, presence of tiny droplets in the coating indicated that better mixing conditions were needed to attain complete dispersion of TiO_2 nanoparticles in the epoxy matrix.

On using 20 g/L of TESP having density 2.47 g/cm^3, the TiO_2 in the system was 300 mg/L, 19% phenol degradation was achieved as shown in Fig. 2a. However, drastic increase in water turbidity was encountered as shown in Fig. 2b. On using 10 g/L of TEG, having density 1.35 g/cm^3, the TiO_2 in the system was 500 mg/L, 34% phenol degradation was achieved accompanied with slight turbidity increase. TEG was more resistant to the high friction forces induced by the rotating impeller of the centrifugal pump. Optimization of TEG grain size is crucial for achieving high photocatalytic degradation efficiency while maintaining easy gravitational separation.

The initial degradation rate and reactor throughput were calculated for the IWBPR and other photocatalytic reactors treating phenol under comparable conditions. Although the reactor performance was comparable with these photocatalytic reactors, the system complexity and operating cost associated with supplying air to the reaction solution and cooling are totally eliminated in the water-bell reactor. Unlike Photocatalytic reactors employing an internal UV illumination source, the water-bell reactor can benefit from solar radiation rendering the treatment more economic.

4 Conclusion

The immobilized water-bell photocatalytic reactor is promising for scale-up and commercialization owing to its modular design, an integrated storage, passive oxygenation, simple and cheap components and easy catalyst separation. TEG is a novel photocatalyst, the first fluidized photocatalyst to be removed by gravity settling. Enhancement of its photocatalytic and mechanical properties can be achieved through adopting an efficient dispersion technique of the TiO_2 in the epoxy matrix as well as optimization of TiO_2 percent in the epoxy matrix.
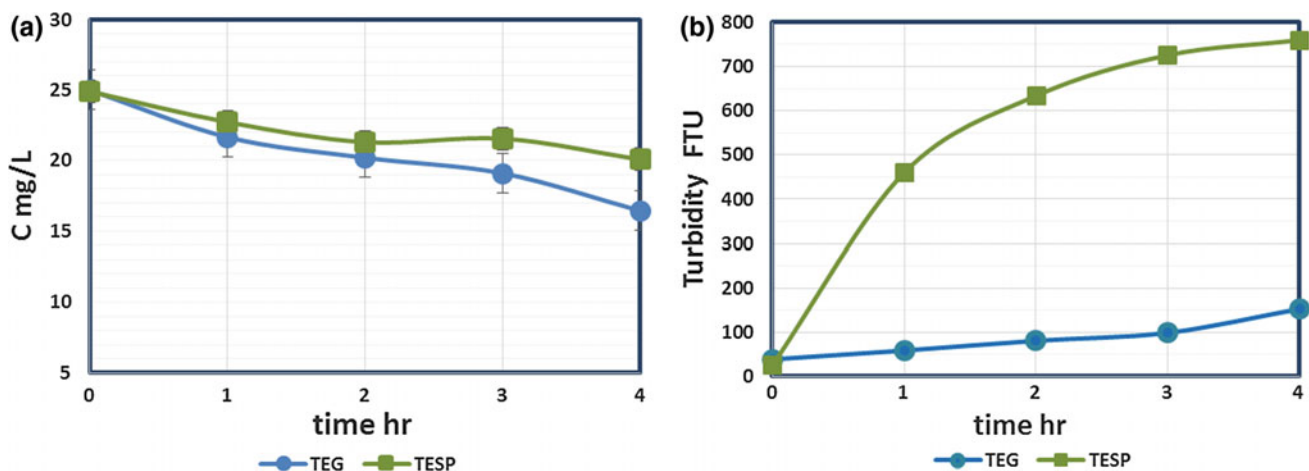
Fig. 2 Photocatalytic activity tests: **a** phenol concenration, **b** turbidity

References

Abdel-Maksoud, Y., Imam, E., & Ramadan, A. (2016). TiO$_2$ solar photocatalytic reactor systems: Selection of reactor design for scale-up and commercialization—Analytical review. *Catalysts, 6* (9), 138. https://doi.org/10.3390/catal6090138.

Abdel-Maksoud, Y., Imam, E., & Ramadan, A. (2018a). TiO$_2$ water-bell photoreactor for wastewater treatment. *Solar Energy, 170,* 323–335.

Abdel-Maksoud, Y., Imam, E., & Ramadan, A. (2018b). Sand supported TiO$_2$ photocatalyst in a tray photo-reactor for the removal of emerging contaminants in wastewater. *Catalysis Today, 313,* 55–62.

Byrne, C., Subramanian, G., & Pillai, S. (2018). Recent advances in photocatalysis for environmental applications. *Journal of Environmental Chemical Engineering, 6,* 3531–3555.

Dong, H., Zeng, G., Tang, L., Fan, C., Zhang, C., He, X., et al. (2015). An overview on limitations of TiO$_2$-based particles for photocatalytic degradation of organic pollutants and the corresponding counter measures. *Water Research, 79,* 128–146.

Sangermano, M., Palmero, P., & Montanaro, L. (2009). UV-cured polysiloxane epoxy coatings containing titanium dioxide as photosensitive semiconductor. *Macromolecular Materials and Engineering, 294,* 323–329.

Santhosh, S., & Natarajan, K. (2015). Antibiofilm activity of epoxy/Ag-TiO$_2$ polymer nanocomposite coatings against Staphylococcus Aureus and Escherichia Coli. *Coatings, 5,* 95–114.

Zangeneh, H., Zinatizadeh, A., Habibi, M., Akia, M., & Isa, M. (2015). Photocatalytic oxidation of organic dyes and pollutants in wastewater using different modified titanium dioxides: A comparative review. *Journal of Industrial and Engineering Chemistry, 26,* 1–36.

Evaluation of Fungal White-Rot Strains for Assisting in Algal Harvest in Wastewater

M. Hultberg and H. Bodin

Abstract

Microalgae co-cultured with certain filamentous fungi form biopellets. Biopellets can be used in microalgae harvesting and in water treatment. White-rot fungi producing laccase are of interest for water treatment. In suitable environmental conditions, certain white-rot fungi can form biopellets with microalgae.

Keywords

Biopellets • Filamentous fungi • Microalgae • Wastewater • White-rot fungi

1 Introduction

The world's population is increasing rapidly, and waste streams such as wastewater are being produced in increasing quantities. This has generated interest in developing sustainable technologies with low energy demand for wastewater treatment that allow recirculation of resources such as nutrients needed for crop production. One possibility is algae-based technologies such as high-rate algal ponds, which are well known for the removal of inorganic nutrients from wastewater (Oswald 1988; Shilton et al. 2012).

A current bottleneck in using microalgae for treatment of wastewater is the harvesting step, which requires methods such as filtration, chemical flocculation and centrifugation.

These harvesting methods may account for as much as 20–30% of the total algal biomass production costs and are also very energy-demanding (Uduman et al. 2010). Recent research has indicated the potential for using filamentous fungi to form pellets with microalgae (biopellets) in order to advance the sustainability and economic feasibility of producing and harvesting microalgal biomass in wastewater (Zhang and Hu 2012; Bhattacharya et al. 2017). In current work, the dominating fungal genus used for algal harvest is *Aspergillus* which is highly efficient in capturing the algal cell (Bhattacharya et al. 2017). However, *Aspergillus* sp. including the species *A. niger*, also known as black mold, is an intense spore-producing species (Schuster et al. 2002), and considering a future large-scale use, this can be a drawback.

In parallel, there is a need to develop techniques for removing micropollutants such as pesticides and pharmaceuticals from wastewater. In some situations, wastewater treatment techniques based on biological processes could be a potential low-cost alternative. Microalgae and fungi have both been demonstrated to effectively remove micropollutants from water (Cai et al. 2007; Pinto et al. 2012; Hultberg et al. 2016). For microalgae, the effect can be partly explained by a synergistic relationship between the photosynthetic microalgae and heterotrophic bacteria degrading the pollutant (Muñoz and Guieysse 2006). For fungi, there are certain species that are of high interest for bioremediation of micropollutants due to their production of extracellular enzymes, such as laccases, capable of degrading recalcitrant xenobiotics (Viswanath et al. 2014). Thus, in the present study four strains of edible white-rot fungi, with a long record of safe use and well known for their production of degrading enzymes such as laccase, were evaluated for their potential to grow in synthetic wastewater and for their ability to form pellets with microalgae to enhance algal harvest.

M. Hultberg (✉)
Department of Biosystems and Technology, Swedish University of Agricultural Sciences, P.O. Box 103 230 53 Alnarp, Sweden
e-mail: malin.hultberg@slu.se

H. Bodin
Division of Natural Sciences, Kristianstad University, Kristianstad, Sweden
e-mail: hristina.bodin@hkr.se

2   Materials and Methods

Microorganisms

The filamentous fungus *Aspergillus niger* ATCC® 16888™ (ATCC, USA), *Ganoderma lucidum* (Ecofungi, Sweden), *Pleurotus ostreatus* M2191 (Mycelia BVA, Belgium), *Pleurotus pulmonarius* (Fungi Perfecti, USA) and *Trametes versicolor* M9912 (Mycelia BVA, Belgium) were used in the study. Also, the microalgal species *Chlorella vulgaris* strain 211/11B from CCAP-SAMS, Scotland, was used.

The microalgal strain was cultivated in synthetic wastewater, SW (OECD 2001) in a climate chamber at 25 °C (photoperiod 16 h) and illumination of 50 μmol/m^2 s (PAR). For fungal inoculum production, all strains were propagated on petri dishes with 25 ml of malt agar for 10 days at 25 °C.

Experimental setup

Experiments were performed as batch reactors in Erlenmeyer flasks on a shaker at 100 rpm at 25 °C. Synthetic wastewater, SW (OECD 2001) with a five-day-old algal culture (OD$_{680}$ 0.400–0.450) was used and inoculated with the fungal strains. Circular slants (diameter 15 mm) from the agar plates were used in all the experiments.

The experimental setup comprised of six treatments: (1) *Control without fungal inoculum*, (2) *A. niger*, (3) *G. lucidum*, (4) *P. ostreatus*, (5) *P. pulmonarius* and (6) *T. versicolor*. Experiment was performed at pH 4.0 as this has previously been applied for pelletization with *A. niger*, pH 7.0 and pH 9.2 (the pH in the algal suspension at the start of the experiment) and with and without an added carbon source (glucose 0.3% w/v). After five days, the experiments were ended, and the fungal biomass was determined by filtration (0.1 mm mesh size) and pelletization of algal cells was determined as percentage reduction in optical density (680 nm) compared to the control.

Statistics

The experiments were set up with three replicates in each treatment, and the data obtained were analyzed statistically using Minitab 17 for Windows. One-way Anova followed by Tukey's multiple comparison test was employed to test for effects of treatment on final concentrations of pesticides in the water. The significance level in all cases was set to $p < 0.05$.

3   Results and Discussion

No biomass production was detected in the control as the algal cells passed through the filter. Thus, the dry weight presented in Table 1 refers to fungal biomass with entrapped algal cells. Lowest biomass production was observed in pH 9.2. This result demonstrates that the pH needs to be modified in the algal culture in order to create an environment conducive for fungal growth. The highest biomass production was observed at neutral pH, and no significant difference in biomass production was observed between the fungal strains at this pH.

The potential for pelletization of the algal cells differed largely between the strains and the highest removal was observed in the treatments with *A. niger*. Almost complete removal of algal cells, corresponding to a reduction of 98.8% of OD$_{680}$ compared to the control, was observed at pH 7 and with an added carbon source. In this treatment, a removal of 55.9%, which was the highest removal of the included white-rots strains, was observed in the treatment with *P. pulmonarius*. This species, commonly known as Phoenix oyster, is edible and produced in large quantities throughout the world (Sánchez 2010) and would be well-suited for large-scale use in industrial processes. However, also the species *G. lucidum*, used for pharmaceutical purposes (Boh et al. 2007), and *T. versicolor*, used

Table 1 Biomass production (g/L, dry weight) of the selected fungal strains when grown in an algal culture in synthetic wastewater. Also, the potential for removing algal cells by entrapment in fungal mycelium was determined and percentage reduction compared to the control are shown (%OD)

Treatment	pH 4		pH 7		pH 9.2		pH 7, glucose 0.3%	
	g/L	%OD	g/L	%OD	g/L	%OD	g/L	%OD
2 (*A. niger*)	1.0a*	64.2	1.0a	80.7	0.5a	69.6	1.9a	98.8
3 (*G. lucidum*)	0.6bc	36.6	0.8a	11.4	0.4a	–	1.3ab	–
4 (*P. ostreatus*)	0.8ab	–**	1.0a	–	0.5a	–	1.4ab	–
5 (*P. pulmonarius*)	0.5c	–	0.8a	10.9	0.4a	–	1.4ab	55.9
6 (*T. versicolor*)	0.4c	–	0.9a	34.2	0.4a	–	0.9b	–

*Values within columns followed by different letters are significantly different ($P < 0.05$)
**no significant decrease compared to the control

for biotechnological purposes (Damle and Shukla 2010) and also eaten in certain parts of the world, showed potential for algal entrapment depending on the environmental conditions.

4 Conclusion

Overall, the highest reduction of algal cells was observed with the fungal species *A. niger*. However, depending on the environmental conditions and the selected strains also the fungal white-rot species showed potential for entrapment of algal cells in their biomass. Developing fungal-assisted algal harvest based on white-rot strains offers several advantages such as access to well-known and safe strains used for mushroom production and potential for inducing laccase production in the wastewater and increased degradation of micropollutants.

References

Bhattacharya, A., Mathur, M., Kumar, P., Kumar Prajapati, S., & Malik, A. (2017). A rapid method for fungal assisted algal flocculation: Critical parameters and mechanism insights. *Algal Research, 21,* 42–51.

Boh, B., Berovi, M., Zhang, J., Zhi-Bin, L. (2007). Ganoderma lucidum and its pharmaceutically active compounds. *Biotechnology Annual Review 13*, 256–301.

Cai, X., Liu, W., Jin, M., & Lin, K. (2007). Relation of diclofop-methyl toxicity and degradation in algae cultures. *Environmental Toxicology and Chemistry, 26,* 970–975.

Damle, A. J., & Shukla, S. R. (2010). Production of laccase from *Coriolus versicolor* and its application in dye decolorization in combination with UV/H2O2 technique. *CLEAN—Soil, Air, Water, 38,* 663–669.

Hultberg, M., Bodin, H., Ardal, E., & Asp, H. (2016). Effect of microalgal treatments on pesticides in water. *Environmental Technology, 37,* 893–898.

Muñoz, R., & Guieysse, B. (2006). Algal-bacterial processes for the treatment of hazardous contaminants: A review. *Water Research, 40,* 2799–2815.

OECD. (2001). OECD guidelines for testing of chemicals. Simulation test-aerobic sewage treatment 303A.

Oswald, W. J. (1988). Microalgae and wastewater treatment. In M. A. Borowitzka & L. J. Borowitzka (Ed.), *Microalgal Biotechnology* (pp. 305–328). Cambridge University Press.

Pinto, A. P., Serrano, C., Pires, T., Mestrinho, E., Dias, L., Teixeira, D. M., et al. (2012). Degradation of terbuthylazine, difenoconazole and pendimethalin pesticides by selected fungi cultures. *Science of the Total Environment, 435–436,* 402–410.

Sánchez, C. (2010). Cultivation of *Pleurotus ostreatus* and other edible mushrooms. *Applied Microbiology and Biotechnology, 85,* 1321–1337.

Schuster, E., Dunn-Coleman, N., Frisvad, J., & van Dijck, P. (2002). On the safety of *Aspergillus niger*—A review. *Applied Microbiology and Biotechnology, 59,* 426–435.

Shilton, A. N., Powell, N., & Guieysse, B. (2012). Plant based phosphorus recovery from wastewater via algae and macrophytes. *Current Opinion in Biotechnology, 23,* 884–889.

Uduman, N., Qi, Y., Danquah, M. K., Forde, G. M., & Hoadley, A. (2010). Dewatering of microalgal cultures: A major bottleneck to algae-based fuels. *Journal of Renewable and Sustainable Energy, 2,* 012701. https://doi.org/10.1063/1.3294480.

Viswanath, B., Rajesh, B., Janardhan, A., Kumar, A. P., Narasimha. (2014). Fungal laccases and their application in bioremediation. *Enzyme Research 163242.* https://doi.org/10.1155/2014/163242.

Zhang, J., & Hu, B. (2012). A novel method to harvest microalgae via co-culture of filamentous fungi to form cell pellets. *Bioresource Technology, 114,* 529–535.

Event Scale Modeling of Experimental Green Roofs Runoff in a Mediterranean Environment

Mirka Mobilia and Antonia Longobardi

Abstract

Event scale analysis of green roofs hydrological performances in a Mediterranean environment. Different green roofs constructive technologies are investigated. Different hydrological models are applied to identify pros and cons of empirical and physically based models.

Keywords

Green roof • Hydrological performances • Event scale analysis

1 Introduction

Green roof (GR) is a technique with a significant potential for reducing outflow peak and runoff water volume compared to traditional roof types (Stovin et al. 2012; Fioretti et al. 2010; Berndtsson 2010). Prediction of hydrological behavior of a vegetated cover is essential for urban planners, policy makers and engineers in order to quantify runoff mitigation before the green roofs retrofit so as to optimize their application. The aim of the present research is to meet this need by testing the accuracy of three different hydrological models in predicting the stormwater management performance of green systems, moving from empirical to physically based approaches. In time, several authors have indeed proposed different hydrological models to predict the GR runoff response (Sartor et al. 2018; Mobilia et al. 2017; Locatelli et al. 2014). Among these, two approaches have been here selected due to their widespread use and demonstrated efficiency, namely the conceptual SWMM model (Rossman 2010) and the physically based 1DHydrus (Hilten et al. 2008). The latter has been further compared with a basic transfer function approach, the Nash model (Nash

1957), typically used to predict the hydrological behavior of natural river basins. Proposed models have been calibrated against observed data at two experimental green roofs test beds for a number of three recorded events.

2 Materials and Methods

2.1 Site Description and Data Acquisition

The two green roof test beds referred to in this study have been described in details in Mobilia and Longobardi (2017). The two benches differ for the composition of the drainage layer, being GR1 made up of expanded clay while GR2 made up of a commercial drainage MODì modules filled with expanded clay (Fig. 1).

The experimental site is fully instrumented with a meteorological station and a runoff measurement system. Three rainfall events recorded by the on-site weather station have been used as input data to calibrate the models. The studied events substantially differ in duration, maximum intensity and cumulative rainfall (Table 1).

2.2 Event Scale Modeling of GR Hydrological Performances

Three models belonging to different hydrological model classes have been applied in the current study for the simulation of the hydrological GR performances, to identify pros and cons of each approach. SWMM (US Environmental Protection Agency, USEPA) is a conceptual model able to simulate hydrology-hydraulic and water quality dynamics within urban areas during single and long-term rainfall events also for SUDS technologies, such as the green roofs. 1DHYDRUS is instead a physically based model that numerically solves Richard's equation for saturated-unsaturated water flow. SWMM and 1DHYDRUS, selected due to their widespread use and demonstrated efficiency,

M. Mobilia (✉) · A. Longobardi
Department of Civil Engineering, University of Salerno, Fisciano, SA, Italy
e-mail: mmobilia@unisa.it
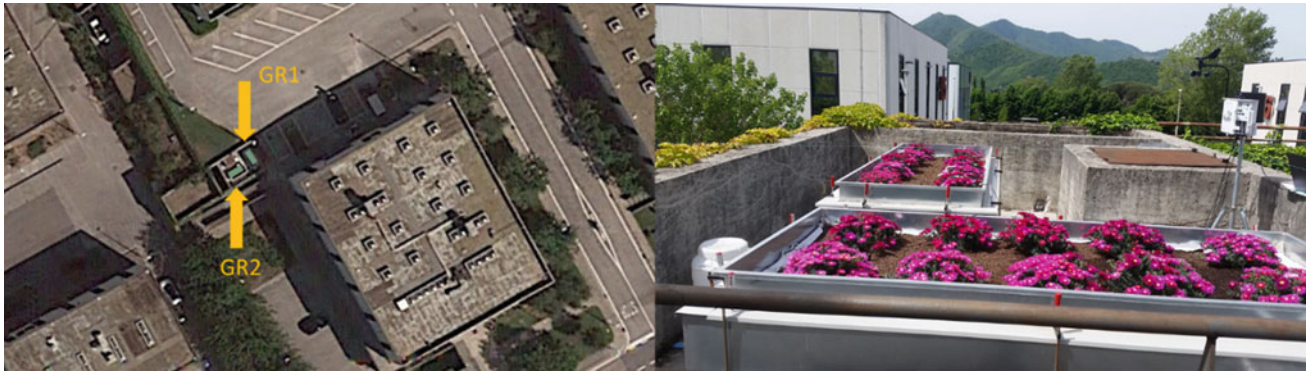
Fig. 1 Green roof test beds located in the University of Salerno campus

Table 1 Rainfall characteristics of the selected events

Events	Duration (h)	Cumulative rainfall (mm)	Maximum intensity (mm/h)
15_01_2018	16	20.1	9.4
09_02_2018	14	11.2	4.8
15_02_2018	4	4.8	2.5

have been further compared with a basic transfer function approach, the Nash model. The Nash cascade model is a transfer function model. The Nash cascade is a chain of linear stores that empty into each other. It has two parameters to govern the shape of the outflow response, namely the number of stores "n" and the outflow coefficient "k", which is identical for all stores. The instantaneous unit hydrograph $h(t)$:

$$h(t) = \frac{t^{n-1}}{(n-1)!k^n} e^{\frac{t}{k}} = \frac{t^{n-1}}{\Gamma(n)k^\wedge n} e^{\frac{t}{k}} \tag{1}$$

is used to transform the net rainfall input $p(t)$ into runoff $q(t)$ according to the convolution integral:

$$q(t) = \int_0^t p(\tau) \cdot h(t-\tau) d\tau \tag{2}$$

where the net rainfall input p is computed as a fraction (loss coefficient) of total rainfall input r:

$$p(t) = \varphi r(t) \tag{3}$$

Event scale models calibration has been based on the comparison between the observed and modeled hourly runoff values (Fig. 2). In order to quantitatively assess the models' accuracy in simulating volumetric rainfall retention from the two eco-roofs, the Nash–Sutcliffe Efficiency index (NSE) has been evaluated:

$$\text{NSE} = 1 - \frac{\sum_{i=1}^{n} \left(R_{\text{obs},i} - R_{\text{mod},i}\right)^2}{\sum_{i=1}^{n} \left(R_{\text{obs},i} - \bar{R}_{\text{mod},i}\right)^2} \tag{4}$$

where n represents the length of the sample, $R_{\text{mod},i}$, $R_{\text{obs},i}$ and $\bar{R}_{\text{obs},i}$ respectively represent the modeled and the observed runoff and mean of the observed runoff. In the case of SWMM, in order to simulate the two green roofs, the module called "Bio-retention cell" included in LID controls group has been used where the parameters subject to calibration have been the berm height and the percentage initially saturated of unit's soil. In the case of 1DHYDRUS, the initial conditions of water content are the only parameter subject to calibration whereas soil parameters have been set on the base of building materials properties. About the Nash cascade model, in the current application, the loss coefficient φ is set a priori based on the results of an empirical analysis of retention coefficients variability of the studied experimental green roof (Mobilia et al. in review 2018). The retention coefficients appear in fact to be function of cumulate rainfall and soil moisture properties which define the initial conditions prior to each event. Furthermore, a number of two stores have been a priori fixed (based on an analysis of hydrograph patterns), and the outflow coefficient has been only considered as a free parameter subject to calibration.

3 Results and Discussion

The Nash–Sutcliffe Efficiency indices describing event runoff predictions for SWMM, Hydrus and Nash cascade models have been reported in Table 2. The average value of 95% for GR1 and 93% for GR2 indicates the best model performances for Nash cascade model. The lowest values of
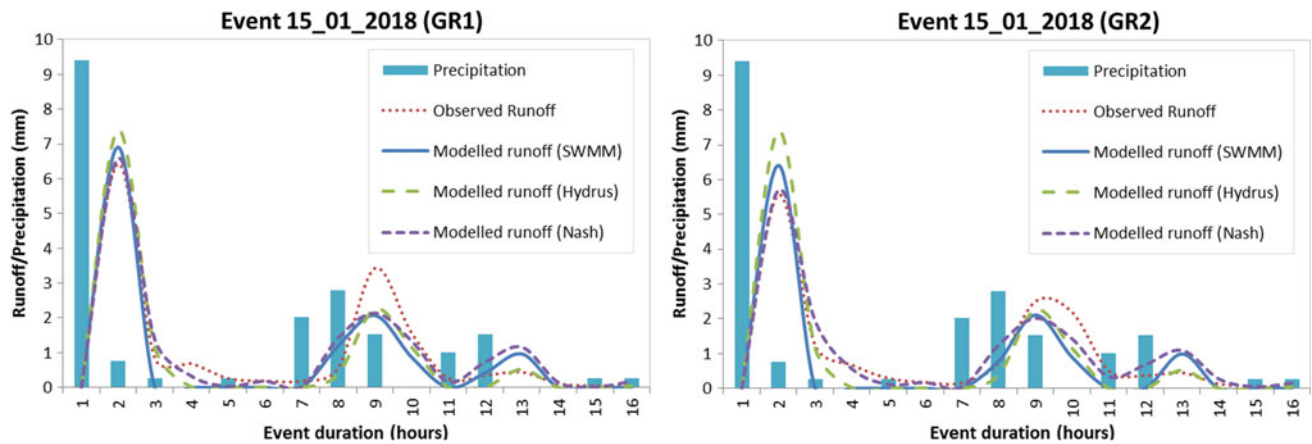
Fig. 2 Observed and modeled runoff for 15/01/2018 event

Table 2 Event scale goodness-of-fit index NSE for the different hydrological models

Events	SWMM		Hydrus		Nash cascade	
	GR1 (%)	GR2 (%)	GR1 (%)	GR2 (%)	GR1 (%)	GR2 (%)
15_01_2018	88	81	92	82	92	94
09_02_2018	95	74	90	87	94	86
15_02_2018	87	89	92	80	99	98
Mean	90	82	91	83	95	93

the model performance indexes, respectively, of 90% for GR1 and 82% for GR2 on average refer to SWMM. For each of the three models, the NSE index is lower for GR2 than GR1 that correspond to a better fitting of the models to the runoff values measured from the green roof with the drainage layer made up of expanded clay than from that one consisting of modular trays.

4 Conclusion

In this paper, three hydrologic models have been calibrated and compared against observed data from two experimental GR benches. The choice of the most appropriate approaches has fallen upon the most commonly and successfully used models for hydrologic assessment (SWMM, Hydrus and Nash model). Model calibration strategy is based on the comparison between the predicted and observed runoff flows. The Nash–Sutcliffe Efficiency index (NSE) has been evaluated to quantitatively assess the model accuracy in the prediction of the response of GRs in terms of runoff production. The results show that each of the three methods can be effectively used for modeling the hydrological behavior of the eco-roofs. Despite Nash cascade model requires few

details in the formulation and schematization of the considered hydrological processes, it returns the best model simulation performances. Finally, the models are better able to reproduce the behavior of a nature-based system like GR1 than of an artificial system with commercial modular trays (GR2).

References

Berndtsson, J. C. (2010). Green roof performance towards management of runoff water quantity and quality: A review. *Ecological Engineering, 36*(4), 351–360.

Fioretti, R., Palla, A., Lanza, L. G., & Principi, P. (2010). Green roof energy and water related performance in the Mediterranean climate. *Building and Environment, 45*(8), 1890–1904.

Hilten, R. N., Lawrence, T. M., Tollner, E. W. (2008). Modeling stormwater runoff from green roofs with HYDRUS-1D. *Journal of Hydrology 358*(3, 4), 288–293.

Locatelli, L., Mark, O., Mikkelsen, P. S., Arnbjerg-Nielsen, K., Jensen, M. B., & Binning, P. J. (2014). Modelling of green roof hydrological performance for urban drainage applications. *Journal of Hydrology, 519,* 3237–3248.

Mobilia, M., D'Ambrosio, R., Longobardi, A. (2018). Climate, soil moisture and drainage layer properties impact on green roofs in a Mediterranean environment. In *2nd WaterEnergyNEXUS International Conference*, in review.

Mobilia, M., Longobardi, A. (2017). Smart stormwater management in urban areas by roofs greening. In *Proceeding International Conference on Computational Science and Its Applications (ICCSA 17)* (pp. 455–463).

Mobilia, M., Longobardi, A., & Sartor, J. F. (2017). Including A-priori assessment of actual evapotranspiration for green roof daily scale hydrological modelling. *Water, 9*(2), 72.

Nash, J. E. (1957). The form of the instantaneous unit hydrograph. *International Association of Scientific Hydrology, Publication, 45,* 114–121.

Rossman, L. A. (2010). Storm water management model user's manual version 5.0, EPA/600/R-05/040, US EPA National Risk Management Research Laboratory, Cincinnati, Ohio, USA.

Sartor, J., Mobilia, M., & Longobardi, A. (2018). Results and findings from 15 years of sustainable urban storm water management. *International Journal of Safety and Security Engineering, 8*(4), 505–514.

Stovin, V., Vesuviano, G., & Kasmin, H. (2012). The hydrological performance of a green roof test bed under UK climatic conditions. *Journal of Hydrology, 414,* 148–161.

Advanced Technologies for Satellite Monitoring of Water Resources

Maria Nicolina Papa, Giuseppe Ruello, Francesco Mitidieri, and Donato Amitrano

Abstract

Exploitation of synthetic aperture radar satellite data. Monitoring of surface water resources with high resolution in time and space. Low-cost technic for freshwater monitoring. Appropriate technology for developing countries. Retrieval of river features: active channels, sediment bars and wet channels.

Keywords

Remote sensing • Reservoirs • Wetlands • Rivers • SAR

1 Introduction

Satellite remote-sensed data provide the opportunity of observing freshwater with high resolution in space and time and covering wide areas. Widespread applications employ data in the visual or infrared band, while the synthetic aperture radar (SAR) data have been until now less exploited. SAR data have significant advantages as the possibility to observe the earth surface also at nighttime and in the presence of cloud cover, the high spatial resolution (up to 1 m) and the short revisit time (about 15 days). The European Space Agency (ESA) distribute SAR data for free and other agencies (like, for example, the Italian Space Agency) provide data, free of charge, for scientific purposes.

In this paper, we investigate the opportunities of exploiting SAR data for the monitoring of different freshwater environments like river, lakes and wetlands. For each of these environments, a pilot project is implemented.

2 Materials and Methods

In order to investigate the potentiality of SAR data for monitoring freshwater resources, we propose the examination of three different study cases, each one dealing with a different environment, and in particular, lakes, rivers and wetlands.

The lakes pilot project (Amitrano et al. 2014a, b) is located in the north of Burkina Faso, where, like in others semi-arid regions, small reservoirs are widely employed for facing water scarcity and climatic variability. The small reservoirs are often built for the initiative of small local communities and even basic data as their location and capacity are not available; therefore, it is extremely hard to optimize their management. The use of remote sensing in this context could really be a breakthrough.

The river pilot project (Mitidieri et al. 2016) is a reach of the Italian River Orco (Piemonte), a wondering river with a mean slope ranging between 1.03 and 0.31% and a mean width ranging between 85 and 200 m. In order to evaluate, enhance or protect the hydro-morphological quality of the river, it is necessary to estimate its future trends moving from the understanding of the evolutions occurred in the past. The exploitation of satellite data is the less expensive, and in some cases the only, way to achieve this.

The SAR data employed for the lakes and river cases were COSMO-SkyMed strip map images (resolution 3 m) provided for free from ASI under the aegis of the 2007 COSMO-SkyMed AO Project and the ASI COSMO-SkyMed OPEN CALL for SCIENCE.

M. N. Papa (✉) · F. Mitidieri
Dipartimento di Ingegneria Civile, Università degli Studi di Salerno, Fisciano, Italy
e-mail: mnpapa@unisa.it

F. Mitidieri
e-mail: fmitidieri@unisa.it

G. Ruello · D. Amitrano
Dipartimento di Ingegneria Elettrica e delle Tecnologie dell'Informazione, Università degli Studi di Napoli Federico II, Naples, Italy
e-mail: ruello@unina.it

D. Amitrano
e-mail: donato.amitrano@unina.it

The third pilot project is the Albufera wetland close to Valencia (Spain). This wetland is exploited for the cultivation of rise and at the same time provides important ecosystem services. For this reason, it is important to monitor the occurrence and duration of flooding and to understand the link between the presence/absence of water and the biological and physicochemical quality of the wetland environment.

The SAR data of Sentinel 1 freely distributed by the European Space Agency (ESA) were used in this case. Data are available since 2017 and provide maps made of rectangular pixels, having sides of 5 and 20 m, with a revisit time of 12 days on average.

All the SAR images were treated through multi-temporal processing, consisting of: co-registration, calibration and despeckling. Due to the very low back signal from water surfaces, these areas can be distinguished in black in the SAR images. Therefore, it is possible to classify the pixels covered by water by applying automatic and semi-automatic procedures (Fig. 1). Two different technics were used to separate the class "water" from the class "no water", the first one was the application of an intensity threshold (lakes and
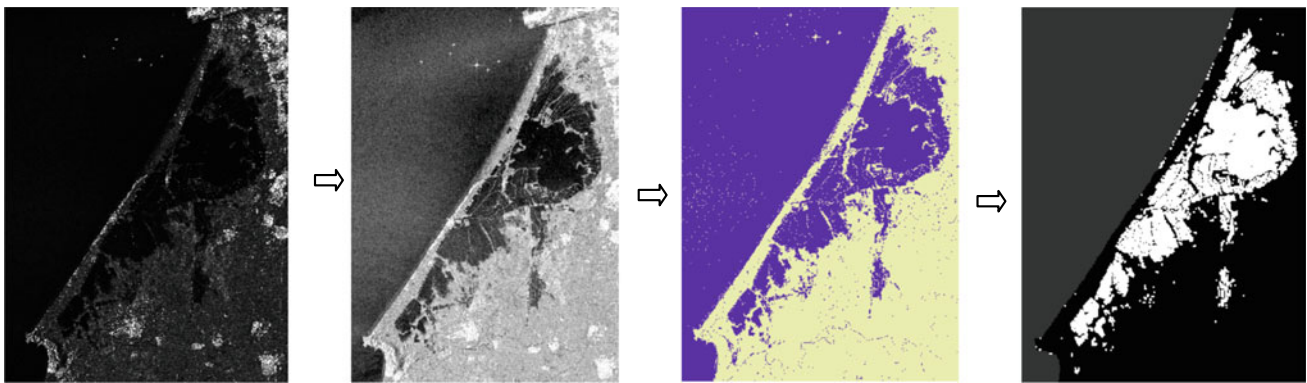
Fig. 1 Processing chain of SAR data for the Albufera wetland. From left to right: result of preprocessing and co-registration; result of the speckle filtering, result of the k-means classification; result of the morphological filtering

Fig. 2 River features extracted from SAR and overlaid to orthophoto. From left to right: Active Channel (AC), Water Channel (WC), Sediment Bars (SB)

river pilot projects) and the second one was a *k*-means clustering procedure (wetland pilot project).

In the river pilot project, apart from the automatic extraction of water pixels, that gives the delimitation of the water channels (WC), also the active channel (AC) and sediment bars (SB) were identified and delimited by a visual interpretation of the SAR images in GIS environment (Fig. 2).

3 Results and Discussion

The use of remote sensed SAR data provided crucial data for the monitoring of water resources in the three different freshwater environments examined. In the reservoirs study case (Burkina Faso), the knowledge of the surface covered by water, integrated with the digital elevation model obtained via interferometric processing, allowed us to estimate the volumes of available water in the observed reservoirs. This data, not available before, allowed for the calibration and validation of a hydrological model for the prediction of future conditions and therefore employable for the optimization of water resources management (Fig. 3).

In the river pilot project, the retrieved data showed that AC areas widen in response to flood events and slowly narrow during low flow. A river mobility index was proposed based on the WC channel time evolution. This allowed for the investigation of the relation between the mobility of the river and the water discharges.

In the wetland pilot project (Albufera), it was possible to provide, for the entire area, the time series of presence/absence of water. This information will be the basis for the investigation of the relation between the duration of dry and wet period and the habitat availability for target species.

4 Conclusions

In this paper, an innovative approach is presented for the effective use of high-resolution SAR data for water-related applications. In particular, we retrieved from SAR images appropriate information to support decisions on water resource management. The approach was implemented in three pilot projects, dealing with the observation of lakes (water reservoirs in the north of Burkina Faso), rivers (Orco River in Italy) and wetlands (Albufera wetland in Spain). In Burkina Faso, we monitored water intake in reservoirs and its evolution in time. With the developed technique, a synoptic view of the total water volume available in the reservoirs of an entire region can be provided. This information, often missing in low-income countries, is crucial for an appropriate management of water use and for the prevention and mitigation of water crisis.

The application of the monitoring approach to the river study case showed great potentiality for the building up of the necessary knowledge of river hydro-morphological evolution in time. It was possible to reconstruct the time evolution of wet channels, active channels and sediment bars. This information is extremely important for the prediction of possible future trends and therefore they constitute the basis for the management of the river.

Finally, the wetland monitoring provided the spatially distributed, time series of the wet and dry periods. The observed dynamic will be correlated with the corresponding effects on the biological and physicochemical quality of the water environment. On the basis of the gained knowledge, it will be possible to optimize the wetland management for the improvement of the environmental quality and the protection of biodiversity.

From the manifold of the implemented pilot cases, it is evident that remote sensing in general and SAR images in
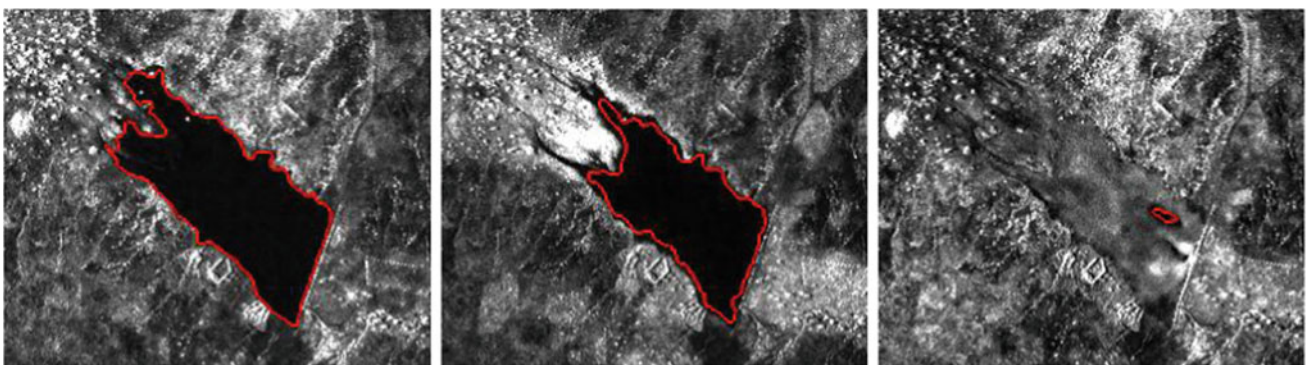
Fig. 3 Shorelines extraction of the Laaba reservoir; acquisitions of (from left to right): 2010/06/12, 2010/08/31 and 2011/03/27

particular, hold enormous potentialities, mainly in the poorest areas of the Earth and that their use can provide significant advantages to all the involved stakeholders.

References

Amitrano, D., Ciervo, F., Di Martino, G., Papa, M. N., Iodice, A., Koussoube, Y., et al. (2014a). Modeling watershed response in semiarid regions with high-resolution synthetic aperture radars. *IEEE Journal of Selected Topics in Applied Earth Observations and Remote Sensing 7*(7).

Amitrano, D., Di Martino, G., Iodice, A., Riccio, D., Ruello, G., Ciervo, F., et al. (2014b). Effectiveness of high-resolution SAR for water resource management in low-income semi-arid countries. *International Journal of Remote Sensing 35*(1).

Mitidieri, F., Papa, M. N., Amitrano, D., Ruello, G. (2016). River morphology monitoring using multitemporal sar data: Preliminary results. *European Journal of Remote Sensing 49*.

Tannery Wastewater Treatment After Biological Pretreatment by Using Electrochemical Oxidation

Tran Le Luu, Tran Tan Tien, Nguyen Ba Duong, and Nguyen Thi Thanh Phuong

Abstract

Tanning industry is receiving a lot of attention due to its pollution levels and discharge legislations toward the environment. Tanerry wastewater treatment by using electrochemical oxidation with SnO_2/Ti and PbO_2/Ti anodes. The tannery wastewater was pretreated using biological method with aerotank process. SnO_2/Ti and PbO_2/Ti anodes effectively treated COD and total nitrogen over 85% after 90 min of electrolysis. The treatment efficiency in tannery wastewater of SnO_2/Ti anode is greater than PbO_2/Ti anode.

1 Introduction

Tanning is an industry that pollutes the environment, including solids, liquids, and gaseous media. Unwanted organic substances such as hair, fat, and meat in the original materials (fresh skin, salted skin) are removed with the excess chemicals with inorganic and organic waste to the wastewater (Dinh et al. 2013). The decomposition of organic matter in the original material creates a foul smell characteristic in the production area and the surrounding area. Evaporation and boiler emissions also contribute negatively to the state of the environment. The pollutants in tannery wastewater require a combination of treatments such as mechanical, physical, chemical like fenton, and biological methods. However, due to economic and technical constraints, the majority of pollutants after treatment at the factories are still high, the basic pollution parameters such as BOD_5, COD, NH_3, and color do not still not meet the effluent discharge standards. Recently, the electrochemical oxidation has been extensively studied for the application of many types of wastewater treatment. Electrochemicals open up new avenues for the treatment of harmful organic pollutants, which can oxidize toxic organic pollutants with phenolic microorganisms into organic substances that can be completely oxidized to CO_2 and water. This technology consists of the direct and/or indirect oxidation of organic matter contained in wastewater in a suitable anode or in a solution of an electrochemical device. However, in the process of electrolysis, the side reactions that make up oxygen can occur and reduce the oxidation efficiency. The electrochemical treatment of industrial wastewater is increasingly in concern because it has its own advantages such as simple equipment, high capacity for medium and small scale, low initial investment, electrical speed control and easy automation, requires very little or no chemicals in the process, environmental friendly, and high selectivity.

2 Materials and Methods

All the experiments were performed at room temperature and analysis followed the Standard Method for the examination of Water and Wastewater (USA). At regular time intervals, wastewater samples were withdrawn and collected in beaker for further analysis. pH, color, and conductivity were measured by using Metrohm 900 multimeter, Switzerland. Chemical oxygen demand (COD) was measured by using Lovibond RD125 Thermoreactor Closed Reflux Titrimetric Method, England. Total Nitrogen (TN) was measured by using TOC Shimadzu 00936, Japan.

T. Le Luu (✉) · T. T. Tien
Department of Mechatronics and Sensor Systems Technology, Vietnamese German University, Thủ Dầu Một, Binh Duong 590000, Viet Nam
e-mail: luu.tl@vgu.edu.vn

N. B. Duong · N. T. T. Phuong
Institute of Environment and Natural Resources, Viet Nam National University, Ho Chi Minh City 700000, Viet Nam

Total Chromium in the wastewater was analyzed by using an atomic absorption spectrometer (Analytic Jena Contraa 300, Germany). Total NO_3^-, NH_4^+, and Cl^- were measured by using ion chromatography (Metrohm IC 883, Switzerland).

3 Results and Discussion

3.1 Effect of pH

The result of treatment of pollutants in tanning effluents with SnO_2/Ti and PbO_2/Ti anodes corresponding to difference pH is presented in Fig. 1. As shown in Fig. 2a, the color treatment efficiency of the SnO_2/Ti electrode was quite high, up to

60.7% at pH 8, equivalent to a drop of color to 186 Pt–Co. Increasing or decreasing pH of the wastewater compared to pH 8 resulted in a reduction of treatment efficiency. The color treatment efficiency in the base medium is higher than the acidic environment. The COD removal efficiency of SnO_2/Ti anode when changing the pH of the wastewater gave similar results to the color treatment, which is due to the colorant compounds in the wastewater treatment is mainly the organic residue remaining after biological pretreatment (e.g., tannic acid). When chemically oxidized organic compound into easily digestible secondary products, like either CO_2 or H_2O, is followed by a reduction in COD and color. The COD and TN treatment efficiencies when using SnO_2/Ti electrode gave the best at pH 8 with 51.8 and 55.2%, equivalent to 149 and
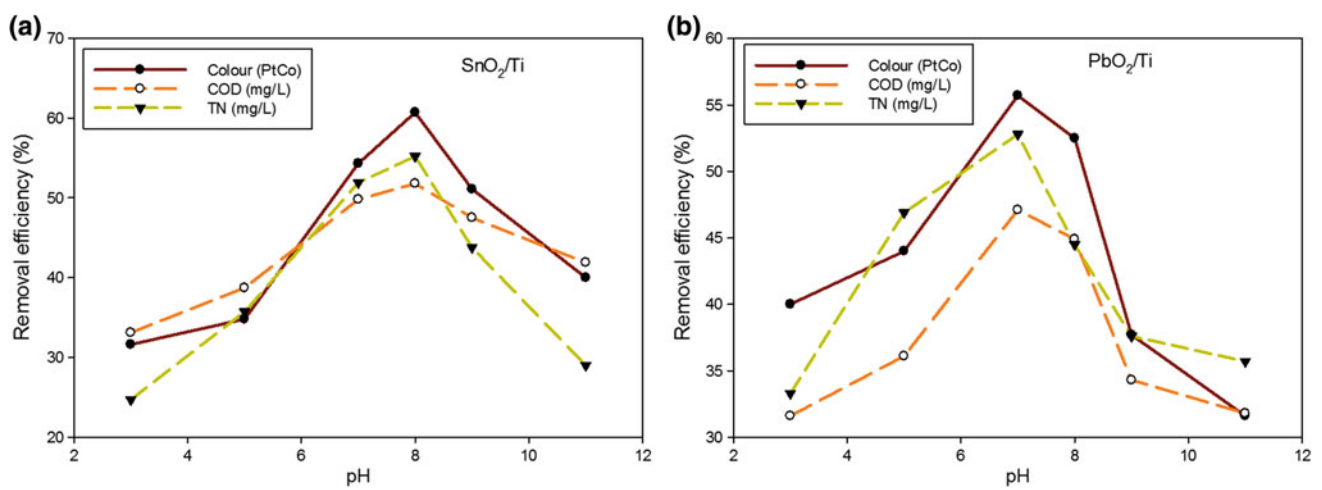
Fig. 1 Effect of pH on tannery wastewater treatment efficiency of SnO_2/Ti (**a**) and PbO_2/Ti (**b**) anodes. Experimental condition: current density 33.3 mA/cm^2, agitation rate 200 rpm and electrolysis time 60 min
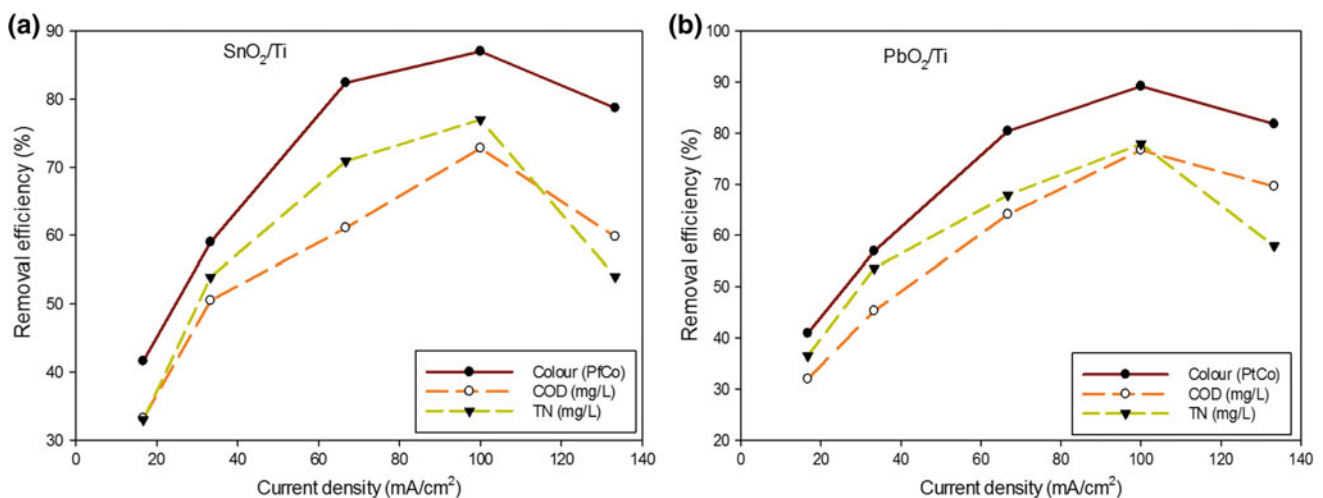
Fig. 2 Effect of current density on the treatment efficiency of SnO_2/Ti and PbO_2/Ti anodes. Experimental condition: pH 8, electrolysis time 60 min, agitation rate 200 rpm

77.4 mg/L, respectively. Similar to the color processing efficiency, total COD and nitrogen removal efficiency were lowest at pH 3 with 37.7 and 24.6%. The pH values significantly influence on the effluent treatment efficiency of the SnO_2/Ti electrode. The color, COD, and TN removal efficiencies are best in neutral medium (pH 7), which results in higher processing efficiency in the acid or base mediums. This result agreed with the study of Xiuping Zhu et al. (2009) reported the N–NH_3 treatment by changing pH that neutral N–NH_3 was more effective than in acidic environments. This is explained by the fact that nitrogen in tannery wastewater after biological pretreatment mainly exists in the N–NH_3 form and is readily decomposed in the base medium according to the following reaction:

$$2NH_4^+ + 6OH^- \rightarrow N_2 + 6H_2O + 2H^+ + 6e-$$
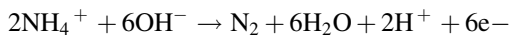
As another aspect showed in Fig. 2b, the color treatment efficiency of the PbO_2/Ti electrode was highest at pH 7 with 56.3%, corresponding a reduction to 196 Pt–Co. Effectively, color treatment in acidic environments showed better performance than in the base environment. The lowest color treatment efficiency was achieved at pH 11 when the treatment efficiency was only 31.6%, equivalent to the color reduction to 299 Pt–Co. Similarly with the color efficiency, COD and TN efficiencies also were best achieved at pH 7 with a COD removal efficiency 47.1%, equivalent to a reduction to 165 mg/L, the TN removal efficiency was 52.81% equivalent to the reduction to 78.2 mg/L. COD removal efficiency was low at pH 3 and pH 11 with 31.6 and 31.8%, respectively. Meanwhile, the TN treatment efficiency was lowest at pH 3, reaching only 35.67%. After treatment, the pH of the wastewater was reduced.

3.2 Effect of Current Density

Figure 2 shows the experimental result of tannery wastewater treatment using electrochemical oxidation at SnO_2/Ti and PbO_2/Ti anodes with different current densities. The current densities significantly affect tannery wastewater after biological pretreatment with SnO_2/Ti anode. Increasing the current density increases the treatment efficiency of pollutants in wastewater. As shown in Fig. 2a with SnO_2/Ti anode, the color treatment efficiency rapidly increased as the current density increased from 16.7 to 100 mA/cm^2 then decreased at 133.3 mA/cm^2. In particular, at current density 16.7 mA/cm^2, the treatment efficiency was 41.6%, equivalent to the reduction of 279 Pt–Co. When increasing the current density to 33.3, 66.6, and 100 mA/cm^2, the color

treatment efficiency achieved 59, 82.4, and 87%, respectively. At the current density 133.3 mA/cm^2, the color treatment efficiency reduced to 78.7%, equivalent to 102 Pt–Co. The trend of decreasing COD and total Nitrogen is quite similar to color, however at a smaller scale. This indicates the stable and comprehensive treatment of SnO_2/Ti anode after biological pretreatment of tannery wastewater.

4 Conclusion

In this study, SnO_2/Ti and PbO_2/Ti anodes can thoroughly treat the pollutants in the tannery wastewater after activated sludge pretreatment. SnO_2/Ti and PbO_2/Ti anodes effectively treated COD and total nitrogen to up to 85% after 90 min of electrolysis at a current density of 66.7 mA/cm^2. From the above results, it was found that the pH of the wastewater directly affected the efficiency of the treatment. SnO_2/Ti electrode gave higher efficiency in wastewater with neutral pH to base, while PbO_2/Ti electrode offered higher processing efficiency in acidic to neutral wastewater. The current density and the rate of agitation affected the treatment efficiency of the two electrodes, while the duration of the treatment is inversely proportional to the depletion of pollutants in the effluent. SnO_2/Ti anode has higher treatment efficiency, lower energy consumption, and lower cost compared to PbO_2/Ti anode in tannery wastewater treatment; however, its stability is not quite good. The combination of biological pretreatment and electrochemical oxidation can treat the tannery wastewater to achieve the Vietnamese discharge standard for effluents.

References

Benhadji, A., Ahmed, M. T., & Maachi, R. (2011). Electrocoagulation and effect of cathode materials on the removal of pollutants from tannery wastewater of Rouïba. *Desalination, 277*, 128–134.

Deghles, A., & Kurt, U. (2016). Treatment of raw tannery wastewater by electrocoagulation technique: Optimization of effective parameters using Taguchi method. *Desalination and Water Treatment, 57*, 14798–14809.

Dinh, H. T. (2013). *Light manufacturing in Viet Nam* (pp. 1–89). The World Bank.

Lofrano, G., Meriç, S., Zengin, G., & Orhon, D. (2013). Chemical and biological treatment technologies for leather tannery chemicals and wastewaters: A review. *Science of the Total Environment, 461*, 265–281.

Zhu, X., Ni, J., & Lai, P. (2009). Advanced treatment of biologically pretreated coking wastewater by electrochemical oxidation using boron-doped diamond electrodes. *Water Research, 43*, 4347–4355.

Numerical Modelling of Integrated OMBR-NF Hybrid System for Simultaneous Wastewater Reclamation and Brine Management

Shadi Wajih Hasan and Vincenzo Naddeo

Abstract

OMBR is a recently developed technology for wastewater treatment. OMBR-NF hybrid system was numerically modelled. Influence of process variables on system performance indicators was investigated.

Keywords

OMBR • NF • Wastewater reclamation •
Brine management • Modelling

1 Introduction

Membrane bioreactors (MBRs), as a highly productive wastewater treatment technology combining biological treatment with membrane separation, have gained great attention for industrial and municipal wastewater treatment. When compared with the conventional activated sludge (CAS) technology, MBRs have an array of advantages such as limited footprint, least sludge production, and better effluent quality. Despite having attained these advantages over CAS, MBRs have several limitations resisting its application in multiple water treatment plants. Energy requirement for MBRs is relatively higher compared to CAS (Meng et al. 2009). Apart from this, membrane fouling results in performance reduction, severe flux decline or expeditious pressure increase, and continual membrane cleaning, which leads to a direct increase in operating and maintenance costs. Osmotic membrane bioreactors (OMBRs) have been introduced as an expansion to conventional MBRs. The use of forward osmosis (FO) dense membranes in OMBR offers several advantages over porous pressure-driven microfiltration (MF)/ultrafiltration (UF) porous membranes used in MBRs (Cornelissen et al. 2008). These include effective membrane rejection, limited membrane fouling, and lower energy consumption (Achilli et al. 2009). Nanofiltration (NF) is the most recent development among the pressure-driven membranes process for liquid-phase separation. NF had been able to replace reverse osmosis (RO) in many fields of applications because of its low energy requirements and higher flux rates. The properties of NF ranges in between non-porous RO membranes, in which the transport is governed by a solution-diffusion mechanism, and porous UF membranes in which the transport is predicted by size exclusion or charge effect is some cases (Gozalvez et al. 2002;

S. W. Hasan (✉)
Department of Chemical Engineering, Center for Membrane and Advanced Water Technology, Khalifa University of Science and Technology, Masdar City Campus, 127788 Abu Dhabi, UAE
e-mail: shadi.hasan@ku.ac.ae

V. Naddeo
Department of Civil Engineering, University of Salerno, Via Giovanni Paolo II 132, Fisciano 84084, SA, Italy
e-mail: vnaddeo@unisa.it

Bowen and Welfoot 2002). These properties make NF extremely useful in practical application such as selective removal of particles, fractionalization, and ultra-purification. Reject brine from seawater desalination plants remains a huge environmental challenge through which methods of brine volume minimization have been investigated by many researchers (Kazner et al. 2014; Martinetti et al. 2009). In OMBR systems, draw solutions (DS) of high salinities are used in order to create sufficient osmotic pressure to withdraw pure water from the feed side (FS) across the FO membrane. Modelling RO rejects brine and wastewater as DS and FS, respectively, was proposed in this paper. Therefore, the main objective of this paper was to model an integrated OMBR-NF hybrid system for simultaneous wastewater reclamation and brine management from energy requirements and water quality perspectives.

2 Materials and Methods

The influence of five key process variables (model inputs) such as K_d (mass transfer coefficient in the draw side), X_{di} (draw solution concentration), K_{ICP} (internal concentration polarization coefficient), SRT (sludge retention time in the feed side), and Q_{fi}/Q_{di} (inlet feed-to-draw mass ratio) on each of the following system performance indicators (model outputs): $\Delta\pi_{eff}$ (effective osmotic pressure), J_w (pure water flux across the membrane), X_{ww} (concentration of pure water that permeates through the membrane), J_s (reverse salt flux), and ECP (external concentration polarization in the draw side) was investigated. The developed model for the OMBR-NF hybrid system consisted of a flat sheet membrane submerged in the bioreactor and a concentrated brine as the DS. FS enters the OMBR system

where water diffuses across the FO membrane thus diluting the DS. Concentrated sludge is rejected from the OMBR, returned and mixed with the FS. Diluted DS is then sent to a NF unit through which pure water is generated while concentrated DS is sent back to the OMBR. Mass balance for water and salts in the OMBR and NF was carried out at steady state.

The driving force of J_w through the FO membrane is the $\Delta\pi_{eff}$, which depends on the internal (ICP) and external concentration polarization effects. The negative driving force of $\Delta\pi_{eff}$ is the hydraulic pressure difference between the DS side and the feed side (i.e. transmembrane pressure; ΔP). Thus, J_w can be calculated using Eq. (1):

$$J_w = A(\Delta\pi_{eff} - \Delta P) \tag{1}$$

where A is the pure water permeability of FO membrane.

The J_s is a function of J_w and can be calculated using Eq. (2):

$$J_s = BJ_w/A\beta R_g T \tag{2}$$

where B is the salt permeability of FO membrane; b is the van't Hoff coefficient; R_g is the universal gas constant; and T is the absolute temperature.

MATLAB R2011b software was used to solve the model equations of the OMBR-NF hybrid system, and sensitivity analysis using one-at-a-time OAT approach was used to obtain the results for the variation of one variable in certain selected parameters.

3 Results and Discussion

See Fig. 1.
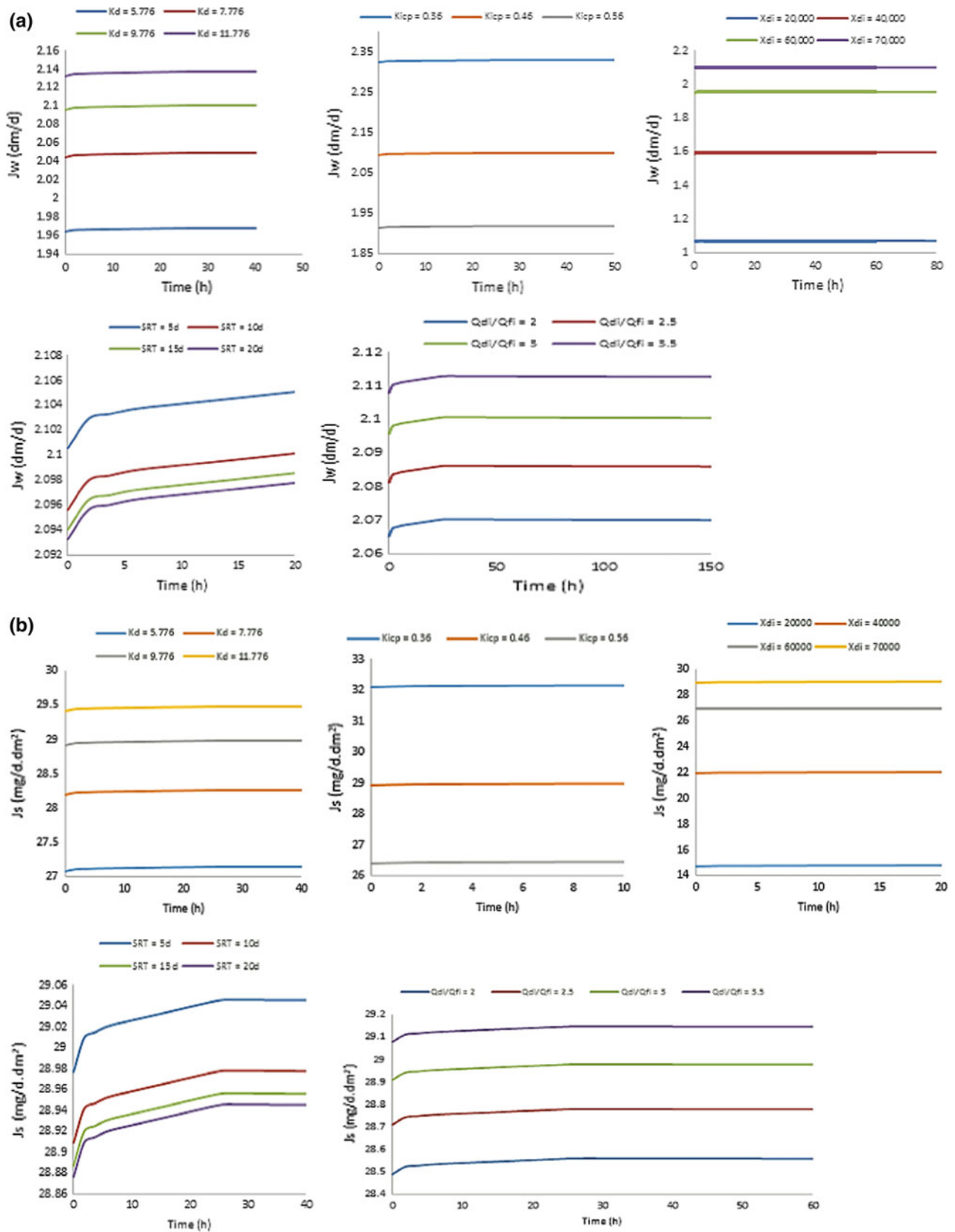
Fig. 1 Impact of K_d, K_{ICP}, X_{di}, SRT and Q_{di}/Q_{fi} process variables on **a** J_w, and **b** J_s

4 Conclusions

The combination of OMBR and NF was demonstrated in this paper. A numerical modelling involving process variables and system indicators was developed. The impact of system variables on performance indicators was investigated for optimal operation of the integrated OMBR-NF hybrid system. Sensitivity analysis results demonstrated a viable system, which can be utilized for wastewater treatment associated with the utilization of reject brine as a draw solution.

References

Achilli, A., Cath, T. Y., Marchand, E. A., Childress, A. E. (2009). The forward osmosis membrane bioreactor: A low fouling alternative to MBR processes. *Desalination 239*, 10–21.

Bowen, W. R., & Welfoot, J. S. (2002). Modelling the performance of membrane nanofiltration critical assessment and model development. *Chemical Engineering Science, 57,* 1121–1137.

Cornelissen, E. R., Harmsen, D., de Korte, K. F., Ruiken, C. J., Qin, J. J., Oo, H., et al. (2008). Membrane fouling and process performance of forward osmosis membranes on activated sludge. *Journal of Membrane Science, 319,* 158–168.

Gozalvez, J. M., Lora, J., Mendoza, J. A., & Sancho, M. (2002). Modelling of a low-pressure reverse osmosis system with concentrate recirculation to obtain high recovery levels. *Desalination, 144,* 341–345.

Kazner, C., Jamil, S., Phuntsho, S., Shon, H. K., Wintgens, T., & Vigneswaran, S. (2014). Forward osmosis for the treatment of reverse osmosis concentrate from water reclamation: Process performance and fouling control. *Water Science and Technology, 69,* 2431–2437.

Martinetti, C. R., Childress, A. E., & Cath, T. Y. (2009). High recovery of concentrated RO brines using forward osmosis and membrane distillation. *Journal of Membrane Science, 331,* 31–39.

Meng, F. G., Chae, S. R., Drews, A., Kraume, M., Shin, H. S., & Yang, F. L. (2009). Recent advances in membrane bioreactors (MBRs): Membrane fouling and membrane material. *Water Research, 43,* 1489–1512.

Climate, Soil Moisture and Drainage Layer Properties Impact on Green Roofs in a Mediterranean Environment

Mirka Mobilia, Roberta D'Ambrosio, and Antonia Longobardi

Abstract

Analysis of event scale hydrological performances of green roofs in a Mediterranean environment. Different green roofs constructive technologies are investigated. Observed soil water contents help describe the impact of cumulative rainfall depth and duration on green roofs hydrological performances.

1 Introduction

In the last few years, due to an increasingly invasive urbanization the scientific community has had to face technologies for hydrogeological risks management in urban environments (Sartor et al. 2018). GRs are considered, in this context, a promising solution able to reduce the risks deriving from the inability of drainage urban systems to collect stormwater. They act as filters that reduce the stormwater production based on the specific retention capacity. Green roof retention capacity depends on numerous factors such as the characteristics of the rain event, the moisture content, the depth and characteristics of the substrate, the vegetation and the slope (Carbone et al. 2015; Speak et al. 2013; Teemusk and Mander 2007; Wong and Jim 2014), and the research in this area is still challenging and affected by large uncertainties (Nawaz et al. 2015; Soulis et al. 2017). In particular, in the Mediterranean regions, characterized by long periods of drought, high temperatures and heavy rainfall, the substrate layer moisture content, which is not routinely measured, is considered the key element that influences the performance of green roofs and is mainly affected by substrate depth and composition of the soil (Chenot et al. 2017). In the reported paper, the importance of observed substrate soil moisture measurements is shown to improve the prediction of hydrological performances of two extensive green roofs test beds, located in the University of Salerno campus, Southern Italy (Mobilia et al. 2017, Mobilia and Longobardi 2017), highlighting the dependence of rainfall depth and duration and on the construction technology.

2 Materials and Methods

2.1 UNISA Experimental Site

In January 2017, two green roof test beds were installed at the Laboratory of Environmental and Maritime Hydraulic, Department of Civil Engineering of the University of Salerno, Southern Italy (Fig. 1a).

They are characterized by the same vegetation layer, made up of succulent Mesembryanthemum, and the same 10 cm peat and zeolite support substrate layer. Different storage layer technologies make distinction between the two test beds. In the case of GR1, it consists of a traditional expanded clay layer of 5 cm depth, while in the case of GR2 it consists of a commercial modular tray panel, MODì, filled with expanded clay (Fig. 1b). A nonwoven filter mat is interposed between the substrate and the storage layer. GR layers are placed on stainless steel benches with a surface of 2.5 m² (1 × 2.5 m) and a double pitch slope of 1%. The experimental site is fully and continuously (5 min resolution) monitored with a meteorological station including a tipping bucket type rain gauge, a thermo hygrometer, a pyranometer and four soil moisture sensors (Fig. 1c). Runoff from GRs is collected within tanks and measured on a 5 min step by digital scales.

M. Mobilia (✉) · R. D'Ambrosio · A. Longobardi
Department of Civil Engineering, University of Salerno, Fisciano, SA, Italy
e-mail: mmobilia@unisa.it
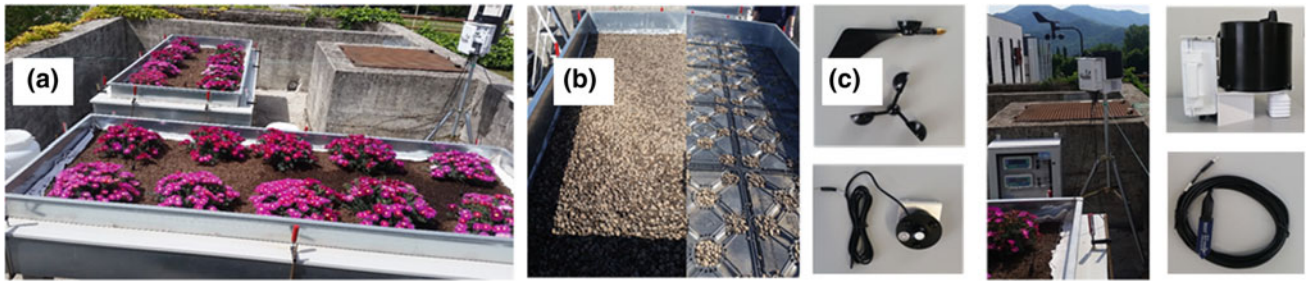
Fig. 1 **a** GR experimental test beds at University of Salerno, **b** drainage layer construction types, **c** the monitoring system

2.2 Retention Capacity of Experimental GRs

The monitoring campaign has started in February 2017, but measurements collected during February and March have been discarded because during that period the system was considered at an early stage. Analyses concern 14 rainfall-runoff events. For each test bed and for each observed event, the hydrological performance in term of retention capacity "RC" has been computed according to:

$$RC = 1 - C^*$$ (1)

where C^* is the discharge coefficient, computed as the ratio between the cumulative observed runoff depth and the cumulative observed rainfall depth at the event scale. Beside the RC coefficient, cumulate rainfall, rainfall duration and observed initial substrate soil water content have been derived for each event.

3 Results and Discussion

To analyze the role played by the soil moisture content VW (%) in the hydrological behavior of the GRs, the relationship between the retention capacity and the soil water content has been firstly investigated (Fig. 2). Data appear characterized by a large amount of scatter, but it is possible to identify groups of events for each of which a different hydrological behavior is detected, reducing the prediction uncertainty. A first group is identified as the events characterized by low cumulative rainfall depth (crosses in Fig. 2). A rainfall threshold of 11 mm has been found. Despite the high soil moisture content approached in some cases (especially for GR2), the stormwater production is negligible for this group of events, with average retention capacity of about 83%.

A second group is represented by initial low soil moisture content events (triangles in Fig. 2). A water content threshold of 5% has been found. For those events, the retention capacity presents a large degree of variability. The rainfall characteristic such as the duration and cumulative precipitation depth of the events are factors to be considered when searching for explanations of the mentioned variability, such as illustrated in Fig. 3. Regardless for the specific soil water content, when the initial soil moisture content is below the 5%, the retention capacity is strongly dependent on rainfall properties, with the largest GR storage occurring for the lower cumulative rainfall and duration.

The remaining group (circles in Fig. 2) describes an almost linear relationship between the soil water content and the retention capacity. The drainage layer building practices appear not be dramatically important for the investigated case study, as the hydrological performances of GR1 and GR2 appear almost similar at the event scale, with a moderate larger retention capacity of about 10% of GR2 over GR1.

4 Conclusion

In this paper, the relationship between the retention capacity of GRs systems, the characteristics of the rainfall triggering stormwater events and the initial substrate soil moisture content has been investigated. The results show that the hydrological response of the green roof systems is driven by threshold mechanisms in which the retention capacity is governed by the rainfall properties, when the moisture content is under a water content threshold of 5%, and almost constant when the rainfall volume is below a threshold of 10 mm. In the remaining cases, the retention capacity is highly affected by the soil water content. The drainage layer building practices only moderately affect the event scale performance as GR1 and GR2 appear to be characterized by similar RC coefficients, but they appear to affect the hydrological processes dynamic occurring at the two GRs as the GR2 observed initial soil moisture contents seem consistently larger than the one observed at GR1.
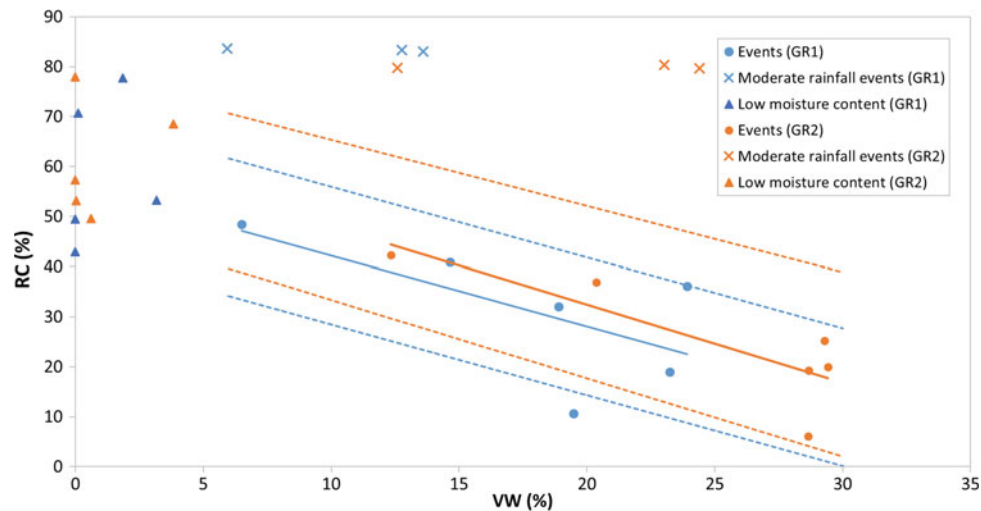
Fig. 2 Retention capacity of the two green roofs as a function of initial soil water content (dashed lines represent prediction boundaries for $\alpha = 0.05$)
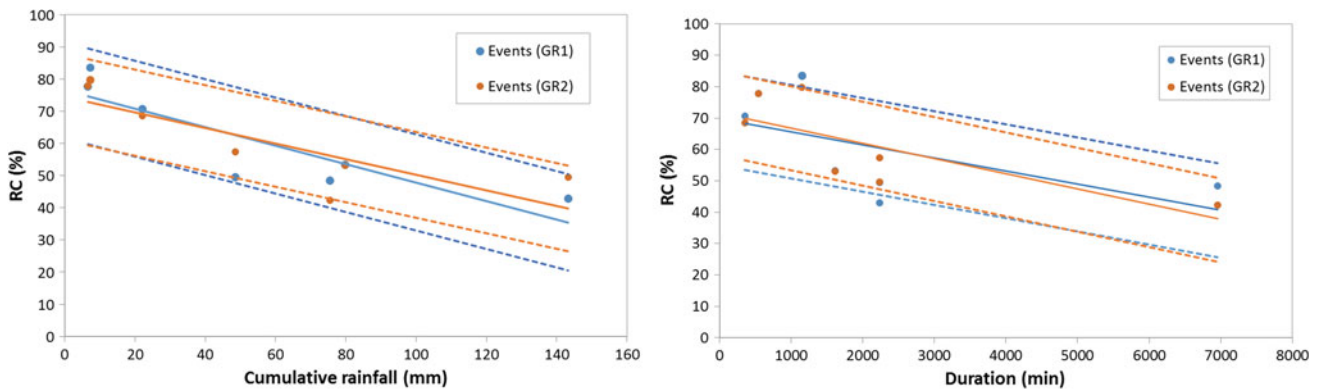
Fig. 3 Retention capacity of the two green roofs as a function of cumulative rainfall and duration (low initial soil water content events group) (dashed lines represent prediction boundaries for $\alpha = 0.05$)

References

Carbone, M., Nigro, G., Garofalo, G., & Piro, P. (2015). Experimental testing for evaluating the influence of substrate thickness on the sub-surface runoff of a green roof. *Applied Mechanics and Materials, 737,* 705–709.

Chenot, J., Gaget, E., Moinardeau, C., Jaunatre, R., Buisson, E., & Dutoit, T. (2017). Substrate composition and depth affect soil moisture behavior and plant-soil relationship on mediterranean extensive green roofs. *Water, 9*(11), 817.

Mobilia, M., Longobardi, A. (2017). Smart stormwater management in Urban areas by roofs greening. In *Proceeding International Conference on Computational Science and Its Applications (ICCSA 17)*, pp.455–463.

Mobilia, M., Longobardi, A., & Sartor, J. F. (2017). Including a-priori assessment of actual evapotranspiration for green roof daily scale hydrological modelling. *Water, 9*(2), 72.

Nawaz, R., McDonald, A., & Postoyko, S. (2015). Hydrological performance of a full-scale extensive green roof located in a temperate climate. *Ecological Engineering, 82,* 66–80.

Soulis, K. X., Ntoulas, N., Nektarios, P. A., & Kargas, G. (2017). Runoff reduction from extensive green roofs having different substrate depth and plant cover. *Ecological Engineering, 102,* 80–89.

Speak, A. F., Rothwell, J. J., Lindley, S. J., & Smith, C. L. (2013). Rainwater runoff retention on an aged intensive green roof. *Science of the Total Environment, 461,* 28–38.

Teemusk, A., & Mander, U. (2007). Rainwater runoff quantity and quality performance from a green roof: The effects of short-term events. *Ecological Engineering, 30,* 271–277.

Sartor, J., Mobilia, M., & Longobardi, A. (2018). Results and findings from 15 years of sustainable urban storm water management. *International Journal of Safety and Security Engineering, 8*(4), 505–514.

Wong, G. K., & Jim, C. Y. (2014). Quantitative hydrologic performance of extensive green roof under humid-tropical rainfall regime. *Ecological Engineering, 70,* 366–378.

Orthophosphate Versus Bicarbonate for Buffering the Acidification in a Bromide Enhanced Ozonation of Ammonia Nitrogen

Barbara Ruffino and Maria Chiara Zanetti

Abstract

The acidification in the process of ammonia nitrogen oxidation must be prevented. The superiority of orthophosphate versus bicarbonate was demonstrated. Ammonia nitrogen removal rate in the presence of $HPO_4^=/H_2PO_4^-$ increased by 15%. Nitrate generation in the presence of $HPO_4^=/H_2PO_4^-$ decreased by 50%. Presence of $HPO_4^=/H_2PO_4^-$ limited the generation of bromate to 0.04% of the bromate yield.

1 Introduction

Ammonia nitrogen, that is the compresence of ammonia (NH_3) and ammonium ion (NH_4^+), is one of the most diffused pollutants in wastewater of both municipal and industrial origin. In a previous work (Ruffino and Zanetti 2011), we demonstrated that bromide enhanced ozonation could be a fast and effective process for ammonia nitrogen removal by avoiding nitrate generation. But both the traditional biological oxidation (autotrophic nitrification) and chemical processes (i.e. by means of ozone or ozone plus bromide) for ammonia nitrogen removal determine a progressive release of H^+ with consequent acidification of the treated wastewater. In order to prevent acidification, buffering agents, if not present in a sufficient amount, should be added to the wastewater.

Bicarbonate (HCO_3^-) is the most used agent for buffering purposes. However, it is known as a strong scavenger of hydroxyl radicals ($HO^\bullet$) in ozonation processes (Ma and Graham, 2000). As shown in reaction (1), bicarbonate reacts with hydroxyl radicals to generate carbonate radicals ($HCO_3^\cdot$), with a rate of $8.5 \times 10^6 \, M^{-1} \, s^{-1}$ (Acero and von Gunten 2000). Then, the presence of bicarbonate in an ozonation process may depress the amount and, subsequently, the oxidizing ability of $HO^\bullet$ radicals in ammonia nitrogen removal. A secondary effect of the reaction is the basification of the system.

$$HCO_3^- + HO^\cdot \rightarrow HCO_3^\cdot + OH^- \qquad (1)$$
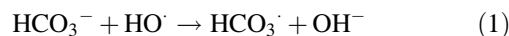
This study wants to demonstrate the superiority of a mixture of orthophosphate ($HPO_4^=/H_2PO_4^-$) over bicarbonate in buffering the acidification caused by the oxidation of ammonia nitrogen in a bromide enhanced ozonation process.

2 Materials and Methods

Tests were carried out in continuous (gas)/batch (liquid) modality in a 350 ml glass gas washing bottle equipped with a sealed-in filter disc (50 mm diameter, P0 porosity, 160–250 um, according to ISO 4793–80 standard) for ozone diffusion. Ozone was generated from oxygen gas (99.95% v/v) using an ozone generator (Ozone Lab TM, Ozone Services Division of Yanco Industries, Canada). Fluxes of oxygen and ozone-enriched oxygen of 100 ml/min were carried to and from the ozone generator through Teflon tubes. All tests took place at a room temperature value of 20 ± 2 °C.

Solutions were prepared by dissolving NH_4Cl and $NaHCO_3$ or a mixture of potassium orthophosphate (K_2HPO_4, 90.8% and KH_2PO_4, 9.2%, so as to obtain a starting pH value of approximately 7.8) in order to have starting concentration of ammonia nitrogen of 10 mM (approx. 180 mg/l) and of the buffering agent (bicarbonate or orthophosphate) of 15 mM. In fact, it was previously

B. Ruffino (✉) · M. C. Zanetti
DIATI, Politecnico di Torino, Turin, Italy
e-mail: barbara.ruffino@polito.it

M. C. Zanetti
e-mail: mariachiara.zanetti@polito.it

demonstrated that a ratio of 1:1.5 mol/mol between ammonia nitrogen and the buffering agent was sufficient to guarantee the complete ammonia oxidation without causing acidification of the system. Aliquots of a 2000 mg/L solution of potassium bromide (KBr) were added in order to obtain bromide concentrations of 266 mg Br$^-$/l (3.33 mM). In this study, the [NH$_4^+$]/[Br$^-$] ratio was equal to 3 mM/mM. All chemicals were of analytical grade and purchased by Sigma Aldrich.

Ammonia, nitrate, bromate and alkalinity were determined according to Standard Methods (APHA, AWWA, WEF 2005).

3 Results and Discussion

Figure 1 shows the depletion of ammonia nitrogen during a bromide enhanced ozonation in the presence of bicarbonate or a mixture of orthophosphate as buffering agents. As demonstrated in previous works, the depletion of ammonia nitrogen in a bromide enhanced ozonation process followed a zero-order kinetic (Ruffino and Zanetti 2011).

Figure 1 shows that, in the presence of the same boundary conditions (initial concentration of ammonia nitrogen and buffering species, concentration of bromide and experimental apparatus), the rate of ammonia nitrogen removal was approximately 15% higher when a mixture of orthophosphate was preferred to bicarbonate as a buffering agent. The rate of ammonia nitrogen removal in the presence of bicarbonate was of 1.93×10^{-3} mM s^{-1}, conversely, in the presence of a mixture of orthophosphate it rose to 2.22×10^{-3} mM s^{-1}. These values were obtained as an average of three tests carried out in different days.

At the end of the ozonation tests, nitrate, residual alkalinity and bromate concentrations were measured. The generation of nitrate after a 60-minute ozonation was in the

order of $8.65 \pm 1.86\%$ (average and standard deviation over three tests) of the theoretical value, when bicarbonate was used as a buffering agent. The theoretical value of nitrate generation is the concentration value that should be registered if all the removed ammonia nitrogen was oxidized to nitrate. In the case of the mixture of orthophosphate (HPO$_4^=$/H$_2$PO$_4^-$), the nitrate generation was in the order of $4.24 \pm 0.82\%$ of the theoretical value that is 50% less of the generation obtained with bicarbonate.

As expected, the process of bromide enhanced ozonation of ammonia nitrogen consumed alkalinity. The initial concentration of alkalinity, that corresponded to 15 mM of bicarbonate or a mixture of orthophosphate, was of 765 ± 1 mg CaCO$_3$eq/l and 667 ± 2 mg CaCO$_3$eq/l, respectively. By considering the amount of nitrogen and alkalinity consumed during the tests, a specific alkalinity consumption of 3.92 ± 0.04 g CaCO$_3$eq/g N–NH$_4^+$ resulted for the system buffered by bicarbonate and of 3.73 ± 0.01 g CaCO$_3$eq/g N–NH$_4^+$ for the system buffered by the mixture of orthophosphate. That meant that the use of orthophosphate allowed to save approximately 5% of the alkalinity necessary for buffering the oxidation of ammonia nitrogen.

Figure 2 relates the residual concentration of ammonia nitrogen after a 30- or 50-minute ozonation processes to the bromate yield. The bromate yield is defined as the ratio between the concentration of the formed bromate and the initial concentration of bromide (Li et al., 2017) as in (2)

$$BrO_3^- \text{ yield}\% = [BrO_3^-]/[Br^-] * 100 \,(mM/mM) \quad (2)$$

It is well known that bromide during an ozonation process may be converted to bromate (BrO$_3^-$) that is classified as a probable or likely human carcinogen and for which many countries have established the maximum allowable level in drinking water at 10 ug/L. Bromate is produced during ozonation through a multistep process involving the oxidation of bromide (Br−), ensuing generation of hypobromous acid
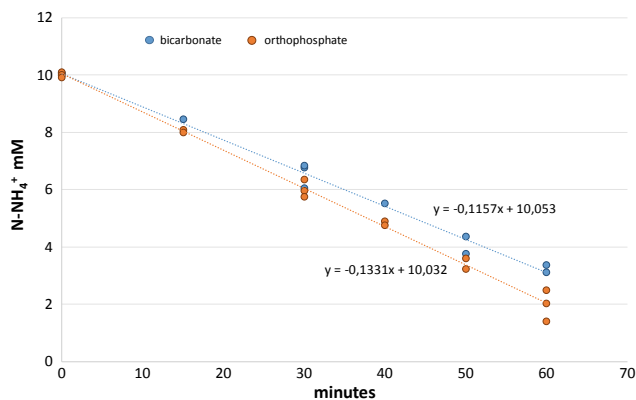
Fig. 1 Depletion of ammonia nitrogen during a bromide enhanced ozonation in the presence of bicarbonate or a mixture of orthophosphate as buffering agents
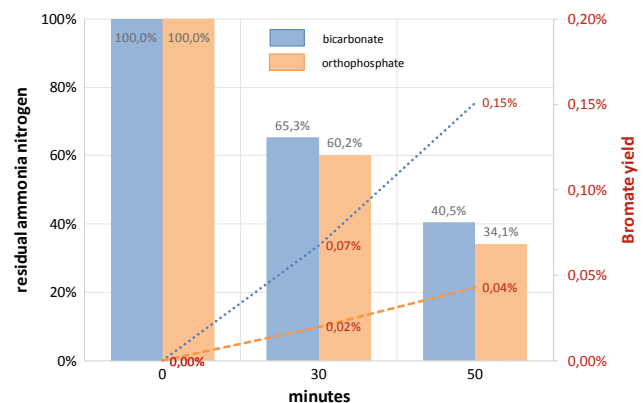
Fig. 2 Residual concentration of ammonia nitrogen and bromate yield

(HOBr) and bromite (BrO_2^-) and their reactions with ozone (Fischbacher et al. 2015; von Gunten 2003; von Gunten and Oliveras 1998). It is of interest the trend of bromate generation observed in these tests. From Fig. 2, it appears that for approximately the same residual ammonia amount, after 50 min, bromate generation for the system containing the mixture of orthophosphate was approximately one-fourth of the system that used bicarbonate as a buffering agent.

4 Conclusion

In this study, we demonstrated the superiority of orthophosphate over bicarbonate in buffering acidification during a bromide enhanced ozonation process of ammonia nitrogen. The use of orthophosphate instead of bicarbonate allowed to obtain:

- rates of ammonia nitrogen removal 15% higher;
- reduction of nitrate generation in the order of 50%;
- saving of buffering species in the order of 5%;
- a bromate yield of approximately one-fourth of the one obtained with bicarbonate as a buffering agent.

References

Acero, J. L., & von Gunten, U. (2000). Peroxide Based Advanced Oxidation Process for Drinking Water Treatment. *Ozone Science and Engineering, 22,* 305–328.

APHA, AWWA, WEF. (2005). *Standard methods for the examination of water and wastewater,* (21st ed.), Washington DC.

Fischbacher, A., Löppenberg, K., von Sonntag, C., & Schmidt, T. C. (2015). A new reaction pathway for bromite to bromate in the ozonation of bromide. *Environmental Science and Technology, 49* (19), 11714–11720.

Li, W. T., Cao, M. J., Young, T., Ruffino, B., Dodd, M., Li, A. M., et al. (2017). Application of UV absorbance and fluorescence indicators to assess the formation of biodegradable dissolved organic carbon and bromate during ozonation. *Water Research, 111,* 154–162.

Ma, J., & Graham, N. J. D. (2000). Degradation of atrazine by manganese-catalysed ozonation—Influence of radical scavengers. *Water Research, 34*(15), 3822–3828.

Ruffino, B., & Zanetti, M. C. (2011). Bicarbonate and ammonia depletion in ozonized systems with bromide ion. *Ozone Science & Engineering, 33,* 425–433.

von Gunten, U. (2003). Ozonation of drinking water: Part II. disinfection and by-product formation in presence of bromide, iodide or chlorine. *Water Research, 37*(7), 1469–1487.

von Gunten, U., & Oliveras, Y. (1998). Advanced oxidation of bromide-containing waters: bromate formation mechanisms. *Environmental Science and Technology, 32*(1), 63–70.

New Approach with Fluidized Bed Reactor Using Low-Cost Pyrophyllite/Alumina Composite Membrane for Real-Metal Plating Wastewater Treatment

Soomin Chang, Deaeun Kwon, and Jeonghwan Kim

Abstract

Hybrid fluidized bed ceramic membrane reactor was developed using low-cost pyrophyllite/alumina composite membrane with GAC particles as fluidized media to treat real metal-plating wastewater. With GAC fluidization, both uncoated and coated ceramic membranes achieved more than 90% of COD removal efficiency. There was no occurrence in membrane fouling under GAC fluidization during one-day of system operation for both membranes.

Keywords

Metal-plating wastewater • Low-cost pyrophyllite/alumina composite ceramic membrane • Fluidized bed membrane reactor

1 Introduction

There have been upsurges of interests in using ceramic membranes for the treatment of industrial wastewater where polymeric membranes may not be applicable due to their low chemical and thermal resistances (Jeong et al. 2017). However, low pressure-driven ceramic membrane process such as microfiltration (MF) or ultrafiltration (UF) does not provide high organic removal efficiency from industrial wastewater. In addition, ceramic membranes still require high costs and additional energy to reduce membrane fouling which is a long-standing problem with membrane technology. Recently, MF or UF membrane processes are combined with adsorbents such as activated carbon particles as a post-treatment to

remove organic compounds while it requires a large footprint. The membranes can be submerged into reactor with the adsorbents to reduce its footprint, but aeration often needs to be applied to suspend the adsorbent particles and thus it requires significant energy usage. In this study, new approach has been attempted for real-metal plating wastewater treatment by combining submerged membrane reactor with granular activated carbon (GAC) particles as fluidized media. The GAC particles are fluidized by recirculating a bulk wastewater alone without aeration through the reactor. In this way, the GAC particles are expected to provide not only adsorption capability for the organic pollutants present in wastewater, but also scouring agents to control membrane fouling (Ahmad et al. 2018). Ceramic membranes consisted of natural minerals have been paid much attention due to their low costs. Pyrophyllite is one of the natural clay minerals abundant in the earth. In this study, new ceramic membrane consisting of pyrophyllite materials as support layer with coated alumina as active layer was also developed and applied in the hybrid fluidized bed membrane reactor with GAC particles for the treatment of real metal-plating wastewater.

2 Materials and Methods

Hybrid fluidized bed membrane reactor was developed by submerging a flat-tubular ceramic membrane into fluidized bed reactor. Here, GAC particles were fluidized by recirculating a bulk wastewater through the reactor. The membrane reactor was operated at a set-point flux of 45 L/m²/hr. The total volume of the reactor and effective surface area of membrane were 4.7 L and 0.0362 m², respectively. In this study, a real metal-plating wastewater was used as a feed wastewater. Permeate produced by membrane was recycled into the reactor to maintain constant wastewater level. The GAC (>0.84 mm in size) particles were fluidized by using a recirculation pump from a bottom of reactor to cover the whole surface area of the membrane to control

S. Chang · D. Kwon · J. Kim (✉)
Department of Environmental Engineering, Inha University, Incheon, Republic of Korea
e-mail: jeonghwankim@inha.ac.kr

S. Chang
e-mail: chessmin91@hotmail.com

D. Kwon
e-mail: kwonde15@gmail.com

membrane fouling. Uncoated flat-tubular ceramic membrane consisted of 80% pyrophyllite and 20% of alumina. Membrane dimension was 7.6 cm width, 23.3 cm height, and 0.4 cm thickness. Nominal pore size of the membrane was 1.0 μm. A flat-tubular ceramic membrane coated by alumina active layer on pyrophyllite support layer was also tested in this study. The nominal pore size of coated membrane was 0.1 μm and dimension of membrane was the same as the uncoated one. Both uncoated and coated ceramic membrane were applied into the hybrid fluidized bed membrane reactor to investigate the effect of GAC dosage and solution pH on organic removal efficiency and fouling rate.

3 Results and Discussion

The pH of real metal-plating wastewater applied in this study was 2.0 with an average particle size of 1255 nm and chemical oxygen demand (COD) concentration of 1000 mg/L. Critical flux without GAC fluidization was measured as about 10 L/m^2/hr. With GAC fluidization, however, the critical flux was increased significantly to 45 L/m^2/hr, indicating that the GAC fluidization should be very effective to mitigate fouling rate. For the uncoated pyrophyllite membrane without GAC fluidization, the TMP increased gradually with time and then jumped to 0.5 bar within 2-h filtration. The fouling rate was reduced by adjusting the wastewater pH to 7.0. At neutral pH, average particle size in raw wastewater was about 18 times bigger than that observed at acidic pH (22,921 nm), suggesting that the fouling layer consisted of bigger particles formed on membrane should be less compact than that formed by smaller particles. For the coated alumina composite membrane, similar results were observed with the uncoated one without GAC fluidization. Regardless of the uncoated or coated membrane tested, however, the GAC fluidization along membrane surface reduced membrane fouling significantly. Under GAC fluidization, the TMP value was maintained below 0.2 bar for all test conditions during the whole operational period applied in this study (24 h). There was no effect of pH change in feed wastewater on fouling rate for both membranes under GAC fluidization. Without GAC fluidization, COD removal efficiency was almost same for both uncoated and coated membranes, which is about 30%. However, the GAC fluidization resulted in more than 90% of the COD removal efficiency for both membranes. No more beneficial effect by increasing GAC dosage to 30% from 10% on COD removal efficiency and fouling reduction was observed. Total suspended solid concentration in permeate from hybrid fluidized bed membrane reactor for alumina composite membrane was near zero regardless of GAC fluidization.

4 Conclusion

Hybrid fluidized bed membrane reactor was developed by submerging pyrophyllite-based membrane with GAC particles as fluidized media for the treatment of raw metal-plating wastewater. Fouling rate was reduced by neutralizing wastewater pH without GAC fluidization. However, GAC fluidization showed great way to reduce membrane fouling with real-metal plating wastewater regardless of wastewater pH applied. Both uncoated pyrophyllite membrane substrate and coated membrane with alumina active layer on the substrate showed more than 90% of COD removal efficiency under GAC fluidization. Total suspended solids were removed almost completely through both membranes. Increasing GAC dosage to 30% from 10% did not result in more beneficial effect on COD removal efficiency and fouling rate.

References

Jeong, Y., Cho, K., Kwon, E., Tsang, Y., Rinklebe, J., & Park, J. (2017). Evaluating the feasibility of pyrophyllite-based ceramic membranes for treating domestic wastewater in anaerobic ceramic membrane bioreactors. *Chemical Engineering Journal, 328,* 567–573.

Ahmad, R., Aslam, M., Park, E., Chang, S., Kwon, D., & Kim, J. (2018). Submerged low-cost pyrophyllite ceramic membrane filtration combined with GAC as fluidized particles for industrial wastewater treatment. *Chemosphere, 206,* 784–792.

Impact of Seasonality on Quorum Quenching Efficacy and Stability for Biofouling Control in Membrane Bioreactors

Kibaek Lee, Jun-Seong Park, Tahir Iqbal, Chang Hyun Nahm,
Pyung-Kyu Park, and Kwang-Ho Choo

Abstract

Low temperatures produce more biopolymers, leading to severe biofouling. Moving QQ sheets mitigate biofouling under cold weather conditions. QQ activities drop sharply with decreasing water temperatures. QQ sheets remain active during long-term field tests using real wastewater. QQ sheets have no impact on activated sludge treatment performance.

1 Introduction

Quorum quenching (QQ) strategies for mitigation on the membrane biofouling in membrane bioreactors (MBRs) have been continuously studied (Kyungmin et al. 2009,

K. Lee · K.-H. Choo
Advanced Institute of Water Industry, Kyungpook National University, Daegu, Republic of Korea
e-mail: lee-male@hanmail.net

J.-S. Park · T. Iqbal · K.-H. Choo (✉)
Department of Environmental Engineering, Kyungpook National University, Daegu, Republic of Korea
e-mail: chookh@knu.ac.kr

J.-S. Park
e-mail: js-park2015@naver.com

T. Iqbal
e-mail: engrtahir5@gmail.com

C. H. Nahm · P.-K. Park
Department of Environmental Engineering, Yonsei University, Seoul, Republic of Korea
e-mail: nemcheng@hotmail.com

P.-K. Park
e-mail: pkpark@yonsei.ac.kr

Weerasekara et al. 2014, 2016), but it is still difficult to evaluate the possibility of applying QQ technology to full-scale plants because the real plants experience significant variations in operating conditions, such as feedwater qualities and water temperatures. In this study, therefore, the QQ efficacy and stability with seasonal variations including water temperature were explored using pilot-scale MBRs (Fig. 1). The biofouling behaviors of two MBRs run in parallel, where one is with vacant sheets and the other with QQ sheets, were investigated using real municipal wastewater.

2 Materials and Methods

2.1 Preparation of QQ Sheets

Rhodococcus sp. BH4 was used as a QQ bacterium to degrade the type-1 signal molecules of acylhomoserine lactones (AHLs) to control membrane biofouling in MBRs. A polymer stock was prepared with polyvinyl alcohol (10 wt%) and sodium alginate (1.0 wt%). The BH4–polymer mixture was cast on a glass plate using a casting knife, and then, the sheets were cross-linked in boric acid (7.0 wt%) and calcium chloride (4.0 wt%) solutions and subsequently soaked in sodium sulfate (0.5 M) overnight (Iqbal et al. 2018, Nahm et al. 2017). The QQ sheet was cut into small pieces by 10 mm × 10 mm in size. Vacan sheets were prepared in the same manner as described above, but no BH4 was added during the casting step.

2.2 MBR Operating Conditions

The pilot-scale MBRs used in this study were designed with a series of anoxic, anaerobic, and oxic membrane (A^2O) processes with working volumes of 36, 36, and 144 L, respectively. Two pilot-scale MBRs were operated in parallel at a constant flux in the range of 15–20 L/m^2 h, with
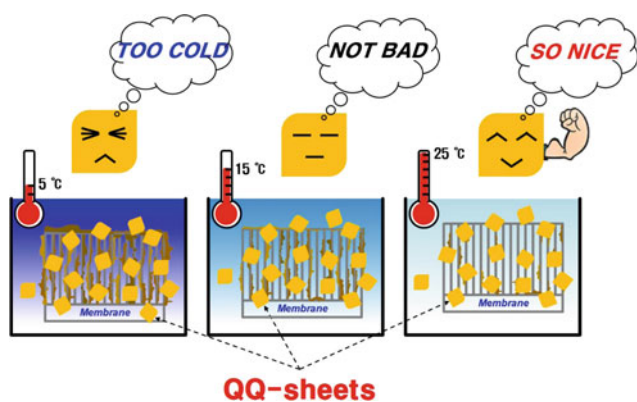
Fig. 1 Impact of water temperature on quorum quenching efficacy

2 min of the relaxation (no filtration) after 8 or 10 min of filtration at the Shincheon municipal wastewater treatment plant in Daegu, Korea. The two reactors were operated as conventional MBRs at first, that is, no sheets were added. Then, Reactor 1 was operated as a vacant MBR with vacant sheets (0.5% v/v), whereas Reactor 2 was operated as a QQ MBR with QQ sheets (0.5% v/v). The entire MBR operation was separated into four phases (Phases 1–4) based on the operating conditions.

2.3 Measurement of QQ Activity of QQ Sheets

The QQ activity of QQ sheets was determined based on the degradation rate of N-octanoyl-L-homoserine lactone, which is known as a dominant signal molecule in MBRs for wastewater treatment (Weerasekara et al. 2014). Briefly, an indicating agar plate was prepared by mixing an overnight culture of *A. tumefaciens* A136 and LB agar at a volume ratio of 1:9. The indicating agar was supplemented with tetracycline (4.5 µg/ml), spectinomycin (50 µg/ml), and X-gal (2 mg/ml). Then, 20 µl of each sample was loaded on the indicating agar. The AHLs were detected by the AHL reporter strain, *A. tumefaciens* A136, with the production of β-galactosidase in response to AHL level, with β-galactosidase decomposing X-gal, resulting in blue color. The AHL level was estimated quantitatively based on the size of color.

2.4 Analytical Procedures

During MBR operations, various water quality parameters, such as chemical oxygen demand, total organic carbon, total nitrogen, and total phosphorus, were determined according to Standard Methods (APHA 1998) unless otherwise noted. Mixed liquor characteristics, such as the amounts of extra-cellular polymeric substances (EPSs) and soluble microbial

products and microbial floc size, were also monitored. The floc size was measured using a laser diffraction particle size analyzer (LS 13 320, Beckman Coulter, USA). The total organic carbon (TOC) concentration was determined using a TOC analyzer (TOC-V CPH, Shimadzu, Japan).

3 Results and Discussion

QQ sheets delayed membrane fouling in pilot-scale MBR operations, but low temperatures (winter season) caused severe biofouling. The greater amount of EPS produced in cold weather was responsible for the quicker biofouling of a membrane, even with the QQ media. There were significant negative relationships between EPS (proteins and carbohydrates) amount and water temperature (Pearson correlation coefficient $r = -0.695$ to -0.782 with p-values <0.05). Cold weather was detrimental to the QQ activity (Fig. 1). The degradation rate of AHLs signal molecules by QQ sheets decreased markedly at low temperatures (i.e., the QQ activity at 5 °C was <20% of that at 25 °C), but was restored with a higher dose of QQ sheets. It was reported that the fouling decay by QQ was more significant with greater QQ bacteria doses to MBRs (Iqbal et al. 2018). The mobile sheets had negligible physical effects on membrane cleaning in MBRs, but they were rather entrapped inside the bundle of hollow fibers. In a previous study, however, it was found that mobile vacant and QQ media, which were added to a membrane bioreactor installed with a plate-and-frame module, had a positive effect on membrane fouling control (Kim et al. 2013). This was because the media added provided physical shears and collisions on the membrane surface resulting in membrane cleaning. It seems that the module geometry may affect the physical impact of media on membrane fouling control. The QQ bacteria in the sheets lost their activity in the early stage of the test, but survived during the long-term pilot-scale MBR operation fed with real municipal wastewater. It is unclear whether the loss of QQ activity was caused by the inactivation of QQ bacteria or by the disintegration of QQ media. Further in-depth studies on media durability are needed. Nonetheless, there was no significant difference in treatment efficiency among the MBR conditions, such as conventional, vacant, and QQ MBRs.

4 Conclusions

The effect of water temperature on QQ efficacy was investigated in the long-term pilot-scale MBR tests, which were operated from autumn through spring. The QQ activity of BH4-encapsulated sheets declined with decreasing water temperature from 25 to 5 °C, showing almost no QQ activity

at 5 °C. Although low water temperatures exacerbated biofouling in MBRs owing to the greater production of EPSs, QQ still enabled biofouling mitigation. The lower activity of QQ sheets at low temperature could be compensated with increasing the QQ bacteria dose to MBRs. QQ technology showed no side effect on the characteristics of activated sludge and treatment efficiency during three-season pilot-scale MBR operations.

References

APHA (Ed.). (1998). *Standard methods for the examination of water and wastewater*. American Public Health Association, American Water Works Association, and Water Environment Federation, Washington, DC.

Iqbal, T., Lee, K., Lee, C.-H., & Choo, K.-H. (2018). Effective quorum quenching bacteria dose for anti-fouling strategy in membrane bioreactors utilizing fixed-sheet media. *Journal of Membrane Science, 562,* 18–25.

Kim, S.-R., Oh, H.-S., Jo, S.-J., Yeon, K.-M., Lee, C.-H., Lim, D.-J., et al. (2013). Biofouling control with bead-entrapped quorum quenching bacteria in membrane bioreactors: Physical and biological effects. *Environmental Science and Technology, 47*(2), 836–842.

Kyungmin, Y., Wonseok, C., Hyunsuk, O., Woonyoung, L., Byung-kook, H., Chunghak, L., et al. (2009). Quorum sensing: a new biofouling control paradigm in a membrane bioreactor for advanced wastewater treatment. *Environmental Science and Technology, 43*(2), 380–385.

Nahm, C. H., Choi, D.-C., Kwon, H., Lee, S., Lee, S. H., Lee, K., et al. (2017). Application of quorum quenching bacteria entrapping sheets to enhance biofouling control in a membrane bioreactor with a hollow fiber module. *Journal of Membrane Science, 526,* 264–271.

Weerasekara, N. A., Choo, K.-H., & Lee, C.-H. (2014). Hybridization of physical cleaning and quorum quenching to minimize membrane biofouling and energy consumption in a membrane bioreactor. *Water Research, 67,* 1–10.

Weerasekara, N. A., Choo, K.-H., & Lee, C.-H. (2016). Biofouling control: Bacterial quorum quenching versus chlorination in membrane bioreactors. *Water Research, 103,* 293–301.

Surface Modification of RO Desalination Membrane Using ZnO Nanoparticles of Different Morphologies to Mitigate Fouling

Revathy Rajakumaran, Boddu Vinisha, Mathava Kumar, and Raghuram Chetty

Abstract

Chemical modification of different morphologies of ZnO nanoparticles (spherical, flowers). Modification of thin-film composite (TFC) using ZnO nanoparticles by surface coating. Measured flux, NaCl rejection and hydrophilicity. Fouling resistance studies on unmodified and modified membrane. Best membrane performance was observed with 0.02 wt% ZnO-S-modified membrane.

Keywords

Reverse osmosis • ZnO nanoparticles • Surface modification • Hydrophilicity • Flux • Fouling resistance

1 Introduction

The shortage of clean and fresh water has become the critical driver for research in sustainable development to meet the ever-growing demand. Desalination of brackish/seawater using membranes is a promising solution to reduce the pressure on natural water resources (Kaldellis and Kondili 2007). Reverse osmosis (RO) is the most significant and energy-effective separation technology (Werber et al. 2016). The most widely used RO membrane is polyamide thin-film composite (PA-TFC) membrane which comprises of bottom polyester fabric as base, a middle porous polysulfone support and a thin polyamide layer at the top (Safarpour et al. 2015). However, the major drawback observed in TFC membrane is fouling. Membrane fouling including biofouling, colloidal fouling, organic and inorganic fouling, which leads to the increase in operating pressure, flux decline, repetitive chemical cleaning and poor membrane performance. Hydrophilicity and surface roughness of polymeric membrane are major properties in mitigating fouling (Baek et al. 2011; Kang and Cao 2012). Surface modification of TFC membranes is one of the methods to improve the performance of the membrane (Emadzadeh et al. 2017). With the improvement in the field of nanotechnology, the hydrophilic nanomaterials are incorporated to enhance membrane properties. Among different nanomaterials used for modification of the membrane, zinc oxide (ZnO) is one of the most popular photocatalyst having a large band gap (3.37 eV) as well as known for its chemical stability, non-toxicity nature and antibacterial activity (Zanni et al. 2016; Malachová et al. 2011). This work aims to understand the effect of two different morphologies of chemically modified zinc oxide nanoparticles (spherical and flowers) for the modification of TFC-RO membranes. The effect of different concentrations of various morphologies of ZnO nanoparticles on the desalination performance and fouling resistance properties of the thin-film RO membranes were studied.

2 Materials and Methods

2.1 Preparation of Different Shapes of Zinc Metal Oxide Nanoparticles

ZnO spherical nanoparticles were prepared by sol–gel method (Chung et al. 2015). Zinc acetate $Zn(CH_3COO)$ and oxalic acid solutions were prepared in ethanol solution at 1:1 molar ratio. The mixtures were stirred vigorously to obtain a zinc oxalate gel. The acquired gel was dried at 60 °C for

R. Rajakumaran · M. Kumar (✉)
Environmental and Water Resource Engineering Division, Department of Civil Engineering, Indian Institute of Technology Madras, Chennai 600036, India
e-mail: mathav@iitm.ac.in

B. Vinisha · R. Chetty
Department of Chemical Engineering, Indian Institute of Technology Madras, Chennai 600036, India

overnight and calcinated for 3 h at 400 °C. The flower-like ZnO nanostructures were synthesized by hydrothermal method, controlling the molar ratio of sodium hydroxide (NaOH) to zinc acetate (Zn(CH$_3$COO)) (Zhang and Mu 2007).

2.2 Preparation of ZnO/RO Polymeric Membrane

Polysulfone porous support was prepared by phase inversion method using 19 wt% polysulfone (Psf) in 81 wt% N-methyl, 2-pyrrolidone solvent. The polymer solution was casted on a polyester non-woven fabric using automatic film applicator of 0.1 mm thickness. The PA layer was coated on membrane by interfacial polymerization (Ali et al. 2016).

2.3 Characterization Methods

Fourier transform infrared (FT-IR, Perkin Elmer) spectrum was obtained to test functional groups of membrane surfaces. Transmission electron microscope (TEM, JEOL-JEM2100) and scanning electron microscope (SEM, Hitachi S4800) were utilized to investigate the surface morphology of the samples. Atomic force microscopy (AFM) analysis was used to calculate the surface roughness parameters and investigate the surface morphology of the active polyamide layer using a dual-scope C-26, DME scanning probe-optical microscope. The static water contact angle of the membrane surface was measured by sessile drop method with a goniometer (GBX-Digidrop MCAT).

2.4 Membrane Separation Performance

The performances of modified membranes were tested, along with a pristine membrane without modification in terms of water flux and salt rejection using a cross-flow unit. The experimental conditions are as follows: operating pressure 20 bar, NaCl solution concentration 2000 mg L^{-1}, temperature 25 °C. The membrane effective area was 42 cm^2. The fouling resistance studies were conducted for 300 min by adding 500 mg L^{-1} of humic acid in feed solution. Water flux (F) and salt rejections (R) were calculated by the following two equations: $F = V/A*t$ and $R\ (\%) = 100 \times (1 - C_p/C_f)$, where V, A and t represent the total volume of permeate collected, cross-sectional area and a fixed time, respectively. C_f and C_p are the salt concentrations of feed and permeate side measured by with salinity meter.

3 Results and Discussion

3.1 Characterization of ZnO Nanoparticles and TFC-RO Membrane

The successful synthesis of ZnO nanoflowers (ZnF) and ZnO spherical nanoparticles (ZnS) was confirmed using SEM and TEM. The micrographs confirm that the average particle sizes of ZnF and ZnS were around 1 μm and 30 nm, respectively.

3.2 Membrane Separation Performance

The study of hydrophilicity of the prepared TFC-RO membrane was performed by contact angle measurement. The decrease in trend of contact angle is consistent with the increase of ZnO concentration for both the morphologies as shown in Fig. 1.

Salt rejection values and water flux were measured to evaluate the desalination performance of modified TFC-RO membranes and compared to that of pristine RO membranes. The water flux value through the membrane was found to increase with the increasing concentration of ZnO and reaches to its maximum value at 0.02 wt% for all ZnO morphologies as represented in Fig. 2a. The results of normalized water flux decline of the optimized membrane during fouling test are given in Fig. 2b. It can be seen that the pristine polyamide membrane has the highest loss of water flux than the modified membrane.
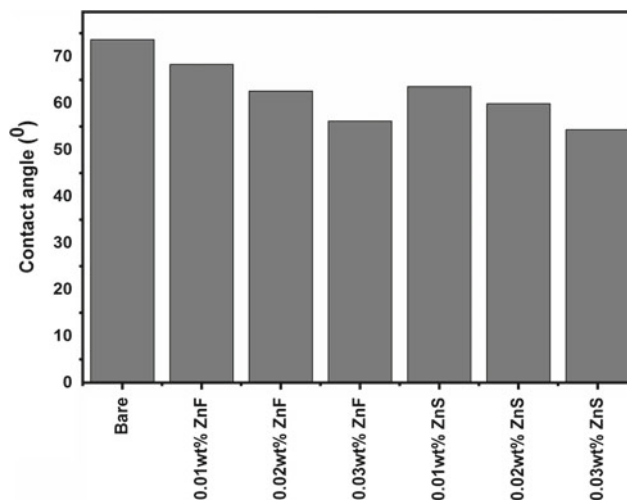
Fig. 1 Contact angle of pristine and modified RO membranes

Fig. 2 a Water flux and salt rejection **b** fouling behaviour of unmodified and modified RO membranes
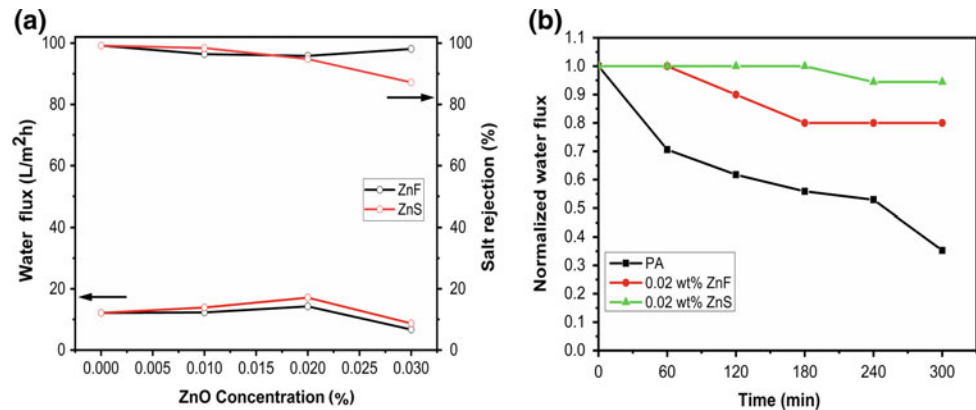
4   Conclusion

ZnO nanoparticles of two different morphologies were synthesized using hydrothermal and sol–gel method and coated on the membrane surface. The incorporation of ZnO improved the performance of RO membrane in the terms of water permeability, salt rejection and anti-fouling property by improving hydrophilicity of polyamide layer. The membrane containing 0.02 wt% ZnS exhibited superior RO performance including 41.18% increase in water flux with respect to pristine membrane, 95% NaCl rejection and superior fouling resistance property compared to 0.02 wt% of ZnF-RO membranes.

References

Kaldellis, J. K., & Kondili, E. M. (2007). The water shortage problem in the Aegean archipelago islands: cost-effective desalination prospects. *Desalination, 216,* 123–138. https://doi.org/10.1016/J.DESAL.2007.01.004.

Werber, J. R., Deshmukh, A., & Elimelech, M. (2016). The Critical Need for Increased Selectivity, Not Increased Water Permeability, for Desalination Membranes. *Environmental Science & Technology Letters, 3,* 112–120. https://doi.org/10.1021/acs.estlett.6b00050.

Safarpour, M., Khataee, A., & Vatanpour, V. (2015). Thin film nanocomposite reverse osmosis membrane modified by reduced graphene oxide/TiO2 with improved desalination performance. *Journal of Membrane Science, 489,* 43–54. https://doi.org/10.1016/J.MEMSCI.2015.04.010.

Baek, Y., Yu, J., Kim, S.-H., et al. (2011). Effect of surface properties of reverse osmosis membranes on biofouling occurrence under filtration conditions. *Journal of Membrane Science, 382,* 91–99. https://doi.org/10.1016/J.MEMSCI.2011.07.049.

Kang, G., & Cao, Y. (2012). Development of antifouling reverse osmosis membranes for water treatment: A review. *Water Research, 46,* 584–600. https://doi.org/10.1016/J.WATRES.2011.11.041.

Emadzadeh, D., Ghanbari, M., Lau, W. J., et al. (2017). Surface modification of thin film composite membrane by nanoporous titanate nanoparticles for improving combined organic and inorganic antifouling properties. *Materials Science and Engineering C, 75,* 463–470. https://doi.org/10.1016/J.MSEC.2017.02.079.

Zanni, E., Chandraiahgari, C., De Bellis, G., et al. (2016). Zinc oxide nanorods-decorated graphene nanoplatelets: A promising antimicrobial agent against the cariogenic bacterium streptococcus mutans. *Nanomaterials, 6,* 179. https://doi.org/10.3390/nano6100179.

Malachová, K., Praus, P., Rybková, Z., & Kozák, O. (2011). Antibacterial and antifungal activities of silver, copper and zinc montmorillonites. *Applied Clay Science, 53,* 642–645. https://doi.org/10.1016/J.CLAY.2011.05.016.

Chung, Y. T., Ba-Abbad, M. M., Mohammad, A. W., et al. (2015). Synthesis of minimal-size ZnO nanoparticles through sol–gel method: Taguchi design optimisation. *Materials and Design, 87,* 780–787. https://doi.org/10.1016/J.MATDES.2015.07.040.

Zhang, Y., & Mu, J. (2007). Controllable synthesis of flower- and rod-like ZnO nanostructures by simply tuning the ratio of sodium hydroxide to zinc acetate. *Nanotechnology, 18,* 075606. https://doi.org/10.1088/0957-4484/18/7/075606.

Ali, M. E. A., Hassan, F. M., & Feng, X. (2016). Improving the performance of TFC membranes via chelation and surface reaction: applications in water desalination. *Journal of Materials Chemistry A, 4,* 6620–6629. https://doi.org/10.1039/C6TA01460G.

Nutrient Removal and Biomass Production by Immobilized *Chlorella Vulgaris*

Marion Lux Y. Castro and Florencio C. Ballesteros Jr.

Abstract

Immobilized cells of Chlorella vulgaris in alginate–chitosan matrix achieved faster growth rates and produced more biomass than their free cell counterpart in synthetic aquaculture wastewater. Higher (89.8%) nitrate-N removal was achieved by immobilized cells than by the free cells (45.9%). Phosphate-P removal was both high at 98.9 and 99.5% by immobilized and free cells, respectively. The alginate–chitosan matrix was found suitable for growth, nutrient removal, and biomass production in synthetic aquaculture wastewater.

Keywords

Microalgae • Chlorella vulgaris • Immobilization • Alginate • Chitosan • Nutrient removal

1 Introduction

Intensified aquaculture production leads to increased waste generation. Wastes discharged without treatment promote eutrophication in water bodies. Microalgal systems have been proven efficient for the treatment of various wastewaters including those from a brewery plant (Mata et al. 2012), piggery farm (Wang et al. 2012), anaerobic digested dairy manure (Singh et al. 2011), and freshwater aquaculture/fish farms (Gao et al. 2016). Cultivation of microalgae using wastewater as media has the advantage of improving water quality while simultaneously producing biomass, which could serve as feedstock for downstream processes to produce protein complements and food additives for aquaculture, animal and human feed, even biogas and fuels, and biofertilizer. However, some disadvantages are the costly separation of biomass from the treated water and the need for large cultivation areas.

Immobilization of microalgae is a promising way to harvest microalgal biomass. Current uses of immobilized microalgae in a variety of matrices include: glycerol and hydrogen production, electricity generation, culture collections storage and handling, biomonitoring of water quality and measurement of toxicity, cultivation for metabolite production and nutrients and pollutants as well as metal removal (Moreno-Garrido 2008). Numerous studies have immobilized microalgae into matrices of natural polymers such as alginate (Yadavalli and Heggers 2013), carrageenan (Rao et al. 2013), and chitosan (Aguilar-May and Sanchez-Saavedra 2009) to remove nutrients from various types of wastewater.

Since the use of combining polymers as matrix for immobilization has not been investigated as extensively as that of alginate, the present study investigated the effects of using a combination of the alginate–$CaCl_2$–chitosan for the immobilization of *Chlorella vulgaris* cells on nutrient removal and biomass production using aquaculture wastewater. A comparison with that of free cells was also done.

2 Materials and Methods

Cultures of *Chlorella vulgaris* were obtained at the Institute of Biological Sciences, UP Los Baños, Laguna, Philippines. The microalgae were pre-cultured in modified BG 11 medium, at room temperature with a constant aeration (0.01 ml-min^{-1}) and light intensity of 55 µmol m^{-2} s^{-1}. Microalgae in the exponential phase were collected, centrifuged (10000 g in 5 min), and re-suspended in distilled water. Microalgae and 3% alginate suspension were

M. L. Y. Castro (✉)
Institute of Agricultural Engineering, College of Engineering and Agro-Industrial Technology, University of the Philippines Los Baños, Laguna, Philippines
e-mail: mycastro@up.edu.ph

F. C. Ballesteros Jr.
Environmental Engineering Program, College of Engineering, University of the Philippines Diliman, Quezon City, Philippines
e-mail: fcballesteros@up.edu.ph

prepared with 1:1 volume ratio and added dropwise to 4% $CaCl_2$ solution by a syringe to form beads. Beads were hardened in the $CaCl_2$ solution for 1 h, rinsed with distilled water, and then added to 0.25% chitosan solution under mild shaking for 30 min. Laboratory scale batch reactors (4 l bottles) were used. Synthetic aquaculture wastewater was prepared using (in g l^{-1}): KNO_3, 1.63; $CaCl_2$–$2H_2O$, 3.6; $MgSO_4$–$7H_2O$, 7.5; K_2HPO_4, 1.83; $C_6H_8O_7$, 0.6; Na_2CO_3, 2.0; H_3BO_3, 2.86; $MnCl_2$–H_2O, 1.81; $ZnSO_4$–$7H_2O$, 0.22; $CuSO_4$–$5H_2O$, 0.08; $(NH_4)_5[Fe(C_6H_4O_7)_2]$, 0.6; $Co(NO_3)_2$–$6H_2O$, 0.05; Na_2MoO_4–$2H_2O$, 0.39; and Na_2EDTA, 0.1 at pH 7.1. Free cells from the pre-culture and immobilized cells were inoculated (20% v/v) in the medium. Reactors were illuminated (222 µmol m^{-2} s^{-1}) with 12-h light, 12-h dark period, under continuous aeration (LowAir—0.5 vvm, HighAir—1.5 vvm) for 10d.

For nutrient analysis, daily samples were filtered by 55 mm filter (Whatman GF/C). Nitrate-N and phosphate-P concentrations were analyzed using Hach DR 890. Ten milliliters from the free cell cultures was used daily for biomass analysis. For immobilized cell cultures, 3 g of beads was dissolved in 10 ml of 0.5 mol trisodium citrate solution (pH 6.5). Cells were filtered and oven-dried at 120 °C for 24 h. Dry weight of biomass was determined in g l^{-1}. Biomass curves were used to determine the specific growth rate (μ) in the exponential phase.

Two setups were used—low aeration rate (LowAir) and high aeration rate (HighAir). For each condition, free and immobilized cells were used. Mean and standard deviation values of the triplicates for each setup were calculated. Nutrient removal and biomass production were evaluated using one-way analysis of variance (ANOVA) ($p < 0.05$).

3　Results and Discussion

3.1　Nutrient Removal

In 10d, the immobilized cells of *Chlorella vulgaris* from both setups under LowAir and HighAir achieved significantly higher nitrate-N removal of 89.8% (6.833–0.7 mg-L^{-1}) and 84.4% (6.833–1.067 mg-L^{-1}), compared to the free cells with 30.7% (6.833–4.733 mg-L^{-1}) and 45.9% (6.833–3.7 mg-L^{-1}), respectively. Using free cells, nitrate-N removal (from 2.4 to 30.7%) under LowAir was significantly lower than under HighAir (from 12.2 to 45.9%), whereas for the immobilized cells of *Chlorella vulgaris*, nitrate-N removal (from 52.2 to 89.8%) under LowAir was significantly higher than under HighAir (from 42.4 to 84.4%) (Fig. 1).

Free cells needed more air to remove more nitrate-N. The immobilized cells did not require as much air as the free cells to be able to remove more nitrate-N. This shows that
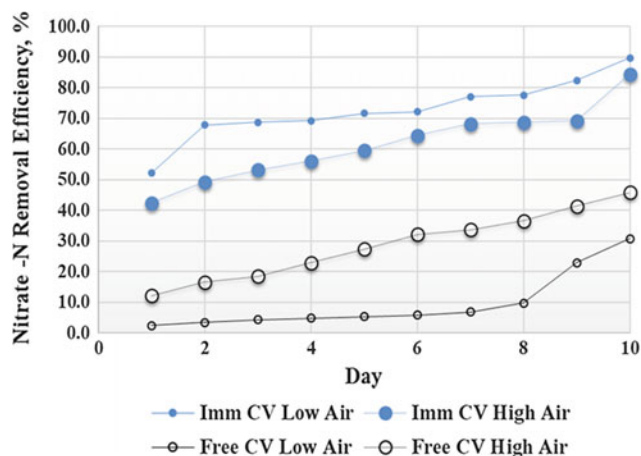
Fig. 1 Nitrate-N removal by free and immobilized *Chlorella vulgaris* under LowAir and High Air

nutrients were diffused and assimilated accordingly even within the matrix. As with the immobilized *Chlorella sorokiniana* GXNN 01 from the work of Liu et al. (2012), cells assimilated carbon sources under micro-aerobic (MNA) conditions, needing low aeration during treatment.

In 10d, phosphate-P removed by free cells from 61.4 to 99.5% (from 1.84 to 0.01 mg-L^{-1}) under LowAir was not significantly different from 82.1 to 98.9% (from 1.84 to 0.02 mg-L^{-1}) under HighAir (Fig. 2a). For setups with immobilized cells, significantly higher phosphate-P removal was achieved under HighAir than LowAir. Phosphate-P removal ranged from 88 to 97.8% (from 1.84 to 0.04 mg-L^{-1}) under LowAir and from 59.2 to 98.9% (from 1.84 to 0.02 mg-L^{-1}) under HighAir (Fig. 2b). As with nitrogen removal, phosphate removal can be attributed to microalgal uptake, assimilation, and adsorption on alginate–chitosan gel matrix.

Liu et al. (2012) reported comparable results when after 5 d in synthetic municipal WW, phosphate-P removed by immobilized cells of *Chlorella sorokiniana* GXNN 01 (87.49, 88.65, and 84.84%) was higher than that by the free cells (20.21, 42.27, and 53.52%) under heterotrophic, mixotrophic, and MNA conditions, respectively. Yadavalli and Heggers (2013) achieved quicker results when they immobilized *Chlorella pyrenoidosa* in alginate for the treatment of a dairy farm effluent. After 4d, phosphate-P removed was 97% (from 30 to 0.87 mg-L^{-1}).

3.2　Biomass Production and Growth Rates

Significantly higher dry weight biomass was achieved by the immobilized cells than the free cells. For both, higher biomass was achieved by setups under HighAir than LowAir. The highest increase in biomass ($17\times$) from 0.26 to
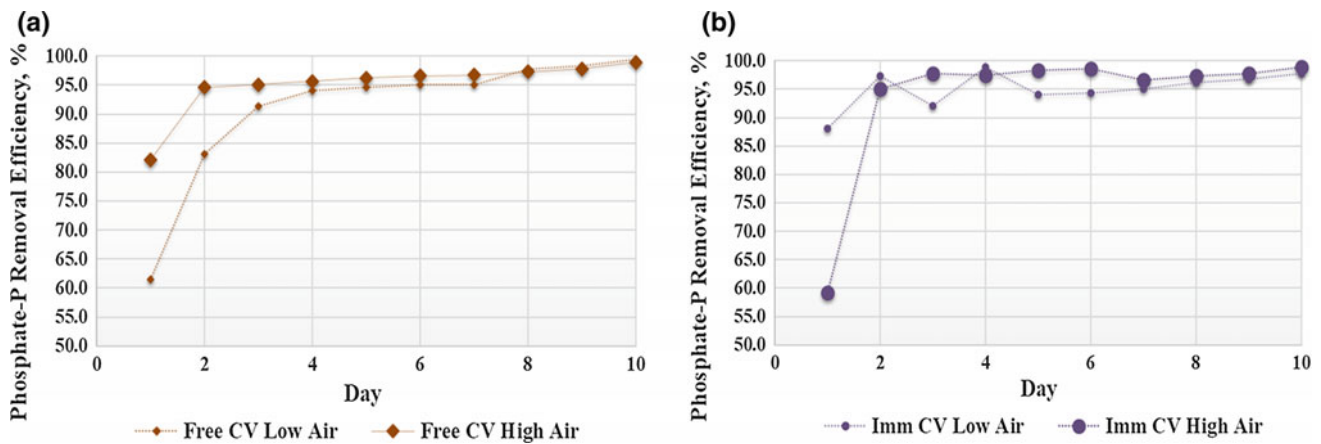
Fig. 2 **a** Phosphate-P removal by free *Chlorella vulgaris* under LowAir and HighAir. **b** Phosphate-P removal by immobilized *Chlorella vulgaris* under LowAir and HighAir

4.411 gDW-L^{-1} was obtained by the setup ImmCV HighAir with μ of 1.1 day^{-1}, followed by ImmCVLowAir (9.2×) from 0.24 to 2.213 gDW-L^{-1} with μ of 0.7 day^{-1}, then by FreeCVHighAir (5.8×) from 0.1 to 0.58 g DW-L^{-1} with μ of 0.8 day^{-1}, and lastly by FreeCVLowAir (3.9 × from 0.06 to 0.235 g DW-L^{-1} with μ of 0.6 day^{-1} (Fig. 3).

High-level aeration produced higher biomass in both free and immobilized setups than low-level aeration. This was due to better mixing, diffusion, and nutrient delivery to the cells. Immobilized cells also acquired more stability to withstand mixing due to aeration. Fiero et al. (2008) also achieved higher growth rates of immobilized cells of *Scenedesmus* sp. strain 1 (0.26 day^{-1}) than the free cells (0.10 day^{-1}). Another strain of Scenedesmus sp. also reached higher growth rates when immobilized (0.06 day^{-1}) than did the free cells (0.03 day^{-1}). Higher growth rates were attributed to an acquired added stability brought by the chitosan.
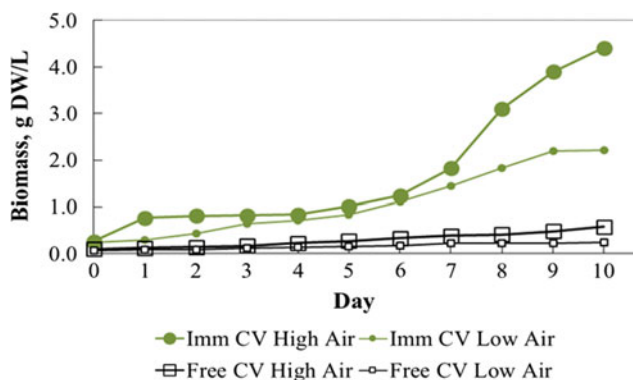
4 Conclusion

The effect of alginate–CaCl$_2$–chitosan immobilization of *Chlorella vulgaris* cells on nutrient removal and biomass production was investigated. Immobilized cells had faster growth rates than the free cells. Nitrate-N and phosphate-P removal by free and immobilized cells was evaluated. Immobilized cells removed 89.8% nitrate-N and 98.9% phosphate-P, while free-living cells removed 45.9% nitrate-N and 99.5% phosphate-P within 10d in aquaculture wastewater. The alginate–CaCl$_2$–chitosan as immobilizing matrix for *Chlorella vulgaris* cells was found suitable for nutrient removal and biomass production. Foregoing results can be used to develop treatment strategies for various aquaculture systems.

References

Mata, T. M., Melo, A. C., Simoes, M., & Caetano, N. S. (2012). Parametric study of a brewery effluent treatment by microalgae *Scenedesmus obliquus*. *Bioresource Technology, 107,* 151–158.

Wang, H., Xiong, H., Hui, Z., & Zeng, X. (2012). Mixotrophic cultivation of *Chlorella pyrenoidosa* with diluted primary piggery wastewater to produce lipids. *Bioresource Technology, 104,* 215–220.

Singh, M., Reynolds, D. L., & Das, K. C. (2011). Microalgal system for treatment of effluent from poultry litter anaerobic digestion. *Bioresource Technology, 102,* 10841–10848.

Gao, Feng, Li, Chen, Yang, Z. H., Zeng, G. M., Feng, L. J., Liu, J., et al. (2016). Continuous microalgae cultivation in aquaculture wastewater by a membrane photobioreactor for biomass production and nutrients removal. *Ecological Engineering, 92,* 55–61.

Moreno-Garrido, I. (2008). Microalgae immobilization: Current technologies and uses. *Bioresource Technology, 99,* 3949–3964.

Yadavalli, R., & Heggers, G. R. (2013). Two stage treatment of dairy effluent using immobilized *Chlorella pyrenoidosa*. *Journal of Environmental Health Science and Engineering, 11,* 36.

Fig. 3 Biomass production curve of free and immobilized *Chlorella vulgaris* under LowAir and HighAir

Rao, P., Saisha, V., Shashidhar, S.B. (2013). Removal of chromium (VI) from synthetic wastewater using immobilized algae. *International Journal of Current Engineering and Technology*. (Special Issue), 157–160.

Aguilar-May, B., & Sanchez-Saavedra, M. P. (2009). Growth and removal of nitrogen and phosphorus by free living and chitosan-immobilized cells of the marine *Cyanobacterium Synechococcus* elongates. *Journal of Applied Phycology, 21,* 353–360.

Liu, Kai, Li, Jian, Qiao, Hongjin, Lin, Apeng, & Wang, G. (2012). Immobilization of *Chlorella sorokiniana* GXNN01 in alginate for removal of N and P from synthetic wastewater. *Bioresource Technology, 114,* 26–32.

Fiero, S., Sanchez-Saavedra, M. D., & Copalcua, C. (2008). Nitrate and phosphate removal by Chitosan immobilized *Scenedesmus*. *Bioresource Technology, 99,* 1274–1279.

Treatment of Printed Circuit Board Wastewater Containing Copper and Nickel Ions by Fluidized-Bed Homogeneous Granulation Process

Nathaniel E. Quimada, Mark Daniel G. De Luna, and Ming-Chun Lu

Abstract

In this study, treatment of synthetic printed circuit board wastewater containing copper and nickel ions was done through fluidized-bed homogeneous granulation process (FBHGP). The treatment occurred in a single reactor, removing and granulating both copper and nickel ions at the same period of time. The effect of total carbonate loading (10, 12, 15, 17, 20 mM) on the treatment of Cu^{2+} (6.3 mM) and Ni^{2+} (3.4 mM) was evaluated in this study with initial precipitant flow rate of 15 mL/min and initial operating pH of 6.5 and shifted to 8.5 pH on the given period of time. The synthetic wastewater containing copper and nickel ions had better result in terms of size of recovered granules, removal and granulation efficiencies when 17 mM of CO_3 was employed in the system, resulting to copper removal of 97.5%, copper granulation of 93.1% and nickel removal and granulation efficiencies of 81.2 and 73.6%, respectively. The granules recovered were >0.42 mm in size with rough surface and EDX analysis identified the presence of oxygen, copper and nickel.

N. E. Quimada
Environmental Engineering Program, National Graduate School of Engineering, University of the Philippines, Diliman, Quezon City, Philippines
e-mail: nathanielquimada@gmail.com

M. D. G. De Luna (✉)
Department of Chemical Engineering, University of the Philippines, Diliman, Quezon City, Philippines
e-mail: mgdeluna@up.edu.ph

M.-C. Lu
Department of Environmental Resources Management, Chia Nan University of Pharmacy and Science, Tainan, 717, Taiwan
e-mail: mmclu@mail.cnu.edu.tw

1 Introduction

Printed circuit boards (PCBs) are essential components in almost all electrical and electronic equipment (EEE) (Jadhav and Hocheng 2015). Due to its demand, the production is increasing in volume; however, the production of PCBs produces wastewaters containing elevated concentrations of copper and nickel ions. These metal ions are toxic, carcinogenic and can impact to the existence of living organisms and the ecosystem (Duda-Chodak and Blaszczyk 2008; Solomon 2009).

There are several methods that dealt on the treatment of heavy metals from wastewater, including coagulation–precipitation, solvent extraction, membrane filtration, electrodialysis, adsorption and ion exchange and electroplating. Chemical precipitation is commonly favored among others due to its low cost and high efficiency features. However, this method produces large volume of sludge that holds high moisture content and may increase its cost due to dewatering (Chen et al. 2015; Salcedo et al. 2016).

The use of fluidized bed is another method that are widely accepted due to fact that it resulted to low recovery of sludge in the reactor (Salcedo and Lu 2015). There are now several studies that use fluidized-bed crystallization process to recover different heavy metals. At present, there are no records treating two metal ions in a single reactor with the same period of time. Thus, the present study evaluated the applicability of the fluidized-bed homogeneous granulation process in the treatment of wastewater containing both copper and nickel ions. This study investigated the effect of the amount of sodium carbonate (Na_2CO_3) as precipitant in the removal and granulation efficiency in the treatment both Cu^{2+} and Ni^{2+} ions in the wastewater. The operation occurred in a FBR with constant operating condition of 6.3 mM of Cu^{2+} mixed with 3.3 mM of Ni^{2+} with constant precipitant flow rate and operating pH. The recovered granules were characterized to validate its composition and its morphology.

2 Materials and Methods

2.1 Chemicals

All solutions were prepared from reagent chemicals. The synthetic wastewater was prepared by dissolving nickel using $NiSO_4 \cdot 6H_2O$ (99%) from Shikmayu's Pure Chemicals, copper using $CuCl_2 \cdot 2H_2O$ (98%) from Choneye Pure Chemicals and the precipitant used was sodium carbonate from Panreac in reverse osmosis water. The initial concentration of 600 ppm copper and 300 ppm nickel was constant throughout the study. The total carbonate loading was varied (10, 12, 15, 17 and 20 mM), and the precipitant flow rate was 10 mL min^{-1} and initial pH was 6.5.

2.2 Fluidized-Bed Reactor

The FBR used in the experiment was a cylindrical Pyrex glass with total volume of 450 mL. The reactor was filled with glass beads with diameters of 4 and 2 mm with fixed depths of 1.5 and 1 cm, respectively. There were three inlets in the reactor, the two horizontal inlets were for the wastewater and for the precipitant, while the vertical inlet at the bottom was for the influent recirculation; effluent was pass through in the outlet located in the upper part of the reactor. The pH meter was mounted at the top of the FBR to monitor the pH throughout the operation.

2.3 Experimental Procedures

The synthetic wastewater containing copper and nickel ions and the precipitant solution was pumped simultaneously with the flow rate (Q) of 10 mL min^{-1}, and the same flow rate was applied to the synthetic wastewater. The recirculation flow rate was initially set to 25 mL min^{-1} and slowly increased up to 100 mL min^{-1} depending on the size of the granules along the treatment process. There were two phases in the adjustment of pH, initial pH of 6.5 was applied until 6 days and then adjusted the pH to 8.5 until day 14. To study the effect of total carbonate loading, varying CO_3 (10, 12, 15, 17 and 20 mM) was done to determine its removal and granulation efficiencies for both copper (6.3 mM) and nickel (3.4 mM) with constant Q and initial pH.

2.4 Water Sample Analysis and Granules Characterization

Effluent samples were taken from the reactor every 24 h for copper and nickel concentration analyses. The analysis was done using atomic absorption spectrometer (AA Analyst 200, Perkin Elmer). Total removal and granulation efficiencies of copper and nickel were attained after the effluent solutions were filtered using 0.45-μm micro-syringe filter paper and using this formula:

$$\%\text{Removal} = \left(1 - \frac{[\text{metal}]_d \times Q_T}{[\text{metal}]_{\text{in}} \times Q_{\text{metal}}}\right) \times 100 \quad (1)$$

$$\%\text{Granulation} = \left(1 - \frac{[\text{metal}]_t \times Q_T}{[\text{metal}]_{\text{in}} \times Q_{\text{metal}}}\right) \times 100 \quad (2)$$

where $[\text{metal}]_d$ is the effluent copper/nickel concentration after filtration; $[\text{metal}]_t$ is the total effluent copper/nickel concentration; $[\text{metal}]_{\text{in}}$ is the influent copper/nickel concentration; Q_{metal} is the flow rate of the wastewater; and Q_T is the flow rate of wastewater and the precipitant.

After a non-stop operation for 14 days, the produced granules were collected, air-dried and analyzed to determine the size distribution of particles. The surface shape and structure of granules were determined by using scanning electron microscopy, and EDX was performed to determine the composition of the granules.

3 Results and Discussion

3.1 Effect of Total Carbonate Loading in Removal and Granulation Efficiencies of Copper and Nickel

The amount of total carbonate loading in the system was greatly affected the removal and granulation efficiencies of both copper and nickel. Figure 1 shows removal and granulation efficiencies over operating time, it is apparent that at lower amount of CO_3 loaded to the system, the removal of metal ions were also low. At 10 mM of CO_3, copper removal and granulation efficiencies were 94.7 and 77%, respectively, while nickel removal efficiency of 62.8% and granulation efficiency 54.6% occurred. The low removal and granulation efficiencies of both copper and nickel happened because of the amount of the carbonate ions available to react to both copper and nickel ions were not enough. The occurrence may due to the fact that there is no excess of carbonate ions in the system. Zhou et al. (1999) mentioned in their study on the removal of metals in FBR using sodium carbonate as the precipitant, when the amount of carbonate is less, precipitation of the copper carbonate or hydroxide is inhibited due to the insufficiency of CO_3^{2-} and OH^- ions.

Both copper and nickel showed unfavorable efficiencies in low amount of CO_3 are used. Shown in Fig. 1 that as the amount of CO_3 is increasing, the removal and granulation efficiencies of copper also increasing resulted to 98 and

Fig. 1 Effect of total carbonate loading on copper removal and granulation (**a**) and nickel removal and granulation (**b**)
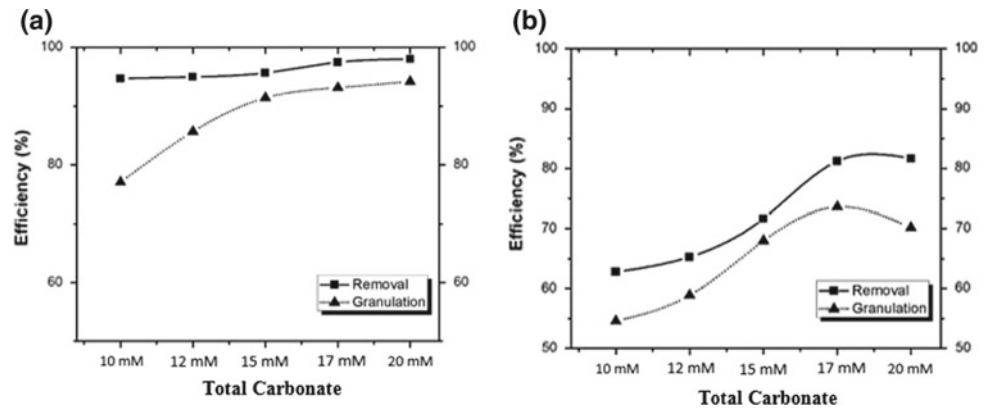
94.2%, respectively. However, at 20 mM of CO_3, there was a slight drop of nickel removal and granulation efficiencies to 0.5 and 3.4%, respectively. The increase in removal and granulation efficiencies at high CO_3 loading in the system is because increased carbonate ions react with both copper and nickel ions.

Hence, a further increase in precipitant leads to spontaneous nucleation and reduction in the mechanical strength of nickel crystals forming more fines(Salcedo et al. 2016). In this study, at 20 mM of CO_3 was used, the large granules produced were less and the formation of fines was extensive.

3.2 Morphology and Composition of Granules

The SEM image of the granules was classified as round with weak structure. This may be due to the mixture of two metal ions and the period of time that the treatment happened. The EDX result showed that the granules recovered were composed of copper = 51.32%, nickel = 9.75%, oxygen = 24.37% and C = 14.56% by weight.

4 Conclusion

Increasing the amount of carbonate precipitant improved the removal and granulation efficiencies for both copper and nickel. However, further increase may cause large amount of produced fines and less formation of bigger granules. Synthetic wastewater with the concentration of 6.3 mM of copper and 3.4 mM of nickel, initial operating pH of 6.5 and

precipitant flow rate of 10 attained the optimum copper removal of 95.5%, copper granulation of 93.13% and nickel removal and granulation efficiencies of 81.2 and 73.6%, respectively. Accordingly, the recovered granules were comprised of carbon, oxygen, copper and trace amount of nickel.

References

Chen, C., Shih, Y., & Huang, Y. (2015). Remediation of lead (Pb (II)) wastewater through recovery of lead carbonate in a fluidized-bed homogeneous crystallization (FBHC) system. *Chemical Engineering Journal, 279,* 120–128. https://doi.org/10.1016/j.cej.2015.05.013.

Duda-Chodak, A., & Blaszczyk, U. (2008). The impact of nickel on human health. *Journal of Elementology, 13*(4), 685–696.

Jadhav, U., & Hocheng, H. (2015). Hydrometallurgical recovery of metals from large printed circuit board pieces. *Scientific Reports, 5* (101), 14574. https://doi.org/10.1038/srep14574.

Salcedo, A. F. M, Ballesteros, F. C., Lu, M. (2015). Recovery of nickel from industrial wastewater by homogeneous fluidized-bed granulation : Effects of influent nickel concentration, CO_3 : Ni ratio and pH of the precipitant, September 3–5, 2015.

Salcedo, A. F. M., Ballesteros, F. C., Vilando, A. C., & Lu, M. (2016). Nickel recovery from synthetic Watts bath electroplating wastewater by homogeneous fluidized bed granulation process. *Separation and Purification Technology, 169,* 128–136. https://doi.org/10.1016/j.seppur.2016.06.010.

Solomon F. (2009). Impacts of copper on aquatic ecosystems and human health. Mining Magazine, January 25–28, 2009. doi: MINING.com.

Zhou, P., Huang, J.-C., Li, A. W. F., & Wei, S. (1999). Heavy metal removal from wastewater in fluidized bed reactor. *Water Research, 33*(8), 1918–1924. https://doi.org/10.1016/S0043-1354(98)00376-5.

Investigation of the Synthesis and Adsorption Kinetics of Biochar-Supported Fe$_3$-XMn$_x$O$_4$ for Imidacloprid Pesticide Removal

Mark Daniel G. De Luna, Michael M. Sablas, Chiu-Wen Chen, and Cheng-Di Dong

Abstract

Simple synthesis procedure for biochar-supported Fe$_3$-xMn$_x$O$_4$ was conducted. Synthesis conditions were examined for optimal metal impregnation yield. Kinetics of adsorption was investigated for imidacloprid removal.

1 Introduction

Global production and application of pesticide have progressively increased with the rising demand for food products. However, water pollution from pesticides poses a serious threat to humans and the environment due to their persistence, toxicity, and high tendency for bioaccumulation (Sanyal et al. 2017; Moschopoulou et al. 2017). Imidacloprid (IMD), a systemic neonicotinoid, is one of the widely used pesticides worldwide (Simon-Delso et al. 2015). This study examined the potency of a synthesized biochar-supported Fe$_3$-xMn$_x$O$_4$ to adsorb IMD in aqueous solution. The synthesized catalyst has two-pronged action: as an adsorbent and as a radical promoter in advanced oxidation processes. The synthesis and use of recyclable catalysts have recently gained more attention since they address the excessive sludge generation problem in classic homogeneous reactions for pollutant removals (He et al. 2015). The introduction of Mn^{2+} was reported to improve the catalytic activity of magnetite (Fe$_3$O$_4$) in the degradation of organic pollutants (Zhong et al. 2014). Metal substitutions improved the surface properties of magnetite, such as specific surface area and superficial hydroxyl amount. The present study focuses only on the adsorptive potential of the Mn-substituted magnetite (Fe$_3$-xMn$_x$O$_4$) by examining its adsorption kinetics. We also examined the optimum synthesis conditions for high metal impregnation yield and stability unto the biochar support.

2 Materials and Methods

The synthesis of biochar-supported Fe$_3$-xMnxO$_4$ was performed by wet impregnation method (Wei et al. 2015; Nguyen et al. 2011). Initially, 100 mL of HNO$_3$ (20%) solution containing FeSO$_4$.7H$_2$O (Shimakyu Pure Chem., 98 + %) and MnSO$_4$.H$_2$O (J. T. Baker, 98 + %) was prepared. The molecular ratio of Mn/Fe was controlled at 1:5 or as desired, while the total concentration of Mn and Fe was kept at 0.9 M. 1 mL hydrazine was added to prevent the oxidation of ferrous cations (Fe^{2+}), and the pH was set low enough (pH < 1) to prevent metals from precipitation. The solution was heated between 60 and 70 °C for 30 min. After heating and constant stirring, the solution was then poured to a beaker with 50 g activated biochar. The mixture was then cooled at 25 °C while stirring at a rate of 150 rpm for another 24 h. The suspension was decanted and dried at 110 °C in the oven for 2 h. Finally, the dried samples were thermally treated at 800 °C for 1 h in the presence of nitrogen to form the biochar-supported Fe$_3$-xMn$_x$O$_4$ catalyst.

M. D. G. De Luna (✉)
Department of Chemical Engineering, University of the Philippines Diliman, Quezon City 1101, Philippines
e-mail: mgdeluna@up.edu.ph

M. D. G. De Luna · M. M. Sablas
Environmental Engineering Program, National Graduate School of Engineering, University of the Philippines Diliman, Quezon City 1101, Philippines
e-mail: mmsablas@up.edu.ph

C.-W. Chen · C.-D. Dong
Department of Marine Environmental Engineering, National Kaohsiung University of Science and Technology, Kaohsiung City 81157, Taiwan
e-mail: cwchen@mail.nkmu.edu.tw

C.-D. Dong
e-mail: cddong@mail.nkmu.edu.tw

IMD adsorption experiments were performed using a batch equilibration technique. 1 mM of IMD (Sigma-Aldrich, 98 + %) spiked solution was prepared. The kinetic experiments were conducted in 50 mL amber bottles by mixing 0.3 g of biochar-supported $Fe_3\text{-}xMn_xO_4$ catalyst with 40 mL of 1 mM IMD solution. The mixture was then agitated on a reciprocating shaker at 25 °C and 120 rpm. Samples were taken at desired intervals and subsequently filtered. Residual IMD concentration in the solution was analyzed using HPLC system (Hitachi Chromaster 5420). Likewise, polarized Zeeman atomic absorption spectrometer (Hitachi ZA3300) was used for the determination of total iron and manganese metals in the biochar.

3 Results and Discussion

3.1 Effects of Synthesis Parameters in $Fe_3\text{-}XMn_xO_4$ Biochar Impregnation

To determine good synthesis conditions that will yield high percent metal impregnation into the biochar with high stability for multiple reuse, three synthesis parameters were investigated: metal concentration, biochar concentration, and pyrolysis temperature. As presented in Fig. 1a, % Fe and Mn impregnation increased when we raised the total metal concentration from 0.1 to 0.9 M. However, highest percent metal impregnations were only 31.7 and 28.4% for Fe and Mn, respectively. The rest were precipitated and lost into the solution. We varied the biochar concentration (i.e., 0.2 and 0.5 g mL^{-1}) to determine if this will improve the metal impregnation. Figure 1b shows the significant improvement in metal impregnation as we raised the biochar concentration from 0.2 to 0.5 g mL^{-1}. From low yield of only 28.4 and 31.7%, metal impregnations improved to 60.7 and 77.7% for Fe and Mn, respectively. This can be attributed to the increased surface contact of metal on the biochar as we raised the latter's concentration. For the effect of calcination temperature, Fe and Mn impregnated biochar were subjected to 200 and 800 °C. The result in Fig. 1c indicated that higher calcination temperature also improved the metal impregnation. Interestingly, metal leaching induced by washing was minimal in both temperatures, suggesting that the catalyst was fairly stable at neutral pH. Percent metal impregnations at 800 °C calcination temperature were 60.7 and 77.7% for Fe and Mn, respectively. On the other hand, calcination at 200 °C only yielded 20.3 and 14.6% metal impregnation for Fe and Mn, respectively.

Fig. 1 Effects of different parameters in biochar metal impregnation: a initial metal concentration, b biochar concentration, and c calcination temperature
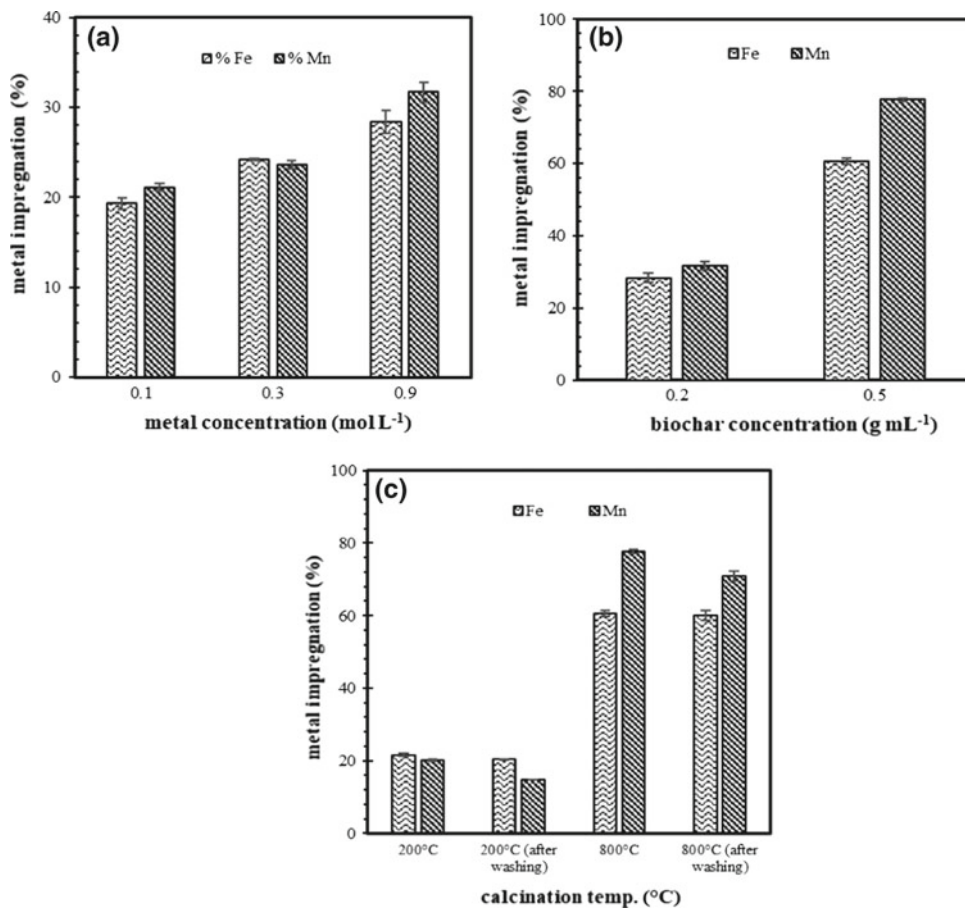
3.2 Kinetics of Adsorption of Biochar-Supported Fe$_3$-XMn$_x$O$_4$

The pseudo-first-order (PFO) and pseudo-second-order (PSO) rate equations have been commonly employed to describe the adsorption kinetics from data obtained under non-equilibrium conditions. The PFO rate equation or the so-called Lagergren equation is expressed as $\ln(q_e - q_t) = \ln q_e - k_1 t$, where q_t is the amount of adsorbate adsorbed at time t, q_e is its value at equilibrium, and k_1 is the PFO rate constant. On the other hand, the PSO equation by Ho and McKay (1998) is expressed as $t/q_t = 1/(k_2 q_e^2) + 1/(q_e t)$, where k_2 is the PSO rate constant. Both PFO and PSO equations were used in parallel, and their respective coefficients of determination (R^2) were used to assess which kinetics best fitted the experimental data. The adsorption of IMD onto the biochar-supported Fe$_3$-xMn$_x$O$_4$ follows the PFO kinetics as observed in the closer-to-unity value of R^2. The computed adsorption capacities from PSO model (52.15 mg g^{-1}) were also in agreement with the experimental adsorption capacities at equilibrium (45.98 mg g^{-1}). This suggested that the rate of pollutant removal was directly proportional to the pollutant concentration. The result implied that one IMD molecule was adsorbed onto one adsorption site on the solid surface. The same observation is applied to adsorption in solid–liquid systems based on the sorption capacity of solids (Boparai et al. 2011).

4 Conclusion

Biochar-supported Fe$_3$-xMn$_x$O$_4$ can be used as an effective adsorbent for removing IMD from contaminated water. The pseudo-first-order kinetic model accurately described the adsorption kinetics. The effects of synthesis conditions on the metal impregnation yield (%) were investigated, and optimal conditions for the study were as follows: 0.9 M total metal concentration, 0.5 g mL^{-1} biochar concentration, and 800 °C calcination temperature. The biochar exemplified stability after several washes with insignificant metal leaching. Results from this study showed that the synthesized material has a high potential as an effective adsorbent of pollutants in water.

References

Boparai, H. K., Joseph, M., & O'Carroll, D. M. (2011). Kinetics and thermodynamics of cadmium ion removal by adsorption onto nano zerovalent iron particles. *Journal of Hazardous Materials, 186,* 458–465. https://doi.org/10.1016/j.jhazmat.2010.11.029.

He, J., Yang, X., Men, B., Yu, L., & Wang, D. (2015). EDTA enhanced heterogeneous Fenton oxidation of dimethyl phthalate catalyzed by Fe3O4: Kinetics and interface mechanism. *Journal of Molecular Catalysis A: Chemical, 408,* 179–188. https://doi.org/10.1016/j.molcata.2015.07.030.

Moschopoulou, G., Dourou, A., Fidaki, A., & Kintzios, S. E. (2017). Assessment of pesticides cytoxicity by means of bioelectric profiling of mammalian cells. *Environmental Nanotechnology, Monitoring and Management, 8,* 254–260. https://doi.org/10.1016/j.enmm.2017.10.004.

Nguyen, T. D., Phan, N. H., Do, M. H., & Ngo, K. T. (2011). Magnetic Fe2MO4 (M:Fe, Mn) activated carbons: Fabrication, characterization and heterogeneous Fenton oxidation of methyl orange. *Journal of Hazardous Materials, 185,* 653–661. https://doi.org/10.1016/j.jhazmat.2010.09.068.

Sanyal, S., Law, A., & Law, S. (2017). Chronic pesticide exposure and consequential keratectasia & corneal neovascularisation. *Experimental Eye Research, 164,* 1–7. https://doi.org/10.1016/j.exer.2017.08.002.

Simon-Delso, N., Amaral-Rogers, V., Belzunces, L., Bonmatin, J., Chagnon, M., Downs, C., et al. (2015). Systemic insecticides (neonicotinoids and fipronil): trends, uses, mode of action and metabolites. *Environmental Science and Pollution Research, 22,* 5–34. https://doi.org/10.1007/s11356-014-3470-y.

Wei, G., Liang, X., He, Z., Liao, Y., Xie, Z., Liu, P., et al. (2015). Heterogeneous activation of Oxone by substituted magnetites Fe$_3$ − xMxO$_4$ (Cr, Mn Co, Ni) for degradation of Acid Orange II at neutral pH. *Journal of Molecular Catalysis A: Chemical, 398,* 86–94. https://doi.org/10.1016/j.molcata.2014.11.024.

Zhong, Y., Liang, X., He, Z., Tan, W., Zhu, J., Yuan, P., et al. (2014). The constraints of transition metal substitutions (Ti, Cr, Mn, Co and Ni) in magnetite on its catalytic activity in heterogeneous Fenton and UV/Fenton reaction: From the perspective of hydroxyl radical generation. *Applied Catalysis B: Environmental, 150–151,* 612–618. https://doi.org/10.1016/j.apcatb.2014.01.007.

A Kinetic Study of Calcium Carbonate Granulation Through Fluidized-Bed Homogeneous Process for Removal of Calcium-Hardness from Raw and Tap Waters

Arianne S. Sioson, Mark Daniel G. De Luna, and Ming-Chun Lu

Abstract

Fluidized-bed technology had been greatly employed to treat wastewater by removal of heavy metals, nutrients, and dissolved minerals through granulation or crystallization. This work focuses to imply the technology of fluidized-bed homogeneous granulation process to remove hardness from raw and tap waters. The paper investigated the granulation kinetics of $CaCO_3$ through fluidized-bed homogeneous granulation (FBHG) process during the homogenous nucleation stage. The mechanism followed the pseudo-second-order (PSO) kinetics, that calcium cation attracts to carbonate anion to form particle of $CaCO_3$ through double displacement chemical reaction. The calcium-to-carbonate molar ratio ($[Ca^{2+}]/[CO_3^{2-}]$) was varied into 1.25, 1.50, 1.75, 2.00, 2.25, and 2.50, with constant values of operating pH = 10 ± 0.2, influent carbonate concentration ($[CO_3^{2-}]$) = 10 mM and total influx flow rate (Q_T) = 60 mL min^{-1}.

A. S. Sioson (✉)
Environmental Engineering Graduate Program College of Engineering, University of the Philippines Diliman, Quezon City, Philippines
e-mail: arianneass@gmail.com

M. D. G. De Luna
Department of Chemical Engineering, University of the Philippines Diliman, Quezon City, Philippines
e-mail: mgdeluna@up.edu.ph

M.-C. Lu
Department of Environmental Resources Management, Chia-Nan University of Pharmacy and Science, Tainan, Taiwan
e-mail: mmclu@mail.cnu.edu.tw

1 Introduction

Freshwater supply available for human consumption is stored beneath the ground, soil or fractured bedrock, and surface waters such as lakes, rivers, and streams. These raw, tap, and other freshwaters contain some levels of dissolved minerals mostly in the form of calcium (Ca^{2+}) (Kalas et al. 2015). This is because of the contact of water as it flows below the surface of the soil and in groundwater to the sedimentary type of rock which is rich in calcium and that latter ions dissolve easily making hard water (Rolence et al. 2014).

The presence of mineral ions in the water had been identified so many decades ago to be a problem in the industries operations and in some domestic uses. The minerals present in the water would react with soap anions which decreases the cleaning efficiency and would induce scaling problems and failures in pipeline of boilers, heat exchangers, and electrical appliances (Bibiano-Cruz et al. 2016). Recently, it has been reported to also cause some serious diseases and illness to human like urolithiasis, cardiovascular disorder, kidney problems, anencephaly, cancer, and toughening of skin and hair (Altundogan et al. 2016). Thus, removal of mineral ions from groundwater and tap water had been considered.

Several techniques commonly used to solve the problem are ion exchange, lime softening, electrochemical, and adsorption. These techniques have some problems such as low removal efficiency, voluminous sludge production, acidic effluent, high power consumption and maintenance, and waste by-products (Park et al. 2007). Thus, various studies were done to address the problems by removal of contaminants in a wastewater and at the same time recovering the contaminants through granulation.

Related studies developed fluidized-bed reactor for water softening, nutrient removal, and heavy metal recovery. The use of the fluidized-bed granulation process enables good solid mixing, high rate of heat and mass transfer, and

increase the purity and size for material recovery, and it is an environmental friendly technology because it reduces the production of waste like sludge (Wei 2009).

2 Materials and Methods

The calcium carbonate homogeneous granulation was done in the laboratory-scale fluidized-bed reactor (FBR). The cylindrical Pyrex glass reactor with total volume of 550 mL was divided into two parts. The upper part which was the effluent region has dimensions of 15 cm in height and 4 cm in inner diameter. The lower part which was the reaction region has dimensions of 80 cm in height and 2 cm in inner diameter.

The reactor was initially loaded with glass beads of the same size up to 1 cm and then filled with 450 mL RO water. Granulation of calcium carbonate was initiated by controlling the parameters, operating pH to 10 ± 0.2, carbonate influent concentration to 10 mM, and influx flow rate to 60 mL min^{-1}, and varying calcium-to-carbonate molar ratio into 1.25, 1.50, 1.75, 2.00, 2.25, and 2.50.

Homogeneous nucleation kinetics of $CaCO_3$ in the FBR at different calcium precipitant dose was studied to determine the rate of chemical reaction occurred and the factors that could affect the rate. The investigation of the mechanism of $CaCO_3$ granulation through FBHG process was done in terms of pseudo-first-order (PFO) and pseudo-second-order (PSO) linear forms. Kinetic models pseudo-first- and second-order equations, linear forms, and plots were shown in Table 1, with parameters q_e (mg g^{-1}) as equilibrium nucleation capacity, h (mg g^{-1} h^{-1}) as initial nucleation rate, and k_1 (h^{-1}) and k_2 (g mg^{-1}h^{-1}) as rate constants.

3 Results and Discussion

The granulation kinetics of $CaCO_3$ were analyzed using PFO model by plotting log $(q_e - q_t)$ versus time (h), where q_e and q_t were the amounts granulated inside FBR in equilibrium and in any time, respectively. The calculated parameters shown in Table 2, with their corresponding correlation coefficients (R^2) in the range of 0.817–0.953, were obtained from the slope and intercept of their generated linear forms. Since the R^2 values obtained in PFO model were found to be much lower than 1, the model was considered not fit (Fierro et al. 2008).

The granulation kinetics of $CaCO_3$ in FBR were also analyzed using PSO model by plotting t/q_t versus time (h). The calculated parameters and R^2 values were also presented in Table 2. The R^2 values were found to be greater than 0.99 in all $[Ca^{2+}]/[CO_3^{2-}]$ condition that was varied. The results indicated that PSO kinetics is the fitted model that could describe the $CaCO_3$ granulation kinetics through FBHG process. Granulation kinetics fitted in the PSO model means that the mechanism relies on the assumption that chemical sorption occurred, the reason why there was nucleation and granulation. Chemisorption describes ion exchange reaction involving valency forces through sharing or exchange of electrons between particles as covalent forces (Ho 2006). The calcium cation attracts to carbonate anion forming particle of $CaCO_3$ through double displacement chemical reaction, and the particle attracts to other particle or surface by forming chemical bonds. PSO applies at higher concentration, which means the lower the concentration, the lower the collision of ions, making precipitation of $CaCO_3$ slower.

There were high initial nucleation rates during the first hours of experiment during homogeneous nucleation, and

Table 1 Pseudo-kinetic models and their forms used in this study

Kinetic model	Equation	Linear form	Plot
Pseudo-first order	$\frac{dq_t}{dt} = k_1(q_e - q_t)$	$\log(q_e - q_t) = \log(q_e) - \frac{k_1 t}{2.303}$	$\log(q_e - q_t)$ vs t
Pseudo-second order	$\frac{dq_t}{dt} = k_2(q_e - q_t)^2$	$\frac{t}{q_t} = \frac{1}{k_2 q_e^2} + \frac{1}{q_e}t$	$\frac{t}{q_t}$ vs t

Table 2 Parameters calculated in pseudo-first- and second-order kinetic models for $CaCO_3$ precipitation through FBHG process

$[Ca^{2+}]/[CO_3^{2-}]$	PFO			PSO			
	k_1	q_e	R^2	k_2	q_e	h	R^2
1.25	0.0031	1.149	0.953	0.661	1.260	1.539	0.9991
1.50	0.0016	1.240	0.923	1.450	1.371	2.723	0.9986
1.75	0.0014	1.330	0.817	2.293	1.435	4.929	0.9999
2.00	0.0011	1.554	0.893	2.515	1.651	6.859	0.9999
2.25	0.0008	1.674	0.941	2.641	1.753	9.042	0.9999
2.5	0.0009	1.897	0.911	2.482	1.991	9.843	0.9999

throughout the experiment reached the equilibrium nucleation capacity, which increased when the $[Ca^{2+}]/[CO_3^{2-}]$ were increased. The high initial nucleation rate was expected because of the unseeding granulation where homogeneous nucleation to form nuclei of new small granules was the dominant mechanism in the first hours to produce granules, and when there were enough granules inside the reactor, the nucleation rate decreases because particles shift into agglomeration to form bigger granules.

The major ions monitored in this study were Ca^{2+} and CO_3^{2-} from solutions of $Ca(OH)_2$ and K_2CO_3, respectively. However, it cannot be neglected that the presence of other ions could affect the granulation of $CaCO_3$ in FBR. Other conditions could also affect the reaction, nucleation, and granulation in which they should be considered and monitored in the investigation of $CaCO_3$ granulation kinetics. Aside from calcium precipitant dose, pH was another important parameter because it determined the dominant ions in the system, whether bicarbonate, carbonate or hydroxide (Skoog and West 1963). Best pH in crystallization of $CaCO_3$ in FBR through homogeneous granulation was found to be at 10–11 (Mahasti et al. 2017). At this pH, dominant ions present in the system was carbonate, thus, higher efficiency of $CaCO_3$ granulation is expected.

4 Conclusion

Kinetics of $CaCO_3$ granulation through FBHG process fitted in the PSO model, which means that the mechanism relies on the assumption that chemical sorption occurred that is why there is nucleation and granulation. Chemisorption describes the ion exchange reaction involving valency forces, where the calcium cation attracts to carbonate anion forming particle of $CaCO_3$ that later on granulate and formed into bigger granules. The amount of calcium precipitant dose could significantly affect the $CaCO_3$ granulation performance through FBHG process. Molar ratio was important because it determined the amount of calcium precipitant that could react with carbonate ions to granulate $CaCO_3$.

Increasing calcium concentration increased the supersaturation state of the solution to granulate $CaCO_3$ resulting in higher granulation.

References

Altundogan, H. S., Topdemir, A., Cakmak, M., & Bahar, N. (2016). Hardness removal from waters by using citric acid modified pine cone. *Journal of the Taiwan Institute of Chemical Engineers, 58,* 219–225. https://doi.org/10.1016/j.jtice.2015.07.002.

Bibiano-Cruz, L., Garfias, J., Salas-Garcia, J., Martel, R., & Llanos, H. (2016). Batch and column test analyses for hardness removal using natural and homoionic clinoptilolite: Breakthrough experiments and modeling. *Sustainable Water Resources Management, 2,* 183–197. https://doi.org/10.1007/s40899-016-0050-y.

Fierro, V., Torné-Fernández, V., Montané, D., & Celzard, A. (2008). Adsorption of phenol onto activated carbons having different textural and surface properties. *Microporous and Mesoporous Materials, 111,* 276–284. https://doi.org/10.1016/j.micromeso.2007.08.002.

Ho, Y. S. (2006). Review of second-order models for adsorption systems. *Journal of Hazardous Materials, 136,* 681–689. https://doi.org/10.1016/j.jhazmat.2005.12.043.

Kalas, K. R., Ghazi, I. N., Abdul-Majeed, M. A. (2015). Hardness removal from drinking water using electrochemical cell. *Engineering and Technology Journal 33*(1), 78–89.

Mahasti, N. N. N., Shih, Y. J., Vu, X. T., & Huang, Y. H. (2017). Removal of calcium hardness from solution by fluidized-bed homogeneous crystallization (FBHC) process. *Journal of the Taiwan Institute of Chemical Engineers, 78,* 378–385. https://doi.org/10.1016/j.jtice.2017.06.040.

Park, J. S., Song, J. H., Yeon, K. H., & Moon, S. H. (2007). Removal of hardness ions from tap water using electromembrane processes. *Desalination, 202*(1–3), 1–8. https://doi.org/10.1016/j.desal.2005.12.031.

Rolence, C., Machunda, R. L., & Njau, K. N. (2014). Water hardness removal by coconut shell activated carbon. *International Journal of Science, Technology and Society, 2*(5), 97. https://doi.org/10.11648/j.ijsts.20140205.11.

Skoog, D. A., & West, D. M. (1963). Fundamentals of analytical chemistry. *Journal of Chemical Education, 40*(11), 614. https://doi.org/10.1021/ed040p614.2.

Wei, Z. (2009). A review of techniques for the process intensification of fluidized bed reactors. *Chinese Journal of Chemical Engineering, 17*(4), 688–702. https://doi.org/10.1016/S1004-9541(08)60264-5.

Destruction of Selected Pharmaceuticals with Peroxydisulfate (PDS): An Influence of PDS Activation Methods

Robert Wolski, Monika Półtorak, Iwona Rykowska,
Sławomir Kaczmarek, and Przemysław Andrzejewski

Abstract

The presence of pharmaceuticals' residual in water is considered as a serious environmental problem. Two of them, i.e., paracetamol and diclofenac were treated with peroxydisulfate activated with ferrous ions and copper oxide. The degradation rates of both compounds versus type activators applied were evaluated by the means of changes of pharmaceutical concentration as well as observed changes of nitrite and nitrate concentrations in the reaction mixtures during the oxidation processes. The results clearly show that paracetamol was relatively easily decomposed independently from the type of PDS activator applied, contrary to the diclofenac, which was more resistant to the oxidation, especially, when CuO activation was used.

Keywords

Pharmaceutical residuals • Peroxydisulfate • PDS

R. Wolski
Faculty of Chemistry, Department of Chemical Education,
Adam Mickiewicz University in Poznan, 89B Umultowska St.,
61-614 Poznan, Poland
e-mail: wola@amu.edu.pl

M. Półtorak
Faculty of Chemistry, Department of Water Treatment
Technology, Adam Mickiewicz University in Poznan,
89B Umultowska St., 61-614 Poznan, Poland
e-mail: poltorak.monika@gmail.com

I. Rykowska · S. Kaczmarek · P. Andrzejewski (✉)
Faculty of Chemistry, Department of Analytical Chemistry,
Adam Mickiewicz University in Poznan, 89B Umultowska St.,
61-614 Poznan, Poland
e-mail: pandrz@amu.edu.pl

I. Rykowska
e-mail: iwona.rykowska@amu.edu.pl

S. Kaczmarek
e-mail: slakac1@amu.edu.pl

1 Introduction

A strong oxidant called peroxydisulfate (PDS, also known as persulfate) is often considered as a very useful oxidant. The behavior of this oxidant is, however, different from other compounds such as ozone or chlorine. Prior to the application of PDS, the compound has to be activated. Several types of activators are pointed out, however, the application of ion of some metals on its lower valence (such as Fe^{+2}) (Anipsitakis and Dionysiou 2003; Anipsitakis and Dionysiou 2004) as well some metals' oxides (such as CuO) (Zhang et al. 2014) or UV radiation (Berlin 1986) seems to be the most promising. PDS activation achieved by some metals' ions of its lower valence leads to the formation of very reactive sulfuric radicals (SO_4^{*-}) according to equation (Anipsitakis and Dionysiou 2003):

$$S_2O_8^{2-} + Fe^{+2} \rightarrow SO_4^{*-} + SO_4^{2-} + Fe^{+3}$$

Furthermore, the UV beam activation of PDS also leads to the formation of the reactive sulfuric radicals (SO_4^{*-}) according to Eq. (2) (Berlin 1986):

$$S_2O_8^{2-} + h\nu \rightarrow 2SO_4^{*-}$$
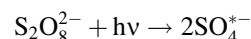
This activation method is two times more effective compared to the Fe^{+2} activation (two SO_4^{*-} radicals vs. one radical). However, the effectiveness of the process could be limited by a low water transparency. Moreover, formation of other radicals can be expected as the UV radiation of water may also result in generation of HO* radicals according to the equation (Berlin 1986):

$$H_2O \xrightarrow{h\nu} 1/2 H_2 + HO^*$$

Contrary to the above activation methods, PDS activation with oxides of some metals, crucially CuO, results in no radical oxidation mechanism (Zhang et al. 2014).

The main aim of the research was to evaluate the PDS's activation method influence on the pharmaceuticals decomposition during peroxydisulfate oxidation. Authors decided to select PDS activation methods, which in authors' opinion, could be applied in a water/wastewater treatment technology. Two pharmaceuticals oxidation by PDS dependency on mechanisms of reactions were considered: paracetamol or diclofenac oxidation by SO_4^{*-} radicals (Fe^{+2} activation) and paracetamol/diclofenac oxidation by no-radical species (CuO activation).

Thus, the main aim of the research was to investigate the PDS activation methods' influence on given pharmaceuticals decomposition.

2 Materials and Methods

2.1 Pharmaceuticals and Oxidant, I.E., Diclofenac, Paracetamol, and PDS

See Figs. 1 and 2.

2.2 Analytical Methods

Amount of both nitrite/nitrate, formed as a result of nitrogen oxidation, and changes of paracetamol/diclofenac concentration during oxidation were chosen as the indicators of pharmaceuticals degradation.

Two indirect methods of spotting PDS's concentration change during the oxidation process were applied: Firstly, sulfate's concentration was determined (one of the molecules of PDS finally generates two molecules of sulfate ions) and secondly, redox potential measurements. Changes in sulfate concentration were compared to changes in, continuously measured, redox potential of the reaction mixture.

Fig. 2 Structure of peroxydisulfate ion (PDS)
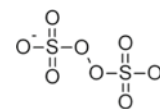
2.3 Experimental

Paracetamol or diclofenac was oxidized by potassium peroxysulfate activated in homogenic condition (Fe^{+2}) or heterogenic one (CuO). pH of these solutions was adjusted by the adding the solution of H_2SO_4 (>95%, Fluka) or NaOH (>98%, Fluka), to reach pH of 5.8. No buffers were added to the reaction mixtures but the pH of reaction mixtures was checked twice, i.e., pharmaceuticals solution prior to PDS's addition and after 60th minute of the reaction. Subsequently, PDS and activators were added to both reactors.

3 Results and Discussion

3.1 PDS Decomposition During Its Activation with Copper Oxide or Ferrous Ions Without Presence of Any Potential or Inorganic and Organic Reducers

PDS decomposition runs very fast, in the presence of ferrous ions, and reached the rate of app. 35%. However, PDS decomposition, in the presence of CuO, runs definitely slower, yet, reached higher value, compared to the PDS/Fe^{+2} reaction, rate app. 43%. This last phenomenon, i.e., a slower activation process, the authors attributed to the fact that this reaction run at the border of two phases: solid (CuO) and liquid (water solution of PDS) (Figs. 3 and 4).

2-[2-(2,6-dichloroanilino)phenyl]acetic acid (diclofenac)

N-(4-hydroxyphenyl)acetamide (paracetamol)

Fig. 1 Diclofenac and paracetamol structure
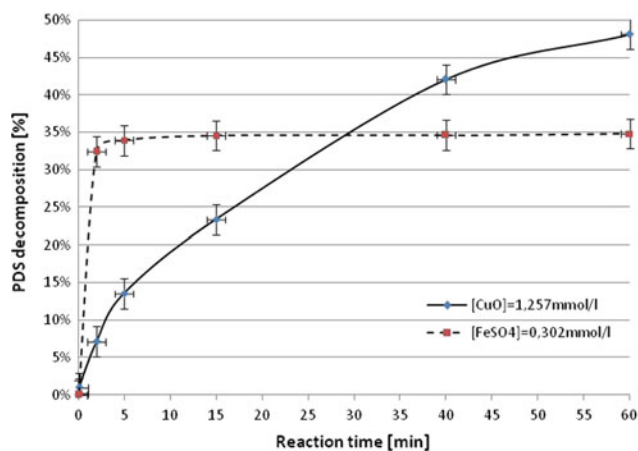
Fig. 3 PDS decomposition during its activation with copper oxide or ferrous ions without the presence of any potential or inorganic and organic reducers. Experiments conditions: pH = 5.8, [PDS] = 0.296 mmol/l, mixing speed = 700 rpm
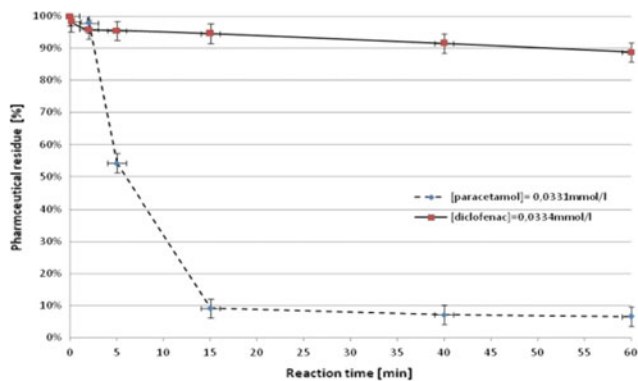
Fig. 4 Paracetamol and diclofenac degradation during its oxidation by CuO activated PDS
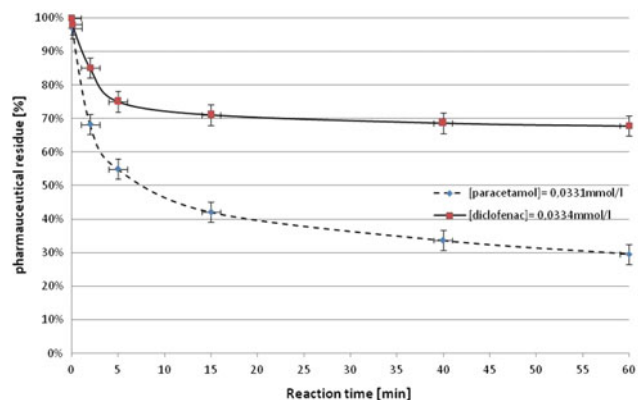
Fig. 5 Paracetamol and diclofenac degradation during its oxidation by Fe^{+2} activated PDS. Experiments conditions: pH = 5.8, [PDS] = 0.296 mmol/l, [Fe^{+2}] = 0.553 mmol/l, mixing speed = 700 rpm Paracetamol and diclofenac underwent degradation by Fe^{+2} activated PDS, but significant differences in degradation rates were observed. Paracetamol was degraded app. two times more effectively than diclofenac

Experiments conditions: pH = 5.8, [PDS] = 0.296 mmol/l, [CuO] = 1.257 mmol/l, mixing speed = 700 rpm Despite quite significant decomposition rate of PDS activated by CuO, diclofenac was hardly decomposed during this reaction—at least in comparison with over 90% of paracetamol destruction (Fig. 5).

4 Conclusion

1. PDS underwent degradation, during its activation, independently from the type of the activator applied.
2. Paracetamol was relatively easy decomposed regardless the type of PDS activator applied, contrary to diclofenac, which was more resistant to oxidation especially, when CuO activation was used.

References

Anipsitakis, G. P., & Dionysiou, D. D. (2003). Degradation of organic contaminants in water with sulfate radicals generated by the conjunction of peroxymonosulfate with cobalt. *Environmental Science and Technology, 37*(20), 4790–4797.

Anipsitakis, G. P., & Dionysiou, D. D. (2004). Radical generation by the interaction of transition metals with common oxidants. *Environmental Science and Technology, 38*(13), 3705–3712.

Berlin, A. A. (1986). Kinetics of radical-chain decomposition of persulfate in aqueous solutions of organic compounds. *Kinetic. Katal, 27,* 34–39.

Zhang, T., Chen, Y., Wang, Y., Le Roux, J., Yang, Y., & Croué, J.-P. (2014). Efficient peroxydisulfate activation process not relying on sulfate radical generation for water pollutant degradation. *Environmental Science & Technology, 48,* 5868–5875.

Non-destructive In Situ Fouling Monitoring in Membrane Processes

L. Fortunato, S. Jeong, and T. Leiknes

Abstract

Fouling is considered the bottleneck of membrane systems. In this study, the fouling occuring in different membrane processes and configurations was studied by using Optical Coherence Tomography (OCT). Fouling formation in membrane system was assessed and quantified non-invasively during operation. The use of the OCT enabled monitoring fouling evolution and correlating it to the membrane performance decline.

1 Introduction

In the last decades, the use of membrane systems for freshwater production has increased strongly to supply the growing water demand due to increasing human population, industrial and agricultural activity, economic growth, and urbanization. Fouling represents one of the major drawbacks of membrane systems. In this work, the suitability of the fouling monitoring in membrane system is presented.

L. Fortunato (✉) · T. Leiknes
Biological and Environmental Science and Engineering Division (BESE), Water Desalination and Reuse Center (WDRC), King Abdullah University of Science and Technology (KAUST), Thuwal, 23955-6900, Saudi Arabia
e-mail: luca.fortunato@kaust.edu.sa

S. Jeong
SungKyunKwan University (SKKU), 2066, Seobu-ro, Jangan-gu, Suwon-si, Gyeonggi-do 16419, Republic of Korea

The optical coherence tomography (OCT) was employed to study in situ non-destructively the fouling formation in membrane processes. The innovative approach consists in acquiring online information about the fouling in the process under continuous operation. The approach was tested in three different membrane configurations and processes (spiral wound for desalination, submerged membrane for wastewater treatment, and membrane distillation for brine treatment).

2 Materials and Methods

An optical coherence tomography (OCT, Thorlabs GANYMEDE spectral domain OCT system with a central wavelength of 930, Thorlabs, GmbH, Dachau, Germany) equipped with a 5X telecentric scan lens (Thorlabs LSM 03BB) was used to investigate the fouling formation on membrane system. The OCT probe was mounted on a motorized frame (Welmex) allowing the movement in a system of coordinates with a precision of 5 μm on the x and y and 0.79 μm on the z.

The OCT scans were acquired under continuous operation in a fixed area for the entire period of observation. Several analytical techniques were used to study the fouling related the membrane performance decrease (flux decrease and pressure drop increase). The samples collected from the autopsy were analyzed using different techniques including: inductively coupled plasma optical emission spectrometry (ICP-OES), liquid chromatography with organic carbon detector (LC-OCD), total organic carbon (TOC), ATP Analyzer, in order to evaluate the nature of the deposits.

3 Results and Discussion

In the submerged membrane system (membrane bioreactor), the continuous monitoring allowed evaluating the dynamic evolution of the fouling layer under continuous operation
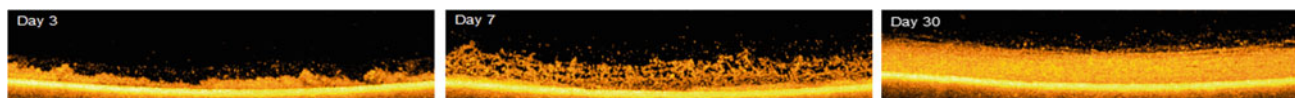
Fig. 1 Changes in biofilm morphology acquired by OCT scan over the time in submerged membrane bioreactor
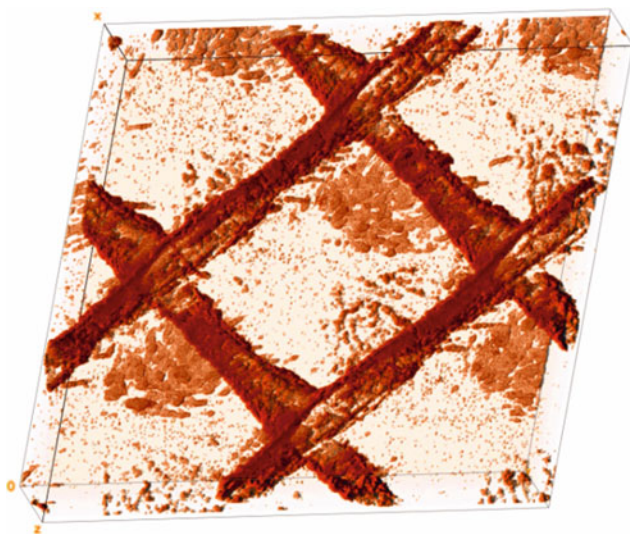
Fig. 2 3D rendered OCT image with biomass in spacer-filled channel

Fig. 3 Membrane distillation. Normalized flux pattern versus volume concentration factor VCF. The OCT scans were acquired non-destructively in situ. The membrane autopsy was performed at different time intervals (VCF 1.20, 2.50, and 3.20)

(Fig. 1) (Fortunato et al. 2017b, c). The OCT scans were employed to validate the filtration mechanism (pore blocking and cake layer). The OCT scans of the biomass morphology were then implemented in computational fluid dynamic model to evaluate the impact of the fouling on the local flux.

In the spiral wound system, the OCT was used to evaluate the spatially resolved distribution of the biofouling in spacer-filled channel membrane elements (Fig. 2). The approach enabled quantifying the amount of biomass deposited over the time. The analysis indicates that most of the biomass accumulates on the feed spacer during the early stage of biofouling (Fortunato et al. 2017a; Fortunato and Leiknes 2017).

In membrane distillation for the treatment of highly saline feed (i.e. brine), the OCT was used to evaluate the impact of scaling on the overall process (Fortunato et al. 2018). The continuous non-destructive monitoring with OCT provided an insight of the fouling mechanism by offering an appropriate timing for the membrane autopsy sampling (Fig. 3).

A correlation between the membrane processes performance decline (i.e., flux decrease, TMP increase, Pressure drop increase, etc.) and fouling development assessed with OCT was observed for all the processes tested. The OCT non-destructive analysis can help to determine the impact of different operational parameters on the overall performance of the filtration processes.

4 Conclusion

- The OCT analysis coupled with destructive techniques is suitable for evaluating the fouling in the membrane systems; the non-destructive analysis under continuous operation enabled the understanding of the fouling mechanism.
- The in situ continuous online monitoring allowed linking the flux trend with the fouling formed on the membrane surface.
- The non-destructive analysis performed with OCT coupled with destructive analysis performed during the membrane autopsy proved a better understanding of the fouling distribution and its nature.

References

Fortunato, L., Bucs, S., Linares, R. V., Cali, C., Vrouwenvelder, J. S., & Leiknes, T. (2017a). Spatially-resolved in-situ quantification of biofouling using optical coherence tomography (OCT) and 3D image analysis in a spacer filled channel. *Journal of Membrane Science, 524,* 673–681.

Fortunato, L., Jang, Y., Lee, J.-G., Jeong, S., Lee, S., Leiknes, T., et al. (2018). Fouling development in direct contact membrane

distillation: Non-invasive monitoring and destructive analysis. *Water Research, 132,* 34.

Fortunato, L., Jeong, S., & Leiknes, T. (2017b). Time-resolved monitoring of biofouling development on a fat sheet membrane using optical coherence tomography. *Scientific Reports, 7*(1), 15.

Fortunato, L., & Leiknes, T. (2017). In-situ biofouling assessment in spacer filled channels using optical coherence tomography (OCT): 3D biofilm thickness mapping. *Bioresource Technology, 229,* 231–235.

Fortunato, L., Qamar, A., Wang, Y., Jeong, S., & Leiknes, T. (2017c). In-situ assessment of biofilm formation in submerged membrane system using optical coherence tomography and computational fluid dynamics. *Journal of Membrane Science, 521,* 84.

Preparation of TiO2/SiO2 Ceramic Membranes Via Solgel Dip Coating for the Treatment of Produced Wastewater

Sarah S. Marzouk, Fawzi Banat, and Shadi Wajih Hasan

Abstract

TiO2-based commercial membranes were coated with SiO2 nanoparticles using solgel dip coating. Membranes were characterized using FTIR, SEM, contact angle and were also tested for the COD removal efficiency. Membrane coating was confirmed from FTIR spectra. SiO2 coating enhanced membranes hydrophilicity.

Keywords

Ceramic membranes • Oil rejection • Solgel dip coating • SiO2 • Produced water

1 Introduction

Oil production is still considered as one of the main energy sources in the globe. In the process of oil extraction from its underground formations, the water produced as a by-product is called produced water. This water is usually characterized by its high oil and salt content. Since such water cannot be directly dumped to the environment; it has to be treated first. Membrane technology has shown high potential in treating wastewater with similar properties (Mustafa et al. 2018; Nasiri and Jafari 2016). The research on the use of ceramic membranes in this area has been widely investigated by researchers. This is because of the ceramic membranes' superior chemical and thermal stability and high mechanical strength (Weschenfelder et al. 2016). They have been tested for their oil removal efficiency, and so far, they have shown promising results in the treatment of oily water as they proved to have high flux, low fouling and good oil removal efficiency. However, different coating and surface modification techniques have been tested on ceramic membranes in order to enhance their properties for the purpose of oil rejection (Puthai et al. 2017), for example, increasing their flux, hydrophilicity, decreasing their pore sizes and enhancing their performance. Therefore, the main objective of this paper was to modify a TiO2 ceramic membrane with SiO2 nanoparticles via solgel dip-coating approach. The modified membrane was used for the treatment of produced water and achieves better rejection of contaminants.

2 Materials and Methods

Commercial ceramic ultrafiltration membranes were used in this research study. The membranes are TiO2-based and have a thickness of 2.5 mm, pore size of 1 kD and a 47 mm diameter. Two of these membranes were coated with SiO2 using the solgel dip-coating method. The SiO2 nanoparticles used have an average diameter of 20 nm and were supplied from EPRUI Nanoparticles & Microspheres Co. Ltd. Membranes, M1 and M2, were dipped in SiO2 solutions of different concentrations: 0.5 and 1 wt%, respectively, for 26 h. The membranes were then left to dry in the oven at 40 °C for 12 h and were calculated after that at 300 °C for 2.5 h and were then left to cool down for 60 min. The membranes were characterized using the Fourier-transform infrared spectroscopy (FTIR) in the range of 4000–400 cm^{-1} using the attenuated total reflectance technique (ATR) to confirm the presence of SiO2. Moreover, scanning electron microscopy (FEI-Nova-nano-SEM) was also employed to confirm the deposition of silica oxide particles on the membrane surface. Finally, the contact angle test was done using the Kyowa contact angle measuring device, CA-A (Kyowa Interface Science Co., Ltd., Japan) in order to measure the hydrophilicity of the membranes.

S. S. Marzouk (✉) · F. Banat · S. W. Hasan
Department of Chemical Engineering, Center for Membrane and Advanced Water Technology, Khalifa University of Science and Technology, Masdar City Campus, 127788 Abu Dhabi, UAE
e-mail: sarah.marzouk@ku.ac.ae

F. Banat
e-mail: fawzi.banat@ku.ac.ae

S. W. Hasan
e-mail: shadi.hasan@ku.ac.ae

3 Results and Discussion

3.1 FTIR

The FTIR was done for the two coated membranes M1, M2 and for an uncoated membrane for comparison. Figure 1 shows the adsorption spectra of the three membranes. It can clearly be seen that the SiO_2 coated membrane M2 (with the 1% solution) had the highest peak at 1080 cm^{-1} which corresponds to the Si–O–Si bond. On the other hand, M1 had a lower peak at the same frequency. This indicates that the different concentration solutions had an effect on the intensity of SiO_2 embedded in the membrane surface. A peak at that frequency, however, was not witnessed on the uncoated membrane spectra. This proves that the membrane itself has no peak at that frequency and that those peaks observed for M1 and M2 are due to the SiO_2 deposition solely.

3.2 SEM

The Nova-SEM images were used to study the morphology of the three membranes surfaces. Figure 2 shows images of the coated membrane surfaces at 200,000× magnification and the uncoated membrane surface at 400,000× magnification. The white particles seen on the coated membranes surfaces are identified as SiO_2 nanoparticles. This was deduced as they show most on membrane M2, less on membrane M1 and are absent on the uncoated membrane.

3.3 Contact Angle

The contact angle test was carried to measure the wettability of the membranes. The results show great enhancement in the hydrophilicity of the coated membranes. Figure 3 shows the water droplets as seen by a high speed camera during the contact angle test when they first hit the membranes surfaces. The contact angle of the uncoated membrane—Fig. (3a)—was 74.7° when it first hit the surface of the membrane, 2700 ms later—when the test was finished—the contact angle was 53.6°. This indicated that the uncoated membrane was fairly hydrophilic. Nevertheless, the hydrophilicity was nearly doubled for the 0.5% coated membrane M1—Fig. (3b)—as the contact angle was 39.7° and took 24 s to completely sink in the membrane. Variously, M2—Fig. (3c)—was super hydrophilic and the water droplet instantly disappeared nearly giving a contact angle of zero.
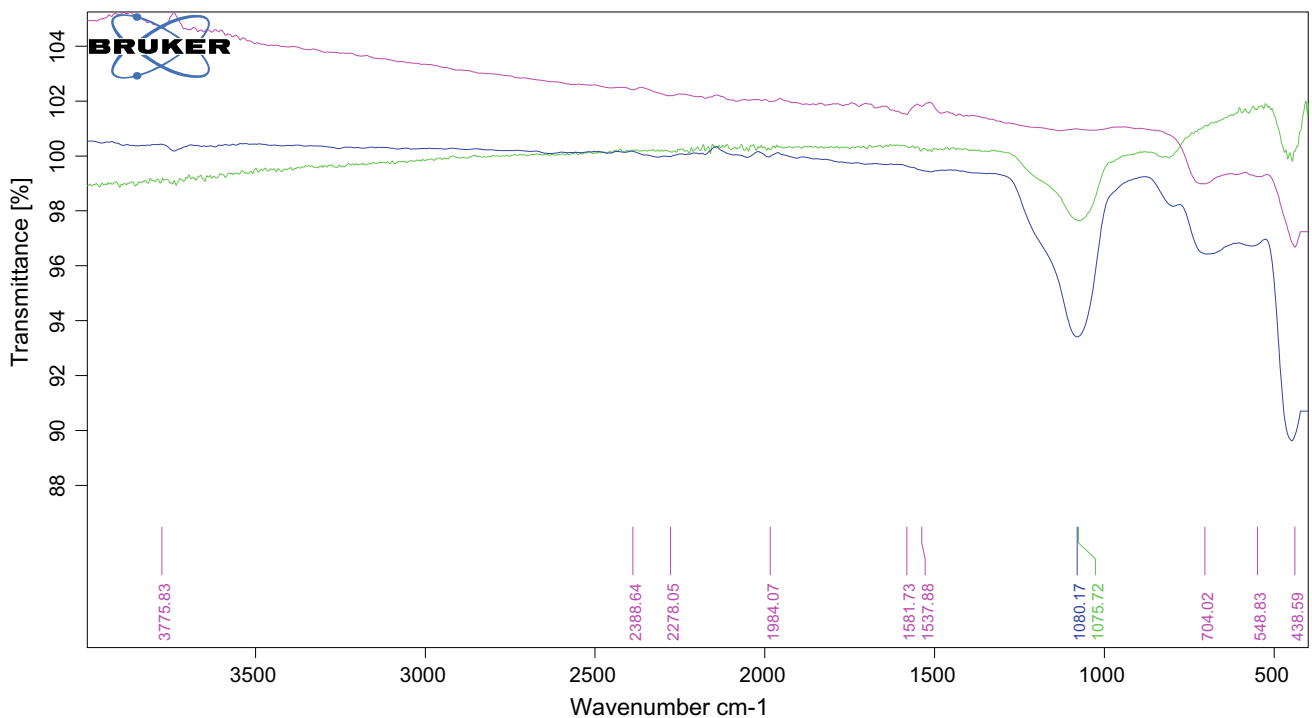
Fig. 1 FTIR spectra **a** purple: uncoated membrane **b** green: M1 **c** blue: M2
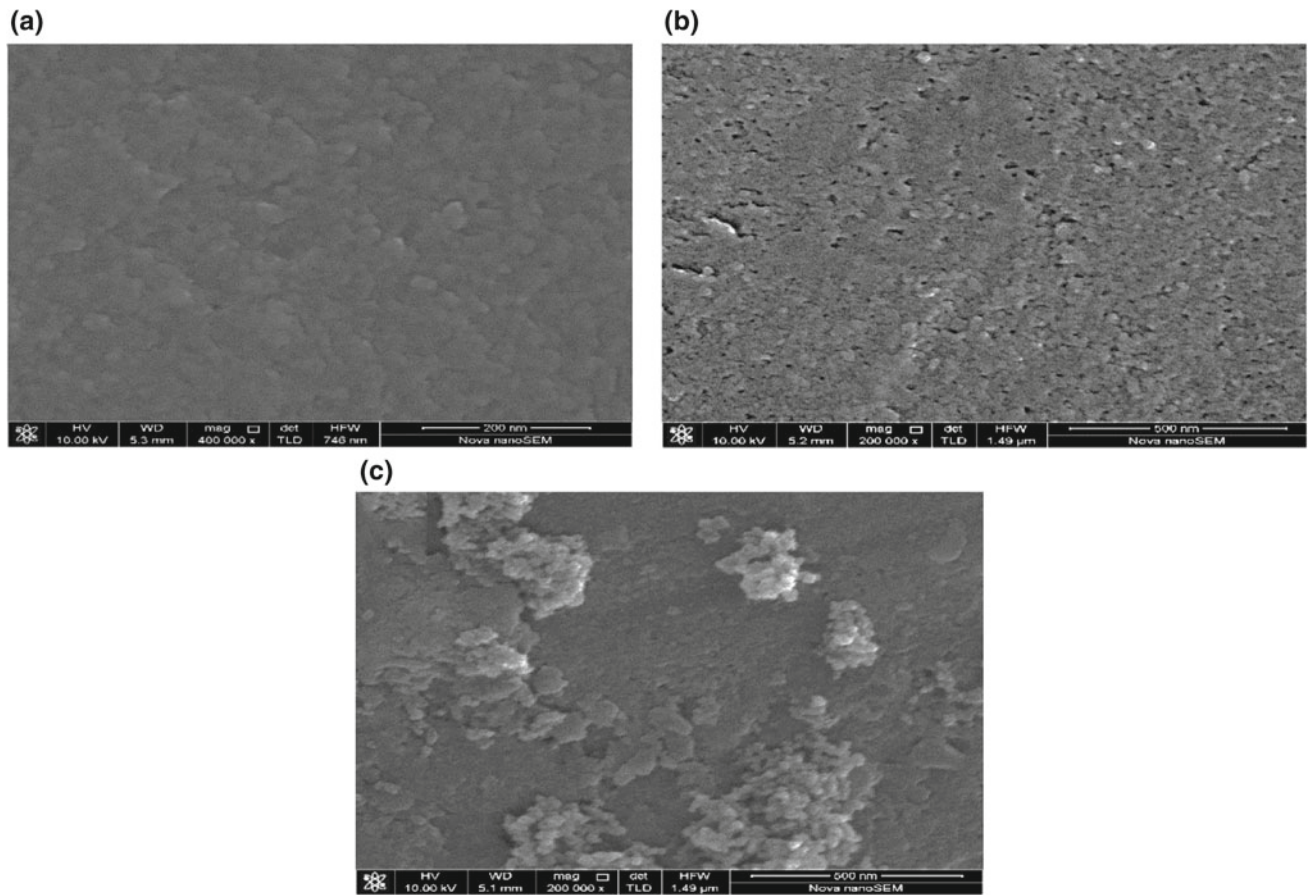
Fig. 2 SEM images for the **a** uncoated membrane **b** M1 **c** M2
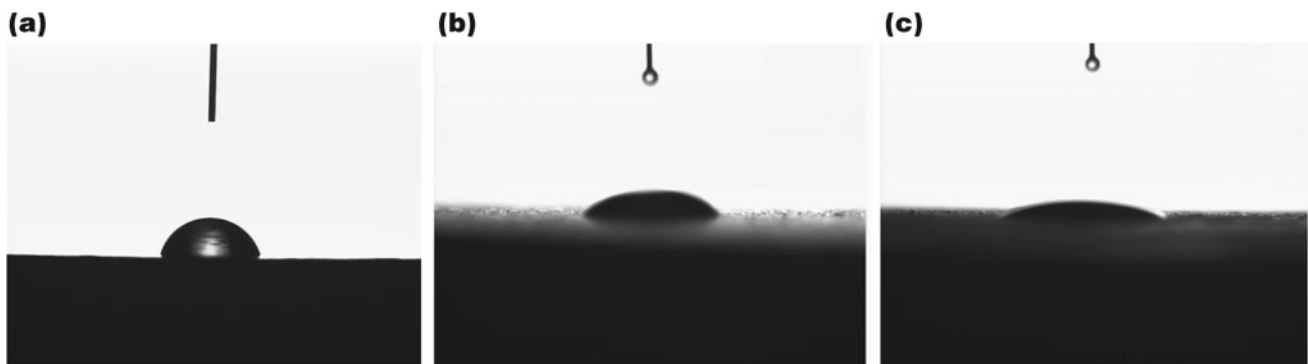
Fig. 3 Water droplets during CA test **a** uncoated membrane **b** M1 **c** M2

4 Conclusion

In conclusion, the SiO$_2$ nanoparticles were successfully deposited on the surface of the ceramic membranes as proved with the Si–O–Si bond frequency shown in FTIR spectra. Moreover, the SEM images also indicated the deposition of the SiO$_2$ particles on the coated membranes. In addition, the contact angle measurements showed a significant improvement in the hydrophilicity of the membranes which makes the membranes better oil rejectors. The future work of the authors would be to test the optimum time of the dip coating of the membranes and the calcination time. The testing of the membranes using produced water from the industry will also be done as well to evaluate the membranes' COD and TOC removal efficiency.

References

Mustafa, G., Wyns, K., Buekenhoudt, A., & Meynen, V. (2018). Antifouling grafting of ceramic membranes validated in a variety of challenging wastewaters. *Water Research, 104*, 242–253.

Nasiri, M., & Jafari, I. (2016). Produced water from oil-gas plants: A short review on challenges and opportunities. *Periodica Polytechnica Chemical Engineering, 61,* 73–81.

Puthai, W., Kanezashi, M., Nagasawa, H., & Tsuru, T. (2017). Development and permeation properties of SiO_2–ZrO_2 nanofiltration membranes with a MWCO of <200. *Journal of Membrane Science, 535,* 331–341.

Weschenfelder, S., Fonseca, M., Borges, C., & Campos, J. (2016). Application of ceramic membranes for water management in offshore oil production platforms: Process design and economics. *Separation and Purification Technology, 171,* 214–220.

Multicriteria Evaluation of Novel Technologies for Organic Micropollutants Removal in Advanced Water Reclamation Schemes for Indirect Potable Reuse

C. Echevarría, I. Martin, M. Arnaldos, X. Bernat, C. Valderrama, and J. L. Cortina

Abstract

Multicriteria evaluation based on technical, economic and environmental assessment shows the benefits and limitations of novel PAC-NF systems versus conventional UF-RO (50%) systems.

Keywords

Organic micropollutants • Indirect potable reuse • Technical-economic assessment • Hybrid systems • PAC-NF • UF-RO (50%)

1 Introduction

Indirect potable reuse (IPR) refers to the addition of purified reclaimed water into a water body (surface water augmentation or groundwater recharge) in order to store it and reuse it as drinking water supply. The application of this system represents a sustainable management of an alternative water resource following the circular economy framework that allows to preserve conventional freshwater resources. One possibility in IPR schemes is the deep well injection of reclaimed water for groundwater replenishment systems (GWRS) or also the prevention of saline barrier intrusion in those coastal regions with overexploitation of groundwater. However, the presence in urban and industrial wastewaters of compounds of anthropogenic origin that are called organic micropollutants (OMP), their unknown effects on public health post-catchment in water treatment plants and the concern associated in public authorities and population represent additional drawbacks in the implementation of IPR schemes. In order to guarantee the removal of these compounds, it is necessary to resort to advanced water reclamation technologies, focused on the removal of these recalcitrant compounds, usually not removed completely in conventional wastewater treatment schemes (Alvarino et al. 2018; Cabeza et al. 2012).

Reverse osmosis (RO), due to its molecular weight cutoff (200–300 Da), is able to remove efficiently the majority of OMP present in urban wastewaters (300–400 Da) apart from a complete removal of salinity, nutrients and organic matter; nevertheless, its efficiency is also associated with a high treatment cost (Verliefde 2008). Usually, in these advanced reclamation schemes, microfiltration (MF) or ultrafiltration (UF) are used as pre-treatment in order to guarantee a free suspended solids (SS) and disinfected influent. Moreover, in case legislation and/or quality requirements allow it, the pre-treatment (MF/RO) and the RO effluents are blended 50% to reduce the overall treatment costs. On the other hand, hybrid technologies represent an alternative to remove efficiently OMP by avoiding the use of RO (and its high energy cost associated) through the combination of different removal technologies. Powdered activated carbon (PAC)-nanofiltration (NF), for example, combines the adsorption potential of PAC with membrane separation provided by a capillary hollow fiber (HF)-NF. Other possibilities are the combination of advanced oxidation systems with membrane technologies or the use of adsorbent filters (usually granular activated carbon (GAC)) or biofilters as final polishing steps.

The aim of this research is to compare from a technical and economic point of view the use of UF/RO systems and hybrid systems based on PAC-NF in order to remove

C. Echevarría (✉) · I. Martin · M. Arnaldos · X. Bernat
CETAQUA, Water Technology Center, Barcelona, Spain
e-mail: cechevarria@cetaqua.com

I. Martin
e-mail: imartin@cetaqua.com

M. Arnaldos
e-mail: marina.arnaldos@cetaqua.com

X. Bernat
e-mail: xbernat@cetaqua.com

C. Valderrama · J. L. Cortina
Chemical Engineering Department, Technical University of Catalonia (UPC), Barcelona, Spain
e-mail: cesar.alberto.valderrama@upc.edu

J. L. Cortina
e-mail: jose.luis.cortina@upc.edu

efficiently OMP from wastewater effluents and use the reclaimed water for groundwater replenishment and as a barrier against aquifer salinization.

2   Materials and Methods

During 18 months, a prototype composed by a PAC contact tank and two capillary HF-NF modules was operated in "El Baix Llobregat" water reclamation plant (WRP) in order to characterize water quality, obtain optimal operating conditions and compare it from a technical-economic point of view with the full-scale plant (15,000 m^3/d) UF-RO (50% blend) used for aquifer recharge. PAC-NF prototype (2 m^3/h) was fed with a MBR prototype (3 m^3/h) effluent, which performance and technical evaluation will remain out of the scope of this study. HF-NF modules (PES; MWCO: 1000 Da) are chlorine tolerant and were operated in inside-out configuration, with a baseline internal recirculation (crossflow) of 12 m^3/h. Due to its MWCO, no salinity removal is obtained. The UF-RO (50% blend) full-scale plant was fed from a conventional basic reclamation (BR) system based on a physico-chemical treatment followed by ballasted sedimentation, disk-filtration and UV disinfection.

The prototype performance was compared with data (hydraulic and energy) gathered from the full-scale UF-RO. In addition, several campaigns were carried out to establish a water quality monitoring of the different streams. Seventeen OMP were selected as target analytes representing a wide range of micropollutants occurring in wastewaters. Solid phase extraction (SPE) coupled online with liquid chromatography and tandem mass spectrometry (LC-MS/MS) with electrospray ionization was used to quantify OMP. These 17 OMP included **nine pharmaceuticals** (Acetaminophen (ACET), Atenolol (ATE),

Cotinine (COT), Codeine (COD), Sulfamethoxazole (SMX), Diclofenac (DCF), Erythromycin (ERY), Carbamazepine (CBZ) and Carbamazepine Epoxide (CAE), which is a metabolite of CBZ), **six pesticides** (Diuron (DIU), Isoproturon (ISO), Atrazine (ATZ), Simazine (SMZ), Pentachlorophenol (PCP) and Terbuthylazine (TBZ)) and **two alkylphenols** (Octylphenol (OCT) and Nonylphenol (NON)).

3   Results and Discussion

In terms of OMP removal, due to the MWCO (1000 Da), tested HF-NF membrane did not represent a physical barrier to these compounds and the addition of PAC allows the major part of the adsorption. No significant variations were found in the removal of target compounds regarding the different tested PAC dosages (20, 50, 100 mg/L). Due to the high cost associated with PAC (2–5 €/kg), and according to resulting water yield and energy demands, low PAC dosage (20 mg/L) was defined as the optimal to operate in a sustainable way the hybrid HF-NF system.

Figure 1 aims to compare the removal efficiencies of conventional advanced wastewater treatment and reclamation systems with the hybrid system tested. RO membranes, due to the MWCO represented a physical barrier to OMP and high removal efficiencies (beyond 90–95%), were obtained for most of detected compounds. Since OMP removal efficiencies obtained through UF are very low (5–15%), the UF-RO (50% blend) system reported removal efficiencies between 40 and 50%. On the other hand, PAC-NF system allowed higher average removal efficiencies (50–70%) for most of detected OMP.

Operational expense (OPEX) (including chemicals, energy and membrane replacement) and capital expense (CAPEX) were evaluated for both advanced water

Fig. 1 Comparison of OMP removal efficiencies between PAC-NF system and conventional advanced water reclamation systems RO & UF-RO(50%)
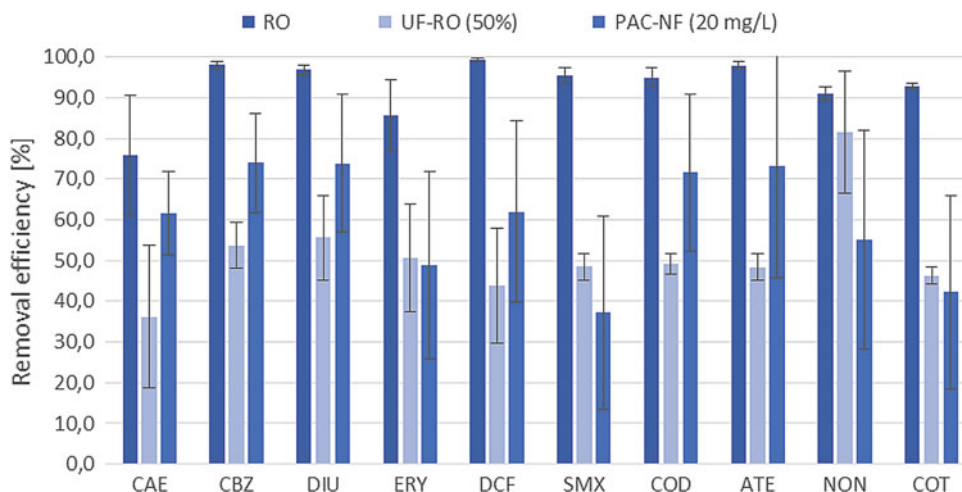
Table 1 Implementation costs of both advanced water reclamation schemes

Application (reuse)	Coastal areas (Saline intrusion barriers)	Inland areas (IPR—GWR or surface water augmentation)
Water quality limitations	Salinity removal-reduction	Nutrients removal
Advanced water reclamation scheme	UF + RO (50% blend)	PAC-NF (20 mg/L)
Average removal of recalcitrant OMP	40–50%	50–70%
Brine generation [m^3/d]	3750 (marine disposal)	4350 (return to headworks)
OPEX [€/m^3]	0.20	0.25
CAPEX [M€]	9	8
Carbon footprint [kg CO_2/m^3]	0.24	0.72

reclamation systems, both sized for a 15,000 m^3/d of capacity. Due to the high inlet pressure in RO membranes (10 bar approximately), energy demand of UF + RO (0.70 kWh/m^3) is twice that of PAC-NF (0.35 kWh/m^3). In terms of chemical consumption, due to the continuous PAC dosing, PAC-NF system is a 90% higher (191 Tn/year) than UF + RO (50%) (101 Tn/year). Operational costs of 0.20 and 0.25 €/m^3 were obtained, respectively, for UF + RO and PAC-NF systems. The higher cost of PAC-NF is mainly associated with the high cost of PAC, which in this study was considered 2 €/kg. Due to the lower water yield, PAC-NF generates a higher volume of brines; nevertheless, the conductivity of these brine allows to return it to headworks. On the contrary, for RO brines, it is necessary to manage it with the submarine emissary. CAPEX was also assessed resulting in 9 M€ for UF-RO plant (50% blend) and 8 M€ for PAC-NF plant. Finally, in terms of environmental impact, the use of PAC has a negative impact in the carbon footprint (0.72 kg CO_2/m^3), resulting to be around three times higher than in the UF + RO system (0.24 kg CO_2/m^3).

4 Conclusion

From a technical point of view, OMP removal efficiencies for the different treatment schemes showed that the hybrid system PAC-NF allows average removal efficiencies between 50 and 70% regarding the inlet (MBR) concentration while efficiencies between 40 and 50% were obtained from UF-RO (50% blend) system.

As it is shown in Table 1, two applications for the implementation of these two treatment schemes were proposed. PAC-NF could be an interesting alternative to UF-RO in IPR in inland zones (in case salinity removal is not required, and there is a proper nitrification-denitrification upstream). In addition, despite a higher OPEX (0.25 €/m^3) and carbon footprint associated, the possibility of returning brines generated headworks is associated with economic savings in brine management and can be also perceived an environmental driver. On the other hand, in coastal areas, were brine management is not an issue since marine disposal is the main alternative, UF-RO (50% blend) seems to be more suitable due to its lower OPEX (0.2 €/m^3). Additionally, in coastal areas with groundwater overexploitation, saline intrusion in aquifers is a recurrent problem and the deep well injection of purified reclaimed water with salinity reduction (obtained through RO membranes) is used as artificial barrier in order to preserve groundwater reservoirs from salinization.

References

Alvarino, T., Suarez, S., Lema, J., & Omil, F. (2018). Understanding the sorption and biotransformation of organic micropollutants in innovative biological wastewater treatment technologies. *Science of the Total Environment, 615,* 297–306. https://doi.org/10.1016/j.scitotenv.2017.09.278.

Cabeza, Y., Candela, L., Ronen, D., & Teijon, G. (2012). Monitoring the occurrence of emerging contaminants in treated wastewater and groundwater between 2008 and 2010. The Baix Llobregat (Barcelona, Spain). *Journal of Hazardous Materials, 239–240,* 32–39. https://doi.org/10.1016/j.jhazmat.2012.07.032.

Verliefde, A. (2008). Rejection of organic micropollutants by high pressure membranes (NF/RO). TU Delft.

Environmental or Economic Considerations in Photo-Fenton Processes: What Choice Has the Most Notable Benefits for Large-Scale Applications?

D. Prato Garcia and A. Robayo Avendaño

Abstract

A marginal increase in operational costs led to a 45% reduction in carbon footprint. Life cycle assessment and multivariable analysis allow identifying an economic and environmentally friendly operational condition. Photo-Fenton in raceway reactors increases biodegradability of recalcitrant effluents at a low cost (0.33 US$/m^3).

1 Introduction

Photo-Fenton processes in tubular reactors (compound parabolic concentrators, CPC; parabolic through concentrators, PTC) have been successfully used during decades for the treatment of recalcitrant compounds and water purification (Belalcázar-Saldarriaga et al. 2018). Technical (pressure drops, dirt on the reflecting surfaces, and fragility of glass tubes) and environmental issues (electricity and reagent consumption) appear to be most notable restrictions for their introduction as an economic and sustainable alternative for large-scale applications (Belalcázar-Saldarriaga et al. 2018; Chavaco et al. 2017). On the other hand, photo-Fenton processes in open pond reactors (raceway, flat plate, and solar lagoons) have a greater operational flexibility, lower operating costs, and a reduced environmental footprint due to their lower energetic consumption and the nature of the materials used for their construction (Belalcázar-Saldarriaga et al. 2018; Chavaco et al. 2017).

Climate change and water scarcity are attracting ever more attention of the scientific community; indeed, environmental aspects of activities, products, and processes draw the attention of stakeholders significantly. This situation has also had a remarkable impact during the conception of new treatment processes as well as in the operation of existing ones. Technical and economic considerations are still prerequisite to ensure the technologies robustness and cost-effectiveness in large-scale applications; however, social pressure has led to an increasingly stringent environmental legislation and the use of more environmentally friendly processes (Klöpffer and Grahl 2014). Therefore, in this study, we evaluated the impact of economic and operational decisions on the environmental footprint and the economic performance of a photo-Fenton process carried out in a raceway-type reactor.

2 Materials and Methods

Acid orange 52 (AO52, $C_{14}H_{14}N_3NaO_3S$, purity = 85%), reactive orange 16 (RO16, $C_{20}H_{17}N_3Na_2O_{11}S_0$, purity = 70%), iron (II) sulfate heptahydrate (FeSO$_4$•7H$_2$O, 99%), hydrogen peroxide (H$_2$O$_2$, 30%). Assays were performed in a raceway-type reactor (total volume, T_V = 5000 cm^3, surface area to reactor volume = 0.33 cm^2/cm^3). A detailed description of the reactor can be found in (Chavaco et al. 2017). Biochemical oxygen demand (BOD$_5$), chemical oxygen demand (COD), and spectrophotometric analyses were performed as indicated in (Chavaco et al. 2017). We used a Box–Behnken experimental design (BBD) to determine the effect of concentrations of dye mixture (X_1), H$_2$O$_2$ (X_2), and Fe^{2+} (X_3) on the percentage of decolorization (PD). The PD was assessed on the basis of absorbance changes at 473 nm that is the wavelength of maximum absorbance for a mixture containing the same proportion of AO52 and RO16

D. Prato Garcia (✉)
Facultad de Ingeniería y Administración, Universidad Nacional de Colombia, Carrera 32 no. 12-00, Sede Palmira, Chapinero, Vía Candelaria, Palmira, Valle del Cauca, Colombia
e-mail: dpratog@unal.edu.co

A. Robayo Avendaño
Facultad de Ingeniería, Universidad Santiago de Cali, Calle 5 no. 62-00, Campus Pampalinda, Cali, Valle del Cauca, Colombia

(from now on dye mixture). This study considered the following phases described in the ISO 14040 standard: (1) goal and scope, (2) inventory analysis, (3) impact assessment, and (4) interpretation (Chavaco et al. 2017; Klöpffer and Grahl 2014; Guinée et al. 2002). Information regarding the unitary processes considered in this study was obtained from the most recent Ecoinvent v 3.4 database. Environmental performance of the process was evaluated via a life cycle assessment (LCA) in the software openLCA 1.7 (GreenDelta$^©$).

3 Results and Discussion

Before starting the formal study of the process, it is worth mentioning that the statistical study pointed out that r^2 (0.988) is in reasonable agreement with the adjusted r^2 (0.9733); in addition, the model F-value of 65.74 implies the model is significant, and there is only a 0.01% chance that a F-value this large could occur due to noise. Values obtained for standard deviation (S.D. = 1.62) and the variation coefficient (V.C. = 1.79%) confirm the proposed model's suitability to represent the PD. The ANOVA suggests that dye and hydrogen peroxide concentration have a significant impact ($p < 0.0001$) on PD. In this study, we used the concept of desirability function (D) to identify the operational conditions that allow meeting the objective established for the process (PD = 97%), minimizing the consumption of reagents.

The optimization module of Design-Expert$^®$ suggested that the following best operational conditions, BOP (concentration of: dye mixture = 54.7 mg/L, H_2O_2 = 47 mg/L, and Fe^{2+} = 10 mg/L) allowed fulfilling the objective of

treatment and generating a biodegradable effluent (BOD_5/COD = 0.45). The BOP led to an average annual cost of 0.33 (US\$/m^3), which can be considered satisfactory taking into account the cost reported in the specialized literature (US\$2/m^3 to US\$10/m^3) for the treatment of synthetic solutions of azo dyes (Belalcázar-Saldarriaga et al. 2018; Chavaco et al. 2017; Klöpffer and Grahl 2014). However, the multivariable analysis pointed out that five operational (Fig. 1) conditions also fulfill the treatment goal but at a higher operating cost.

As shown in Fig. 1, these conditions led to quite different economic and environmental performance for the process. For example, run 3 allowed the decolorization and biocompatibilization of the wastewater in 20 min. Compared to the suggested BOP, run 3 allowed reducing treatment time by 67% (from 60 to 20 min), which would lead to a reduction in carbon footprint. However, the LCA reveals that energy consumption does not play an important role in the carbon footprint of the process. In this study, the carbon footprint is influenced by the consumption of H_2O_2 (c.a. 20%) and the reagents used for pH adjustment (c.a. 50%). BOP and runs 3, 5, and 7 drive to very low operating costs (US\$0.33/m^3 to US\$0.35/m^3); however, in these operating conditions, the lower dye-to-reagents ratio promotes the occurrence of undesirable reactions that reduce the oxidant power of the medium. This behavior is common in photo-Fenton processes and is attributed to the temporal abundance of iron and peroxide required for the generation of HO$^•$ radicals as well as the reactivity of this radical (10^9–10^{10} M/s) (Belalcázar-Saldarriaga et al. 2018; Chavaco et al. 2017; Klöpffer and Grahl 2014). The treatment of concentrated effluents (100 mg/L, see experimental runs 10 and 12) allows making a better use of reagents (mainly H_2O_2),

Fig. 1 Economic and environmental performance of the studied process
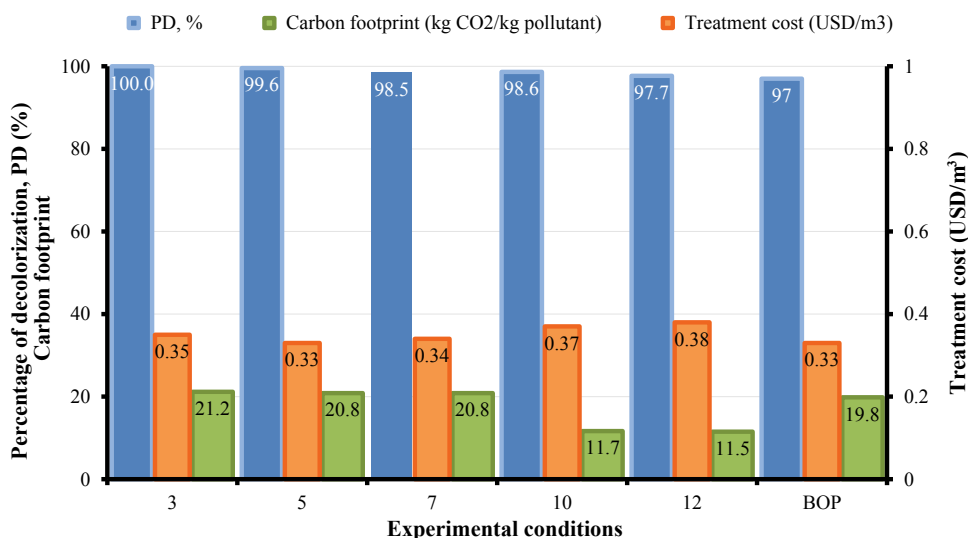
reducing up to 45% the carbon footprint of the process. In addition, these operational conditions increase treatment cost in less than five cents (from 0.33 to 0.38 US$/m^3).

4 Conclusion

The LCA reveals that energy consumption does not play an important role in the carbon footprint of the process. Furthermore, pH adjustment and oxidant consumption (to a lesser extent) emerge as the most aggressive activities of the process. In this study, the use of multivariable analysis and life cycle assessment reveals that a process optimization strategy based on cost reduction led to an increase in the carbon footprint. From a purely economic point of view, our study reveals that even non-optimal operational conditions can lead to a substantial reduction in the carbon footprint of

the process (45%) without generating an appreciable increase (15%) in treatment cost.

References

Belalcázar-Saldarriaga, A., Prato-Garcia, D., & Vasquez-Medrano, R. C. (2018). Photo-Fenton processes in raceway reactors: Technical, economic, and environmental implications during treatment of colored wastewaters. *Journal of Cleaner Production, 182,* 818–829.

Chavaco, L. C., Arcos, C. A., & Prato-Garcia, D. (2017). Decolorization of reactive dyes in solar pond reactors: Perspectives and challenges for the textile industry. *Journal of Environmental Management, 198,* 203–212.

Guinée, J., Gorrée, M., & Heijungs, R. et al. (2002). *Handbook on life cycle assessment operational guide to the ISO Standards*. The Netherlands.

Klöpffer, W., & Grahl, B. (2014). *Life cycle assessment (LCA). A guide to best practice*. Weinheim: Wiley-VCH.

Optimization of Energy Consumption in Activated Sludge Process Using Deep Learning Selective Modeling

Rafik Oulebsir, Abdelouahab Lefkir, Abdelmalek Bermad, and Abdelhamid Safri

Abstract

Optimization of Energy consumption in activated sludge plants. Selection approach of the best observation that will be used in a supervised deep learning model. The model was applied to learning and validation period in order to show its performance.

1 Introduction

Reducing energy consumption has become a global concern, and the need for technology and tools for modeling, management, and optimization is growing in the field of wastewater treatment; 60–70% of the total energy consumption of the wastewater treatment plant (WWTP) is used for the aeration tanks in the activated sludge process (ASP) (Hreiz 2015). Several optimization methods use the activated sludge model (ASM) which is classified in the white-box plant models coupled with a settling tank (see Maachou et al. 2017; Chachuat et al. 2005; Henze et al. 2000); but, because of their complex calibration process, this model cannot be applied on a large scale in different wastewater treatment plants (Gillot and Choubert 2010),

and the number of the parameters to determine is disadvantageous, especially in the Algerian context. Artificial neural network (ANN) is normally very effective to capture the nonlinear relationships that exist between variables in complex systems and can also be applied in situations where insufficient process knowledge is available to construct a white-box model of the system (Melcer et al. 2003; Gernaey 2004). Considerable progress has been made in ANN technology, using now deep learning techniques to increase their performances(Deep Learning A Practitioner's Approach 2017).

2 Materials and Methods

In order to create a model that can determine optimal energy consumption for a degree of pollution of the incoming wastewater, we need to select data that can be used to train this model. We used a simple method that consists of first select the data that satisfy the purification efficiency for which the WWTP was designed with a percentage of error noted Estandards, and second to select the data that gave a minimal energy consumption for criteria of selection(Lefkir et al. 2016). We used three criteria of selection that are: degree of pollution abatement, pollution index, and Brown's water quality index (Water Quality Indices 2012).

The results of the selection will be used to train an artificial neural network to predict the optimal energy consumption of the ASP, due to the complexity of the process we used a deep neural network (DNN). Deep learning is making major advances in solving problems that have resisted the best attempts of the artificial intelligence community for many years. It has turned out to be very good at discovering intricate structures in high-dimensional data and is therefore applicable to many domains of science, business, and government (LeCun 2015).

R. Oulebsir · A. Safri
Laboratoire d'environnement Géotechnique et Hydraulique, USTHB, Algiers, Algeria

A. Lefkir (✉)
LTPiPE Laboratory, ENSTP, BP 32, Vieux Kouba City, Algiers, Algeria
e-mail: a.lefkir@enstp.edu.dz

A. Bermad
Laboratoire Matériaux de Génie Civil et Environnement, ENP, Algiers, Algeria

Table 1 Data selection and number of data used for training and testing the deep neural network

Number of data for each period	Degree of pollution abatement	Pollution indices	Water quality indices
Number of data selected	90	62	51
Number of data used for training	72	49	40
Number of data used for testing	18	13	11
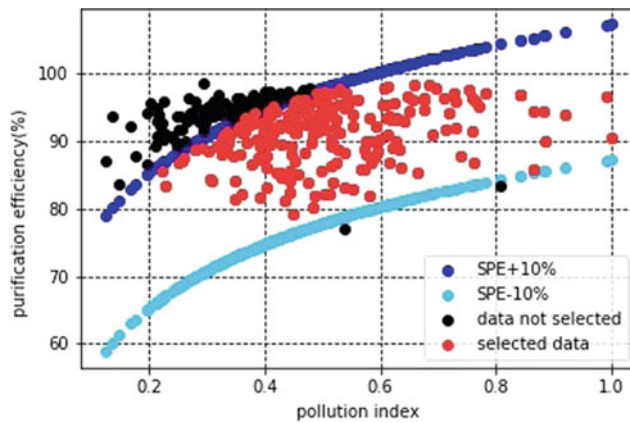
Fig. 1 First selection of the data that satisfy the purification efficiency

3 Results and Discussion

The results of the first selection of optimal data for the training of the optimal DNN are presented in Fig. 2. The percentage of data that pass the first selection is 69, 0.2% of all data represent where the purification efficiency is insufficient, and 30.4% represent the percentage of data where energy consumption needed for the aerobic treatment is exceeded and indicates a waste of energy.

For the second selection, the results are different according to the criteria used to judge the efficiency of the treatment (see Table 1), but the number of data selected for the modeling is small due to the number of database used.

We used four variables as inputs for the deep neural network that are: temperature of the incoming wastewater, recirculated sludge flow, the incoming flow of wastewater, and the criteria of selection that is one of the criteria used for the second selection, the output is the energy consumption. For every selection criteria, a DNN was trained (Figs. 1 and 2).

The DNN trained using degree of pollution abatement has the best performances; this is due to the fact that the criteria measure the degree of pollution using the mass of each pollutant, unlike the other pollution criteria that using the concentration of each pollutant, which can give a false value of energy needed to treat the wastewater.

The DNN trained was applied to the data selected in the first selection but was not selected in the second, in order to determine the estimated optimal energy. The model is not powerful for all the data, and this is due to number of small number of data used for training. The savings made are of 10% of the total energy consumption of the experiences used (Fig. 3).

4 Conclusion

Many standard measurements are usually used for the control of the process and the quality of incoming and outcome wastewater; this measurement represents information that can be used for the optimization of the process. A powerful model can be used to combine with a selection of the optimal experiences of the WWTP, to create a model for the optimization of the ASP, and the selection can be based on different criteria according to the desired objective of the manager.

In this paper, we used a simple method of selection to determine the best experiences based on pollution criteria combined with a DNN, but due to the small number of data used for training, the DNN does not learn efficiently, but the results are optimistic. The DNN trained makes a gain of 10% of the total energy used in 144 experiences.
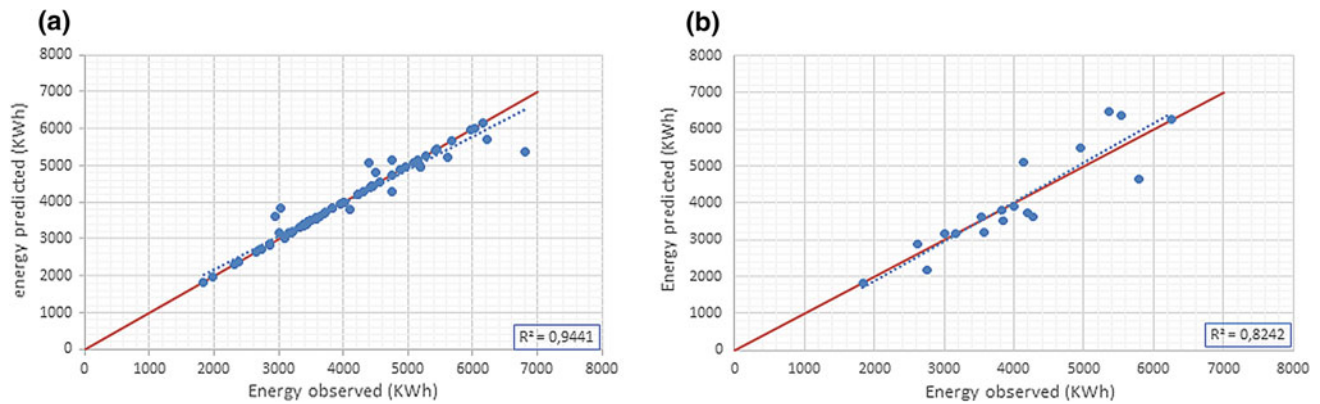
Fig. 2 Deep neural network modeling results using the degree of pollution abatement **a** training **b** testing period
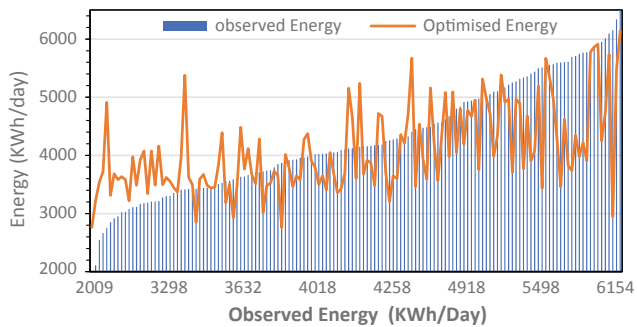
Fig. 3 Savings made by using the deep neural network model on non-selected data

The use of the model to determine efficient energy consumption and using the results to retrain the model can lead the model to predict the optimal energy consumption.

References

Lefkir, A., Maachou, R., Bermad, A., & Khouider, A. (2016). Factorization of physicochemical parameters of activated sludge process using the principal component analysis. *Desalination and Water Treatment.*

Henze, M., Gujer, W., Mino, T., & van Loosdrecht, M.C. (2000). *Activated Sludge Models ASM1, ASM2, ASM2d and ASM3.* IWA Publishing.

Chachuat, B., Roche, N., & Latifi, M. A. (2005). Long-term optimal aeration strategies for small-size alternating activated sludge treatment plants. *Chemical Engineering and processing: Process intensification.*

Water Quality Indices (2012). Elsevier.

Gernaey K.V., van Loosdrecht Mark C.M., Henze Mogens, Lind Morten, & Jørgensen Sten, B. (2004). Activated sludge wastewater treatment plant modelling and simulation: State of the art. *Environmental Modelling & Software.*

Melcer, H., Dold, P.L., Jones, R.M., Bye, C.M., Takacs, I., Stensel, H. D., Wilson, A.W., Sun, P., & Bury, S. (2003). Methods for wastewater characterization in activated sludge modeling. *Water Environment Research Foundation (WERF).*

Hreiz, R., Latifi, M.A., & Roche, N. (2015). Optimal design and operation of activated sludge processes: State-of-the-art. *The Chemical Engineering Journal.*

Deep Learning A Practitioner's Approach (2017). O'Reilly Media, Inc.

Maachou, R., Lefkir, A., Bermad, A., Djaoui, T., & Khouider, A. (2017). Statistical analysis of pollution parameters in acti- vated sludge process. *Desalination and Water Treatment.*

Gillot, S., & Choubert, J.M. (2010). Biodegradable organic matter in domestic wastewaters: Comparison of selected fractionation techniques. *Water Science and Technology.*

LeCun, Y., Bengio, Y., & Hinton, G. (2015). Deep learning, nature.

Electrochemical Sensors for Emerging Contaminants: Diclofenac Preconcentration and Detection on Paper-Based Electrodes

E. Costa-Rama, Henri P. A. Nouws, Cristina Delerue-Matos, M. C. Blanco-López, and M. T. Fernández-Abedul

Abstract

A paper-based electrochemical sensor has been developed as a green tool for analysis of diclofenac. The electrochemical behaviour of diclofenac has been studied on carbon-paper-based electrodes. A miniaturized device combining paper electrodes and reusable connections allows to perform decentralized analysis. The employment of a paper-based electrode allows simple on-site preconcentration of the analyte improving the sensitivity of the methodology.

Keywords

Emerging contaminants • Diclofenac •
Electroanalysis • Paper-based electrodes •
Green technologies

1 Introduction

Nowadays, the presence of emerging contaminants is a worldwide problem of increasing environmental concern. The term emerging contaminants (ECs) is referred to a heterogeneous group of substances, such as personal care products, pharmaceuticals and flame retardants, characterized by a widespread distribution due to their massive everyday use and persistence in the environment (Albero et al. 2015). Additionally, current wastewater treatment plants are not specifically designed for eliminating these contaminants and, in consequence, these may reach environmental waters and so, potentially, drinking waters. Hence, it is mandatory to develop analytical devices for ECs determination not only sensitive enough for their application in environmental waters but also miniaturized, simple, portable and mainly sustainable.

Diclofenac (Fig. 1a) is a non-steroidal anti-inflammatory drug widely prescribed as analgesic and in the treatment of rheumatic complaints and acute joint inflammation. Because of its broad consumption, diclofenac residues are detected in surface waters (Paíga et al. 2016). Thus, in this work, a paper-based analytical device, that combines a paper-based working electrode with pseudoreference and counter electrodes based on metallic wires, was developed for the electrochemical detection of diclofenac. The sustainability of the device is noticeable since electrochemical techniques are *green* in essence because (Kreysa et al. 2014): (i) they employ the electron as a cheap and clean reagent, (ii) most of the reactions can be performed at room temperature, avoiding energy consumption and costs associated to temperature control, (iii) they involve safe operations in low or null volatility reaction media reducing accidental solvent releases to atmosphere and (iv) they are cost-effective since the required equipment and operations are usually simpler and cheaper than other techniques. Moreover, the employment of paper as substrate allows to reduce costs of fabrication and transportation since it is a widely available, light and flexible material, easy to transport and store (Martinez et al. 2010). Its porosity and high surface area, as well as its easy modification and printing, make it a versatile material, very suitable for combination with electrochemical techniques (Mettakoonpitak et al. 2016; Glavan et al. 2014; Amor-Gutiérrez et al. 2017; Núñez-Bajo et al. 2017).

E. Costa-Rama · H. P. A. Nouws · C. Delerue-Matos
REQUIMTE/LAQV, Instituto Superior de Engenharia do Porto, Politécnico do Porto, Rua Dr. António Bernardino de Almeida, 431, 4200-072 Porto, Portugal
e-mail: estefaniarama@graq.isep.ipp.pt

H. P. A. Nouws
e-mail: han@isep.ipp.pt

C. Delerue-Matos
e-mail: cmm@isep.ipp.pt

M. C. Blanco-López · M. T. Fernández-Abedul (✉)
Departamento de Química Física y Analítica, Facultad de Química, Universidad de Oviedo, 33006 Oviedo, Spain
e-mail: mtfernandeza@uniovi.es

M. C. Blanco-López
e-mail: cblanco@uniovi.es
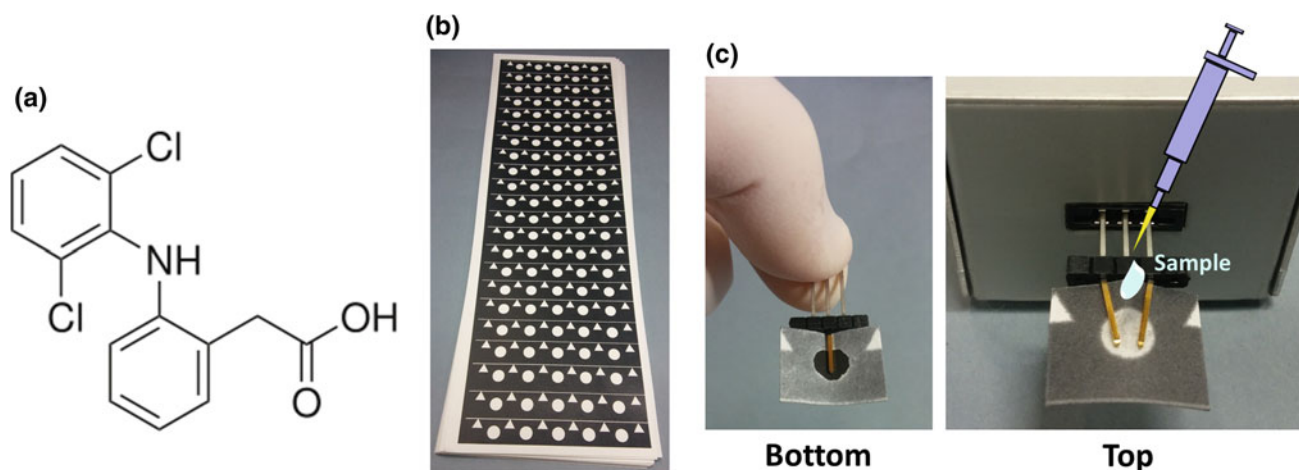
Fig. 1 **a** Diclofenac structure. **b** Photograph of several sheets of paper after wax printing. **c** Photograph of the bottom and top views of the paper-based electrochemical cell. In the right photograph (top side), the paper-based platform is ready to use after being directly inserted in a commercial connector. The gold-plated header connector provides the RE and CE as well as the connection for the WE

In addition, the small size of the developed device together with the availability of commercial portable potentiostats, make possible to perform decentralized analysis (out of laboratory). This is very interesting for environmental pollutants monitoring (especially in developing countries and remote locations) since it allows completing the analysis on-site and taking decisions in real time.

2 Materials and Methods

The main reagents and materials needed were: diclofenac disodium salt (DCF), N,N-dimethylformamide (DMF), carbon paste, Whatman™ paper grade 1, gold-plated connector headers and an edge connector. Working solutions of diclofenac were prepared in purified water or in 0.1 M phosphate buffer (PB) solution pH 7.0. The carbon ink was prepared dispersing carbon paste in DMF (40%, w/w) by sonication (1 h).

The instrument employed was an Autolab potentiostat controlled by Nova 2.1.2 software. A wax printer ColorQube 8570 (XEROX) was used to wax-print the paper (Fig. 1b).

The electrochemical cell constructed combined a paper-based working electrode (WE) with pseudoreference and counter electrodes (RE and CE) based on metallic wires (provided by the gold-plated connector header) (Amor-Gutiérrez et al. 2017) (see Fig. 1c). The WE was constructed depositing a 2-μL drop of the carbon ink in a wax-defined paper area and leaving to dry at room temperature. To perform the measurements, a 10-μL drop of working solution was deposited on the topside of the electrochemical cell covering the three electrodes. The paper-based WE is single use while the gold-plated connector header can be reused for several measurements after cleaning it with water in between.

3 Results and Discussion

First, the electrochemical behaviour of DCF on carbon paper-based electrodes was studied performing cyclic voltammetry (CV). For a DCF concentration of 100 μM, an oxidation peak appeared at +0.48 V with a peak current intensity of 2.2 μA (Fig. 2a) and no reduction peak was present. Hence, the current intensity of this anodic peak was chosen as analytical signal. Differential pulse voltammetry (DPV) was also tested in order to increase the sensitivity. When DPV was performed (employing the same parameters as in a previous work (Fernández-Llano et al. 2007)) in a 100-μM DCF solution, an oxidation peak with a peak current intensity of 3.5 μA was observed at +0.45 V (Fig. 2b). Therefore, employing DPV a better-defined and higher peak was obtained.

In order to increase the analytical signal, even more, a different strategy was chosen. We took advantage of the porous nature of paper to preconcentrate DCF in the paper-based WE. Then, a 40-μL drop of a 100-μM DCF solution in water was deposited on the topside of the WE and was left to dry at room temperature. In a second step, CV was performed in 10 μL of 0.1 M PB pH 7.0 obtaining the CV of Fig. 2c (continuous line). Two anodic peaks, at +0.44 V (peak I) and +0.88 V (peak II) with current intensities of 58.8 and 28.0 μA, respectively, and one cathodic peak (peak III) at +0.18 V with a current intensity of 2.0 μA were obtained. The presence of those peaks is in agreement with previous works (Blanco-López et al. 2004). The effect
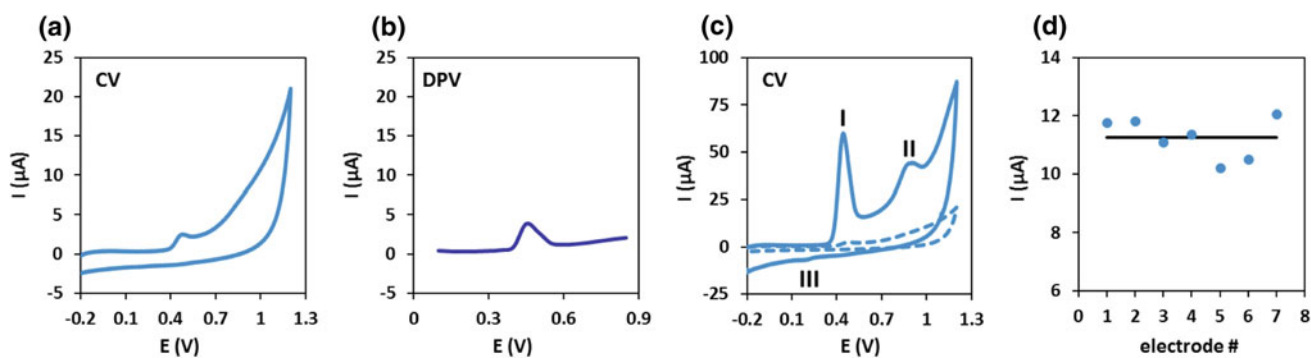
Fig. 2 Cyclic (**a**) and differential pulse (**b**) voltammograms performed in 10 μL of 100 μM DCF in 0.1 M PB pH 7.0. **c** Comparison between cyclic voltammograms performed in 10 μL of a 100 μM DCF solution in 0.1 M PB pH 7.0 (dashed line) and in 10 μL of 0.1 M PB pH 7.0 after preconcentration of 40 μL of 100 μM DCF in water (continuous line). **d** Comparison of peak current intensities of the first anodic peak obtained employing seven different paper-based WE when CVs are recorded in 10 μL of 0.1 M PB pH 7.0 after preconcentration of 40 μL of 20 μM DCF in water (the black line indicates the mean value)

of preconcentration is clear in Fig. 2c, where voltammograms recorded with and without preconcentration are compared. The current intensity of the first anodic peak (peak I) is more than 24 times higher (58.8 vs. 2.2 μA) after preconcentration. Therefore, the porous nature of the paper-based electrode allowed on-site preconcentration of DCF and, consequently, a notorious improvement of the sensitivity. Moreover, the paper-based device offers a good reproducibility as shown in Fig. 2d. Seven different paper-based WEs were tested (employing the same RE and CE) preconcentrating 40 μL of 20 μM DCF. A peak current intensity of 11.3 ± 0.7 μA (RSD < 6.3%) was obtained.

Optimizing key parameters such as the volume of the DCF solution deposited and temperature of drying, low limits of detection for DCF could be achieved. Moreover, this simple preconcentration methodology allows to perform the measurement in a different medium from that of the sample, optimum for the detection.

4 Conclusion

Electrochemical paper-based platforms are attractive tools for the evaluation of water quality due to the combination of the great advantages of electrochemical techniques together with the friendly inherent characteristics of paper. Thus, small-size and portable devices can be developed for water analysis with good analytical characteristics achieved by simple on-site preconcentration without the need of external preconcentration systems that increase not only the complexity of the determination but also the cost and the waste generated.

References

Albero, B., Sánchez-Brunete, C., García-Valcárcel, A. I., Pérez, R. A., & Tadeo, J. L. (2015). *TrAC - Trends in Analytical Chemistry, 71*, 110–118.

Amor-Gutiérrez, O., Costa Rama, E., Costa-García, A., & Fernández-Abedul, M. T. (2017). *Biosensors Bioelectronics, 93*, 40–45.

Blanco-López, M. C., Fernández-Llano, L., Lobo-Castañón, M. J., Miranda-Ordieres, A. J., & Tuñón-Blanco, P. (2004). *Analytical Letters, 37*, 915–927.

Fernández-Llano, L., Blanco-López, M. C., Lobo-Castañón, M. J., Miranda-Ordieres, A. J., & Tuñón-Blanco, P. (2007). *Electroanalysis, 19*, 1555–1561.

Glavan, A. C., Christodouleas, D. C., Mosadegh, B., Yu, H. D., Smith, B. S., Lessing, J., et al. (2014). *Analytical Chemistry, 86*, 11999–12007.

Kreysa, G., Ota, K., & Savinell, R. F. (Eds.). (2014). *Encyclopedia of applied electrochemistry*. New York: Springer.

Martinez, A. W., Phillips, S. T., Whitesides, G. M., & Carrilho, E. (2010). *Analytical Chemistry, 82*, 3–10.

Mettakoonpitak, J., Boehle, K., Nantaphol, S., Teengam, P., Adkins, J. A., Srisa-Art, M., et al. (2016). *Electroanalysis, 28*, 1420–1436.

Núñez-Bajo, E., Blanco-López, M. C., Costa-García, A., & Fernández-Abedul, M. T. (2017). *Biosensors Bioelectronics, 91*, 824–832.

Paíga, P., Santos, L. H. M. L. M., Ramos, S., Jorge, S., Silva, J. G., & Delerue-Matos, C. (2016). *Science of the Total Environment, 573*, 164–177.

Optimization of the Wastewater Treatment Plant: From Energy Saving to Environmental Impact Mitigation

D. Panepinto, V. Riggio, Barbara Ruffino, G. Campo, A. Cerutti,
S. Borzooei, M. Ravina, I. Bianco, and Maria Chiara Zanetti

Abstract

This paper outlines a multi-objective, integrated approach to analyse various possibilities for increasing energy efficiency of the largest Italian wastewater treatment plant (WWTP) at Castiglione Torinese. In this approach, wastewater and sludge treatment units are thoroughly investigated to find the potential ways for improving the energy efficiency of the system. Firstly, a multi-step simulation-based methodology is proposed to make a full link between treatment processes and the energy demand and production. Further, a scenario-based optimization approach is proposed to find the non-dominated and optimized performance of the WWTP. The results prove a potential to save up to 5000 MWh of the annual energy consumption of the plant, in addition to improve the effluent quality through operational changes only. Even for what concerns the sludge line a model was proposed for the optimization of the energy recovery from the processes that in a WWTP are devoted to the management of sewage sludge. The obtained results show that the introduction of an advanced thickening stage and sludge pre-treatment, together with the optimized production and use of biomethane, would have a positive impact on the energy and greenhouse gas balance of the plant. The preliminary tests were conducted with microalgae, under different light intensities (3 and 5 fluorescent lamps equal to 44 and 76 μmol/m^2/s), that had shown a total CO_2 reduction of 80 and 70%, respectively.

D. Panepinto (✉) · V. Riggio · B. Ruffino · G. Campo · A. Cerutti · S. Borzooei · M. Ravina · I. Bianco · M. C. Zanetti
DIATI (Department of Engineering for Environmental, Land and Infrastructures), Politecnico Di Torino, Corso Duca Degli Abruzzi 24, Turin, Italy
e-mail: deborah.panepinto@polito.it

1 Introduction

Wastewater treatment (WWT), removing biological and chemical pollutants from water, assumed a major role to protect the environment and public health. During the past years, WWT plants have been developing the adopted technologies to increase the reclamation efficiency to comply with the discharge limits imposed by the law, which become year by year more restrictive.

The main concern of the WWT industry has always been to meet water-quality standards in order to keep public trust (Focus on Energy 2006). Thus, WWT plants are usually designed to meet certain effluent requirements, without any major energy considerations (Ahmetović et al. 2014). As a result, WWT plants were hardly ever designed with energy efficiency in mind (Panepinto et al. 2016). However, this attitude was definitely changing, in recent years, in the general framework of the achievement of 20-20-20 goals defined for Climate and Energy by Directive 2009/28/EU.

This paper presents various attempts made for process optimization of the WWTP to increase the plant energy efficiency resulting in the economic savings and simultaneous improvement in pollutant removal and environmental impact mitigation.

The introduction of mathematical models in the field of the wastewater treatment engineering could supply important evaluating and decision-making tools for engineers to move forward toward the optimization of treatment plants. The application of mathematical models for mimicking the biological processes, hydraulic and settling phenomena's and energy consumption and production of different treatment units in WWTP were undertaken. Based on simulation results, optimum operational parameters were proposed to managing company (Borzooei et al. 2016). The importance of modelling project in performance investigation of the treatment units as a troubleshooting tool was also highlighted (Borzooei et al. 2017). Further several practical

scenarios were evaluated for the plant under various operational modes and extreme weather conditions which will be used as the practical tool to increase the preparedness of the managing company in these challenging conditions.

In the last years, anaerobic digestion has become widespread throughout Europe, since anaerobic digestion provides the possibility to recover energy from the produced biogas starting from different natural materials. Among the factor that is influencing on the mass transfer in each biological step of anaerobic digestion, both the composition and the quality of the substrate play a fundamental role.

The production of methane by anaerobic digestion of sludges of a wastewater treatment plant is maximum when into the bio-digesters the optimal conditions for the activity of microorganisms operating the hydrolysis and the transformation of its products in methane (CH_4) are realized (Panepinto and Genon 2016).

In order to increase the production of biogas and so to improve the electric energy yield of the process, the use of pretreatment was evaluated. There are different types of pretreatment and in this study, in particular, the thermal pretreatment (at low temperature, 100 °C), the chemical pretreatment with use of NaOH and $Ca(OH)_2$ and the thermo-alkaline pretreatment with use of NaOH (at low temperature) were analysed. Intermediate pretreatments, i.e. after a first AD stage, were analysed too (Campo et al. 2018).

Subsequently, two possibilities for the use of produced biogas will be evaluated: the vaporization in internal combustion engine in order to produce electric and thermal energy or the upgrading of biogas-to-biomethane (analysing the most frequently used technologies such as pressurized water scrubbing—PWS-, pressure swing absorption—PSA-, chemical absorption with amine solutions—MEA-, membrane permeation—MB- and cryogenic separation—CRY-) and subsequent injection to the gas grid or use in transports. In order to obtain the biomethane from the biogas, an innovative technology will be also analysed: the use of microalgae as biofilter for CO_2. In fact, these organisms can be taken into account for trapping CO_2 coming from exhaust gases, as they require carbon dioxide to breathe. As a second result, microalgae can be used for the production of bioproducts.

The increasing interest in the production and use of biogas and biomethane by anaerobic digestion plants necessitates developing a plausible prediction model aiming to determinate biogas and biomethane flows. Understanding the amount of material and energy flows necessary in input and produced as output is important in the economic-environmental feasibility study of biogas/biomethane production plant during its preliminary assessment (e.g. to fix the incentive scheme to apply).

In this work, a computational model (called $MCBioCH_4$) created at the DIATI Department is used. The model focuses on triple targets. The first one is to obtain information about the productivity of biogas/biomethane plants regarding achievable gas flow rates. The second one consists to acquire the plant energy expenditure and subsequently, the economically exploitable energy flows share (electrical and/or thermal energy produced or biomethane addressed being introduced into the national distribution grid of natural gas or as a fuel for mobility). The last one is to outline the whole environmental impact system starting from the substrates fed to the plant, up to reach the use of biogas/biomethane as alternative energy sources to fossil fuels.

From the point of view of the environmental impact reduction of a WWTP, another important topic is the characterization and reduction of odour emissions. Odour nuisances are connected to a large number of chemical substances, mostly detectable at low-concentration thresholds. Direct estimation of odour impacts through olfactometry is not always applicable, as this approach requires air sampling and a pool of trained panellists. Measuring the concentration of odorous substances (known as the indirect method) may be preferable in case a continuous monitoring of such impacts is needed. In our work, the design and development of an integrated odour emission monitoring system at the wastewater treatment plant (WWTP) using an indirect approach was also performed. The monitoring system is composed by a set of fixed measuring stations of the main chemical species responsible of odour impacts (VOC, H_2S and NH_3) and a modelling tool supporting the control and evaluation of odour nuisance episodes.

The implementation of continuous monitoring is going to provide important information on concentration distribution, detecting the occurrence of possible short-term emission peaks. A conversion method is then applied to calculate and classify total odour intensity.

The main challenge in the implementation of the modelling chain is that the sources of gaseous effluents are discontinuous and diffused (not punctual). In addition, emission intensity depends on the operating conditions of the plant and on the quality of treated wastewater, as well as on local weather conditions.

As a final result, the WWTP will be equipped with a complete and integrated monitoring system of odour emissions, able to detect possible episodes of odour nuisances and immediately warn WWTP operators and environmental control agencies.

Finally, the evaluation of the overall process environmental compatibility will be performed. The overall scenario will be analysed on global scale with the implementation of the life cycle assessment—LCA (Blengini et al. 2011).

The tool of LCA will be also used in order to rationalize technological choices and to define management strategies.

References

Focus on Energy. (2006). Water and wastewater energy best practice guidebook. Prepared for Wisconsin Department of Administration by the Focus on Energy Program. Madison, WI, US.

Ahmetović, E., Ibrić, N., & Kravanja, Z. (2014). Optimal design for heat-integrated water-using and wastewater treatment networks. *Applied Energy, 135,* 791–808.

Blengini, G. A., Brizio, E., Cibrario, M., & Genon, G. (2011). LCA of bioenergy chains in Piedmont (Italy): A case study to support public decision makers towards sustainability. *Resources, Conservation and Recycling, 57,* 36–47.

Borzooei, S., Zanetti, M., Genon, G., Ruffino, B., Godio, A., Campo, G., Panepinto, D. (2016). Modelling and calibration of the full scale WWTP with data scarcity.

Borzooei, S., Zanetti, M. C., Lorenzi, E., Scibilia, G. (2017). Performance investigation of the primary clarifier-case study of Castiglione Torinese. In *Frontiers International Conference on Wastewater Treatment and Modelling* (pp. 138–145). New York: Springer.

Campo, G., Carutti, A., Zanetti, M. C, Scibilia, G., Lorenzi, E., Ruffino, B. (2018). Enhancement of waste activated sludge (WAS) anaerobic digestion by means of pre- and intermediate treatments. Technical and economic analysis at a full-scale WWTP. *Journal of Environmental Management*, *216*, 372–382.

Panepinto, D., & Genon, G. (2016). Analysis of the extrusion as a pretreatment for the anaerobic digestion process. *Industrial Crops and Products, 83,* 206.

Panepinto, D., Fiore, S., Zappone, M., Meucci, L., Genon, G. (2016). Evaluation of the energy efficiency of a large wastewater treatment plant in Italy. *Applied Energy*, 404–411.

Influence of Microalgae–Bacteria Consortium on Pathogens Removal (*Pseudomonas aeruginosa* and *Escherichia coli*) from Domestic Wastewater

Graziele Ruas, Mayara Leite Serejo, Priscila Guenka Scarcelli, and Marc Árpád Boncz

Abstract

The potential of microalgae, bacteria, and a microalgae–bacteria consortium for the removal of *Pseudomonas aeruginosa* and *Escherichia coli* during domestic wastewater treatment was investigated; *P. aeruginosa* was removed mainly by microalgae action when in the microalgae–bacteria consortium; *E. coli* was removed by both microalgae and bacterial action; The effect of the LEDs was higher on *E. coli* than *P. aeruginosa* removal; The symbiotic system is more advantageous than just microalgae system, because the biomass productivity is higher and pathogens removal is almost similar for both systems.

1 Introduction

The development of economic and accessible technologies promoting wastewater disinfection more efficiently is a current concern, especially given the increasing threat of antibiotic-resistant bacteria (Rizzo et al. 2013; Bouki et al. 2013). A Microalgae–bacteria system is an eco-friendly and low-cost treatment alternative traditionally used in the removal of nutrients (Nurdogan and Oswald 1995) and recently as an alternative for disinfection, removal of emerging contaminants (pharmaceuticals and personal care products) and heavy metals (Ruas et al. 2017; Matamoros et al. 2015; Talaiekhozani and Rezania 2017), becoming a prominent alternative for post-treatment of domestic wastewater treated anaerobically. Recent researches showed that the microalgae–bacteria consortium can be applied in the disinfection of domestic wastewater; however, many questions regarding the removal mechanisms remained unanswered (Ruas et al. 2017). In this context, this work investigated if the microalgae–bacteria consortium (a mixture of mainly *Chlorella vulgaris* and activated sludge) is a good system for removal of *P. aeruginosa* and *E. coli* during domestic wastewater treatment.

2 Materials and Methods

Six conditions for pathogen removal were investigated in batch culture systems: using only microalgae, in dark (MD) and in light (ML) conditions; using a microalgae–bacteria consortium, in open (MBO) and closed (MBC) conditions; using only bacteria (B); and a blank, only wastewater without microorganisms (W). The microalgae–bacteria consortium used in the tests consisted of a culture mainly composed of *Chlorella vulgaris* and nitrifying–denitrifying aerobic activated sludge. All conditions, except MD, were performed at light intensity of $439 \pm 100 \ \mu mol \ m^{-2} \ s^{-1}$ with 16:8 h light/dark cycles (from white LEDs), temperature of 30 °C, and shaking at 200 rpm. *E. coli* was determined using the methodology Colilert® kit (IDEXX Laboratories, USA) and *P. aeruginosas* was determined using the membrane filtration method with M-PA Agar Base—M1121 (HIMEDIA, India).

G. Ruas (✉) · M. L. Serejo · P. G. Scarcelli · M. Á. Boncz
Faculty of Engineering, Architecture and Urbanism and Geography, Federal University of Mato Grosso do Sul,
Av. Costa e Silva, Campo Grande, Mato Grosso do Sul, Brazil
e-mail: graziele.ruas@gmail.com

M. L. Serejo
e-mail: mayara.serejo@ufms.br

P. G. Scarcelli
e-mail: priscilaguenkascarcelli@gmail.com

M. Á. Boncz
e-mail: marc.boncz@ufms.br
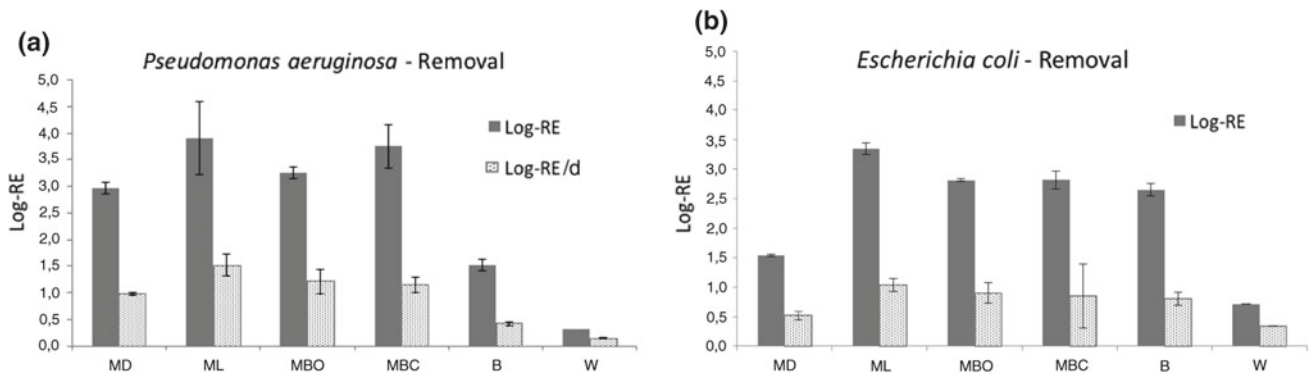
Fig. 1 Removal efficiency in logarithmic units after 3.3 days of the experiment (Log-RE) and daily removal (Log-RE/d) for *Pseudomonas aeruginosa* (**a**) and *Escherichia coli* (**b**) under different conditions tested

3 Results and Discussion

P. aeruginosa logarithmic removal efficiencies (P-Re), after 3.3 days of experiment, were 3.0 ± 0.1 (MD), 3.9 ± 0.7 (ML), 3.3 ± 0.1 (MBO), 3.8 ± 0.4 (MBC), 1.5 ± 0.1 (B) and 0.3 ± 0.0 (W), while the logarithm of the removal efficiencies of *E. coli* (E-Re) was 1.5 ± 0.1 (MD), 3.3 ± 0.1 (ML), 2.8 ± 0.2 (MBO), 2.8 ± 0.5 (MBC), 2.6 ± 0.1 (B), and 0.7 ± 0.0 (W) (Fig. 1). Using a Student's t-test, no difference was observed between ML, MBO, and MBC conditions for *P. aeruginosa,* and between MBO, MBC, and B conditions for *E. coli.* The higher P-Re obtained for the ML condition, when compared to the B condition, suggested that *P. aeruginosa* was removed mainly by microalgae when it was in consortium, while *E. coli,* on the other hand, was removed by both microalga and bacterial action. In addition, it can be observed that the effect of the LEDs was higher on *E. coli* than *P. aeruginosa* removal, comparing the MD and W condition (Fig. 2).

The microalgal productivity rate was 92 ± 0 (ML), 133 ± 8 (MBO), and 138 ± 10 (MBC). Therefore, the microalga–bacterial symbiosis is more suitable for the production of biomass. Considering that biomass productivity is also one of the objectives of effluent treatment in microalgae systems and that the *P. aeruginosa* and *E. coli* removal efficiencies were not statistically different in the systems (ML, MBC, and MBO), the symbiotic system is more advantageous than just the microalga.

4 Conclusion

The best performances for P-Re and E-Re were ML, MBO, and MBC, suggesting that these microorganisms can be removed quantitatively by both microalgae and microalgae–bacteria consortia. The higher P-Re obtained for the MD condition, when compared to the B condition, implied that *P. aeruginosa* was removed mainly by microalgae when it was in consortium, while *E. coli,* on the other hand, was removed by both microalga and bacterial action. The effect of the LEDs was higher on *E. coli* than *P. aeruginosa* removal. The symbiotic system is more advantageous than just microalgae system, because the biomass productivity is higher and the *P. aeruginosa* and *E. coli* removal is statistically similar for both systems.
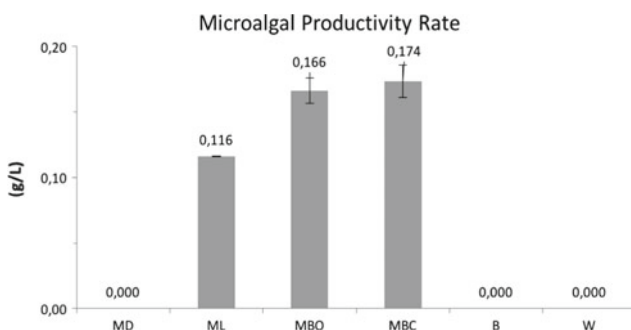
Fig. 2 Microalgal productivity rate after 3.3 days of the experiment under different conditions tested

References

Bouki, C., Venieri, D., & Diamadopoulos, E. (2013). Detection and fate of antibiotic resistant bacteria in wastewater treatment plants: a review. *Ecotoxicology and Environmental Safety, 91,* 1–9.

Matamoros, V., Gutiérrez, R., Ferrer, I., García, J., & Bayona, J. M. (2015). Capability of microalgae-based wastewater treatment systems to remove emerging organic contaminants: a pilot-scale study. *Journal of Hazardous Materials, 288,* 34–42.

Nurdogan, Y., & Oswald, W. J. (1995). Enhanced nutrient removal in high-rate ponds. *Water Science and Technology, 31*(12), 33–43.

Rizzo, L., Manaia, C., Merlin, C., Schwartz, T., Dagot, C., Ploy, M. C., et al. (2013). Urban wastewater treatment plants as hotspots for antibiotic resistant bacteria and genes spread into the environment: a review. *Science of the Total Environment, 447,* 345–360.

Ruas, G., Serejo, M. L., Paulo, P. L., & Boncz, M. Á. (2017) Evaluation of domestic wastewater treatment using microalgal-bacterial processes: effect of CO_2 addition on pathogen removal. Journal of Applied Phycology.

Talaiekhozani, A., & Rezania, S. (2017, September). Application of photosynthetic bacteria for removal of heavy metals, macro-pollutants and dye from wastewater: A review. Journal of Water Process Engineering **19**, 312–321.

Fuzzy-Assisted Ultrafiltration of Wastewater from Milk Industries

Francesco Villecco, Rita Patrizia Aquino, Vincenza Calabrò,
Maria Ida Corrente, Antonio Grasso, and Vincenzo Naddeo

Abstract

The whey is a by-product rich in organic substances; the system, as conceived, is self-learning.

Keywords

Fuzzy logic • Dairy farm • Ultrafiltration •
Wastewater treatment

1 Introduction

The dairy sector is one of the driving forces of the Italian food. In 2015, the Italian dairy farms were characterized by a turnover of 16 billion euros (Federalimentare elaborations on ISTAT data) larger than that of all other sectors of the food industry. The effluent coming from dairy farms can be divided into two categories: (i) wastewater resulting from the production process: milk residue; serum residues; curds; brines exhausted; buttermilk; spinning water; and water washing products and (ii) waste materials derived from support activities: washing machines and plants and local water containing residues of detergents and chemicals; cooling water; and sewage sewer sanitation. Serum composition varies as a function of several factors, such as farmed species, power supply, milk production season, stage of lactation, type of cheese, type of processing adopted. Whey constitutes about 85–88% by weight of the treated milk (Pizzichini 2006).

The whey is a by-product rich in organic substances and, consequently, a difficult waste to be disposed. Even if no toxic agents or inhibitors of bacteria are present, it may not be directly discharged into water bodies, nor its biological treatment is simple. The current Environmental Consolidation Act Decree. 152/2006 classifies it as a special non-hazardous waste, thus subjected to the relevant waste disposal procedures (GURI 2006). The whey used for livestock increases more than solving the disposal difficulties, as it merely transfers the problem from serum to animal excreta. It is well known that serum may cause intestinal diseases and even bleeding to animals, thus generating large production of manure hard to treat, so much so that its use in farming practices is continuously reducing.

As a matter of fact, wastewaters contain significant quantities of valuable products that can, therefore, represent a significant source of profit, once recovered (see, e.g., whey proteins and lactose useful in food and pharmaceutical industries or for production of biofuels). A drawback can thus be transformed into a resource.

Milk and whey drying issues on an industrial scale are better approached with an intensified process, i.e. high efficiency and low cost. The process intensification is a strategy that aims at gaining benefits during production through small scale of equipment, increasing efficiency, saving energy, reducing costs, mitigating environmental impact, improving security, automation and control devices. The membrane techniques, among the ones available, allow to differentially

F. Villecco (✉)
Department of Industrial Engineering, University of Salerno,
Via Giovanni Paolo II 132, 84084 Fisciano, SA, Italy
e-mail: fvillecco@unisa.it

R. P. Aquino · M. I. Corrente
Department of Pharmacy, University of Salerno,
Via Giovanni Paolo II 132, 84084 Fisciano, SA, Italy
e-mail: aquinirp@unisa.it

M. I. Corrente
e-mail: mcorrente@unisa.it

V. Calabrò
DIMES, University of Calabria, Via Pietro Bucci, 87036
Arcavacata di Rende, CS, Italy
e-mail: vincenza.calabro@unical.it

A. Grasso
CSI, University of Salerno, Via Giovanni Paolo II 132, 84084
Fisciano, SA, Italy
e-mail: agrasso@unisa.it

V. Naddeo
Department of Civil Engineering, University of Salerno,
Via Giovanni Paolo II 132, 84084 Fisciano, SA, Italy
e-mail: vnaddeo@unisa.it

recover all chemical serum components, without causing denaturation of proteins. Ultrafiltration is specially applied to the separation of macromolecules and colloidal materials from solvents or solutes, but is also used in other fields. The ultrafiltration is widely used in the dairy industry because it allows the removal and then the recovery of the whey proteins from milk, thereby reducing the pollution load and, in turn, the economic exploitation of components at highest biological value.

2 Materials and Methods

Experimental

The washing of the membrane is a critical step in the process. It has the purpose of activating the filtering properties of the membrane (in the case of a new membrane) or to restore them when the fouling, occurred during the process, compromises the success of the operations.

To even only partly retain the smaller whey protein, i.e. α-lactalbumin, the membrane should have an MWCO between 5 and 20 KDa (Nunes 2007). Based on the analysis of the parameters, the most suitable filter to our process, selected among those available on the market, was polymeric membranes made from polysulphone. With the progress of the ultrafiltration, a progressive reduction of the permeate flow was observed. The flow decay during the ultrafiltration process is the progressive decrease per unit time of the mass of permeate passing through the membrane. It reduces, until a steady state is attained (Song 1998). Actually, the flow rate decay is caused by an increase in the resistance to the mass transfer due to the membrane fouling, i.e. the accumulation of material (cake) on the filter surface that greatly reduces the membrane permeability and thus the process efficiency. The rate of the membrane fouling was determined by the variation of permeability over time: fouling rate = dLP/dt.

The choice of the flow–flow filtration mode, in which only a part of the fluid permeates the filter while the retentate is recirculated with a flow direction parallel to the filter surface, reduces, but not eliminates, the gradual clogging of the membrane, which has then to undergo a cleaning process.

In the case of a new membrane, washing is performed: with distilled water for 15 min; with a 1% ultraclean basic solution, at the temperature of 30 °C for 30 min; and with distilled water to restore the pH.

The maintenance operations are periodically carried out to prevent the irreversible membrane fouling, thus allowing its operability. This involves the entire system, including: a pump washing with a basic solution of ultraclean to 5% for 1 h, with the purpose of removing impurities that may clog the pores; a membrane and plant washing with the basic solution of ultraclean 1%, at a temperature of 30 °C for 30 min to remove the deposited material; a membrane immersion in distilled water with the mechanical removal of the cake formed on its surface; and a flushing with distilled water to restore the pH. Operations are repeated for each series of tests, and each time the process fluid is changed.

The plant

The plant consists of a supply and recycling tank; a centrifugal pump; a linear membrane reactor; a tank for the permeate collection; and a refrigeration system (if necessary). Pressure regulating valves are considered auxiliary elements. A cooling system keeps the temperature of the process fluid, at a constant value counterbalancing the pump compression work, by means of: a thermocouple; a coil in which water flows at a temperature of 15 °C; and a control valve of the water flow that flows through the coil. In this way, characteristics of the process fluid are preserved. It has to be noted that a temperature rise causes a change in the fluid viscosity, being permeability inversely proportional to viscosity. The centrifugal pump consists of an impeller with blades communicating with the suction tube and with the supply–discharge pipe. During operations, the impeller blades ensure the fluid rotation which is conveyed towards the delivery pipe. Finally, the pump guarantees a pressure difference (TMP) through the membrane to allow the ultrafiltration.

The flow decay

The decay of the permeate flow is caused by the membrane fouling. Systems have been developed, based on fluid dynamics or chemical methods, to improve the membrane performance. They basically consist in the variation of the speed profiles on the membrane surface so as to increase the shear stresses, thus removing the deposited material. Chemical methods provide structural modifications of the membrane surface to reduce the affinity between the surface and the compounds that tend to deposit (Curcio et al. 2004). A periodic variation of the flow speed profile, coupled with the TMP variations applied, appears to provide encouraging results (Curcio et al. 2006). The idea is, then, to apply pulsing conditions, as this could be useful in reducing the decay of the permeate flow. Figure 1 depicts the plant.

3 Results and Discussion

The process optimization

The proposed method to get rid of the gradual accumulation of solid on the membrane and then to optimize the UF process is the implementation of a pulse function η on the
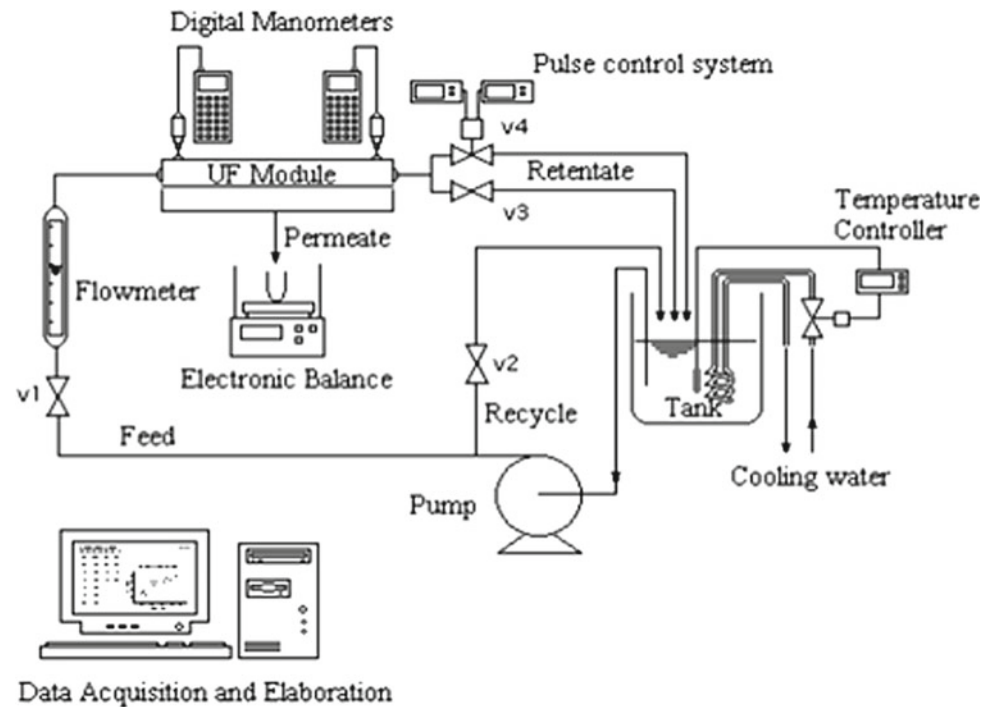
transmembrane pressure, TMP. The function makes the transmembrane pressure to oscillate, between high values (operational TMP) and relatively low values. During the pulse phase, an instantaneous reduction of the transmembrane pressure is obtained, leading to the relaxation of the membrane itself which, rising up, pushes upwards the fouling cake (cake) deposited on it. The tangential flow of retentate drags away the fouling materials, thus removing deposits on the membrane and consequently increasing the efficiency of ultrafiltration. Furthermore, the sudden pressure decrease has an effect of "suction" on the permeate: in fact, a small amount of permeate is sucked into the part of the retentate, passing through the membrane in the opposite direction, thus cleaning the membrane pores. The deformation undergoing the effect of the TMP appears thus to play a crucial role, even if little is found in the literature on this parameter.

It should be remembered that the final goal of this work is to optimize the UF process by developing a control system that may allow the UF by the pressure oscillations, rather than to develop an efficient membrane cleaning method. The system will have either to monitoring the fouling and to schedule the intervention on the controlled variables. An intelligent algorithm has thus been developed based on the fuzzy logic. It has thus been necessary to rationalize the

process; to identify the sequence of operations; and to develop the control algorithm.

The fuzzy controller

We define two input variables: (i) the ΔP variable, which is the difference between the pressure upstream and the pressure downstream the filter, and (ii) the variable D, which is the membrane deformation. As an output variable, we chose the number of times the solenoid valve opens in a given time interval (Zhai et al. 2010).

After the filtration process has begun, the membrane deformation is measured via optical image analysis. Then, the value is compared to a given threshold. If this latter has been reached or overcome, the pulse function is activated by a sudden decrease of the pressure holding on the membrane, being the number of pulses a function of the transmembrane pressure. If the deformation is lower than the threshold, then flow is checked: if a no-flow condition occurs, a pulse is sent to the plant to remove the cake that is presumably hindering the flow through the membrane (Ghomshei et al. 2009).

Differently, if flow holds, the plant is working as required and the algorithm goes to the end. It has to be noted that the system, as conceived, is self-learning. As an example, the pulsation value used in a circumstance is recorded and used as a starting value for the next action (Sena et al. 2013a, b).

4 Conclusion

The control system developed shows a number of features, altogether heading to the process optimization. As a first, the system guarantees a continuous filtration process, as no interruptions are necessary to restore the filter functionality, increasingly spoiled by the material deposited on the membrane surface until the pulse function is applied by the fuzzy controller. This also helps in avoiding the overload on the membrane surface, due either to the weight of the cake formed or to the increase in the transmembrane pressure caused by the filter clogging, thus preserving the membrane integrity. Finally, it is noteworthy that the system does not suffer at all from the lack of information about the membrane elasticity coefficients, since the fuzzy approach allows to overcome the mathematical complexity of the process.

References

Curcio, S., Scilingo, G., Calabró, V., Iorio, G. (2004). Ultrafiltration of BSA in pulsating condition: an artificial neural network approch.

Curcio, S., Scilingo, G., Calabró, V., Iorio, G. (2006). Reduction and control off lux decline in cross-flow membrane processes modeled by artificial neural network.

Ghomshei, M., Villecco, F., Porkhial, S., Pappalardo, M. (2009). Complexity in energy policy: A fuzzy logic methodology. In *6th International Conference on Fuzzy Systems and Knowledge Discovery, FSKD 2009* (pp. 128–131).

GURI, Gazzetta Ufficiale Repubblica Italiana, D.lgs n.152 del 3/4/2006, "Norme in materia ambientale", Pubblicato sul Supplemento Ordinario n. 96 del 14/2006.

Nunes, S. P. (2007). Organic-inorganic membranes for gas separation. *Annales de Chimie: Science des Materiaux, 32,* 119–126.

Pizzichini, M. (2006). *Tecnologia di processo per la valorizzazione delle component del siero di latte*. Enea.

Sena, P., D'Amore, M., Pappalardo, M., Pellegrino, A., Fiorentino, A., & Villecco, F. (2013a). Studying the influence of cognitive load on driver's performances by a fuzzy analysis of lane keeping in a drive simulation. *IFAC Proceedings, 46*(21), 151–156.

Sena, P., Attianese, P., Pappalardo, M., Villecco, F. (2013b). FIDELITY: Fuzzy inferential diagnostic engine for on-line support to physicians. *IFMBE Proceedings*. Springer. https://doi.org/10.1007/978-3-642-32183-2_95.

Song, L. (1998). Flux decline in cross-flow microfiltration and ultrafiltration: mechanism and modeling membrane fouling. *Journal of Membrane Science*. https://doi.org/10.1016/s0376-7388(97)00263-9.

Zhai, Y., Liu, L., Lu, W., Li, Y., Yang, S., Villecco, F. (2010). The application of disturbance observer to propulsion control of sub-mini underwater robot. Lecture Notes in Computer Science (LNCS). https://doi.org/10.1007/978-3-642-12156-2_44.

Performance of Electro-Fenton Water Treatment Technology in Decreasing Zebrafish Embryotoxicity Elicited by a Mixture of Organic Contaminants

João Amorim, Carlos Pinheiro, Isabel Abreu, Pedro Rodrigues,
M. Ángeles Sanromán, Emílio Rosales, Marta Pazos, António Soares,
Cristina Delerue-Matos, Aurélia Saraiva, Luís Oliva-Teles,
António Paulo Carvalho, and Laura Guimarães

Abstract

Electro-Fenton technology was able to decrease zebrafish embryotoxicity of fluoxetine and pirimicarb, when single or in mixture.

Keywords

Fluoxetine • Pirimicarb • Advanced oxidation process • Zebrafish embryo and larvae • Ecotoxicity evaluation

1 Introduction

Water depletion and loss of water quality have become a global problem contributed by population growth, ensuing agriculture and energy demands, increased frequency of extreme weather events (drought in particular), transboundary water competition, as well as intensification of man-made chemical and physical pollutions (e.g., endocrine disruptors, microplastics) (World Bank Water Group). Altogether, these stressors are jeopardizing economic, social, and environmental health, and threatening population well-being. Such a situation calls for a paradigm shift in terms of water resources and their management to comply with water quality and quantity demands as a function of their use. If adequately treated and evaluated in relation to environmental risks and economic considerations, reclaimed water can provide a useful resource to be directed toward agricultural irrigation. However, reclaimed water is very often contaminated by metabolites and/or degradation products of pharmaceutical products and pesticides, which are only partially eliminated during secondary and tertiary wastewater treatments (Campo et al. 2013; Paíga et al. 2016). Treatment technologies are thus under improvement to address this limitation to wastewater reuse. Electro-Fenton is a hybrid technology for advanced oxidation combining electrochemical reactions with Fenton's reagent. Electro-Fenton technology (EF) has been proven useful to improve removal of organic compounds that can be refractive to biological remediation (Meijide et al. 2016). Though

J. Amorim (✉) · C. Pinheiro · I. Abreu · P. Rodrigues · A. Saraiva ·
L. Oliva-Teles · A. P. Carvalho · L. Guimarães
Interdisciplinary Centre of Marine and Environmental Research
(CIIMAR), University of Porto, Terminal de Cruzeiros de Leixões,
Av. General Norton de Matos, 4450-208 Matosinhos, Portugal
e-mail: jamorim@ciimar.up.pt

A. P. Carvalho
e-mail: apcarval@fc.up.pt

L. Guimarães
e-mail: lguimaraes@ciimar.up.pt

J. Amorim · C. Pinheiro · I. Abreu · P. Rodrigues · A. Saraiva ·
L. Oliva-Teles · A. P. Carvalho
Faculty of Sciences, University of Porto, Rua do Campo Alegre,
4169-007 Porto, Portugal

M. Á. Sanromán · E. Rosales · M. Pazos
Centro de Investigación Tecnolóxico Industrial-MTI, University
of Vigo, Campus as Lagoas, Marcosende, 36310 Vigo, Spain
e-mail: biosuv@uvig.es

E. Rosales
e-mail: biosuv@uvig.es

M. Pazos
e-mail: biosuv@uvig.es

A. Soares · C. Delerue-Matos
REQUIMTE/LAQV, Instituto Superior de Engenharia, Instituto
Politécnico Do Porto, Rua Dr. António Bernardino de Almeida,
431, 4200-072 Porto, Portugal
e-mail: cmm@isep.ipp.pt

243

refinements to the technology have been successively introduced to improve its ability to remove pharmaceuticals from wastewater, limited information is still available on its performance on combined mixtures of pharmaceuticals and pesticides typically occurring in reclaimed water. To tackle this knowledge gap, the present study therefore aimed at assessing EF efficacy for toxicity removal of a mixture of antidepressant fluoxetine and carbamate pesticide pirimicarb.

2 Materials and Methods

Fluoxetine is a well-known antidepressant capable of selectively inhibiting the reuptake of serotonin, a mono-amine neurotransmitter present in both humans and aquatic organisms (Airhart et al. 2012). Pirimicarb is a selective carbamate acaricide–insecticide that acts by inhibiting cholinesterase activity (Natale et al. 2018; Vera-Candioti et al. 2015). Chemical quantification and the zebrafish embryotoxicity assay (ZET) were used to evaluate EF influence on the concentrations and toxicity elicited by a mixture (MIX) of fluoxetine (FLX) and pirimicarb (PIRI). For the bioassays, test solutions of FLX, PIRI and MIX were prepared with filtered dechlorinated tap water. Concentrations of FLX and PIRI in the parent solutions and the MIX were 152 and 180 mg L^{-1}, respectively. The EF experiments were prepared as previously described (Meijide et al. 2016). Dechlorinated water, and the Fe^{+2} and sodium sulfate were used as control treatments. Because Fenton's reaction occurs in acidic environments (pH 3), pH correction was applied to all treatments containing Fenton's reagent, so that adequate conditions to embryos and larvae development could be achieved. Five dilutions (increasing in order of magnitude from 10 to 100000×) with dechlorinated water of the treatments containing the test substances and Fenton's reagent were also tested, to ensure effects observed were related to FLX, PIRI or the MIX. After pH adjustment, precipitation was detected in the original test treatments containing Fenton's reagent. Hence, bioassays were carried out with treatments diluted 10× and higher, before and after the passage of the EF electrical current. The assays were conducted according to OECD guidelines with slight adaptations. If performed with embryos, and/or larvae before they attain the complete self-feeding stage, these assays comply with the 3R principles of relative replacement of animal tests (EC 2010; Embry et al. 2010). Briefly, 1 h post-fertilization (hpf) embryos were transferred to a 24-well plate (12 embryos per well) and exposed for 7 days to test treatments. Test media were renewed daily for the whole duration of the experiments. During the exposure period, embryos were observed with an inverted microscope for selected endpoints: mortality, 75% epiboly, delay/arrest of cell division,

abnormal cell masses, developmental delay, pericardial edema, head, eye and tail abnormalities. Cross-tabulation analysis was used to investigate effects elicited by the test treatments before and after EF application.

3 Results and Discussion

Upon EF application, very high removal rates were obtained for FLX (99%), PIRI (98%) or the MIX (97%), as indicated by the total organic content determined in the samples. For the bioassays, total mortality in the control treatment (13%) was within expected levels for ZET. Before EF application, very high mortality rates ($p < 0.05$) were observed in the 10× dilution at 72 hpf for FLX (87%) and the MIX (100%) treatments (Fig. 1). At 144 hpf, mortality also reached 100% in the FLX treatment. According to Kalichak et al. (2016), zebrafish larvae mortality (35–48%) was significantly affected at 95 hpf by FLX exposure (0.009–99 µg L^{-1}), when compared to the control (18%). No significant mortality was found for the subsequent dilutions (100× to 100000×) tested before EF application. After EF, no significant mortality relative to the control was found for any of the treatments tested and their respective dilutions (Fig. 1), indicating this technology would be effective in decreasing the toxicity of FLX and MIX treatments. Given the high mortality rate recorded in the 10× dilution, the remaining parameters were only assessed on the subsequent dilutions tested. Results obtained in the 100× dilution for hatching, side-wise position and active swimming are presented in Fig. 1. For higher dilutions tested, no significant differences could be depicted for side-wise position and active swimming, compared to the control. For hatching, the response pattern was similar to that found for the 100× dilution.

Results obtained for the 100× dilution, before EF application, revealed that the hatching rate was significantly ($p < 0.05$) delayed in FLX (only 64% of the larvae were hatched at 72 hpf, compared to 93% recorded in the control for the same time period), PIRI (56%) and the MIX (50%) treatments (Fig. 1). After EF application, delayed hatching was still detected for FLX (59%) and the MIX (58%), but was no longer detected for PIRI (Fig. 1). In addition, a hatching delay, not previously observed, was detected for ELY after EF application (60% of hatched larvae recorded at 72 hpf). At 144 hpf, hatching rates were similar among test treatments, except for the MIX, which still presented a significant ($p < 0.05$) decrease in hatching (69% of hatched larvae, compared 98% recorded in the control). A previous study (Pan et al. 2018) also reported a significant decrease in hatching (5%, $p < 0.05$), following exposure of zebrafish embryos to 1000 µg L^{-1} FLX for 48 h. According to these authors, FLX seemed to be capable of delaying, or postpone, the hatching time window. Concerning PIRI, studies
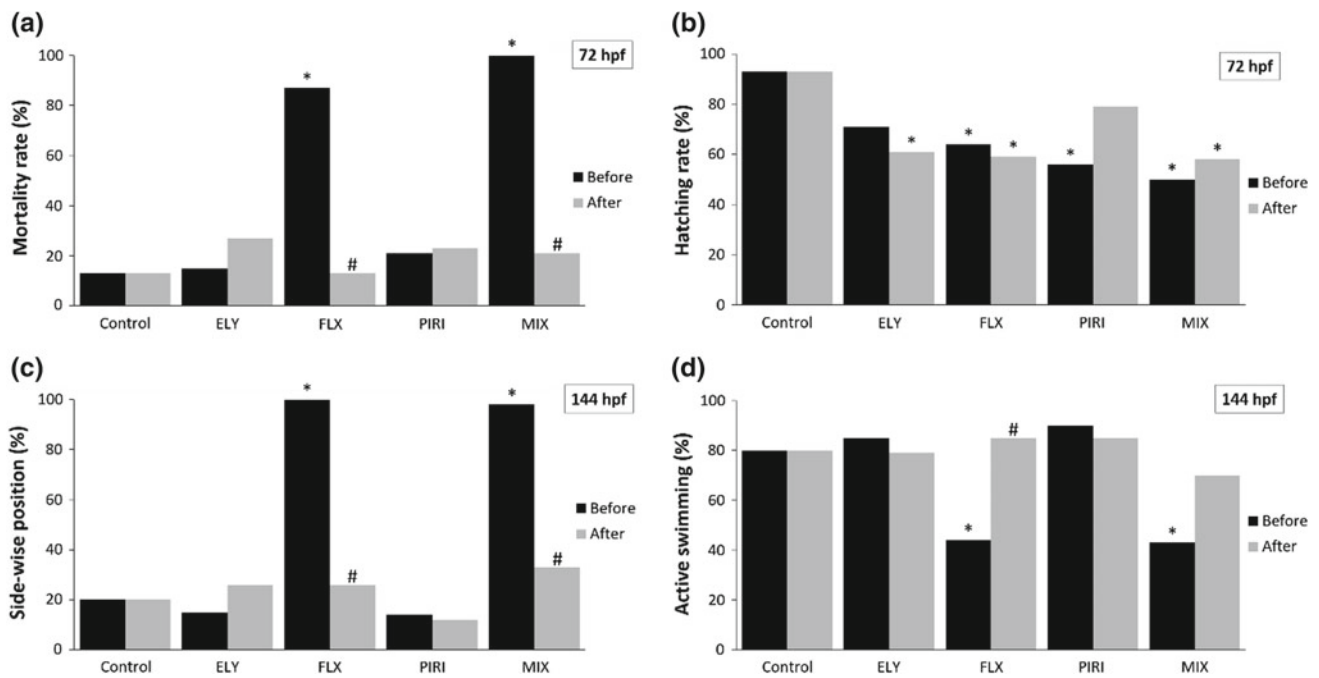
Fig. 1 Results obtained for mortality ($10\times$ dilution), hatching ($100\times$ dilution), side-wise position ($100\times$ dilution) and active swimming ($100\times$ dilution) endpoints in the zebrafish embryotoxicity bioassays carried out before and after application of the electro-Fenton technology (EF). Tested treatments were the control (dechlorinated water), Fenton's reagent only (ELY), fluoxetine (FLX), pirimicarb (PIRI) and a mixture (MIX) of fluoxetine and pirimicarb. * identifies significant differences ($p < 0.05$) between ELY, FLX, PIRI or the MIX, relative to the control, either before or after EF application; # identifies significant differences ($p < 0.05$) within each treatment before and after EF application

addressing its impact on aquatic organisms are scarce, with only a few evaluating its toxicity toward fish (Tomlin 1994; Vera-Candioti et al. 2015; Aragon et al. 2017). Most of these assessed PIRI medial lethal concentration (LC_{50}), with no reference to effects on hatching. However, Aragon et al. (2017) reported a no-observed-effect concentration (NOEC) of 23.8 mg L^{-1} for zebrafish development after 120 hpf of exposure to PIRI, a concentration far higher than the one tested in our study. The present results further suggest EF could elicit a possible synergistic interaction of components in the MIX (including Fenton's reagent), as indicated by the decreased hatching rate still found at 144 hpf.

The response pattern found for side-wise position and active swimming endpoints ($100\times$ dilution) was similar and closely resembled the results obtained for mortality in the 10% dilution tested (Fig. 1). Before EF application, at 144 hpf most larvae were in side-wise position in the FLX (100% compared to 20% in the control, $p < 0.05$) and MIX (98%) treatments. After EF application, no differences in larvae position were found among treatments (Fig. 1), so that side-wise larvae exposed to FLX and the MIX were within the control range. Active swimming was significantly reduced ($p < 0.05$) at 144 hpf in FLX and the MIX before EF application. In these treatments, only 44% (FLX) and

43% (MIX) of the larvae displayed active swimming behavior even after stimulation, compared to 80% recorded in the control. After EF application, all test groups showed similar rates of active swimming larvae (Fig. 1). Previous alterations of larvae swimming caused by fluoxetine exposure were reported by Pan and co-workers (2018). In their study, zebrafish larvae (120 hpf) exposed to 100 µg FLX L^{-1} exhibited longer swimming distance and faster swimming speed than the control group. Nonetheless, studies analyzing swimming behavior in fish larvae are scarce and need further analysis to better understand the influence of FLX on zebrafish early swimming behavior. Taken together, the results obtained for mortality ($10\times$ dilution), and side-wise position and active swimming ($100\times$ dilution), suggest that EF application would be effective in reducing FLX toxicity even when in mixture with the insecticide.

4 Conclusion

Fluoxetine was able to affect zebrafish embryo and larvae mortality, hatching and behavior. Individually, pirimicarb affected hatching only. When in mixture, toxicity appeared to be mostly driven by fluoxetine. Application of the EF was

generally able to decrease the toxicity of fluoxetine and pirimicarb, either individually or combined. Further molecular, biochemical, histological and behavioral studies evaluating neurotransmitter receptors, transporters and enzymes known to be involved in the modes of action of these contaminants will deepen our knowledge on the processes by which the effects observed take place. Importantly, they may provide useful biomarkers to early diagnose EF efficiency toward such mixtures, leading to the identification of useful tools to monitor reclaimed water quality and improve its reuse.

References

Airhart, M. J., et al. (2012). *Neurotoxicology and Teratology, 34*(1), 152–160.

Aragon, A., et al. (2017). *Analytical and Bioanalytical Chemistry, 409* (11), 2931–2939.

Campo, J., et al. (2013). *Journal of Hazardous Materials, 263,* 146–157.

EC. (2010). Directive on the protection of animals used for scientific purposes. Directive 2010/63/EU, Brussels, Belgium.

Embry, M. R., et al. (2010). *Aquatic Toxicology, 97,* 79–87.

Kalichak, F., et al. (2016). *Environmental Toxicology and Pharmacology, 41,* 89–94.

Meijide, J., et al. (2016). *Journal of Hazardous Materials, 319,* 43–50.

Natale, G. S., et al. (2018). *Ecotoxicology and Environmental Safety, 147,* 471–479.

Paíga, P., et al. (2016). *Science of the Total Environment, 573,* 164–177.

Pan, C., et al. (2018). *Chemosphere, 205,* 8–14.

Tomlin, C. D. S. (Ed.). (1994). *The pesticide manual-world compendium* (10th ed.). Surrey, UK: The British Crop Protection Council.

Vera-Candioti, J., et al. (2015). *Toxicology and Industrial Health, 31* (11), 1051–1060.

An Overview of Photocatalytic Drinking Water Treatment

Miray Bekbolet

Abstract

Photocatalytic disinfection of *Escherichia coli* was assessed. Removal of natural organic matter by advanced oxidation processes more specifically photocatalysis was considered. Application of first-, second- as well as third-generation photocatalysts was evaluated. Photocatalytic degradation process was evaluated for drinking water quality aspects.

1 Introduction

Photocatalysis has been applied for the treatment of drinking water either for inactivation of pathogenic bacteria or degradation of natural dissolved organic matter for almost three decades.

In aqueous solutions, photocatalytic reactions rely on the use of a semiconductor and a suitable light source. Upon irradiation, absorbed light energy by the semiconductor ($E > E_{bg}$) produces e$^-$/h$^+$ pair that leads to the formation of reactive oxygen species (ROS) primarily hydroxyl radicals through reactions with dissolved oxygen. Based on these primary events, in the presence of a substrate various degradation reactions take place mostly via oxidation mechanism.

In natural waters, two major components require to be treated to obtain safe drinking water. The presence of dissolved organic matter poses a risk of formation of disinfection by-products that the presence of pathogenic microorganisms also creates serious public health problems. The powerful oxidation mechanism of photocatalysis is capable of eliminating both components under mild reaction conditions. Even under sunlit surface waters due to the recent developments on visible light active photocatalysts, both reactions could proceed simultaneously and consecutively.

TiO$_2$ has been utilized as a successful photocatalyst for decades for the degradation of a wide range of organic compounds including pesticides and emerging pollutants. Moreover, the degradation of dissolved organic matter has also been presented covering almost all aspects of water matrix effects by Bekbolet and colleagues (Bekbölet 1996; Uyguner-Demirel and Bekbolet 2011; Sen Kavurmaci and Bekbolet 2014; Bekbolet and Sen-Kavurmaci 2015). Dissolved organic matter has been modeled by simple compounds as humic and fulvic acids, although they also express complex structural diversity and heterogeneity. TiO$_2$ P-25 composed of anatase and rutile phases has been utilized and accepted as a standard photocatalyst. Second-generation visible light active TiO$_2$ and third-generation non-TiO$_2$ photocatalysts have also been studied in comparison with TiO$_2$ P-25 (Birben et al. 2015).

TiO$_2$ photocatalysis has also been applied for inactivation of a wide range microorganisms, i.e., bacteria, fungi and algae. Bekbolet and colleagues demonstrated successful efficiency of TiO$_2$ photocatalysis for *Escherichia coli* inactivation. Further interest was directed to the use of VLA TiO$_2$ specimens upon solar irradiation (Bekbölet and Araz 1996; Birben et al. 2017; Uyguner-Demirel et al. 2018).

Due to the co-presence of both substrates in natural waters, research studies should cover simultaneous removal of components. Bekbolet and colleagues presented two major studies on the *i.* role of dissolved organic matter on the photocatalytic treatment of emerging pollutants and *ii.* role of dissolved organic matter on inactivation of microorganisms via photocatalysis (Uyguner-Demirel et al. 2018).

M. Bekbolet (✉)
Institute of Environmental Sciences, Bogazici University, 34342 Bebek, Istanbul, Turkey
e-mail: bekbolet@boun.edu.tr

2 Materials and Methods

Natural organic matter analog compounds will be used. TiO_2, doped TiO_2, ZnO, Ce-doped ZnO as well lanthanide ferrites will be used as photocatalysts. Solar irradiation will be applied. Humic matter will be characterized by UV–Vis and fluorescence spectroscopic parameters along with organic carbon contents. Advanced fluorescence techniques, i.e., excitation–emission matrix (EEM), and fluorescence features will also be applied.

3 Conclusion

The present work will primarily focus on basic principles and applications of TiO_2 photocatalysis on the degradation of dissolved organic matter as followed by UV–Vis and fluorescence spectroscopic techniques as well as organic carbon contents. Secondly, TiO_2 photocatalytic inactivation of microorganisms will be presented focusing on *E. coli* as an indicator organism. Findings on this subject matter will be evaluated with reference to the literature reports to highlight future research interests.

References

Bekbolet, M., & Sen-Kavurmaci, S. (2015). The effect of photocatalytic oxidation on molecular size distribution profiles of humic acid. *Photochemical & Photobiological Sciences, 14*(3), 576–582.

Bekbölet, M. (1996). Destructive removal of humic acids in aqueous media by photocatalytic oxidation with illuminated titanium dioxide. *Journal of Environmental Science and Health. Part A: Environmental Science and Engineering and Toxicology, 31*(4), 845–858.

Bekbölet, M., & Araz, C. V. (1996). Inactivation of *Escherichia coli* by photocatalytic oxidation. *Chemosphere, 32*(5), 959–965.

Birben, N. C., Uyguner-Demirel, C. S., Kavurmaci, S. S., Gürkan, Y. Y., Turkten, N., Cinar, Z., et al. (2017). Application of Fe-doped TiO_2 specimens for the solar photocatalytic degradation of humic acid. *Catalysis Today, 281,* 78–84.

Birben, N. C., Uyguner-Demirel, C. S., Sen-Kavurmaci, S., Gurkan, Y. Y., Turkten, N., Cinar, Z., et al. (2015). Comparative evaluation of anion doped photocatalysts on the mineralization and decolorization of natural organic matter. *Catalysis Today,* 240, Part A, 125–131.

Sen Kavurmaci, S., & Bekbolet, M. (2014). Tracing TiO_2 photocatalytic degradation of humic acid in the presence of clay particles by excitation–emission matrix (EEM) fluorescence spectra. *Journal of Photochemistry and Photobiology A: Chemistry, 282,* 53–61.

Uyguner-Demirel, C. S., & Bekbolet, M. (2011). Significance of analytical parameters for the understanding of natural organic matter in relation to photocatalytic oxidation. *Chemosphere, 84*(8), 1009–1031.

Uyguner-Demirel, C. S., Birben, C. N., Bekbolet, M. (2018). A comprehensive review on the use of second generation TiO_2 photocatalysts: Microorganism inactivation. *Chemosphere, 211*, 420–448.

Solar Light-Initiated Photoinactivation of *E. coli*: Influence of Natural Organic Matter

Ceyda S. Uyguner-Demirel, Ezgi Lale, Nazmiye Cemre Birben, and Miray Bekbolet

Abstract

Increasing need for clean potable water around the world, have led researchers to focus on water disinfection using natural and/or artificial sunlight for the inactivation of a wide range of microorganisms. In this study solar light-initiated photoinactivation of pathogenic bacteria i.e. *Escherichia coli (E. coli)*. The effect of natural organic matter (NOM) type and water matrix was evaluated. Both NOM and bacteria removal by solar irradiation was followed by UV-vis and fluorescence spectroscopic analysis to characterize NOM and reveal inactivation data of *E. coli* to kinetics.

1 Introduction

Due to the increasing demand of clean drinking water around the world, disinfection of water by the application of different treatment methods has attracted significant interest. Water disinfection using natural and/or artificial sunlight has been widely investigated for the inactivation of a wide range of micro-organisms (McGuigan et al. 2012). Natural organic matter (NOM), namely, humic substances as a representative group are complex macromolecules of ill defined structure that are important sunlight absorbers in natural waters. Depending on the source, both the amount and the composition of NOM vary spatially and temporarily; therefore, the effect of NOM on solar light-initiated inactivation of micro-organisms requires significant attention. The aim of the present study was to evaluate the effect of various NOM model compounds and inorganic components on the solar photoinactivation of *Escherichia coli* which is a common pathogenic indicator for water disinfection. Due to various characteristics of surface waters, humic acid (HA), a lower molecular size fraction of HA and Suwannee River natural organic matter (SRNOM) were selected as model compounds of NOM. Although humic acid derived from the soil is considered as a low-quality humic matter, relative to that derived from aquatic NOM, it has been utilized as a standard material in bench-scale laboratory studies for NOM characterization and removal by photocatalytic degradation (Uyguner and Bekbolet 2005; Uyguner-Demirel and Bekbolet 2011). Throughout the application of solar light-initiated photoinactivation of bacteria, the release of organic matter can be observed and characterized with UV–Vis absorption spectra and specific fluorescence techniques (Castro-Alferez et al. 2016). Excitation–emission matrix (EEM) fluorescence contour plots of NOM and inactivated bacteria exhibit maximum fluorescence intensities in specific regions. Relating this information to NOM characterization and bacteria inactivation would be crucial to understand the mechanism of photolytic degradation.

2 Materials and Methods

Three different types of NOM model compounds were used: (i) humic acid sodium salt (HA, Aldrich), (ii) a lower molecular size fraction of HA (30 kDa) and (iii) Suwannee River natural organic matter (SRNOM) reference sample (International Humic Substance Society, IHSS). Synthetic source waters containing varying concentrations and types of NOM were prepared and inoculated with *E. coli* to an initial concentration of approximately 10^6 CFU/mL *E. coli* (strain O157). Stock suspension was prepared in Luria-Bertani (LB) medium. Working solutions were subjected to the solar photolytic treatment, and enumeration was carried out according to standard methods by membrane filter method. Effect of water matrix (WM) on *E. coli* photoinactivation

C. S. Uyguner-Demirel (✉) · E. Lale · N. C. Birben · M. Bekbolet
Bogazici University, Institute of Environmental Sciences,
34342 Bebek, Istanbul, Turkey
e-mail: uygunerc@boun.edu.tr

was also investigated by adding cations (Ca^{2+}, Mg^{2+}, Na^+, K^+) as well as accompanying common anions (e.g. Cl^-, NO_3^-, SO_4^{2-}, $H_2PO_4^-$ and HCO_3^-/CO_3^{2-}). Simulated solar photodegradation and photoinactivation experiments (Atlas Suntest CPS+ solar simulator, light intensity, $I_o = 250$ W/m^2) were carried out in Pyrex reaction vessels. Spectroscopic characterization prior to and following the solar photolytic treatment was measured by specific UV–Vis and fluorescence parameters. EEM contour plots were constructed based on the fluorescence data recorded in the excitation wavelength of 200–500 nm and emission wavelength of 200–600 nm.

3 Results and Discussion

Humic acids representing the main colour producing component of NOM in natural waters have a broad and intense absorbance spectrum due to their large and highly conjugated molecular structures. DOC contents of HA, 30 kDa HA and SRNOM are in the range of 3–10 mg L^{-1} resembling that of natural waters. In order to make concentration-independent comparisons, carbon-normalized specific

Fig. 1 Characteristics of NOM analogues

absorbance ($SUVA_{254}$, L/m mg) was calculated by dividing the intensity of UV absorbance at 254 nm by DOC concentration of the sample. $SUVA_{254}$ values which have been shown to be strongly correlated with the hydrophobic organic acid fraction and aromatic content vary in the range of 4–13 L/m mg for NOM analogues. Low $SUVA_{254}$ value for SRNOM reflects that a large portion of this particular NOM includes low molecular weight mostly aliphatic compounds (Fig. 1).

Following a stepwise approach, photoinactivation of *E. coli* in the presence of different NOM types and inorganic components was investigated under simulated solar light (Fig. 2). Upon photolytic irradiation period of 60 min, 4-log reduction of *E. coli* was achieved in the presence of HA and 30 kDa molecular size fraction of HA, whereas 3-log reduction of *E. coli* was attained in the presence of SRNOM. The variations in water quality significantly affect microbial inactivation. Reduction of UV transmittance depending on the humic content is one of the most important factors that influences the efficiency of the solar photoinactivation. Based on the results of the present study, it can be stated that the high DOC content of SRNOM caused decreasing inactivation rates. The observed impact of humic concentration on *E. coli* photoinactivation was expected in accordance with previous studies (Cantwell et al. 2008). A slight retardation effect of water matrix on photoinactivation of *E. coli* was also observed.

Solar photodegradation of natural organic matter can lead to the conversion of NOM to inorganic compounds and alteration of the chemical properties that can easily be followed by spectroscopic parameters. EEM fluorescence contour plots of NOM following 60 min of treatment in the presence and absence of WM and *E. coli* are presented in Fig. 3. In EEM fluorescence contour plots, natural organic matter exhibits fluorescence in the excitation wavelength range of $\lambda_{exc} = 200$–500 nm and emission wavelength range of $\lambda_{emis} = 280$–600 nm (Baker et al. 2008). When the destruction of bacteria occurs, the presence of aromatic
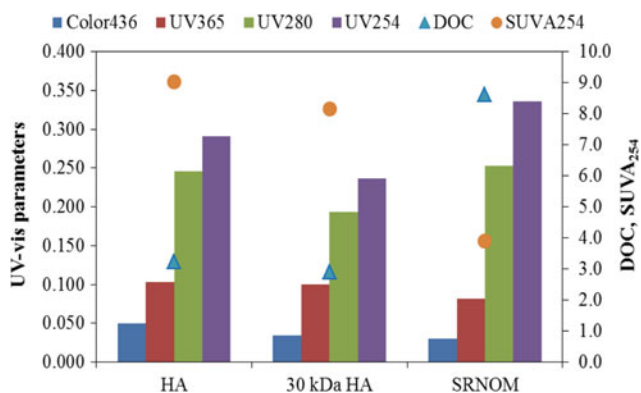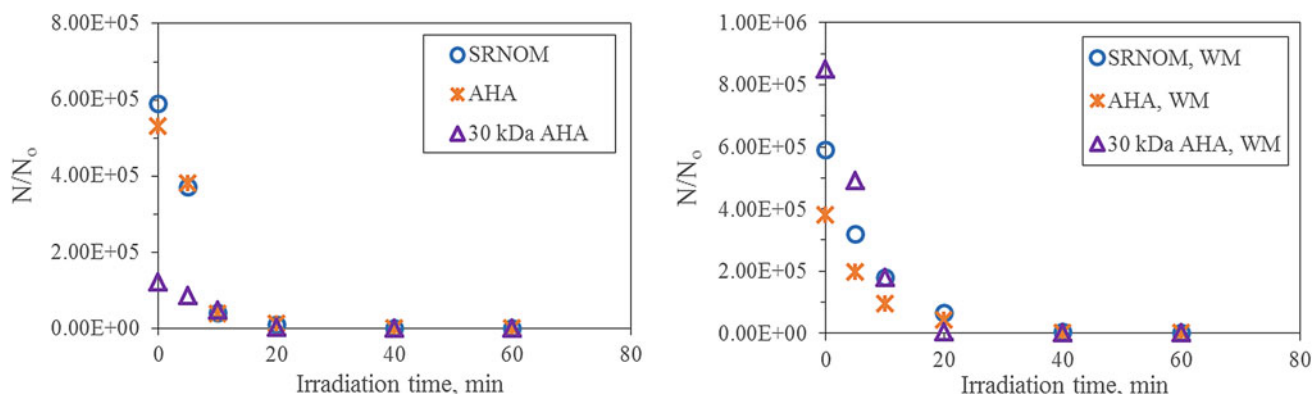
Fig. 2 Comparative presentation of *E. coli* removal in the presence of NOM analogues: effect of WM
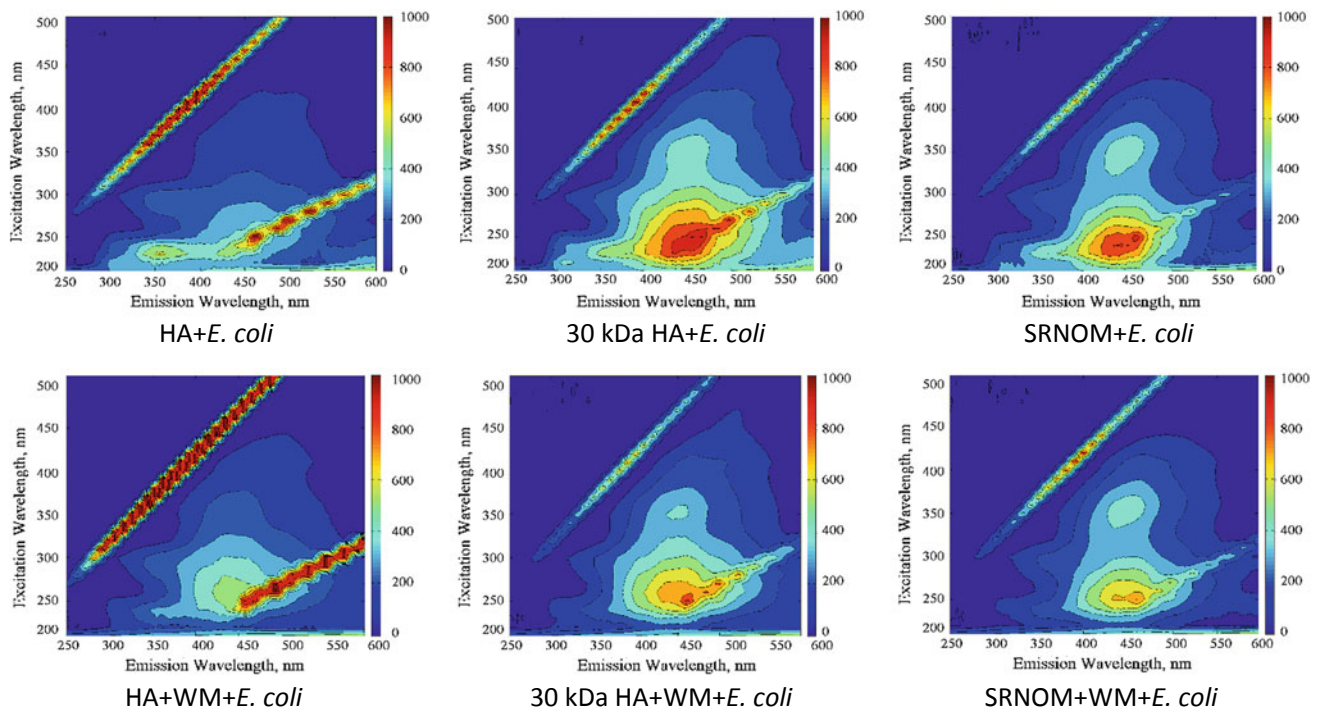
Fig. 3 EEM fluorescence contour plots of NOM following 60 min treatment in the presence of WM and *E. coli*

proteins I (λ_{exc} 220–250 and λ_{emis} 280–332), aromatic proteins II (λ_{exc} 220–250 and λ_{emis} 332–380) and microbial by-products (λ_{exc} 250–470 and λ_{emis} 280–380) can be observed in EEM fluorescence plots (Coble 1996). Relating this information to NOM characterization and bacteria inactivation would be crucial to understand the mechanism of photolytic degradation.

4 Conclusion

Simultaneous removal of both NOM and *E. coli* by solar irradiation could be attained under specified experimental conditions. A slight retardation effect of water matrix on photoinactivation of *E. coli* was observed. Besides UV–Vis and fluorescence spectroscopic analysis covering EEM fluorescence contour plots to characterize NOM and revealing inactivation data of *E. coli* to kinetics, the structure of the "inactivated" bacteria and in situ produced organic matrix should be deeply investigated. Application of EEM fluorescence spectroscopy as a more sophisticated method can bring about a detailed understanding of the qualification of microbial products and can help distinguish NOM quality by distinguishing non-living organic matter from bacteria.

References

Baker, A., Tipping, E., Thacker, A., & Gondar, D. (2008). Relating dissolved organic matter fluorescence and functional properties. *Chemosphere, 73*(11), 1765–1772.

Cantwell, R. E., Hofmann, R., & Templeton, M. R. (2008). Interactions between humic matter and bacteria when disinfecting water with UV light. *Journal of Applied Microbiology, 105*, 25–35.

Castro-Alférez, M., Polo-López, M. I., & Fernández-Ibáñez, P. (2016). Intracellular mechanisms of solar water disinfection. *Science Reports, 6*(38145), 1–10.

Coble, P. G. (1996). Characterization of marine and terrestrial DOM in seawater using excitation-emission matrix spectroscopy. *Marine Chemistry, 51*, 325–346.

McGuigan, K. G., Conroy, R. M., Mosler, H.-J., du Preez, M., Ubomba-Jaswa, E., & Fernandez-Ibañez, P. (2012). Solar water disinfection (SODIS): A review from bench-top to roof-top. *Journal of Hazardous Materials, 235–236*, 29–46.

Uyguner, C. S., & Bekbolet, M. (2005). A comparative study on the photocatalytic degradation of humic substances of various origins. *Desalination, 176*(1–3), 167–176.

Uyguner-Demirel, C., & Bekbolet, M. (2011). Significance of analytical parameters for the understanding of natural organic matter in relation to photocatalytic oxidation. *Chemosphere, 84*(8), 1009–1031.

Molecular Size Distribution Profiles of Organic Matrix in Reverse Osmosis Concentrate Under Oxidative and Non-oxidative Conditions

Nazmiye Cemre Birben and Miray Bekbolet

Abstract

Photolytic/photocatalytic degradation of synthetic ROC samples was evaluated. Role of various photocatalysts on ROC degradation was evaluated. Molecular size fractionation was performed following photodegradation/ photocatalytic degradation. Advanced fluorescence techniques used for detecting changes in fluorophores.

Keywords

Molecular size distribution • Novel photocatalysts • Photocatalysis • Reverse osmosis concentrate

1 Introduction

The major aim of this study was to investigate the applicability of solar photocatalysis on the removal of organics present in reverse osmosis concentrate (ROC) mainly comprised of humics and emerging contaminants (ECs) using both commercial photocatalysts and synthesized ones. To this purpose, TiO_2 P-25 and ZnO were selected as commercial photocatalysts, whereas N-doped TiO_2 and TiO_2/ZnO nanocomposite were nominated as synthesized photocatalysts. Organic matrix composed of humic matter and selected ECs (SMX and CMZ) constituted the major consortia of ROC_m and ROC_{ECm}. Being as the major organic component of ROC_m, removal of humic-like matter via photodegradation and photocatalysis was targeted. Considering the hydrophobic, hydrophilic, multi-ligand, polydisperse character of humic-like matter in NOM composition that significantly change with molecular size distribution profiles, the employment of fluorescence spectroscopic techniques, i.e., EEM and PARAFAC, was assessed to measure the intrinsic fluorescence of emerging contaminants in the solution matrix during photocatalytic degradation.

2 Materials and Methods

2.1 Experimental Setup

Solar photolysis and photocatalysis reactions were performed by using an ATLAS Suntest CPS+ simulator equipped with an air-cooled xenon lamp ($I_o = 250$ W/m^2 and emission spectrum range between $\lambda = 300$–800 nm) as the light source (Ref. 56052371, Atlas). Detailed information on experimental procedure has been presented elsewhere (Birben et al. 2015).

2.2 Analytical Methodology

Non-Purgeable Organic Carbon (NPOC, mg/L) Analyses: NPOC contents of all samples prior to and following each process were determined by using total organic carbon analyzer (Shimadzu TOC VWP).

UV-vis spectroscopic measurements: UV-vis absorption spectra were recorded in the 200–600 nm wavelength range using Perkin Elmer Lambda 35 UV-vis double beam spectrophotometer employing Hellma quartz cuvettes of 1.0 cm optical path length. Humic matter was characterized by specified UV-vis parameters. Absorbance values at 436 nm ($Color_{436}$), 365 nm (UV_{365}), 280 nm (UV_{280}), and 254 nm (UV_{254}) were recorded in all samples to track the change of UV-vis parameters (m^{-1}) following each experimental run.

Fluorescence spectroscopic measurements: Fluorescence spectra acquired in the synchronous scan mode were recorded on a Perkin Elmer LS 55 Luminescence Spectrometer

N. C. Birben (✉) · M. Bekbolet
Institute of Environmental Sciences, Bogazici University, 34342 Istanbul, Turkey
e-mail: cemre.birben@boun.edu.tr

M. Bekbolet
e-mail: bekbolet@boun.edu.tr

equipped with a 150 W xenon arc lamp and a red-sensitive photomultiplier tube. Detailed information regarding EEM measurements was presented elsewhere (Sen-Kavurmaci and Bekbolet 2014; Birben et al. 2015).

PARAFAC modeling was conducted according to the methodology described by Stedmon and Bro (2008). EEM fluorescence data were modeled using the DOMFluor Toolbox in MATLAB R according to the recommended procedure (Stedmon and Bro 2008).

Molecular size fractionation by ultrafiltration: Prior to and following each treatment processes, ROC_m and ROC_{ECm} samples were fractionated using a 50-mL Amicon Model 8050 ultrafiltration stirred cells into appropriate molecular size fractions, i.e., 100, 30, 10, 3, and 1 kDa. Prior to and following treatment processes, ROC_{m1}, ROC_{m2}, ROC_{ECm1},

and ROC_{ECm2} were fractioned into six nominal molecular weight cut-offs, and each fraction (F) was defined as follows: 0.45 μm ff $> F1 > 100$ kDa,   100 kDa $> F2 > 30$ kDa, 30 kDa $> F3 > 10$ kDa,   10 kDa $> F4 > 3$ kDa,   3 kDa $> F5 > 1$ kDa, and $F6 < 1$ kDa.

3 Results and Discussion

Molecular size distribution profiles provide information on (i) degradation of each molecular size fraction $F1$–$F6$ via oxidation, (ii) in situ fragmentation of higher molecular size fractions to lower molecular size fractions.

Owing to its insignificant change in NPOC removal efficiencies with respect to increasing irradiation periods,
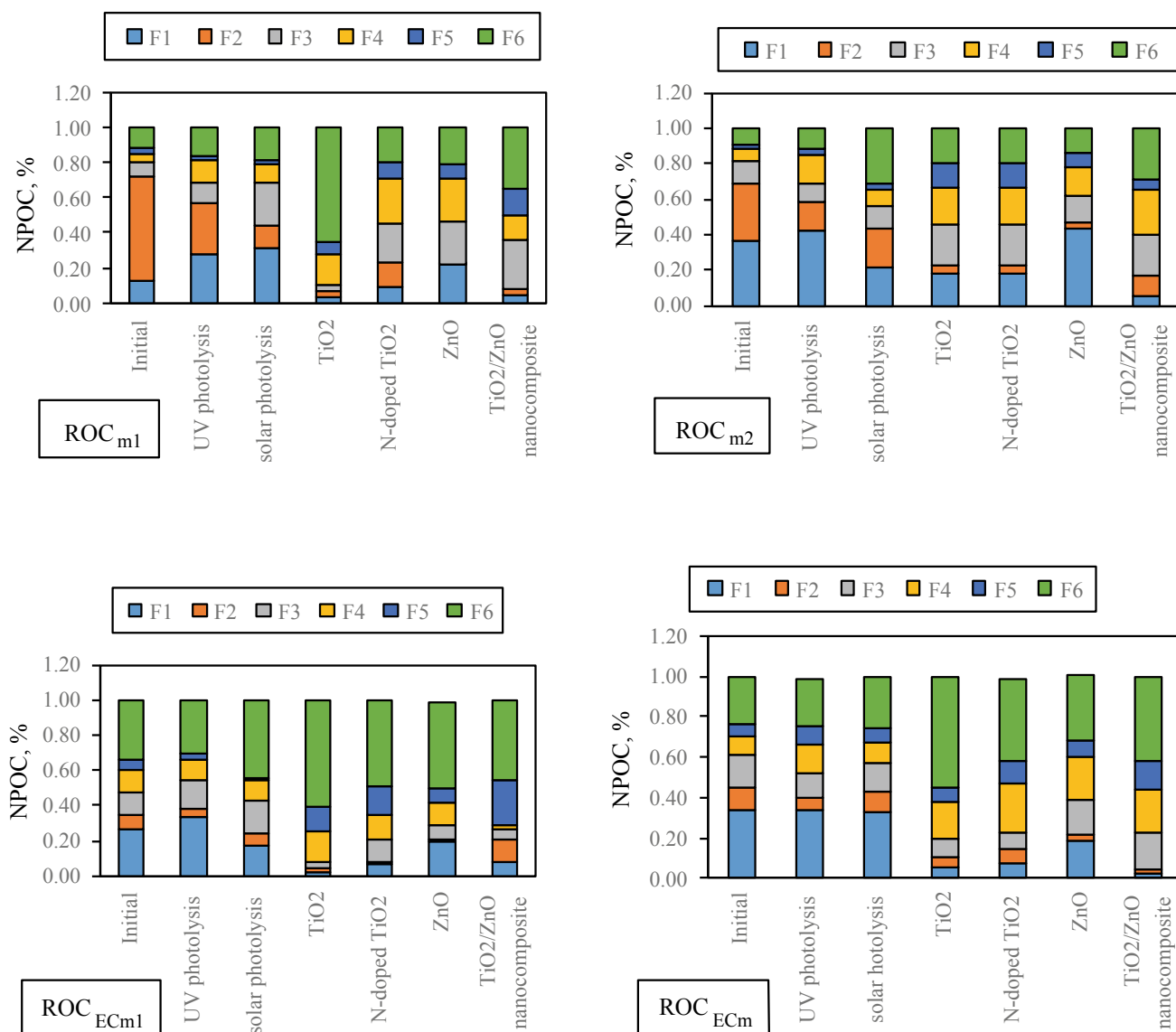
Fig. 1 Changes in molecular size distribution profiles of ROC_m and ROC_{ECm} prior to and following photodegradation and photocatalytic degradation processes expressed in terms of NPOC

molecular size fractionation of ROC samples was carried out by using samples exposed to UV photodegradation and solar photodegradation following irradiation period of 60 min. On the other hand, for photocatalytic degradation experiments, upon 50–60% NPOC removal was achieved, samples were subjected to molecular size fractionation in the presence of selected photocatalysts. Transformations observed on the fractional distribution percentages of each ROC_m and ROC_{ECm} samples were expressed in terms of NPOC, and results were presented in Fig. 1.

4   Conclusion

Transformation of higher molecular size organics of ROC_m and ROC_{ECm} into lower molecular size organics was noticeably observed by the application of molecular size fractionation procedure as well as EEM fluorescence features. Moreover, EEM fluorescence features in combination with PARAFAC modeling would bring further insight into the understanding transformation of fluorophobic components of ROC samples exposing to photodegradation and photocatalytic degradation.

References

Birben, N. C., Uyguner-Demirel, C. S., Sen-Kavurmaci, S., Gurkan, Y. Y., Turken, N., Cinar, Z., et al. (2015). Comparative evaluation of anion doped photocatalysts on the mineralization and decolorization of natural organic matter. *Catalysis Today, 240*, 125–131.

Sen-Kavurmaci, S., & Bekbolet, M. (2014). Tracing TiO_2 photocatalytic degradation of humic acid in the presence of clay particles by excitation–emission matrix (EEM) fluorescence spectra. *Journal of Photochemistry and Photobiology A, 82*, 53–61.

Stedmon, C. A., & Bro, R. (2008). Characterizing dissolved organic matter fluorescence with parallel factor analysis: A tutorial. *Limnology and Oceanography Methods, 6*, 572–579.

Solar Photocatalytic Degradation of Humic Acids Using Copper-Doped TiO$_2$

Miray Bekbolet and Nazli Turkten

Abstract

Preparation of undoped and Cu-doped TiO$_2$ photocatalysts using sol–gel method. Characterization of photocatalysts using XRD, SEM, XPS, UV-DRS, BET and FTIR techniques. Visible light photocatalytic degradation of humic acid in drinking water. Investigation of degradation pathway using humic acid fluorescence excitation emission matrix contour plots. Evaluation of adsorption characteristics of TiO$_2$ photocatalysts on humic acid solution.

Keywords

Adsorption • Copper doping • Humic acid • Photocatalysis • Sol–gel • TiO$_2$

1 Introduction

Humic substances mainly humic acids (HAs) constitute the major fraction of natural organic matter. In the past several decades, applications of advanced oxidation techniques (AOTs) are considered as effective tools for the removal of humic acids from natural waters. Titanium dioxide (TiO$_2$) photocatalysis gained great attention among these AOTs. However, TiO$_2$ has a wide band gap and is only excited by UV light. Therefore, to activate TiO$_2$ photocatalysts efficiently under visible light irradiation, several new photocatalysts are made using impurity doping approach in recent years. Doping with metals has been considered one of the most effective approaches to improve the photocatalytic

M. Bekbolet · N. Turkten (✉)
Institute of Environmental Sciences, Bogazici University, 34342 Bebek, Istanbul, Turkey
e-mail: nazli.turkten@boun.edu.tr

M. Bekbolet
e-mail: bekbolet@boun.edu.tr

activity of TiO$_2$ in visible region. In the present study, both photocatalytic performance and adsorption characteristics of TiO$_2$ photocatalysts on the degradation of natural organic matter (NOM) were represented by a model humic acid (HA). Undoped TiO$_2$ and copper-doped TiO$_2$ (Cu–TiO$_2$) were synthesized by a sol–gel method from an alkoxide precursor. Prepared TiO$_2$ photocatalysts were characterized by XRD, SEM, XPS, UV-DRS, BET and FTIR methods. Their photocatalytic activities were assessed with regard to degradation kinetics of humic acid in terms of UV–vis spectroscopic parameters and organic contents. Humic acid fluorescence excitation emission matrix (EEM) contour plots expressed indicated that solar photocatalytic degradation pathway for a TiO$_2$-type specific regardless of Cu dopant.

2 Materials and Methods

Working HA (Aldrich, humic acid sodium salt) solution was prepared by appropriate dilution of the stock solution (1000 mg/L). 30 kDa molecular size fraction of humic acid was prepared using 50 mg/L HA, filtered through 0.45-µm cellulose acetate membrane filter (Millipore) and followed by ultrafiltration process with using (Amicon 8050 ultrafiltration stirred cell unit) (UV$_{254}$: 0.3973 cm^{-1}, DOC: 3.46 mg/L). Suwannee River Natural Organic Matter (SRNOM, IHSS) solution supplied form IHSS was also used. TiO$_2$ was synthesized using a sol–gel method previously developed (Turkten and Cinar 2017). Two different Cu-doped photocatalysts containing 0.25 wt% Cu (0.25-Cu TiO$_2$) and 0.50 wt% Cu (0.50-Cu TiO$_2$) were prepared by an incipient wet impregnation method using Cu(NO$_3$)$_2$·3H$_2$O as Cu source. Cu-doped TiO$_2$ samples were calcined at 773 K for 5 h and grinded. Undoped and Cu-doped synthesized TiO$_2$ photocatalysts were examined by using XRD, SEM, XPS, UV-DRS, BET and FTIR techniques. Organic matrix was characterized by monitoring mineralization extend in terms of dissolved organic carbon content (DOC, mg/L) and by spectroscopic parameters based on absorbance values

measured at specified wavelengths of 436 nm (Color$_{436}$, cm^{-1}), 365 nm (UV$_{365}$, cm^{-1}), 280 nm (UV$_{280}$, cm^{-1}) and 254 nm (UV$_{254}$, cm^{-1}). Moreover, fluorescence index (FI) and excitation emission matrix (EEM) features were also assessed (Uyguner and Bekbolet 2005; Uyguner-Demirel and Bekbolet 2011; Sen Kavurmaci and Bekbolet 2014).

In adsorption experiments, both undoped and Cu-doped TiO$_2$ photocatalysts were used. Batch adsorption experiments were carried out by the addition of different amounts of TiO$_2$ photocatalysts to the HA solution for each flask. The tests were held in the dark, at 25 ± 2 °C in a water bath shaker for 24 h. Then, the samples were filtered through 0.45-µm Millipore membrane filters.

3 Results and Discussion

In XRD diffractogram of undoped TiO$_2$, both anatase and rutile phases were present. Six distinctive peaks corresponding to the (101), (004), (200), (211), (118) and (116) planes of anatase were found. In XRD diffractograms, the peak at 25.5° (2θ) corresponded to the characteristic peak of (101) plane in anatase and at 27.7° (2θ) corresponded to the characteristic peak of (1 1 0) of rutile. Cu-doped TiO$_2$ diffractograms indicated predominantly anatase phase with a trace portion of rutile. The reason could be explained that Cu has a promoting effect on the transformation of anatase to rutile crystalline phase. SEM micrographs obtained for undoped and Cu-doped TiO$_2$ photocatalysts samples consisted of small, nearly spherical and some larger elongated particles. An enhancement of Cu-doping has an effect on the

aggregation of particles. Characteristic peaks of Ti 2p, O 1s and Cu 2p were evident in all samples as displayed by XPS diffractograms. Two peaks at ca. 458 and 463 eV corresponded to the photo-splitting electrons Ti^{4+} 2p$_{3/2}$ and Ti^{4+} 2p$_{1/2}$ indicating the presence of Ti^{4+}. O 1s binding energies of Cu-doped TiO$_2$ photocatalysts samples were located at a higher energy than 529.3 eV of synthesized TiO$_2$ which was assigned to the metallic oxide (O$_2^-$) in the TiO$_2$ lattice. Peaks of Cu 2p$_{3/2}$ and Cu 2p$_{1/2}$ appeared at around 933 and 953 eV, respectively, confirming the presence of Cu^{2+}. UV-DRS spectra of the undoped specimens had an absorption edge at around 410 nm; however, the absorption threshold of Cu-doped specimens shifted towards the visible region as 420–600 nm. This absorption edge indicated that Cu^{2+} ions were localized in the TiO$_2$ lattice occupying Ti^{4+} positions. Band gap energies and respective effective wavelength indicated a red shift to the possible use of solar irradiation. BET surface area measurements revealed that TiO$_2$ specimen would expose the highest surface area for interaction with 30 kDa humic components (Table 1).

Based on the irradiation time-dependent logarithmic decay profiles, photocatalytic degradation of HA was approximated to first order kinetic model (Table 2). Photocatalytic mineralization extents as presented by DOC removal rates (kxDOC, mg/L min), revealed an enhancement was attained upon use of Cu-doping.

Besides kinetics of specific parameters, UV–vis parameters also hold prime importance revealing information as further evaluated with respect to organic carbon contents. More significantly, carbon-based UV–vis parameters (CbColor$_{436}$, CbUV$_{365}$, CbUV$_{280}$ and CbUV$_{254}$) could be calculated as the ratio of the absorbance values (m^{-1}) to the

Table 1 Properties of photocatalyst specimens

Photocatalyst specimen	Crystallite size (nm)	BET surface area (m^2/g)	Pore volume (cm^3/g)	Pore size (nm)	Anatase/rutile (%)
Synthesized TiO$_2$	33.14	50.25	0.169	4.442	87/13
0.25-Cu TiO$_2$	16.23	55.29	0.110	5.120	98/2
0.50-Cu TiO$_2$	17.01	44.22	0.0938	3.336	97/3

Table 2 Pseudo-first-order kinetic constants

Photocatalyst specimen	Pseudo-first-order kinetic reaction constant, k $\times 10^{-2}$ (min^{-1})				
	UV–vis spectroscopic parameters				DOC
	Color$_{436}$	UV$_{365}$	UV$_{280}$	UV$_{254}$	
Synthesized TiO$_2$	1.136	1.246	1.237	1.214	0.515
0.25-Cu TiO$_2$	0.650	0.732	0.770	0.775	0.852
0.50-Cu TiO$_2$	0.795	0.762	0.730	0.692	0.575
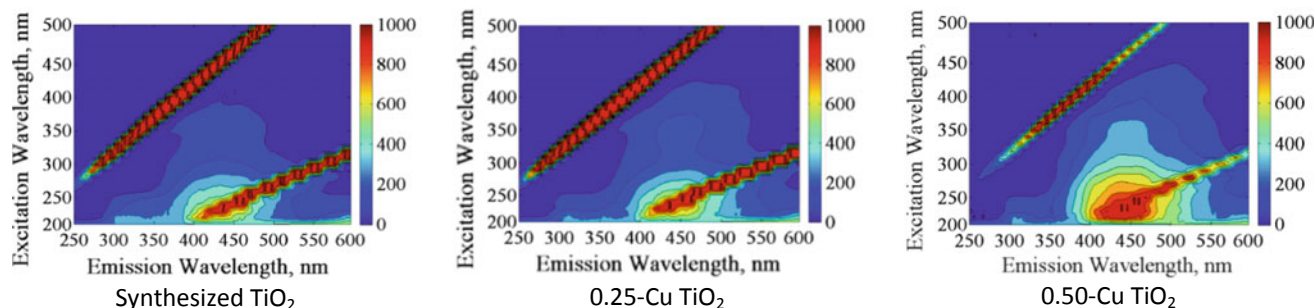
Fig. 1 EEM contour plots of HA for undoped and Cu-doped TiO$_2$ photocatalysts

respective organic carbon contents (mg/L), *i.e.,* absorbance/DOC (L/m.mg). Moreover, EEM fluorescence features of HA for undoped and Cu-doped photocatalysts at irradiation time 60 min were presented in Fig. 1.

4 Conclusion

Upon photocatalytic treatment under solar light irradiation, based on the obtained UV–vis parameters and NPOC removal data, Cu-doped TiO$_2$ photocatalysts samples showed a higher photocatalytic performance with regard to undoped sol–gel synthesized TiO$_2$. Further assessment on the influence of dose effect, 0.25-Cu TiO$_2$ was performed a better photocatalytic performance than 0.50-Cu TiO$_2$ sample. EEM fluorescence contour plots displayed the removal of humic-like fluorophores in accordance with the irradiation periods. Kinetic performances of TiO$_2$ photocatalysts on the degradation of both Suwannee River and Aldrich humic acid solutions were compared. In adsorption experiments, primary adsorption for undoped TiO$_2$ and 0.25-Cu TiO$_2$ photocatalysts was slightly similar and was determined ca. 8%.

On the other hand, ca. 22% was assigned for primary adsorption of 0.50–Cu TiO$_2$ photocatalyst.

References

Sen Kavurmaci, S., & Bekbolet, M. (2014). Tracing TiO$_2$ photocatalytic degradation of humic acid in the presence of clay particles by excitation–emission matrix (EEM) fluorescence spectra. *Journal of Photochemistry and Photobiology A: Chemistry, 282,* 53–61.

Turkten, N., & Cinar, Z. (2017). Photocatalytic decolorization of azo dyes on TiO$_2$: Prediction of mechanism via conceptual DFT. *Catalysis Today, 287,* 169–175.

Uyguner, C. S., & Bekbolet, M. (2005). Evaluation of humic acid photocatalytic degradation by UV–vis and fluorescence spectroscopy. *Catalysis Today, 101*(3), 267–274.

Uyguner-Demirel, C. S., & Bekbolet, M. (2011). Significance of analytical parameters for the understanding of natural organic matter in relation to photocatalytic oxidation. *Chemosphere, 84*(8), 1009–1031.

Hyperspectral Monitoring of a Constructed Wetland as a Tertiary Treatment in a Wastewater Treatment Plant for Domestic Sewage

Agostina Chiavola, Cecilia Bagolan, Monica Moroni, and Simona Bongirolami

Abstract

Constructed wetlands are an efficient technology for wastewater treatment; environmental monitoring via the analysis of hyperspectral data has a huge potentiality; vegetation indices make it possible to synthesize reflectance characteristics related to health state.

Keywords

Constructed wetlands • Hyperspectral sensors • Monitoring • Vegetation indices

1 Introduction

Constructed wetlands (CWs) have been proven to be an efficient technology for wastewater treatment, especially as a tertiary process. Compared to conventional treatment systems, constructed wetlands require lower costs and are more easy to operate and manage. However, the main issue concerning this type of systems lies on the choice of the suitable plants and their distribution within the wetland unit. To ensure that the constructed wetland will work properly, vegetation has to be continuously monitored to verify its health state. This paper presents the application of a ground spectroscopy technique traditionally employed in different sectors of environmental monitoring as: (i) vegetation characterization to identify different plants and the eventual start and evolution of stress situations (Sims and Gamon 2002); (ii) soil monitoring to highlight degradation situations that may determine desertification processes within the wetland plant (Stocking and Clark 1999); (iii) determination of the pollution level of superficial water bodies (Gowen et al. 2011). Wetland vegetation is an important component of wetland ecosystems that plays a vital role in environmental function. It is also an excellent indicator for early signs of any physical or chemical degradation in wetland environments. Mapping and monitoring vegetation species distribution, quality, and quantity are important technical tasks in sustainable management of wetlands (Adam et al. 2010).

In the present case, the spectroscopy-based monitoring technique was used to determine the health state of the plants in a constructed wetland unit of a wastewater treatment plant for domestic sewage. Via the acquisition and analysis of hyperspectral data, it was possible to obtain a qualitative description of selected vegetation species; furthermore, a quantitative analysis was performed by determining the values of vegetation indices (VI) of the investigated species. Broadband and narrowband indices, related to chlorophyll content and to chlorophyll-carotenoid ratio, were computed. The quality of water in the wetland was also detected and related to spectral data.

2 Materials and Methods

2.1 Study Area

The object of this study is the constructed wetland unit located, as a tertiary treatment, in the wastewater treatment plant (WWTP) for domestic sewage of Latina Mare, managed by Acqualatina S.p.A. It has an extension of 5000 m^2, and it is divided into three different sections, from upstream to downstream:

A. Chiavola (✉) · C. Bagolan · M. Moroni
DICEA-Sapienza University of Rome, via Eudossiana 18, 00184 Rome, Italy
e-mail: agostina.chiavola@uniroma1.it

C. Bagolan
e-mail: cecilia.bagolan@gmail.com

M. Moroni
e-mail: monica.moroni@uniroma1.it

S. Bongirolami
Acqualatina S.p.A., Viale P. L. Nervi snc—C.com, Latinafiori—Torre 10 Mimose, 04100 Latina, Italy
e-mail: simona.bongirolami@acqualatina.it

- Section 1: at the beginning of the wetland, is a deep pond with a water level of 1.50 m;
- Section 2: in the middle of the wetland, is a free water surface system with a water level of 0.5 m;
- Section 3: at the end of the wetland, is a deep pond with a water level of 1 m.

Many types of plants have been implanted in the wetland area. In the present work, it was decided to investigate three species: *Iris pseudacurus, Juncus effusus,* and *Nymphaea Alba.* These species are the most diffused in the wetland area and are more resistant to the local weather conditions. Of the three species, *Juncus* and *Nymphaea* are present in Sects. 2 and 3, while *Iris* in all the sections. In general, *I. pseudacurus* is among the most commonly used plants for constructed wetlands because it never goes on vegetative rest and is effective throughout the whole year.

2.2 Data Acquisition

The survey was carried out by collecting data twice a month from April 2018 to May 2018, which is the period when the plants in the wetlands are verdant. Data collection involved the above mentioned three sections. The aim was to correlate the plant health state with the concentrations of pollutants and nutrients in the wetland water. Reflectance values were acquired by means of the field-portable spectroradiometer FieldSpec 4–ASD that operates in the range of wavelengths 350–2500 nm. For each measurement, 2151 data points were collected covering the entire spectral range (350–2500 nm) with a resolution of 1 nm. The spectroradiometer was mounted at a height of 0.15 m above the foliage to ensure a large field of view including the plant only (0.005 m^2). Calibration and optimization were conducted before each spectral measurement using a Spectralon panel as the reference white. For each sample, three spectra were collected and then averaged in order to detect one representative spectral measurement for plant and to reduce noise on the reflectance data. Spectral data were measured between 11:30 a.m. and 1:00 p.m. on clear days.

2.3 Vegetation Hyperspectral Features

Stressful situations, as well as plant senescence, modify the spectral response of vegetation. In the phase of plant senescence, chlorophyll degrades faster than carotene. This entails a significant increase in the visible red area reflectance (600–700 nm), with a measurable decrease of chlorophyll absorption (at 420, 490, and 660 nm). In this situation, carotenoids and xanthophylls become dominant pigments in the leaves, which appear yellow (chlorosis) because these chemical compounds absorb blue light while

reflecting the green and red parts of the visible spectrum. A combination of green and red provides the yellow color observed. When the leaf dies, brown pigments (tannins) appear, reducing the reflectance in the spectral range 400–750 nm (Piro et al. 2017).

The red edge position changes in response to an increase or a decrease in the amount of chlorophyll. In particular, a shift toward lower wavelengths means a decrease of chlorophyll content, which can be associated with an unhealthy condition for the plant.

The leaf maturation sees a gradual increase in the reflection in the NIR (near infrared, 720–1200 nm), while, during the senescence reflectance in the NIR, first increases and then decreases when cells deteriorate.

2.4 Spectral Indices Selection

Spectral signature of leaves or canopies may be used to quantify vegetation indices. These are the result of mathematical operations between reflectance values both in the visible and near-infrared portions of the spectrum. VIs are used to capture essential characteristics of the spectra, in order to reduce the large volume of data usually collected with hyperspectral devices. VIs play also the role of indicators of plant pigment content linked to their eco-physiological state.

Three primary types of indices have been developed for plant stress estimation: simple ratio (SR), normalized difference (ND), and combinations of reflectance (CoR) values at key wavelengths (Moroni et al. 2013).

VIs may be also classified as broadband and narrowband indices. Broadband vegetation indices take into account wavelengths from green, red, VIS, and NIR bands, as vegetation shows specific reflectance properties in these bands. These properties can reveal the health state of the canopy.

In this paper, five broadband indices (TVI, RVI, DVI, NDVI, RDVI) and ten narrowband indices ($NBR_{1,2}$, $NDVI_{705}$, SIPI, $PSND_{A,B,C}$, $PSSR_{A,B,C}$) were considered (Moroni et al. 2013).

3 Results and Discussion

Figure 1 shows one of the determinations of the reflectance spectra of the *Iris* plants in Sect. 1 (blue), Sect. 2 (orange), and Sect. 3 (red). The spectral signatures of the species in the three sections reflect the typical behavior of healthy vegetation. In fact, the spectral signatures present a high value of the green peak (550 nm) and a consistent red edge (700–750 nm). Nevertheless, the spectral response of the plants presents some differences in terms of reflectance values from upstream to downstream. The value of the green peak of the plant in Sect. 1 results much higher than in Sects. 2 and 3. This is related to the

Fig. 1 Comparison between the reflectance spectra of *Iris* in the three sections
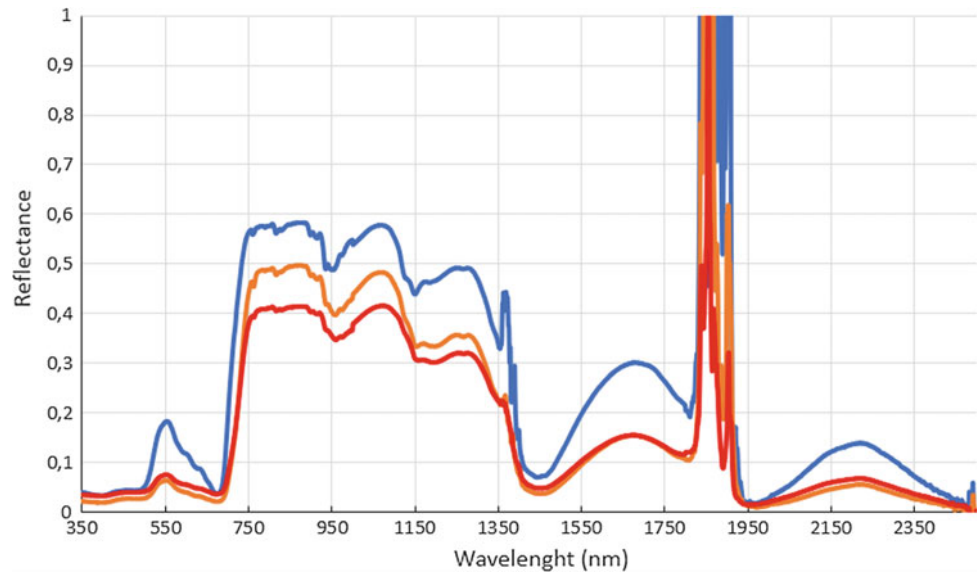
chlorophyll content: The *Iris* plant in Sect. 1 presents a higher concentration of pigments than in the other sections. Furthermore, comparing the NIR plateau and the red edge, the decrease of the reflectance values is significant. Again, this is related to the larger concentration of pigments in the *Iris* plant of Sect. 1 rather than the plants in Sects. 2 and 3. It is worth noting that from a visual inspection, the plants always appear in a good state of health, whereas their observation with the hyperspectral device makes it possible to highlight the differences described above.

The qualitative observations derived from the analysis of the spectral signatures can be quantified via the introduction of vegetation indices. All the investigated indices agree with the results of the qualitative analysis. The value of all the indices decreased from upstream to downstream. The better health state of the plant at the beginning of the wetland unit is likely to be attributed to the higher load of nutrients released by the incoming effluent from the previous treatments.

4 Conclusion

Hyperspectral monitoring of vegetation turned out to be a potentially useful tool to identify and prevent unhealthy conditions. To the authors' knowledge, its extensive application to constructed wetland monitoring has not yet been made. Although it was not possible, due to the unfavorable weather conditions, to study the evolution of the plants under investigation from vegetative rest to flowering, this contribution demonstrates also that hyperspectral data make it possible to

define vegetation indices which may be usefully employed as plant health status indicators. The qualitative analysis of the spectra and the quantitative analysis through the vegetation indices pointed out that most of the plants appear in a good health state, with the plants at the beginning of the pond being in a better state compared to the plants at the end. The preliminary results obtained with this investigation will be complemented in the future investigations.

References

Adam, E., Mutanga, O., & Rugege, D. (2010). Multispectral and hyperspectral remote sensing for identification and mapping of wetland vegetation: A review. *Wetlands Ecology and Management, 18,* 281–296.

Gowen, A., Tsuchisaka, Y., O'Donnell, C., & Tsenkova, R. (2011). Investigation of the potential of near infrared spectroscopy for the detection and quantification of pesticides in aqueous solution. *American Journal of Analytical Chemistry, 2*(8), 53–62.

Moroni, M., Lupo, E., & Cenedese, A. (2013). Hyperspectral proximal sensing of Salix Alba Trees in the Sacco River Valley (Latium, Italy). *Sensors, 13*(11), 14633–14649.

Piro, P., Porti, M., Veltri, S., Lupo, E., & Moroni, M. (2017). Hyperspectral monitoring of green roof vegetation health state in Sub-Mediterranean climate: Preliminary results. *Sensors, 17,* 662.

Sims, A. D., & Gamon, J. A. (2002). Relationships between leaf pigment content and spectral reflectance across a wide range of species, leaf structures and developmental stages. *Remote Sensing of Environment, 81,* 337–354.

Stocking, M. A., & Clark, R. (1999). Soil productivity and erosion: Biophysical and farmer-perspective assessment for hillslopes. *Mountain Research and Development, 19*(3), 191–202.

Applicability of WQI and Scientific Communication for Conservation of River Ganga System in India

Gagan Matta

Abstract

Water one of the most important vital source for the survival of living forms on earth. In the last two decades, a rapid increase in population has given a tremendous increase in uncontrolled development activities leading to the destruction of all major water bodies on earth. River Ganga System, covering 2525 km from the Himalayas to the Bay of Bengal nourishing millions of peoples of India and one of the major source of water and other use in India. With its tremendous use and importance, it is very much important to monitor it on regular basis and categorize its water quality on the basis of water quality indexing. This categorization will help to aware mass depended on the water body for various uses and to policy makers to improve the decision-making system for the betterment of the River Ganga System for its conservation and rejuvenation.

1 Introduction

Surface water quality has increasing importance worldwide especially in developing countries where all the developments from commercial to industrial and domestic are depended on surface water bodies. The concern that fresh water will be a scarce resource in the future has forced the developing countries into the evaluation of the river water quality in recent years. It is necessary to safeguard human health and to protect valuable freshwater resources.

G. Matta (✉)
Hydrological Research Lab., Research Wing, Department of Zoology and Environmental Science, Gurukula Kangri Vishwavidyalaya, Haridwar, India
e-mail: profgaganmatta@gmail.com

Monitoring and assessment of water resources for different purposes are well defined, but sometimes due to large number of samples and it is difficult to evaluate the water bodies. To overcome these difficulties, mathematical or statistical expressions are used to assess the large and complex data. The usefulness of water quality indexes as the indicators of water pollution, with the assessment of ecological changes and classification of river water quality. The WQI is one such tool providing a simple and understandable platform for scientist and policy makers to assess the respective water body more accurately. During the current research work were used to assessed the water quality of dynamic and static flow of River Ganga System in Himalayan Region. Outcome has no values till it reaches to mass in the respective study areas who are directly affected due to changes in water quality. During the study, we have used techniques of scientific communication to share the findings, to understand the decline of water quality and aware the mass that how with small changes in our routine we can help in conservation of River Ganga System.

2 Materials and Methods

Study Area: Himalaya region—north east zone of Garhwal area, India India.
Coordinates: 30° 19′ 48″N to 78° 03′ 36″E.
Water Body: River Ganga System
Sampling Sites: Ten different location (Uttarkashi, Rudrapur, Srinagar, Tehri Dam, Devprayag, Rishikesh, Haridwar, Bahadarabad, Bhogpur and Roorkee)
Number of Samples: 120 samples in triplicate
Duration: Bimonthly
Note: Acid-washed Nalgene wide-mouth natural HDPE polypropylene, 1000 ml bottles were used to collect the samples and transported to the lab for chemical analysis. The samples were stored in the insulated, ice-cooled container.
Water quality parameters: 19 in number

Analytical Procedures:

Onsite Assessment: pH, temperature (Temp.), dissolved oxygen (DO) and total dissolved solids (TDS) were measured by a portable multi-parameter instrument, model—TMULTI 27 (TOSHCON) (Kamboj et al. 2017);

Laboratory analysis: free CO_2, turbidity, total hardness (TH), biochemical oxygen demand (BOD_5), chemical oxygen demand (COD), total suspended solid (TSS), Chloride (Cl^-), Phosphate (PO_4^-), sulphate (SO_4^-), nitrate (NO_3^-), nitrite (NO_2^-), lead (Pb), Copper (Cu), Iron (Fe) and Zinc (Zn) were analysed in laboratory using standard protocol of APHA (2012).

Scientific Communication

Workshops and camps were organized to share the findings among locals, sharing the reason behind the downfall in the water quality methods how we can improve the water quality with minimum changes into the daily routine at domestic, commercial and agricultural level (Matta and Kumar 2017a).

Mode of Demonstrations: Audio-Visual mode

Information shared to individual for water conservation, precautionary measure of water hygiene. Medical camps are organized for the residential colonies of knowledge will be given to the community that how to be safe from polluted water. To share and update the precautionary knowledge with locals how to make water clean before drinking and other uses living near to industrial sites (Matta and Kumar 2017b).

3 Results and Discussion

The minimum value of pH varied from 7.6 to 8.7 throughout the study period, which indicates that the water quality of the Ganga River system was slightly alkaline. The turbidity values represent that the river water was highly turbid especially for the monsoon season (218.2–550.1 NTU) which is the consequence of developmental activities as debris were dumped into river water and run-off water of heavy rainfall in the study area. Only few of the downstream sites showed slightly high values of BOD (4.50 mg/L at site—8 and 3.56 mg/L at site—10). The range of COD was observed between 3.0 and 7.9 mg/L. The monthly variation in TSS ranged from 118.1 to 324.5 mg/l during the study period. The minimum value (93.9 mg/l) of TDS was observed in the autumn season, and the maximum value (290.5 mg/l) was reported in the summer season. The minimum level (0.95 mg/L) of free CO_2 was recorded in winter season, and the maximum level (1.85 mg/L) was noticed in the monsoon season. The lower range (58.01–70.05 mg/L)

of TH was examined in the winter season, and the higher range (89.7–210.0.5 mg/L) was noticed in monsoon season. In this work, five essential nutrients were analysed and observed that the range of the Cl^- (6.9–10.5 mg/L), NO_3^- (0.05–0.06 mg/L) and NO_2^- (0.008–0.012 mg/L) was higher during the summer season. The level of PO_4^- (0.39–0.56 mg/L) and SO_4^- (12.6–43.8 mg/L) was recorded high in monsoon season. The range of all metals analysed, found higher in the summer season except the range of Pb (0.15–0.52), which was higher in the winter season. The range of Cu, Fe and Zn was found 0.59–2.23, 0.06–0.27 and 2.01–9.00 mg/L, respectively.

Water Quality Indexing

The computation of the WQI was done for observed data by a weighted arithmetic index method for the different parameters, implemented by many researchers (Matta et al. 2018a, b). The equation used for the computation of WQI is

$$WQI = \sum_{i=0}^{n} \frac{W_i q_i}{W_i} \qquad (1)$$

where q_i = subindex or quality rating for the ith parameter, W_i = unit weight for the ith parameter.

The calculation of WQI involves four steps: first is the selection of parameters, in this study 13 hydro-chemical variables were selected out of 19 due to the lack of proposed standard limit of drinking water by BIS (2012). The second is the computation of subindex or quality rating (q_i), the equation is expressed as (Brown et al. 1972):

$$q_i = \left\{ \frac{(V_a - V_i)}{(V_s - V_i)} \right\} \times 100 \qquad (2)$$

where q_i = subindex for the ith parameter, V_a = actual value present of the ith parameter at a given sampling station, V_i = ideal value for the ith parameter, V_s = standard value for the ith parameter.

If quality rating = zero, it means the complete absence of pollutants. While, quality rating $0 < q_i < 100$ implies that the pollutants are above the standards (Ahmad 2014). The third step is the calculation of unit weight (W_i) for the ith parameter, which is inversely proportional to the standard value of that particular variable.

$$W_i = \frac{k}{S_i} \qquad (3)$$

where S_i = standard value for the ith parameter, k = proportionality constant, which can be calculated as:

$$k = \frac{1}{\sum \frac{1}{S_i}} \qquad (4)$$

Table 1 Calculated values of WQI of various seasons for Ganga River system

Season	Calculated WQI	Quality status
Autumn	41.69	Good water quality
Winter	39.4	Good water quality
Summer	35.6	Good water quality
Monsoon	65.3	poor water quality

The fourth step is the categorization of computed WQI values into five class for water quality is given as: 0–25 is excellent; 26–50 is good; 51–75 is poor; 76–100 is very poor and above 100 is unsuitable for drinking purposes (Table 1).

4 Conclusion

An assessment of the various physico-chemical parameters along with different heavy metals, the study was carried out to understand the present water quality status of River Ganga system, using WQI and on the basis of findings, awareness among the locals using scientific communication techniques. The comparison of the analytical result of the various parameters indicated that the turbidity, TH, Pb, Cu and Zn concentrations were beyond the acceptable limit specified by Beuro of India (BIS 2012) which makes the river water unfit for potable purposes. After the applicability of WQI, the seasonal river water quality is represented into different quality classes. In this study, the river water quality was found in poor condition during autumn, winter and summer season due to the numerous developmental activities, dumping of agricultural and industrial wastes directly into the river water. However, in monsoon season, the water quality was reported on a very poor condition. Therefore, proper care, maintenance, disposal of waste, chemical and biological treatment are required before using for drinking purposes. A proper scientific communication through workshop, banner, personal interaction with locals and farmers was also conducted to share the finding and to update with methods to how to overcome with it.

References

Ahmad, A. B. (2014). Evaluation of groundwater quality index for drinking purpose from some villages around Darbandikhan district, Kurdistan Region-Iraq. *IOSR Journal of Agriculture and Veterinary Science, 7,* 34–41.

APHA. (2012). *Standard methods of water and wastewater analysis* (22nd ed.). New York, Washington, DC: American Public Health Association.

BIS (Bureau of Indian Standards). (2012). Specification for drinking water IS 10500: 2012, New Delhi, India.

Brown, R. M., McLellend, N. I., Deininger, R. A., & O'Connor, M. F. (1972). A water quality index crashing the psychological barrier. *Indicators of Environmental Quality, 1,* 173–182.

Government of Uttarakhand. (2014). *Uttarakhand Action Plan on Climate Change.*

Kamboj, N., Matta, G., Bharti, M., Kumar, A., Kamboj, V., & Gautam, R. K. (2017). Water quality categorization using WQI in rural areas of Haridwar, India. *ESSENCE-International Journal for Environmental Rehabilitation and Conservation, 8*(2), 108–116.

Matta, G., & Kumar, A. (2017a). Health risk, water hygiene, science and communication. *ESSENCE-International Journal for Environmental Rehabilitation and Conservation, 1,* 179–186.

Matta, G., & Kumar, A. (2017b). Role of science and communication in health and hygiene: a case study. *ESSENCE-International Journal for Environmental Rehabilitation and Conservation, 2,* 95–101.

Matta G, Kumar A, Kumar A, Naik PK, Kumar A. (2018a). Applicability of heavy metal indexing on Ganga River system assessing heavy metals toxicity and ecological impact on river water quality. *INAE Letters, An Official Journal of the Indian National Academy of Engineering.* https://doi.org/10.1007/s41403-018-0041-4.

Matta, G., Kumar, A., Naik, P. K., Tiwari, A. K., & Berndtsson, R. (2018b). Ecological analysis of nutrient dynamics and phytoplankton assemblage in the Ganga river system, Uttarakhand. *Taiwan Water Conservancy, 66*(1), 1–12.

Techno-Economic Feasibility of Membrane Bioreactor (MBR)

Paolo Roccaro and Federico G. A. Vagliasindi

Abstract

MBR CAPEX is higher than CAS+coagulation CAPEX; MBR OPEX is lower than CAS CAPEX; MBR may be economically competitive with CAS +coagulation systems.

1 Introduction

The use of membrane bioreactor (MBR) technology has been steadily growing in the wastewater industry. Initially, the technology was being used on smaller plants mostly treating industrial wastewater. Nowadays, MBR is considered a well established, mature technology with many full-scale plants around the world treating large municipal and industrial wastewater (Judd and Judd 2011; Krzeminski et al. 2017).

Overall, membrane fouling and energy consumption still remain serious operational obstacles and challenges in the wider spread of the MBR technology. However, other technical and economic factors could make the MBR competitive with the conventional activated sludge (CAS) system. Therefore, the objective of the study is to develop cost curves in order to compare the techno-economic feasibility of MBR and CAS systems.

2 Materials and Methods

Estimated costs of wastewater treatment trains represent an important aspect to assess the feasibility and sustainability of wastewater treatment projects for the protection of environment and health.

In order to evaluate and compare the feasibility, MBR with CAS, capital costs, operation and maintenance costs (O&M) and total unit costs (TUC) has been calculated for each treatment train, considering five different sizes (8000, 15,000, 60,000, 110,000, 200,000 equivalent population related to a water supply of 180, 200, 250, 275, 300 L per capita per day, respectively). The total unit cost (TUC) is a useful parameter for a direct comparison of the treatment costs of different schemes. The treatment costs were computed based on the actual price whenever possible according to the methodology proposed by Roccaro et al. (2013). The capital costs include construction costs of building works, costs of electromechanical components, taxes, design costs, contingency costs, etc. The operation and maintenance costs include costs for personnel, energy, reagents, sludge disposal and ordinary and extraordinary repairs. These costs were assessed according to metric estimates, data provided by companies, data based on the literature review and simplify estimates (Roccaro et al. 2013). In the costs calculation, biological processes included nitrogen and phosphorus removal. The total unit cost was computed by the operation and maintenance costs and annual depreciation charge of capital costs as shown in Eq. (1).

$$\mathrm{TUC} = \frac{\mathrm{ADC} + \mathrm{OMC}}{Q} \tag{1}$$

ADC = annual depreciation charge of capital costs (€/y);
OMC = operation and maintenance costs (€/y);
Q = flow rate (m^3/y).

P. Roccaro (✉) · F. G. A. Vagliasindi
Dipartimento di Ingegneria Civile e Architettura, Università degli Studi di Catania, Viale A. Doria, 6, 95125 Catania, Italy
e-mail: paolo.roccaro@unict.it

3   Results and Discussion

Figure 1 shows the cost curves for CAS and MBR systems. The developed cost curves can be used to estimate the CAPEX, OPEX and TUC of different size of wastewater treatment plants employing CAS with tertiary treatment (coagulation based) or MBR systems.

CAPEX of MBR are higher than those found for CAS, while the reverse is in terms of OPEX. This result is corroborated prior research (Iglesias et al. 2017). While the higher CAPEX of MBR is expected due to the cost of the membrane that is expensive, the lower OPEX of MBR is the result of the balance between the higher energy cost of MBR with its lower cost for sludge treatment and disposal. The latter result is also in agreement with prior research (Ozdemir and Yenigun 2013).

Although the presented data is in agreement with prior studies (Ozdemir and Yenigun 2013; Iglesias et al. 2017), local factors may influence the techno-economic feasibility of MBR vs. CAS systems as reported in other prior research (Bertanza et al. 2017).

There are several factors that influence the CAPEX and OPEX of MBR that need deeper investigation. Following are listed as the main advantages and disadvantages of MBR that have a relevant impact on treatment costs.

The advantages offered by the MBR system compared to CAS system are

- operation at biomass concentration and sludge retention time higher than those used for CAS;
- less use of soil thanks to the lower size of reactors;
- elimination of the primary settling unit;
- possible elimination of the disinfection stage;
- better quality of the effluent that is considered osmotizable or suitable for agricultural reuse;
- reduced production and disposal of excess sludge;
- possible production of stabilized sludge;
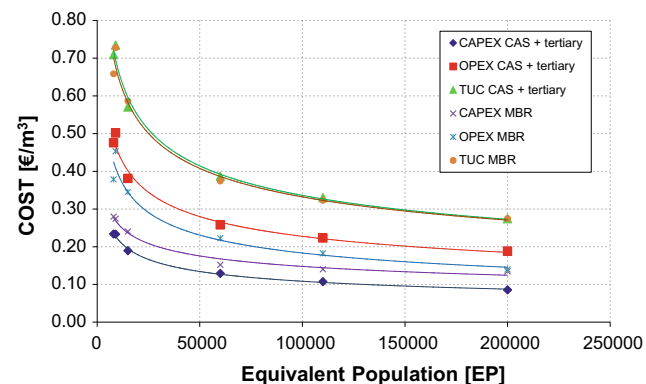
- for ex novo plants, the reduction of the sludge in excess can allow significant savings across the sludge line, which would treat a reduced flow rate compared to a CAS configuration.

MBR plants have also several disadvantages that include:

- membrane fouling resulting in the decline of the permeate flow and short lifetime of membrane;
- foaming issues;
- need of more efficient screens for solid removal;
- need for an equalization tank to control the hydraulic peak load;
- higher process air insufflation due to the higher concentration of biomass in the mixed liquor;
- greater air insufflation for fouling control.

4   Conclusion

Although in many cases, the costs of the MBR are higher than of CAS; the comparison of the data carried out in this study highlights the possibility that the MBR are economically competitive mainly thanks to the production of less excess sludge.

Other factors such as the reduction of membranes cost, the longer life of the membranes and design choices need more investigation to evaluate their impact on MBR cost and resulting techno-economic feasibility.

References

Bertanza, G., Canato, M., Laera, G., Vaccari, M., Svanström, M., & Heimersson, S. (2017). A comparison between two full-scale MBR and CAS municipal wastewater treatment plants: Techno-economic-environmental assessment. *Environmental Science and Pollution Research, 24*(21), 17383–17393.

Iglesias, R., Simón, P., Moragas, L., Arce, A., & Rodriguez-Roda, I. (2017). Cost comparison of full-scale water reclamation technologies with an emphasis on membrane bioreactors. *Water Science and Technology, 75*(11), 2562–2570.

Judd, S., Judd, C. (2011). *The MBR book. Principles and applications of membrane bioreactors for water and wastewater treatment*, 2nd edn. Elsevier Ltd. ISBN: 9780080966823.

Krzeminski, P., Leverette, L., Malamis, S., & Katsou, E. (2017). Membrane bioreactors—A review on recent developments in energy reduction, fouling control, novel configurations, LCA and market prospects. *Journal of Membrane Science, 527*, 207–227.

Ozdemir, B., & Yenigun, O. (2013). A pilot scale study on high biomass systems: Energy and cost analysis of sludge production. *Journal of Membrane Science, 428*, 589–597.

Roccaro P., Sgroi M., Vagliasindi F. G. A. (2013). Removal of xenobiotic compounds from wastewater for environment protection: Treatment processes and costs. *Chemical Engineering Transactions, 32*, 505–510. ISSN: 1974-9791.

Fig. 1 Cost curves (CAPEX, OPEX and TUC) for CAS (employing a tertiary treatment) and MBR systems

Electrochemical Wastewater Treatment with SnO$_2$-Based Electrodes: A Review

Duong Hieu Linh and Tran Le Luu

Abstract

This review paper focuses on discussing SnO$_2$-based electrodes with regard to the stability, their application to water treatment. The approaches have been based on developing new doping routes, new fabrication routes, or combining TiO$_2$ nanotubes with SnO$_2$ catalyst. Operation parameters also need considering thoroughly when SnO$_2$ electrodes are applied to treat wastewater. More effort should be put on optimizing the catalysts and the preparation routes. SnO$_2$-based electrode is a very promise electrode material for electrochemical wastewater treatment.

1 Introduction

The establishment and enforcement of more strict pollution regulations, together with economic and social pressures in order to achieve the goals of sustainable development have stimulated "zero-effluent" processes and have required the development and research of new or more efficient wastewater treatment technologies. On the other hand, because industrial waste is usually composed of organic and inorganic compounds, exhibiting a highly diverse feature, a comprehensive strategy of treatment is unfeasible. Regarding effluents contaminated with organic matters, biological oxidation is certainly the most cost-effective process to treat this type of wastewater, yet this method may be hampered when toxic or bio-refractory substances are present in the wastewater. Because of these facts, industrial effluents are currently treated employing advanced approaches such as physical-chemical methods (coagulation, flocculation), chemical oxidation (use of chlorine, ozone, hydrogen peroxide), and advanced oxidation processes (AOP) (Fenton's reaction, photo-chemistry). Nevertheless, all these methods display a number of considerable disadvantages. In this context, electrochemical oxidation is a promising approach to many environmental problems owing to its easy operation and the fact that it uses a versatile, efficient, cost-effective, and clean reagent, the electron (Martínez-Huitle and Ferro 2006). Moreover, thanks to the intensive studies, electrochemical technologies may be effectively used for disinfection and purification of wastewater contaminated with organic matters. Concerning this, the key factor which has to be considered in order to develop electrochemical oxidation technique is electrode material, and the desired electrodes must be highly efficient in pollutant treatment, must be highly stable under anodic polarization conditions, and must have low investment costs (Meaney and Omanovic 2007). For the electrochemical oxidation of organic compounds, the electrodes possessing high oxygen evolution over-potential are favored, and the typical electrodes of this type which have been extensively studied in the past include graphite, glassy carbon, platinum, boron-doped diamond (BDD), and various metal oxide electrodes including PbO$_2$, IrO$_2$, RuO$_2$, and SnO$_2$. Among these, the metal oxide electrodes, particularly Sb-doped SnO$_2$ electrodes are claimed to be ideal for oxidizing organic matters. However, a major drawback of SnO$_2$ electrodes is their insufficient electrochemical stability (Chen 2004), making the application limited. In this regard, this review paper focuses on discussing SnO$_2$-based electrodes with regard to the stability, their application to water treatment as well as future research directions to make this type of electrode more attractive. Specifically, this paper provides a

D. H. Linh · T. Le Luu (✉)
Department of Mechatronics and Sensor Systems Technology, Vietnamese German University, Thủ Dầu Một, Binh Duong 590000, Viet Nam
e-mail: luu.tl@vgu.edu.vn

short review of SnO_2 properties and mechanisms regarding pollutant electrochemical oxidation. Some typical methods of preparing SnO_2 electrodes, together with the nanostructures synthesized by respective preparation methods are also summarized and presented. Next, the application of SnO_2-based electrodes to water treatment is considered. Last but not least, we describe some studies concerning recent development and future research with SnO_2-based electrodes.

2 Mechanisms for Electrochemically Oxidizing Pollutants

2.1 Indirect Electro-oxidation Processes

Contaminants can be electrochemically oxidized through various ways. One of the popular methods is the utilization of the chlorine and hypochlorite produced at the anode. At a high chloride level, typically higher than 3 g/L, a high number of inorganic and organic contaminants can be effectively degraded. Because chlorinated organic compounds, intermediates or final products are possibly generated, it is difficult for this technique to be widely applied. If the raw wastewater contains a low chloride level, the addition of a large salt quantity is needed to enhance the process efficiency. The electrically produced hydrogen peroxide is also reported for degrading pollutants. This system is based on the electro-Fenton reaction with an addition of Fe^{2+} salts or the in situ formation from a dissolving iron anode. Another electrochemically generated product which can be applied for wastewater treatment is ozone. Another type of electro-oxidation, mediated electro-oxidation is applied by Farmer et al. to remove mixed and hazardous wastes. Metal ions including Ag^{2+}, Co^{3+}, Fe^{3+}, Ce^{4+}, and Ni^{2+}, usually called mediators, are anodically oxidized to a reactive, high valence state. As a result, organic compounds will be attacked by these reactive ions. Additionally, hydroxyl-free radicals which may be also generated in the process can contribute to the removal of the pollutants. However, a highly acidic media needed for the operation and the addition of the heavy metals resulting in the secondary pollution hamper the application of this technique (Panizza and Cerisola 2009).

2.2 Direct Anodic Oxidation

Anodic oxidation or direct oxidation can be done by producing physically adsorbed "active oxygen" (adsorbed hydroxyl radicals, ·OH) or chemisorbed "active oxygen" (oxygen in the oxide lattice, MO_{x+1}). In this process, organic compounds can be completely destroyed by the adsorbed hydroxyl radicals, while selective oxidation products can be generated from the chemisorbed "active oxygen." Generally, pollutants are oxidized more effectively by ·OH than by O in MO_{x+1}.

3 Properties of SnO_2

Tin can attain an oxidation state of 2^+ (stannous oxide SnO) or 4^+ (stannic oxide SnO_2) due to having a dual valence which facilitates a fluctuation of the surface oxygen composition. SnO_2 possesses a tetragonal rutile structure with space group D_{4h}[14] [P4$_2$/mnm], and the unit cell is composed of six atoms, two tin and four oxygen atoms. The unit cell of SnO_2 shows the structure of 6/3 coordination. The lattice parameters are $a = b = 4.737$ Å and $c = 3.185$ Å, hence the c/a ratio standing at 0.673. The ionic radii for O^{2-} and Sn^{4+} are 1.40 and 0.71 Å, respectively. The density of SnO_2 is 6.85 g/cm^3, and the melting point is 1630 °C. As a mineral, the stannic oxide is also called Cassiterite. Noticeably, pure SnO_2 is an n-type broad-band gap (3.6 eV) semiconductor exhibiting the properties of high conductivity and nearly complete, insulator-like transparency. Besides, the carrier density of un-doped SnO_2 is up to 10^{20} cm^{-3} which is comparable to that of semimetals (10^{17}–10^{20} cm^{-3}). In addition, SnO_2 is chemically inert, mechanically hard, and high-temperature resistant. Pure SnO_2 has a very high electrical resistance property and is unsuitable for electrode fabrication. Nevertheless, mixing with Ar, B, Bi, F, P, and Sb makes the conductivity of SnO_2 considerably improved. Among these doping agents, Sb is the most frequently used for SnO_2 for electrochemical applications. The application of doped SnO_2 films as transparent electrodes can be found in high-efficiency solar cells, gas detectors, far IR detectors and transparent heating elements. The onset potential for O_2 evolution on SnO_2 doped with Sb is approximately 1.9 V versus NHE in 0.5 M H_2SO_4 solution, similar to that on PbO_2. Owing to the property of high oxygen evolution over-potential (i.e., poor catalyst for oxygen evolution reaction), the antimony-doped tin oxide is considered as a "non-active" anode and favor complete oxidation of organic matters to CO_2. Hence, Sb-doped SnO_2 electrodes are thought to be ideal for treating wastewater and particularly for oxidizing organic compounds. The additional advantage of SnO_2 is its low cost compared with many other precious metal oxides such as Pt and boron-doped diamond.

4 Fabrication Methods

Generally, fabricating the SnO_2 films can be based on chemical vapor deposition, thermal decomposition, sol-gel dip-coating, spray pyrolysis, and electrodeposition. On the other hand, because of their small size and large surface area,

metal oxide nanostructures show excellent chemical and physical properties which are different from those of bulk materials. Additionally, these nanostructures can be useful for enhancing the performance and stability of the electrode. Therefore, apart from describing typical fabrication methods, this section presents the nanostructures formed by respective preparation methods and provides an overview about the stability of SnO$_2$-based electrodes.

5 Application in Wastewater Treatment

It is indicated that contaminants are oxidized at anode fabricated from titanium coating with Sb-doped SnO$_2$ (Ti/SnO$_2$-Sb$_2$O$_5$), and the efficiency of the oxidative treatment of organic substances at this anode was roughly five times higher than that at Pt electrode. In another study, Bonfatti et al. investigated the reactivity of glucose toward mineralization based on the electrochemical incineration at Pt, SnO$_2$-Pt composite, and PbO$_2$ electrodes with the supporting electrolyte of 1 M H$_2$SO$_4$. It is pointed out that this type of tin dioxide-based electrode was inefficient in incinerating electrochemically organic compounds. Glucaric acid which was found as the main oxidation intermediate is seemingly difficult to be attacked at this electrode.

Comninellis reported that the current efficiency for Ti/SnO$_2$–Sb$_2$O$_5$ was 0.58 in order to degrade 71% of phenol, whereas the figures obtained on PbO$_2$, IrO$_2$, RuO$_2$, and Pt were 0.18, 0.17, 0.14, and 0.13, respectively, at the experiment conditions including the current density of 500 A/m^2, pH 12.5, initial concentration of 10 mM, reaction temperature of 70 °C. Grimm et al. studied phenol oxidized in a means of cyclic voltammetry using Ebonex/PbO$_2$ and Ti/SnO$_2$ electrodes. The best results were achieved on the Ti/SnO$_2$ electrode fabricated with a sol-gel dip-coating technique. Moreover, it is shown that doping the sol-gel solution with 10% Sb helped to improve the conductivity of the SnO$_2$-films and get higher current density for the oxidation. Zanta et al. investigated p-chlorophenol oxidation on SnO$_2$–Sb$_2$O$_5$-based anodes and found that 75% of the organic compounds were degraded. Adams et al. researched the treatment of 2-nitrophenol (2-NPh), 3-nitrophenol (3-NPh), and 4-nitrophenol (4-NPh) using SnO$_2$-based mixed oxide electrodes, namely Ti/SnO$_2$–Sb$_2$O$_5$, Ti/SnO$_2$–Sb$_2$O$_5$–PtO$_x$, Ti/SnO$_2$–Sb$_2$O$_5$–RuO$_2$, and Ti/SnO$_2$–Sb$_2$O$_5$–IrO$_2$ and pointed out that Ti/SnO$_2$–Sb$_2$O$_5$–IrO$_2$ would be promising in the application of electrochemical wastewater treatment due to its long lifetime and being highly active in the removal of nitrophenols. Additionally, the study results confirmed that the most efficient current was at 100 mA, and the rate constants for the electrochemical oxidation decreased in the order of: 2-NPh > 4-NPh > 3-NPh. Polcaro et al. used PbO$_2$-based and SnO$_2$-based anodes to research the electrochemical oxidation of 2-chlorophenol. It was concluded that Ti/SnO$_2$ anode was preferable because it can better oxidize toxic substances with the faradaic yield of approximately 50%. Nevertheless, the presence of only a small quantity of easily biodegradable oxalic acid in the effluent could stop electrolysis at SnO$_2$ electrode.

6 Conclusion

Electrochemical oxidation is a promising approach to many environmental problems in general and water treatment in particular. Among electrode materials, Sb-doped SnO$_2$ is claimed to be ideal for oxidizing organic matters due to its high oxygen evolution over-potential and its low cost compared with many other metal oxides. However, as mentioned above, insufficient electrochemical stability makes the application of SnO$_2$ electrodes limited. In order to overcome this disadvantage and also increase electrochemical performance, many advanced and intensive studies have been conducted based on developing new doping routes (e.g., IrO$_2$-doped SnO$_2$–Sb$_2$O$_5$, SnO$_2$–Sb$_2$O$_3$–PtO, Ti, Ru, Sn, Sb metal oxide coating), together with new preparation routes (such as block copolymer-based soft template, or the combined application of several methods to fabricate the anode, or the traditional fabrication routes developed to form the nanostructures of the electrode). Combining TiO$_2$ nanotubes with SnO$_2$ catalyst (e.g.,) is also a promising strategy producing TiO$_2$ nanotubes-based unique micro-structured electrodes with remarkable oxidation ability and strong stability. Concerning the application of the SnO$_2$-based electrodes to water treatment, besides electrode material, operation parameters (e.g., pH, current density, with or without chloride added to the solution) are crucial factors affecting removal efficiency. Therefore, in order to develop further electrochemical oxidation technique with SnO$_2$-based electrodes and achieve the goals of "zero-effluent," more effort should be put on optimizing the catalysts and the preparation routes. In addition, advanced SnO$_2$-based electrodes should be applied to research the treatment of various kinds of wastewater and find out the optimized operation parameters.

References

Chen, G. (2004). Electrochemical technologies in wastewater treatment. *Separation and Purification Technology, 38,* 11–41.

Martínez-Huitle, C. A., & Ferro, S. (2006). Electrochemical oxidation of organic pollutants for the wastewater treatment: direct and indirect processes. *Chemical Society Reviews, 35,* 1324–1340.

Meaney, K. L., & Omanovic, S. (2007). $Sn_{0.86}$–$Sb_{0.03}$–$Mn_{0.10}$–$Pt_{0.01}$-oxide/Ti anode for the electro-oxidation of aqueous organic wastes. *Materials Chemistry and Physics, 105,* 143–147.

Panizza, M., & Cerisola, G. (2009). Direct and mediated anodic oxidation of organic pollutants. *Chemical Reviews, 109,* 6541–6569.

Rajeshwar, K., Ibanez, J. G., & Swain, G. M. (1994). Electrochemistry and the environment. *Journal of Applied Electrochemistry, 24,* 1077–1091.

Walsh, F. C. (2001). Electrochemical technology for environmental treatment and clean energy conversion. *Pure and Applied Chemistry, 73,* 1819–1837.

Control of Hazardous Substances in Water and Recovery of Renewable/Valuable Resources from Wastewater

Statistical Analysis of the Quality Indicators of the Danube River Water (in Romania)

Alina Bărbulescu, Lucica Barbeş, and Anita Dani

Abstract

Analysis of the distribution of the water quality indicators of the Danube River during the period 2010–2012 for the surface water in Chiciu area (km 375). Analysis of the correlation of the quality indicators at the observation points. Similarity and dissimilarity studies of the parameters' series at the observation points. Mathematical modeling of the indicators series.

1 Introduction

Nowadays, in most regions of the world, there is a continuing degradation of water quality. Water quality is a major issue for the sustainable development of any country. For its preservation, it is necessary to initiate and implement strategic programs for monitoring the physicochemical and ecological parameters. According to the Water Framework Directive 2000/60/EC, approved by the European Commission, it is necessary to ensure the "very good" status for all water bodies.

In most cases, the rivers' water is used for human needs, such as water supply, irrigation, and power generation. But, due to the erosion and sedimentation processes, surface water undergoes continuous changes that influence the water quality parameters (Issa et al. 2015). Surface water quality is increasingly affected by pollution with different chemical compounds. In aquatic systems, pollutants are distributed through diffusion and advection processes. Their transport can be described and forecast by mathematical models (Hakanson and Boulion 2003).

Water quality is assessed by the following categories of indicators: hydromorphological (water depth, flow, width and level); physical (water temperature, pH, electrical conductivity, transparency, turbidity, temporary, permanent and total hardness); chemical (dissolved oxygen, COD-Mn, COD-Cr, BOD) (Teodosiu et al. 2015), nutrients (nitrogen and phosphorus compounds), metals (Cd, Hg, Zn, Cr, Cu, Ni, As, Ag, Mo, Se, Co), organic and inorganic micropollutants (detergents, pesticides, phenols, cyanides, hydrocarbons); biological (plankton, benthic algae and macroozobentos); and microbiological (coliforms and streptococci). Pollution sources of surface waters are different and are classified in diffuse and point-to-point. The diffuse ones are pollutants from agricultural and industrial activities, while the others arise from the chemical industry, mining or households, and so on.

Surface water quality parameters can be modelled using neural networks (Antanasijevic et al. 2014). For example, two models have been proposed for modelling the total phosphorus: a simple one, with an input variable and another more complex, with 14 input variables. The relationships between phosphorus and other water quality parameters have been established. Five different types of neural networks—linear, generalized regression neural network (GRNN), radial basis function (RBF), multilayer perceptron with one or two hidden layers—have been used (Mozejko et al. 2008).

COMSOL Multiphysics software for dynamic simulation of accidental pollution on a flowing water sector can be also applied (Cristea et al. 2010). Descriptive statistics, graphical

A. Bărbulescu · L. Barbeş (✉)
Ovidius University of Constanta, Romania, 124 Mamaia Blvd.,
900527 Constanta, Romania
e-mail: lucille.barbes2009@gmail.com

A. Bărbulescu
e-mail: emma.barbulescu@yahoo.com

A. Dani
Higher Colleges of Technology, Sharjah, United Arab Emirates
e-mail: adani@hct.ac.ae

analysis and multivariate statistical analysis are used to study the water hydrogeochemical characteristics (Lu et al. 2015). Graphic methods include the Durov diagram, the Stiff diagram, the Piper diagram, and the Gibbs diagram. Common methods of multivariate statistical analysis include factorial analysis (Zhu et al. 2006; Zhang et al. 2006; Marusic and Ciufudean 2016), principal component analysis (Wang et al. 2010), and cluster analysis (Chattopadhyay and Singh 2013).

In this article, we aim at analysing the Danube River water quality based on data collected at three points at Chiciu, in Romania. We conduct a similarity study and compare the resulted parameters with the admissible limits in order to observe the number of exceedances in the study period.

2 Materials and Methods

2.1 Study Area and Water Quality Data

The Danube River is the collector to the Black Sea of all discharges from upstream countries, affecting the quality of the Danube Delta waters and the Black Sea coast. Chiciu (the "crossing place" in Slavonic) is the area of the ferryboat terminals on DN3 national road in Romania. Chiciu km 375 is located in the Dobrogea catchment area, which is situated in the southeastern part of Romania.

The monitored sections are part of the highly modified water body (CAPM)—Chiciu-Isaccea RORW14.1_B4, with a length of 275.5 km and the typical typology RO14. The data set used in this study was collected twice a month during the period 2010–2012 on the Danube River at Chiciu km 375 station at three sites: left bank—RO142900_1, middle—RO142900_2, right bank—RO142900_3, latitude 44.13 and longitude 27.27 (Fig. 1).

All water samples collected during the study period were analyzed for a large number of water quality parameters, including pH, alkalinity, BOD, COD-Cr, COD-Mn, N-NH4,

N-NO3, P, conductivity, fix residue, Cu, Cr, As, Ni, Pb dissolved. These elements were monitored and analyzed based on the quality standards imposed by the Romanian legislation.

2.2 Methodology

Statistical tests are performed for assessing the types of data distribution. The outliers and change points' existence is checked as well.

Multivariate analysis of variance, multiresponse Permutation Procedures, analysis of group similarities and the Mantel test are used to distinguish if the groups of data collected at the three sites differ one from the other.

To determine which variables best distinguish among the groups, classification and regression trees, the discriminant analysis and the logistic regression are employed.

3 Results and Discussion

The distributions of all parameters, but the pH, are right-skewed, some of them, with outline values (especially As, Cr, Ni, Pb). Some series present change points, as, for example, the concentration of As (Fig. 2). A high variation of the pollution level has been recorded in the middle of the period.

Comparing the pollution levels with the maximum admissible ones, it resulted that during the study period, the maximum admissible has been exceed only few times.

The similarity analysis applied to the series registered at the same site for the three years showed that there are some variations of the species' concentrations at each site and each river bank. Also, the similarity analysis applied to the series registered during the observation period at the three sites suggested a dissimilarity of the pollution with different species on the river's banks, the left bank being more polluted than the right one or the middle of the river.
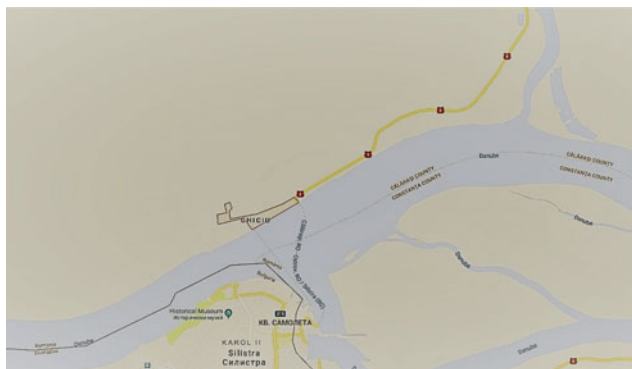
Fig. 1 Danube River and the monitoring stations (Chiciu km 375)
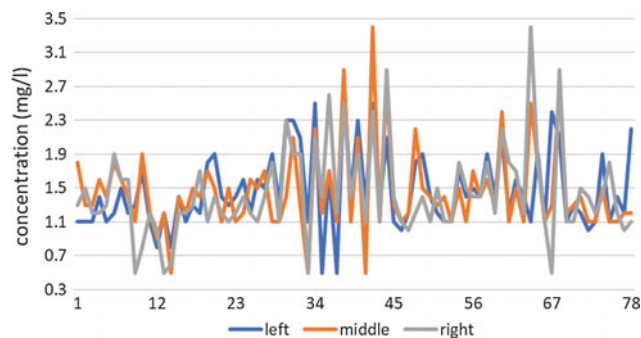
Fig. 2 Series of As concentration

4 Conclusion

The integrated water resources management issued from the necessity of an efficient approach of diminishing the water pollution, since the release of a big quantity of metals and organic compounds in the environment raised concerns related to their accumulation and negative effect for the human life (Teodosiu et al. 2015).

The evaluation of the chemical state and ecological potential of water of the main watercourse of the Danube River in the Chiciu area km 375 has been done during the period 2010–2012 by applying the monitoring methodologies in conformity to the Water Framework Directive Water 2000/60/EC. It was found that the ecological state of the main watercourse of the Danube River in the Chiciu area km 375 was good during the study period. The results proved that there are only a few significant differences among the water quality parameters at the three sites.

This research will be extended for other zones along the Danube River, especially in the Nature Reserve Danube Delta.

References

Antanasijevic, D., Pocajt, V., Peric-Grujic, A., & Ristic, M. (2014). Modelling of dissolved oxygen in the Danube River using artificial neural networks and Monte Carlo Simulation uncertainty analysis. *Journal of Hydrology, 519,* 1895–1907.

Chattopadhyay, P. B., & Singh, V. S. (2013). Hydrochemical evidences: Vulnerability of atoll aquifers in Western Indian Ocean to climate change. *Global and Planetary Change, 106,* 123–140.

Cristea, V., Bagiu, E., Agachi, P.: Simulation and control of pollutant propagation in Someş River using COMSOL multiphysics. In *Proceedings of the 20th European Symposium on Computer Aided Process Engineering–ESCAPE 20*, Italy, pp. 985–991 (2010).

Hakanson, L., & Boulion, V. (2003). A general dynamic model to predict biomass and production of phytoplancton in lakes. *Ecological Modelling, 165*(2–3), 285–301.

Issa, I. E., Al-Ansari, N., Knutsson, S., & Sherwany, G. (2015). Monitoring and evaluating the sedimentation process in Mosul dam reservoir using trap efficiency approaches. *Engineering, 7,* 190–202.

Lu, S. B., Pei, L., & Bai, X. (2015). Study on method of domestic wastewater treatment through new-type multi-layer artificial wetland. *International Journal of Hydrogen Energy, 40*(34), 11207–11214.

Marusic, G., & Ciufudean, C. (2016). The use of Navier-Stokes equations in modeling water quality in river-type systems. *International Journal of Mathematical Models and Methods in Applied Sciences, 10,* 317–320.

Mozejko, J., Gniot, R., & Polish, J. (2008). Application of neural networks for the prediction of total phosphorus concentrations in surface waters. *Polish Journal of Environmental Studies, 17*(3), 363–368.

Teodosiu, C., Robu, B., Cojocariu, C., & Barjoveanu, G. (2015). Environmental impact and risk quantification based on selected water quality indicators. *Natural Hazards, 75*(1), 89–105.

Wang, Y., Wang, L., Xu, C., Ji, J., Xia, X., An, Z., et al. (2010). Hydro-geochemistry and genesis of major ions in the Yangtze River, China. *Geological Bulletin of China, 29*(2–3), 446–456.

Zhang, Y., Wu, Y., Wen, X., & Su., J. (2006). Application of environmental isotopes in water cycle. *Advances in Water Science*, *17*(5), 738–747.

Zhu, X., Wang, Z., Li, J., Yu, L., & Wang, J. (2006). Applications of SWAT model in Zhang Wei River Basin. *Progress in Geography, 25*(5), 106–111.

Statistical Analysis of the Water Quality of the Major Rivers in India

Anita Dani and Alina Bărbulescu

Abstract

This study presents a longitudinal analysis of pollution profiles of rivers in India. Pollution profiles of 40 in India are created based on the levels of the biochemical oxygen demand (BOD). The cluster analysis has been used to represent groups of rivers with similar levels of pollutants. The longitudinal analysis has been used to reveal how the profiles change over six years from 2007 to 2012. The analysis is used for detecting rivers which remained polluted throughout.

Keywords

Pollutants • BOD • Statistical analysis • Clustering

1 Introduction

Nowadays, water pollution is one of the most important issues all over the world, and particularly, in India. More than 70% of the fresh water in this country cannot be used for consumption[1] (Dwivedi 2017). Water pollution has an adverse effect not only on the health of people using the polluted water or living in its vicinity but also on the soil fertility and the crops' quality. Consumption of polluted water can provoke diseases (cholera, diarrhoea, dysentery, jaundice and tuberculosis) that can affect the entire community in a region.

Given the importance of freshwater for human life, scientists raised their concern about the accelerating pollution of the freshwater and the importance of maintaining the water quality for the future generation (Falkenmark 1993). The pollution sources are the sewage discharge, industrial effluents and agricultural run-off. Their effects have been studied in many articles (Gleick 1993), while the effect of water pollution on the ecosystems has also been analysed (Dugan 1972).

The report of Ministry of Environment and Forest [2] presents the situation of the water pollution in India, the trend of water quality in the main rivers' basins, while the criteria for identification of polluted rivers are given in (Sahoo et al. 2017). Other studies contain the results of the analysis of the water quality of selected rivers in India (Bora and Goswami 2017; Kaushik et al. 2010; Singh et al. 2018; Trivedi and Vediya 2012)

Pollution level of water is determined by the concentration of several pollutants. The indicators of the water quality, measured at different sites are the pH level, electrical conductivity (EC), total dissolved solids (TDS), total suspended solids (TSS), dissolved oxygen (DO) and biochemical oxygen demand (BOD).

In this article, we discuss the level of BOD in more than 40 rivers in India during a period of six years and we classify those rivers in clusters function of the levels of pollution.

2 Materials and Methods

Data used in this study was collected by ENVIS Centre on Control of Pollution Water, Air and Noise (see Footnote 1). In the present analysis, only one variable was considered—biochemical oxygen demand (BOD).

The total amount of oxygen required by aerobic micro-organisms for complete degradation of organic wastes

---

[1]ENVIS Centre on Control of Pollution Water, Air and Noise, http://www.cpcbenvis.nic.in/water quality_ data.html.

A. Dani (✉)
Higher Colleges of Technology, Sharjah, United Arab Emirates
e-mail: adani@hct.ac.ae

A. Bărbulescu
Ovidius University of Constanţa, Constanţa, Romania
e-mail: alinadumitriu@yahoo.com

---

[2]www.indiaenvironmentportal.org.in/files/file/GhaggarReport.pdf.

present in a water body is termed as biochemical oxygen demand (BOD). This is an indicator of organic pollution, higher values indicating higher levels of organic pollution. BOD values above 5 mg/l are undesirable (Bora and Goswami 2017).

Firstly, the statistical analysis of the distribution of the main pollutants was performed for each river, given that on each there are many observation points.

The second important step is the classification of the rivers function of the level of pollution with different pollutants, using a two-step clustering method on the mean value of the variable BOD. Cluster analysis was done using SPSS. Five clusters were determined in order to define differentiated profiles indicating different levels of BOD. Based on the mean value of BOD in each cluster, five profiles were defined on the scale of Very low, Low, Medium, High and Very high levels of BOD. These profiles were created for each year.

In the third stage, pollutants' profiles evolution is presented. Due to this longitudinal analysis, it is possible to detect changes in the pollution profile of each year. For example, some rivers may be found highly polluted in comparison with other rivers in the first year, but may become less polluted in the following years. On the other hand, some rivers may remain in the cluster of highly polluted rivers all the years.

Finally, the comparison of results is provided.

3 Results and Discussion

Table 1 contains the cluster sizes (expressed as %) for each year. It can be seen that in the year 2007, almost 71% of rivers were having very low levels of BOD but this number decreased drastically during the subsequent years. This is an indication of the increase in pollution levels. The percentage of rivers in the Very high cluster was the highest during the year 2010 but decreased in the following year. Unfortunately, this decline was not steady.

As mentioned before, those profiles indicated levels of BOD but the levels are not constant. The mean values of pollutant levels in each group indicate the cluster centres.

Table 2 shows the cluster centres for each cluster in each year. The rivers in the cluster Very low level in 2007 have BOD levels less than 5, which is an indicator of drinkable water. The same year, the remaining 29% of rivers had BOD levels beyond the accepted level, indicating that the water in those rivers is not suitable for drinking. In the year 2009, only 3% of rivers had BOD levels greater than 5 mg/l. The data for the year 2010 indicate that all rivers had BOD levels of less than 5 mg/l. This is not sufficient to conclude about overall purity of water as other parameters are not considered. Figures 1 and 2 summarize the distribution and the changing of BOD values in each cluster.

The classification provides the rivers with major pollution that require urgent attention from the authorities. The pollution decrease has been emphasized for another group of rivers, for which amelioration measures have been implemented.

After doing a comparative study, looking at individual records, the rivers which showed decline in the pollutant level and those that constantly belonged to the Very high cluster each year were investigated.

Sabarmati River, which had a very high level of BOD during the year 2007, indicated drastic decline in the following years, whereas river Ghaggar and rivers in Andhra Pradesh and Madhya Pradesh were always included in the Very high cluster.

4 Conclusion

We proposed a new method of comparative analysis, which can be used for monitoring pollution levels of a large number of rivers. The cluster analysis resulted in disjoint groups of rivers, such ad the rivers with similar levels of BOD were included in the same group. The advantage of such clustering is that the grouping is not done on the fixed

Table 1 Cluster sizes

Year	Very low (%)	Low (%)	Medium (%)	High (%)	Very high (%)
2007	70.6	14.7	5.9	5.9	2.9
2008	29.4	41.2	23.5	2.9	2.9
2009	26.3	47.4	15.8	7.9	2.6
2010	42.1	28.9	18.4	5.3	5.3
2011	29.7	32.4	32.4	2.7	2.7
2012	30.6	25.0	33.3	5.6	5.6

Table 2 Cluster centres for each cluster in each year

	2007	2008	2009	2010	2011	2012
Very low	2.09	0.25	0.35	0.37	1.36	0.38
Low	6.58	0.95	0.8	0.93	2.77	0.91
Medium	10.18	2.21	1.55	1.79	4.65	1.76
High	14.37	3.85	2.86	2.7	18.26	4.57
Very high	52.23	5.61	4.05	5.3	25.92	5.91
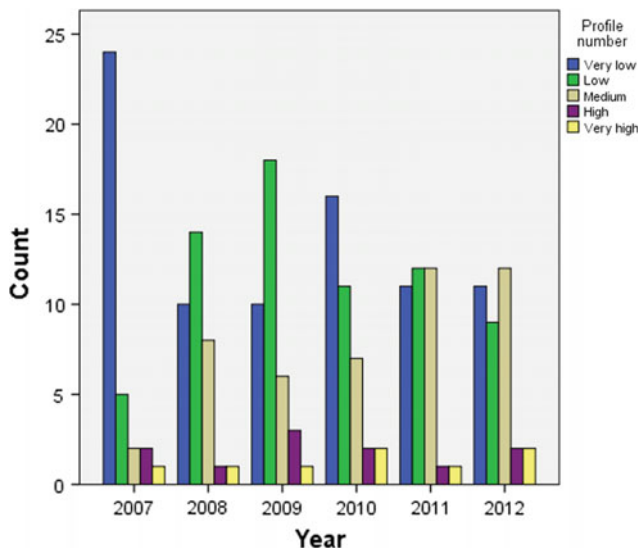
Fig. 1 Distribution of percentages in each cluster per year
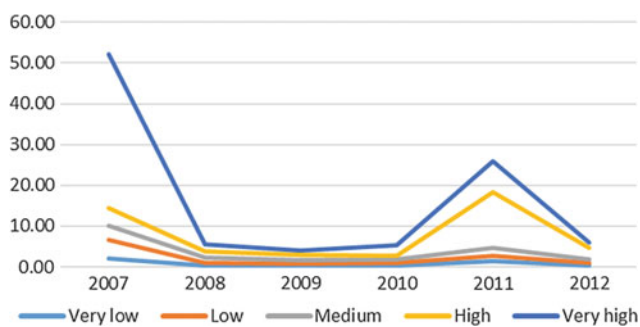
Fig. 2 Changes in the mean BOD for each cluster per year

values, but the mean of each cluster was calculated on the basis of actual values, which may change each year. This study can be extended by creating comprehensive purity profiles of rivers based on more than one parameter. The results of our study can be used by the authorities for taking decisions on implementing the necessary measures for cleaning the water and stopping its pollution.

References

Dwivedi, A. K. (2017). Researches in water pollution: A review. *International Research Journal of Natural and Applied Sciences, 4*(1), 118–142.

Falkenmark, M. (1993). Water scarcity: Time for realism. *Populi, 20*(6), 11–12.

Gleick, P. (1993). An introduction to global freshwater issues. In P. Gleick (Ed.), *Water in crisis* (pp. 3–12). New York: Oxford University Press.

Dugan, R. (1972). *Biochemical ecology of water pollution*. New York: Plenum Publishing Co., Ltd.

Sahoo, M. M., Patra, K. C., Swain, J. B., & Khatua, K. K. (2017). Evaluation of water quality with application of Bayes' rule and entropy weight method. *European Journal of Environmental and Civil Engineering, 21*(6), 730–752.

Bora, M., & Goswami, D. C. (2017). Water quality assessment in terms of water quality index (WQI): Case study of the Kolong River, Assam, India. *Applied Water Science, 7*(6), 3125–3135.

Kaushik, A., Sharma, H. R., Jain, S., Dawra, J., & Kaushik, C. P. (2010). Pesticide pollution of river Ghaggar in Haryana, India. *Environmental Monitoring and Assessment, 160*(1–4), 61–69.

Singh, G., Kumari, B., Sinam, G., Kumar, N., & Mallick, S. (2018). Fluoride distribution and contamination in the water, soil and plants continuum and its remedial technologies, an Indian perspective—a review. *Environmental Pollution, 239,* 95–108.

Trivedi, H. B., & Vediya, S. D. (2012). Assessment of nitrate contamination of the groundwater samples in Bhiloda Taluka of Sabarkantha district, Gujarat. *International Journal of Pharmacy & Life Sciences, 3*(11), 2103–2106.

Methane and Hydrogen Production from Cotton Wastes in Dark Fermentation Process Under Anaerobic and Microaerobic Conditions

Gaweł Sołowski, Izabela Konkol, and Adam Cenian

Abstract

Dark fermentation of textile wastes is discussed in the paper. The fermentation was carried out under the following conditions: load 5 g/L, pH was varied in the range 6.23–7.8, and oxygen in small quantities was added. The oxygen flow rates (OFR) were between 1 and 4.6 mL/h. The highest volumes of methane were obtained under anaerobic conditions (pH 6.23 and 7.8), while production of hydrogen was larger under oxygen flow rate 4.6 mL/h and pH value 6.23.

1 Introduction

Dark fermentation (DF) is a type of anaerobic digestion process, where various substrates are converted into hydrogen, carbon dioxide and low organic acids (Chaganti et al. 2012). Before viable DF industrialization, a methane generation, the process that removes hydrogen from the biogas, must be inhibited. Another problem is hydrogen sulphur formation; this can be prevented by addition of oxygen in small amounts (Terry 2010; Duangmanee 2009; Khosh-nevisan et al. 2017). Thus, it seems worth checking which process, methanogenesis or hydrogenesis, is more sensitive to the presence of oxygen. The addition of 2–8% oxygen helped in hydrogen production in photofermentation and

was called microaerobic dark fermentation (Abo-Hashesh and Hallenbeck 2012). Due to the high content of cellulose and low of lignin, cotton wastes can be considered as a promising material for fermentation (Sołowski 2016)—this was checked in this paper.

2 Materials and Methods

The fermentation process of cotton wastes was performed in reactors (jars) of volume 2 dm^3. As inoculum, sludge from a biogas plant in Lubań (Pomerania Region), 5 g/L volatile suspended solids (VSS), were applied to each batch of cotton waste. The reactors were kept under mesophilic conditions (37 °C). The substrate (load 5 g/L) used was obtained from a 100% cotton lab coat, milled and hydrolysed using 0.1 M acidic solution for 2 h. After adding cotton to the inoculum, the pH value of mixture in some reactors was lowered (using 50% H_2SO_4) from 7.8 to 6.23. The oxygen flow rates: 0, 1, 1.5 and 4.6 mL/h were applied. The oxygen was added twice a day for 26 days. The results obtained are compared to the earlier studies (Sołowski et al. 2018) for higher pH value 7.54. The biogas production was determined using the Owen method, but its content was registered using a TCD Gas Chromatograph (GC).

3 Results and Discussion

The GC analysis allowed determination of methane, hydrogen, hydrogen sulphide, carbon dioxide and nitrogen concentrations. The biogas production was continued ~ 27 days. In the case of VSS = 5 g/L, the pH value, shortly after H_2SO_4 addition, was 6.23 or 6.4. The methane production after ~ 27 days were 0.94 and 2.94 dm^3 for OFR 4.6 mL/h (pH 6.4) and 1 mL/h (pH 6.23), respectively. The ratio of concentrations of the main biogas components CH_4: $CO_2 = 60.5:34.3$ and $58.6:29.7$ for OFR 1 mL/h (pH 6.23) and 4.6 mL/h (pH 6.4).

G. Sołowski (✉) · I. Konkol · A. Cenian
Instytut Maszyn Przepływowych im R. Szewalskiego, Polskiej Akademii Nauk, Gdańsk, Poland
e-mail: gsolowski@imp.gda.pl

I. Konkol
e-mail: iz.konkol@gmail.com

A. Cenian
e-mail: cenian@imp.gda.pl

Fig. 1 Time evolution of methane production for cotton waste and sour cabbage for VSS 5 g/L; cotton under strict anaerobic conditions—pH 7.8 (blue rhombi) and OFR 1.5 mL/h (blue asterisks). and OFR 1 mL/h (pH 6.23—green triangles) and OFR 4.6 mL/h (pH 6.5—violet crosses). The methane production from sour cabbage under anaerobic conditions (red squares) and for OFR 0.63 mL/h (orange dots)
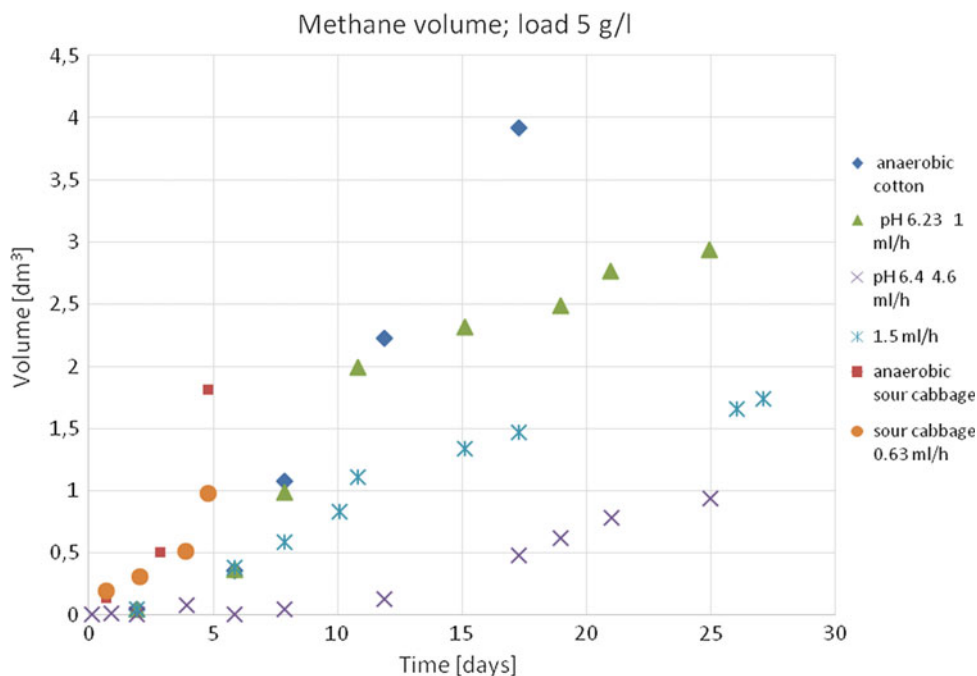
The methane production under anaerobic conditions (pH 7.8) was 3.92 dm^3 (after 415 h–17.1 days), and 1.74 dm^3 for OFR 1.5 mL/h (after 650 h–27 days). In the first anaerobic case, the concentration of methane was 63.8% (22.3% of carbon dioxide). The hydrogen production (during almost 25 days) was very low: 0.002 and 0.006 dm^3 for OFR 1 mL/h (pH 6.23) and OFR 4.6 mL/h (pH 6.4), respectively. Under anaerobic conditions (and pH 7.8), hydrogen production was 0.0003 dm^3 (during 415 h– 17.1 days) which is much smaller than in the case of OFR 1.5 mL/h, i.e. 0.0019 dm^3.

The data are compared with results for VSS 5 g/L of sour cabbage (Sołowski et al. 2018). The results of the comparison are shown in Fig. 1.

The methane production is 2.1 times larger (in volume) for cotton than for sour cabbage (although over 5 times longer fermentation time).

The hydrogen production from sour cabbage and OFR 0.63 mL/h was 3 times higher than for waste cotton and OFR 1.5 mL/h and 12% higher than for OFR 4.6. Similarly, to hydrogen production from sour cabbage (Sołowski et al. 2018), also for cotton waste, the microaerobic fermentation conditions lead to 6 times higher yields than the anaerobic conditions. In contrast, microaerobic conditions lead to lower methane generation (even more than 2 times) although the period of methane production can be longer (e.g. 10 days).

OFR rates suitable for hydrogen production are higher for cotton waste than for sour cabbage.

4 Conclusions

Waste cotton is a potential source of methane. Under anaerobic conditions and VSS 5 g/L, methane production was 3.92 dm^3 during 17.1 days (methane content up to 63.8%). The cotton was a weak hydrogen source under conditions of the experiment. Microaerobic conditions support not only hydrogen production from sour cabbage but also from cotton waste. Microaerobic conditions in the case of cotton waste prolonged the process of methane production up to 27.1 days but decreased methane production (its lower content in obtained biogas). A lowering pH value (e.g. 6.4) lead to an increase of hydrogen and decrease of methane production. The oxygen seems to play the role of a stress factor for bacteria, and when carefully controlled can lead to stable hydrogen production via dark fermentation. These phenomena need further research.

References

Abo-Hashesh, M., & Hallenbeck, P. C. (2012). Microaerobic dark fermentative hydrogen production by the photosynthetic bacterium, *Rhodobacter capsulatus* JP91. *International Journal of Low-Carbon Technologies, 7*(2), 97–103.

Chaganti, S. R., Kim, D. H., & Lalman, J. A. (2012). Dark fermentative hydrogen production by mixed anaerobic cultures: Effect of inoculum treatment methods on hydrogen yield. *Renewable Energy, 48*, 117–121. Available at: http://dx.doi.org/10.1016/j.renene.2012.04.015.

Duangmanee, T. (2009). *Micro-aeration for hydrogen sulfide removal from biogas*. Iowa State University. Available at: http://lib.dr.iastate.edu/etd/10748.

Khoshnevisan, B., et al. (2017). A review on prospects and challenges of biological H_2S removal from biogas with focus on biotrickling filtration and microaerobic desulfurization. *Biofuel Research Journal, 4*(4), 741–750. Available at: https://www.biofueljournal.com/article_53413.html.

Sołowski, G. (2016). Theoretical potential of hydrogen production from textiles wastes in pomeranian region by means of dark fermentation. *Globalizacja a Regionalna Ochrona Srodowiska, 1*, 313–317.

Sołowski, G., et al. (2018). Hydrogen and methane production under conditions of dark fermentation process with low oxygen concentration. In T. Sabu (Ed.), *Proceedings of the International Conference on Reuse and Recycling (ICRM 2018)*, Kottayam, Kerala, India.

Terry, P. A. (2010). Application of ozone and oxygen to reduce chemical oxygen processing plant. *International Journal of Chemical Engineering, 2010*, 1–6.

Microalgae Production Coupled with Simulated Blackwater Treatment

Luan de Souza Leite, Maria Teresa Hoffmann, and Luiz Antonio Daniel

Abstract

Efficiency of simulated blackwater treatment by UASB was analyzed. Removal of N, P, and DOC by *Chlorella sorokiniana* was evaluated. Total ammonia removal was obtained.

1 Introduction

The microalgae cultivation may be practiced for different aims, such as producing a wide range of bioenergy, including bioelectricity and biodiesel (Baicha et al. 2016), removing emerging contaminant (Norvill et al. 2016), being used as organic slow-release fertilizer (Coppens et al. 2016) and wastewater treatment (Ramsundar et al. 2017).

Microalgae growth and wastewater treatment combination appears as a promising solution to overcome current high costs of microalgae cultivation (Franchino et al. 2016). It also ensures a wastewater safe disposal reducing the nutrient discharge in which may cause severe prob-lems in aquatic environmental, like the eutrophication phenomenon.

In Brazil, between 6 and 20 L is used per flush, what promotes the domestic wastewater dilution. This condition becomes impossible to obtain a considerable biomass, and a possible solution could be the mixing of the wastewater with another kind of wastewater. Piggery wastewater has been used by many researchers showing good results (de Godos et al. 2009) and is very available in Brazil, once the country occupies the third place in swine meat production in the world (EMBRAPA 2018).

In this work, *Chlorella sorokiniana* production using blackwater simulated (a mixture between domestic and piggery wastewater) was investigated, aiming its production characterization by nutrient removing during the variation of both physical and chemical wastewater quality parameters.

2 Materials and Methods

2.1 Sample Collection

Wastewater for the experiment was taken from full-scale wastewater treatment plant (WWTP) of São Carlos, São Paulo State, Brazil. The population served by WWTP is approximately 200,000 inhabitants. This plant is characterized as a separated sewer system treatment around 20 million m^3 of wastewater per year. The piggery wastewater was collected from the Santo Inácio de Loyola Farm, located in the city of Brotas, São Paulo State, Brazil (22° 14′ 12.0″S, 47° 58′ 06.3″W). This farm contains around 23,000 pigs, producing about 250 m^3 of piggery wastewater per day.

2.2 Experimental Unit

In a laboratory situated inside the WWTP installations, the simulated blackwater was weekly prepared (mixture between 400 L of piggery and 1200 L of domestic wastewater) and

L. de S. Leite (✉) · M. T. Hoffmann · L. A. Daniel
Department of Hydraulics and Sanitation, São Carlos School of Engineering, University of São Paulo, Av. Trabalhador São-Carlense, 400, São Carlos, São Paulo 13566-59, Brazil
e-mail: luanleite@usp.br

M. T. Hoffmann
e-mail: mariateresa@usp.br

L. A. Daniel
e-mail: ldaniel@sc.usp.br

was treated in an upflow anaerobic sludge blanket (UASB). The reactor is 4 m of length and 450 mm of diameter with treatment capacity of 650 L and hydraulic retention time (HRT) of 3 days.

The UASB effluent was collected and left in three-flat-panel photobioreactors (PBRs) operating in batch, with 50 L in each one. The microalgae cultivation was carried out during 4 weeks, with average light intensity of 196 μmol m^2 s^{-1}, aeration rate of 0.6 vvm, 10 L of microalgae acclimated in wastewater as inoculum, photoperiod of 16:8 (day:night), 30 °C of temperature and hydraulic retention time (HRT) of 7 days.

2.3   Analysis

Simulated blackwater and UASB effluent were monitored weekly using the following parameters: pH, alkalinity (2320 A), biochemical oxygen demand BOD (5210 B), chemical oxygen demand (COD, 5220 D), soluble COD filtrated in membrane 0.45 μm (sCOD, 5220 D), total solids (TS, 2450 B), total suspended solids (TSS, 2450 D) and volatile total solids (VTS, 2450 E).

The samples from the FBR effluent were taken daily in order to monitor the dry weight, absorbance (wavelength of 680 nm), COD, sCOD, dissolved organic carbon (DOC, 5310 B), total suspended solids (TSS, 2450 D), pH, alkalinity, ammonia (NH$_3$, 4500 C), soluble phosphorus (PO$_3^{-4}$, 4500 E), nitrite (NO$_2^-$, HACH 8507) and nitrate (NO$_3^-$, HACH 10020) concentrations. All analyses were performed in triplicate and the methodology number shown is equivalent to Standard Methods (APHA 1998).

3   Results and Discussion

The organic matter characterization of simulated blackwater and UASB effluent is shown in Table 1. The large range of simulated blackwater showed a large variability of mixture characteristics, similar to those reported previously (Chys et al. 2018).

In Table 2, the effluent characteristics after 7 days of cultivation in each batch are shown. Due to the variation in organic matter, there are a large range of nutrient concentrations. The final pH value is similar to other microalgae cultivation studies without artificial pH control (chemicals products or with CO$_2$ application) (Vadlamani et al. 2017). The alkalinity tendency varied during the cultivation, decreasing until a minimum value and rising up after. The carbon form present in the wastewater has already reported by other study (Zhang et al. 2014).

In addition to the nutrient absorption by microalgae, the physical conditions like high pH range (range 9–10) and aeration might also promote the ammonia remotion by air stripping (Zhang et al. 2012). This remotion does not allow a higher nutrient uptake by microalgae because of the N:P ratio, since the nitrogen decays drastically in the first few days (Zhang and Chen 2015).

4   Conclusion

The experimental results showed an improvement in the final effluent quality using simulated blackwater treatment by UASB followed by PBRs. Even with a large variability in physical and chemical wastewater parameters, considerable

Table 1 Characterization of simulated blackwater treatment by UASB

Parameters	Simulated blackwater		UASB effluent	
	Range	Average	Range	Average[a]
pH	6.4–7.4	6.8	7.4–7.6	7.5
Alkalinity (mg/L)	1071–2077	1642	1253–1991	1620
COD (mg/L)	3507–9757	6992	378–884	547 (92.2)
BOD (mg/L)	1955–5410	3643	164–330	207 (94.3)
sCOD (mg/L)	954–1953	1450	175–304	262 (81.9)
TS (mg/L)	1369–7030	3737	957–1616	1286 (65.6)
VTS (mg/L)	1873–5163	3518	325–485	414 (88.2)

[a]Average removal in %

Table 2 Analysis of parameters and efficiency in the FBR effluent after 7 days of cultivation

Parameters	Influent range	Week 1[a]	Week 2[a]	Week 3[a]	Week 4[a]
Dry weight (g/L)	–	0.98 ± 0.06	0.95 ± 0.14	0.94 ± 0.09	0.95 ± 0.04
pH (–)	8.8–9.0	9.2 ± 0.0	9.0 ± 0.2	9.2 ± 0.2	9.0 ± 0.2
Alkalinity (mg/L)	1036.9–1753.9	664.5 ± 24.9 (62.1)	422.8 ± 60.8 (59.2)	561.7 ± 52.7 (56.4)	474.2 ± 42.6 (67.0)
COD (mg/L)	573–777	970 ± 37	976 ± 5	1480 ± 50	953 ± 9
sCOD (mg/L)	211–351	281 ± 10 (15.3)	204 ± 20 (8.5)	224 ± 18 (24.8)	220 ± 7 (37.2)
TSS (mg/L)	323–520	672 ± 28	784 ± 92	680 ± 16	672 ± 25
DOC (mg/L)	61–150	109.4 ± 2.8 (27.1)	58.9 ± 0.5 (3.7)	70.2 ± 3.7 (13.7)	70.3 ± 2.8 (38.4)
NH_3 (mg/L)	178.6–298.4	0.0 ± 0.0 (100)	0.0 ± 0.0 (100)	0.0 ± 0.0 (100)	0.0 ± 0.0 (100)
NO_3^- (mg/L)	0.87–1.67	0.6 ± 0.5 (37.9)	1.3 ± 1.3 (24.0)	1.3 ± 1.3	1.0 ± 0.2
NO_2^- (mg/L)	0.52–3.61	3.4 ± 0.5	0.6 ± 0.5 (76.7)	8.8 ± 1.3	5.6 ± 0.1
PO_3^{-4} (mg/L)	15.8–20.5	7.3 ± 0.8 (57.4)	8.9 ± 1.0 (58.6)	9.4 ± 1.1 (40.8)	8.4 ± 0.2 (59.2)

[a]Average removal in %

nutrient removals were obtained. The pH control might be the key to improve the microalgae growth in these conditions. Due to the alkaline condition, the ammonia removal occurs by air stripping reducing the nitrogen available and consequently limiting microalgae growth.

References

APHA. (1998). *Standard methods for examination of water and watewater* (20th ed.). Washington: American Public Health Association.

Baicha, Z., Salar-garcía, M. J., Ortiz-martínez, V. M., Hernández-fernández, F. J., & Ríos, A. P. D. L. (2016). A critical review on microalgae as an alternative source for bioenergy production: A promising low cost substrate for microbial fuel cells. *Fuel Processing Technology Journal, 154,* 104–116. https://doi.org/10.1016/j.fuproc.2016.08.017.

Chys, M., Demeestere, K., Nopens, I., Audenaert, W. T. M., & Van Hulle, S. W. H. (2018). Municipal wastewater effluent characterization and variability analysis in view of an ozone dose control strategy during tertiary treatment: The status in Belgium. *Science of the Total Environment, 625,* 1198–1207. https://doi.org/10.1016/j.scitotenv.2018.01.032.

Coppens, J., Grunert, O., Van Den Hende, S., Vanhoutte, I., Boon, N., Haesaert, G., et al. (2016). The use of microalgae as a high-value organic slow-release fertilizer results in tomatoes with increased carotenoid and sugar levels. *Journal of Applied Phycology, 28*, 2367–2377. https://doi.org/10.1007/s10811-015-0775-2.

de Godos, I., Blanco, S., García-Encina, P. A., Becares, E., & Muñoz, R. (2009). Long-term operation of high rate algal ponds for the bioremediation of piggery wastewaters at high loading rates. *Bioresource Technology, 100,* 4332–4339. https://doi.org/10.1016/j.biortech.2009.04.016.

EMBRAPA. (2018). *Estatísticas - Desempenho da produção* (WWW Document). https://www.embrapa.br/suinos-e-aves/cias/estatisticas (in Portuguese).

Franchino, M., Tigini, V., Varese, G. C., Mussat Sartor, R., & Bona, F. (2016). Microalgae treatment removes nutrients and reduces ecotoxicity of diluted piggery digestate. *Science of the Total Environment, 569–570,* 40–45. https://doi.org/10.1016/j.scitotenv.2016.06.100.

Norvill, Z. N., Shilton, A., & Guieysse, B. (2016). Emerging contaminant degradation and removal in algal wastewater treatment ponds: Identifying the research gaps. *Journal of Hazardous Materials, 313,* 291–309. https://doi.org/10.1016/j.jhazmat.2016.03.085.

Ramsundar, P., Guldhe, A., Singh, P., & Bux, F. (2017). Assessment of municipal wastewaters at various stages of treatment process as potential growth media for *Chlorella sorokiniana* under different modes of cultivation. *Bioresource Technology, 227,* 82–92. https://doi.org/10.1016/j.biortech.2016.12.037.

Vadlamani, A., Viamajala, S., Pendyala, B., & Varanasi, S. (2017). Cultivation of microalgae at extreme alkaline pH conditions: A novel approach for biofuel production. *ACS Sustainable Chemistry and Engineering, 5,* 7284–7294. https://doi.org/10.1021/acssuschemeng.7b01534.

Zhang, B., & Chen, S. (2015). Optimization of culture conditions for *Chlorella sorokiniana* using swine manure wastewater. *Journal of Renewable and Sustainable Energy, 7.* https://doi.org/10.1063/1.4923326.

Zhang, L., Lee, Y. W., & Jahng, D. (2012). Ammonia stripping for enhanced biomethanization of piggery wastewater. *Journal of Hazardous Materials, 199–200,* 36–42. https://doi.org/10.1016/j.jhazmat.2011.10.049.

Zhang, Q., Wang, T., & Hong, Y. (2014). Investigation of initial pH effects on growth of an oleaginous microalgae Chlorella sp. HQ for lipid production and nutrient uptake. *Water Science and Technology, 70,* 712–719. https://doi.org/10.2166/wst.2014.285.

Waterborne Diseases in Sebou Watershed

Rachida El Morabet, Mohamed Aneflouss, and Said El Mouak

Abstract

Starting from an extremely important territory from an ecological and socioeconomic point of view but subject to a strong constraint linked to anthropic pressures. We show in this work how global change has the potential to affect human health through the deterioration of water quality.

Keywords

Sebou watershed • Water pollution • Sources of water pollution • Infectious diseases • Human health

1 Introduction

The water resources of the Sebou watershed are one of the most important water resources in Morocco (30% of Morocco's surface water resources and 20% of the national groundwater potential). However, pollution at the Sebou watershed level that exceeds by far all national standards (SWA 2014). Its negative effects on biodiversity, agricultural development may/will probably constitute a potential risk of constituting a potential vector for the proliferation of epidemics. The current situation can be considered catastrophic. This region is under an increasing anthropogenic pressure from a variety of uses, resulting in significant levels of pollution and a vulnerable socioecological system.

2 Materials and Methods

This work has been executed on the basis of the information provided by: (a) field investigations: the analysis of the files (of water disease) of the regional hospital Al Idrissi of 2014 (b) report on the assessment of water quality in the Sebou watershed. 2014 (c) remote sensing.

3 Results and Discussion

The Sebou watershed is the second most populated basin of the Kingdom of Morocco. It has 7.4 million inhabitants [2014 statistics, (HCP)], and approximately 21.7% of the total population of Morocco, with an average annual growth rate of 1.8% compared to 1.4% for the rest of the country between 2004 and 2014. Its population is growing faster than the national average. The increase in industrial facilities, the development of the agricultural sector and the extension of urban areas are causing rapid and uncontrolled degradation of the water quality of Sebou watershed. The high pollutant load contaminated the groundwater which circulates at shallow depths (from 4 to 15 m) under a permeable substratum (Fig. 1).

The water microbiological quality remains the most important concern in worldwide public health. Water contamination plays a very important role in disease propagation due to lack of sanitation; water contaminated by human, animal or chemical waste can lead to the local population getting multiple sicknesses like cholera, typhoid, polio, hepatitis A and E, and diarrhea. The results of the survey conducted in the main hospital of the Gharb region in 2014 show the extent of the spread of water diseases in the region (Fig. 1; Tables 1, 2 and 3).

The data show that:

- The percentage of diarrhea and gastroenteritis is bigger than other diseases. There are many contaminants that can cause it (57.1%) (Table 1).

R. El Morabet (✉)
LADES Lab., CERES Center, FLSH-M,
Hassan II University of Casablanca, Casablanca, Morocco
e-mail: rachidaelmorabet@yahoo.fr

M. Aneflouss · S. El Mouak
LADES Lab., FLSH-M, Hassan II University of Casablanca,
Casablanca, Morocco
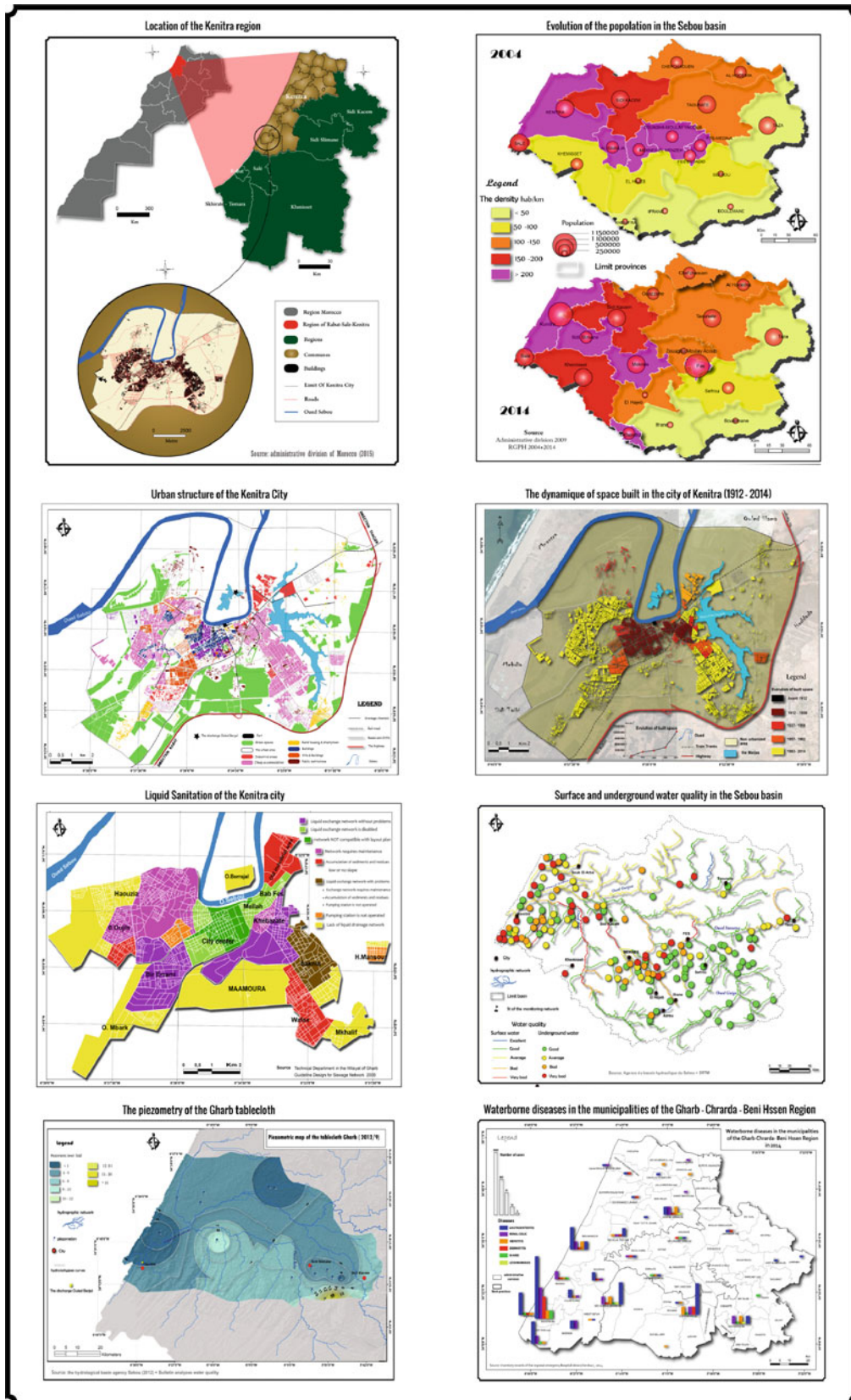
Fig. 1 Data from the study area

Table 1 Frequency of some diseases associated with water pollution at the Idrissi regional hospital by age, 2014

The type of disease	Age												Total
	<5	05–10	11–15	16–20	21–25	26–30	31–35	36–40	41–45	46–50	51–60	60>	
Anemia	*33*	*34*	*14*	*19*	*20*	*20*	*9*	*11*	*9*	*11*	*20*	*36*	*236*
Renal colic	*5*	*3*	*7*	*5*	*17*	*22*	*9*	*13*	*17*	*12*	*15*	*15*	*140*
Dermatitis	*7*	*5*	*6*	*3*	*6*	*5*	*1*	*1*	*4*	*0*	*3*	*6*	*47*
Hypothyroidism	0	0	0	2	1	1		2	0	0	1	2	9
Hepatitis A + E	*1*	*1*	*5*	*4*	*3*	*5*	*4*	*4*	*2*	*3*	*10*	*10*	*52*
Gastroenteritis Diarrhea	**52**	**33**	**47**	**70**	**67**	**70**	**54**	**47**	**40**	**31**	**73**	**75**	**659**
Leishmaniasis	0	0	0	0	0	0	0	0	0	1	0	0	1
Meningitis	0	0	1	1	0	1	0	0	2	1	1	1	8
Typhoid	0	1	0	0	0	0	0	0	0	0	0	1	2
Total	98	77	80	104	114	124	77	78	74	59	123	146	1154

Table 2 Frequency of waterborne diseases by sex at the Idrissi regional hospital, 2014

The type of disease	Men		Women		
	Number	%	Number	%	Total
Anemia	*78*	*6.8*	*158*	*13.7*	*236*
Renal colic	*66*	*5.7*	*74*	*6.4*	*140*
Dermatitis	*18*	*1.6*	*29*	*2.5*	*47*
Hypothyroidism	3	0.3	6	0.5	9
Hepatitis A + E	*26*	*2.3*	*26*	*2.3*	*52*
Gastroenteritis Diarrhea	**253**	**21.9**	**406**	**35.2**	**659**
Leishmaniasis	0	0.0	1	0.1	1
Meningitis	3	0.3	5	0.4	8
Typhoid	2	0.2	0	0.0	2
Total	449	*39.0*	704	*61.0*	1154

Table 3 Monthly distribution of some diseases associated with water pollution at the Idrissi regional hospital, 2014

Month	Anemia	Renal colic	Dermatitis	Diarrhea	Hypothyroidism	Hepatitis A + E	Inflammation of the stomach and intestines	Leishmaniasis	Meningitis	Typhoid	Total
January	15	5	2	7	0	40	1	0	1	5	76
February	17	6	1	8	1	39	0	0	0	5	77
March	20	7	4	5	2	50	0	0	0	6	94
April	18	7	6	4	2	58	0	1	0	*3*	99
May	18	17	12	8	1	66	0	0	0	*5*	**127**
June	18	21	8	4	2	59	0	1	0	*4*	**117**
July	20	10	5	6	0	67	0	0	1	*3*	**112**
August	19	12	3	3	1	54	0	1	0	*3*	**96**
September	34	16	2	3	0	47	0	2	0	*5*	**109**
October	14	15	3	7	0	32	0	1	0	5	77
November	19	10	1	5	0	36	0	1	0	5	77
December	24	14	0	15	0	36	0	1	0	3	93
Total	236	140	47	75	9	584	1	8	2	52	1154

- Women are the major affected category (61%) (Table 2).
- There is a high incidence of diseases in warm months (Table 3). In the Tables 1, 2 and 3; the bold font of the type of disease represents the most widespread and dangerous diseases, while the bold font in months indicates the high number of patient cases in the hot season. Font in italic refers to the second dangerous class of disease prevalent in the study area.

4 Conclusion

The achievement of water security requires the coordination of the actors in an appropriate regulatory framework. The depollution in the Sebou watershed is urgent if we want to insure the economic and social development of the region.

References

HCP. (2014). *Report (Statistics) of the High Commission to the Plan (HCP)*.

SWA. (2014). *Report of the Sebou Watershed Agency (SWA)*.

Chances and Barriers of Wastewater Heat Recovery from a Multidisciplinary Perspective

Florian Kretschmer and Thomas Ertl

Abstract

The heating sector is a key energy sector in the European Union. Wastewater contains significant amounts of thermal energy. Heat recovery from wastewater can support the energy transition. Wastewater heat recovery concerns a multitude of different disciplines.

1 Introduction

Climate change is one of the grand challenges of our times. Consequently, the energy strategy of the European Union (European Commission s.a.) proposes staggered targets for renewables, energy efficiency and emission reductions to finally reducing greenhouse gas emissions by at least 80% until 2050. In this context, it is of crucial importance not only to focus on the energy and mobility sectors but on the heating (and cooling) sector as well. This is due to the fact that the latter already is and expectedly remains the biggest energy sector in the European Union (European Commission 2016). Currently, this sector still strongly depends on fossil resources.

Already more than ten years ago, Sanden and Azar (2005) described that short-term climate targets might be achieved by an increased application of "customary" technologies (e.g. biomass, wind power, solar energy), improved energy efficiency and the substitution of coal by natural gas.

Concerning long-term goals, they state the need for broad application of far more advanced technologies. However, also the development of unexploited renewables could be an option to support the energy turn. Consequently, the energy content of wastewater has become a focal point of interest in recent years. Wastewater contains two forms of energy, chemical-bound energy from organic matter as well as thermal energy (Nowak et al. 2015). While the former can be recovered as methane-containing biogas by means of anaerobic sludge treatment (digestion), the latter will be made accessible through heat exchangers and heat pumps. Kretschmer et al. (2016) estimated degrees of electrical and thermal self-sufficiency for several wastewater treatment plants (WWTPs) with anaerobic sludge treatment. Their investigations showed that electrical self-sufficiency might only be achieved under optimised operational conditions. Thermal self-sufficiency, in contrast, seems much easier to be reached even under average performance. The considerations of both heat sources, digester gas-based heat and recoverable heat from wastewater reveal potential degrees of thermal self-sufficiency beyond 800%.

Based on the above said, two core messages can be derived: (1) Renewable heat supply is of tremendous importance for the success of the energy transition and (2) wastewater contains notable amounts of surplus heat, which still have remained rather untapped so far. Consequently, the question arises about the possible role wastewater could play as a source of renewable thermal energy (heat). To answer this question, this article presents and (briefly) discusses different chances and barriers related to wastewater heat recovery from an interdisciplinary perspective. Although elaborated under Austrian national circumstances, the results obtained are of general nature and thus easily transferable to other countries to provide guidance and orientation for multidisciplinary planning of wastewater heat recovery also under other specific boundary conditions.

F. Kretschmer (✉) · T. Ertl
University of Natural Resources and Life Sciences, Vienna,
Institute of Sanitary Engineering and Water Pollution Control,
Muthgasse 18, 1190 Vienna, Austria
e-mail: florian.kretschmer@boku.ac.at

T. Ertl
e-mail: thomas.ertl@boku.ac.at

297

2 Materials and Methods

The materials used for defining the chance and barriers related to wastewater heat recovery were the following: (1) An analysis of the heat potential available at more than 600 Austrian WWTPs considering wastewater related and spatial criteria, (2) results from seven Austrian national case studies concerning the economic and environmental feasibility of wastewater heat recovery, (3) an Austrian regional stakeholder analysis for identifying key stakeholder groups to be involved in wastewater heat recovery planning also considering their related level of knowledge, general attitude and information paths, (4) a measurement campaign for wastewater flow and temperature of very high spatial and temporal resolution (18 measurement sites along a flow distance of 18 km during a period of five months) in an Austrian sewer system and (5) comprehensive literature review concerning wastewater as a resource, wastewater heat recovery in the context of sewer and WWTP operation and maintenance as well as policy instruments to support practical application of wastewater heat recovery.

The methodological approach for defining the different chances and barriers followed a three-stage approach. In the process, depending on the specific research question, the existing material was hermeneutically analysed and interpreted: First, to prepare a multidisciplinary understanding of the issue, an integrated analysis of the system "wastewater heat recovery" was carried out. This included the identification of all relevant disciplines (sub-systems) as well as their systemic connections. Second, to reduce complexity and make the system analysis more tangible for practical considerations, different thematic fields concerning wastewater heat recovery were aggregated. This process step included both, theoretical aspects from the integrated system analysis as well as practical experiences from the case studies and the stakeholder analysis. Third, for each thematic field, chances and barriers were identified based on the experiences from the preliminary working steps and the related contents of the available material. Their final discussion considered again the available material as well as further international literature.

3 Results and Discussion

The above described analysis revealed seven thematic fields relevant to wastewater heat recovery from a multidisciplinary perspective: (1) Availability, (2) economic efficiency, (3) climate protection, (4) wastewater management and water pollution control, (5) stakeholder management, (6) spatial planning and (7) institutionalisation.

Availability on the one hand concerns the energy supply and on the other hand the heat demand. For Austria, Neugebauer et al. (2015) estimate the available thermal energy in the effluent of more than 600 WWTPs beyond 3.000 GWh/a. Furthermore, their spatial analysis showed that about two third of the investigated plants are in close distance or even within existing settlements. Consequently, the availability of significant amounts of heat in the adequate distance to potential consumers provides a great chance for wastewater heat recovery.

In the context of economic efficiency, it can be noted that according to Meeten (2017) there are estimated 700–1000 wastewater heat recovery facilities already being installed on a global level, and tendencies are further increasing. Kollmann et al. (2017) calculate and proof the economic chances related to wastewater heat recovery for an Austrian case study. Consequently, the economic efficiency of wastewater heat recovery appears feasible at many places around the world.

Concerning climate protection, Neugebauer et al. (2015) calculate CO_2 emissions and global warming potentials of different heat generation systems (wastewater heat pump, wood chip combustion, heat from natural gas). In this context, depending on the electricity mix applied to run the heat pump, wastewater heat recovery can be very competitive. Consequently, wastewater heat recovery can also provide a promising opportunity in regard with climate protection.

Wastewater management and water pollution control concern the operation of sewers and WWTPs. According to Kretschmer and Ertl (2010), in sewer wastewater heat recovery can have negative impacts on the functionality of sewers as well as on the temperature sensitive processes of wastewater treatment. Consequently, wastewater management related requirements can represent a certain barrier for wastewater heat recovery. However, problems will be avoided, if wastewater heat recovery takes place in the effluent of a WWTP. Furthermore, wastewater heat recovery can generate additional income for operators of wastewater utilities.

Regarding stakeholders, Lindemann (2016) identifies 12 different stakeholder groups being affected by the energetic use of wastewater. Due to the multidisciplinary character of the issue, stakeholder management is a key aspect of wastewater heat recovery (whom to involve how and when). A large variety of management methods and tools are available today. Targeted stakeholder management requires skill, experience and certain effort, but it provides a great chance for developing optimal, durable and widely accepted solutions.

Also, spatial planning plays an important role in the context of wastewater heat recovery. This is due to the fact that transport distances between the heat source and

consumption point have a great influence of the efficiency of the supply system (transport heat loss). Targeted spatial planning (settlement development towards existing heat sources) and optimisation of existing and future settlement structures can support an efficient heat supply. However, a lack of planning guidelines and legal requirements concerning integrated spatial and energy planning might hamper respective activities.

Finally, institutionalisation concerns the establishment of a (national, regional, local) framework to promote the practical application of wastewater heat recovery. Suitable framework conditions (application of policy instruments, definition of implementation goals, etc.) can catalyse the activation of available wastewater heat sources. In contrary, their lack as well as a missing political initiative certainly represents a great barrier regarding large-scale practical implementation of wastewater heat recovery.

4 Conclusion

The evaluation of chances and barriers related to wastewater heat recovery gives clear evidence that wastewater as a source of renewable heat could offer great chances in fighting climate change. Considerable quantities of wastewater heat are available, and already today a competitive and climate friendly supply is possible in many places. In any case, we consider the potential barriers related to wastewater heat recovery (e.g. undisturbed operation of wastewater infrastructure, lack of planning guidelines, missing institutional framework conditions) surmountable. Consequently, wastewater could be a valuable element of a future, diversified and local energy mix. This article shall mark a step in this direction.

References

European Commission. (2016). *Communication from the commission to the European parliament, the council, the European economic and social committee and the committee of the regions—An EU strategy on heating and cooling*. COM (2016) 51 final, Brussels.

European Commission. (s.a.). *Energy strategy and energy union—Secure, competitive, and sustainable energy*. https://ec.europa.eu/energy/en/topics/energy-strategy-and-energy-union. Accessed May 18, 2018.

Kollmann, R., Neugebauer, G., Kretschmer, F., Truger, B., Kindermann, H., Stoeglehner, G., et al. (2017). Renewable energy from wastewater—Practical aspects of integrating a wastewater treatment plant into local energy supply concepts. *Journal of Cleaner Production, 155,* 119–129.

Kretschmer, F. (2017). *Abwasser als erneuerbare Energiequelle—Potenziale, Chancen und Barrieren im oesterreichischen Kontext* (English translation of the title: *Wastewater as a source of renewable energy—Potentials, chances and barriers in the Austrian context*). Wiener Mitteilungen, Band 246.

Kretschmer, F., & Ertl, T. (2010). *Thermische Abwassernutzung aus siedlungswasserwirtschaftlicher Sicht* (English translation of the title: *Wastewater heat recovery from a wastewater management perspective*). Energiemanagement in der Abwasserwirtschaft - Kanal und Kläranlage, OEWAV. ISBN: 978-3-902084-85-9.

Kretschmer, F., Neugebauer, G., Kollmann, R., Eder, M., Zach, F., Zottl, A., et al. (2016). Resource recovery from wastewater in Austria: Wastewater treatment plants as regional energy cells. *Journal of Water Reuse and Desalination, 06*(3), 421–429.

Lindemann, N. (2016). *Akteursanalysen als Grundlage für die Verbreitung der energetischen Nutzung von Abwasser* (English translation of the title: *Stakeholder analysis as a basis for establishing energetic use of wastewater*). Master thesis at the University of Natural Resources and Life Sciences, Vienna.

Meeten, N. (2017). *Wastewater thermal energy mapping* (pp. 32–34). Water New Zealand, September/October 2017. https://www.waternz.org.nz/Attachment?Action=Download&Attachment_id=2648. Accessed May 23, 2018.

Neugebauer, G., Kretschmer, F., Kollmann, R., Narodoslawsky, M., Ertl, T., & Stoeglehner, G. (2015). Mapping thermal energy resource potentials from wastewater treatment plants. *Sustainabilty, 7*(10), 12988–13010.

Nowak, O., Enderle, P., & Varbanov, P. (2015). Ways to optimize the energy balance of municipal wastewater systems: Lessons learned from Austrian applications. *Journal of Cleaner Production, 88,* 125–131.

Sanden, B. A., & Azar, C. (2005). Near-term technology policies for long-term climate targets—Economy wide versus technology specific approaches. *Energy Policy, 33*(2005), 1557–1576.

Mine Water in the Closure of a Coal Basin: From Waste to Potential Resources

Javier Menéndez and Jorge Loredo

Abstract

The closure of the coal mines originates underground water reservoirs. The stored water can be used to produce energy. The water is at a temperature between 20 and 25 °C. A potential use consists in the production of thermal energy with heat pump.

Keywords

Mine water • Coal mines • Coal mining closure • Geothermal resources • Underground reservoir

1 Introduction

The Asturian Central Coal Basin (ACCB) is located in northern Spain. With an area of about 1400 km^2, the ACCB is the largest carboniferous outcrop of the peninsula and the main Spanish coal mining district. It has been an exploited coal mining area for more than 200 years, through open pit and underground mining, with indoor mining predominating in the last decades.

Mining operations have altered the natural flow of groundwater. The mining voids, together with the spaces created due to the fracturing induced by mining, can be filled up with water, once the mines are closed and inundated, materializing then a new aquifer or "mining reservoir."

When mining ends, one option is to abandon pumping, gradually flooding both the mine voids and the open pores; this "groundwater rebound" (Henton 1981) continues until potentiometric equilibrium is reached (Younger et al. 2002). If the lithological units connected to any part of the flooded system intersect the surface at a level lower than that of the mouth of the mine shaft, water upwelling (a spring) will occur. If pumping is resumed such that its discharge is equal to the recharge, the water level can be stabilized throughout the ductwork of the new aquifer. The stored volume is then equivalent to that of the filled voids, and an underground reservoir has been created. Estimating the capacity of this reservoir requires a rigorous analysis of the void space, the local mining history, and interconnections that may exist with adjacent mining works, as very often a mine shaft does not constitute an isolated system.

New studies on the framework of a circular economy have led to find new possibilities for mine water which can be considered as a potential resource, converting mining exploitations into storage and production facilities of renewable energy and generating new economic activities in the mining regions. Then, mine water, either coming from the pumps or from the stage rebound after flooding during the closure period, could be used with economic and social benefits for energy generation.

The temperature of water from the coal mining reservoirs in Europe is usually above 14 °C, so modern heat pumps using it as cold source are competitive, considering current prices of electricity and fuel (Jardón 2010). There has been research and applications of mine water as a source of low-enthalpy geothermal energy in the world: Poland (Malolepszy 2000), UK (Sutton 2002; McLoughlin 2006),

J. Menéndez (✉)
Hunaser Energía, Avda. Galicia, 44,
33005 Oviedo, Asturias, Spain
e-mail: javiermenendezr@gmail.com

J. Loredo
University of Oviedo, School of Mines,
Independencia, 13, 33004 Oviedo, Asturias, Spain
e-mail: jloredo@uniovi.es

Slovakia (Bajtos 2001), Germany, The Netherlands and France (Demollin et al. 2005), USA (Watzlaf and Ackman 2006).

2 Materials and Methods

One of the more attractive applications of mine water is to use it as geothermal resource. The energy use of mine water in the CCB by means of heat pumps is ideal, due to the high performance that can be reached with an average temperature of 20 °C. Considering an average total flow of 40 hm^3 year^{-1} pumped in the entire coal mining reservoirs in the ACCB, 1.700 h year^{-1} for heating (Ochsner 2008), the thermal potential of the cool (P_c) and the warm (P_w) sides are, in W (Bajtos 2001; Jardón 2010):

$$P_c = \Delta T \cdot F \cdot SH \cdot \rho$$

$$P_w = P_c \cdot COP \cdot (COP - 1)^{-1}$$

where

ΔT = Difference of temperature of mine water going in and out of the evaporator, which is generally 5 °C for common heat pumps
F = Pumped flow (6.53 m^3 s^{-1})
SH = Water specific heat = 4186.8 J kg^{-1} (°C)$^{-1}$
ρ = Water density = 1000 kg m^{-3}
COP = Heat pump coefficient of performance (amount of heat in relation to the drive power required).

To produce hot water at 35 °C, a COP = 6.73 can be considered. Thus, $P_c \approx 136.8$ MW and $P_w \approx 160.7$ MW, so the work contributed to the compressor of the heat pump is $P_w - P_c \approx 23.9$ MW. A heat pump available 1700 h year^{-1} would produce 273.2 thermal GWh, consuming 40.6 electrical GWh (Jardón 2010).

Producing energy by means of heat pumps using mine water, compared to conventional systems using natural gas, in several applications, means economic savings above 70%

Fig. 1 Project scheme. Winter (heat mode)
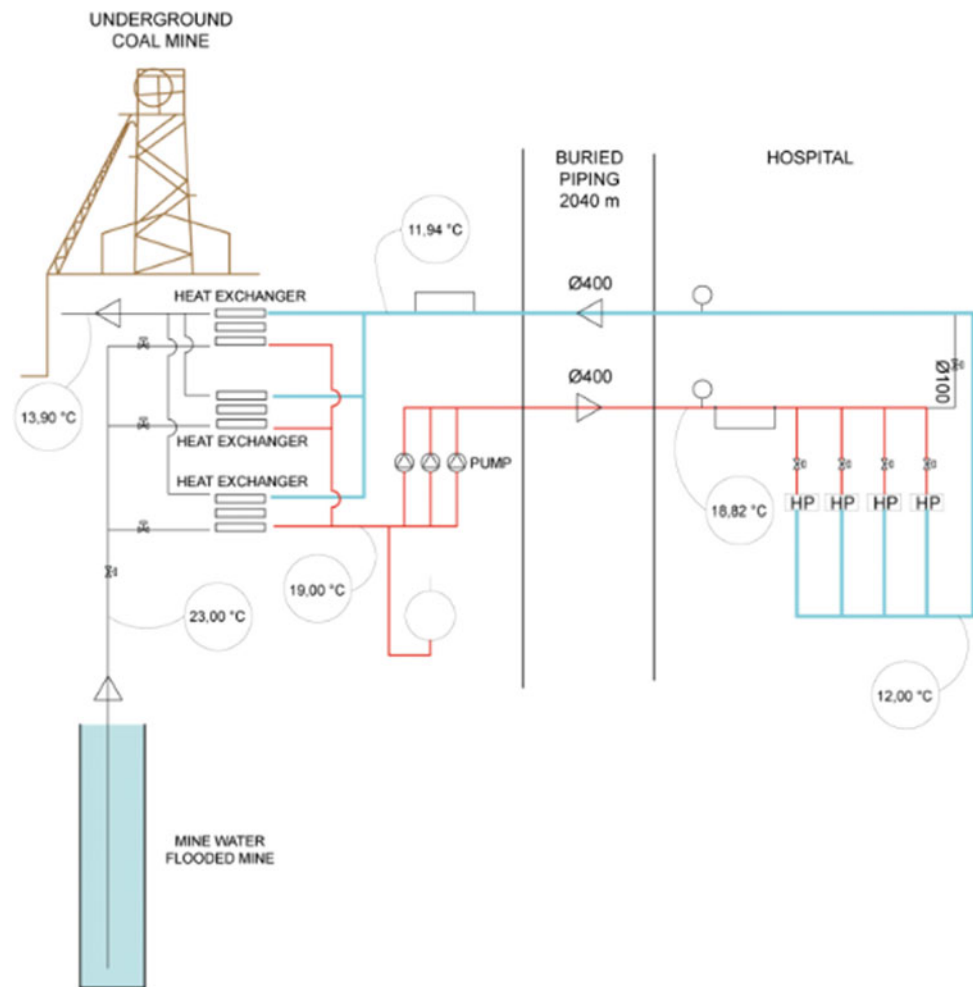
Fig. 2 Project scheme. Summer (cool mode)
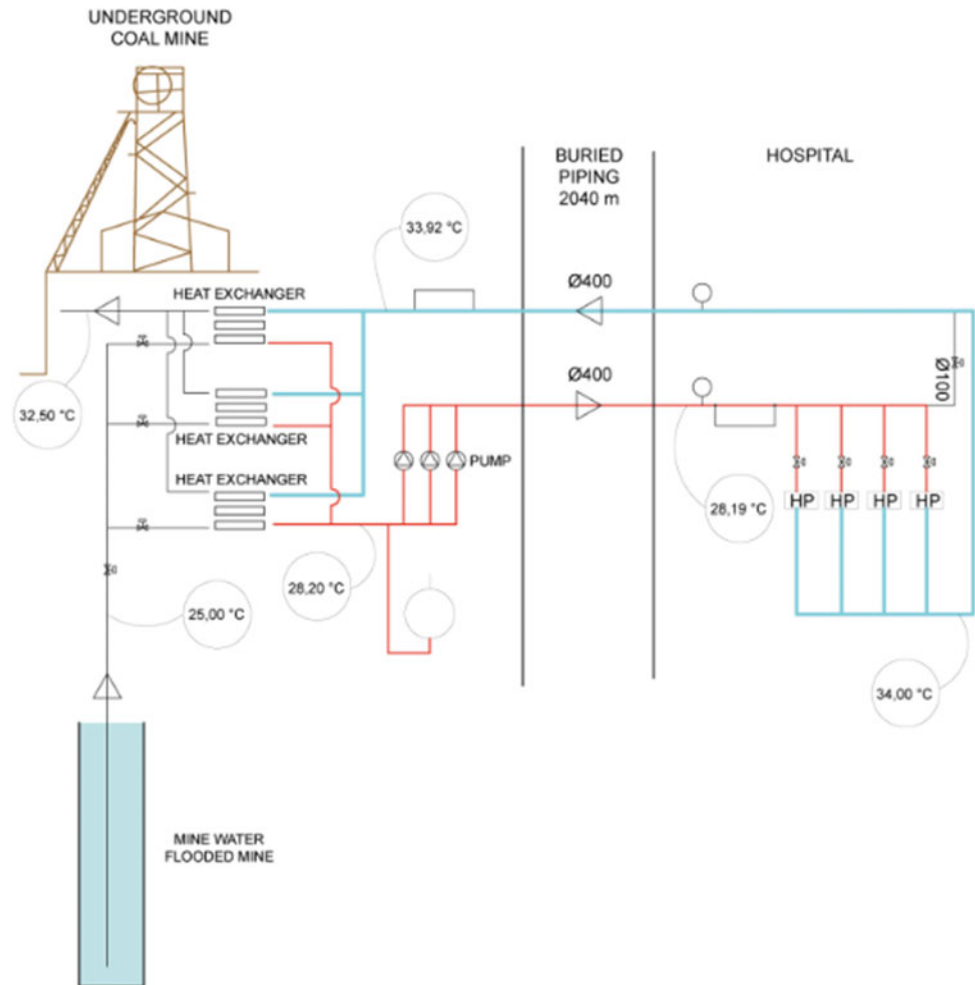
and reductions of CO_2 emissions between 20 and 40% (Jardón 2010; Cordero et al. 2010). Mine water from a mining reservoir in the ACCB (Barredo-Figaredo) has been already used as geothermal resource to heat and cool some buildings, and there are ongoing projects to extend these applications to other potential future users in the area.

3 Results and Discussion

In the case of the hospital, that is located 2 km far from the shaft, the mine water goes directly to heat exchanger placed on the mine installations. It is a tubular heat exchanger with a thermal exchanging power of 3500 kW. After the exchange, the mine water is discharged into a river. The heat is given to a secondary circuit that is a secondary closed loop of clean water of 4 km made with polyethylene pipes, Ø 400 mm. Three Grundfos HS-150-125-381 320 5/1 FA pumps (3 x 55 kW) are used to pump this clean water to the heat pumps in the hospital.

Hospital thermal installation includes two Carrier 30XWH-1.152 chillers, which can provide heat (1509 kW each one) or cold (1141.4 kW each one) to the building, depending on the climate conditions and the specific needs of the climate system. Another chiller, a CARRIER 30XWH-652, produces simultaneous heating and cooling in a compensated generation system. Figures 1 and 2 show the scheme of the project for the winter and summer situations. In "summer scenario," the heat pumps supply cold, and in the "winter scenario," it supplies heat. First data of the geothermal systems allow us to establish that use of mine water energy in these buildings has reduced emissions more than a 60%, comparing actual systems with conventional natural gas boilers and air chillers.

4 Conclusion

Closed and inundated coal mines in the ACCB can constitute mining reservoirs which could be regulated and used as water and energy resource. It is essential to define the

hydrogeological model, the water balance, and the volume of voids of the mining reservoir system previously to these applications, which fit with an integrated management of water resources, allowing regulating simultaneously both surface and underground resources.

Considering the pumping rates and the high COP values that can be reached for mine water in the CCB, their energy use by means of water–water heat pumps for heating and cooling is optimal.

The entire coal mining reservoirs in the ACCB involve a potential of energy supply higher than 250 thermal GWh year^{-1}. Compared to conventional systems, economic savings and a reduction in CO_2 emissions are achieved. These applications are encouraging and might be profitably extended to other minor coal mining basins in Asturias and other areas.

References

Bajtos, P. (2001). Low enthalpy geothermal energy from mine waters in Slovakia. In *Proceedings of the International Scientific Conference of Geothermal Energy in Underground Mines*, Poland.

Cordero, C., Garzón, M. B., & Álvarez, C. J. (2010). Aprovechamiento geotérmico de las aguas de mina. Universidad de Oviedo: Campus geotérmico. In *Proceedings of the Congress GEOENER 2010*.

Demollin, E., Malolepszy, Z., & Bowers, D. (2005). Potential use of geothermal energy from mine water in Europe for cooling and heating. In *Proceedings of the International Conference "Passive and Low Energy Cooling for the Built Environment"*, Greece.

Henton, M. P. (1981). The problem of water table rebound alter mining activity and its effects on ground and surface water quality. In W. van Duijvenbooden, P. Glasbergen, & H. Van Lelyveld (Eds.), *Quality of Groundwater, Proceedings of the International Symposium Noordwijkerhout* (pp. 111–116). The Netherlands: Elsevier.

Jardón, S. (2010). *Aprovechamiento de las aguas de mina en la Cuenca Central Asturiana como recurso energético. Aplicación al embalse minero Barredo-Figaredo* (Ph.D. thesis). University of Oviedo.

Malolepszy, Z. (2000). Low-enthalpy geothermal waters in coal mines, Upper Silesia coal basin, Poland. In *Proceedings of the World Geothermal Congress 2010* (pp. 1401–1406), Japan.

McLoughlin, N. (2006). *Geothermal heat in Scotland*. http://www.scottish.parliament.uk/business/research/briefings-06/SB06—54.pdf.

Ochsner, K. (2008). *Geothermal heat pumps. A guide to planning & installing*. London: Earthscan.

Sutton, K. (2002). UK abandoned mines could provide low cost heating. *Heat Pump News*. Saving Energy (Issue 1). http://www.heatpumps.org.uk/PdfFiles/HeatPumpNewsNo.1.pdf.

Watzlaf, G. R., & Ackman, T. E. (2006). Underground mine water for heating and cooling using geothermal heat pump systems. *Mine Water and the Environment, 25*(1), 1–14.

Younger, P. L., Banwart, S. A., & Hedin, R. S. (2002). *Mine water. Hydrology, pollution, remediation*. Dordrecht, The Netherlands: Kluwer Academic Publishers.

Water Pollution by Polychlorinated Biphenyls from the Energy Sector of Armenia

A. Aleksandryan, A. Khachatryan, and Yu. Bunyatyan

Abstract

Polychlorinated biphenyls (PCBs) were wildly used in electrical equipment of various types in the industry, power engineering and other branches of National Economy. Being absorbed from water and accumulated in media and tissue to concentrations greater than those found in surrounding water, PCBs bioaccumulate and increase up the food chain. The greatest danger to environment and people originates from lack of information about the related hazards among owners of PCB and PCB-filled equipment. Monitoring study was performed on surface waters, bottom sediment, foodstuffs, and soil samples. PCBs accumulation occurred from the lower to the higher trophic level.

1 Introduction

Energy generation is one of the leading economic sectors in the Republic of Armenia, yet energy sector is one of the main sources of environmental pollution by polychlorinated biphenyls (PCBs). PCBs have been wildly used in electrical equipment of various types: power transformers, capacitors, greasing/lubricating systems, rectifiers, high-voltage switches and breakers, compressors, etc. The mentioned equipment is functioning in the industry, power engineering, and other branches of National Economy in a considerable quantity.

Ecological exposure to PCBs is primarily an issue of bioaccumulation resulting in chronic effects rather than direct toxicity. PCBs bioaccumulate in biota by both bio-concentration (being absorbed from water and accumulated in tissue to concentrations greater than those found in surrounding water) and biomagnification (increasing in tissue concentrations as they go up the food chain through two or more trophic levels). At most contaminated sites, PCBs are predominantly bound to particles or strongly associated with an organic fraction (National Research Council 2001).

Therefore, aquatic organisms are exposed to a combination of dissolved, sediment-associated, and food-associated PCBs (National Research Council 2001). However, in terrestrial ecosystems, lower trophic-level organisms are exposed to PCBs primarily through the ingestion of soil and prey, although dermal absorption and inhalation might be important exposure routes for certain species. At each higher trophic level, certain PCB congeners are selectively enriched or depleted because of selective metabolism and excretion of metabolites. As a result, organisms at the top of the food chain are generally at the greatest risk of adverse effects due to exposure to PCBs. However, foraging preferences, species sensitivity, and other site-specific factors can modify the magnitude of those risks (National Research Council 2001; Aleksandryan et al. 2013).

The daily risk of PCB-related affections in big groups of population in the course of professional activity of humans is extremely great. The greatest danger to environment and people originates from incompetent handling of these compounds, ignorance among owners of PCB and PCB-filled equipment about the hazards of the given substances, as well as contact to soils, foodstuff and other objects polluted by PCBs.

A. Aleksandryan (✉)
Ministry of Nature Protection of the Republic of Armenia, Yerevan, Armenia
e-mail: anahit.aleksandryan@yahoo.com

A. Khachatryan · Yu. Bunyatyan
Environmental Monitoring and Information Center SNCO, Yerevan, Armenia
e-mail: khachart7@yahoo.com

Yu. Bunyatyan
e-mail: bunyatyan43@rambler.ru

2 Materials and Methods

Environmental samples were taken according to the unified sampling method.

Analyses for PCBs were done using "Gas-Chromatograph/Mass-Spectrometer GCMS-QP2010 SE EI 230V CELV incl. GC-2010 Plus" (Shimadzu Corporation, Japan).

3 Results and Discussion

In order to study the trend of environmental pollution by PCBs, a monitoring study was performed on surface waters, bottom sediment, foodstuffs, and soil samples (Table 1; Figs. 1 and 2).

Monitoring data showed that soil concentration of PCBs declined, water concentration increased, but bottom sediment concentration increased approximately six times. The reason for the increase in PCB concentration of the biological samples is that most of the samples have been taken in close proximity to transformer installations, while in the earlier study in 2002–2003 the PCBs were analyzed in samples collected for POPs-pesticides analysis.

As a result of studies, the peculiarities of POPs transformation along the trophic chains of the Republic of Armenia hydroecosystem were revealed: The process of PCBs accumulation occurred from the lower to the higher trophic levels (Figs. 1 and 2).

4 Conclusion

PCBs high concentrations were mainly revealed due to the activity of hydropower plants at different sites. At sites, where the flow rate is not so high, the quantity of PCBs in bottom sediment was higher. At the sites, where water was "rich" in PCBs, but the river drift was high, no significant amounts of PCBs were observed (Aleksandryan and Khachatryan 2012).

It is necessary to exclude application of PCBs used in oils and electrical equipment of the energy production/
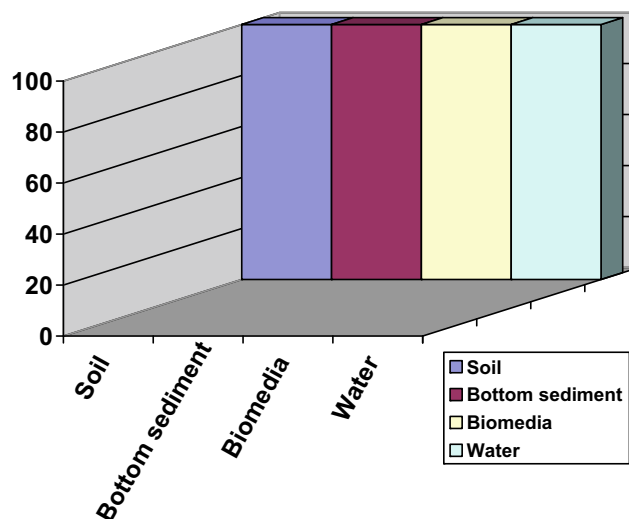
Fig. 1 PCBs in various environmental media (%)
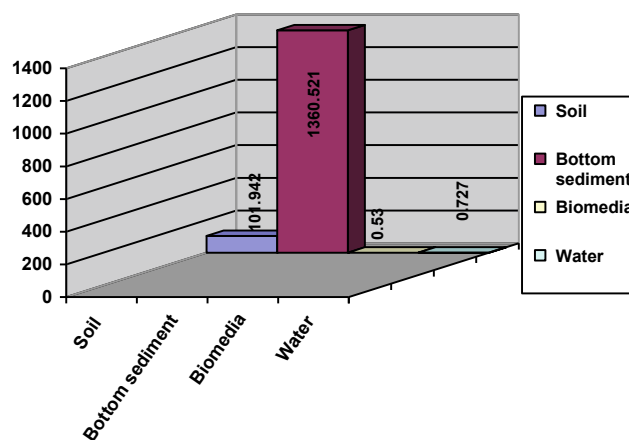
Fig. 2 Average content of PCB in different media

distribution sector that is regulated by Stockholm Convention on Persistent Organic Pollutants (POPs), the principles of which require phasing-out the use and further treatment of PCB-containing oils. This will eliminate PCBs-related pollution of water resources caused by energy sector-specific equipment.

Table 1 Average and maximum values of PCBs revealed in environmental media of the Republic of Armenia

Media	Revealed amounts of PCBs	
	Average value	Maximum value
Water, mcg/L	0.727	6.831
Biomedia, mcg/g	0.530	0.743
Bottom sediment, mcg/kg	1360.521	2166.052
Soil, mcg/kg	101.942	434.980

References

Aleksandryan, A., & Khachatryan, A. (2012). Polychlorinated biphenyls in bottom sediment and water from hydroecosystems of Armenia. In *EcoSummit 2012*, Columbus, OH, USA, September 30–October 5, 2012. Poster No. 107.

Aleksandryan, A., Holoubek, I., & Khachatryan, A. (2013). *Distribution of persistent organic pollutants in environmental media* (174 pp.). Yerevan. ISBN 978-9939-0-0754-0.

National Research Council. (2001). *A risk-management strategy for PCB-contaminated sediments*. Washington, DC: The National Academies Press. https://doi.org/10.17226/10041.

Semi-continuous Anaerobic Digestion of Orange Peel Waste: Preliminary Results

Paolo S. Calabrò, Filippo Fazzino, Adele Folino, and Dimitrios Komilis

Abstract

Orange peel waste (OPW) is a promising substrate for anaerobic digestion. The problems related to the presence of d-Limonene in OPW need to be overcome. Alkaline pretreatment of OPW and addition of granular activated carbon are promising remedies.

1 Introduction

Orange peel waste (OPW) is produced in large quantities in many parts of the world (Calabrò et al. 2016, 2018b) but a sustainable solution for its valorisation has not been found until now. A promising solution is using OPW as substrate for anaerobic digestion; however, problems linked to the seasonality of its production and to the presence of d-Limonene, a well-known antimicrobial agent, must be resolved first. A conventional solution is to co-digest OPW with other substrates; however, this option is not practical when large quantities of this residue must be managed.

In this paper, three sets of semi-continuous anaerobic digestion experiments, designated as experiments A, B1 and B2, C1 and C2, respectively, are presented. In experiment A, the effect of pH and nutrients on the sustainable OPW loading was analysed. In experiments B1 and B2, the effect of activated carbon on high OPW loadings was evaluated. Finally, in experiments C1 and C2, the effect of alkaline pretreatment on OPW digestion was assessed.

2 Materials and Methods

The substrate used was a lyophilized OPW collected in an orange transformation industry in Sicily (Table 1). Lyophilization allows to preserve as much as possible the characteristics of OPW. In experiments C1, C2 lyophilized OPW was subjected to NaOH (5% TS) pretreatment at room temperature for 24 h (Calabrò et al. 2018a).

In experiments B and C, granular activated carbon was also added (CARBOSORB 2040 −20 × 40 mesh—was provided by Comelt srl—Milan, Italy).

The inoculum used in the experiments was liquid digestate coming from a full-scale plant treating manure and various residues from the agro-industry. It was sieved to remove fibrous materials (e.g. straw) and then kept in anaerobic conditions in an oven at 35 °C before the experiments to reduce as much as possible the non-specific biogas production.

Semi-continuous reactors (three-neck bottles, volume 1.1 L, WTW-Germany, equipped with valves allowing biogas collection and sludge withdrawal) were placed in a thermostatic cabinet at 35 ± 0.5 °C and mixed by a magnetic stirrer throughout the test period. Two or three times per week, biogas was slowly transferred into a second bottle (alkaline trap) containing 1 L of a 3 N NaOH solution using a 100 mL syringe. Through a side opening of the second bottle, a tube allowed to transfer biogas via the syringe. The carbon dioxide present in the biogas was absorbed into the alkaline solution. The pressure increase in the alkaline trap provoked the displacement of a certain volume of that alkaline solution that was transferred by a tube connected to another side

P. S. Calabrò (✉) · F. Fazzino · A. Folino
Dipartimento di Ingegneria Civile, dell'Energia, dell'Ambiente e dei Materiali, Università Mediterranea di Reggio Calabria, Via Graziella- loc. Feo di Vito, Reggio Calabria, Italy
e-mail: Paolo.calabro@unirc.it

D. Komilis
Department of Environmental Engineering, Democritus University of Thrace, Xanthi, Greece

Table 1 Substrate and inocula characteristics

	TS (%)	VS (%TS)	pH
Inoculum (Exp. A)	4.8	71.9	7.9
Inoculum (Exp. B)	4.0	65.7	7.9
Inoculum (Exp. C)	4.1	64.6	8.1
Raw lyophilized OPW	93.2	96.9	–

opening of the bottle to a graduated volumetric cylinder. The total volume of the alkaline solution displaced by the gas was considered equal to the volume of methane present in the biogas. The volume of carbon dioxide was, therefore, calculated by the difference of the methane volume from the total biogas volume (Calabrò et al. 2016, 2018b).

In experiment A, $NaHCO_3$ was added several times during the experiment to increase the pH.

Since the C/N of the OPW is about 51, a nutrient solution compliant with the UNI/TS 11703:2018 norm recently introduced in Italy was periodically added to reduce C/N ratio. The norm includes the use of three different nutrient solutions defined as Solutions A, B and C. Solution A contains specified quantities of KH_2PO_4, $Na_2HPO_4 \cdot 12H_2O$, NH_4Cl, distilled water; the amount to be used was assessed to supplement nitrogen present in OPW so that to reach a C/N of about 30. Solution B contains $CaCl_2 \cdot 2H_2O$, $MgCl_2 \cdot 6H_2O$, $FeCl_2 \cdot 4H_2O$, distilled water and the amount to be used is the same as Solution A. Solution C contains $MnCl_2 \cdot 4H2O$, H_3BO_3, $ZnCl_2$, $CuCl_2$, $Na_2MoO_4 \cdot 2H_2O$, $CoCl_2 \cdot 6H_2O$, $NiCl_2 \cdot 6H_2O$, Na_2SeO_3, distilled water and the amount to be used is 1/5 of the volume of Solution A.

During experiment A, designed to verify the maximum OPW loading applicable to the process, the substrate loading was set to 1 gVS/(L day) (days 1–81; HRT 46 days) and then to 2 gVS/(L day) (days 82–100; HRT 23 days). Due to pH reduction, 2 and 4 g of $NaHCO_3$ were added on days 52 and 56, respectively. Since pH stabilization and the biogas production achieved were unsatisfactory, nutrient Solutions B and C were added on day 63 and Solution A on day 70. The experiment was stopped due to excessive pH reduction on day 105.

Experiment B was designed to assess if reducing HRT a higher loading was sustainable and if GAC could help the process. During this experiment, two bottles (B1 and B2) were prepared; the only difference was the presence of 2% GAC in bottle B2. GAC was supplied with the substrate at each loading so that to keep its concentration constant. HRT was kept equal to 14.7 days, similar to that used in many full-scale plants fed with agro-industrial residues. The substrate loading was set to 2 gVS/(L day), then after a week feeding was suspended for 12 days, then for a week (days 19–26) it was reduced to 1 gVS/(L day) and then (days 27–33) increased to 3 gVS/(L day). Nutrient solutions (A, B and C) directed at supplementing nitrogen down to a C/N of

30 were added on days 16 and 33. The experiment was stopped due to excessive pH drop on day 35.

Experiment C was designed to verify if alkaline pre-treatment and GAC (added only in bottle C2) can make sustainable a loading of 2 gVS/(L day). In this experiment, due to the necessity of preparing pre-treated substrate, feeding was reduced to twice a week. The 2% GAC concentration was confirmed and the HRT was set to 13 days. The loading was gradually increased from 0.5 gVS/(L day) for days 1–3 to 1 gVS/(L day) (days 4–11) and finally to 2 gVS/(L day). Nutrient solutions were added every two weeks. The experiment was designed to last 45 days but was still in progress while writing this abstract and only data for the first 36 days are available.

Total, volatile solids and pH were measured according to standard methods (APHA et al. 2012).

3 Results and Discussion

During experiment A, pH slowly decreased from the initial value (7.9) down to 6.7 during the first 46 days, then it decreased to 6.1 (day 52). The addition of $NaHCO_3$ and of nutrient solutions raised pH to about 7 (until day 81), in this period, it is possible that pH decrease was due to an accumulation of VFA and that nutrients addition helped to stimulate bacterial activity. Then, in correspondence to OLR increase (2 gVS/(L day)), pH decreased and neither sodium bicarbonate nor nutrient solutions addition was able to successfully raise it. The experiment was terminated at day 100 (pH = 4.9). Methane yield was fairly stable during days 18–81 and remained between 0.35 and 0.43 NL/gVS$_{added}$ (average 0.38 NL/gVS$_{added}$, %CH_4 in biogas, 63% on average) then it decreased almost steadily down to 0.3 NL/gVS$_{added}$ on day 100.

During experiment B, in both reactors, the pH decreased very fast during the first phase of feeding (down to 6.05 and 6.2 in reactor 1 and 2, respectively, with reactor 2 being the one in which GAC was added). Then, it slightly recovered when feeding was suspended. In the following period, especially when feeding was increased up to 3 gVS/(L day), pH decreased but reactor 2 performed slightly better.

Experiment C (Fig. 1) demonstrated that from day 21 onward, reactor 2, the one where GAC was added, performed better in terms of pH and from days 28 also in terms of methane production. In the period, when OLR was set at
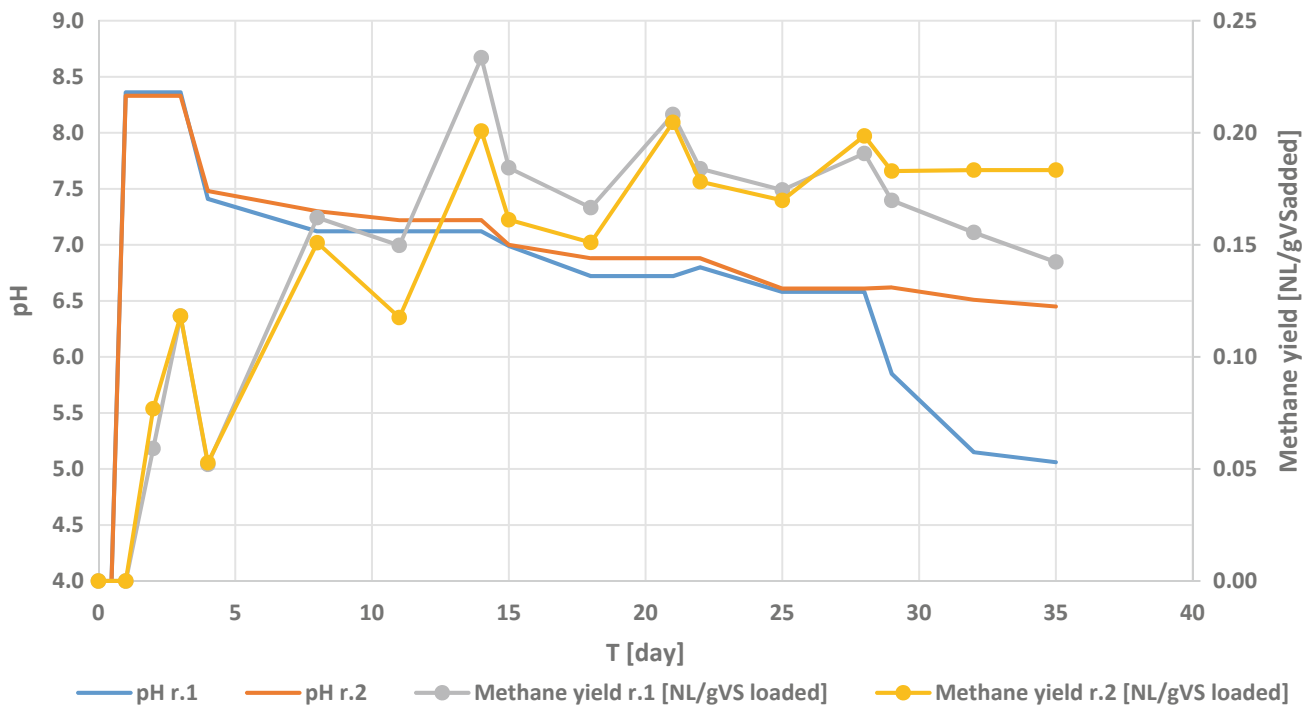
Fig. 1 Profiles of pH and methane yield in experiment C

2 gVS/(L day) (days 11–35), methane yield in both reactors was identical and equal to 0.18 NL/gVS$_{added}$. This value is about half of that registered during experiment A when, however, HRT was set at about 46 days, about 4 times the value set in experiment C. The organic loading for experiment C was close to the higher values signalized in literature (Zema et al. 2018 and references therein) It is possible that, as signalized in literature, the presence of GAC helps in controlling inhibiting substances and in gradually selecting acclimated biomass (Chen et al. 2008; Lee et al. 2016).

4 Conclusions

These preliminary results demonstrate that OPW pretreatment with the addition of a moderate amount of GAC can render anaerobic digestion of pure OPW sustainable in terms of process stability and applicable loading (up to 2 gVS/(L day)). However, the supplementation of nutrients is necessary which can be achieved either by the direct addition of nutrients or by the addition of an appropriate N rich co-substrate.

References

APHA, AWWA, & WEF. (2012). *Standard methods for the examination of water and wastewater* (22nd ed.). American Public Health Association, American Water Works Association, Water Environment Federation.

Calabrò, P. S., Pontoni, L., Porqueddu, I., Greco, R., Pirozzi, F., & Malpei, F. (2016). Effect of the concentration of essential oil on orange peel waste biomethanization: Preliminary batch results. *Waste Management, 48,* 440–447. https://doi.org/10.1016/j.wasman.2015.10.032.

Calabrò, P., Catalán, E., Folino, A., Sánchez, A., & Komilis, D. (2018a). Effect of three pretreatment techniques on the chemical composition and on the methane yields of *Opuntia ficus-indica* (prickly pear) biomass. *Waste Management & Research, 36,* 17–29. https://doi.org/10.1177/0734242X17741193.

Calabrò, P. S., Paone, E., & Komilis, D. (2018b). Strategies for the sustainable management of orange peel waste through anaerobic digestion. *Journal of Environmental Management, 212,* 462–468. https://doi.org/10.1016/j.jenvman.2018.02.039.

Chen, Y., Cheng, J. J., & Creamer, K. S. (2008). Inhibition of anaerobic digestion process: A review. *Bioresource Technology.* https://doi.org/10.1016/j.biortech.2007.01.057.

Lee, J. Y., Lee, S. H., & Park, H. D. (2016). Enrichment of specific electro-active microorganisms and enhancement of methane production by adding granular activated carbon in anaerobic reactors. *Bioresource Technology.* https://doi.org/10.1016/j.biortech.2016.01.054.

Zema, D. A., Fòlino, A., Zappia, G., Calabrò, P. S., Tamburino, V., & Zimbone, S. M. (2018). Anaerobic digestion of orange peel in a semi-continuous pilot plant: An environmentally sound way of citrus waste management in agro-ecosystems. *Science of the Total Environment, 630.* https://doi.org/10.1016/j.scitotenv.2018.02.168.

Nonwoven Wet Wipes Can Be Hazardous Substances in Wastewater Systems—Evidences from a Field Measurement Campaign in Berlin, Germany

Raja-Louisa Mitchell, Michel Gunkel, Jan Waschnewski, and Paul Uwe Thamsen

Abstract

Nonwoven wet wipes can be hazardous substances for wastewater systems. The study investigates the composition of physical constituents in the wastewater. The solid fractions per m^3 wastewater are determined. The amount of nonwoven wet wipes in the sewer samples ranges from 0 to 116 g/m^3. The accumulation of wet wipes along the path of wastewater transport is shown.

Keywords

Pump blockages • Clogging • Nonwoven wet wipes • Physical constituents • Wastewater composition • Wastewater fractions

1 Introduction

Disposable wet wipes made from nonwoven fabrics are increasingly being used in households, especially in bathroom settings. These include baby wipes, facial tissues and moist toilet paper (EDANA 2017). In recent years, the increasing consumption of disposable nonwoven wet wipes is increasingly causing operational problems in sewer systems in terms of, e.g., blockages of pumps, deposits in sewers and an increase in screenings (Flegenheimer 2015; Bjorkman 2015; DWA 2016). Wastewater system operators usually associate these problems with nonwoven wet wipes that were disposed of via the toilet (Wessex Water 2016). The operational problems, especially the blockage of

R.-L. Mitchell (✉) · P. U. Thamsen
Chair of Fluid System Dynamics, Technische Universität Berlin, Berlin, Germany
e-mail: raja-louisa.mitchell@tu-berlin.de

M. Gunkel · J. Waschnewski
Berliner Wasserbetriebe, Berlin, Germany
e-mail: michel.gunkel@bwb.de

J. Waschnewski
e-mail: jan.waschnewski@bwb.de

wastewater pumps, are not only a serious hazard for the critical infrastructure, but also imply high costs for wastewater system operators, due to increased energy consumption and maintenance costs.

This paper presents the first part of a larger research effort addressing the problem of wet wipes in sewer systems. The focus of this publication is a field measurement campaign that assessed the amounts of flushed materials (with a focus on nonwoven wet wipes) in Berlin, Germany.

2 Materials and Methods

The field measurement campaign gathered sample data in two catchment areas (combined sewer system, catchment 1 mainly residential area and catchment 2 residential with hotels and old peoples' homes) within the Berlin district Wilmersdorf. We considered a 1-year period between summer 2014 and summer 2015 (except for winter months) to account for seasonal changes. Samples of wastewater (~ 2.8 m^3 respectively) were gathered three times a day by means of a suction vehicle: multiple samples per day area needed to avoid sampling only extreme (low or high) flow conditions. Flaps on the nozzle of the suction hose ensured that the total wastewater flow at the time of sampling was collected. The samples remained in the suction vehicle until the end of the day, with the total daily mixed sample amounting to 8.3 m^3. The complete sample was then discharged into the sewer through a basket screen (mesh size ~ 5 mm^2). The basket screen retained all the solids contained in 8.3 m^3 wastewater collected throughout the day. After weighing (wet weight) and mixing, a random grab sample (~ 0.8–3.5 kg) was extracted for further analysis. Additionally, one sample was taken from a pumping station suction chamber and one from a clogged pump. The suction chamber sample was taken from a large inner city pumping station with dry-installed pumps after the daily cleaning cycle, to ensure optimal mixing of the wastewater in the suction chamber. Using a suction vehicle, 8.3 m^3 were extracted from the suction chamber and released

back into the sewer system via the basket screen. A random grab sample was extracted from the total solids retained in the basket for further analysis. The pump sample was extracted by hand from a clogged pump of an inner city pumping station located in the same district as the catchments used for sewer sampling. A random sample was extracted from the pump clog for further analysis.

The textile research institute *Thüringisches Institut für Textil- und Kunststoff-Forschung e.V. (TITK)* was commissioned with the following further analysis of the samples. First, the samples were dried to determine the dry weight. Drying was either conducted in a drying oven (8 h at 80 °C) or at room temperature for 4–7 days, followed by additional drying using a hairdryer. Unfortunately, the same drying procedure could not be ensured for all samples, due to procedural problems (mainly caused by sample contamination).

Second, the following fractions were analysed and the dry weight of each fraction was determined: plastics, textiles (nonwovens, fibres, threads, textile areas, composite materials, knitted fabrics, woven fabrics), paper, wood/leaves and rests (e.g. hair and cigarette butts). For this analysis, sediments were disregarded, as they do not have the potential to clog pumps or screens.

3 Results and Discussion

We here report and comment the results in terms of composition and amount of the solid fractions in the wastewater samples.

Both composition and amount vary greatly: Fig. 1 depicts the dry weight of the fractions per m³ of wastewater. The data were compared with relevant precipitation data. However, no correlation with weather or seasons could be inferred.

The total amount of solids per m³ wastewater varies from 57.7 g/m³ (sample 4) to 1109.3 g/m³ (sample 12). The

Average percentage distribution of solids in sampled wastewater (n=12)
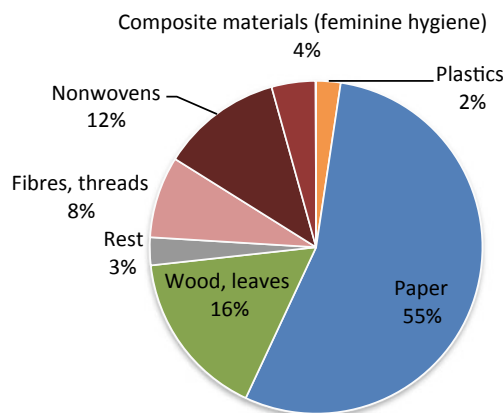
Percentage distribution of solids in sample of pumping station suction chamber (n=1)

Fig. 2 Average distribution of solids in samples from Berlin wastewater

composition of the total solids (the amount of the individual fractions) also varies strongly. Paper is the fraction which has the largest range (from 0 to 886 g/m³). The amount of nonwoven wet wipes ranges from 0 g/m³ wastewater (sample 2) to 117 g/m³ wastewater (sample 8).

In terms of composition, the wastewater in the sampled catchment areas contained, on average, 319 g/m³ of solid constituents, made up mainly of paper (206.15 g/m³), followed by 40.37 g/m³ wood/leaves, 40.23 g/m³ nonwoven wet wipes, 21.8 g/m³ of other textiles (such as cloth rests), 7.52 g/m³ of various rests (cigarette butts, etc.) and 3.18 g/m³ of plastics (see Fig. 1).

The three diagrams in Figs. 2 and 3 show the average percentage distribution of solids in the samples taken from

Fig. 1 Solids per m³ wastewater in samples of Berlin wastewater

the sewer, the suction chamber of the pumping station and the pump blockage, respectively. By comparing these three distributions, the change in the composition of physical constituents along the path of wastewater transport can be shown. The top diagram, showing the distribution of solids in the sewer itself, before the wastewater has been pumped for the first time, is composed mainly of paper (55%), while nonwoven wet wipes make up 12% of total constituents.

The suction chamber of pumping stations is often the first critical point in the wastewater system, with respect to blockages and other problems, such as deposits. Here, problematic components can become concentrated, e.g. in the scum on the wastewater, which develops due to FOG (fat, grease, oils) and wet wipes. Whenever the layer of scum is broken, e.g. after the pumping station cleaning cycle, these concentrated components have to be pumped and cause problems.

Accordingly, the amount of nonwoven wet wipes is much higher in this sample, making up 1/3 of total physical constituents. The fraction of composite materials (mainly

feminine hygiene products such as tampons and sanitary napkins) is also higher, while the paper fraction is lower, compared to the sewer samples, due to break up and dissolution.

In the sample of the pump blockage, the concentration of the nonwoven wet wipes is even higher, making up nearly half of the sample (47%). The composite materials (feminine hygiene products), too, are greatly increased, accounting for 37% of the total sample. In contrast, easily disintegratable materials such as paper cannot be found in the blockage sample.

4 Conclusions

The results of the field measurements show that the physical constituents found in wastewater vary greatly in type and amount. While this was to be expected, due to the inhomogeneous character of the medium and the multiple factors influencing wastewater generation, the degree of variance was greater than heretofore assumed. Most interestingly, these variations could not be correlated with precipitation data or expected seasonal variations (such as more organic material like wood and leaves in autumn).

Furthermore, for the first time, data regarding specific g/m^3 values of the different physical fractions in wastewater could be collected for an inner city wastewater system. These data give an important insight into the composition of wastewater, which in turn is important for designing operational processes.

It could also be shown that nonwoven wet wipes make up a relevant fraction in the wastewater. While the amount of nonwoven wet wipes is fairly low in the sewers, compared to other constituents, they become more concentrated in the suction chamber of pumping stations and even more so in pump blockages. This shows that even a small amount of nonwoven wet wipes in the wastewater system can lead to operational problems.

The authors are aware that a distinction has to be made regarding "flushable" and "non-flushable" wet wipes and that there is a lot of discussion surrounding this issue. In this study, the type of wet wipe identified in the samples (flushable/non-flushable) was not determined. Accordingly, no statement as to what type of wipes was found in the wastewater system can be made. Further research regarding the type of wet wipes causing problems in wastewater systems around the world is necessary.
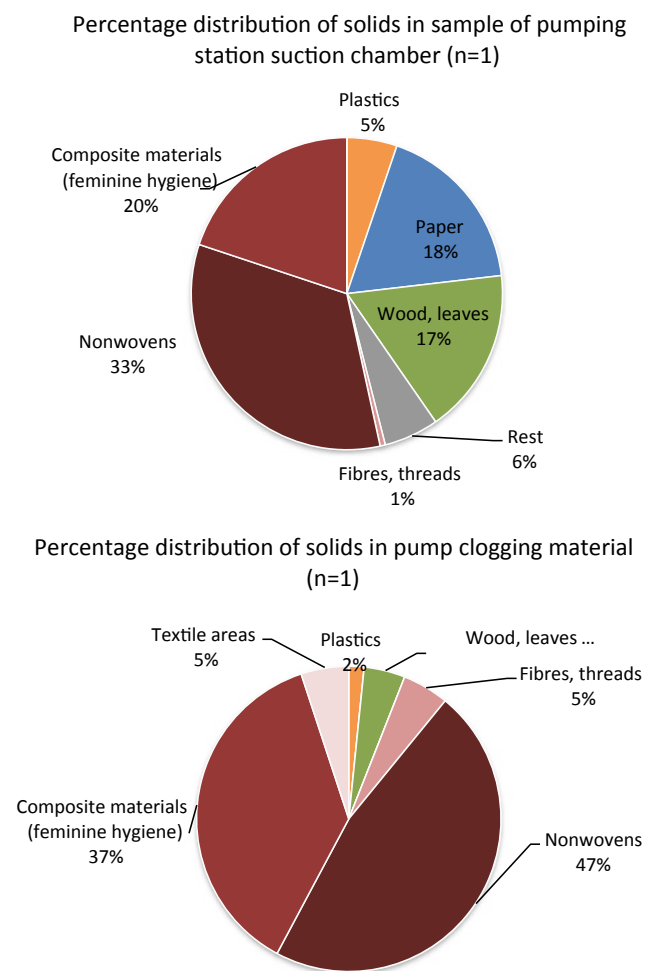
Fig. 3 Average distribution of solids in samples of suction chamber and pump blockage

References

Bjorkman, M. (2015). Disposable wipes threaten wastewater systems. *Pumps & Systems*.

DWA. (2016). *Feuchttücher*, pp. 2428–2434. KA Betriebsinfo.

European Disposables and Nonwovens Association (EDANA). (2017). *Facts and figures, nonwoven statistics 2017 (data 2016)*. https://www.edana.org/discover-nonwovens/facts-and-figures. Accessed 11.7.2018.

Flegenheimer, M. (2015). Wet wipes box says flush. New York's sewer system says don't. *The New York Times*. http://www.nytimes.com/2015/03/15/nyregion/the-wet-wipes-box-says-flush-but-the-new-york-city-sewer-system-says-dont.html?_r=1. Published 13.3.2015. Accessed 12.7.2018.

Wessex Water UK. (2016). *Flushable wet wipes evidence report*. Wessex.

Wastewater to Energy: Relating Granule Size and Biogas Production of UASB Reactors Treating Municipal Wastewater

Isaac Owusu-Agyeman, Elzbieta Plaza, and Zeynep Cetecioglu

Abstract

The effect of granular size distribution and temperature on the performance of UASB reactors treating municipal wastewater was studied. Larger granular size distribution favours stable methane production. Increase in temperature increases UASB performance. SMA of sludge decreases with increasing height along the reactor.

Keywords

Biogas • UASB • Municipal wastewater • Granular size distribution • Microbial community • Specific methanogenic activity

1 Introduction

Recovery of energy from wastewater treatment directly is getting the needed attention due to the shift of wastewater treatment plants from energy consuming to energy producing systems. Direct treatment of municipal wastewater with high rate anaerobic digestion reactors including upflow anaerobic sludge blanket (UASB) reactors can enhance bioresource recovery from wastewater and make treatment plants net-energy producing systems. UASB reactors are mainly applied to treat concentrated wastewaters, and there are only a few studies on UASB for treating low strength municipal wastewaters. Size of UASB granules is known to influence the performance of the reactor (Jijai et al., 2015; Wu et al., 2016). However, the influence of the structure of different granular size on the performance of UASB treating diluted municipal wastewater are yet to be studied. To fill the gap, a holistic approach is taken by systematically studying two identical pilot scale UASB reactors with different granular size distribution but treating the same municipal wastewater. The study aims to maximize energy recovery from UASB by understanding the granular size and operational parameters' effects of the reactors.

2 Materials and Methods

Each of the two pilot scale UASB reactors has a volume of 2.5 m^3 and flowrates are set at ≈ 0.88 m^3/h. The reactors are operated at 20 ± 3 and 28 ± 3 °C. The UASB reactors are fed with the same municipal wastewater of soluble chemical oxygen demand (COD) concentration of 243 ± 47 mg/L. COD, alkalinity, NH_4–N, pH, total suspended solids, volatile suspended solids, volatile fatty acid are analysed routinely.

The size distribution of the granules is determined from a digital image using ImageJ software (version 1.51, National Institutes of Health, USA). Settling velocity of the granules is measured using a measuring cylinder and stopwatch. The granular morphologies are studied with scanning electron microscope (SEM) (TM-1000, Hitachi High-Technologies Corporation, Japan).

Specific methanogenic activities (SMA) of sludge at different levels of reactors are measured using automatic methane potential test system (AMPTS II, Bioprocess Control, Sweden).

3 Results and Discussion

UASB Reactors 1 and 2 have modal granular sizes of 3–4 and 1–2 mm with settling velocities of 86–225 and 27–180 m/h, respectively. The typical settling velocity of

I. Owusu-Agyeman (✉) · Z. Cetecioglu
Department of Chemical Engineering,
KTH Royal Institute of Technology, Stockholm, Sweden
e-mail: isaacoa@kth.se

Z. Cetecioglu
e-mail: zeynepcg@kth.se

E. Plaza
Department of Sustainable Development,
Environmental Science and Engineering,
KTH Royal Institute of Technology, Stockholm, Sweden
e-mail: elap@kth.se

methane-producing granular sludge is ≥ 60 m/h (Hulshoff Pol et al., 2004; Yi et al., 2016). The superior settling characteristics of the granular sludge of UASB 1 favour methanogenesis.

The COD removal efficiency and the methane production by the reactors indicate that UASB 1 performs better especially in terms of biogas production (Fig. 1b). The average COD removal efficiencies by UASB 1 and 2 at operating temperature of 20 °C were 45 and 41%. There was a huge fluctuation in the biogas production by the UASB 2 (Fig. 1). On the other hand, the biogas production by the UASB 1 was stable with an average of 610 L CH4/d. The results suggest that the UASB with larger granular size distribution performs better in biogas production which confirms other studies (Jijai et al., 2015; Wu et al., 2016). The stable biogas production for the larger granular-sized UASB reactor is attributed to their internal structure including bigger pore size, higher porosity and shorter diffusion distances which promote better substrate transport and improve biogas production (Wu et al., 2016). SEM image of the cross section of UASB 1 granules confirmed a well-developed internal layered structure.

As expected increase in temperature to ~ 28 °C resulted in an increase in COD removal efficiency and biogas production. The average COD removal efficiency increased to 51 ± 8 and $51 \pm 5\%$ for reactor 1 and 2, respectively. There was an increased biogas production by UASB1 from 610 to 808 L CH4/d when temperature increased from 20 to 28 °C. The increase in performance with temperature is explained by an increase in the methanogenic activities (Lucas et al. 2018) and reduction in the methane solubility in the effluent (Crone et al., 2016).

SMA results for sludge taken from different levels of the reactors during operation at 20 °C show maximum methane potential (PMP) of 349–437 and 230–260 mL g^{-1} VS d^{-1} from lower to upper sludge level of UASB reactors 1 and 2, respectively (Fig. 2). However, the actual methane productions (AMP) are only 7 and 1.0 mL g^{-1} VS d^{-1} at the influent COD concentration of 243 mg/L. The decrease in the SMA with height (Fig. 2a and b) can be explained by the fact the substrate (dissolved COD) decreases as wastewater flows from bottom to top which results in lower methanogenic activity at the upper level.

Fig. 1 **a** COD removal efficiency and **b** biogas production rate for the two pilot scale UASB reactors operated temperature of ~ 20 and ~ 28 °C
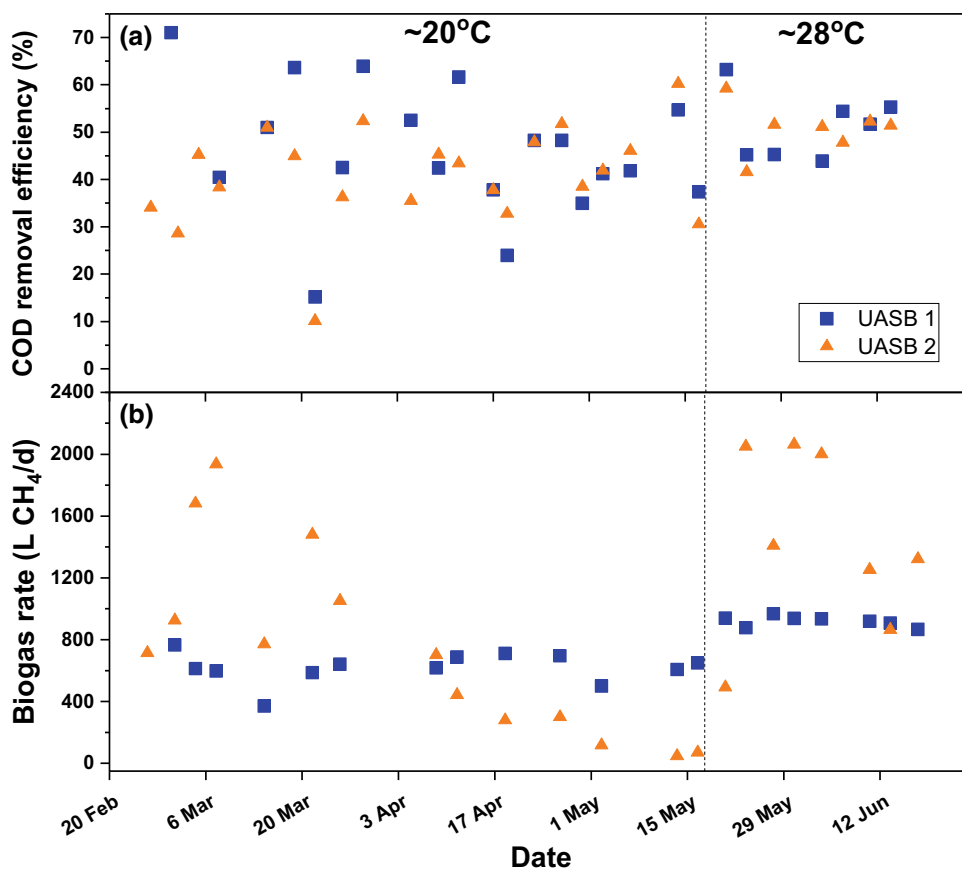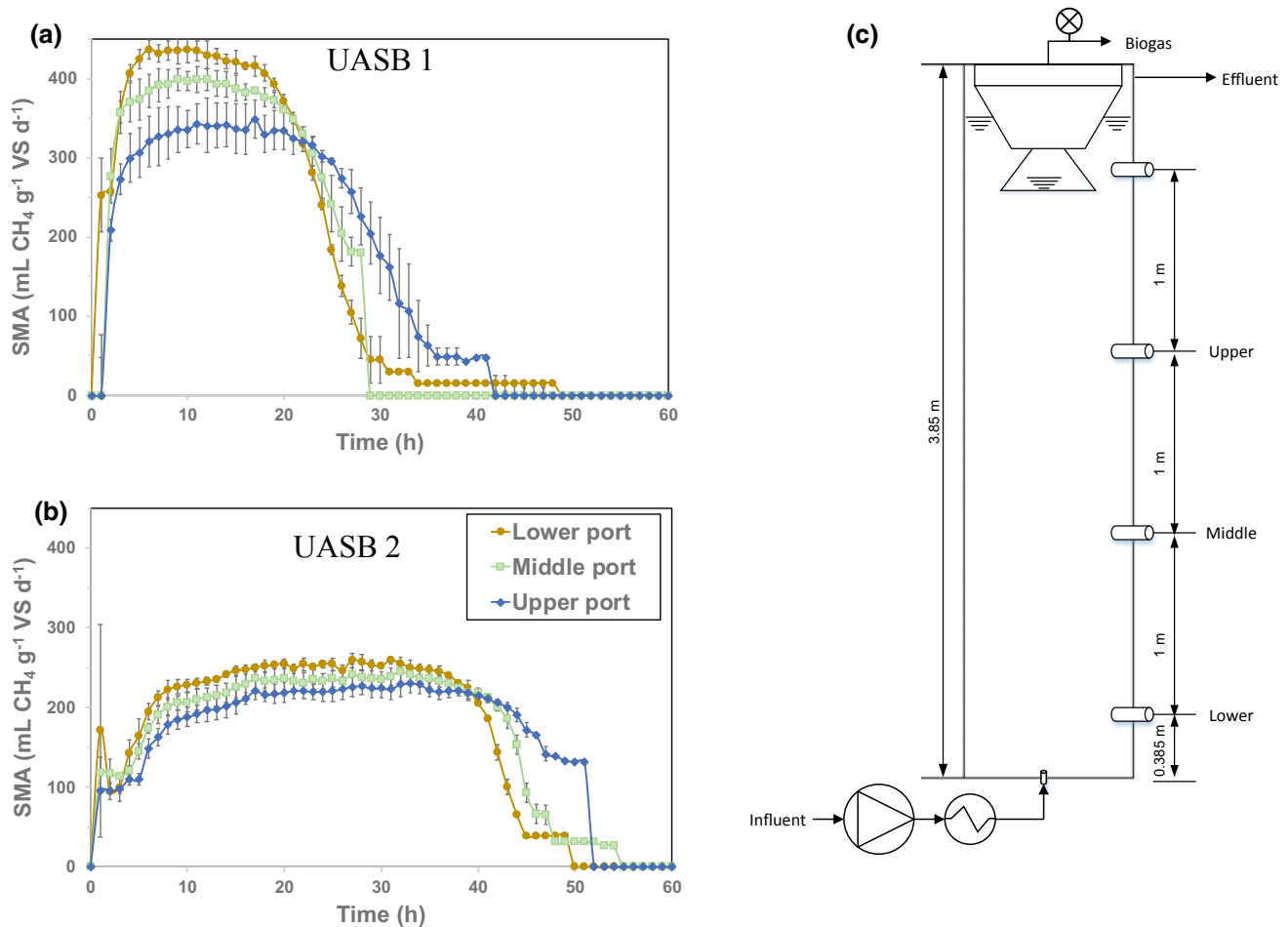
Fig. 2 SMA results of granular sludge taken at an operation temperature of 20 °C for **a** UASB reactor 1 (larger granule size) and **b** UASB reactor 2 (smaller granule size). **c** Schematic of the pilot scale reactors showing the sampling points (lower, middle and upper) of sludge used (SMA test was performed at 35 °C with 2000 mg/L volatile solids (VS) and sodium acetate concentration of 3000 mg/L)

4 Conclusion

The effect of granular size distribution and temperature on the performance of UASB reactors treating municipal wastewater is studied. The studies show that granular size can significantly influence the UASB performance in terms of methane production. UASB reactor with larger granular size distribution produces a stable amount of methane when compared with a reactor with low granular size treating the same influent wastewater. This was attributed to the well-developed pore structure which aids methane production. The PMP of the sludge were significantly higher than the AMP for both reactors, with a decrease in PMP with height increase which was attributed to substrate decrease from bottom to top.

References

Crone, B. C., Garland, J. L., Sorial, G. A., & Vane, L. M. (2016). Significance of dissolved methane in effluents of anaerobically treated low strength wastewater and potential for recovery as an energy product: A review. *Water Research, 104,* 520–531.

Hulshoff Pol, L. W., De Castro Lopes, S. I., Lettinga, G., & Lens, P. N. L. (2004). Anaerobic sludge granulation. *Water Research*.

Jijai, S., Srisuwan, G., O-Thong, S., Ismail, N., & Siripatana, C. (2015). Effect of granule sizes on the performance of upflow anaerobic sludge blanket (UASB) reactors for cassava wastewater treatment. *Energy Procedia, 79,* 90–97.

Lucas, S., Raphaele, S., Chaves, M., & Van Haandel, A. (2018). Influence of temperature on the performance of anaerobic treatment systems of municipal wastewater. *Water SA, 44,* 211–222.

Wu, J., Afridi, Z. U. R., Cao, Z. P., Zhang, Z. L., Poncin, S., Li, H. Z., et al. (2016). Size effect of anaerobic granular sludge on biogas production: A micro scale study. *Bioresource Technology, 202,* 165–171.

Yi, X. H., Wan, J., Ma, Y., & Wang, Y. (2016). Characteristics and dominant microbial community structure of granular sludge under the simultaneous denitrification and methanogenesis process. *Biochemical Engineering Journal, 107,* 66–74.

CO$_2$ Biofixation by *Chlamydomonas reinhardtii* Using Different CO$_2$ Dosing Strategies

Nilesh R. Badgujar, Franscesco Di Capua, Stefano Papirio, Francesco Pirozzi, Piet N. L. Lens, and Giovanni Esposito

Abstract

The CO$_2$ sequestration potential of the green microalga *Chlamydomonas reinhardtii* was investigated with different CO$_2$ dosing strategies. A gas mixture containing 30% CO$_2$ and 70% N$_2$ was used in these experiments in order to simulate the treatment of flue gases from various industries containing high concentrations of CO$_2$. Alongside the CO$_2$ sequestration, the results suggest that the microalgal biomass was rich in carbohydrates and lipids, and thus suitable to be used for biofuel production.

Keywords

Periodic CO$_2$ dosing • CO$_2$ sequestration • Biochemical profiles • Chlorophyll • *Chlamydomonas reinhardtii*

1 Introduction

The atmospheric carbon dioxide (CO$_2$) concentrations reached 411.31 parts per million (ppm) in May 2018, i.e. 2.54% higher than the 400.83 ppm registered in 2015. This recent unusual increase in CO$_2$ emissions is due to overuse of fossil fuels and the strong 2015–16 El Niño event, which has ultimately reduced the natural capacity of forests and oceans to absorb CO$_2$ from the atmosphere (CO$_2$ Earth 2018).

The natural photosynthetic capacity of microalgae has grabbed world's attention due to their stronger CO$_2$ biofixation capacity and the potential to couple this CO$_2$ sequestration to the production of wide range of products (biofuels and value-added compounds). Microalgae can also use wastewater as source of nutrients, contributing to an environmental benefit along with biofuel production (Kumar et al. 2010). It was found that the green microalga *Chlamydomonas reinhardtii* can capture the CO$_2$ at a high rate, because of its well-developed photosynthetic apparatus and active ribulose-1,5-bisphosphate carboxylase/oxygenase (RuBisCO) enzyme. Most of the studies on CO$_2$ fixation by *C. reinhardtii* were based on the production of biomass and biofuel like bio-H2, bio-ethanol. Very little information exists about the growth of *C. reinhardtii* under elevated concentrations of CO$_2$ (Fan et al. 2017).

In this research, *C. reinhardtii* was cultivated under various CO$_2$ dosing strategies with the objective to increase the biomass growth rate as well as biochemical compounds production. In our previous study, the highest CO$_2$ sequestration rates were observed at a CO$_2$ concentration of 30%, which was used as a fixed CO$_2$ concentration in this study. The production rate of sugars, proteins, lipids and pigments with different CO$_2$ feeding strategies was also investigated. A detailed understanding of the effect of dosing strategies is essential to apply the CO$_2$ sequestration process by microalgae for the treatment of industrial flue gases containing high concentrations of CO$_2$.

2 Materials and Methods

2.1 Microalgae Culture

The microalgae culture of *C. reinhardtii* used in this study was obtained from the algae collection centre of the University of Naples Federico II. The high salt medium (HSM) used for the cultivation of *C. reinhardtii* consisted of (mg L^{-1}): NH$_4$Cl (500), MgSO$_4$·7H$_2$O (20), CaCl$_2$·2H$_2$O (10), K$_2$HPO$_4$ (1440), KH$_2$PO$_4$ (720), EDTA disodium salt (50), ZnSO$_4$·7H$_2$O (22), H$_3$BO$_3$ (11), MnCl$_2$·4H$_2$O (5.01),

N. R. Badgujar (✉) · G. Esposito
University of Cassino and Southern Lazio, Cassino, Italy
e-mail: badgujarnilesh89@gmail.com

F. Di Capua · S. Papirio · F. Pirozzi
University of Napoli Federico II, Naples, Italy

P. N. L. Lens
IHE, Delft, The Netherlands

$CoCl_2 \cdot 6H_2O$ (1.61), $CuSO_4 \cdot 5H_2O$ (1.57), $(NH_4)_6Mo_7O_{24} \cdot 4H_2O$ (1.1), $FeSO_4 \cdot 7H_2O$ (4.99), KOH (15).

2.2 CO₂ Sequestration Experiments

Batch experiments for CO_2 sequestration were carried out in 500 mL glass flasks containing 300 mL of HSM and inoculated with microalgae in exponential growth phase. The bottles were kept on rotary shakers at 160 rpm, while a 30% CO_2–70% N_2 gas mixture was supplied using a DAS GIP MX 4/4 gas mixer. Continuous light was supplied by Philips TLD Eco 51 W/840 fluorescent lamps at an intensity of 130 μmol m^{-2} s^{-1} and measured with Digital Lux metre (Dr. Meter, China). Temperature was kept between 22 and 25 °C. Prior to starting the biosequestration experiments, the initial pH of the medium was adjusted to 7.0.

In our previous study, the effect of different concentrations of CO_2 in the feed gas on the growth of *C. reinhardtii* was investigated by sparging the gas just once per day for 10 min. According to Ying et al. (2015), periodic dosing of CO_2 helps to achieve a higher gas/liquid mass transfer rate than continuous dosing and increase the biofixation capacity of microalgae. In the present study, besides a single sparging for 10 min each day at a flow rate of 1 L/h, CO_2 was sparged with the same flow rate for 10 min two and three times a day (double and triple sparging, respectively) and twice a day for 10 min each by doubling the volume of fed gas using a flow rate of 2 L/h (double volume–double sparging).

2.3 Analytical Methods

2.3.1 Measurement of Cell Growth

Absorbance was measured by spectrophotometric method using an UV/Visible spectrophotometer (Agilent G1103A 8453) at 680 nm wavelength.

2.3.2 Biochemical Analysis

Samples for biochemical analyses were collected each day to measure the concentrations of sugars, proteins and lipids. Samples were pretreated using ultrasonication at 60 °C for 10 min in order to break the cell wall so that the biochemical compounds could be more accurately measured. The sugars were estimated using phenol sulphuric acid assay (Dubois et al. 1956), proteins using Lowry's assay (Lowry et al. 1951) and lipids using sulfo-phospho-vanillin assay (Mishra et al. 2014).

2.3.3 Measurement of Total Pigments

A spectrophotometric method was used to measure the total pigments (chlorophyll and carotenoids) produced by the microalgae. 1 mL sample was centrifuged at 8000 rpm for 5 min, and the supernatant was discarded. The algal pellet was dissolved in 1 mL preheated dimethyl sulfoxide at 60 °C using vortex shaker, then the solution was centrifuged at 8000 rpm for 5 min. The supernatant was transferred to another tube and used to measure the absorbance at different wavelengths (480, 630, 649, 665 and 710 nm). The measured absorbance was used to calculate the amount of chlorophyll a and b as well as the carotenoids by using the equations developed by Wellburn (1994).

3 Results and Discussion

The first significant result shown in Fig. 1 is the gradual decrease of pH from 7.0 to approximately 4.5 (triple dosing and double dosing + double volume), 4.2 (double dosing) and 3.8 (single dosing) over the period of sequestration. This decrease of pH can be attributed to the CO_2 solubilization and conversion into carbonic acid as well as ammonium (NH_4^+) uptake by microalgae. The cell density increased significantly until the pH dropped to 5.5 (day 8), since a further decrease of pH did not correspond to an extra cell density increase (Fig. 1).

The biochemical analyses (Fig. 1) were performed to study the fate of the carbon captured by the microalgae inside the cells. The total sugar concentration obtained with the single and double dosing strategy was comparatively higher compared to that achieved with the other two strategies. While the protein and lipid concentration was
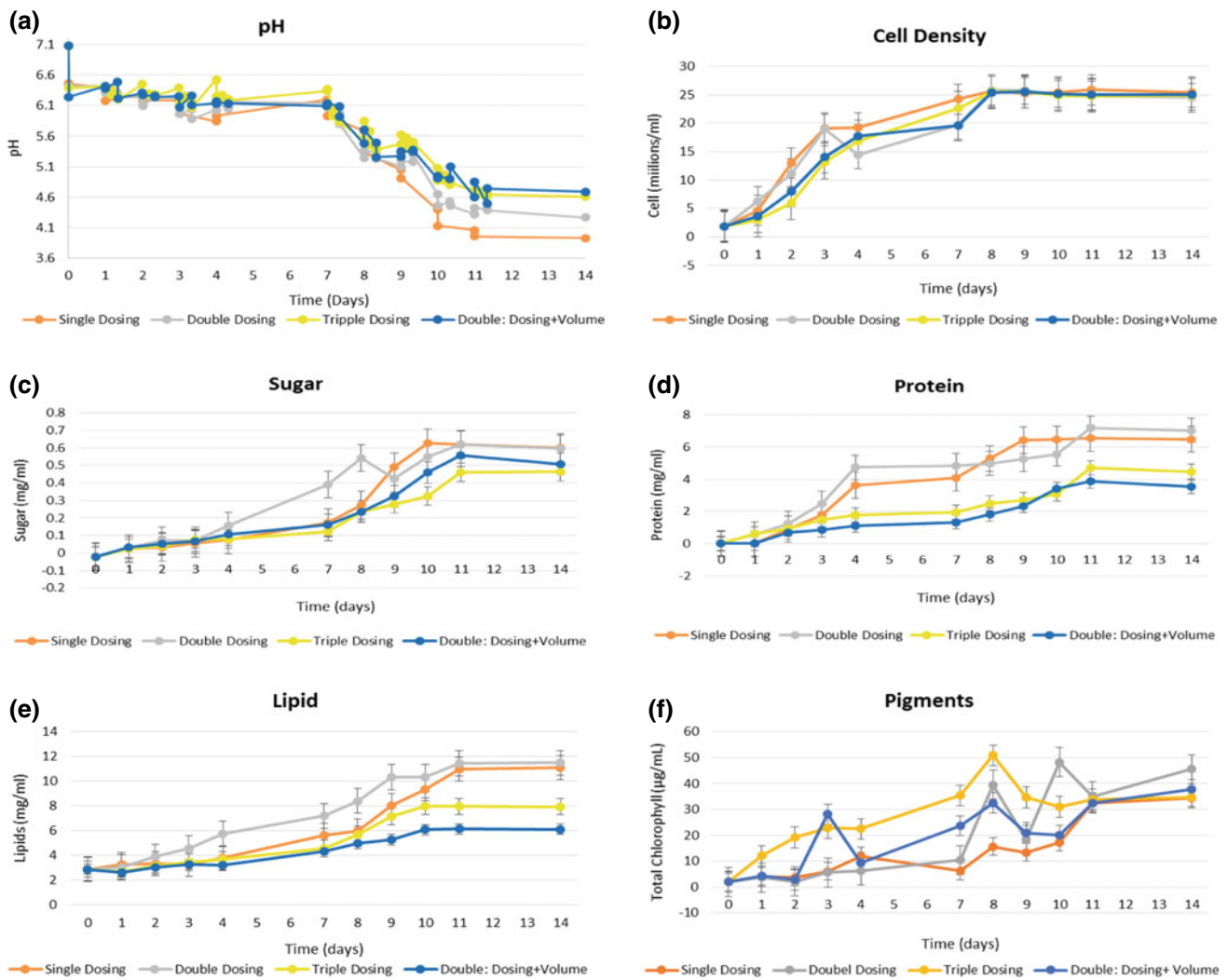
Fig. 1 Different parameters investigated during the biosequestration of CO_2 by *C. reinhardtii*. **a** pH of the medium, **b** cell density, **c** sugar concentration, **d** protein concentration, **e** lipid concentration, **f** pigment concentration

higher with the double dosing strategy, the total pigment concentration was substantially the same under all conditions.

4 Conclusion

The CO_2 sequestration experiments with *C. reinhardtii* showed that the double dosing strategy resulted in a significantly higher concentration of biochemical compounds compared to the other strategies tested. In particular, the production of sugars, proteins and lipids at the end of the experiments was 0.6, 6.8 and 11.5 mg/mL, respectively. Cell density at the end of the experiments was approximately the same (25 millions/mL) with all dosing strategies. In order to better understand the rate and pathways of CO_2 biofixation by

C. reinhardtii, the effect of different gas flow rates on the growth of microalgae, cell dry weight and total organic carbon should be analysed. However, the results of this study show that the flue gases from industries containing 30% CO_2 can be efficiently used for enhancing the growth of *C. reinhardtii* and the production of biomolecules of commercial interest.

References

CO₂ Earth. (2018). *Are we stabilizing yet?* https://www.co2.earth/.

Dubois, M., Gilles, K. A., Hamilton, J. K., Rebers, P. A., & Smith, F. (1956). Colorimetric method for determination of sugars and related substances. *Analytical Chemistry, 28*(3), 350–356.

Fan, Q., Yan, X., Yi, Y., Xiaosheng, L., Li, Z., Hui, Z., et al. (2017). Enhancing growth of *Chlamydomonas reinhardtii* and nutrient

removal in diluted primary piggery wastewater by elevated CO_2 supply. *Water Science and Technology, 75*(10), 2281–2290.

Kumar, A., Ergas, S., Yuan, X., Sahu, A., Zhang, Q., Dewulf, J., et al. (2010). Enhanced CO_2 fixation and biofuel production via microalgae: Recent developments and future directions. *Trends in Biotechnology, 28,* 371–380.

Lowry, O. H., Rosebrough, N. J., Farr, A. L., & Randall, R. J. (1951). Protein measurement with the Folin phenol reagent. *Journal of Biological Chemistry, 193*(1), 265–275.

Mishra, S. K., Suh, W. I., Farooq, W., Moon, M., Shrivastav, A., Park, M. S., & Yang, J. W. (2014). Rapid quantification of microalgal lipids in aqueous medium by a simple colorimetric method. *Bioresource technology, 155,* 330–333.

Wellburn, A. R. (1994). The spectral determination of chlorophylls a and b, as well as total carotenoids, using various solvents with spectrophotometers of different resolution. *Journal of Plant Physiology, 144,* 307–313.

Ying, K., Gilmour, D., & Zimmerman, W. (2015). Periodic CO_2 dosing strategy for *Dunaliella salina* batch culture. *International Journal of Molecular Sciences, 16*(5), 11509–11521.

A Suggestion on Nutrient Removal/Recovery from Source Separated Human Urine Using Clinoptilolite Combined with Anaerobic Processing

B. Beler-Baykal, M. N. Taher, and M. Altinbas

Abstract

Source separated human urine is a renewable alternative source of fertilizers. Plant nutrients therein may be concentrated upon clinoptilolite to be made available to plants in due course. The remaining liquid phase is a saline solution containing appreciable amounts of organics which may be converted into biogas to be used as energy while it is treated anaerobically. The preliminary results reveal that in addition to high levels of nutrient recovery and considerable organics removal, the remaining liquid waste may possibly be treated using anaerobic processes and that the outcomes can be improved especially after determining the best choices for process variables.

1 Introduction

Containing over 80% of nitrogen (N) and over 50% of both phosphorus (P) and potassium in conventional domestic wastewater, human urine is an effective and renewable source of fertilizers. Human urine makes up only 1% of conventional domestic wastewater by volume and may easily be separated using urine diverting toilets, as well as through urinals which are already being used widely across the world. Nutrients may then be removed from the liquid phase, i.e., source separated human urine, and recovered to be used further as fertilizer. One efficient way of doing that is through processing urine with ammonium selective natural zeolite clinoptilolite to transfer and concentrate nutrients onto this natural solid phase mainly through ion exchange/adsorption and subsequently make them available to plants through desorption into water, either through irrigation or precipitation (Beler-Baykal 2015). The effectiveness of the process had been demonstrated in a number of previous work (Beler-Baykal et al. 2004, 2009, 2011; Kocaturk and Beler-Baykal 2012; Allar and Beler-Baykal 2016; Dogan et al. 2017) indicating recoveries which exceed 80% for N and 90% for P. This route provides a short cut in returning plant nutrients back to soil for crop production. This will provide further benefits in terms of energy conservation especially as 1% of the global energy use goes to the production of nitrogen fertilizers through the Haber–Bosch process (Kongshaug 1998; IFA/UNEP 1998). This makes urine diversion and processing a meaningful practice from the perspective of valorizing wastes, in this case from (a portion of) domestic wastewater, which will aid food security and environmental sustainability.

Separation of urine and its contents from the rest of domestic wastewater constituting 99% by volume, alleviates the need for nitrification/denitrification units in conventional domestic wastewater treatment plants which is a sensitive process using significant amounts of energy. Hence diversion of human urine also provides benefits in terms of reducing the treatment trend as well as energy in domestic wastewater plants, and it aids in controlling domestic wastewater oriented water pollution.

As on a global basis, the equivalent of nutrients from human excreta is about 35% of the entire global fertilizer use; the potential is appreciable and should not be underestimated. Processing urine with clinoptilolite is a proven method of nutrient recovery, yet the remaining liquid phase,

B. Beler-Baykal (✉) · M. N. Taher · M. Altinbas
Department of Environmental Engineering, Istanbul Technical University, Ayazaga, 34469 Istanbul, Turkey
e-mail: baykalb@itu.edu.tr

M. N. Taher
e-mail: mustafan80@gmail.com

M. Altinbas
e-mail: altinbasm1@itu.edu.tr

nutrient-devoid urine solution, is a waste stream which should be taken care of for environmental protection. The primary aim of this work is to find a remedy for this highly saline residue after nutrient removal which contains considerable amounts of organic matter, and anaerobic processing is suggested to deal with this liquid phase. With that, the intention is to make a preliminary observation to investigate the possible use of anaerobic processes which will yield biogas which may be used as energy while reducing the pollution potential imposed by the residue originating from nutrient recovery using clinoptilolite from source separated urine.

2   Materials and Methods

The experiments were performed in the laboratory scale setups in two segments: nutrient removal from source separated stored urine using clinoptilolite in an up flow fixed bed column, followed by elution of nutrients using tap water in the first segment, and to observe the possibility of COD removal to be accompanied by biogas production in an anaerobic expanded granular sludge bed reactor using source separated urine in the second segment. Within the scope of this work, emphasis is placed on N and P as nutrients. Characteristics of the urine samples used in the experiments are summarized in Tables 1 and 2 as appropriate. Urine samples were collected from urinals of ITU's Environmental Engineering Department. As can be observed from the tables, it is highly saline and rich in organic matter as well as nutrients. A Turkish clinoptilolite from Gordes region was used after conditioning with NaCl to obtain the Na form, which had previously been shown to be the best surface form for ammonium removal, in the particle size range of 1–2 mm. Anaerobic sludge was obtained from a confectionary wastewater treatment plant. As the liquid phase is highly saline, adaptation was started with 25% urine and was stepwise raised to 65% which reasonably represents the COD concentration expected in the liquid phase resulting from nutrient removal.

3   Results and Discussion

Characterization of the liquid phase for nutrient removal experiments is presented in Table 1. As the ratio of ortho-P to total-P was 93%, ortho-P was used to represent phosphorus, which was in line with previous experiments and literature. It may be observed that the success of clinoptilolite was high for nutrient removal with 87% for N and 100% for P, also compatible with the literature. For the purpose of the present study, it was also important to determine COD removal in the clinoptilolite column, which was also significant with 39%. This is important (for) evaluating expected COD concentrations in relation to the possibility of using anaerobic processes and to decide about the dilutions for adaptation of the anaerobic sludge to salinity. Following the removal step, the inlet was shifted to tap water for elution of nutrients from the surface for recovery, and the results show that in the first 100 h, recovery levels were 45 and 100% for nitrogen and phosphorus, respectively. However, it has to be kept in mind that thereafter a low but steady release of N is expected for extended periods of time as the nutrient enriched clinoptilolite is considered as a slow release fertilizer. Further release of N from the surface in time will lead to an increase in N recovery efficiency. Figures 1 and 2 are provided to show N and P concentrations in time during removal and recovery of urine-based nutrients.

Table 2 shows that COD may be represented well through soluble COD. It may further be observed from Table 2 that with 25% urine, COD removals could reach 75% which decreased to about 40% with 65% urine. Evolution of biogas was observed through the use of Teddler bags. It is important to realize that in this segment, fresh urine without nutrient removal had been used as the main aim was to observe COD removal under saline conditions. Shifting the feed solution to nutrient-devoid urine will most probably improve performance through alleviating any negative effects due to high ammonium concentrations. Also, the results have revealed that optimization of process variables including choosing the best salinity and COD

Table 1 Characterization of influent and effluent of fixed bed clinoptilolite columns

Parameters	Units	100% Urine		
		Initial	Final	% Removal
COD	mg COD/L	4450	2700	39
NH_4	mg NH_4^+-N/L	7130	940	87
TKN	mg N/L	7620	1624	–
Ortho-phosphate	mg PO_4^{3-}/L	165	1	100
Potassium	Mg K^+/L	4050	1065	74

Table 2 Characterization of anaerobic processing Influent and effluent with different adaptation stages

Parameter	Unit	25% urine			50% urine			65% urine		
		Inf.	Eff.	RE%	Inf.	Eff.	RE%	Inf.	Eff.	RE%
Total COD	mg/L	1220	440	64	2130	1465	45	2900	1720	35
Soluble COD	mg/L	1200	300	75	2100	1020	60	2900	1430	40
NH_4^+	mg NH_4–N/L	906	930	–	1811	1800	–	2900	2950	–
TKN	mg NH_3–N/L	2660	2690	–	4360	4020	–	7640	7540	–
E. conductivity	µS/cm	8100	8800	–	22,500	22,000	–	25,500	26,700	–
Calculated CH_4 production	L CH_4/day	1.7			2.0			2.8		
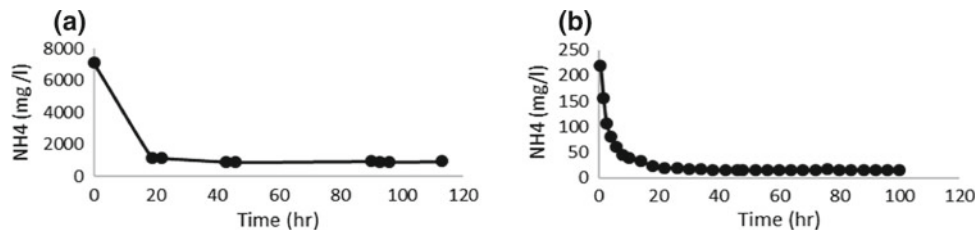
Fig. 1 **a** NH_4^+ removal from liquid phase, **b** NH_4^+ recovery from solid phase
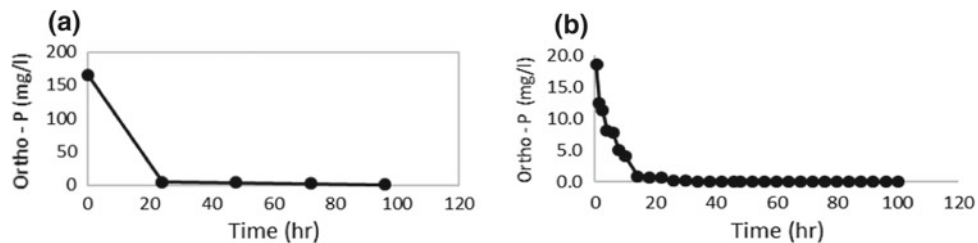
Fig. 2 **a** PO_4^{3-} removal from liquid phase, **b** PO_4^{3-} recovery from solid phase

levels in the feed solution will be a key factor for improving performance. Nevertheless, the preliminary results under conditions employed in this work have provided evidence that an efficiency of 40–75% may be expected in terms of COD removal which is calculated to lead to the generation of 1.3–2.8 L CH_4/day in this 9.2 L reactor which corresponds to 0.31-0.51 l CH_4/l urine.

employed in the preliminary experiments reported in this work, there seems to be a good chance of improving the process efficiency by determining best choices of process variables upon further work. Moreover, with a holistic perspective, the approach described in this work provides a promising route to reduce the energy demand for integrated domestic wastewater treatment and fertilizer production.

4 Conclusion

It was demonstrated that 87% of N and 100% of P can be removed from source separated human urine through processing with clinoptilolite, while nearly 40% of COD is also removed in the process. Anaerobic processing seems to be a promising route for reducing the pollution potential of the saline solution remaining after nutrient removal, while generating biogas from a waste stream. Although COD removals between 40 and 75% could be attend under the conditions

References

Allar, A.D., & Beler-Baykal, B. (2016, February). An investigation into the potential use of nutrients recovered from urine diversion on a summer housing variables site: Self-sufficiency based on nitrogen balance. *Water Science and Technology, 73*(3), 576–581. https://doi.org/10.2166/wst.2015.527.

Beler-Baykal, B. (2015). Stream segregation in household use: A review of grey water as an alternative source of water and yellow water as an alternative source of fertilizers. *Water Qual Expo Health, 7*, 27–37.

Beler-Baykal, B., Allar, A. D., & Bayram, S. (2011). Nitrogen recovery from source separated human urine using clinoptilolite and preliminary results of its use as fertilizer. *Water Science and Technology, 63*(4), 811–817.

Beler-Baykal, B., Bayram, S., Akkaymak, E., & Cinar, S. (2004). Removal of Ammonium from human urine through ion exchange with clinoptilolite and its recovery for further reuse. *Water Science and Technology, 50*(6), 149–156.

Beler-Baykal, B., Kocaturk, N. P., Allar, A. D., & Sari, B. (2009). The effect of initial loading on the removal of Ammonium and Potassium from source separated human urine via clinoptilolite. *Water Science and Technology, 60*(10), 2515–2520.

Dogan, G., Giresunlu, E., & Beler-Baykal, B. (2017). A preliminary investigation on the use of segregated wastewater streams as fertilizer and irrigational water upon pepper. In *IWA Resource Recovery Conference*, August 5–9, 2017, New York, USA.

IFA/UNEP. (1998). *The fertilizer industry, world food supplies and the enviro*nment. Paris: International Fertilizer Industry Association, December 1998.

Kocaturk, N. P., & Beler-Baykal, B. (2012). Recovery of plant nutrients from dilute solutions of human urine and preliminary investigations on pot trials. *Clean, 40*(5), 538–544.

Kongshaug, G. (1998). Energy consumption and greenhouse gas emissions in fertilizer production. In *IFA Technical Conference*, Marrakech, Morocco, 28 September–1 October, 1998.

Niches for Bioelectrochemical Systems in Wastewater Treatment Plants

Miguel Osset-Álvarez, Laura Alsina, Narcis Pous,
Ramiro Blasco-Gómez, Jesús Colprim, M. Dolors Balaguer,
and Sebastià Puig

Abstract

Climate change and future depletion of resources are two of the most important environmental challenges that humankind have ever faced. This chapter aims to give a second chance to contaminated water and recalcitrant carbon dioxide (CO_2) streams by putting forward a resilience and sustainable technology-based electron-driven microbial reactions.

Keywords

Carbon capture • Electro bioremediation • Microbial electrosynthesis • Water

1 Introduction

Bioelectrochemical systems (BES) have been explored in wastewater treatment plants (WWTPs) according to three main concepts: to produce energy from organic substrates, to generate/recovery products and to provide specific environmental services. This abstract contains a critical examination of the current application of BES in the field of bioremediation of contaminated water and bio-electro carbon dioxide recycling in WWTPs. Data from lab-scale and pilot-plant studies will be shown to prove that BES is a highly promising and cost-effective technology for the sustainable remediation of contaminated sites and production biofuels and/or commodity chemicals from recalcitrant CO_2 streams emitted in WWTPs.

2 Water Recovery as a Need not a Wish

Water, food and energy are essential interrelated resources for sustainable development, whose demands expected to increase in the next decades. The environmental clock is ticking: climate change and depletion of fossil resources are around the corner. Because of this, all major stakeholders involved in water management agree that a change of paradigm is needed: wastewater (contaminated water) is not only waste that must be treated, but also a valuable source of resources.

BES are a promising platform through which we can provide reducing power (as electrons) to the cathode (Majone et al. 2015). In our European Patent (Puig et al. 2012), we drove oxidised nitrogen compounds (nitrate, nitrite and nitrous oxide) reductions in biocathodes by controlling the electron availability. The cathode potential influences the removal rate, the presence of undesirable intermediates (nitrite and nitrous oxide) and the stability of the biocathode (Pous et al. 2015). Microcosms isolated from denitrifying biocathodes were successfully used for the elucidation of the underlying extracellular electron transfer (EET) fundamentals as well as microbiome analyses. Cyclic voltammetry analysis for a denitrifying biocathode dominated by *Thiobacillus* sp showed nitrate reduction to nitrite proceeds at -0.30 V and nitrite reduction at -0.70 V (Pous et al. 2014). Finally, a novel and scalable tubular d-BES was developed. The system was able to achieve the highest denitrification rates with BES (up to 850 gN·m^{-3} NCC·day^{-1}) at low HRTs (0.5 h) while simultaneously achieving final disinfection of the treated stream (Pous et al. 2017).

Wastewater treatment is a highly energy demanding process. The removal of organic matter and nitrogen (mainly ammonium; NH_4^+) as the main hazardous products in sewages is necessary for protecting the quality of the water bodies. In WWTPs, about 4.6 kWh kg^{-1} N are required for aeration (Ekman et al. 2006). Avoiding the disadvantages of the so far established technologies, in Vilajeliu-Pons et al. (2018), we

M. Osset-Álvarez · L. Alsina · N. Pous · R. Blasco-Gómez · J. Colprim · M. Dolors Balaguer · S. Puig (✉)
LEQUIA, Institute of the Environment, University of Girona, Girona, Catalonia, Spain
e-mail: sebastia@lequia.udg.cat

suggested an alternative effective autotrophic and anoxic nitrogen removal strategy based on BES that are microbial electrochemical devices coupling the microbial metabolism to an electric current flow. The complete anoxic conversion of ammonium (NH_4^+) to dinitrogen gas (N_2) in continuously operated bioelectrochemical systems was comparable to conventional WTTP, with 35 ± 10 g N m^{-3} d^{-1} at the litre-scale. In contrast to classical aerobic nitrification, the energy consumption was considerable lower (1.16 ± 0.21 kWh kg^{-1} N, being more than 35 times less energy than the conventional wastewater treatment as no aeration was needed) and no intermediate nitrogen species (NO_2^-, NO_3^-, N_2O) accumulate.

3 A Bioelectrochemical Platform for CO$_2$ Recycling

EU annual production of biofuels climbed from approximately 8.2 billion L in 2006 to nearly 30.8 billion L in 2015 (source: Eurostat). Despite this growth, the market is still dominated by the so-called first and second-generation biofuels, which have raised numerous ethical and environmental concerns, such as the effects on food and feed availability and prices (the "fuel vs. food debate").

There is a general consensus that third-generation sustainable biofuels from non-crop feedstocks will play a major role in meeting European's energy and climate targets for 2030 on greenhouse gases (GHG) emissions reduction and in boosting the EU strategies for the bioeconomy and the circular economy. Firstly, the Indirect Land Use Change Directive (the so-called iLUC Directive) established in 2015 that every Member State should account a max 7% crop-based biofuels towards the 10% target of renewables in transport by 2020 fixed by the Renewable Energy Directive (RED). Secondly, current EU regulations also require biofuels to meet several environmental and cost-reduction criteria, such as a minimum of GHG emissions saving of 50% compared to fossil fuels and 60% for new installations. The potential of carbon capture and utilisation (CCU) for producing third-generation biofuels able to meet these sustainable requirements is very high. Waste off gases or, directly, recalcitrant CO_2 from industrial sources or WWTPs are feedstocks whose conversion could delay carbon emissions to the atmosphere while reducing the consumption of the original feedstocks (e.g. fossil resources, crops).

Acetogenic bacteria are capable to convert carbon dioxide into biofuels or commodity chemicals. In our case, bacteria do not utilise sunlight or external dosage of hydrogen (H_2) as an energy source; instead, electrons are fed from renewable electricity. The reduction typically occurs in a BES where the biocatalyst (i.e. bacteria) is grown as a biofilm on the cathode accepting electrons from the electrode. However, reduction of CO_2 to alcohols such as butanol can occur directly (i.e. bacteria donate electrons) or through the intermediate production of H_2 that acts as electron transfer molecule (as it is the case of many acetogenic bacteria). This reduction process is called "H_2-mediated electron transfer" and has previously proven to be an efficient pathway for butyrate production at lab scale (Puig et al. 2017).

To maintain the supply chain in chemical feedstocks in the long-term, the use of CO_2 as an alternative to petrochemical feeds is considered essential. Bioelectrochemical technologies have evolved into a rapidly growing research domain where CO_2 is converted into value-added products like carboxylic acids, bioalcohols, biodiesel, bioplastics, etc. (Batlle-Vilanova et al. 2017; Ganigué et al. 2015; Pepè Sciarria et al. 2018; Blasco-Gómez et al. 2019). Thereby, CO_2 fermenting organisms like *Clostridium ljungdahlii* and related species, which are also researched and applied for reduced synthesis gas fermentation, are especially interesting. The natural products of these organisms are acetic acid and ethanol, which can be upgraded to higher-value end products (e.g. butanol) through genetic engineering of the production strain, or through coupling of two microbial production strains to achieve up to eight-carbon products (Köpke et al. 2010).

References

Batlle-Vilanova, P., et al. (2017). Microbial electrosynthesis of butyrate from carbon dioxide: Production and extraction. *Bioelectrochemistry, 117,* 57.

Blasco-Gómez, R., Ramió-Pujol, S., Bañeras, L., Colprim, J., Balaguer, M. D., & Puig, S. (2019). Unravelling the factors that influence the bio-electrorecycling of carbon dioxide towards biofuels. *Green Chemistry, 21,* 684–691.

Ekman, M., Bjorlenius, B., & Andersson, M. (2006). Control of the aeration volume in an activated sludge process using supervisory control strategies. *Water Research, 40*(8), 1668–1676.

Ganigué, R., et al. (2015). Microbial electrosynthesis of butyrate from carbon dioxide Chem. *Communication, 51,* 3235–3238.

Köpke, M., Held, C., Hujer, S., Liesegang, H., Wiezer, A., Wollherr, A., et al. (2010). Clostridium ljungdahlii represents a microbial production platform based on syngas. *Proceedings of the National Academy of Sciences, 107*(29), 13087–13092.

Majone, M., Verdini, R., Aulenta, F., Rossetti, S., Tandoi, V., Kalogerakis, N., et al. (2015). In situ groundwater and sediment bioremediation: Barriers and perspectives at European contaminated sites. *New Biotechnology, 32*(1), 133–146.

Pepè Sciarria, T., Batlle-Vilanova, P., Colombo, B., Scaglia, B., Balaguer, M. D., Colprim, J., et al. (2018). Bio-electrorecycling of carbon dioxide into bioplastics. *Green Chemistry, 2018*(20), 4058–4066.

Pous, N., Koch, C., Colprim, J., Puig, S., & Harnisch, F. (2014). Extracellular electron transfer of biocathodes: Revealing the potentials for nitrate and nitrite reduction of denitrifying microbiomes dominated by Thiobacillus sp. *Electrochemistry Communications, 49,* 93–97.

Pous, N., Puig, S., Balaguer, M. D., & Colprim, J. (2015). Cathode potential and anode electron donor evaluation for a suitable treatment of nitrate-contaminated groundwater in bioelectrochemical systems. *Chemical Engineering Journal, 263,* 151–159.

Pous, N., Puig, S., Balaguer, M. D., & Colprim, J. (2017). Effect of hydraulic retention time and substrate availability in denitrifying bioelectrochemical systems. *Environmental Science: Water Research & Technology, 3*(5), 922–929.

Puig, S., Ganigué, R., Batlle-Vilanova, P., Balaguer, M. D., Bañeras, Ll, & Colprim, J. (2017). Tracking bio-hydrogen-mediated production of commodity chemicals from carbon dioxide and renewable electricity. *Bioresource Technology, 228,* 201.

Puig, S., Pous, N., Balaguer, M. D., & Colprim, J. (2012). European Patent (WO 2014082989 A1). Bioelectrochemical treatment of contaminated water with oxidised nitrogen compounds.

Vilajeliu-Pons, A., Koch, C., Balaguer, M. D., Colprim, J., Harnisch, F., & Puig, S. (2018). Microbial electricity driven anoxic ammonium removal. *Water Research, 130,* 168–175.

Degradation of Gaseous VOCs by Ultrasonication: Effect of Water Recirculation and Ozone Addition

Jose Comia Jr., Giuseppina Oliva, Tiziano Zarra, Vincenzo Naddeo, Florencio C. Ballesteros Jr., and Vincenzo Belgiorno

Abstract

Ultrasonication with water recirculation slightly enhanced the removal of toluene compared to water recirculation alone due to conjunction of pyrolysis and hydroxyl radical oxidation with absorption. On the other hand, the addition of ozone with ultrasonication decreased the removal efficiency due to scavenging of hydroxyl radicals. The reaction rate for ozone and OH radicals produced during the US process was faster compared to the rate for ozone and toluene.

Keywords

VOCs • Toluene • Ultrasonication • Ozonation • Absorption

1 Introduction

Emissions of volatile organic compounds (VOCs) have become great concerns due to their undesirable health and environmental effects (Rahmani et al. 2014). Sources of these emissions are related to various industries such as petrochemicals, paints, solvents, and even waste and wastewater treatment plants (Carabineiro et al. 2015; Huang et al. 2016). The regulations on air pollution and the air quality expectation of the population necessitate the need for the treatment of waste gases from different emission sources (Lebrero et al. 2014). However, conventional abatement processes have different drawbacks and limitations prompting the need for researches to focus on advanced oxidation processes (AOPs). These processes rely on the effects of highly reactive oxidants—hydroxyl radicals—that can degrade a broad range of organic compounds (Yao et al. 2014).

Ultrasonication (US), an AOP, promotes the formation of hydroxyl radicals to degrade aromatic VOCs. In this process, three subsequent steps occur: the formation of liquid voids, growth of bubbles, and implosive collapse of cavity bubbles (Kidak and Ince 2007). When these bubbles, which entrap water vapor and gases into the liquid, implode, pyrolysis takes place and generates reactive species such as hydroxyl radicals (Mahamuni and Adewuyi 2010). Several studies investigated the degradation of VOCs such as pyridine (Elsayed 2015) and toluene (Goel et al. 2004) considering the influences of various operating conditions such as ultrasound frequency, pH, and initial VOC concentration.

This work aims to investigate the degradation of gaseous VOCs using ultrasonication, with toluene as a representative compound, considering the influence of water recirculation and ozone addition.

2 Materials and Methods

Research studies were carried out at the Sanitary Environmental Engineering Division (SEED) Laboratory of the Department of Civil Engineering of University of Salerno. The ultrasonication (US) setup, shown in Fig. 1, consisted of the US bath equipment (ELMA Transsonic TI-H-10, 135 kHz frequency), two 1 L glass reactors in series both containing 0.5 L deionized water, recirculation tank, and ozonation equipment. The synthetic contaminated stream was obtained by bubbling air in pure toluene (CAS No 108-88-3, Sigma-Aldrich) without moisture. Airflow was set at 0.5 L min^{-1}, and toluene flow was adjusted to achieve the desired concentration. Entering air was diffused in the first

J. Comia Jr. (✉) · F. C. Ballesteros Jr.
Environmental Engineering Program, University of the Philippines Diliman, 1101 Quezon City, Philippines
e-mail: josecomiajr@gmail.com

G. Oliva · T. Zarra · V. Naddeo · V. Belgiorno
Sanitary Environmental Engineering Division, Department of Civil Engineering, University of Salerno, Via Giovanni Paolo II, Fisciano, SA, Italy

reactor and the outlet gas to the second reactor. Water in both reactors was recirculated by a peristaltic pump at 250 mL min^{-1} flow from a recirculation tank. Direct air sampling was done directly using the photoionization detector (PID, Tiger, Ion Science) for both the inlet (S_1) and outlet ports (S_2) at specific intervals until 300 min. Tests were performed with the control (no US) and US frequency of 130 kHz. Additional ozone was provided by the UV/O_3 reactor as denoted by unit G. Ozone produced from two lamps merged with the toluene before entering the reactors in the ultrasound bath. The volume of water in the recirculation tank was 9 L.

The removal efficiency (RE) was analyzed using the equation below where C_i and C_o are the inlet and outlet concentrations, respectively.

$$RE\,(\%) = \frac{C_i - C_o}{C_i} \times 100$$

3 Results and Discussion

For the effect of water recirculation, ultrasonication slightly enhanced the removal of toluene up to 300 min as shown in Fig. 2a. At around 105 min, both the removal for the control and 130 kHz became almost constant, implying steady state at 37% removal. From around 80 ppm toluene initial removal, it decreased to around 30 ppm toward the 300 min period for 130 kHz. The decrease in removal for both tests implies the saturation of the system as the influx of toluene was constant. Continuous absorption was the predominant mechanism in the removal process. A maintained gas to liquid mass transfer due to the water recirculation acted as a driving force in absorption. With US, the enhanced removal was due to pyrolysis and production of OH radicals. To further improve the removal of the system, the suggestion of the scrubbing liquid should be done which was also noted by Tokumura et al. (2008).

To further enhance the removal of toluene, ozone with a dosage of 17.40 mg min^{-1} was introduced in the recirculation step. Figure 2b shows the effects of ozone addition to the US degradation process. At around 10 min reaction time, removal was 73% for O_3/US system and 93% for lone ozonation. Steady-state removal was achieved around 240 min. Based on the results, the addition of ozone proved to be antagonistic in conjunction with the US. As the toluene and ozone mixture was bubbled into the reactors, OH radicals produced from the decomposition of ozone and ultrasonication were scavenged by the ozone molecules leading to lower degradation The reaction rates for ozone and hydroxyl radicals (7.30×10^{-14} cm^3 molecule^{-1} s^{-1}) are faster compared to the reaction of ozone and toluene (1.20×10^{-20} cm^3 molecule^{-1} s^{-1}) (Atkinson et al. 2003; Subrahmanyam et al. 2010). Pyrolysis was also inhibited due to toluene accumulation in the gas–liquid interface. This, in turn, leads to a lower driving force for toluene absorption.

Ozone solubility was enhanced due to bubbling and the simultaneous agitation. It was observed that 98% removal was achieved up to 5 min reaction time. It can be inferred that the reaction of O_3 with toluene is the predominant mechanism in the removal as ozone accumulated in the recirculation water and hydroxyl radicals are short-lived. Higher removal for O_3 compared to O_3/US was also observed by Kidak and Ince (2007) for the degradation of phenol at basic pH.
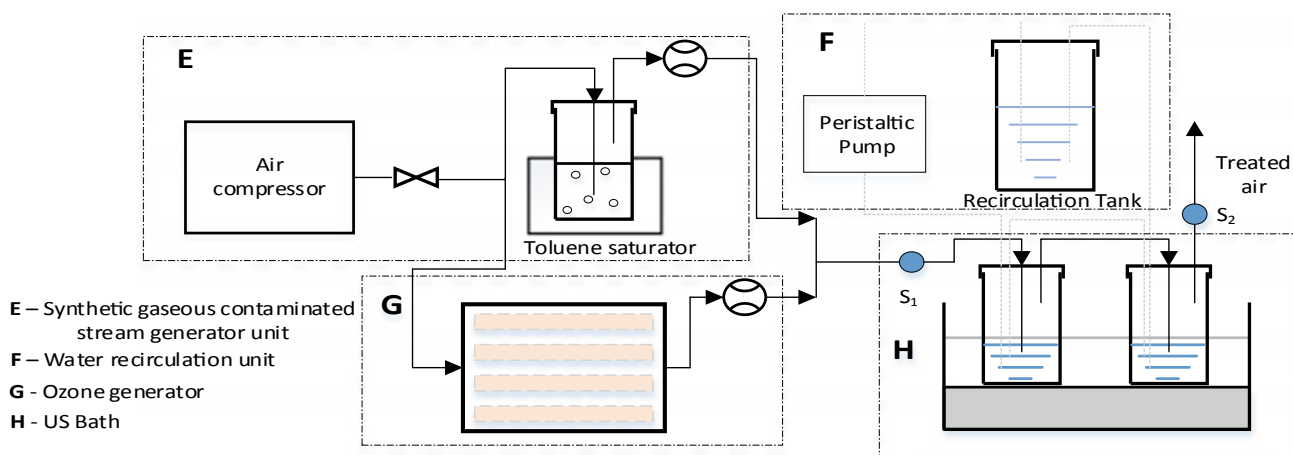
Fig. 1 US treatment setup with water recirculation and ozonation
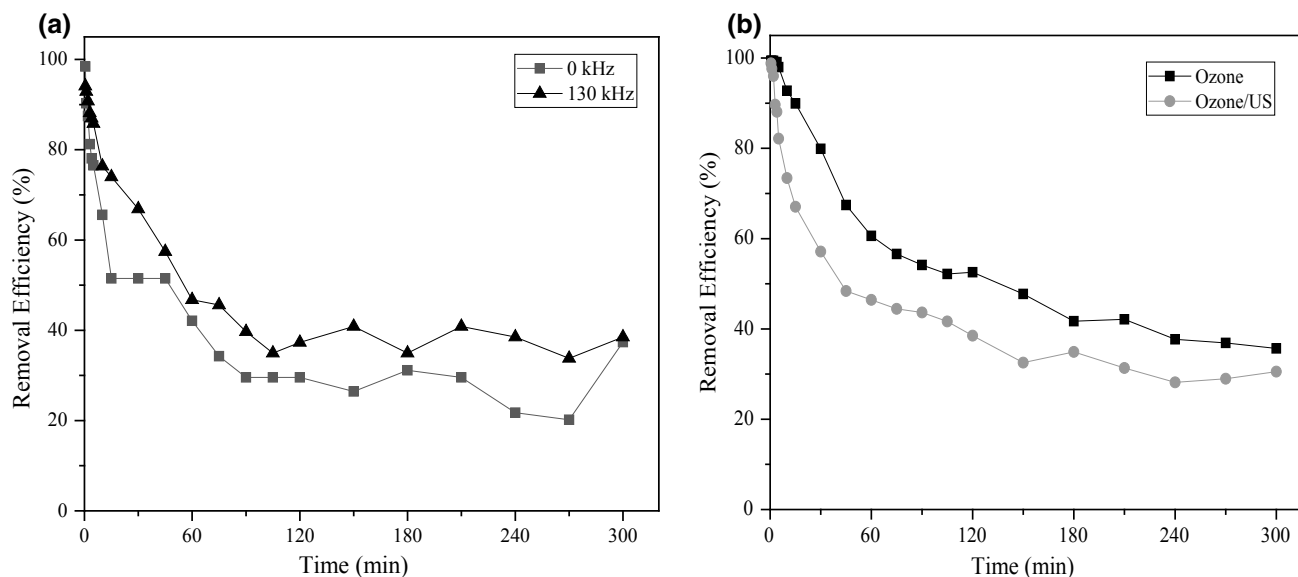
Fig. 2 **a** Removal of toluene at various US frequencies with water recirculation (C_i = 60–80 ppm), **b** effect of ozone addition and water recirculation on toluene degradation (C_i = 250 ppm)

4 Conclusion

Ultrasonication, an advanced oxidation process, relies on the generation of hydroxyl radicals for VOC degradation. The effect of water recirculation and ozone addition was determined in the ultrasonic degradation of gaseous VOCs, using toluene as a representative compound. Ultrasonication with water recirculation slightly enhanced the removal of toluene compared to water recirculation alone due to conjunction of pyrolysis and hydroxyl radical oxidation with absorption. On the other hand, the addition of ozone with ultrasonication decreased the removal efficiency due to scavenging of hydroxyl radicals.

References

Atkinson, R., Baulch, D. L., Cox, R. A., Crowley, J. N., Hampson, R. F., Hynes, R. G., et al. (2003). Evaluated kinetic and photochemical data for atmospheric chemistry: Part 1—Gas phase reactions of O_x, HO_x, NO_x and SO_x species. *Atmospheric Chemistry and Physics Discussions*, *3*(6), 6179–6699. https://doi.org/10.5194/acpd-3-6179-2003.

Carabineiro, S. A. C., Chen, X., Konsolakis, M., Psarras, A. C., Tavares, P. B., Órfão, J. J. M., et al. (2015). Catalytic oxidation of toluene on Ce-Co and La-Co mixed oxides synthesized by exotemplating and evaporation methods. *Catalysis Today*, *244*, 161–171. https://doi.org/10.1016/j.cattod.2014.06.018.

Elsayed, M. A. (2015). Ultrasonic removal of pyridine from wastewater: Optimization of the operating conditions. *Applied Water Science, 5* (3), 221–227. https://doi.org/10.1007/s13201-014-0182-x.

Goel, M., Hongqiang, H., Mujumdar, A. S., & Ray, M. B. (2004). Sonochemical decomposition of volatile and non-volatile organic compounds—A comparative study. *Water Research, 38*(19), 4247–4261. https://doi.org/10.1016/j.watres.2004.08.008.

Huang, H., Huang, H., Zhan, Y., Liu, G., Wang, X., Lu, H., … Leung, D. Y. C. (2016). Efficient degradation of gaseous benzene by VUV photolysis combined with ozone-assisted catalytic oxidation: Performance and mechanism. *Applied Catalysis B: Environmental, 186*, 62–68. https://doi.org/10.1016/j.apcatb.2015.12.055

Kidak, R., & Ince, N. H. (2007). Catalysis of advanced oxidation reactions by ultrasound: A case study with phenol. *Journal of Hazardous Materials, 146*(3), 630–635. https://doi.org/10.1016/j.jhazmat.2007.04.106.

Lebrero, R., Gondim, A. C., Pérez, R., García-Encina, P. A., & Muñoz, R. (2014). Comparative assessment of a biofilter, a biotrickling filter and a hollow fiber membrane bioreactor for odor treatment in wastewater treatment plants. *Water Research, 49,* 339–350. https://doi.org/10.1016/j.watres.2013.09.055.

Mahamuni, N. N., & Adewuyi, Y. G. (2010). Advanced oxidation processes (AOPs) involving ultrasound for waste water treatment: A review with emphasis on cost estimation. *Ultrasonics Sonochemistry, 17*(6), 990–1003. https://doi.org/10.1016/j.ultsonch.2009.09.005.

Rahmani, F., Haghighi, M., & Estifaee, P. (2014). Synthesis and characterization of Pt/Al_2O_3-CeO 2 nanocatalyst used for toluene abatement from waste gas streams at low temperature: Conventional vs. plasma-ultrasound hybrid synthesis methods. *Microporous and*

Mesoporous Materials, 185, 213–223. https://doi.org/10.1016/j.micromeso.2013.11.019.

Subrahmanyam, C., Renken, A., & Kiwi-Minsker, L. (2010). Catalytic non-thermal plasma reactor for abatement of toluene. *Chemical Engineering Journal, 160*(2), 677–682. https://doi.org/10.1016/j.cej.2010.04.011.

Tokumura, M., Nakajima, R., Znad, H. T., & Kawase, Y. (2008). Chemical absorption process for degradation of VOC gas using heterogeneous gas-liquid photocatalytic oxidation: Toluene degradation by photo-Fenton reaction. *Chemosphere, 73*(5), 768–775. https://doi.org/10.1016/j.chemosphere.2008.06.021.

Yao, H., Hansen, M., & Feilberg, A. (2014). DMS removal in a bubble reactor using peroxone (O_3/H_2O_2) reactions. *Chemical Engineering Transactions, 40,* 229–234. https://doi.org/10.3303/CET1440039.

Optimal Chlorination Station Scheduling in an Operating Water Distribution Network Using GANetXL

Roya Peirovi, Alireza Moghaddam, Carol Miller, Asiyeh Moteallemi, Mahdi Rouholamini, and Mohammadamin Moghbeli

Abstract

Chlorination is the process of adding chlorine to drinking water to disinfect it prior to transmission and distribution to the receiving community. In order to maintain the drinking water quality, the chlorine level must remain within certain minimum and maximum values. This paper aims at applying GANetXL optimization tool to a real-world water network to best determine where and how much disinfectant should be injected. GANetXL is a software module that relies on the use of a genetic algorithm (GA) interfaced with EPANET 2.0. The results clearly demonstrate the positive performance of GANetXL to optimize both the disinfectant dosage value as well as the dosing location (i.e., the proper nodes to which the chlorine should be injected).

R. Peirovi
Department of Environmental Health Engineering, Gonabad University of Medical Sciences, Gonabad, Iran
e-mail: peirovi.r@gmu.ac.ir

A. Moghaddam
Department of Civil Engineering, University of Urmia, Gonabad, Iran
e-mail: Alireza.moghaddam@yahoo.com

C. Miller
Department of Civil and Environmental Engineering, Wayne State University, Detroit, MI, USA
e-mail: ab1421@wayne.edu

A. Moteallemi (✉)
Department of Environmental Health Engineering, Torbate Jam Faculty of Medical Sciences, Torbat Jam, Iran
e-mail: rahil_0m0@yahoo.com

M. Rouholamini
Electrical and Computer Engineering Department, Wayne State University, Detroit, MI, USA
e-mail: gj9598@wayne.edu

M. Moghbeli (✉)
University of Politecnico di Milano, Milan, Italy
e-mail: m.moqbeli@gmail.com

1 Introduction

Chlorine is one of the most common disinfectants used in water treatment facilities. As required by drinking water quality guidelines, it is important to maintain the chlorine level of water between the minimum (0.2 mg/L) and maximum (4 mg/L) allowable limits (Munavalli and Kumar 2003). High doses of residual chlorine in a drinking water distribution network might lead to the development of disinfection by-products, such as trihalomethanes and haloacetic acids. These compounds are carcinogenic and harmful to a wide variety of organisms. This underscores the importance of maintaining appropriate chlorine levels throughout the water distribution network. In general, the closer a node is to a chlorine injection point, the greater the concentration of the residual chlorine. The possibility exists that chlorine levels at the most distant nodes (nearby downstream users) may reach dangerously low levels. Various experts have pointed out the key role of chlorine-injecting boosters in maintaining the quality of water (Boccelli et al. 1998). The concentration levels in the injection must lie within a certain range to ensure that the concentration of the residual chlorine will be within desired bounds. To this end, iterative and enumeration techniques may be employed to find the best scenario of nodal chlorine injection. However, these methods are computationally demanding and time consuming and, as a result, not applicable to large-scale networks (Rouhiainen et al. 2003). Therefore, it is clear that we have to utilize optimization algorithms. Having taken into account relevant constraints, Boccelli et al. used a linear objective function to best operate booster pumps of a water network for maintaining the residual chlorine level within a permissible band (Boccelli

Fig. 1 Screenshots of GANetXL

et al. 1998). Ayvaz et al. employed fuzzy decision-making framework, genetic algorithm (GA), and linear programming (LP) to find the optimal location for the booster pumps in a drinking water distribution network. The aforesaid model used a multi-objective optimization, simultaneously optimizing for the minimal total amount of chlorine injected and a minimal number of booster pumps—while also satisfying all constraints imposed by the water quality concerns (Ayvaz and Kentel 2014). In this paper, GANetXL optimization tool, for the very first time, is applied to a real-world water network to best determine where and how much disinfectant should be injected. GANetXL is an Excel module that depends on the use of a genetic algorithm (GA) interfaced with EPANET 2.0.

2 Method and Materials

EPANET 2.0 is capable of tracking how a specific material grows or decays when reacting with water in pipelines. The convective transfer of disinfectants across pipe i is expressed by the classic transfer equation as follows:

$$\frac{\partial c_i}{\partial t} = -u_i \frac{\partial c_i}{\partial x} \pm R(c_i) \qquad (1)$$

where c_i in mg/L represents chlorine concentration in ith pipe. c_i is nodal-dependent and time-variant. u_i in m/s denotes velocity of the flow in pipe i, and finally, $R(c_i)$ is representative of the reaction rate proposed by Rossman (2000).

2.1 GANetXL

Bicik et al. (2008) have developed a novel optimizer, GANetXL, which allows users with little/no background in coding and programming to handle optimization. GANetXL utilizes genetic algorithms (GA) for the optimization tasks.

The most recent version of this software module supports both single and multi-objective GAs. It is quite user-friendly and enables the users to define, configure, and solve optimization problems, and then visualize the results (Fig. 1).

2.2 Objective Function

The objective function of the optimization problem is represented as:

minimize

$$E = \sum_{j=1}^{M} \sum_{k=1}^{N_j} \left[Cn_{jk} - C_{\min} \right]^2, \quad j = 1, \ldots, M; \quad k = 1, \ldots, N_j$$

subject to:

$$Cn_{jk} \geq C_{\min}$$
$$Cn_{jk} \leq C_{\max}$$

(2)

where M denotes the number of determining nodes; N_j is the number of time intervals of jth node; $C_{\min}$ and $C_{\max}$ in mg/L are the minimum and maximum allowable concentration limits, respectively; and Cn_{jk} denotes the amount of residual chlorine at node j in the kth time interval.

3 Results and Discussion

In this section, the performance of GANetXL in optimizing the injection of chlorine to a real-world water network (Shokoohi et al. 2017) situated in the south of Iran is discussed. Figure 2 shows the location of booster pumps (A, B, and C) within this network. Table 1 indicates four different scenarios of booster operation that were simulated in this investigation.

According to Table 1, in scenario S_2, in which both boosters (A and B) are employed simultaneously, not only is
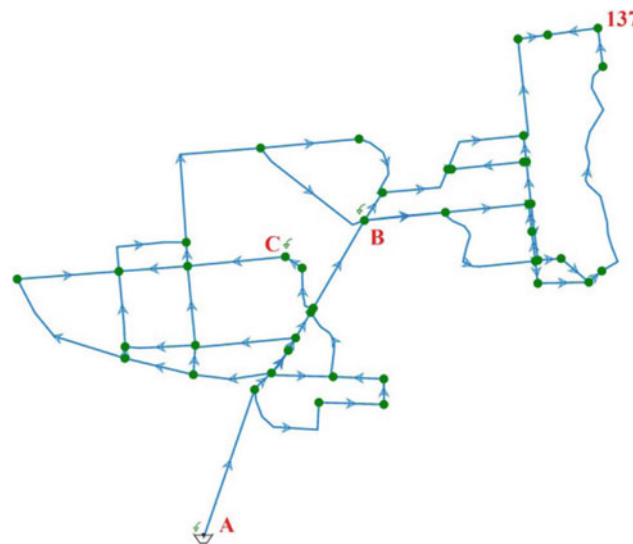
Fig. 2 Location of the booster pumps in the network application

Table 1 Simulated scenarios of chlorine injection

Scenarios	Injection location	Injection timeframe (h)	Objective function	Acceptable nodes (%)
S1	A	1	3050.8	99.22
S2	A/B	1	843.2	100
S3	A/B/C	1	1689.4	98.74
S4	A/C	1	2364.79	98.83

the objective function lower than those of other scenarios, but also the percentage of unacceptable nodes is minimum (by unacceptable nodes, we mean those that have chlorine level outside the acceptable boundaries). This means that S_2 is the best scenario from both health and cost standpoints.

Although S_1 is just slightly different from S_2 in the number of unacceptable nodes, the objective function is significantly larger. Scenarios S_3 and S_4 are not acceptable, as the residual chlorine requirements are not met in these scenarios. The amount of chlorine injected in S_2 (the best scenario) is shown in Fig. 3 in terms of boosters. It should be mentioned that the sum of chlorine injected by booster A and B is 70.13 mg/L in 24 h.

Figure 4 shows the hourly values of the residual chlorine at the 137th node for one day. For the case of chlorine injection at the reservoir node (S_4), the level of residual chlorine is too close to the lower boundary. This necessitates the use of the boosters throughout the network to maintain the desired level of residual chlorine.
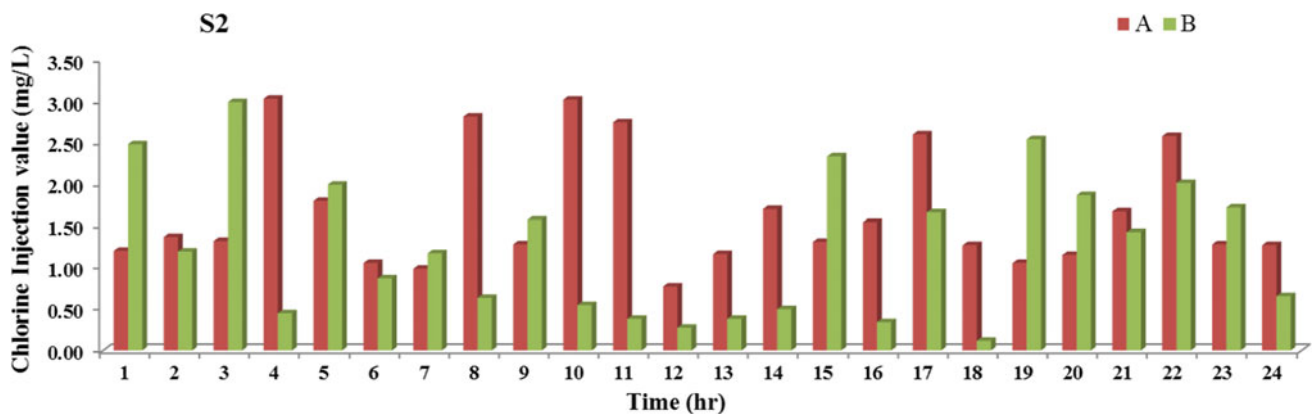
Fig. 3 Chlorine injected by boosters A and B under scenario S_2
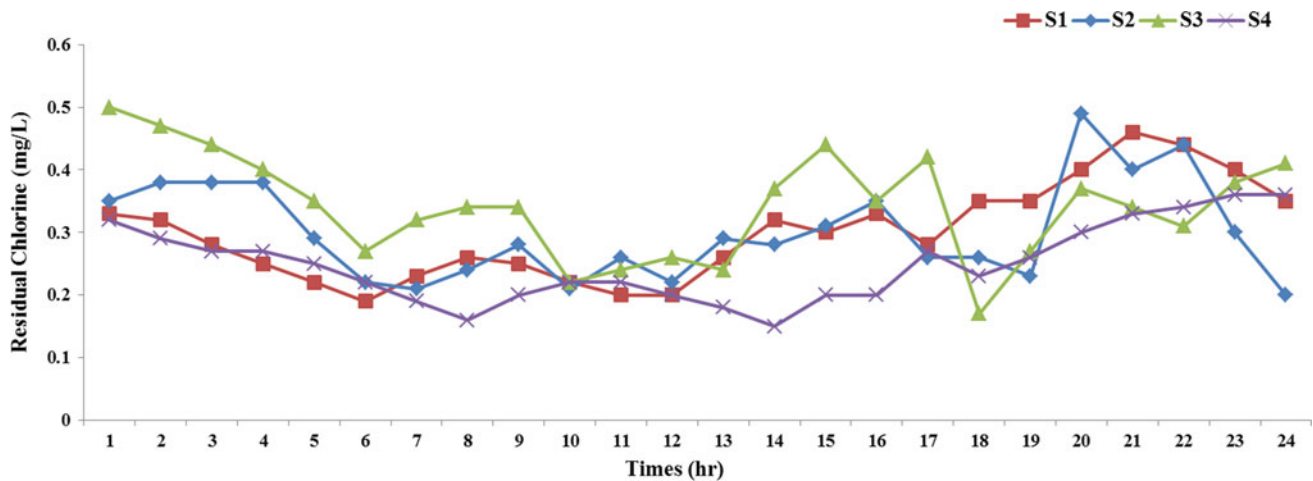
Fig. 4 Changes in residual chlorine at the 137th node (a critical node)

4 Conclusions

This paper aimed at applying GANetXL optimization tool to a real-world water network to best determine the location(s) and dosage of disinfectant. The results clearly demonstrate the powerful performance of GANetXL to calculate the amount of disinfectant needed as well as to identify the proper nodes to which the chlorine should be injected. The results obtained also showed that injecting the disinfectant at an interior node improves the residual chlorine levels in the pipes.

References

Ayvaz, M. T., & Kentel, E. (2014). Identification of the best booster station network for a water distribution system. *Journal of Water Resources Planning and Management, 141*(5), 04014076.

Bicik, J., Morley, M., & Savić, D. (2008). A rapid optimization prototyping tool for spreadsheet-based models. *Water Distribution Systems Analysis*, 1–11.

Boccelli, D. L., Tryby, M. E., Uber, J. G., Rossman, L. A., Zierolf, M. L., & Polycarpou, M. M. (1998). Optimal scheduling of booster disinfection in water distribution systems. *Journal of Water Resources Planning and Management, 124*(2), 99–111.

Munavalli, G., & Kumar, M. M. (2003). Optimal scheduling of multiple chlorine sources in water distribution systems. *Journal of Water Resources Planning and Management, 129*(6), 493–504.

Rossman, L. A. (2000). EPANET 2: User's manual. US Environmental Protection Agency Office of Research and Development National Risk Management Research Laboratory.

Rouhiainen, C., Tade, M., & West, G. (2003). Multi-objective genetic algorithm for optimal scheduling of chlorine dosing in water distribution systems. *Advances in Water Supply Management*, 459–469.

Shokoohi, M., Tabesh, M., Nazif, S., & Dini, M. (2017). Water quality based multi-objective optimal design of water distribution systems. *Water Resources Management, 31*(1), 93–108.

Utilization of Microalgae Cultivated in Municipal Wastewater for CO$_2$ Fixation from Power Plant Flue Gas and Lipid Production

R. J. Tu, S. F. Han, W. B. Jin, X. Zhou, Q. Wang, H. Y. Chen, F. Z. Zeng, Z. Q. He, and J. Q. Wang

Abstract

This study established a combined culture system for microalgae, wastewater, and flue gas. The microalgae growth rate could be greatly enhanced by feeding with CO$_2$ of flue gas. The maximum carbon sequestration and average carbon sequestration rate were 1.203 g/L and 0.225 g/(L·d).

Keywords

Microalgae • Power plant flue gas • Lipid production • CO$_2$ fixation

1 Introduction

Microalgae are considered as one of the most promising feedstocks for biodiesel production nowadays (Abomohra et al. 2014). However, the main drawback for economical biodiesel production from microalgae is the high cost of algal cultivation for the huge consumption of freshwater resources, nitrogen and phosphate, and CO$_2$ (Jiang et al. 2011). One possible solution to overcome this problem is to cultivate algae in municipal wastewater due to its abundance and enrichment of nutrients (Tu et al. 2015). Microalgae contain about 50% of carbon, which means that a total of 1.83 ton of CO$_2$ is needed to produce 1 ton of microalgae. The cost of CO$_2$ supply for microalgae large-scale cultivation should be considered and the low CO$_2$ fixation efficiency by microalgae will lead to much more expenditure of CO$_2$.

The CO$_2$ fixation technology was the focus of developed county since the 1970s (Um and Kim 2009). It was reported that microalgae could be cultivation in the air-lift reactor (Gordana et al. 2005). The pure culture green microalgae were used for CO$_2$ absorption by Douskova et al. (2009). Hsueh et al. (2007) absorbed CO$_2$ using pure culture hot-spring microalgae. Doucha et al. (2005) carried out the study on pilot-scale cultivation of microalgae by flue gas and production costs. In China, the explore studies have been carried out on the growth of microalgae on flue gas (Yue et al. 2002).

There was still short of research report about the CO$_2$ fixation by microalgae although this technology has been the concern of the world. At present, the microalgae pure culture was used in the study. However, it was easy to be competed out of the pure culture cultivated in the laboratory. Thus, it was necessary to establish a combined culture system for microalgae, wastewater, and flue gas with industrial application, and through the optimization of the selection of algae and ventilation conditions to improve lipid yield and carbon sequestration efficiency of microalgae. In this study, the mutant microalgae were cultivated in municipal wastewater using simultaneous flue gas. The effects of carbon dioxide concentration on the growth of microalgae as well as the lipid production were investigated during outdoor expansion cultivation. This study will provide information for further study on the removal of CO$_2$ from flue gas.

2 Materials and Methods

2.1 Algae Strain and Growth Conditions

Chlorella pyrenoidosa obtained from Freshwater Algae Culture Collection at the Institute of Hydrobiology (strain number FACHB-9) was cultivated outdoors in a columnar photobioreactor made of plexiglass with working volume of 8 L (1200 mm in height, 140 mm in diameter) using municipal wastewater as the medium. The experiments were

R. J. Tu · S. F. Han · W. B. Jin (✉) · X. Zhou · Q. Wang · H. Y. Chen · F. Z. Zeng · Z. Q. He · J. Q. Wang
Shenzhen Engineering Laboratory of Microalgal Bioenergy, Harbin Institute of Technology, 518055 Shenzhen, China
e-mail: 13828830095@139.com

performed at Harbin Institute of Technology, Shenzhen, China (N 22° 35′ 25″, E 113° 59′ 01″) during autumn. During the experiment, the weather was in a stable condition, and all were sunny days with maximum intensity of illumination from 70,000 to 100,000 lx average temperature between 24 and 27 °C.

2.2 Wastewater Used in the Experiment

Wastewater was collected by pumping from sewage well at the campus of Harbin Institute of Technology, Shenzhen Graduate School, Shenzhen, China. The main source of the wastewater comes from student domes and teaching building complex. After settled in a plastic bucket, the supernatant was collected for the algal cultivation, and the water quality parameters were as follows: COD 130 ± 10 mg/L, TN 31 ± 5 mg/L, NH_3-N 28 ± 5 mg/L, TP 4.5 ± 0.5 mg/L, pH 7.5 ± 0.8.

3 Results and Discussion

3.1 Grough and Lipid Production of *C. pyrenoidosa*

The lipid yield and lipid content of *C. pyrenoidosa* were compared when the maximum biomass was reached under two aeration conditions (Fig. 1).

The maximum lipid yield of *C. pyrenoidosa* in the treatment of flue gas and air is 0.193 and 0.111 g/L, respectively, the former is 74.44% higher than the latter. It can be seen that the treated tail gas can greatly increase lipid production.

3.2 The Carbon Content of *C. pyrenoidosa*

Microalgae were harvested on the last day of culture and then their carbon content was determined. The carbon content of each algae under two different gas conditions was shown in Table 1. As can be seen from Table 1, the carbon content of several algae was slightly higher than 40%.

3.3 The Amount of Carbon Fixation by *C. pyrenoidosa* Under Different Aeration Conditions

Carbon fixation by *C. pyrenoidosa* under different aeration conditions reached the maximum on the fourth and fifth
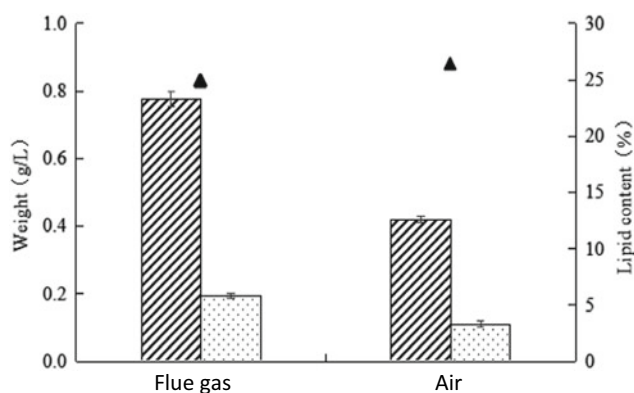
Fig. 1 Lipid content under different ventilation conditions

Table 1 Carbon content of *C. pyrenoidosa*

Ventilation type	TC (%)	IC (%)
Flue gas	42.24	0.00279
Air	41.14	0.00447

days. The rate and amount of carbon fixation on the fourth and fifth days are shown in Fig. 2.

On the fourth day of aeration, the amount of carbon fixation by *C. pyrenoidosa* reached the maximum of 0.634 g/L, while on the same day, the amount of carbon fixation by *C. pyrenoidosa* was 0.878 g/L, 38.53% higher than that of the former. On the fifth day, the amount of carbon fixation by *C. pyrenoidosa* reached the maximum of 1.203 g/L, 89.87% higher than the maximum under air conditions. The average carbon fixation rate of *C. pyrenoidosa* reaching the maximum carbon sequestration was 0.140 g/(L·d) and 0.225 g/(L·d), respectively, under the
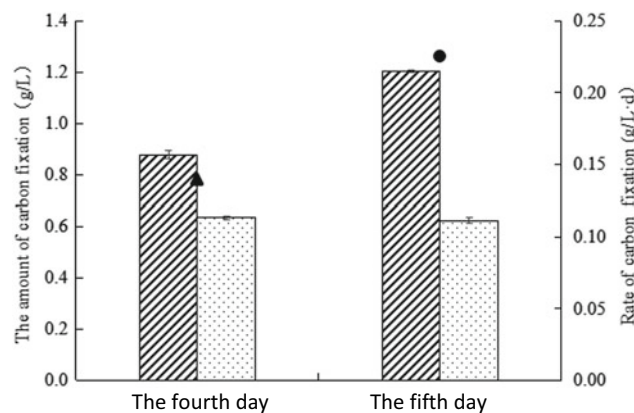
Fig. 2 Amount of carbon fixation by *C. pyrenoidosa* under different aeration conditions

condition of air entrainment and exhaust treatment. The latter is 61.34% higher than the former.

4 Conclusion

The results showed that the microalgae growth rate could be greatly enhanced by feeding with CO_2 of flue gas. The maximum carbon sequestration and average carbon sequestration rate were 1.203 g/L and 0.225 g/(L·d), 89.87 and 61.34% higher than that feeding with air, respectively.

References

Abomohra, A., El-Sheekh, M., & Hanelt, D. (2014). Pilot cultivation of the chlorophyte microalga *Scenedesmus obliquus* as a promising feedstock for biofuel. *Biomass and Bioenergy, 64,* 237–244.

Doucha, J., Straka, F., & Livansky, K. (2005). Utilization of flue gas for cultivation of microalgae (*Chlorella* sp.) in an outdoor open thin-layer photobioreactor. *Journal of Applied Phycology, 5,* 403–412.

Douskova, I., Doucha, J., & Livansky, K. (2009). Simultaneous flue gas bioremediation and reduction of microalgal biomass production costs. *Applied Microbiology and Biotechnology, 1,* 179–185.

Gordana, V. N., Yoojeong, K., & Wu, X. X. (2005). Air-lift bioreactors for algal growth on flue gas: Mathematical modeling and pilot-plant studies. *Industrial Engineering Chemistry Research,* 6154–6163.

Hsueh, H. T., Chu, H., & Yu, S. T. (2007). A batch study on the bio-fixation of carbon dioxide in the absorbed solution from a chemical wet scrubber by hot spring and marine algae. *Chemosphere, 5,* 878–886.

Jiang, L., Luo, S., Fan, X., Yang, Z., & Guo, R. (2011). Biomass and lipid production of marine microalgae using municipal wastewater and high concentration of CO_2. *Applied Energy, 88,* 3336–3341.

Tu, R. J., Jin, W. B., Xi, T. T., Yang, Q., Han, S. F., & Abomohra, A. (2015). Effect of static magnetic field on the oxygen production of *Scenedesmus obliquus* cultivated in municipal wastewater. *Water Research, 86,* 132–138.

Um, B. H., & Kim, Y. S. (2009). Review: A chance for Korea to advance algal-biodiesel technology. *Journal of Industrial and Engineering Chemistry, 1,* 1–7.

Yue, L. H., Chen, B. Z., &Wang, L. (2002). Isolation and determination of cultural characteristics of microalgae for greenhouse gases fixation from the stack gases. *Journal of Northeastern University (Natural Science), 3,* 289–292.

Techno-Economic Assessment of Combined Heat and Power Units Fuelled by Waste Vegetable Oil for Wastewater Treatment Plants: A Real Case Study

Simona Di Fraia, Nicola Massarotti, Laura Vanoli, Riccardo Bentivoglio, and Gianfranco Milani

Abstract

An integrated system for sewage sludge drying and electricity production is proposed. The system is powered by waste vegetable oil from separate collection. The system significantly reduces the sludge to be disposed of and the electricity to be supplied by the grid.

1 Introduction

Wastewater treatment is high-energy-consuming. Electrical energy is required to supply all the treatments aimed at wastewater purification and sludge treatment, accounting for 25–50% of the total operating costs of such plants (Gude 2015). Thermal energy is mainly needed for sludge treatment, usually anaerobic digestion and drying. Due to contemporary demand for electrical and thermal energy, the use of cogeneration systems has been demonstrated to be particularly appropriate for wastewater treatment plants (Di Fraia et al. 2018). The most common practice for energy self-production in wastewater treatment plants is the use of biogas from anaerobic digestion of sludge, used for heating and electricity generation (Gu et al. 2017). However, biogas is usually insufficient to supply thermal and electrical demand for wastewater and sludge treatment (Di Fraia et al. 2018; Silvestre et al. 2015). The use of renewable energy systems has been also suggested to reduce both economic costs and environmental impact of wastewater treatment plants (Chae and Kang 2013). Depending on their availability, different renewable energy sources can be employed —solar panels and photovoltaic, wind power, geothermal energy and hydropower (Di Fraia et al. 2018).

In this work, waste vegetable oil (WVO) is proposed as bioenergy source to supply energy demand of a wastewater treatment plant. In the European Waste Catalogue, WVO is classified as municipal wastes. The European potential amount has been estimated between 700 and 1000 ktons per year (Hribernik and Kegl Hribernik and Kegl 2009), with an expected increase of around 2% per year. However, the major part of WVO is discharged into the environment (Chhetri et al. 2008), with significant damage to the aquifers, water surfaces, and sewage systems. For this reason, WVO collection and recovery should be encouraged. The high viscosity of WVO causes several operational problems when they used as fuel, such as difficulty in starting, poor atomization of fuel, carbon deposition, filter plugging (Pugazhvadivu and Jeyachandran 2005; Kalam et al. 2011). Therefore, WVO is usually converted into biodiesel, through the processes of transesterification, neutralization, washing and distillation (Knothe et al. 2015). These processes improve the fuel chemical–physical characteristics of raw WVO, but they cause high economic and environmental costs as well (Enweremadu and Mbarawa 2009). Hence, direct use of WVO as fuel, after mechanical pre-treatments and with suitable operational strategy, has been suggested to reduce energy demand and environmental impact with

S. Di Fraia (✉) · N. Massarotti · L. Vanoli
Dipartimento di Ingegneria, Università degli Studi di Napoli "Parthenope", Naples, Italy
e-mail: simona.difraia@uniparthenope.it

N. Massarotti
e-mail: massarotti@uniparthenope.it

L. Vanoli
Dipartimento di Ingegneria Civile e Meccanica, Università degli Studi di Cassino e del Lazio Meridionale, Cassino, Italy
e-mail: laura.vanoli@uniparthenope.it

R. Bentivoglio · G. Milani
GRASTIM JV, Naples, Italy
e-mail: riccardo.bentivoglio@grastim.it

G. Milani
e-mail: gianfranco.milani@grastim.it

respect to biodiesel production (Kalam et al. 2011; Capuano et al. 2017). Viscosity of WVO for direct use can be reduced through pre-heating or mixing with other fuels (Pugazhvadivu and Jeyachandran 2005). It has been observed that pre-heating of WVO to 55.0 °C reduces viscosity, increasing the flow passing through the filter (Bari et al. 2002).

In the present work, WVO is used to fuel a combined heat and power (CHP) unit serving a wastewater treatment plant (WWTP). As case study, a real WWTP located in the Campania region, southern Italy, is considered, with WVO collected by a real company of the same region operating in this sector.

2 Materials and Methods

The authors carry out a feasibility analysis of the proposed system focused on energy recovery, energy consumption and process costs. The data concerning WVO collection are provided by a company which operates in 177 municipalities of Campania region, Southern Italy. The average collection is of 5800 t/year, which is reduced by 2.00% due to refining treatments loss. According to the analysis carried out, the calorific value of WVO is 36.9 MJ/kg. The WWTP considered serves an equivalent population of 1,200,000 inhabitants, with an electrical energy demand of 31,916 MWh/year and a sludge production of 36,498 t/year. Currently, the sludge is only thickened and mechanically dewatered, with an average final moisture content of 75.0%.

Considering the available WVO and its characteristics, the design of the CHP unit is based on analytical modelling and manufacturer data regarding the operation of a real diesel engine. Stationary operation at full load is considered. The electricity produced is used to supply a fraction of the WWTP demand, whereas the heat is used to produce the desiccant flow for sludge drying and to pre-heat WVO at 60.0 °C, in order to decrease its viscosity for a correct operation of the engine.

Thermal demand of the WWTP is only due to sludge drying, which is simulated through the commercial software

Aspen Plus (Advanced System for Process Engineering). A convective belt dryer is considered, which operates with a fixed sludge flow rate, characterized by constant average properties measured at the plant. In order to increase the efficiency of the process, a fraction of the desiccant flow is recycled and heated through the low-grade heat of the CHP unit. Thermodynamic properties of the exhausts and the air are determined through Raoult's and Henry's laws, implemented in Aspen Plus. Sewage sludge is modelled as a carbonaceous fuel (Brambilla 2014) and the kinetic of the process is implemented through an experimental drying curve.

An auxiliary boiler is included to meet the temperature required by the system for drying the sludge at a final moisture content lower than 10.0%. The layout of the proposed system is shown in Fig. 1.

The feasibility of the developed layout is assessed through an economic analysis, performed on the basis of the proposed system cost and achievable economic savings. The cost of the dryer and the natural gas auxiliary boiler are derived from a market survey, performed on the basis of manufacturer cost data. Cost functions are adopted in order to evaluate the cost for the tank and the CHP unit (Di Fraia et al. 2018). For electrical energy cost, a market-based time-dependent tariff is considered. The sludge disposal tariff and the WVO cost are based on the information provided by the managers and stakeholders of the case study plant.

3 Results and Discussion

Two working conditions are considered in this work and their results are compared. As mentioned before, the CHP system is designed considering the available WVO. In particular, the analysis is carried out for two different engine sizes, 1135 kW$_{el}$ and 1600 kW$_{el}$, which correspond to 8000 and 6000 h of operation per year. In both cases, two units are supposed to be installed and operated. The main results obtained for the two cases considered, case A and B from now on, are reported in Table 1. In the cases A and B, the system allows to reduce the sludge to be disposed of 72.2

Fig. 1 Layout of the proposed system
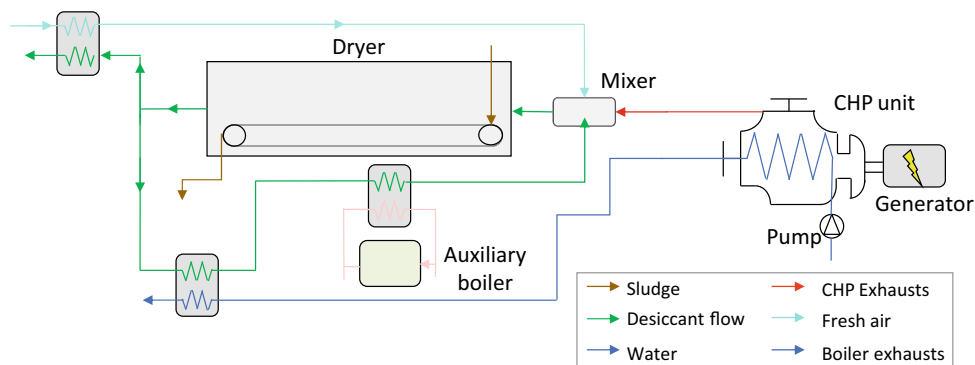
Table 1 Main results of the analysis

	Parameter		Case A	Case B
CHP unit	Electrical energy produced	MWh$_{el}$/year	18,160	19,200
	Thermal energy recovered from the CHP exhausts	MWh$_{th}$/year	8925	9011
	Thermal energy recovered from the cooling system	MWh$_{th}$/year	8728	8292
	Thermal energy recovered to pre-heat WVO	MWh$_{th}$/year	213	84.0
	Total efficiency	–	66.0%	65.8%
Dryer	Final moisture content of the sludge	–	9.89%	8.92%
	Thermal energy recovered from the dryer exhausts	MWh$_{th}$/year	1478	1956
	Electrical energy demand	MWh$_{el}$/year	1600	1200
Auxiliary boiler	Thermal energy produced	MWh$_{th}$/year	2960	1380
	Natural gas consumption	t/year	243	113
Economic analysis	Investment costs	k€	5391	6754
	Operation and maintenance costs	k€/year	4378	4315
	Avoided electrical energy cost	k€/year	2981	3240
	Avoided sludge disposal cost	k€/year	3416	3423
	Simple payback	year	2.67	2.88
	Net present value	k€	19,760	22,000

and 72.4%, respectively, and it covers the 54.2 and the 58.0% of the electrical energy demand of the WWTP and the dryer. The case B appears to be more convenient due to the higher electrical energy production and the lower amount of thermal energy supplied by the auxiliary boiler. The higher engine size is characterized by a higher electrical efficiency and consequently by a higher electricity production. However, it has to be noticed that the total efficiency of the CHP unit is lower in case B, due to the lower usage of the available low-grade heat.

4 Conclusion

The feasibility analysis of an integrated system for sewage sludge drying and electricity production is carried out. In the proposed layout, waste vegetable oil is used to fuel a combined heat and power unit serving a wastewater treatment plant. As case study, a real wastewater treatment plant located in southern Italy is considered, and the waste vegetable oil is collected by a real company of the same region, operating in this sector. The results of the analysis are very promising. The system reduces the sludge to be disposed of more than 70.0%, and it covers more than 50.0% of the electrical energy demand of the wastewater treatment plant and the dryer, with a simple payback lower than 3.00 years.

References

Brambilla, M. (2014). Testing, modeling and performance evaluation of a sewage sludge fluidized bed gasifier.

Gude, V. G. (2015). Energy and water autarky of wastewater treatment and power generation systems. *Renewable and Sustainable Energy Reviews, 45,* 52–68.

Di Fraia, S., Figaj, R. D., Massarotti, N., & Vanoli, L. (2018a). An integrated system for sewage sludge drying through solar energy and a combined heat and power unit fuelled by biogas. *Energy Conversion and Management, 171,* 587–603.

Gu, Y., et al. (2017). The feasibility and challenges of energy self-sufficient wastewater treatment plants. *Applied Energy, 204,* 1463–1475.

Silvestre, G., Fernández, B., & Bonmatí, A. (2015). Significance of anaerobic digestion as a source of clean energy in wastewater treatment plants. *Energy Conversion and Management, 101,* 255–262.

Chae, K.-J., & Kang, J. (2013). Estimating the energy independence of a municipal wastewater treatment plant incorporating green energy resources. *Energy Conversion and Management, 75,* 664–672.

Di Fraia, S., Massarotti, N., & Vanoli, L. (2018b). A novel energy assessment of urban wastewater treatment plants. *Energy Conversion and Management, 163,* 304–313.

Hribernik, A., & Kegl, B. (2009). Performance and exhaust emissions of an indirect-injection (IDI) diesel engine when using waste cooking oil as fuel. *Energy & Fuels, 23*(3), 1754–1758.

Chhetri, A. B., Watts, K. C., & Islam, M. R. (2008). Waste cooking oil as an alternate feedstock for biodiesel production. *Energies, 1*(1), 3–18.

Pugazhvadivu, M., & Jeyachandran, K. (2005). Investigations on the performance and exhaust emissions of a diesel engine using

preheated waste frying oil as fuel. *Renewable Energy, 30*(14), 2189–2202.

Kalam, M., et al. (2011). Emission and performance characteristics of an indirect ignition diesel engine fuelled with waste cooking oil. *Energy, 36*(1), 397–402.

Knothe, G., Krahl, J., & Van Gerpen, J. (2015). The biodiesel handbook. Amsterdam: Elsevier.

Enweremadu, C., & Mbarawa, M. (2009). Technical aspects of production and analysis of biodiesel from used cooking oil—a review. *Renewable and Sustainable Energy Reviews, 13*(9), 2205–2224.

Capuano, D., et al. (2017). Direct use of waste vegetable oil in internal combustion engines. *Renewable and Sustainable Energy Reviews, 69,* 759–770.

Bari, S., Yu, C., & Lim, T. (2002). Filter clogging and power loss issues while running a diesel engine with waste cooking oil. *Proceedings of the Institution of Mechanical Engineers, Part D: Journal of Automobile Engineering, 216*(12), 993–1001.

Eco-LCA of Biological Wastewater Treatments Focused on Energy Recovery

Alexander Meneses-Jácome and Adriana Ruiz-Colorado

Abstract

This work presents a novel methodology for sustainability assessment of biological wastewater treatment systems (Bio-WWTs) promoting the energy valorization of their by-products (e.g. biogas). The methodology combines analytical identification of principles-criteria of sustainability (PCS), life cycle assessment (LCA) and energy analysis (EmA) to obtain a set of sustainable development indicators (SDIs). Synergy among single SDIs is required to confirm an overall sustainable condition.

1 Introduction

LCA has been used to study environmental compatibility of domestic WWTs undertaking higher treatment standards (Ontiveros and Campanella 2013), as well as agro-industrial WWTs promoting biogas valorization (Papong et al. 2014). Improved methodologies based on LCA have been also applied for WWTs implementing both, more stringent discharge standards and resource recovery activities (Wang et al. 2012). However, LCA is even lacking of the full capacity to quantify impacts due to ancillary sustainability goals and have limitations to incorporate economic aspects in its appraisal. "Eco-LCA" is an alternative approach that combines LCA with eco-economics methods such as EmA (Raugei et al. 2014; Zhang et al. 2010), offering a promising route towards a more complete sustainability analysis of WWTs (Zhang et al. 2014). This work presents a methodology for sustainability assessment of agro-industrial Bio-WWTs, where LCA, EmA and PCS are merged to obtain SDIs made up of an environmental and an "eco-economic" term. The latter is related to changes in the supply of ecosystem services as Bio-WWTs enforce energy recovery. A "proof of concept" of this methodology is presented through two case studies in Colombia.

2 Materials and Methods

LCA stage. A consequential LCA approach was applied for Bio-WWTs taken on the role of waste-to-energy system (Meneses-Jácome et al. 2015). Thus, Bio-WWTs got a productive connotation and LCA can be combined with EmA to appraise ecosystem service changes linked to this energy function. **Study case #1:** Anaerobic-EGSB unit coupled to an activated sludge process (ASP) to treat poultry-viscera processing effluents. Biogas valorization (120 m^3 day^{-1}) was evaluated for two scenarios: (i) biogas mixed with natural gas for self generation in a micro-turbine; (ii) biogas fuelled in an industrial boiler while ASP ran on national electricity. **Study case #2**: Former EGSB unit treating beer industry effluents, time later coupled to an aerobic-MBBR. Biogas for exclusive industrial use (1600 m^3 day^{-1}). **Unit function**: 1 m^3 of raw biogas. **Inventory**: available elsewhere (Meneses-Jácome 2017), it includes conventional energy sources shifted in the system borders. **Environmental assessment**: based on five mid-point impact categories (Table 1) considered as equally relevant for bio-energy production (Dressler et al. 2012) and WWTs (Corominas et al. 2013). This reduced number of

A. Meneses-Jácome (✉) · A. Ruiz-Colorado
Grupo de Investigación en Bioprocesos y Flujos Reactivos, Universidad Nacional de Colombia—Sede Medellín, Carrera 80 No. 65-223, Núcleo Robledo, Medellín, Colombia
e-mail: amenesesj@unal.edu.co

A. Ruiz-Colorado
e-mail: aaruiz@unal.edu.co

A. Meneses-Jácome
Programa de Ingeniería Ambiental, Unidades Tecnológicas de Santander—UTS, Calle de los Estudiantes # 9-82, Ciudadela Real de Minas, Bucaramanga, Colombia

Table 1 Statement of PCS and SDIs for Bio-WWTs focused on energy recovery

PCS	Environmental impact term (LCA)					Eco-economic term (Energy)				SDIS	
	Mid-point impact categories[a]			Indicators (NEB approach)		Indirect impacts or environmental pressure indicators	Physical flows accounted as energy[c]	AVI_i	$NAVI_i$	Ecoefficiency pairs	Description
	Descrip.	Indicator (Unit)	Method	NEB_i	AEI_i						
Use of the environment as a sink	Discharge of organic pollutants and nutrients in the effluent	EP (kg $PO_{4\text{-}eq}$/ UF)	CML2001	NEB_{EP}	AEI_{EP}	Ecosystem services for dilution of discharged pollution in water	Water masses for liquid pollutants dilution	AVI_{wd}	$NAVI_{wd} = AVI_{wd}/Em_{ef}$	SDI_{HY}: (AEI_{EP}, $NAVI_{wd}$)	Hydric resources quality
	Local airborne emissions	AP (kg $SO_{2\text{-}eq}$/ UF)	CML2001	NEB_{AP}	AEI_{ATM}^{b}	Ecosystem services for dilution of atmospheric pollution in local air	Air masses for diluting airborne emissions	AVI_{ATM}	$NAVI_{ATM} = AVI_{ATM}/Em_{ef}$	SDI_{AIR}: (AEI_{ATM}, $NAVI_{ATM}$)	Local air quality
		Rel (kg PM_{eq}/ UF)	Impact 2002+	NEB_{Rel}		Potential to promote respiratory diseases.	DALVs(d)				
	Greenhouse gases emissions	GWP_{100} (kg $CO_{2\text{-}e}$/ UF)	$IPCC_{100a}$	NEBQWP		Changes in the capacity to capture CO^. emissions	Biologically productive area required for CO_2 emissions capture	AVI_{CO_2}	$NAVI_{CO_2} = AVI_{CO_2}/Em_{ef}$	SDI_{CC}: (AEI_{GWP}, $NAVI_{CO_2}$)	Capacity la control or reduce climate charge factors
Sustainable use of renewable and nonrenewable resources	Renewable energy, fossil energy and mineral resources	NRE (MJ_{PE}/ UF)	Impact 2002+	NEB_{NRE}	AEI_{NRE}	Shifting of conventional renewable energy sources	Consumption of hydroelectricity	AVI_{TE}	$NAVI_{TE} = AVI_{TE}/EM_{ef}$	SDI_{RES}: (AEI_{NRE}, $NAVI_{TE}$)	Sustainable use of resources

[a] *EP* eutrophication potential; *AP* acidification potential; *ReI* respiratory inorganics; GWP_{100} global warming potential 100 year.; *NRE* non-renewable energy; *UF* unit function

[b] AEI_{ATM} computes acid emissions and inorganic emissions promoting respiratory diseases

[c] Procedures to estimate energy fluxes in (Meneses-Jácome 2017)

[d] DALYs, disability-adjusted life years

[e] Raw–effluent energy ($Em_{ef} = 2.54 * 10^{16}$ seJ day^{-1}), it includes contributions from chemical potential and from COD, N and P loads (Meneses-Jácome 2017)

indicators was reached by means of analytical identification of PCS (Grunwald and Rosch 2011). Mid-points were progressively transformed into Net Environmental Benefit Indicators (NEBs) (Godin et al. 2012) and then into Average Environmental Influence Indicators (AEIs).

EmA and SDIs. The environmental character embedded inside the PCS aims to identify co-benefits, as well as detrimental changes in the supply or quality of some ecosystem services due to the changes in the Bio-WWTs' life cycle. Thereby, some environmental pressure indicators can be used to assess the environmental economic dimension as "sense of fulfilment" of the PCS. Conveniently, co-benefits and detriments are referred as to "add-value" indicators (AVIs) making sense with the economic notion of "additionality" (Müller 2009). AVIs, firstly accounted as energy flows, are afterwards divided by the raw-effluent's energy flux to obtain normalized add-value indicators (NAVIs). Table 1 summarizes the relationships among PCS, mid-points, NNEBs, AEIs and the pressure indicators acting as a bridge in the NAVIs setting up. Each AEI coupled to an NAVI gives a single SDI (SDI_{CC}, SDI_{RES}, SDI_{HY}, and SDI_{AIR}). Aggregated environmental (AEI_P) and eco-economic terms ($NAVI_T$) were tailored to obtain an overall SDI (SDI_{Ag}). Since AEIs and NAVIs are normalized dimensionless values ranging from −1 to 1, SDIs were interpreted by representing them as ordered pairs (AEI_i and $NAVI_i$) on an Cartesian plane (Fig. 1) as follows: Positive values of both terms confirm a co-benefit or "additionality" (quadrant I); a strong
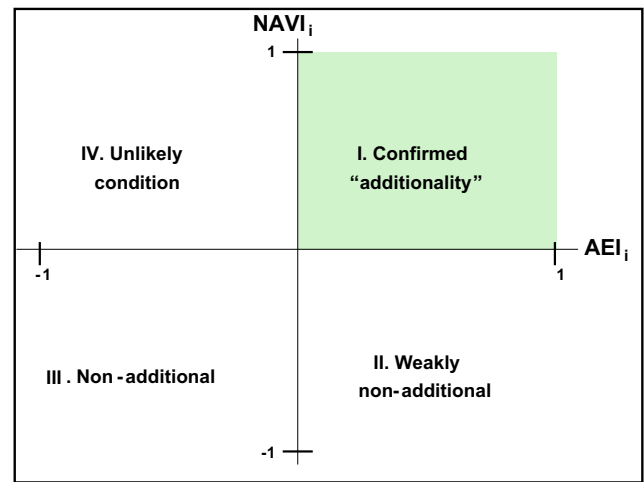
Fig. 1 Standard plot for SDIs interpretation

non-additional condition results from both terms being negative scores (quadrant III); a weak non-additional condition occurs when NAVI is negative, but the AEI is not (quadrant II); a positive NAVI due to a negative AEI is an unlikely and ethically unacceptable scenario (quadrant IV).

3 Results and Discussion

Study Case #1: Table 2 summarizes intermediate indicators serving as a pathway for AEIs. In turn, Table 3 presents AEIs and NAVIs estimated for different data sets. According

Table 2 Primary LCA results for study case #1

Mid-point impact category	Scenario 1	Scenario 2	Null option[a]	$NNEB_{i,n}$[b]		
				$NNEB_{i,1}$	$NNEB_{i,2}$	$NNEB_{i,null}$
AP (kg $SO_{2\text{-eq}}$/UF)	0.00558	0.00363	0	−1	−0.65062	0
ReI (kg $PM_{2.5\text{-eq}}$/UF)	0.00079	0.00059	0	−1	−0.73994	0
EP (kg $PO_{4\text{-eq}}$/UF)	−0.08459	−0.09017	0.11651	0.97302	1	−0.56372
GWP_{100} (kg $CO_{2\text{-eq}}$/UF)	0.337	0.334	1.828	0.8156	0.8173	−1
NRE (MJ/UF)	−3.75	−18.81	0	0.19940	1	0

[a]Null option: untreated effluent
[b]$NNEB_{i,n}$: Normalized net environmental benefit indicator assessed for the "*i*" mid-point impact category at the "*n*" scenario

Table 3 SDIs for the study case #1

SDI_i[a]	Environmental term[b]				Eco-economic term			
	AEI_i	(i)	(ii)	(iii)	$NAVI_i$	(i)	(ii)	(iii)
SDI_{HY}	AEI_{EP}	0.7819	0.0135	0.7819	$NAVI_{wd}$	5.27E−2	0.0	5.27E−2
SDI_{AIR}	AEI_{ATM}	−0.3476	0.1524	0.1524	$NAVI_{ATM}$	−6.69E-5	2.27E−5	2.27E−5
SDI_{CC}	AEI_{GWP}	0.9087	0.0009	0.0009	$NAVI_{CO_2}$	1.07E−2	2.16E−5	2.16E−5
SDI_{RES}	AEI_{NRE}	0.5	0.4003	0.4003	$NAVI_{TE}$	−2.02E−3	−0.81E−3	−0.81E−3
SDI_{Ag}	AEI_P[c]	0.4608	0.1418	0.3339	$NAVI_T$[d]	0.0613	−0,0008	0.05196

[a]Data sets for SDIs evaluation: (i) scenario 1 versus null option as baseline; (ii) scenario 2 versus scenario 1 as baseline; (iii) scenario 2 versus null option as baseline, but conserving NEB for the EP category
[b]$AEI_i = (NNEB_{i,n} − NNEB_{i,b})/2$, subindex "*b*" of baseline
[c]$AEI_P = \sum(w_i * AEI_i)$; weighting factors, $w_i = 0.25$
[d]$NAV_T = \sum NAV_j$

to these results, scenario 2 is non-additional as regards scenario 1, since $NAVI_T$ is a negative score (−0.0008). $NAVI_T$ can be fairly improved by taking the SDI_{HY} referred to data set (I), since the end-effluent quality is equal for both scenarios (1 and 2). Then $NAVI_T$ would become a positive value (0.05196). Figure 2 shows as the single SDI_{CC} mostly determines a better $NAVI_T$ for scenario 1 (solid black triangle) as regards scenario 2 (solid red spot). **Study Case #2:** Fig. 3 sums up the most important results for this case. Solid black arrows show how SDIs are shifted as Bio-WWTs is upgraded from EGSB (triangles) to ESGB + MBBR process (red spots), indicating that the exclusive pursuits of a

high-quality effluent get worse scores in most of SDIs, because external energy consumption and sludge production are increased. The end disposal site for sludge requires to be changed in order to reduce transportation and offset this trend, as shown by the respective SDI_{Ag} (hole-blue rhombus). The ESGB + MBBR process could claim a better environmental performance if the aggregated AEI_P was estimated by using weighting factors giving priority to local SDIs (solid blue rhombus).

4 Conclusion

A methodology unique that combines LCA, EmA and PCS has been developed for sustainability assessment of Bio-WWTs focused on energy recovery. It introduces a set of four single SDIs and the notion of "additionality" to elucidate overall sustainability conditions. This "proof of concept" points out that the additionality depends on synergy among different SDIs and is not only reliant on climate change control, so far the most accepted sustainability criterium for WWTs. Likewise, Bio-WWTs committed with energy recovery activities or improved treatment practices foster a negative score for the $NAVI_{TE}$. This "emergy cost" is a single non-additional condition required to improve other SDIs in order to reach overall "additionality". In the study context, Bio-WWTs would operate with national electricity ($\sim 67\%$ hydro.) allocating biogas to shift natural gas use.
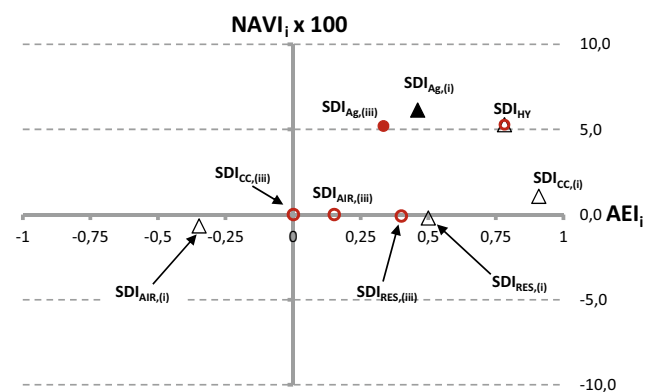
Fig. 2 Plot for SDIs interpretation: study case #1 (**a**, **b**). **a** Single (open triangle) and aggregated (filled traingle) SDIs based on data set (i) from Table 3. **b** Single (open circle) and aggregated (filled circle) SDIs based on data set (iii) from Table 3
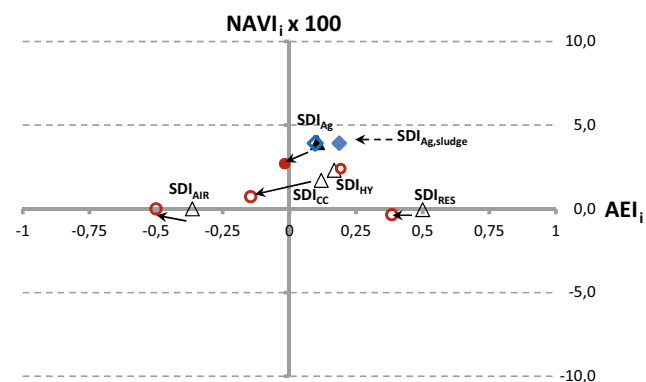
Fig. 3 Plot for SDIs interpretation: study case #2 (**a**–**d**). **a** Single (open triangle) and aggregated (filled triangle) SDIs for the former EGSB unit; **b** Single (open circle) and aggregated (filled circle) SDIs for the upgraded EGSB + MBBR process; **c** Aggregated SDIs for the upgraded EGSB + MBBR process with a new sludge disposal route, calculated with all weighting factors, $w_i = 0.25$, (open diamond); **d** Idem to **c**, calculated with the following set of weighting factors: $w_{EP} = 0.558$, $w_{Atm} = 0.122$, $w_{GWP} = 0.057$ and $w_{NRE} = 0.263$ (filled diamond)

References

Corominas, L., et al. (2013). *Water Research, 47*(15), 5480–5492.

Dressler, D., Loewen, A., & Nelles, M. (2012). *The International Journal of Life Cycle Assessment, 17*(9), 1104–1115.

Godin, D., Bouchard, C., & Vanrolleghem, P. A. (2012). *Water Science & Technology, 65*(9), 1624–1631.

Grunwald, A., & Rosch, C. (2011). *Energy, Sustainability and Society, 1*(1), 3.

Meneses-Jácome, A. (2017). PhD. Thesis: Sustainability of the water-energy nexus … (224 p.). National University of Colombia.

Meneses-Jácome, A., et al. (2015). *Water Science and Technology, 71*(2), 211–219.

Müller, B. (2009). *Additionality in the clean development mechanism—EV44*. Oxford Institute for Energy Studies.

Ontiveros, G. A., & Campanella, E. A. (2013). *Bioresource Technology, 150*, 506–512.

Papong, S., et al. (2014). *Renewable Energy, 65*, 64–69.

Raugei, M., et al. (2014). *Ecological Modelling, 271*, 4–9.

Wang, X., et al. (2012). *Environmental Science and Technology, 46*(10), 5542–5549.

Zhang, Y., Baral, A., & Bakshi, B. R. (2010). *Environmental Science and Technology, 44*(7), 2624–2631.

Zhang, X., et al. (2014). *Resources, Conservation and Recycling, 92*, 95–107.

Optimization of Nutrient Recovery from Synthetic Swine Wastewater Using Response Surface Methodology

Ralf Ruffel M. Abarca, Remegio S. Pusta Jr.,
Rea B. Labad, Jenz Lawrence A. Andit,
Claudine M. Rejas, and Mark Daniel G. De Luna

Abstract

Phosphorus and nitrogen were recovered as struvite in an FBC reactor. Nutrients recovery performance was optimized by using synthetic swine wastewater. Upflow velocity of 20 cm min^{-1} and influent PO$_4^{3-}$ of 162.32 mg L^{-1} yield the best nutrient recovery conditions. Model validation proved that RSM-generated models are robust.

Keywords

Fluidized bed crystallization • Optimization • Struvite • Swine wastewater

R. R. M. Abarca (✉) · R. S. Pusta Jr. · R. B. Labad ·
J. L. A. Andit · C. M. Rejas
Department of Chemical Engineering and Technology,
Mindanao State University—Iligan Institute of Technology,
9200 Iligan City, Philippines
e-mail: ralfabarca@gmail.com

R. S. Pusta Jr.
e-mail: remegiopustajr@gmail.com

R. B. Labad
e-mail: labadrea@gmail.com

J. L. A. Andit
e-mail: jnzlwrnz@gmail.com

C. M. Rejas
e-mail: rejasclaudine@gmail.com

M. D. G. De Luna
Department of Chemical Engineering, University of the
Philippines-Diliman, 1101 Quezon City, Philippines
e-mail: mgdeluna@up.edu.ph

1 Introduction

Swine breeding industry is one of the sources of livestock waste stream with considerable amount of phosphorus and nitrogen that when discharged to the environment without prior treatment could cause eutrophication (Tong et al. 2009). Removal of nutrients from this waste stream is important to maintain water quality and reduce environmental impact. On the other hand, phosphate rock, like oil, is a non-renewable resource currently dwindling in global scale as extraction and usage outstripped discovery. This situation urges researchers to investigate not only on nutrient removal but also on the recovery of phosphate from waste streams (Chen et al. 2009; Cordell et al. 2011).

One of the promising nutrient removal technologies is fluidized bed crystallization (FBC) of struvite as it simultaneously removes nitrogen and phosphorus efficiently with good by-product recyclability (Zhao et al. 2012; Morse et al. 1998). The recovered by-product (struvite pellets) from this process can be used as a substitute for phosphate mineral used in commercial applications or as slow-release agricultural fertilizer (Wang et al. 2006). FBC of struvite can use process optimization schemes such as black box modeling using response surface methodology in developing, improving and optimizing the process (de Luna et al. 2014a).

This study aims to optimize nutrient recovery in synthetic swine wastewater via FBC of struvite with mixing energy expressed as upflow velocity and influent phosphate concentration as factors for optimization.

2 Materials and Methods

Struvite seed crystals were prepared by a precipitation method as reported to our previous work (Abarca et al. 2016). The synthesis was carried out by slowly mixing 0.370 M KH$_2$PO$_4$ (Sharlau, 99.5%), 0.555 M NH$_4$Cl (Sharlau, 99.5%) and 0.370 M MgCl$_2$ (Sharlau, 99%) at pH

8.5. Recovered crystals were washed and dried at 37 °C for two days.

Synthetic swine wastewater (SSW) was prepared using KH_2PO_4 and NH_4Cl and the precipitant solution from $MgCl_2 \cdot 6H_2O$ with deionized water as solvent. FBC was performed in a 0.48 L reactor equipped with a pH meter and a peristaltic pump for recirculation. The reactor was filled with distilled water and seed crystals prior to treatment of SSW. Solution pH of precipitant and SSW were adjusted to 9.53 (De Luna et al. 2014a) prior to dosing at 6.0 ml min^{-1} (De Luna et al. 2014b). The system operated at ambient temperature of 25 °C. Upflow velocity and influent phosphate concentration were varied from 13.79 to 56.21 cm min^{-1} and 98.22 to 451.78 mg L^{-1} (ppm)—alpha values as determined by central composite design (CCD).

Inorganic phosphate ion concentration was determined using molybdenum blue method scanned at 698 nm while ammonium ion concentration was determined by indophenol blue method scanned at 640 nm.

3 Results and Discussion

RSM was used to assess the relationship between the responses (total and dissolved phosphate and ammonium ion concentration) and factors (upflow velocity and influent phosphate), as well as to optimize the factor levels for best nutrient recovery conditions. CCD as experimental design has good statistical properties as it allows reasonable amount of information to test lack of fit when a sufficient number of experimental values exist. The complete conditions and values of responses of the 13 CCD experimental runs, inclusive of replicated central point, are shown in Table 1.

Linear model is fitted to the experimental data for total NH_4^+ concentration and quadratic models for dissolved NH_4^+, total PO_4^{3-} and dissolved PO_4^{3-} concentration. The model F-values of total PO_4^3, dissolved PO_4^{3-}, total NH_4^+ and dissolved NH_4^+ are 4.42, 57.94, 37.98 and 54.33, respectively, implied that models were significant with p-values less than 0.05.

The quality of the model developed was evaluated based on the correlation coefficient R^2 and standard deviation value. The R^2 values for total and dissolved PO_4^{3-} are 0.7596 and 0.9764, and 0.9644 and 0.9749 for total and dissolved NH_4^+, respectively.

The dependence of response values on upflow velocity and influent phosphate concentration is shown in Fig. 1. These response surface plots were used to investigate the effect of factors on the crystallization of struvite from SSW. Highest nutrient removal can be achieved between upflow velocity of 20 and 35 cm/min and influent phosphate concentration between 150 and 275 ppm.

Setting upflow velocity and influent phosphate in range and minimizing response variables resulted in optimum operating conditions of 20 cm min^{-1} upflow velocity and 162.32 mg L^{-1} influent phosphate. This set condition was validated by performing additional FBC runs, and the average response values showed close agreement between the verified and predicted values with relative errors ranging from 5.26 to 9.10%.

Table 1 Central composite design matrix of factor and response values

Run	Factors		Responses			
	Upflow v, (cm min^{-1})	Influent PO_4^{3-} (mg L^{-1})	Total PO_4^{3-} (mg L^{-1})	Dissolved PO_4^{3-} (mg L^{-1})	Total NH_4^+ (mg L^{-1})	Dissolved NH_4^+ (mg L^{-1})
1	35	275	64.33	42.24	2566.94	66.39
2	50	150	110.22	61.64	4649.77	95.14
3	13.79	275	106.75	41.53	166.38	83.55
4	20	150	77.60	30.26	2058.38	68.65
5	35	275	63.30	41.15	3038.34	73.50
6	50	400	63.87	38.15	3584.33	119.41
7	20	400	72.78	61.78	604.89	103.68
8	35	275	63.59	41.38	2512.78	74.65
9	35	98.22	73.20	58.38	2917.18	77.55
10	35	451.78	58.78	58.95	1413.15	109.66
11	56.21	275	73.48	43.56	4564.91	123.84
12	35	275	66.83	44.09	3044.73	72.92
13	35	275	63.59	42.11	2709.30	65.97
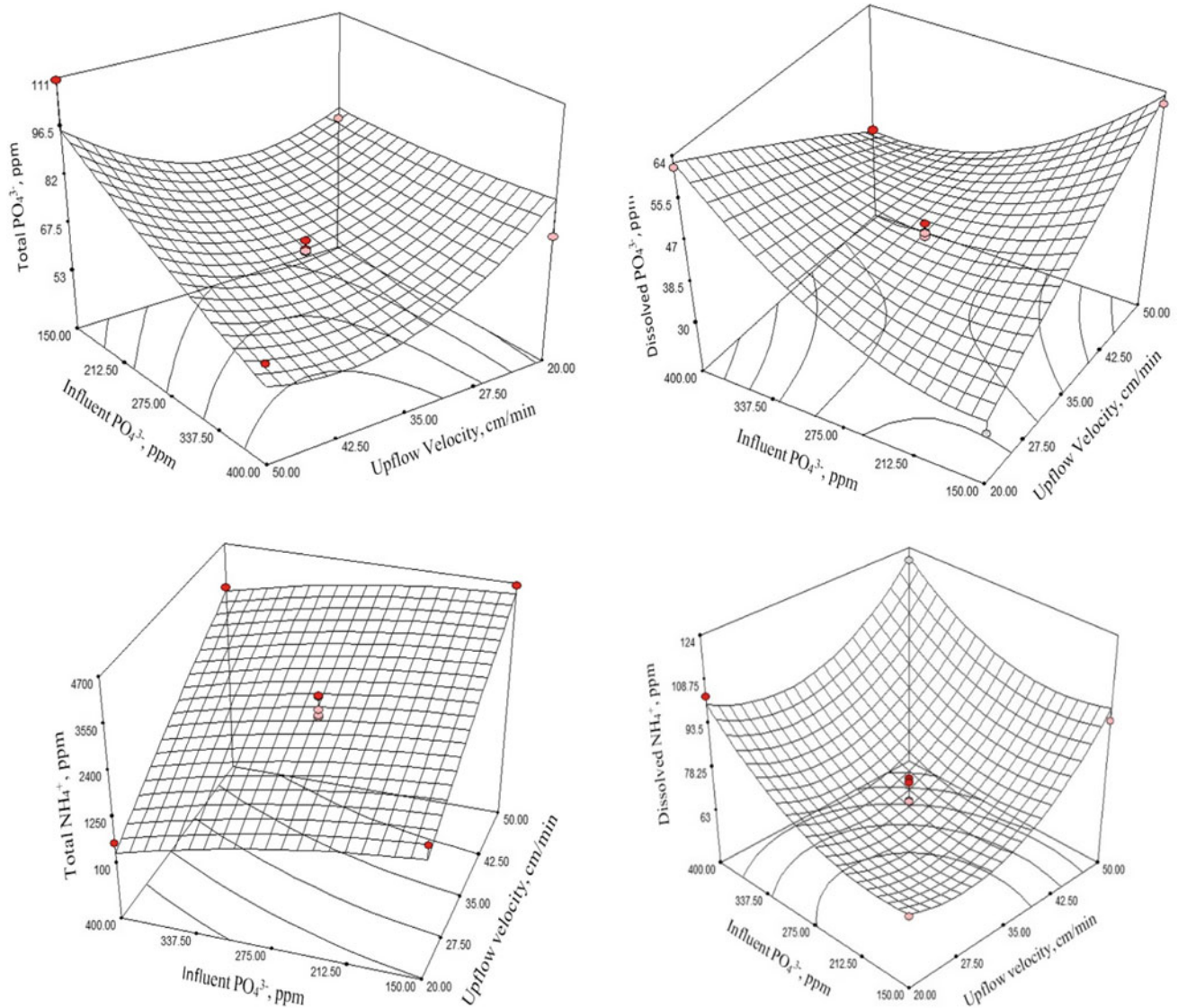
Fig. 1 Response surface plots of total and dissolved PO_4^{3-} and NH_4^+

4 Conclusion

Response surface methodology results confirmed the dependency of responses to upflow velocity and influent phosphate concentration with significant factor interaction for dissolved PO_4^{3-} concentration. Moreover, model validation experiments gave less than 10% relative error from the predicted values, implying that the models generated were robust and insensitive to noise. The process conditions for optimum nutrient removal and recovery are 20 cm min^{-1} and 162.32 mg L^{-1} PO_4^{3-} for the levels of factors studied.

References

Abarca, R.R.M., Pusta, R.S., Labad, R.B., et al. (2016) Effect of upflow velocity on nutrient recovery from swine wastewater by fluidized bed struvite crystallization.

Chen, X., Kong, H., Wu, D., et al. (2009). Phosphate removal and recovery through crystallization of hydroxyapatite using xonotlite as seed crystal. *Journal of Environmental Sciences, 21,* 575–580. https://doi.org/10.1016/S1001-0742(08)62310-4.

Cordell, D., Rosemarin, A., Schröder, J. J., & Smit, A. L. (2011). Towards global phosphorus security: A systems framework for phosphorus recovery and reuse options. *Chemosphere, 84,* 747–758. https://doi.org/10.1016/j.chemosphere.2011.02.032.

De Luna, M.D.G, Abarcam, R.R.M., Su, C.-C., et al. (2014a). Multivariate optimization of phosphate removal and recovery from aqueous solution by struvite crystallization in a fluidized-bed reactor. *Desalin Water Treat*, 1–10. https://doi.org/10.1080/19443994.2014.915584.

De Luna, M. D. G., Abarca, R. R. M., Huang, Y.-H., & Lu, M.-C. (2014b). Phosphate recovery by crystallization process using magnesium ammonium phosphate crystals as seed material. *International Proceedings of Chemical, Biological and Environmental Engineering, 70,* 152–156. https://doi.org/10.7763/IPCBEE.

Morse, G., Brett, S., Guy, J., & Lester, J. (1998). Review: Phosphorus removal and recovery technologies. *Science of the Total Environment, 212,* 69–81. https://doi.org/10.1016/S0048-9697(97)00332-X.

Tong, L., Li, P., Wang, Y., & Zhu, K. (2009). Chemosphere analysis of veterinary antibiotic residues in swine wastewater and environmental water samples using optimized SPE-LC/ MS/MS. *Chemosphere, 74,* 1090–1097. https://doi.org/10.1016/j.chemosphere.2008.10.051.

Wang, J., Song, Y., Yuan, P., et al. (2006). Modeling the crystallization of magnesium ammonium phosphate for phosphorus recovery. *Chemosphere, 65,* 1182–1187. https://doi.org/10.1016/j.chemosphere.2006.03.062.

Zhao, Y., Xi, B., Li, Y., et al. (2012). Removal of phosphate from wastewater by using open gradient superconducting magnetic separation as pretreatment for high gradient superconducting magnetic separation. *Separation and Purification Technology, 86,* 255–261. https://doi.org/10.1016/j.seppur.2011.11.014.

Enzymatic Pretreatment of Chicken Manure for Improved Biogas Yield

Seyedmehdi Emadian, Murat Kuzulcan, Mehmet Ali Küçüker, Burak Demirel, and Turgut Tüzün Onay

Abstract

Chicken manure is an important substrate for biogas production. Enzymatic pretreatment of chicken manure was investigated. A higher biodegradability of chicken manure was the primary aim. Batch anaerobic digestion tests were conducted after pretreatment. Enzymatic pretreatment provided higher biogas yields.

1 Introduction

A higher attention has recently been directed towards the utilization of renewable energy sources in order to substitute fossil fuel sources and to decrease emissions of greenhouse gases (GHGs) released into the atmosphere to mitigate climate change. Among the renewable energy sources, biomass plays a very significant role for both developed and developing countries to reduce GHGs' emissions. Particularly, the production of biogas from biomass has significantly developed worldwide during the last couple of decades, since biogas can easily be used for the production of power and heat. In addition, after upgrading, biomethane can be used as a substitute for natural gas or as a fuel in vehicles. Energy crops, manure, agricultural residues and organic wastes can be used for biogas production in agricultural or centralized biogas plants. Agricultural resources and particularly, animal manure is an important substrate for agricultural biogas plants for renewable energy production (Ward et al. 2008). Furthermore, there exit many studies covering the use of various pretreatment methods applied for biomass for enhanced biogas yields. The role of enzymatic pretreatment in anaerobic digestion has recently been discussed in a review paper as well (Bremond et al. 2018). Therefore, this laboratory-scale work investigated the application of an enzymatic pretreatment step for chicken manure prior to batch anaerobic digestion tests in order to attain higher biogas and methane yields.

2 Materials and Methods

Batch anaerobic digestion tests were conducted according to the guidelines outlined in German VDI 4630 method (VDI 4630 2016). Chicken manure was obtained from a farm. The seed sludge (inoculum) was obtained from a sewage wastewater treatment plant in Istanbul. The samples were kept at 4 °C prior to use. Two sets of experiments were performed at mesophilic temperature (37 ± 1 °C). In the first set (Set 1), chicken manure without pretreatment was mixed with seed sludge at various ratios (w/w) in order to determine the most optimum loading conditions within a total solids (TS) range of 2–8% to attain the highest biogas and methane yields. In the second set (Set 2), the enzymatically pretreated chicken manure was used at the most optimum conditions determined before in Set 1. The biogas experiments lasted for 21 days. Two parallel reactors were run and the average results are reported. Biogas production was daily measured using Milligascounters (Ritter, Bochum, Germany). The composition of biogas, namely methane (CH_4) and carbon dioxide (CO_2), was determined using a GC-TCD. The measurements of pH and solids were conducted according to the guidelines outlined in Standard Methods (APHA 1998).

S. Emadian · M. Kuzulcan · B. Demirel (✉) · T. T. Onay
Boğazici University, Bebek, 34342 Istanbul, Turkey
e-mail: Burak.demirel@boun.edu.tr

S. Emadian
e-mail: mehdi.emadian@gmail.com

M. A. Küçüker
Hamburg University of Technology, Harburg, 21079 Hamburg, Germany
e-mail: mehmetali.kucuker@gmail.com

3 Results and Discussion

The TS contents of chicken manure and seed sludge were initially measured to be 31 and 4%, respectively, prior to the experiments. In Set 1, in total 12 reactors were operated at different TS percentages in order to determine the most optimum TS range for a high biogas and methane yields from chicken manure without enzymatic pretreatment. For instance, in Set 1, for 6% TS reactors, the cumulative biogas and methane production values were 1780 and 1146 N mL, respectively. The biogas and methane yields were 453 and 291 N mL/g $VS_{removed}$, respectively. The most optimum TS range was determined to be from 4 to 6% in the first round of the experiments, where no pretreatment was conducted for the substrate.

In Set 2, in total 10 reactors were run under the most optimum TS conditions as determined in Set 1. The chicken manure was subjected to enzymatic pretreatment in this trial prior to batch anaerobic digestion tests. The results of the experiments indicated that the enzymatic pretreatment resulted in increased biogas and methane yields. For instance, in Set 2, the reactors operated at 5% TS produced cumulative biogas and methane values of 1256 and 767 N mL, respectively. In terms of biogas and methane yields, the values were 840 and 513 N mL/g $VS_{removed}$, respectively. The findings of this laboratory-scale work showed that the enzymatic pretreatment could increase the biodegradability of the chicken manure so that relatively higher biogas and methane yields could be achieved as a result of the anaerobic digestion process.

4 Conclusion

Energy crops and residues from livestock production are the most commonly used substrates in agricultural biogas plants for the production of power and heat. Particularly, cattle and poultry manure are converted into biogas in centralized and farm-scale biogas plants. In addition to the production of power and heat, after upgrading, biogas can also be used as fuel in vehicles or can be fed into the natural gas grid as a substitute of natural gas, making it a very flexible energy source. In Turkey, each year, a huge amount of animal manure is generated from the livestock production sector and management of manure plays a significant role to protect the environment and to reduce greenhouse gas emissions into the atmosphere. Therefore, anaerobic conversion of manure in agricultural biogas plants would result in the production of renewable power and heat, and also digestate as well, that can be further used in agriculture as an organic fertilizer. This laboratory-scale investigation focused on the application of an enzymatic pretreatment for chicken manure in order to achieve higher biogas and methane yields using batch anaerobic digestion experiments. The objective of using enzymatic pretreatment was to improve the biological degradability of the chicken manure for increased biogas production rates. The results obtained in this study showed that the enzymatic pretreatment of chicken manure could provide relatively higher biogas and methane production rates than those without pretreatment.

References

APHA. (1998). *Standard methods for the examination of water and wastewater, Washington, DC.*

Bremond, U., de Buyer, R., Steyer, J. P., Bernet, N., & Carrere, H. (2018). Biological pretreatments of biomass for improving biogas production: an overview from lab to full-scale. *Renewable and Sustainable Energy Reviews, 90,* 583–604.

Ward, A. J., Hobbs, P. J., Holliman, P. J., & Jones, D. L. (2008). Optimization of the anaerobic digestion of agricultural resources. *Bioresource Technology, 99,* 7928–7940.

VDI 4630. (2016). *Fermentation of organic materials. Characterisation of the substrate, sampling, collection of material data, fermentation tests.*

Integration of Liquid–Liquid Membrane Contactors and Electrodialysis for Ammonia Recovery from Urban Wastewaters

X. Vecino, M. Reig, B. Bhushan, J. López, O. Gibert, C. Valderrama, and J. L. Cortina

Abstract

The liquid-liquid membrane contactor (LLMC) is an innovative and eco-friendly technology for ammonium salts production; Electrodialysis (ED) can concentrate efficiently ammonium salts; Concentrated ammonium salts can be obtained by means of integration processes (LLMC and ED); Ammonium salts produced can be used as liquid fertilizers.

Keywords

Ammonium valorization • Ammonium salts • Wastewater treatment • Liquid fertilizers • Liquid–liquid membrane contactors • Electrodialysis concentration

1 Introduction

Nowadays, reactive nitrogen compounds are excessive released into the environment due to industrial and urban wastewaters. A huge environmental challenge exists due to these compounds, such as nitrogen oxides (NO and NO_2), nitrous oxide (N_2O), ammonia (NH_3), ammonium (NH_4^+), and nitrate (NO_3^-) pollute the environment and endanger human health (Sareer et al. 2016). In addition, the circular economy policy proposes actions that will contribute to "closing the loop" of product lifecycles through greater recycling and reuse and bring benefits for both the environment and the economy. From this point of view, two innovative membrane technologies are proposed to valorize the ammonia present in urban wastewaters by separating and concentrating it as ammonium salts: liquid–liquid membrane contactors (LLMCs) (Licon Bernal et al. 2016) and electrodialysis (ED) (Reig et al. 2014).

Using LLMC is possible to separate and recover the ammonia from urban wastewater as ammonium phosphate ($NH_4H_2PO_4$), using an acid stripping solution (e.g., phosphoric acid). Besides, ED allows to increase the $NH_4H_2PO_4$ concentration in order to reach the required nitrogen and phosphorus concentration to be used as liquid fertilizer (Fig. 1).

2 Materials and Methods

A liquid–liquid membrane contactor was supplied from 3 M Company (USA) to conduct the experiments at lab-scale (2.5 × 8 Liqui-Cel X-50 PP fiber). Urban wastewaters from regenerated zeolites were used as feed solution, containing 1.6 g NH_3/L at pH 12 in a 60 L tank (lumen side), whereas 0.5 L of 0.4 mol/L phosphoric acid were used as stripping solution (shell side). Both streams circulated through the LLMC pumped at 450 mL/min and recirculated back into its respective tanks at room temperature during 12 h.

Afterward, the ammonium phosphate solution obtained from LLMC was fed into an ED system supplied by PCCell GmbH (Germany), named PCCell ED 64-004. The ED system worked with 5 cell pairs of membranes (64 cm^2 active area each one) from two different companies: Fujifilm and PCCell. 1 L of $NH_4H_2PO_4$ solution was used to feed the electrode rinse, dilute, and concentrate compartments. The first one was pumped at 90–100 L/h, while the others were pumped at 15–20 L/h through the ED stack. Experiments were carried out at a constant voltage of 7.5 V, taking into account the voltage drop of the system (2.5 V across the electrodes and 1 V for each cell pair (5 V)), using a power

X. Vecino · M. Reig · B. Bhushan · J. López · O. Gibert · C. Valderrama · J. L. Cortina (✉)
Chemical Engineering Department, UPC-Barcelona TECH, Barcelona Research Center for Multiscale Science and Engineering, C/Eduard Maristany 10-14, Campus Diagonal-Besòs, 08930 Barcelona, Spain
e-mail: jose.luis.cortina@upc.edu

J. L. Cortina
CETaqua, Carretera d'Esplugues, 75, 08940 Cornellà de Llobregat, Spain

Fig. 1 Integration of LLMC and ED membrane technologies for ammonia valorization as liquid fertilizers
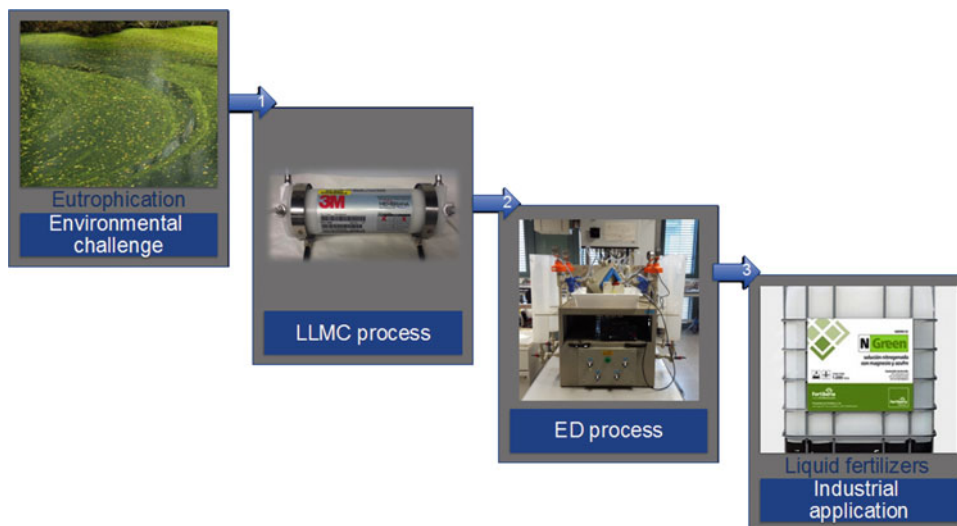
cell HCS-3202, supplied by Manson Engineering Industrial (Hong Kong).

The liquid fertilizer composition, after these processes, was expressed for ammonia as %N and for phosphate as %P_2O_5.

3 Results and Discussion

Ammonia removal from urban wastewaters using LLMC was 86 $\pm$ 3% (at the lumen side), whereas its concentration factor was 34 $\pm$ 2% after 12 h (in the shell side). Moreover, it was possible to recover it as ammonium phosphate at the shell side, containing 5.0 $\pm$ 0.1% of N and 14.9 $\pm$ 2.2% of P_2O_5 (Fig. 2).

The ammonia phosphate produced in the LLMC was subsequently concentrated by ED. It was possible to concentrate the ammonium salt by 51 $\pm$ 1% and 54 $\pm$ 2% using PCCell and Fujifilm membranes, respectively, after almost 4 h of operation process (Fig. 3).

Fig. 3 $NH_4H_2PO_4$ evolution in concentrated stream by ED process

4 Conclusion

To summarize, by the integration of LLMC and ED as innovative membrane technologies were possible to separate, concentrate and valorize ammonia present in urban

Fig. 2 **a** Ammonia evolution in the feed side and **b** N and P_2O_5 evolution in the stripping side over time

wastewaters as ammonium phosphate. This salt solution could be used as a liquid fertilizer in the agriculture sector, promoting in this way a circular economy scheme.

References

Licon Bernal, E. E., Maya, C., Valderrama, C., & Cortina, J. L. (2016). Valorization of ammonia concentrates from treated urban wastewater using liquid-liquid membrane contactors. *Chemical Engineering Journal, 302,* 641–649.

Reig, M., Casas, S., Aladjem, C., Valderrama, C., Gibert, O., Valero, F., et al. (2014). Concentration of NaCl from seawater reverse osmosis brines for the chlor-alkali industry by electrodialysis. *Desalination, 2,* 107–117.

Sareer, O., Mazahar, S., Al Khanum Akbari, W. M. A., & Umar, S. (2016). Nitrogen pollution, plants and human health. In *Plants, pollutants and remediation* (Vol. 1, pp. 27–61).

Remediation of Water Contaminated by Pb(II) Using Virgin Coniferous Wood Biochar as Adsorbent

Agostina Chiavola, Simone Marzeddu, and Maria Rosaria Boni

Abstract

Charcoal from vegetable wastes showed good adsorbent properties for lead-contaminated water. Adsorption capacity at equilibrium was about 10 and 20 mg/g at 50 and 100 mg/L Pb, respectively. Breakthrough curves highlighted longer operation times of column plant filled with charcoal mixed sand than with sand only.

1 Introduction

A wide number of low-cost adsorbents produced from waste products of various activities (e.g. agriculture and industry) have been applied to the removal of pollutants from water and wastewater. The general goal was to give to waste products a new purpose, within the framework of the principles of the circular economy. This would allow to avoid the impacts related to their disposal as well as those due to the industrial production of commercial adsorbents (Kolodynska et al. 2017). Charcoal produced from pyrolysis of vegetable wastes has been so far used in Italy as a soil amendment in agriculture practices. However, some experimental tests have also shown its capability as adsorbent to remove heavy metals from contaminated water (Mohan et al. 2014; Tan et al. 2015; De Gisi et al. 2016; Inyang et al. 2016; Li et al. 2017; Oliveira et al. 2017). In this paper, charcoal obtained by pyrolysis of virgin coniferous wood has been investigated as a potential adsorbent for remediation of waters contaminated by Pb(II). The experimental study was carried out with the aim to determine the main physical and chemical properties of charcoal and its adsorption capacity.

2 Materials and Methods

Charcoal used in the present study (named RE-CHAR®) is produced by a pyrolysis process carried out at 600 °C as average temperature. It complies with the A1/A2 quality classes of the UNI EN ISO 17225-4: 2014 standard and is usually employed as a fertilizer.

The experimental tests were performed using lead-containing solutions prepared by dissolving lead nitrate salt into ultrapure water, in order to have a lead concentration of 50 or 100 mg/L. Charcoal was firstly characterized by means of the following physical–chemical characteristics: bulk density, porosity, field capacity, moisture content, ash content, pH and pH point of zero charge. Scanning electron microscope (SEM) was used to investigate the microscopic structure and for elemental analysis. Adsorption kinetics and isotherms were determined through batch tests; the effects of different experimental parameters, such as adsorbent dosage and initial lead concentration, were also studied. The best fitting kinetic model of the experimental data was evaluated. Batch experiments were conducted in duplicate and the results obtained were averaged. Charcoal behaviour was also investigated as adsorbent media in column plants fed by lead-contaminated solutions, following the procedure outlined in Boni et al. (2018). Breakthrough curves were determined by recording lead concentration in the eluate from the columns with time.

A. Chiavola · S. Marzeddu · M. R. Boni (✉)
Faculty of Civil and Industrial Engineering, Department of Civil, Constructional and Environmental Engineering (DICEA), Sapienza University of Rome, Via Eudossiana 18, 00184 Rome, Italy
e-mail: mariarosaria.boni@uniroma1.it

A. Chiavola
e-mail: agostina.chiavola@uniroma1.it

S. Marzeddu
e-mail: simone.marzeddu@uniroma1.it

3 Results and Discussion

Results of the physical and chemical characterization of RE-CHAR® are listed in Table 1. Figure 1 shows SEM images of RE-CHAR® surface at various magnifications: (a) one chip at 100x; (b) the transversal cut cross section at 500x; (c) the longitudinal vertically cut cross section at 1.00Kx; and (d) variously sized pores at 100.00Kx.

Figure 2 shows lead percentage removal versus time in the batch tests conducted with concentrations of 50 and 100 mg/L of lead and RE-CHAR®. The equilibrium time of the adsorption process was found to be about 4 h.

The linearized form of the equation of the kinetic models was used to find out the best fitting based on the value of R^2. Among the tested models, the pseudo-second order (Ho and McKay 1999) provided a higher value of R^2 at both initial Pb concentration (C_0) tested. By plotting of t/q versus t, as shown in Fig. 3, it was possible to determine the values of the equilibrium adsorption capacity, q_e, and the constant rate, k_s, of the model based on the intercept and slope of the line. Values are listed in Table 2, along with $q_{e,exp}$, i.e. the equilibrium adsorption experimentally determined.

Between the Langmuir and Freundlich adsorption isotherms, the Langmuir model (Langmuir 1918) better fitted the equilibrium data for both contaminated solutions. Figure 4 reports the plots of q_e/C_e versus q_e, where C_e represents the equilibrium Pb concentration in solution. Values of the maximum adsorption capacity, q_{max}, the constant, b, and the dimensionless constant separation factor, R_L, (Weber and Chakravorti 1974) are shown in Table 3.

Figure 5 shows the breakthrough curves obtained by the column plants filled with RE-CHAR® charcoal mixed with soil and with soil only. The plots report the percentage ratio of Pb in the eluate and in the feeding solution (C/C_0).

It can be noted that both breakthrough ($C/C_0 = 5\%$) and exhaustion ($C/C_0 = 95\%$) times were reached faster in the column containing only soil.

4 Conclusions

In the present paper, the efficiency of RE-CHAR® charcoal as a possible sustainable adsorbent media for lead-contaminated solution remediation was evaluated. The goal was to determine if this charcoal, currently mainly used as a soil improver, could also have a further environmental application, i.e. as an adsorbent in place of commercial media. Firstly, the characterization through the main physical and chemical properties was provided. Adsorption was very fast in the first minutes of the tests and then decreased sharply. The Langmuir isotherm better fitted the equilibrium data, while the pseudo-second-order model provided the best agreement of the kinetic experimental data. Application of RE-CHAR® as adsorbent media in column plant showed longer operation time before breakthrough and exhaustion conditions as compared to the same column filled with sand only. Based on these results, it can be assessed that RE-CHAR® can be considered as a valid alternative to commercial activated carbons for the removal of Pb from liquid solutions. More details of the experimental activities and a deeper discussion of the results obtained will be presented at the conference.

Table 1 Physical and chemical properties of RE-CHAR® (% on dry weight)

Property	Symbol	Unit	Values
Bulk density	γ_s	g/cm^3	1.931
Specific weight	γ_d	g/cm^3	0.167
Field capacity	ω_c	g in 100 g	700
Porosity	n	%	91.35
Carbon	C	%	92.56
Oxygen	O	%	5.87
Calcium	Ca	%	0.81
Potassium	K	%	0.53
Magnesium	Mg	%	0.18
Phosphorous	P	%	0.04
Moisture content	ω	%	2.94
Ash content	cc	%	56.87
Potential of Hydrogen	pH	–	12.40
Point of zero charge	pH$_{PZC}$	–	12.98
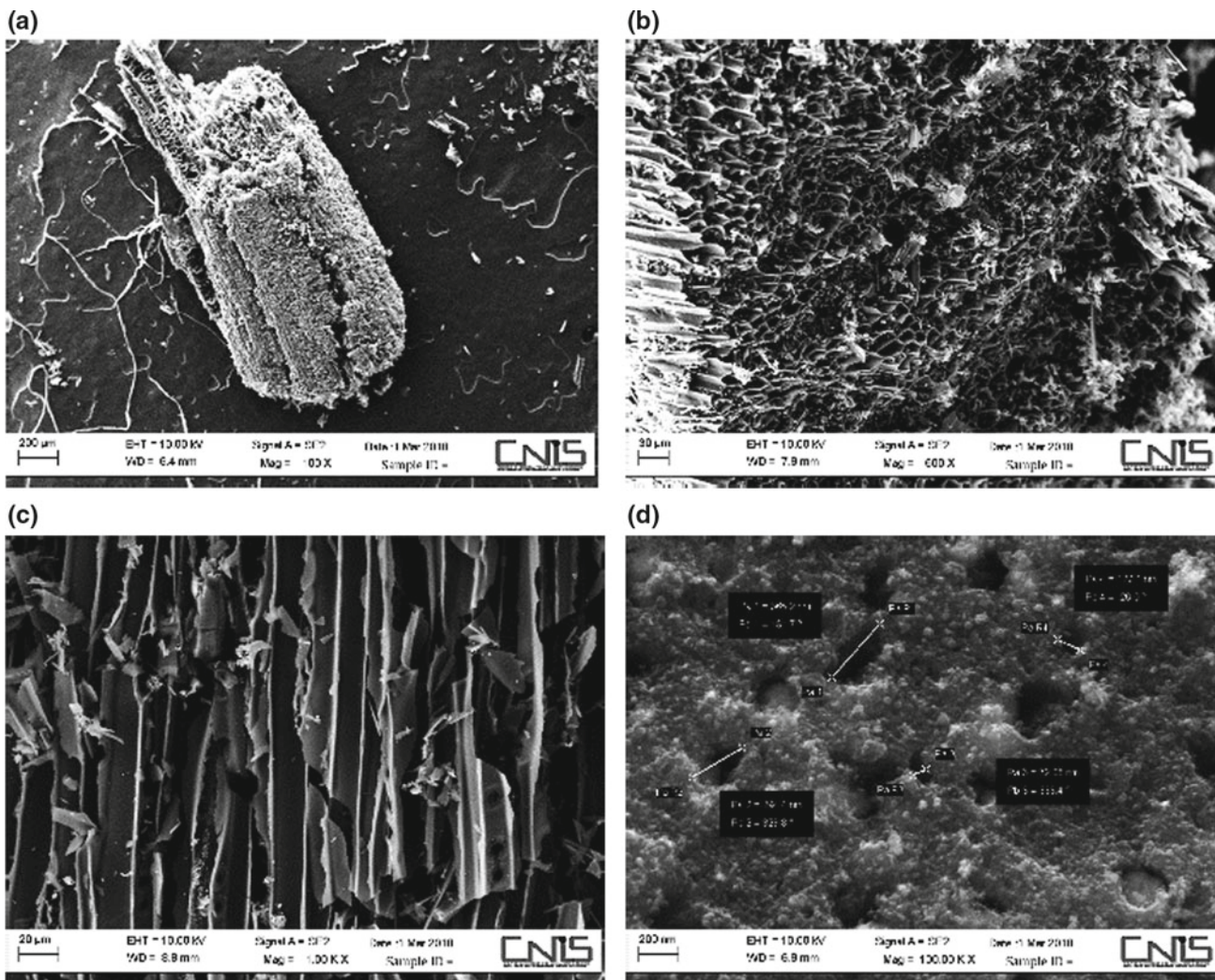
Fig. 1 SEM images of RE-CHAR® surface
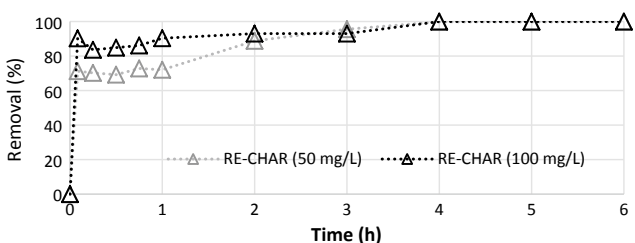
Fig. 2 Lead percentage removal versus contact time

Table 2 Pseudo-second-order kinetic constants

C_0 (mg/L)	$q_{e,exp}$ (mg/g)	q_e (mg/g)	k_s (g/mg min)	R^2 (–)
50	9.7340	9.9957	0.0091	0.9959
100	20.0800	20.1462	0.0128	0.9988
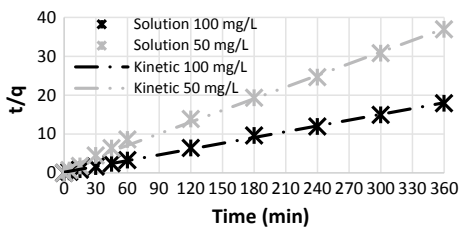
Fig. 3 Linear fitting of experimental data by the pseudo-second-order kinetic model
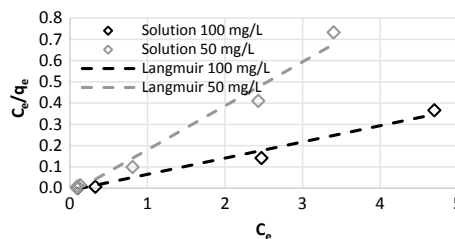
Fig. 4 Experimental isotherm points fitting by the Langmuir linearized equation

Table 3 Langmuir isotherm constants

C_0 (mg/L)	q_{max} (mg/g)	b (L/mg)	R^2 (–)	R_L (–)
50	4.6116	11.5804	0.9967	0.0017
100	9.5895	2.8933	0.9863	0.0032

Fig. 5 Breakthrough curves
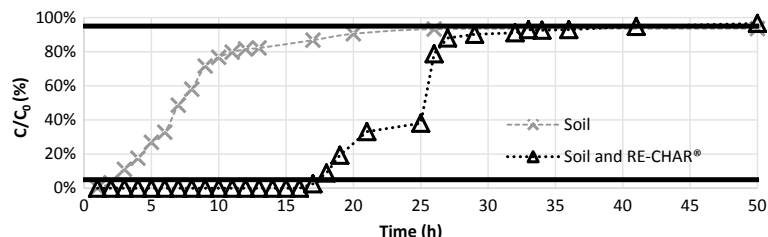
References

Boni, M. R., Chiavola, A., Antonucci, A., Di Mattia, E., & Marzeddu, S. (2018). A novel treatment for Cd-contaminated solution through adsorption on beech charcoal: the effect of bioactivation. *Desalination and Water Treatment, 127*, 104–110.

De Gisi, S., Lofrano, G., Grassi, M., & Notarnicola, M. (2016). Characteristics and adsorption capacities of low-cost sorbents for wastewater treatment: A review. *Sustainable Materials and Technologies, 9*, 10–40.

Ho, Y. S., & McKay, G. (1999). Pseudo-second order model for sorption processes. *Process Biochemistry, 34*(5), 451–465.

Inyang, M. I., Gao, B., Yao, Y., Xue, Y., Zimmerman, A., Mosa, A., Pullammanappallil, P., Sik, Y., & Cao, X. (2016). A review of biochar as a low-cost adsorbent for aqueous heavy metal removal. *Critical Reviews in Environmental Science and Technology, 46*(4), 406–433.

Kołodyńska, D., Krukowska, J., & Thomas, P. (2017). Comparison of sorption and desorption studies of heavy metal ions from biochar and commercial active carbon. *Chemical Engineering Journal, 307*, 353–363.

Langmuir, I. (1918). The adsorption of gases on plane surfaces of glass, mica and platinum. *Journal of the American Chemical Society, 40*, 1361–1403.

Li, H., Dong, X., da Silva, E. B., de Oliveira, L. M., Chen, Y., & Ma, L. Q. (2017). Mechanisms of metal sorption by biochars: Biochar characteristics and modifications. *Chemosphere, 178,* 466–478.

Mohan, D., Sarswat, A., Ok, Y. S., & Pittman, C. U. (2014). Organic and inorganic contaminants removal from water with biochar, a renewable, low cost and sustainable adsorbent—A critical review. *Bioresource Technology, 160,* 191–202.

Oliveira, F. R., Patel, A. K., Jaisi, D. P., Adhikari, S., Lu, H., & Khanal, S. K. (2017). Environmental application of biochar: Current status and perspectives. *Bioresource Technology, 246*, 110–122.

Tan, X., Liu, Y., Zeng, G., Wang, X., Hu, X., Gu, Y., et al. (2015). Application of biochar for the removal of pollutants from aqueous solutions. *Chemosphere, 125,* 70–85.

Weber, T. W., & Chakravorti, R. K. (1974). Pore and solid diffusion models for fixed-bed adsorbers. *AIChE Journal, 20,* 228–238.

A Simplified Model to Simulate a Bioaugmented Anaerobic Digestion of Lignocellulosic Biomass

Alberto Ferraro, Giulia Massini, Valentina Mazzurco Miritana, Antonella Signorini, Marco Race, and Massimiliano Fabbricino

Abstract

Normalized root mean square error (NRMSE) results from calibration and validation phases confirmed the model robustness and stability; k_d calibrated values were consistent with the initial faster process kinetic observed in the anaerobic digestion (AD) configuration; α values from model calibration step further confirmed the beneficial effects of F210 and ARF on the hydrolysis step enhancement of wheat straw (WS).

Keywords

Mathematical modelling • Lignocellulosic substrates • Methane • Bioaugmentation • Anaerobic fungi • Fermenting bacteria

A. Ferraro (✉) · M. Fabbricino
Department of Civil, Architectural, and Environmental Engineering, University of Naples "Federico II", Via Claudio 21, 80125 Naples, Italy
e-mail: alberto.ferraro3@gmail.com

M. Fabbricino
e-mail: fabbrici@unina.it

G. Massini · V. Mazzurco Miritana · A. Signorini
Department of Energy Technologies, Italian National Agency for New Technologies, Energy and Sustainable Economic Development (ENEA), Via Anguillarese 301, 00123 Rome, Italy
e-mail: giulia.massini@enea.it

V. Mazzurco Miritana
e-mail: valentina_mazzurco@yahoo.it

A. Signorini
e-mail: antonella.signorini@enea.it

M. Race
Department of Civil and Mechanical Engineering, University of Cassino and Southern Lazio, Via di Biasio, 03043 Cassino, Italy
e-mail: marcorace@gmail.com

1 Introduction

The energetic valorization of waste biomass through anaerobic digestion (AD) is considered an environmental sustainable strategy to solve two major social problems, organic waste disposal and energy demand. The present work shows the results of an experimental study on bioaugmented anaerobic digestion (BAD) carried out on wheat straw (WS), simulating two different process configurations: (i) single-stage (I-BAD) and (ii) two-stage (II-BAD) at increasing reactor scale. In order to determine and compare process kinetic of the different experimental conditions, it proposed a simplified mathematical model based on a set of ordinary differential equations (ODEs). The model is calibrated and validated using two independent sets of experimental data. The differences obtained among the kinetic parameters in the different configurations are carefully addressed.

2 Materials and Methods

2.1 Batch Bioaugmented Tests

Tests were carried out in batch reactors, at 37 °C, in triplicates. Bioaugmentation conditions were obtained using two functional microbial components, in addition to the methanogenic inoculum (MI): (i) a mix of two strains of anaerobic ruminal fungi (ARF) and (ii) hydrogen-producing bacteria (F210), with a hydrolytic and a fermenting role respectively. ARF and F210 were mixed together with MI in I-BAD configuration, while only ARF and F210 were added in the first stage of II-BAD configuration, followed by MI inoculum addition at the end of hydrogen production phase. Conventional AD tests were conducted too (blank tests). Each experiment was repeated both in 120 mL reactors, and in 120×100 mL ones ($100 \times$ I-BAD and $100 \times$ II-BAD), to have two independent data sets. In all cases, pH was maintained at 6.8 ± 0.2 using a 0.1 M phosphate buffer

solution. Other experimental conditions were similar to the ones reported elsewhere (Ferraro et al. 2018).

2.2 Mathematical Model Calibration and Validation

Mathematical model calibration was performed using Matlab®. Most sensitive parameters were initially identified, and their optimal values were successively determined adopting a response surface methodology, commonly used for model optimization purposes (Boels et al. 2012). In details, the chosen function was the normalized root mean square error (NRMSE) expressed as follows:

$$\text{NRMSE} = \frac{\sqrt{\frac{\sum_{i=1}^{K}\left(y_i - y_i'\right)^2}{K}}}{y_M} \tag{1}$$

with K representing the number of observed values, y_i representing the simulated values, y_i' representing the observed values, and y_M representing the average of the observed values. Calibration was performed using the experimental data set obtained at smaller scale. Validation was instead conducted using the experimental data set obtained at higher scale ($100 \times$ I-BAD and $100 \times$ II-BAD).

3 Results and Discussion

3.1 Mathematical Model Description

The ODEs system was represented by four mass balance equations describing the main phenomena occurring during the process: (i) substrate mass balance (Eq. 2), (ii) soluble hydrogen mass balance (Eq. 3), (iii) soluble methane mass balance (Eq. 4), and (iv) gaseous methane mass balance (Eq. 5).

The substrate mass balance equation was expressed as:

$$\frac{dC}{dt} = -k_d \cdot C_0 \tag{2}$$

with C and C_0 (gCOD L^{-1}) equal, respectively, to the substrate concentration at time t and time zero, and k_d (d^{-1}) defined as substrate degradation constant. The initial degradation phase of lignocellulosic substrates, in facts, generally represents the rate-limiting step of the overall process. For this reason, substrate hydrolysis was assumed as the controlling process, and no other equation related to the acidogenesis, acetogenesis, and methanogenesis phases was added to the simplified model.

For the mass balance equations related to the hydrogen in the liquid phase and methane in the liquid and gaseous phases, it was followed the approach suggested by Pauss et al. (1990) for continuously fed fermenters and homogeneous gas and liquid phases. Of course, the equations were modified to take into account the experimental batch conditions. The final expressions resulted the following ones:

$$\frac{dS_H}{dt} = \alpha \cdot k_d \cdot C + (1 - Y_H) \cdot k_{m,H} \cdot \frac{S_H}{k_s + S_H} \cdot X_H - k_{L,H}$$
$$\cdot (S_H - 16 \cdot k_H \cdot p_H) \cdot \frac{V_L}{V_G} \tag{3}$$

$$\frac{dS_M}{dt} = (1 - \alpha) \cdot k_d \cdot C + (1 - Y_H) \cdot k_{m,H} \cdot \frac{S_H}{k_s + S_H} \cdot X_H$$
$$- k_{L,M} \cdot (M - 64 \cdot k_M \cdot p_M) \cdot \frac{V_L}{V_G} \tag{4}$$

$$\frac{dM}{dt} = k_{L,M} \cdot (M - 64 \cdot k_M \cdot p_M) \cdot \frac{V_L}{V_G} \tag{5}$$

where S_H (gCOD L^{-1}) represents the soluble hydrogen concentration, Y_H (gCOD gCOD^{-1}) is the biomass yield, $k_{m,H}$ (d^{-1}) is the Monod maximum specific uptake rate of hydrogenotrophic biomass, k_s (gCOD L^{-1}) is the hydrogen semi-saturation constant, X_H (gCOD L^{-1}) is the concentration of the hydrogenotrophic biomass, $k_{L,H}$ (d^{-1}) is the hydrogen gas transfer constant, k_H (M atm^{-1}) is the Henry constant for hydrogen, p_H (atm) is the hydrogen partial pressure, S_M (gCOD L^{-1}) is the soluble methane concentration, M (gCOD L^{-1}) is the gaseous methane concentration, $k_{L,M}$ (d^{-1}) is the methane gas transfer constant, k_M (M atm^{-1}) is the Henry constant for methane, and p_M (atm) is the methane partial pressure. The coefficient α, in turns, represents a partition coefficient between the hydrolysis and the methanogenesis process.

3.2 Mathematical Model Calibration and Validation

Results related to NRMSE values obtained from the experimental data fitting in the calibration phase are reported in Fig. 1a (AD test), b (I-BAD test), and c (II-BAD test). The calibration was performed optimizing k_d and α values.

Minimum NRMSE values were 0.1480, 0.0818, and 0.1324 respectively for AD, I-BAD, and II-BAD. Corresponding optimal k_d and α were: (i) AD tests, $k_d = 0.13$ d^{-1} and $\alpha = 0.87$; (ii) I-BAD tests, $k_d = 0.05$ d^{-1} and $\alpha = 0.44$; (iii) II-BAD $k_d = 0.05$ d^{-1} and $\alpha = 0.49$. Overall the highest values were obtained for AD tests. In particular, k_d resulted 2.6 times higher in AD than in BAD tests. This result was consistent with the initial faster production of CH$_4$, which characterized AD tests (Fig. 2a) and with the initial similar slower production of CH$_4$ which characterized both configurations of BAD tests (Fig. 2b, c). Indeed k_d is the kinetic
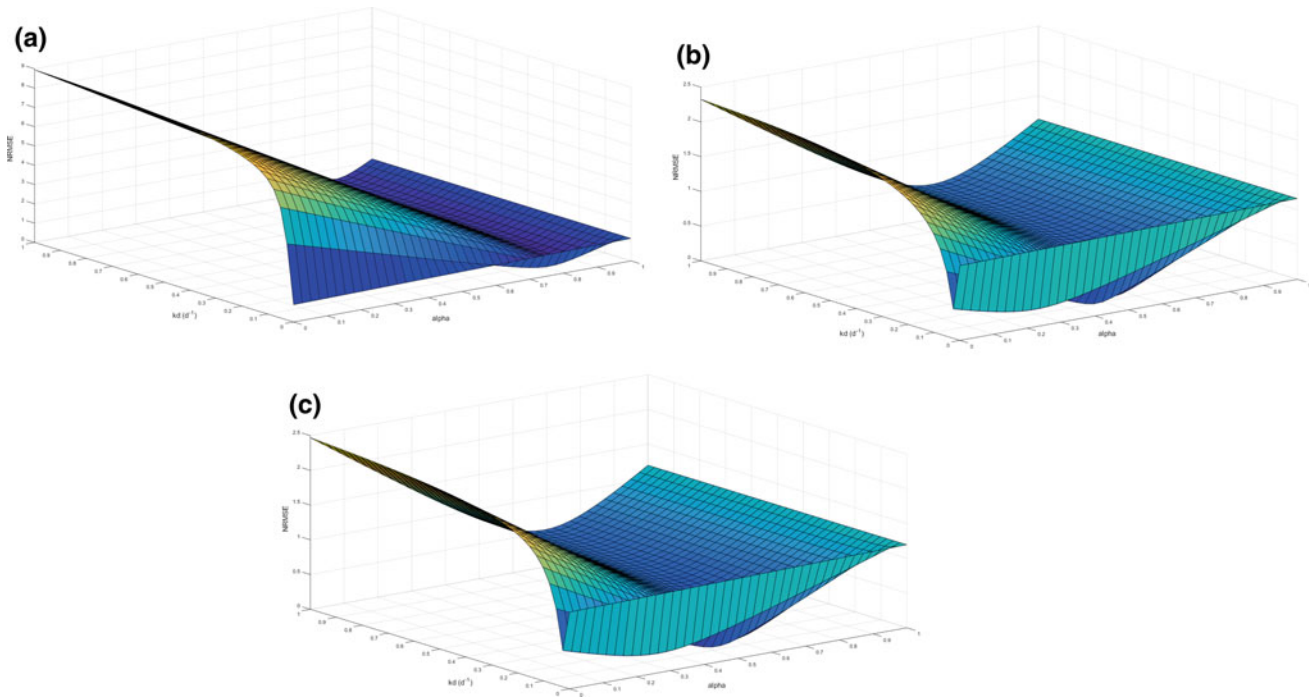
Fig. 1 NRMSE values (z-axis) from calibration step of k_d (x-axis) and α (y-axis) on **a** AD, **b** I-BAD, and **c** II-BAD tests
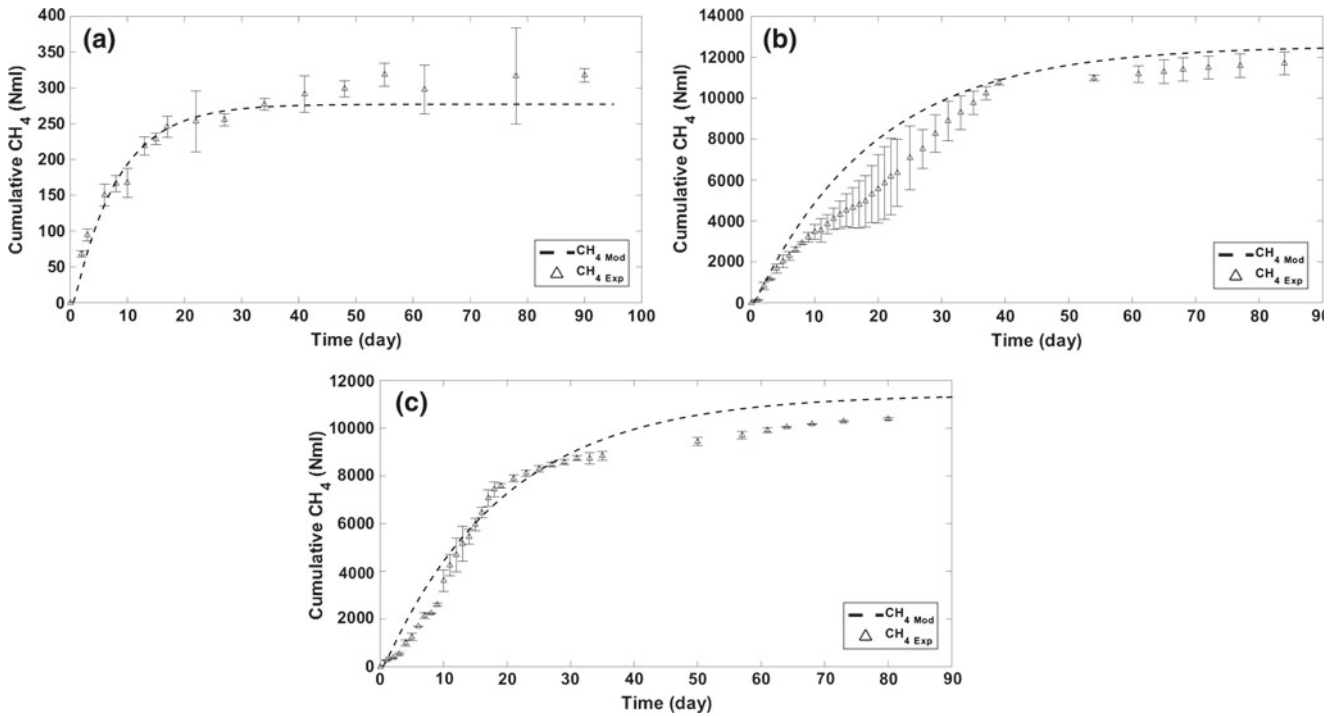
Fig. 2 Fitting of simulated (line) and experimental (dot) data for CH_4 cumulative production (N mL) from validation step for **a** 10 × AD, **b** 100 × I-BAD, and **c** 100 × II-BAD tests

parameter representative of substrate consumption. At the same time, α resulted almost 2 times higher in AD than in I-BAD, and more than 1.5 times higher in AD than in II-BAD tests. Since α indicates the significance of the hydrolysis as limiting step of the whole process, a higher CH_4 production should be expected for lower α values,

accounting for an enhanced methanogenic phase. Experimental results were, once more, in agreement with the expected trend and confirmed the beneficial effect of F210 and ARF components addition in terms of WS hydrolysis phase enhancement.

Results of validation are reported, once more, in Fig. 2. In this case, NRMSE index was equal to 0.0958 (AD), 0.2454 (I-BAD), and 0.1239 (II-BAD). These values assessed the validity and the applicability of the proposed simplified model for CH_4 production simulations, both in case of conventional AD process and in case of bioaugmented ones, at different operational scales.

4 Conclusion

Results reported in the present work highlighted the suitable applicability of the suggested simplified mathematical model as a useful tool for CH_4 production prediction during conventional and bioaugmented AD process. The optimal NRMSE values obtained from both the calibration and the validation phases at different operational scales further confirmed the model robustness and stability. Moreover, the differences observed between the calibrated k_d and α values of AD and BAD tests showed a strong correlation with the experimental results. In fact, lower parameter values from I- and II-BAD configurations were consistent with an initial slower process kinetic as well as with a CH_4 production enhancement due to the improved substrate hydrolysis obtained by ARF and F210 microbial community bioaugmentation. A deeper insight of the explored topic could derive from microbiological investigation aimed at better characterizing the microbial community and further confirming the mathematical model suitability.

References

Boels, L., Keesman, K. J., & Witkamp, G.-J. (2012). Adsorption of phosphonate antiscalant from reverse osmosis membrane concentrate onto granular ferric hydroxide. *Environmental Science and Technology, 46,* 9638–9645.

Ferraro, A., Dottorini, G., Massini, G., Mazzurco Miritana, V., Signorini, A., Lembo, G., et al. (2018). Combined bioaugmentation with anaerobic ruminal fungi and fermentative bacteria to enhance biogas production from wheat straw and mushroom spent straw. *Bioresource Technology, 260,* 364–373.

Pauss, A., Andre, G., Perrier, M., & Guiot, S. R. (1990). Liquid-to-gas mass transfer in anaerobic processes: Inevitable transfer limitations of methane and hydrogen in the biomethanation process. *Applied and Environment Microbiology, 56,* 1636–1644.

Dissolved Oxygen Perturbations: A New Strategy to Enhance the Removal of Organic Micropollutants in Activated Sludge Process

Camilla Di Marcantonio, Amrita Bains, Agostina Chiavola,
Naresh Singhal, and Maria Rosaria Boni

Abstract

Cycles of dissolved oxygen perturbation can affect emerging contaminants removal. The nitrification process can also be enhanced by oxygen perturbations. Perturbation frequency is a sensitive parameter.

1 Introduction

Among the removal treatments for organic micropollutants (OMPs) from wastewater, the biological treatments represent interesting and promising possibilities, in terms of cost and environmental impact. In this field, an innovative approach was proposed by Singhal and Perez-Garcia (2016), based on enzyme biocatalysis processes. Several studies confirm that an increase of OMPs removal could be achieved by stimulating the production of specific enzymes (Alneyadi et al. 2018). This production is due to the establishment of oxidative stress, which is a condition reached when certain environmental stresses or genetic defects cause the production of reactive oxygen species (ROS) that exceed the management capacity of the cells (Mishra et al. 2005). Microorganisms alter their metabolism and defense strategies in order to take advantage of the accumulated oxygen and to avoid the damage caused by oxidative stress. Indeed, a small change in cellular oxidant status can be sensed by specific proteins which regulate a set of genes encoding antioxidant enzymes, in order to induce the adaptive metabolism including ROS elimination and reparation of oxidative damages (Gambino and Cappitelli 2016). In the present study, an approach is proposed to induce the synthesis of OMP-degrading enzymes, based on exposing microbes to cycles of stressing and non-stressing environmental conditions. The hypothesis is that oxidative stress could be caused by a fast change of the dissolved oxygen concentration in the environment which leads to a different oxygen concentration inside the cell. The present paper shows the first results of the experimental activity carried out to verify the effect of dissolved oxygen perturbations on the microbial mixed cultures of activated sludge from domestic sewage. In this first step, feed-batch tests were performed at laboratory scale, testing three different perturbation pathways. The study focused on the effect of the main reactions occurring in a secondary treatment, i.e., carbon removal and nitrification, as well as on the OMPs' degradation. For instance, the effects were tested on a OMPs' mixture of selected not easily biodegradable compounds within the classes of pharmaceuticals [sulfamethoxazole (SMX), sulfadiazine (SDZ), lincomycin (LCM), carbamazepine (CBZ), and naproxen (NPX)] and pesticides [atrazine (ATZ)] and artificial sweeteners [sucralose (SCL)].

C. Di Marcantonio (✉) · A. Chiavola · M. R. Boni
Department of Civil, Constructional and Environmental Engineering (DICEA), Sapienza University of Rome, Rome, Italy
e-mail: camilla.dimarcantonio@uniroma1.it

A. Chiavola
e-mail: agostina.chiavola@uniroma1.it

M. R. Boni
e-mail: mariarosaria.boni@uniroma1.it

A. Bains · N. Singhal
Department of Civil and Environmental Engineering and School of Biological Sciences, The University of Auckland, Auckland, New Zealand
e-mail: abai920@aucklanduni.ac.nz

N. Singhal
e-mail: n.singhal@auckland.ac.nz

2 Materials and Methods

Three perturbation pathways (Fig. 1) were tested to stimulate oxydoreductase enzyme production by microbial cells in activated sludge reactors at laboratory scale. ON–OFF aeration cycles (using air and oxygen mixed flow) were applied in order to obtain different dissolved oxygen (DO) conditions, by varying the set point and the perturbation frequency (f = number of perturbations per hour). Particularly, the following DO pathways were applied: E1) from 0 to ≈ 7 mg O_2/L with $f = 0.5$; E2) from 0 to ≈ 7 mg O_2/L with $f = 1$; E3) from 0 to 2 mg O_2/L with $f = 4$. A non-perturbed condition test (C1) was also run as a control, maintaining an aerobic constant level of dissolved oxygen, to use as a comparison of the performances of a traditional activated sludge treatment without DO control.

The activated sludge was collected from the sludge recycle loop of the secondary treatment of a wastewater treatment plant (WWTP) in Auckland. Sludge was washed by tap water several times and then stored at −20 °C until the use. Prior to each experimental test, biomass was acclimatized by maintaining it under aerobic conditions for at least 24 h and feeding with the same synthetic wastewater used in the laboratory work but without OMPs, in order to reach the steady state for nitrogen removal. The tests were performed in a feed-batch mode bioreactors (volume equal to one liter), with a volatile suspended solids (MLVSS) concentration equal to 3000 mg/L, 50 mL of phosphate-buffered saline (PBS) solution made according to Stoll and Blanchard (1990), an initial concentration of 0.1 mg/L of each OMPs and tap water to ensure the right intake of minerals and micronutrients for biomass activity. The bioreactors were continuously fed with a flow equal to 0.0347 mL/min of synthetic wastewater (SyWW) during all the test duration (48 h). The synthetic wastewater composition followed (Bassin et al. 2011) modified in order to have a C/N/P ratio equal to 100/5/1. pH was maintained around the optimal values for nitrification, i.e., 7.2–8 pH range, by adding 50 mL of PBS (0.2 M, pH 7.6), and monitored during the tests. Samples were collected at 0, 5, 24, and 48 h. The perturbations were performed by Millennium 3 CD 20 logic controller connected to solenoids valves, setting the ON and OFF times of the aeration system. The oxygen monitoring system was composed by a Hamilton Device Manager 1.0.0 software equipped with wireless sensor which was connected to VisiFerm DO sensors. Tests were performed in duplicate, and the results obtained averaged. Nitrification and carbon removal were monitored by measuring the following parameters: acetate (the main source of carbon in the system), NH_3–N, NO_2–N, and NO_3–N concentration. Analytical determination of these compounds (except ammonium nitrogen) was performed by using the Thermo Scientific Dionex ICS-2100 Ion Chromatography System following APHA methods 4110 B (APHA methods, 2005). NH_3–N was measured by the Thermo Scientific Orion 4 ammonia ion-selective electrode following the APHA methods 4500-NH_3 D (APHA methods, 2005). Quantitative analysis of OMPs was carried out by means of Shimadzu Liquid Chromatograph-Mass Spectrometry (LC–MS) 8040 equipped with Agilent ZORBAX Eclipse Plus C18 column. Two specific analytical methods were developed, one in negative mode for naproxen and one in positive mode for all the other compounds based on EPA Method 1694 (Imma Ferrer 2008). The samples were stored for less than one week at −20 °C and subjected to a solid-phase extraction procedure before injection.

3 Results and Discussion

The concentrations of OMPs were analyzed during the tests at different sampling times. The results obtained were used to calculate the removal efficiency of each compound at the end of the tests (Fig. 2), in order to compare the effect of the different DO pathways.

The results summarized in Fig. 2 show a different behavior of the tested contaminants. The removal of LNC results improved with the increasing of the perturbation frequency, while for NPX the process was enhanced only in the test where the oxygen was kept between 0 and 2 mg
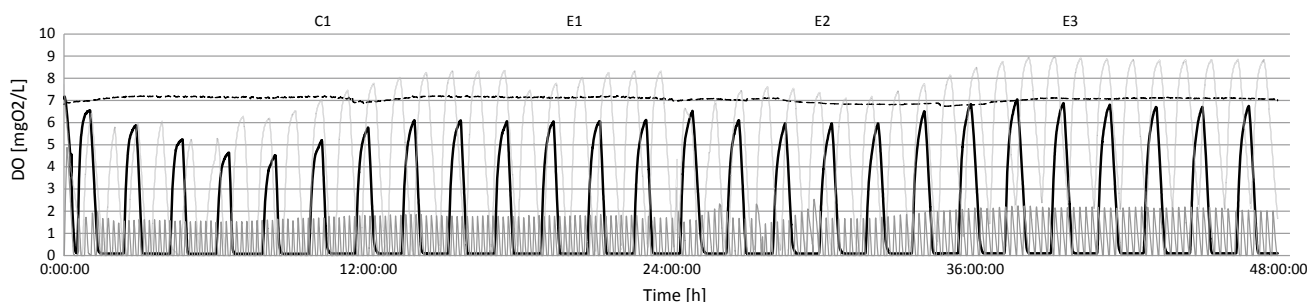
Fig. 1 DO pathways

Fig. 2 OMPs removal after 48 h for each DO pathway

O_2/L. Both SLD and SMX removals were not significantly affected by the DO perturbations. SCL removal was slightly improved only during test E1. For CBZ and ATZ, the best results were obtained when the oxygen level was low for most of the duration of the tests (E1 and E3).

Figure 3 shows concentrations of nitrogen species (in terms of mg N/L) during the tests under the different DO pathways; nitrite values are not shown because always below the detection limit of the analytical method (0.1 mg N/L). The values measured at the beginning of test are related to the 24 h of acclimatization phase, where the steady state of nitrification was achieved due to the constant aerobic condition and the continuous feeding. In the control test, nitrification showed complete ammonium nitrogen oxidation into nitrate, as expected. During the test E2 (oxygen range = 0–7 mg O_2/L and $f = 1$), the higher value of NH_3 was recorded at the end of the test while nitrate remained pretty constant after 20 h, indicating a partial hindrance of the reaction. Moreover, in tests E1 and E3, denitrification reaction was identified, because a low
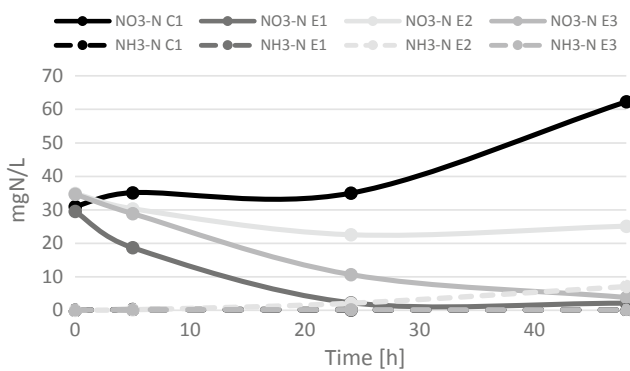
concentration of NH_3 and NO_3^- was revealed, suggesting a final reduction of nitrate into N_2.

4 Conclusion

The results obtained in the present study showed that perturbations frequency and dissolved oxygen ranges are both sensitive parameters for the removal of a mixture of selected OMPs in activated sludge process. Indeed, degradation of some OMPs compounds improved with a high perturbations frequency (e.g., LNC), whereas that of others, OMPs were more affected by the specific DO range. Moreover, a wide difference in the nitrogen removal reactions was observed during the tests depending on the DO pathway. Further investigations and microbiological studies, focusing on the specific enzymes involved in OMPs' degradation reactions, are needed to optimize the oxygen perturbations to improve their removal.

References

Alneyadi, A. H., Rauf, M. A., & Ashraf, S. S. (2018). Oxidoreductases for the remediation of organic pollutants in water—A critical review. *Critical Reviews in Biotechnology, 38*(7), 1–18. https://doi.org/10.1080/07388551.2017.1423275. (Informa Healthcare USA, Inc.).

Bassin, J. P., Pronk, M., Kraan, R., Kleerebezem, R., & Van Loosdrecht, M. C. M. (2011). Ammonium adsorption in aerobic granular sludge, activated sludge and anammox granules. *Water Research, 45*(16), 5257–5265. https://doi.org/10.1016/j.watres.2011.07.034. (Elsevier Ltd.).

Eaton, A. D., Clesceri, L. S., Rice, E. W., & Greenberg, A. E. (2005). *Standard methods for the examination of water and wastewater, centennial edition.*

Gambino, M., & Cappitelli, F. (2016). Mini-review: Biofilm responses to oxidative stress. *Biofouling, 32*(2), 167–178. https://doi.org/10.1080/08927014.2015.1134515. (Taylor & Francis).

Imma Ferrer, E. M. T. (2008). *EPA method 1694 : Agilent's 6410A LC/MS/MS solution for pharmaceuticals and personal care products in water, soil, sediment, and biosolids by HPLC/MS/MS application note.* Group, p. 12.

Mishra, S., Noronha, S. B., & Suraishkumar, G. K. (2005). Increase in enzyme productivity by induced oxidative stress in *Bacillus subtilis* cultures and analysis of its mechanism using microarray data. *Process Biochemistry, 40*(5), 1863–1870. https://doi.org/10.1016/j.procbio.2004.06.055.

Singhal, N., & Perez-Garcia, O. (2016). Degrading organic micropollutants: The next challenge in the evolution of biological wastewater treatment processes. *Frontiers in Environmental Science, 4*, 1–5. https://doi.org/10.3389/fenvs.2016.00036.

Stoll, V. S., & Blanchard, J. S. (1990). Buffers: Principles and practice. *Methods in Enzymology, 182*(1966), 24–38. https://doi.org/10.1016/0076-6879(90)82006-N.

Fig. 3 Nitrification with time for each DO pathway

PFOA and PFOS Removal Processes in Activated Sludge Reactor at Laboratory Scale

Agostina Chiavola, Camilla Di Marcantonio, Maria Rosaria Boni, Stefano Biagioli, Alessandro Frugis, and Giancarlo Cecchini

Abstract

Adsorption was the main removal process of PFOS and PFOA in activated sludge reactors at laboratory scale. Some biodegradation of the two tested contaminants was also detected, after adsorption. Respirometric tests showed inhibition of the nitrifying bacteria up to 30% due to the presence of PFOS and PFOA. COD removal was not affected by the presence of PFOS and PFOA.

Keywords

Activated sludge • Biodegradation • Emerging contaminants • Inhibition effect • Perfluoroalkyl substances • Respirometric test

1 Introduction

Perfluorinated compounds (PFCs) is a class of industrial compounds largely used in the last fifty years, due to their great chemical and thermal resistance, high hydrophobicity and lipophobicity. The extensive range of PFCs applications (from plastic polymers to textile fibres and cosmetics) has resulted in an environmental ubiquity and a worldwide presence in the human body (Ahrens et al. 2011; Castiglioni et al. 2015). Furthermore, scientific research has confirmed their endocrine-disrupting properties (White et al. 2011). Perfluorooctane sulphonic acid (PFOS) and perfluorooctanoic acid (PFOA) are the two PFCs most investigated for their persistence and bioaccumulation in the trophic chain (Castiglioni et al. 2015). An Environmental Quality Standard (EQS) for priority substances (Directive 2013/39/EU) was fixed for PFOS in surface water and biota. Wastewater treatment plants (WWTPs) are among the main sources of PFCs in the environment. Indeed, being resistant to biological and chemical degradation, they are not significantly removed during secondary biological treatment, whereas potential transformation of precursor compounds to PFCs during same processes may lead to an increase of the concentrations in treated water (Pan et al. 2016). Additional understanding about the removal processes in a conventional activated sludge reactor [the most common secondary treatment (Grassi et al. 2013)] can contribute to reduce the environmental impact due to the WWTPs. So far, the number of reports examining the biodegradation and biotransformation of PFOS and PFOA by aerobic and anaerobic microbial populations is limited. However, in scientific literature it is possible to find conflicting results about the biodegradability of PFOS and PFOA (Arvaniti and Stasinakis 2015). Kwon et al. (2014) found that PFOS can be decomposed up to 67% by a specific microorganism present in activated sludge. On the contrary, other authors concluded that PFOS is microbiologically inert under aerobic conditions. PFOA is considered biologically inactive under all the examined conditions (Liou et al. 2010). An important mechanism of removal seems to be the adsorption onto sludge flocs; indeed the use of biomass as adsorbent material has already demonstrated its remarkable performances towards various pollutants, such as heavy metals and organics (Quirantes et al. 2017; Vilardi et al. 2017).

A. Chiavola · C. Di Marcantonio (✉) · M. R. Boni
Department of Civil, Building and Environmental Engineering (DICEA), Sapienza University of Rome, Rome, Italy
e-mail: camilla.dimarcantonio@uniroma1.it

A. Chiavola
e-mail: agostina.chiavola@uniroma1.it

M. R. Boni
e-mail: mariarosaria.boni@uniroma1.it

S. Biagioli · A. Frugis · G. Cecchini
Acea Elabori SpA, Via Vitorchiano 165, Rome, Italy
e-mail: stefano.biagioli@aceaspa.it

A. Frugis
e-mail: alessandro.frugis@aceaspa.it

G. Cecchini
e-mail: giancarlo.cecchini@aceaspa.it

The focus of the present study was to investigate the contribution of biodegradation and adsorption to the removal of PFOS and PFOA in the biological reactor of a WWTP. The response of the biomass activity to different contaminant concentrations was also evaluated.

2   Materials and Methods

Removal processes and potential inhibition of biomass activity in the activated sludge reactor were investigated through a series of batch tests. A 600-mL glass flask (500 mL operating volume) was used for conducting the experiments. The tests were performed in duplicated, and the results averaged. Each flask was placed on a jar tester to provide mechanical stirring in order to maintain the content under completely mixed conditions; it was also aerated for the duration of the test. The flasks were covered with aluminium foils to avoid photo-degradation phenomena, and the temperature was maintained within the range 22 ± 2 °C. pH was controlled through a solution of NaOH 30% (w/v) to fall within 7.2–8.0 range, which is considered optimal for nitrification. The experiments were carried out using the following initial concentrations: 500, 250, and 100 ng/L PFOA and PFOS. These values were chosen because they belong to the range reported by the specialized literature as found in the influent of WWTPs (Arvaniti and Stasinakis 2015; Roh et al. 2009). The overall duration of each test was fixed at 24 h based on preliminary tests, with the aim to guarantee the achievement of equilibrium conditions. During the tests, samples at fixed time intervals (i.e. 0, 3, 6 and 24 h) were collected to determine the kinetics of the processes. Nitrification and COD removal were also monitored by measuring the following parameters: COD, NH_3–N, NO_2–N and NO_3–N, MLSS and MLVSS concentrations. Furthermore, PFOA and PFOS concentrations were measured in the sludge phase at the beginning and at the end of each test. The potential inhibition effect of contaminants on biomass activity was evaluated by following the activated sludge, respiration inhibition test, Carbon and Ammonium Oxidation OECD 209 method (OECD 2010). With this method, it is possible to determine how different concentrations of a tested compound may affect the activity of microorganisms based on oxygen uptake rate (OUR) measurements. The specific oxygen uptake rate (SOUR) was also calculated, by normalizing the OUR to the MLSS content. All the experiments were performed using samples of activated sludge taken from the oxidation tank of a full-scale WWTP for domestic sewage. Three series of tests were performed: (1) with activated sludge, nutrient solutions and PFOA or PFOS at the fixed concentrations; (2) with activated sludge previously inhibited by the addition of sodium azide, nutrient solutions and PFOA or PFOS at the fixed concentrations; (3) activated sludge and nutrient solutions (i.e. without PFOA or PFOS). The nutrient solution had a composition simulating that of domestic sewage as far as C, N and P and microelement components. Quantitative analysis of PFCs was carried out by means ultra-performance liquid chromatography coupled to tandem mass spectrometry.

3   Results and Discussion

Contaminant removals at the end of the tests are shown in Fig. 1a, b for PFOA and PFOS, respectively (error bar indicates the standard deviation calculated on the concentration values of two replicates).

Data show comparable results for the two compounds in terms of total removal from the liquid phase, i.e. from 80 to 89% for PFOA and from 76 to 89% for PFOS, at the increasing initial concentration. Removal associated with the two main processes, i.e. biodegradation and adsorption, was calculated based on the total mass balance of contaminants between solid and liquid phases. The main removal could be ascribed to adsorption, but also some biodegradation occurred: indeed, biodegradation of PFOA varied from 21, 33 and 42%, while for PFOS from 15, 27 and 21%, at the increasing initial concentration. As far as the kinetics are concerned, total removal did not change significantly during the test for both compounds (around 6% for PFOA and 5% for PFOS, data not here shown). This suggests that the first and faster removal mechanism was the adsorption onto sludge flocs; afterwards, a limited biodegradation of the adsorbed contaminants occurred. These results are partially in accordance with scientific knowledge, where PFOA is considered non-biodegradable under aerobic conditions and while PFOS is only partly removed (Kwon et al. 2014). Different kinetic models were applied to the experimental data of residual liquid concentration: the second- and first-order models provided the best fitting for PFOA and PFOS, respectively. Figure 2 shows the trend of COD removal and nitrification reactions (as ammonium removal and nitrate production) in all the tests at different PFCs' initial concentrations and in the blank test; the same figure displays the inhibition % on biomass activity obtained by means of the respirometric tests. The results highlight inhibition of 30% at the two lowest concentrations and 34% at the highest, while COD removal was not affected by the presence of the two compounds, by contrast the nitrification in all the tests.
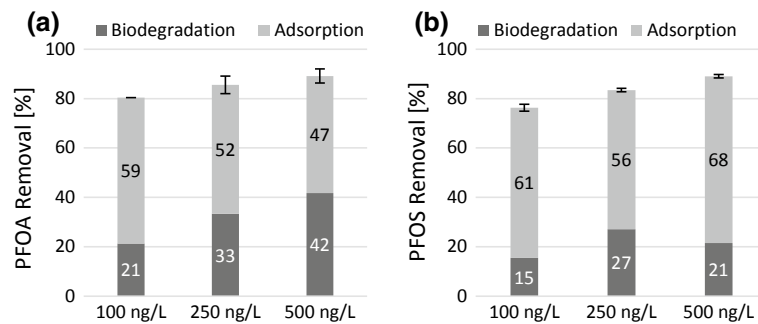
Fig. 1 Removal efficiency of **a** PFOA and **b** PFOS after 24 h of treatment
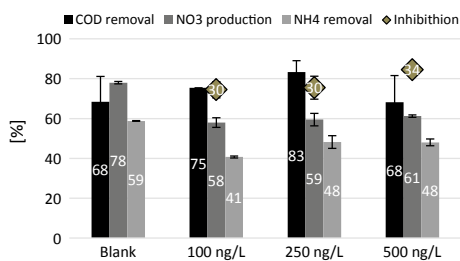
Fig. 2 COD removal, nitrification efficiency, and biomass activity inhibition

4 Conclusion

The results obtained in the present study showed a removal of PFOA and PFOS up to 80 and 76%, respectively, in the activated sludge treatment tests at laboratory scale. The main removal process was observed to be adsorption, which is in accordance with the specialized literature (Arvaniti and Stasinakis 2015). However, some biodegradation was also observed for the two compounds, which started only after adsorption on the sludge. The results obtained from the respirometric tests indicate that the presence of PFOS and PFOA at the tested concentrations affects the activity of nitrifying bacteria.

References

Ahrens, L., Yeung, L. W. Y., Taniyasu, S., Lam, P. K. S., & Yamashita, N. (2011). Partitioning of perfluorooctanoate (PFOA), perfluorooctane sulfonate (PFOS) and perfluorooctane sulfonamide (PFOSA) between water and sediment. *Chemosphere, 85*(5), 731–737. https://doi.org/10.1016/j.chemosphere.2011.06.046. Elsevier Ltd.

Arvaniti, O. S., & Stasinakis, A. S. (2015). Review on the occurrence, fate and removal of perfluorinated compounds during wastewater treatment. *Science of the Total Environment, 524–525*, 81–92. https://doi.org/10.1016/j.scitotenv.2015.04.023. Elsevier B.V.

Castiglioni, S., Valsecchi, S., Polesello, S., Rusconi, M., Melis, M., Palmiotto, M., et al. (2015). Sources and fate of perfluorinated compounds in the aqueous environment and in drinking water of a highly urbanized and industrialized area in Italy. *Journal of Hazardous Materials, 282*, 51–60. https://doi.org/10.1016/j.jhazmat.2014.06.007. Elsevier B.V.

Grassi, M., Rizzo, L., & Farina, A. (2013). Endocrine disruptors compounds, pharmaceuticals and personal care products in urban wastewater: Implications for agricultural reuse and their removal by adsorption process. *Environmental Science and Pollution Research, 20*(6), 3616–3628. https://doi.org/10.1007/s11356-013-1636-7.

Kwon, B. G., Lim, H. J., Na, S. H., Choi, B. I., Shin, D. S., & Chung, S. Y. (2014). Biodegradation of perfluorooctanesulfonate (PFOS) as an emerging contaminant. *Chemosphere, 109*, 221–225. https://doi.org/10.1016/j.chemosphere.2014.01.072. Elsevier Ltd.

Liou, J. S. C., Szostek, B., DeRito, C. M., & Madsen, E. L. (2010). Investigating the biodegradability of perfluorooctanoic acid. *Chemosphere, 80*(2), 176–183. https://doi.org/10.1016/j.chemosphere.2010.03.009. Elsevier Ltd.

Oecd. (2010). Test no. 209: Activated sludge, respiration inhibition test. In *OECD guidelines for the testing of chemicals, section 2: Effects on biotic systems* (No. 209, pp. 1–18). https://doi.org/10.1787/9789264070080-en.

Pan, C.-G., Liu, Y.-S., & Ying, G.-G. (2016). Perfluoroalkyl substances (PFASs) in wastewater treatment plants and drinking water treatment plants: Removal efficiency and exposure risk. *Water Research, 106*, 562–570. https://doi.org/10.1016/j.watres.2016.10.045. Elsevier Ltd.

Quirantes, M., Nogales, R., & Romero, E. (2017). Sorption potential of different biomass fly ashes for the removal of diuron and 3,4-dichloroaniline from water. *Journal of Hazardous Materials, 331*, 300–308. https://doi.org/10.1016/j.jhazmat.2017.02.047. Elsevier B.V.

Roh, H., Subramanya, N., Zhao, F., Yu, C. P., Sandt, J., & Chu, K. H. (2009). Biodegradation potential of wastewater micropollutants by ammonia-oxidizing bacteria. *Chemosphere, 77*(8), 1084–1089. https://doi.org/10.1016/j.chemosphere.2009.08.049. Elsevier Ltd.

Vilardi, G., Di Palma, L., & Verdone, N. (2017). Heavy metals adsorption by banana peels micro-powder. Equilibrium modeling by non-linear models. *Chinese Journal of Chemical Engineering*. https://doi.org/10.1016/j.cjche.2017.06.026. Elsevier B.V.

White, S. S., Fenton, S. E., & Hines, E. P. (2011). Endocrine disrupting properties of perfluorooctanoic acid. *Journal of Steroid Biochemistry and Molecular Biology, 127*(1–2), 16–26. https://doi.org/10.1016/j.jsbmb.2011.03.011. Elsevier Ltd.

Selectrodialysis and Ion-Exchange Resins as Integration Processes for Copper and Zinc Recovery from Metallurgical Streams Containing Arsenic

M. Reig, X. Vecino, M. Hermassi, J. López, C. Valderrama, O. Gibert, and J. L. Cortina

Abstract

SED is an innovative technology for metallurgical effluents treatment; IEX resin is an efficient methodology for metal separation and concentration steps; Cu and Zn were recovered by means of integration processes (SED and IEX resins).

Keywords

Selectrodialysis • Ion-exchange processes • Metal recovery • Free-arsenic stream • Metallurgical industry • Circular economy

1 Introduction

Nowadays, the shortage of water and the need to reduce the associated environmental impacts make necessary not only to treat wastewaters but also to reuse them. In addition, all industrial sectors generate waste effluents with great potential to be valorized. The metallurgical sector produces acid currents that contain heavy metals [e.g. copper (Cu), zinc (Zn)] and impurities [e.g. arsenic (As)]. Heavy metals have an added value, which could be obtained by the metallurgical waste stream treatment.

In this study, a circular economy scheme is proposed in order to be able to take advantage of an acidic effluent produced in the copper and zinc metallurgical industries. From this point of view, two ion-exchange (IEX) technologies were used to separate and concentrate its main elements (Cu, Zn and As): (i) selectrodialysis (SED) followed by (ii) IEX resins. Figure 1 shows the flow chart of integrated processes (SED and IEX resins) for copper and zinc recovery and arsenic removal from acidic metallurgical streams.

By means of a novel electrodialysis-based technology, named SED, is possible to separate different charged ions when electrical current is applied, using standard and mono-selective membranes (Zhang et al. 2012; Reig et al. 2018). In this study, SED was used to separate As from Cu and Zn. Afterwards, the obtained As-rich stream could be treated properly for external disposal, taking into account the arsenic toxicity. Besides, after the SED process, a Cu/Zn-rich stream was also obtained. Sequently, two ion-exchange resins were used to separate both ions (Cu and Zn) in order to reuse both streams in the copper and zinc metallurgical industries, respectively (Juang and Su 1992).

2 Materials and Methods

An ED laboratory-scale set-up (ED 64-4) supplied by PCCell (Germany) was employed to conduct the SED experiments. Fujifilm Manufacturing Europe B.V. (Netherlands) membranes (standard anionic, standard cationic and monovalent selective cation-exchange) were placed between two electrodes, and constant voltage of 7 V was applied. An acidic metallurgical stream containing 170 mM Cu(II), 70 mM Zn(II) and 110 mM As(V) was treated in order to be able to separate the As from Cu and Zn. Initial solution in the Cu/Zn-rich compartment was 300 mM H_2SO_4, whereas initial solutions in the As-rich compartment and electrode rinse streams were 100 mM Na_2SO_4. Samples collected during the experiments were analysed by inductively coupled plasma (ICP) to determine Cu, Zn and As concentrations in each stream along the time.

Once an As-free stream was obtained, the Cu/Zn-rich stream was treated by IEX resins in a fixed-bed configuration (1.1 cm internal diameter and 7.5 cm height), using 2.75 g

M. Reig · X. Vecino · M. Hermassi · J. López · C. Valderrama · O. Gibert · J. L. Cortina (✉)
Chemical Engineering Department, UPC-Barcelona TECH, Barcelona Research Center for Multiscale Science and Engineering, C/Eduard Maristany 10-14, Campus Diagonal-Besòs, 08930 Barcelona, Spain
e-mail: jose.luis.cortina@upc.edu

J. L. Cortina
CETaqua, Carretera d'Esplugues, 75, 08940 Cornellà de Llobregat, Spain
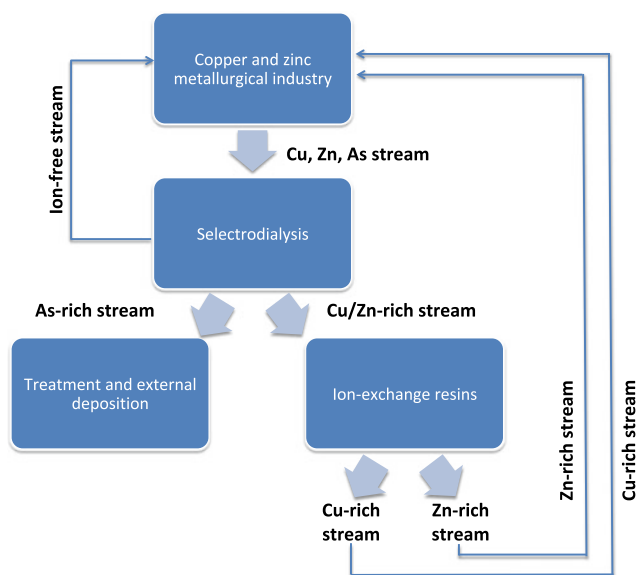
Fig. 1 Circular economy scheme purposed for copper and zinc recovery and arsenic removal in the metallurgical industry

of resin at 1.95 mL/min of flow rate, in order to separate Cu from Zn. Two different IEX resins were used: Purolite S960 (chelating resin) and Lewatit OC VP 1026

(solvent-impregnated resin), for testing which resin had the highest separation factor of both cations (Cu and Zn).

3 Results and Discussion

SED experiments were stopped when the feed solution conductivity was reaching a value around zero. For this reason, conductivity was monitored in each stream during the trials. The electrode rinse stream had no interactions with the other operational streams, so its conductivity remained constant during the tests. As exhibited in Fig. 2, As concentration increased in the As-rich stream, while Cu and Zn concentrations increased in the Cu/Zn-rich stream one. Overall, SED process allowed to recover 49.1% of As (for its subsequent treatment and disposal) and 81.9% of Cu/Zn. The energy consumption of the SED process was about 4.8 kWh/kg Cu + Zn produced.

Afterwards, IEX resins were used to treat the Cu/Zn-rich stream in a fixed-bed column set-up. Best Cu and Zn separation factors were obtained using the Lewatit 1026 resin. In this case, the acidic metallurgical stream (at pH 2.7) was treated by the IEX solvent-impregnated resin followed by an elution step using H_2SO_4 1 M, which allowed to recover

Fig. 2 SED results **a** in the Cu/Zn-rich stream and **b** in the As-rich stream, over time
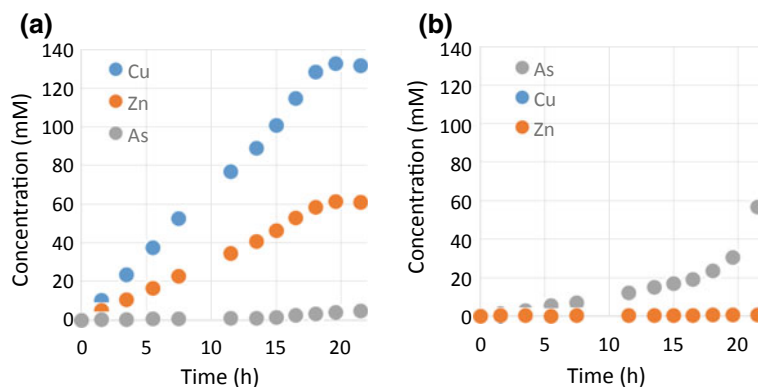
Fig. 3 IEX elution curves by Lewatit 1026 resin for **a** Zn and **b** Cu recuperation, respectively

69% of Zn (Fig. 3a). Then, the pH was increased up to 4.7 to exchange Cu ions (elution step was also conducted using H_2SO_4 1 M) achieving 97% of Cu recovery (Fig. 3b).

4 Conclusion

To summarize, it was possible to separate As from an acidic metallurgical stream containing mainly As, Cu and Zn by SED technology and also it was possible to separate and concentrate Cu and Zn streams by IEX resins. Furthermore, copper and zinc streams can be reused in the copper and zinc metallurgical industries, respectively, promoting in this way the circular economy in the metallurgical sector.

References

Juang, R. S., & Su, J. Y. (1992). Separation of zinc and copper from aqueous sulfate solutions using bis(2-ethylhexyl)phosphoric acid-impregnated macroporous resin. *Industrial and Engineering Chemistry Research, 31*(12), 2779–2783.

Reig, M., Vecino, X., Valderrama, C., Gibert, O., & Cortina, J. L. (2018). Application of selectrodialysis for the removal of As from metallurgical process waters: Recovery of Cu and Zn. *Separation and Purification Technology, 195,* 404–412.

Zhang, Y., Paepen, S., Pinoy, L., Meesschaert, B., & Van der Bruggen, B. (2012). Selectrodialysis: Fractionation of divalent ions from monovalent ions in a novel electrodialysis stack. *Separation and Purification Technology, 88,* 191–201.

Microalgae Cultivation for Pretreatment of Pharmaceutical Wastewater Associated with Microbial Fuel Cell and Biomass Feed Stock Production

Jagdeep Kumar Nayak and Uttam Kumar Ghosh

Abstract

This study evaluated the potential of microalgae Scenedesmus abundance for pretreatment of pharmaceutical wastewater in photobioreactor (PBR) associated with photosynthetic microbial fuel cell (PMFC). At the end of pretreatment process, the removal efficiency of COD of 75 % along with nitrate and phosphate of 78 and 83 % was obtained, respectively. In continuation of treatment process, the pretreated wastewater was used as a substrate for further treatment in PMFC and was succeeded to achieve maximum COD removal of 87.8 % calculating the total (combined of PBR and PMFC) removal efficiency of 95 %. A maximum voltage of 740.13 mV and power density of 838.68 mW/m2 was achieved. A maximum biomass of 0.71 g/L from PBR after pretreatment and 0.78 g/L from PMFC process was obtained.

1 Introduction

The increase of contaminated water with refractory toxicants from pharma industry effluent has become a serious environmental issue due to their significant eco-toxicities and associated health issues (Xiong et al. 2018). Pharmaceutical wastewater treatment needs to involve a series of the treatment process for considerable removal of toxic contaminants. Microalgae assisted bioremediation of pharma effluent has recently gained importance in scientific communities, as microalgae bioremediation process has some positive aspects like solar power assisted, sustainable and ecologically feasibility. Microalgae are well recognized for biological wastewater treatment which leads to remove the pollution load and the potential to grow in wastewaters also maintain the energy neutrality and environmental sustainability (Hemalatha and Mohan 2016). Microalgae bioremediation is also an upcoming approach as compared to the other conventional tertiary treatment for absolute pollutant removal. With the above capabilities, microalgae are cultivating in municipal wastewater as well as in industrial effluents such as pharmaceutical wastewater pulp and paper mill wastewater, distillery spent wash, dairy industry wastewater, and piggery wastewater (Amit and Ghosh 2018).

Microbial fuel cell (MFC) is an emerging technology which uses microbial metabolism for the conversion of biochemical energy to bioelectric energy and some value-added product such as carbon dioxide, water, and bio-energy (Nayak et al. 2018). A generalize design of a "H-type" dual-chambered MFC consists of both anodic and cathodic chamber inoculate with microorganisms (Fig. 1). The electrons, generated in the intermediate process of anaerobic process through anodic chamber, which transfer through external circuit. Protons are transferred through a proton exchange membrane (PEM) such as nafion-117, react with oxygen, an oxidizing agent, at the cathodic chamber which completes the circuit and generation of electricity.

The ability of microalgae to utilize phosphorous (P) and nitrogen (N) is considered as an efficient technique of bioremediation for wastewater treatment. Taking into consideration of the benefits, both microalgae and MFCs, the current study is intended to incorporate microalgae cultivation as a pretreatment or a process for converting inorganic nutrient to biomass and bio-energy from raw pharmaceutical wastewater following the secondary treatment process through MFCs. The study planned to find out the potential of

J. K. Nayak (✉) · U. K. Ghosh
Department of Polymer and Process Engineering, Indian Institute of Technology Roorkee, Roorkee, India
e-mail: jagdeepn220@gmail.com

U. K. Ghosh
e-mail: uttamghosh.iitr@gmail.com

microalgae to utilize the pharma effluent for the biomass growth along with MFCs process for the production of bioelectricity. With this integrated treatment process of microalgae and MFCs, the whole process will get the output of treated water, biomass, and bioelectricity.

2 Materials and Methods

2.1 Sample Collection and Characterization

The raw pharmaceutical wastewater (PW) was collected from the outlet of a pharma industry. Sample was collected and preserved at 4 °C. COD, TDS, TSS, TS, nitrate and phosphate were determined using method instructed by APHA (2005).

2.2 Culture Collection and Cultivation

Pure bacterial culture was isolated from pharmaceutical effluent by serial dilution method. Isolated pure culture was incubated at 25 ± 2 °C in NA (nutrient agar media) with sodium chloride for 48 h. After incubation period, the pure bacterial culture was poured in 250-mL Erlenmeyer conical flasks in pharma effluent to develop an acclimatized bacterial community. The freshwater microalgae, *Scenedesmus abundans* (NCIM No. 2897), were procured from National Chemical Laboratory (NCL), Pune, India. Culture was maintained in Bold's Basal Medium (BBM) with the following elements per liter: $CaCl_2 \cdot 2H_2O$, 0.025 g; $NaNO_3$, 0.25 g; $MgSO_4 \cdot 7H_2O$, 0.075 g; EDTA, 0.05 g; NaCl, 0.025 g; K_2HPO_4, 0.075 g; KH_2PO_4, 0.175 g; H_3BO_3,

0.011 g; KOH, 0.031 g; $FeSO_4 \cdot 7H_2O$ 0.0049 g; H_2SO_4, 0.001 mL and trace element under (16:08 h) dark and light cycle with light illumination of intensity of 94.6 μ mol m^{-2} s^{-1} at 25 ± 1 °C. Aquarium pump was used for the supply of CO_2.

3 Results and Discussion

3.1 Pollutant Removal

The organic concentration is an important factor which limits the growth of microorganism and bioelectricity generation. A cylindrical reactor ($H = 30$ cm, $D = 10$ cm) is used to cultivate and pretreat the pharmaceutical wastewater which is attached with "H-type" dual-chambered microbial fuel cell ($H = 15$ cm, $D = 10$ cm). Graphite rod with 17 cm length and 1.2 cm diameter was used as electrodes in both the chambers. Experiment was run for 21 days. The correlation between COD removal in both process over the incubation period is shown in Fig. 1, and the correlation between biomass growth along with COD is shown in Fig. 2. COD removal showed of 75% from the microalgae pretreatment process and 87.8% from the MFCs process accounting of the total removal efficiency of 95%. Maximum removal efficiency was obtained in 20th day for microalgal pretreatment and in 17th day for MFC treatment. Microalgae utilize phosphate and nitrate in inorganic form for its metabolic activities and growth (Oliver and Ganf 2000). The obtained results suggest that the pollutant can utilize and remove by microalgae that consume inorganic nutrients along with carbon effectively for its growth which leads to bioremediation.

Fig. 1 Diagram of experimental setup
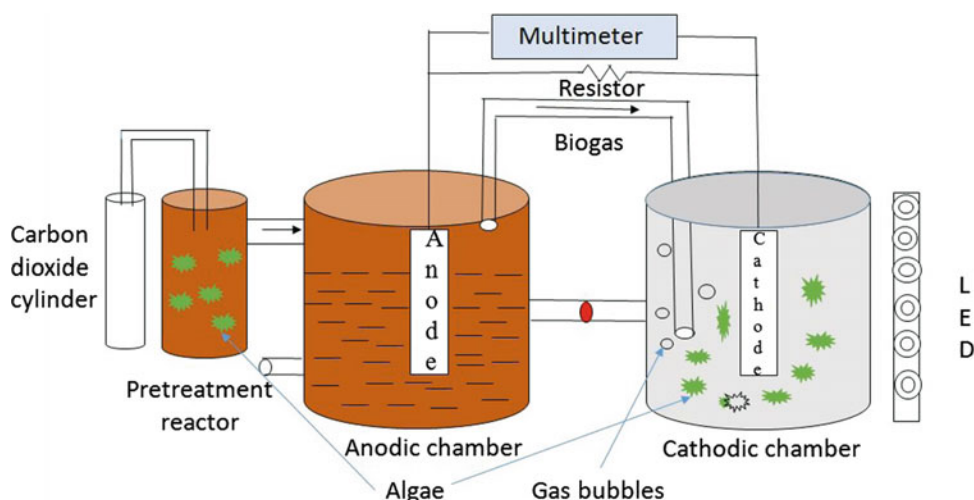
3.2 Biomass Production

Generally, microalgal growth depends on the nutrients present in media, illumination, and optimized condition, etc. In this experiment, the required nutrients for the microalgal growth were present in pharmaceutical wastewater which leads to the growth of microalgae in pretreatment process (Figs. 2, 3 and 4). Figure 2 showed the correlation between COD removal (%) with biomass production in pretreatment process. Similarly, Fig. 4

showed the same pattern with biomass production in MFC process Fig. 5. The maximum growth (0.71 g/L) was seen on 19th day in pretreatment process where the maximum growth (0.78 g/L) of microalgae showed in 17th day in MFC process. Maximum nitrate and phosphate removal of 160.05 mg/L (78%), 90.99 mg/L (73%) was noticed, respectively, in the first process. In the second process, the maximum removal of nitrate and phosphate was 27.02 mg/L (83%), 19.11 mg/L (80.89%), respectively. The significant growth of microalgae in both processes

Fig. 2 Relation between days and COD removal in both process
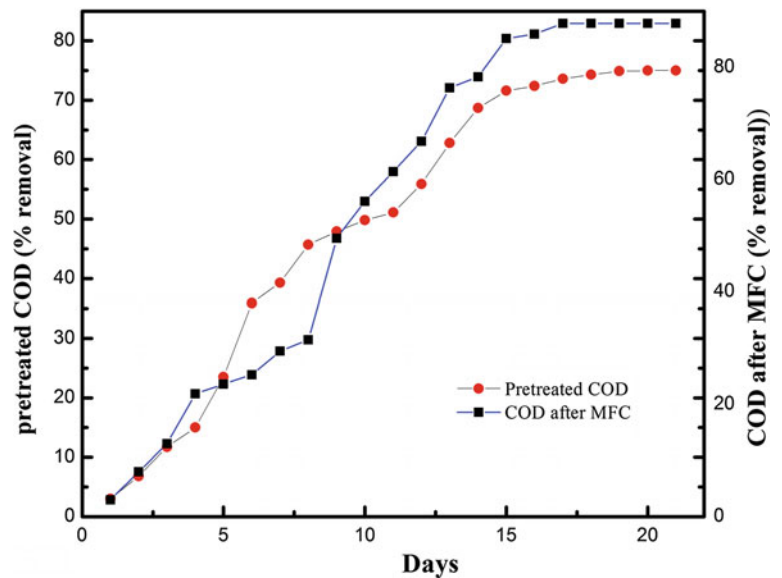
Fig. 3 Relation between COD and biomass in pretreatment
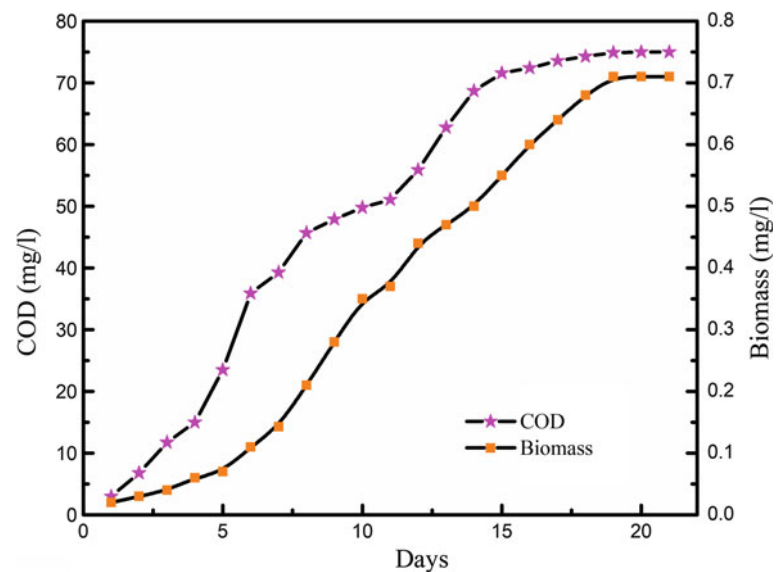
Fig. 4 Nitrate and phosphate removal along with biomass
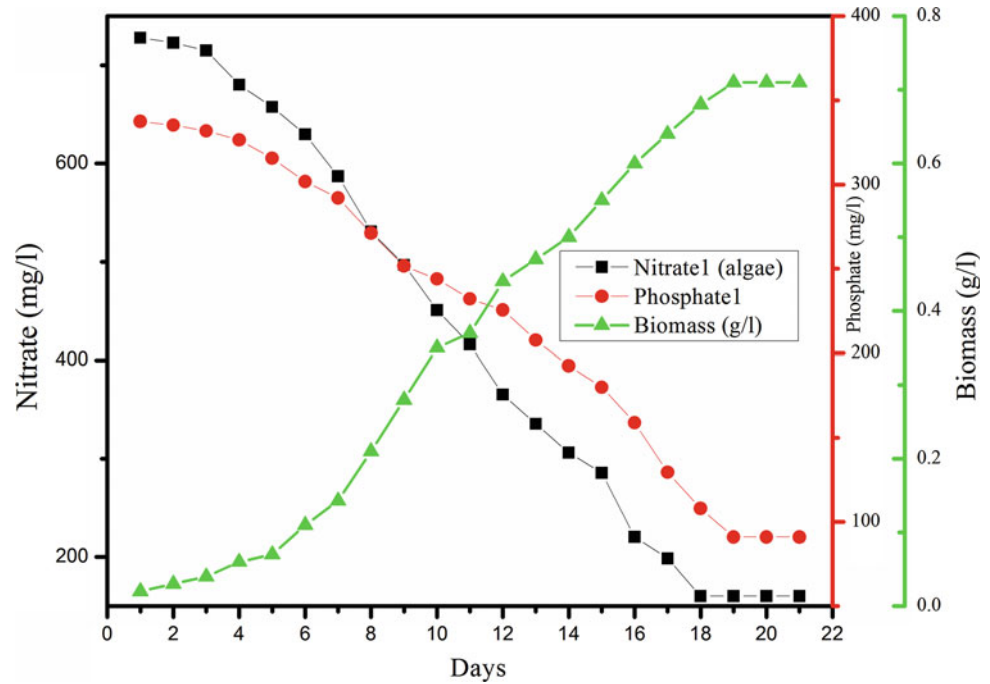
Fig. 5 COD removal and biomass production in MFCs
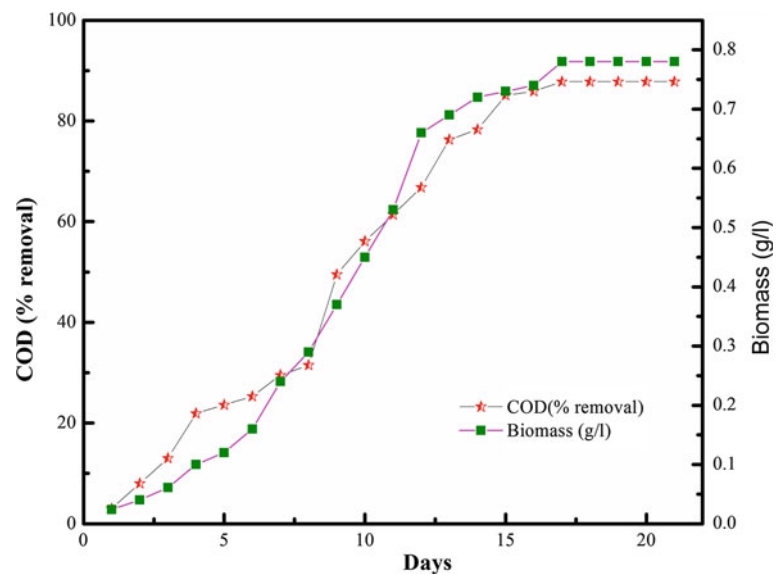
indicates the presence of required nutrient and effective uptake of those nutrient by microalage.

3.3 Bioelectricity Production

Generally, the presence of organic content in wastewater effect the production of electricity through the anaerobic process. MFCs was connected with multimeter along with resistor and was run for 21 days. Production of voltage was measured by multimeter as shown in Fig. 6. Maximum voltage of 740.133 mV and power density of 822.79 mW/m^2 were noticed. The significant increase in electricity generation was due to the simplification of organic component by microalgae in pretreatment process.

Fig. 6 Voltage generation and power density with COD removal in 21 days
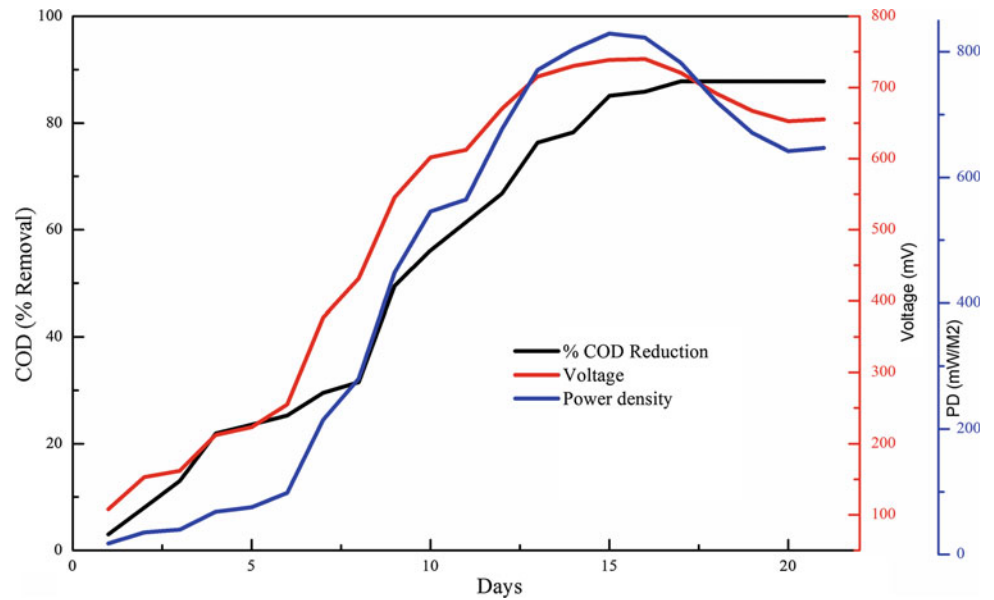
4 Conclusion

Significant removal of pollutant, increase of bioelectricity, and biomass production were noticed with the integration of pretreatment process. The maximum removal of COD, nitrate, phosphate was 87.8, 83, 80.89%, respectively, and the production of electricity and biomass was 0.78 g/L and 740.133 mV, respectively.

References

Amit, & Ghosh, U. K. (2018). An approach for phycoremediation of different wastewaters and biodiesel production using microalgae. *Environmental Science and Pollution Research, 25*, 18673–18681.

Hemalatha, M., & Venkata Mohan, S. (2016). Microalgae cultivation as tertiary unit operation for treatment of pharmaceutical wastewater associated with lipid production. *Bioresource Technology, 215*, 172–177.

Nayak, J., Ghosh, U. K., & Amit. (2018). An innovative mixotrophic approach of distillery spent wash with sewage wastewater for biodegradation and bioelectricity generation using microbial fuel cell. *Journal of Water Process Engineering, 23*, 306–313.

Oliver, R. L., & Ganf, G. G. (2000). Freshwater blooms. In B. A. Whitton & M. Potts (Eds.), *The ecology of cyanobacteria: Their diversity in time and space* (pp. 149–194). Dordrecht: Kluwer.

Xiong, J.-Q., Kurade, M. B., & Jeon, B.-H. (2018). Can microalgae remove pharmaceutical contaminants from water? *Trends in Biotechnology, 36*(1).

Embryotoxicity and Molecular Alterations of Fluoxetine and Norfluoxetine in Early Zebrafish Larvae

Pedro Rodrigues, V. Cunha, M. Ferreira, and Laura Guimarães

Abstract

Embryos and larvae exposed to FLX showed higher mortality rates at 32 hpf than those exposed to NFLX. At 80 hpf gross malformations, mainly in pigmentation, were higher in NFLX exposed larvae than in FLX exposed larvae. In general, strong positive correlations were found between the expression of 34 target genes. Negative correlations were associated with opposite patterns of gene expression in NFLX and FLX larvae. Adrenergic receptors, and some correlated genes, can be responsible for anomalies in pigmentation.

P. Rodrigues (✉) · V. Cunha · M. Ferreira · L. Guimarães
CIIMAR—Interdisciplinary Centre of Marine and Environmental Research, University of Porto, Terminal de Cruzeiros do Porto de Leixões Av. General Norton de Matos s/n, 4450-208 Matosinhos, Portugal
e-mail: pedromcrodrigues93@gmail.com

V. Cunha
e-mail: vfpmc83@gmail.com

M. Ferreira
e-mail: marta.ferreira@usp.ac.fj

L. Guimarães
e-mail: lguimaraes@ciimar.up.pt

P. Rodrigues
ICBAS—Instituto de Ciências Biomédicas de Abel Salazar, Rua de Jorge Viterbo Ferreira n.º 228, 4050-313 Porto, Portugal

M. Ferreira
School of Marine Studies, Faculty of Science, Technology and Environment, The University of South Pacific, Suva, Fiji

1 Introduction

Psychopharmaceuticals in aquatic ecosystems are nowadays recognised as emerging contaminants (EC) of public and scientific concern, largely because the effects towards non-target organisms are still barely known. Fluoxetine (FLX) is an antidepressant of the selective serotonin reuptake inhibitor (SSRI) class (Mennigen et al. 2011). The mode of action of SSRI antidepressants involves the inhibition by presynaptic receptors of serotonin reuptake. This increases the overall concentration of active serotonin in the synaptic cleft, potentiating its effects (Kreke and Dietrich 2008; Mennigen et al. 2011). Beyond FLX, its main metabolite, norfluoxetine (NFLX), can also be of concern to aquatic organisms. In humans, FLX is metabolised in the liver and catabolised by different genes from the Cyp (Cytochrome P450) family, giving rise to NFLX by demethylation reactions (Fong and Molnar 2008; Ring et al. 2001). NFLX has been detected in water samples in the ng/L order (Santos et al. 2010). Both compounds have been reported to negatively affect aquatic organisms (Fong and Molnar 2008; Cunha et al. 2016, 2018), though few studies have addressed the effects of NFLX. In this study, zebrafish (*Danio rerio*) was used to investigate and compare embryotoxicity and effects on gene expression of FLX and NFLX, adding to the knowledge base about their modes of action (MoA).

2 Materials and Methods

Zebrafish reproducers were maintained under standard culture conditions to obtain test embryos and assays were performed according to Cunha et al. (2016). In brief, embryos (~ 1 hpf) were placed in 24-well plates (10 embryos per well) and exposed until 80 hpf to a low concentration (0.0014–0.0015 µM) range of either FLX or NFLX. Stock solutions were prepared in DMSO for FLX

and water for NFLX. Water and DMSO control groups were also included in the experimental design (DMSO (0.004%) and water for FLX; water for NFLX). Observations were made at 8, 32 and 80 hpf for mortality and developmental endpoints. Expression of 34 target genes was measured by qRT-PCR. These were monoamine receptors and transporters related to FLX and NFLX MoA, and genes involved in their metabolism. The complete list is indicated in Fig. 2; primers used are described in Cunha et al. (2016, 2018). Differences in embryotoxicity endpoints were evaluated by *T*-test using the Bonferroni correction (SPSS 25, IBM). A bivariate correlation map was performed with R Corrplot package. An expression heatmap was generated with MORPHEUS (Broad Institute).

3 Results and Discussion

Mortality in the control treatment (16%) was slightly above expected levels for zebrafish embryo assays (OECD 2012), and occurred mainly at 32 hpf (Fig. 1). No differences in mortality between either SSRI or the control could be observed. The mortality rate was, however, significantly higher ($p < 0.05$) at 32 hpf for embryos exposed to FLX than for those exposed to NFLX. Differences in the MoA and pharmacokinetics of these substances may contribute to the results observed. Monoaminergic systems start to develop from 1 to 5 dpf (Kastenhuber et al. 2010; Airhart et al. 2012). Upon this, differences in the metabolism of FLX and NFLX, together with differing potency and ratio of their enantiomers may elicit different adverse outcomes (Hiemke and Härtter, 2000). For gross malformations, at 80 hpf, a significant lower frequency ($p < 0.05$) was found for larvae

exposed to FLX in comparison to those exposed to NFLX. Anomalies in pigmentation were most commonly found in NFLX larvae; spinal abnormalities were also found but at a much lower frequency. Compared to FLX, this can be a result of a stronger effect of NFLX on fish adrenergic receptors, which are present in the melanophores (Xu and Xie 2011). The latter are pigment cells, containing eumelanin, responsible for the black or dark-brown pigmentation of larvae, through the involvement of the tyrosine kinase pathway. Given their relation to neural crest tissue and the importance of somites in patterning neural crest migration, the results point to the need to further investigate possible somites' defects in NFLX exposed embryos (Svetic et al. 2007).

Gene expression analysis revealed significant downregulation in FLX exposed larvae, relative to the control group, of the dopamine transporter and vesicular monoamine transporter (threefold change), serotonin receptor 1a and monoamine oxidase ($\sim$twofold), serotonin transporter, retinoic acid receptor gamma and peroxisome proliferator-activated receptor beta ($\sim$1.5-fold) and peroxisome proliferator-activated receptors alpha and gamma ($\sim$onefold). For NFLX larvae, significant differences relative to the control group were only found for antioxidant enzyme superoxide dismutase ($\sim$onefold). Results from the correlation map show a majority of positive associations between the target genes, with some clusters exhibiting very strong correlation values ($\rho \geq 0.8$) (Fig. 2). One such cluster was found for oxidative stress enzymes, retinoid x receptor gamma, abc transporter b4, cytochrome p450 1a1, pregnane x receptor and adrenergic receptor 2b and 2c. As previously mentioned, adrenergic receptors are involved in embryo pigmentation (Xu and Xie 2011). This cluster could be

Fig. 1 Cumulative mortality and gross malformations observed in zebrafish embryos and larvae exposed to 0.0014–0.0015 µM FLX or NFLX. Results are expressed as mean ± SE. [*]Indicates significant differences in the NFLX group related to FLX ($p < 0.05$)
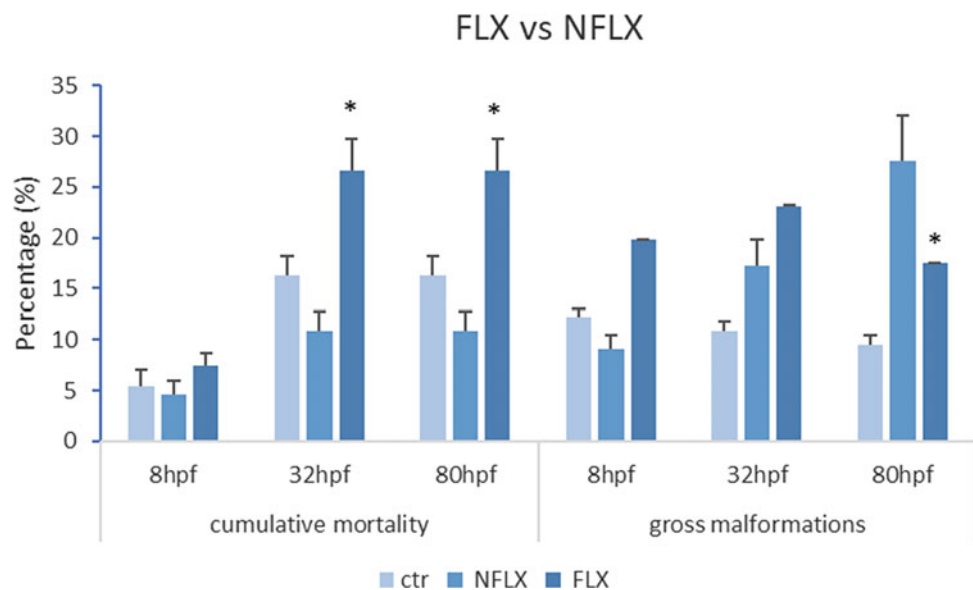
Fig. 2 Correlation map of target genes assessed at 80 hpf in zebrafish larvae exposed to NFLX and FLX
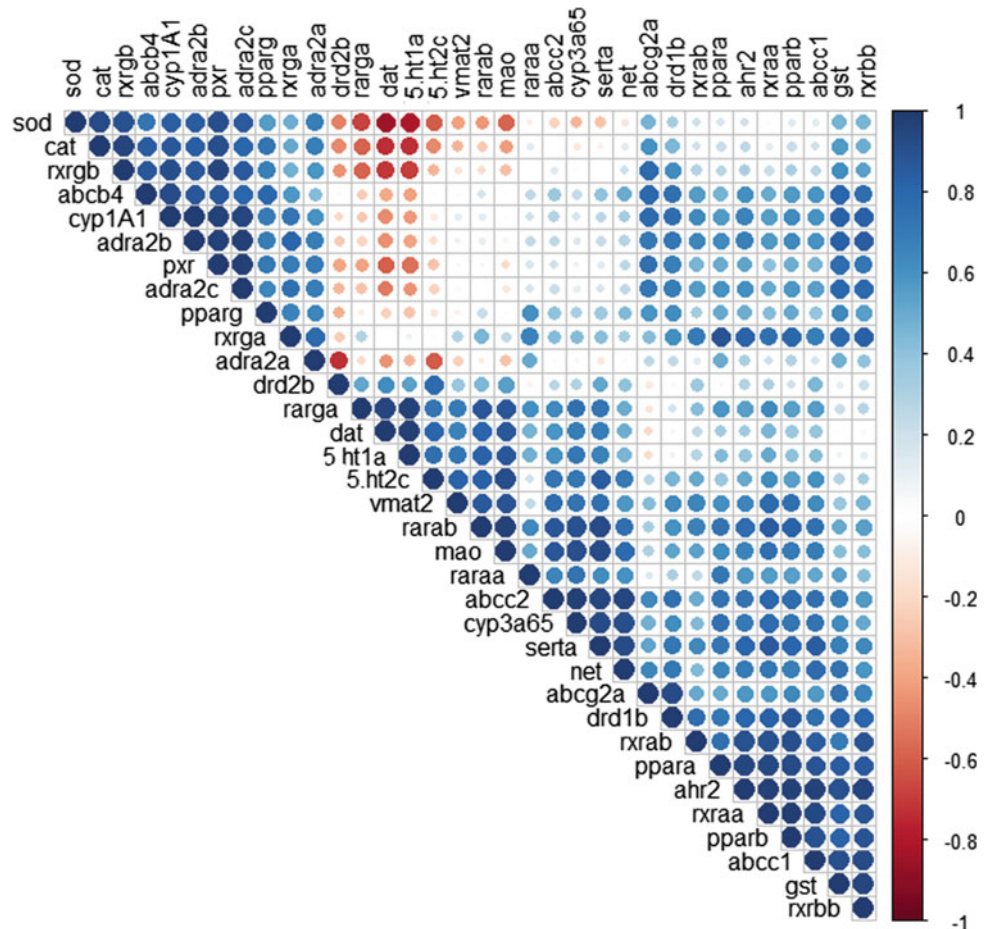
related to the affected pathway responsible for pigmentation anomalies for NFLX larvae. Another cluster was related to peroxisome proliferator-activated receptors alpha and beta, aryl hydrocarbon receptor, retinoid x receptors alpha and beta, abc transporter c1 and gluthatione *S*-transferase. This may be due to the capacity of retinoid x receptors to form heterodimers with other nuclear receptors to regulate several physiological processes in organisms (Xu et al. 2005). A small cluster of three genes (dopamine transporter; serotonin receptor 1a and retinoid acid receptor gamma) showing strong negative correlations between them was also found.

Monoamine receptors and transporters: dopamine receptors D1B (drd1b) and D2B (drd2b); serotonin receptors 2c (5-htc2) and 1a (5-ht1a); noradrenaline receptors alpha-2a (adra2a), 2b (adra2b) and 2c (adra2c); vesicular monoamine transporter (vmat 2); monoamine oxidase (mao); serotonin transporter (serta); dopamine transporter (dat); norepinephire transporter (net).
Nuclear receptors: pregnane x receptor (PXR); peroxisome proliferator-activated receptors alpha (ppara), beta (pparb) and gamma (pparg); retinoid x receptors alpha (rxraa), beta (rxrab, rxrbb) and gamma (rxrga, rxrgb); retinoid acid

receptors alpha (raraa), beta (rarab) and gamma (rarga); aryl hydrocarbon receptor (Ahr).
ABC transporters: abcb4, abcc1, abcc2 and abcg2.
Biotransformation enzymes: cytochrome P450 1A1 (cyp1A1) and 3a65 (cyp3a65); glutathione *S*-transferase (gst).
Oxidative stress enzymes: Cu/Zn superoxide dismutase (sod); catalase (cat).

Gene expression results were further investigated through heatmap analysis to depict differences in patterns of gene expression between FLX and NFLX larvae (Fig. 3). Opposite differences in expression were detected for the two compounds. Globally, genes upregulated in FLX larvae showed no alteration or downregulation in the NFLX treatment, relative to the control; those upregulated in FLX (rxrgb, pxr, cat) showed no alteration or slight downregulation in NFLX larvae. Only three genes showed a fairly similar variation (i.e. downregulation); these were the adrenergic receptors alpha 2a (adra2a) and 2c (adra2c) and the peroxisome proliferator-activated receptor gamma (pparg). It is also of note that gene expression variation was overall more accentuated in FLX larvae, compared to NFLX. This fact appears to counteract the idea that NFLX is more
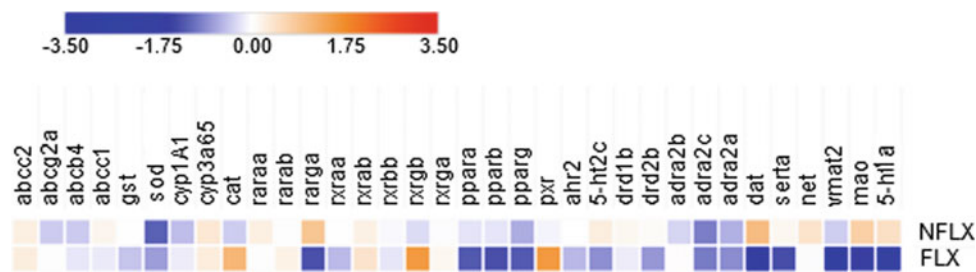
Fig. 3 Heatmap of gene expression variation in zebrafish exposed to NFLX and FLX for 80 hpf. The colour scale reflects the direction and magnitude of variation in relation to the control group. Legend as in Fig. 2

potent than the parental compound as suggested by Hiemke and Härtter (2000). Nevertheless, differences in the metabolism of the two compounds possibly influencing the ratio of their enantiomers and potency warrant further elucidation of effects induced by FLX and NFLX in zebrafish larvae to better understand this.

4 Conclusions

The parental compound (FLX) caused increased mortality at 32 hpf maintained up to 80 hpf. Its metabolite (NFLX), in contrast, increased the number of malformations in zebrafish embryonic development at 80 hpf; with pigmentation anomalies as, main alteration detected. At the expression level, a cluster of altered genes associated with the adrenergic pathway responsible for pigmentation anomalies was identified. Overall, NFLX and FLX mostly appear to cause opposite toxicological effects in zebrafish early development, eventually resulting from differences in their intrinsic pharmacokinetic properties. Future research will focus on clarifying this aspect and develop more studies comparing the toxicity of EC parental compounds and their metabolites, to improve monitoring and risk assessment routines of antidepressants.

References

Airhart, M. J., Lee, D. H., Wilson, T. D., Miller, B. E., Miller, M. N., Skalko, R. G., et al. (2012). Adverse effects of serotonin depletion in developing zebrafish. *Neurotoxicology and Teratology, 34,* 152–160.

Cunha, V., Rodrigues, P., Santos, M. M., Moradas-Ferreira, P., & Ferreira, M. (2016). *Danio rerio* embryos on Prozac—Effects on the detoxification mechanism and embryo development. *Aquatic Toxicology, 178,* 182–189.

Cunha, V., Rodrigues, P., Santos, M. M., Moradas-Ferreira, P., & Ferreira, M. (2018). Fluoxetine modulates the transcription of genes involved in serotonin, dopamine and adrenergic signalling in zebrafish embryos. *Chemosphere, 191,* 954–961.

Fong, P. P., & Molnar, N. (2008). Norfluoxetine induces spawning and parturition in estuarine and freshwater bivalves. *Bulletin of Environmental Contamination and Toxicology, 81,* 535–538.

Hiemke, C., & Härtter, S. (2000). Pharmacokinetics of selective serotonin reuptake inhibitors. *Pharmacology & Therapeutics, 85,* 11–28.

Kastenhuber, E., Kratochwil, C. F., Ryu, S., Schweitzer, J., & Driever, W. (2010). Genetic dissection of dopaminergic and noradrenergic contributions to catecholaminergic tracts in early larval zebrafish. *The Journal of Comparative Neurology, 518,* 439–458.

Kreke, N., & Dietrich, D. R. (2008). Physiological endpoints for potential SSRI interactions in fish. *Critical Reviews in Toxicology, 38,* 215–247.

Mennigen, J. A., Stroud, P., Zamora, J. M., Moon, T. W., & Trudeau, V. L. (2011). Pharmaceuticals as neuroendocrine disruptors: Lessons learned from fish on prozac. *Journal of Toxicology and Environmental Health. Part B, Critical Reviews, 14,* 387–412.

OECD. (2012, July). *OECD guideline for the testing of chemicals.*

Ring, B. J., Eckstein, J. A., Gillespie, J. S., Binkley, S. N., VandenBranden, M., & Wrighton, S. A. (2001). Identification of the human cytochromes p450 responsible for in vitro formation of R- and S-norfluoxetine. *Journal of Pharmacology and Experimental Therapeutics, 297,* 1044–1050.

Santos, L. H., Araujo, A. N., Fachini, A., Pena, A., Delerue-Matos, C., & Montenegro, M. C. (2010). Ecotoxicological aspects related to the presence of pharmaceuticals in the aquatic environment. *Journal of Hazardous Materials, 175,* 45–95.

Svetic, V., Hollway, G. E., Elworthy, S., Chipperfield, T. R., Davison, C., Adams, R. J., et al. (2007). Sdf1a patterns zebrafish melanophores and links the somite and melanophore pattern defects in choker mutants. *Development, 134*(5), 1011–1022.

Xu, J., & Xie, F. K. (2011). α- and β-Adrenoceptors of zebrafish in melanosome movement: A comparative study between embryo and adult melanophores. *Biochemical and Biophysical Research Communications, 405,* 250–255.

Xu, C., Li, C. Y., & Kong, A. N. (2005). Induction of phase I, II and III drug metabolism/transport by xenobiotics. *Archives of Pharmacology Research, 28,* 249–268.

Biological Treatment of Municipal Wastewater Using Green Microalgae and Activated Sludge as Combined Culture

Ghulam Mujtaba, Muhammad Rizwan, and Kisay Lee

Abstract

This paper highlights the use of the combined culture system in municipal wastewater treatment. Removal of nutrients was significantly increased in properly inoculated combined culture system. Release of organic matter from Chlorella biomass decreased the COD removal performance.

Keywords

Microalgae • *Chlorella vulgaris* • Activated sludge • Combined culture • Wastewater treatment • Biofuel production

1 Introduction

Microalgae have a capability to uptake nutrients from wastewater and recycle them into their biomass which can be further utilized for biofuel production (Beuckels et al. 2015). Microalgal technology provides cost-effective treatment, controls sludge generation, and avoids eutrophication (Aslan and Kapdan 2006). The use of the combined culture of microalgae and activated sludge (as bacterial consortium) in wastewater treatment offers a sustainable and cost-effective alternative to conventional biological nutrient removal methods because of their free oxygenation potential and efficient nutrient removal (Posadas et al. 2015). This study aims to remove nutrients (nitrogen and phosphorus) and organic pollutants (as COD) from municipal wastewater through symbiotically driven combined culture. This combined culture is composed of immobilized green microalga that is *Chlorella vulgaris* and activated sludge which is suspended in the culture medium. The effects of the initial ratios of *C. vulgaris* and activated sludge were also investigated on the pollutants removal.

2 Materials and Methods

The microalgal strain *Chlorella vulgaris* AG30007 was maintained in a sterilized BG-11 medium which contained around 250 mg L^{-1} nitrogen, 10 mg L^{-1} phosphorus, and the other macro- and micronutrients. The aerobic activated sludge and municipal wastewater were obtained from the Respia wastewater treatment plant (Yongin-si, Republic of Korea) and stored in a refrigerator at 4 °C. Wastewater was being pre-treated prior to utilize for biological treatment. According to de-Bashan et al. (2004), *C. vulgaris* was immobilized in a matrix of alginate polymer using fully axenic environmental conditions when microalgal cells obtained greater cell density such as >1 g/L. The various biological cultures that were compared for the removal of nutrients and COD are (i) suspended activated sludge, (ii) pure immobilized strain of *C. vulgaris*, and (iii) combined culture of both suspended activated sludge and immobilized *C. vulgaris* with their different inoculum ratios such as 0.2, 0.5, 1.0, 2.0, 5.0, and 10 (activated sludge/*C. vulgaris*). The experiments were performed in a shaking incubator under controlled environmental conditions with a continuous light intensity of 50 μmol m^{-2} s^{-} and constant temperature at 25 °C. Aeration and/or CO_2 source was not supplied externally into the incubator; flasks-driven shaking at 150 rpm was the only source of uniform mixing. Analyses for nutrients and COD removal were made using test kits.

G. Mujtaba (✉)
Dawood University of Engineering and Technology, Karachi, Pakistan
e-mail: ghulam.mujtaba1@duet.edu.pk

M. Rizwan
U.S-Pakistan Centre for Advanced Studies in Water, Mehran University of Engineering and Technology, Jamshoro, Pakistan
e-mail: drmrizwan.uspcasw@faculty.muet.edu.pk

G. Mujtaba · M. Rizwan · K. Lee
Myongji University, Yongin, South Korea
e-mail: kisay@mju.ac.kr

3 Results and Discussion

The removal of nitrogen in the single and combined culture system with different inoculum ratios is compared in Fig. 1. The reactor contained activated sludge did not contribute to nitrogen removal since the performance of nutrients removal is not good enough in a conventional activated sludge process. In general, organic pollutants are mostly removed by utilizing aerobic activated sludge. In contrast, significant removal of nitrogen was achieved in the reactor containing microalga *C. vulgaris*. It is confirmed that microalgae have a high assimilative capacity of nutrient from wastewater. *C. vulgaris* in a single culture system removed almost 80% of nitrogen at the end of treatment (after 84 h of incubation). The role of microalgae was predominant in the co-culture system in the reduction of nitrogen (He et al. 2013). When the initial concentration of NH_4^+–N was around 13–21 mg L^{-1}, *C. vulgaris* assimilated all of the nitrogen from wastewater and removal efficiency was decreased by increasing the concentration further (Aslan and Kapdan 2006), indicating that the initial concentration of nutrient has a profound effect on the removal performance by microalgae. Nitrogen is usually present as ammonia, nitrate, and/or nitrite in wastewater. In this study, using municipal wastewater, ammonia was at larger concentrations and this is the most preferred form of nitrogen which is assimilated by microalgae (Cai et al. 2013). The co-culture system of suspended activated sludge and immobilized *C. vulgaris* exhibited different removal performances depending upon the inoculum ratio. A substantial effect of inoculum ratio between activated sludge and *C. vulgaris* was observed on the efficiency of nitrogen removal which was decreased by

increasing the inoculum ratio from 0.5 to 10. The reactors with lower ratios such as 0.5 and 1.0 obtained more removal of nitrogen than in the pure culture of *C. vulgaris*, which indicates the benefit of exploiting symbiotic association between *C. vulgaris* and activated sludge in wastewater treatment. The reactor with 0.5 (sludge/microalgae) showed the highest performance representing 66% removal after 24 h and 95% removal after 84 h (at the end of treatment). Near to this, the reactor with 1.0 removed 59% of nitrogen after 24 h and 91% at the end of treatment (after 84 h). However, the reactors having higher ratios such as 2.0, 5.0, and 10 displayed 65, 42, and 30% of nitrogen removal after 84 h (lower than in pure *C. vulgaris* culture), which is indicated that too much concentration of activated sludge is not good in the co-culture system. Therefore, there should be an optimum inoculum ratio in order to achieve efficient removal of nutrient from wastewater. For nitrogen removal, the inoculum ratio of 0.5 was found to be the optimum.

Figure 2 shows that the reactors containing *C. vulgaris* either in single or co-culture systems exhibited significantly more removal of phosphorus as compared to the reactor having activated sludge. Although it was insignificant, however, activated sludge contributed in phosphorus reduction showing 36% of removal after 84 h unlikely to nitrogen removal. Phosphorus was completely eliminated (100%) in the co-culture system with inoculum ratios of 0.5 and 1.0 (activated sludge/*C. vulgaris*) after 24 h and in the pure *C. vulgaris* culture after 36 h. In the other reactors with 2.0, 5.0, and 10 inoculum ratios of co-culture, 94, 84, and 76% of phosphorus was removed, respectively, up to 36 h of treatment. After that, some extents of phosphorus were released in the culture medium from all the tested reactors.

Fig. 1 Removal of nitrogen by activated sludge (AS), *C. vulgaris* (CV), and combined culture (CC) with various inoculums ratio of AS and CV after 3.5 days treatment
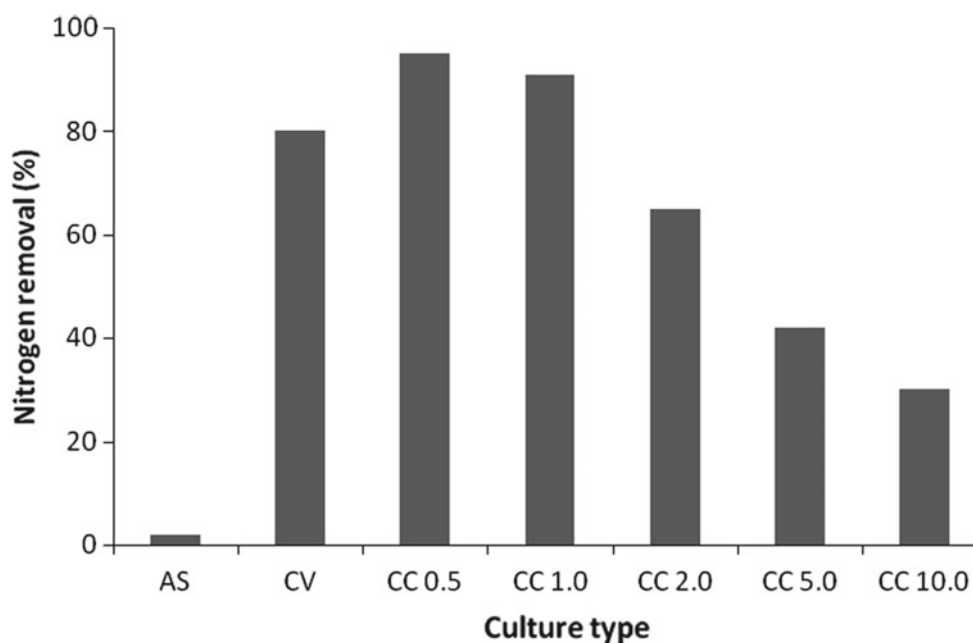
Fig. 2 Removal of phosphorus by activated sludge (AS), *C. vulgaris* (CV), and combined culture (CC) with various inoculums ratio of AS and CV after 3.5 days treatment
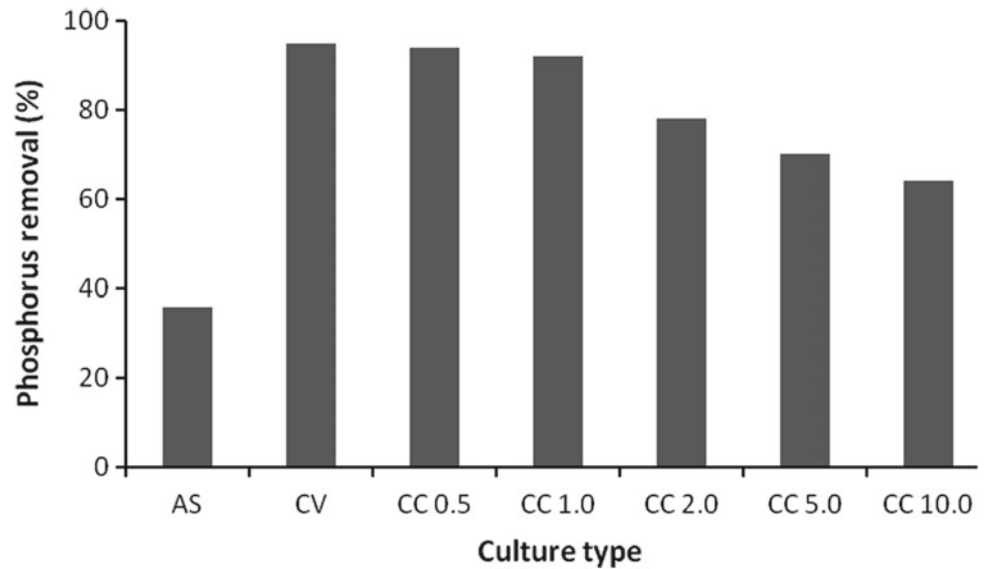
Martinez et al. (2000) observed that removal performance was decreased due to the spilling of phosphorus contents into the culture medium by ruptured algal cells. Likewise, to nitrogen removal, the performance of phosphorus removal was decreased by increasing the inoculum ratio between *C. vulgaris* and activated sludge. Most of the phosphorus was removed within 12 h of incubation, which implied that *C. vulgaris* has high efficiency to uptake phosphorus as well other than nitrogen from wastewater. After 12 h of incubation, 21, 85, 92, 89, 80, 74, and 54% of phosphorus was removed in the reactors containing activated sludge, pure *C. vulgaris*, and co-culture with 0.5, 1.0, 2.0, 5.0, 10 inoculum ratios, respectively. A symbiotic promotion in the reduction of phosphorus occurred at the lower ratios as observed for nitrogen removal.

Activated sludge reduced 50% of COD in the first 12 h, 17% further in the next 12 h (67% removal in 24 h), and only 8% up to 48 h (75% removal) (figure not shown). After that, a minute amount of organic matter (only 7%) was excreted from the biomass of activated sludge in the culture medium. Consequently, the performance of COD removal in the activated sludge reactor was 68% at the end of treatment (after 84 h). *C. vulgaris*, on the other hand, showed the interesting behavior for removing COD and IC in municipal wastewater. The level of COD was decreasing in pure *C. vulgaris* culture up to 24 h of incubation due to mixotrophic metabolism; however, it gradually started to increase until the end of treatment, which indicated that some organic matter may be secreted from algal biomass in the culture

medium. In the first 24 h, the removal of IC was not significant by *C. vulgaris*, because, at this phase, microalgae were engaged in COD removal. And, when *C. vulgaris* stopped consuming organic carbon after 24 h (maybe further biodegradation of organic material was not possible), they started to uptake IC even though it was not so significant. Therefore, it can be concluded that *C. vulgaris* was releasing organic matter by consuming IC through photoautotrophic metabolism which is a general mechanism for algal uptake of IC. At the lower ratios (such as 0.5 and 1.0), microalgae contributed enough in the increment of organic carbon as the levels of COD were raised, however, this increment in the co-culture system was lower as compared to that of pure *C. vulgaris* culture.

4 Conclusion

The combined culture system with lower inoculum ratios exhibited considerably better removal performances for nitrogen and phosphorus, representing a benefit of a symbiotic association of *C. vulgaris* and activated sludge in municipal wastewater. Nutrient assimilative capacity of microalgae could be enhanced in the reactor employed with the low inoculum ratio. Too much concentration of activated sludge may not be helpful for microalgae in wastewater treatment. COD removal performance in the combined culture system was not satisfactory due to the extensive release of carbon materials in the culture medium by *C. vulgaris*.

References

Aslan, S., & Kapdan, I. K. (2006). Batch kinetics of nitrogen and phosphorus removal from synthetic wastewater by algae. *Ecological Engineering, 28,* 64–70.

Beuckels, A., Smolders, E., & Muylaert, K. (2015). Nitrogen availability influences phosphorus removal in microalgae-based wastewater treatment. *Water Research, 77,* 98–106.

Cai, T., Park, S. Y., & Li, Y. (2013). Nutrient recovery from wastewater streams by microalgae: Status and prospects. *Renewable and Sustainable Energy Reviews, 19,* 360–369.

de-Bashan, L.E., Hernandez, J.P., Morey, T., Bashan, Y. (2004). Microalgae growth promoting bacteria as "helpers" for microalgae: a novel approach for removing ammonium and phosphorus from municipal wastewater. *Water Research 38,* 466–474.

He, P. J., Mao, B., Lu, F., Shao, L. M., Lee, D. J., & Chang, J. S. (2013). The combined effect of bacteria and *Chlorella vulgaris* on the treatment of municipal wastewaters. *Bioresource Technology, 146,* 562–568.

Martinez, M. E., Sanchez, S., Jimenez, J. M., Yousfi, F. E., & Munoz, L. (2000). Nitrogen and phosphorus removal from urban wastewater by the microalga *Scenedesmusobliquus*. *Bioresource Technology, 73,* 263–272.

Posadas, E., Morales, M. D. M., Gomez, C., Acien, F. G., & Munoz, R. (2015). Influence of pH and CO_2 source on the performance of microalgae-based secondary domestic wastewater treatment in outdoors pilot raceways. *Chemical Engineering Journal, 265,* 239–248.

Fouling Morphologies on Ion-Exchange Membranes in Reverse Electrodialysis with Effluent from Sewage Treatment Plant

Hanki Kim, Won-Sik Kim, Joo-Youn Nam, Ji-Yeon Choi,
Kyo-sik Hwang, Yong Seog, and Nam-Jo Jeong

Abstract

Fouling occurred on the ion-exchange membranes under practical condition, Reversible fouling occurred on the CEM, Irreversible fouling occurred on the AEM.

1 Introduction

Salinity gradient energy (SGE), also known as 'blue energy,' generates electrical energy by mixing different concentrations of solutions (Vermaas et al. 2013; Di Salvo et al. 2018). The global water cycle has a tremendous SGE energy potential of over 27,000 TWh/year, some of which are 2000 TWh/year, more than 10% of the total global energy potential of renewable energy sources. SGE is very clean energy compared to conventional energy source including solar and wind power. It does not depend on weather fluctuations does not require an additional energy storage system (ESS). Consequently, SGE is a very affordable renewable energy source. Beside natural salinity, anthropogenic (e.g., reclaimed wastewater, brine, etc.), artificial and/or engineering solutions (e.g., ammonium bicarbonate, amine-based solution) are a very attractive source for SGE, which have a huge SGE potential. In order to overcome the geographical limitation, it is essential to develop a low salinity source except for the site of the estuary. Furthermore, the use of fresh water sources is inadequate because it can compete with drinking water, agriculture water and industrial water resources. As an effective and economical low salinity source for SGE, reclaimed wastewater has long been considered. The discharge of reclaimed wastewater into the coast has an SGE potential of 18 GW. In South Korea, 3,696,769 ton/days of reclaimed wastewater was discharged into the coast in 2015, and it has 1257 GWh/year of SGE potential. In this study, the viability of the practical RED was evaluated by using effluent from sewage treatment plant as low salinity source. Especially, underground (Lava) seawater was used for the high salinity source of the RED. RED performances were compared according to characteristics of IEMs and fouling phenomena in the RED stack were considered.

2 Materials and Methods

A RED stack consists of 100–300 unit-cell pairs with an effective membrane area of 19.63 cm². A unit-cell consisted of a LC compartment, an anion exchange membrane (AEM), a high concentration (HC) compartment and a cation exchange membrane (CEM). 100 μm thickness of woven-shaped spacer (SEFAR 03-160/53, open area: 53%) was used to prevent the junction of AEM and CEM. Woven shape spacer is not a preferred option for continuous operation of the RED stack because of pressure drop. However,

H. Kim · W.-S. Kim · J.-Y. Nam · J.-Y. Choi · K. Hwang ·
Y. Seog · N.-J. Jeong (✉)
Marine Energy Convergence and Integration Laboratory,
Jeju Global Research Center (JGRC), Korea Institute
of Energy Research (KIER), Yuseong-gu, South Korea
e-mail: njjeong@kier.re.kr

H. Kim
e-mail: hankikim@kier.re.kr

W.-S. Kim
e-mail: kws@kier.re.kr

J.-Y. Nam
e-mail: jynam@kier.re.kr

J.-Y. Choi
e-mail: jychoi@kier.re.kr

K. Hwang
e-mail: kshwang@kier.re.kr

Y. Seog
e-mail: ysseo@kier.re.kr

Table 1 Major characteristics of ion-exchange membranes used in this study

		Type	IEC (meq/g)	Permselectivity (%)	Area resistance (Ω cm^2)
CEM	Homogeneous	FUJIFILM TYPE-I	1.836	92.0	2.105
	Heterogeneous	Lab-made PF-IEMs	1.793	95.7	0.421
AEM	Homogeneous	FUJIFILM TYPE-I	1.677	92.0	1.34
	Heterogeneous	Lab-made PF-IEMs	1.809	92.4	0.402

it prevents deformation of IEMs that is the main reason of occlusion in flow channels, and it reduces the diffusion boundary layer thickness by generating fluid vortex on the surface of the membrane. As gasket, 100 μm thickness of glass fiber reinforced polytetrafluoroethylene (PTFE) film was used to prevent leakage. For the practical applications of the RED stack, two types of IEMs were compared. One is the commercial RED-specific IEMs (TYPE-I, FUJIFILM Manufacturing Europe BV, Tilburg, Netherlands) and the other is the lab-made pore-filling ion-exchange membranes (PF-IEMs). Each IEMs property was compared in Table 1. Prior to use, IEMs were soaked in 0.5 M NaCl for swelling for 24 h. After preparation and swelling, they were trimmed using a laser cutter and stored in 0.5 M NaCl in a refrigerator at 4 °C to prevent biological contamination.

3 Results and Discussion

Figure 1 shows the contaminated FUJIFILM TYPE-I membranes and lab-made PF-IEMs. Commonly (but not exclusively), organic foulants are negatively charged and favor adsorption on the AEM surface. However, foulants were not adsorbed on the CEM. In some cases, colloidal fouling was observed on the CEM, but it was washable and it can be removed by back-washing. Because fugacity of the

Fig. 1 Pictures of used FUJIFILM TYPE-I membranes (up) and lab-made pore-filling membranes (down). **a** Used CEM, **b** used AEM and **c** poisoned AEM by $[Fe(CN)_6]^{3-/4-}$ redox species
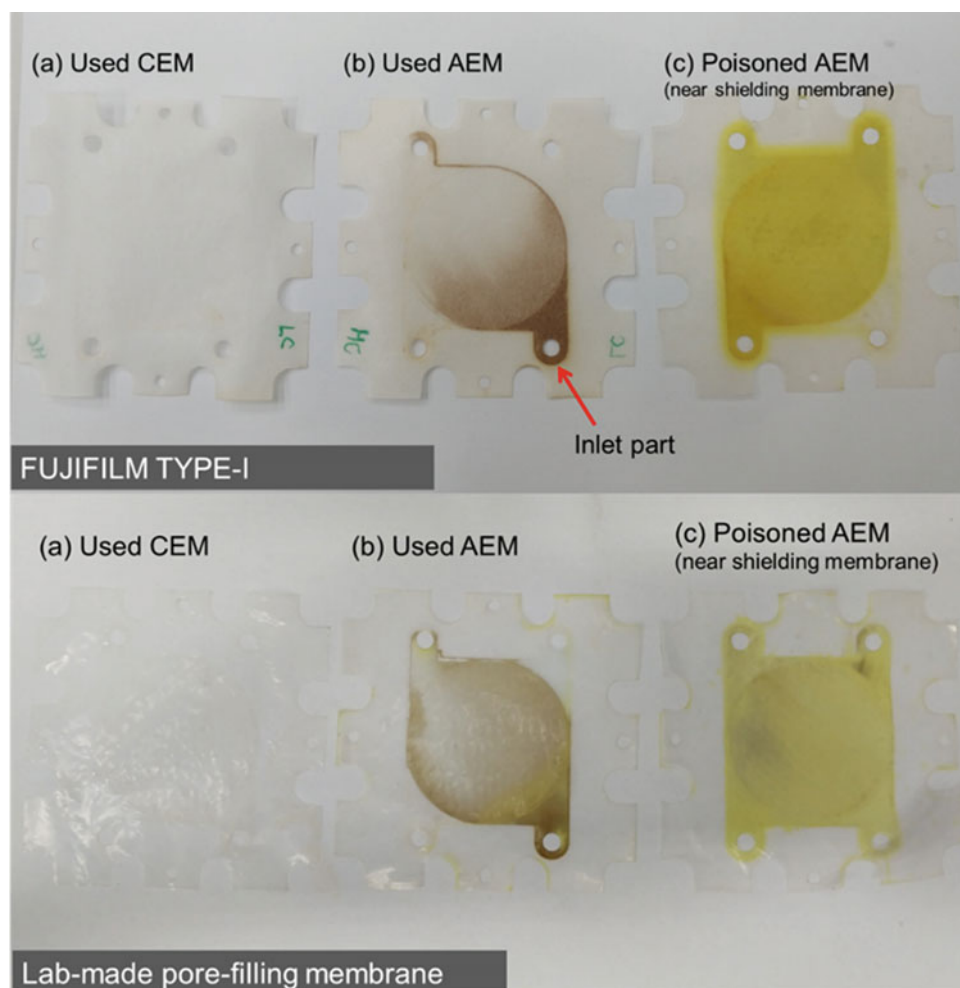
foulants is higher under high pressure, fouling was more progressed at inlet parts where pressure drop was the highest at flow channel. Hence, proper design of inlet parts and manifolds are significantly important to develop feasible RED stack. A promising option to decrease the pressure drop in the inlet parts is the cross-flow type RED stack. Because of the imperfection in the shielding membranes, redox species in the electrode compartment were leaked to the high concentration (HC) and low concentration (LC) flow channels near the electrode. The $[Fe(CN)_6]^{3-/4-}$ redox species was negatively charged thus AEM near the shielding membranes were poisoned by $[Fe(CN)_6]^{3-/4-}$. Undesirable poisoning of a little AEM is not a significant problem for the sustainability of the RED stack. However, fouling in the RED stack (especially on the spacer in LC flow channel) increases pressure drop, and it is the critical problems in continuous operations of RED.

Figure 2 shows the fouling morphologies on the FUJI-FILM TYPE-I. Both AEM and CEM contained debris as the substrate. However, physicochemical properties of debris and electrolyte, especially swelling degree, are not same thus there was the large number of cracks and pin-holes on the membrane surface after swelling. The surface of the membrane due to the debris was severely curved. This further facilitated the adsorption of organic foulant and weakened the resistance to membrane contamination. Figure 2c, d shows the fouling morphologies on the FUJIFILM TYPE-I AEM and CEM at the LC flow channel. It can be seen that the organic fouling formed a firm cake layer on the AEM surface. However, on the surface of the CEM, thin amorphous layer covered the membrane surface. This layer is colloidal fouling, and it seems to be unstable because fouling on the AEM was triggered by electrostatic attraction while the formation of fouling on the CEM was caused by physical

Fig. 2 Fouling morphology on the commercial FUJIFILM TYPE-I AEM and CEM
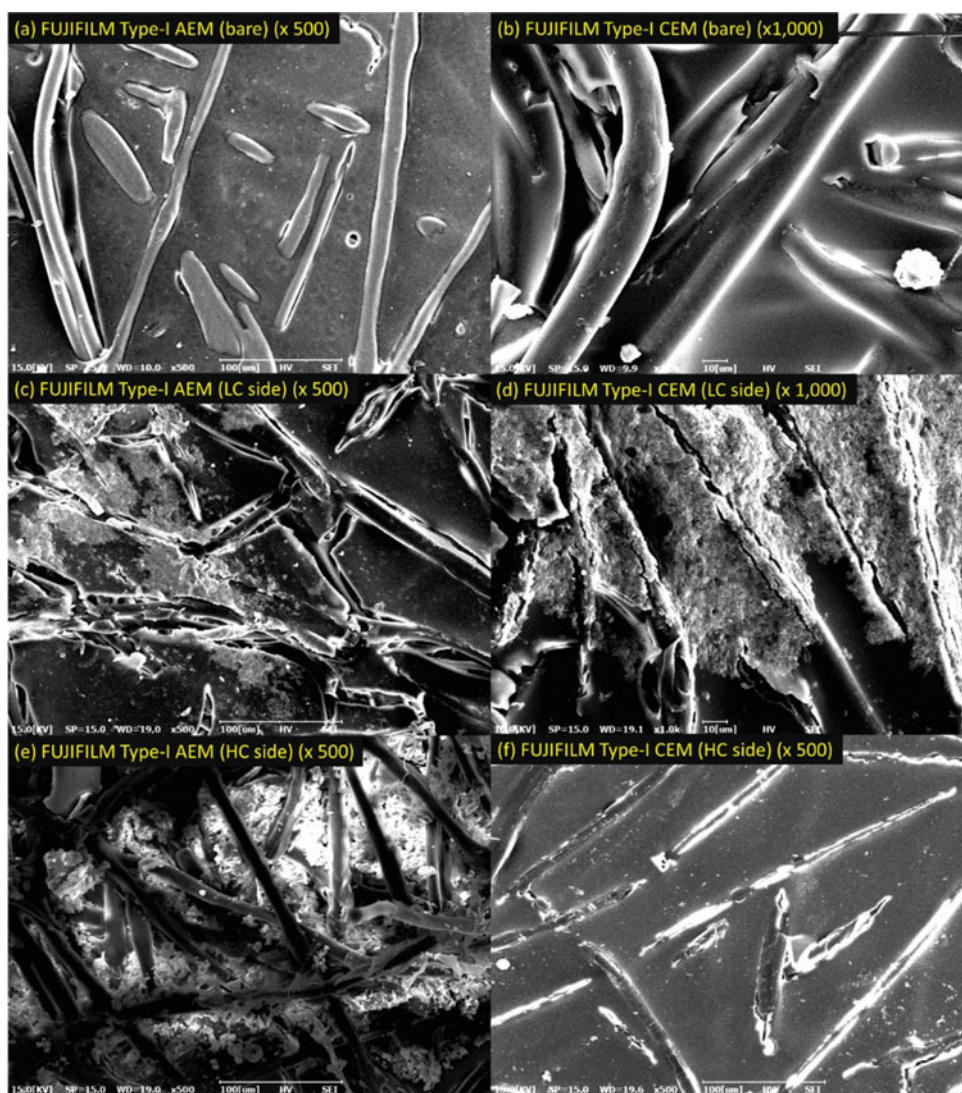
adsorption. Organic foulants were penetrated into the AEM, and formation of the colloidal fouling was enhanced by the electric double layer compression of foulants near the HC flow channel. Hence, the colloidal fouling was observed in the AEM polymer structure. However, CEM surface was clean at the HC flow channel.

electrostatic interaction of negatively charged fouling on the AEM is irreversible; hence, advanced cleaning is required.

4   Conclusion

In this study, fouling morphologies on the ion-exchange membranes in RED stack under the practical conditions were studied. According to the type of membranes, fouling characteristics and morphologies were different. Colloidal foulings are physically adsorbed on the membranes, and they are easily removed from the surface but chemical or

References

Vermaas, D. A., Kunteng, D., Saakes, M., & Nijmeijer, K. (2013). Fouling in reverse electrodialysis under natural conditions. *Water Research, 47*(3), 1289–1298.

Di Salvo, J. L., Cosenza, A., Tamburini, A., Micale, G., & Cipollina, A. (2018). Long-run operation of a reverse electrodialysis system fed with wastewaters. *Journal of Environmental Management, 217,* 871–887.

Co-composting Biosolids and Organic Fraction of Municipal Solid Waste or Carbonized Rice Hull and *Trichoderma harzianum* Augmented Inoculum

Analiza Palenzuela Rollon, Enrico Luis Coquico, Fredie More Pablo, and Angelene Paradero

Abstract

Through composting, biosolids can be converted to a soil conditioner provided pathogen control is ensured. Carbonized rice hull is a promising bulking agent for composting, while OFMSW can provide more organic matter needed for achieving higher peak temperatures. Augmenting with *T. harzianum* improves quality of compost product, thereby providing resistance to plant diseases and promotes growth.

Keywords

Biosolids • C/N ratio • OFMSW • Plant nutrients • Septage

1 Introduction

As the human population rapidly grows, the amount of domestic wastewater and septage, i.e. slurry from septic tanks, and thus, also the amount of biosolids generated from their treatment is increasing. Composting as a sustainable solution to increasing amount and cost of biosolids disposal has been explored by a water district in a suburban setting near Metro Manila. Composting is a sustainable process as it recycles plant nutrients to the soil, thus, improving soil quality and agricultural productivity. Composting can reduce health risks associated with pathogens in biosolids, which are usually hauled and disposed in the uncontrolled dumping area. Towards this goal, a prior pilot-scale windrow composting of dewatered biosolids was done in the water district.

The bulking agent used was carbonized rice hull (CRH) based on the experience of local farmers that mixing it with the top soil of crop planting beds improves the root structure of the vegetable plants in a manner that plants can better take up water and nutrients. Moreover, carbonized rice hull is abundant in the region. In that study, the achieved final organic matter content of the mixture was ca. 20%, which needs to be improved, versus $\geq 20\%$ (PNS/BAFS 2016 Standard for Soil Conditioner). Although the temperature achieved was at most 42 °C, after 50–60 days windrow composting, the detected total coliforms were 32 cfu/g (vs. <500 PNS/BAFS), Faecal Streptococci was negative (vs. <500 PNS/BAFS) and Salmonella was also not detected.

This study explored co-composting the biosolids with the organic fraction of municipal solid waste (OFMSW) as a means of improving compost organic matter content and compost mixture peak temperature during the active phase of the process. While biosolids provide the necessary N, P and K, the OFMSW gives more carbon. *Trichoderma harzianum* was added to augment the composting seed microbes. Trichoderma spp., is among the most common fungi found in soil. Several Trichoderma spp. can suppress soil-borne plant diseases such as Fusarium wilt and Rhizoctonia solani (Vinale et al. 2008; Mehta et al. 2014). This study aimed to compare the effects of CRH and OFMSW as bulking agent or co-substrate at various bulking agent to biosolids ratio on compost temperature during the active phase, organic matter content of final compost and compost quality pertaining to plant growth. The effect of bioaugmentation with *T. harzianum* was also determined.

2 Materials and Methods

Dewatered biosolids were obtained from BWD. Shredded OFMSW was obtained from the University of the Philippines Diliman Materials Recovery Facility (UPD MRF). *T. harzianum* was obtained from BioSpark UPLB.

A. P. Rollon (✉) · E. L. Coquico · F. M. Pablo · A. Paradero
Department of Chemical Engineering, College of Engineering, University of the Philippines Diliman, Quezon City, Philippines
e-mail: aprollon@up.edu.ph

A. P. Rollon
Environmental Engineering Graduate Program, College of Engineering, University of the Philippines Diliman, Quezon City, Philippines

Compost mixtures were of various combinations of three treatments: bulking agent or co-substrate: CRH or OFMSW; bulking agent to biosolids ratio: 1:2 or 2:1; and with or without *T. harzianum* (2 mg/kg mixture). Each combination was duplicated. The OFMSW was 50% wet fresh kitchen waste and 50% dry garden plant leaves. Compost mixtures (2.25 kg each) were placed inside perforated plastic bags. The compost mixtures were turned every ten days. The temperature was measured in about five randomly scattered points in the mixture. Electrical conductivity (EC) and pH were measured on the water extract of compost samples at 1:10 dilution. Samples were composite with respect to space in a compost bag. All the compost mixtures were placed inside covered greenhouse during composting.

The effect of the different compost products on growth of *Brassica oleracea* var. alboglabra (aka. Chinese kale) was determined. Each compost product was applied on the soil at two dosages: 25 and 50% of soil-compost mixture. Prior to planting, seeds of *B. oleracea* var. alboglabra were soaked in water for ca. three hours. The seeds were allowed to germinate on same soil (without compost) and transplanted into the different compost-soil mixtures after seven days of seed germination. After four weeks, the leaf length, width and total plant biomass were measured. There were three replicates for each type of soil-compost mixture.

3   Results and Discussion

Higher peak temperatures (as high as 48 °C) were achieved in most compost mixtures with OFMSW as bulking agent or co-substrate than those with CRH (as high as 43 °C). This indicates that OFMSW contain more highly biodegradable organic matter than CRH. Higher temperatures were achieved in mixtures having *T. harzianum*. Such higher temperature confirms that with the fungus, hydrolysis and further conversion of the biodegradable solids in the compost are faster because *T. harzianum* produces enzymes that break down complex molecules in compost, such as lignocellulose (El-Din et al. 2000).

During composting, electrical conductivity (EC) increased as the process involves mineralization of organic matter thereby releasing plant nutrients as mineral salts or ions. The EC values of water extracts from biosolids-OFMSW compost mixtures were higher than those from biosolids-CRH. Higher EC values indicate that there are higher concentrations of the mineral forms of plant nutrients in the compost. The mineral forms, e.g. ammonium, nitrates, phosphates, sulphates, potassium salts, are those that are readily available for plant uptake. Instances of decrease in EC indicate possible loss of ammonium ions through ammonia volatilization, which is accelerated at higher pH.

Despite probable ammonium losses, EC of biosolids-OFMSW compost was higher suggesting that ammonia loss is replenished through further mineralization of organic matter.

The pH levels in biosolids-OFMSW compost were higher than those in biosolids-CRH compost. This must be due to a higher fraction of easily degraded substances in OFMSW, which releases ammonium. In compost with OFMSW, and with 2:1 OFMSW: biosolids ratio, pH level decreased faster than those of lower OFMSW: biosolids ratio (1:2). This more rapid decrease is attributable to a higher amount of volatile fatty acids produced from hydrolysis and acid fermentation of a larger amount of OFMSW. Between the same ratio, OFMSW: biosolids of 2:1, pH in the mixture with *T. harzianum* is lower than that without it. This is probably because when *T. harzianum* is present, hydrolysis occurs at a faster rate because the fungus produces enzymes that can break down lignocellulosic matter in the OFMSW. Without it, the effect of VFA production on pH is minimal.

In most cases where CRH or OFMSW was part of the compost mixture, organic matter level is higher (24–51%) with *T. harzianum* than without it (10–37%). Probably, the growth of the fungi converts some of the mineral products obtained from the breakdown of complex organic matter to fungal biomass.

At low compost dosage, the total biomass, leaf width and length of plants grown on biosolids-CRH compost were higher compared to those of biosolids-OFMSW and to the soil without compost. This better plant growth may be due to better texture consistency and sufficient nutrients provided by the applied biosolids-CRH compost compared to that of biosolids-OFMSW compost. The higher amount of mineral salts in biosolids-OFMSW compost may have caused lower plant yield. Among biosolids-CRH compost applied at a lower dosage (25%), those where *T. harzianum* was added yielded higher total biomass.

Infestations were observed in some of the plants. The plants that were severely infested were all on soil-compost mixture without *T. harzianum*. None of the plants on compost with *T. harzianum* were severely infested. Five out of six plants that were not infested were grown on compost with *T. harzianum*. This shows that the compost with *T. harzianum* enhances resistance of the plants to infestation.

Thus, better compost mixtures are those with CRH and with *T. harzianum* provided they are added at the right amount. It may be beneficial to explore composting mixtures containing biosolids, OFMSW and CRH and optimize their proportion in order to take advantage of their individual characteristics and role in composting. It has been noted that biosolids-OFMSW compost mixture achieved higher peak temperatures, which should be beneficial in view of pathogen control.

4 Conclusion

At a controlled composting process condition, dewatered biosolids can be converted into a valuable soil amendment product. Higher peak temperatures can be achieved in biosolids-OFMSW than biosolids-CRH composting mixtures. Higher temperatures were achieved in mixtures having *T. harzianum* augmented inoculum than without the added fungi. For achieving high temperature, the best bulking agent to biosolids ratio depends on the bulking agent used. Compost of sufficient organic matter content (at least 20%) can be achieved with CRH or OFMSW as bulking agent and co-substrate. Those, where *T. harzianum* was added, have higher organic matter contents than those without the fungi.

The compost products show good potentials as a soil conditioner, as demonstrated in the plant assay, provided they are added at the right amount. At low compost application rate, the biosolids-CRH composts yielded higher plant biomass than biosolids-OFMSW composts and soil without any of the compost products. The compost products in which *T. harzianum* was added show promising potential for providing plants with resistance against infestation. Based on plant growth and compared at two application rates, compost mixtures with CRH and with *T. harzianum* perform better, provided they are added at the right amount. The application rate of biosolids-OFMSW compost must be adjusted based on soil composition and resulting soil-compost mixture salt level.

References

El-Din, S. M. S. B, Attia, M., & Abo-Sedera, S.A. (2000). Field assessment of composts produced by highly effective cellulolytic microorganisms. *Biology and Fertility of Soils, 32*(1), 35–40.

Mehta, C. M., Palni, U., Franke-Whittle, I. H., Sharma, A. K.: Compost: Its role, mechanism and impact on reducing soil-borne plant diseases. *Waste Management, 34*(3), 607–622 (2014).

Vinale, F., Sivasithamparam, K., Ghisalberti, E. L., Marra, R., Woo, S. L., & Lorito, M. (2008). Trichoderma–plant–pathogen interactions. *Soil Biology & Biochemistry, 40*(1), 1–10.

Production of Bioenergy and Biochemicals from Organic Solid Waste: Influence of the Pretreatment Operating Parameters

A. Conte, A. Cesaro, H. Carrère, E. Trably, F. Paillet, and Vincenzo Belgiorno

Abstract

The organic solvent pretreatment promotes the bioconversion of the organic solid waste. A low acid concentration increases the hydrogen production. Lactate production is favoured by high acid concentration and temperature of the pretreatment.

Keywords

Biorefinery • Energy • Organic waste • Organic acid pretreatment • Building blocks • Recovery

1 Introduction

The anaerobic bioconversion of the organic fraction of municipal solid waste (OFMSW) into a wide range of competitive value-added biochemicals represents a circular economy strategy for the management of this kind of waste (Moscoviz et al. 2018).

Anaerobic processes of the organic solid waste are well-established waste-to-energy technologies and, in recent years, the ability of the dark fermentation (DF) to synthesize hydrogen has raised great scientific attention (Capson-Tojo et al. 2016; Cappai et al. 2014). Nevertheless, the DF appears also as an important sustainable synthesis process of valuable chemicals, which serve as precursors of ubiquitous petrochemical-derived products. However, suitable pretreatments of the substrate are necessary to improve the efficiency of the bioconversion during the anaerobic process (Karthikeyan et al. 2018).

The organic solvent pretreatment, which is already widely used for lignocellulosic substrates (Kabir et al. 2015), seems a promising method to enhance the conversion of OFMSW into more amenable bioproducts.

The aim of this study was to evaluate the effects of formic acid pretreatment on the production of both hydrogen and biomolecules from the DF of differently composed OFMSW. For this purpose, physical–chemical characteristics of raw and treated substrates were studied, and the production of both metabolites and hydrogen at the end of dark fermentation was estimated. The correlations among the resulting data were discussed in order to evaluate the potential commercial and environmental benefits of the proposed treatment.

2 Materials and Methods

The combination of the chemical pretreatment and the DF tests for the organic solid waste was studied, and different operating conditions were explored in order to identify the most relevant ones with reference to the production of both metabolites and biohydrogen.

Differently composed organic solid wastes were used as substrates.

A sequential organic acid pretreatment (Sindhu et al. 2010; Amnuaycheewa et al. 2016) was carried out in the autoclave with specific solid–liquid ratio. The acid concentration, the temperature and duration of the pretreatment were varied according to 2^3 factorial design. The pretreated substrates were used for biohydrogen production potential (BHP) tests, which were performed with a heat-treated inoculum and a substrate (S)-to-inoculum (X) ratio (S/X) of 10 g VS substrate/g VS inoculum (Ghimire et al. 2018).

The effluents of both the pretreatment and the dark fermentation tests were analysed in terms of total solid (TS),

A. Conte · A. Cesaro (✉) · V. Belgiorno
SEED—Sanitary Environmental Engineering Division, Department of Civil Engineering, University of Salerno, Via Giovanni Paolo II, 84084 Fisciano, SA, Italy
e-mail: acesaro@unisa.it

H. Carrère · E. Trably · F. Paillet
LBE, University of Montpellier, INRA, Avenue Des Étangs, 11100 Narbonne, France

volatile solid (VS), pH, soluble chemical oxygen demand (sCOD), total Kjeldahl nitrogen (TKN) and total organic carbon (TOC). Soluble metabolites, like volatile fatty acids (VFAs) and organic acids, were measured at the beginning and the end of each experiment by gas chromatography (GC) and high-performance liquid chromatography (HPLC).

The produced gas composition in hydrogen was quantified with a multiplexed gas chromatograph. A modified Gompertz equation was used to model hydrogen production in DF experiments.

3 Results and Discussion

The substrate conversion was greatly affected by the different operating conditions of the organic acid pretreatment.

The overall hydrogen production increased after the pretreatement of the substrate at the low organic acid concentration. A maximum yield of 31.6 mLH$_2$/g VS was achieved.

Various quantities of organic acids, like acetate, propionate and butyrate, along with ethanol were also observed in the substrates pretreated under the different operating conditions, and this result was consistent with previous reports (Cappai et al. 2014). Significant lactate production was found to be promoted when high acid concentration and high temperature were applied simultaneously; in this case, the hydrogen production from the subsequent DF test drastically decreased. Indeed, in these pretreated substrates, the homoacetogenesis contributed to hydrogen consumption for acetate production (Ghimire et al. 2018).

4 Conclusion

The organic solvent pretreatment is an excellent method for the bioconversion of the OFMSW, and its integration with DF tests enhances the recovery of both bioenergy and biochemicals.

This study highlighted the effects of different operating conditions on the substrate conversion, showing the effects of the main process parameters on different metabolic and energy production pathways. The organic acid concentration plays a key role in the conversion of the investigated

substrates into a variety of reduced products such as hydrogen, ethanol, lactate and organic acids: adjusting the other pretreatment parameters, the subsequent biological process can be targeted towards the production of either building blocks or energy carriers.

The combination of the organic solvent pretreatment and DF could thus contribute to the bio-based society, reducing organic residues and increasing the efficiency of the biomass-based production of energy and valuable commodities, while addressing the biorefinery concept in waste management.

References

Amnuaycheewa, P., Hengaroonprasan, R., Rattanaporn, K., Kirdponpattara, S., Cheenkachorn, K., & Sriariyanun, M. (2016). Enhancing enzymatic hydrolysis and biogas production from rice straw by pretreatment with organic acids. *Industrial Crops and Products, 87,* 247–254.

Cappai, G., De Gioannis, G., Friargiu, M., Massi, E., Muntoni, A., Polettini, A., et al. (2014). An experimental study on fermentative H$_2$ production from food waste as affected by pH. *Waste Management, 34,* 1510–1519.

Capson-Tojo, G., Rouez, M., Crest, M., Steyer, J.-P., Delgenès, J.-P., & Escudié, R. (2016). Food waste valorization via anaerobic processes: A review. *Reviews in Environmental Science and Bio/Technology, 15,* 499–547.

Ghimire, A., Trably, E., Frunzo, L., Pirozzi, F., Lens, P. N. L., Esposito, G., et al. (2018). Effect of total solids content on biohydrogen production and lactic acid accumulation during dark fermentation of organic waste biomass. *Bioresource Technology, 248,* 180–186.

Kabir, M. M., Rajendran, K., Taherzadeh, M. J., & Sárvári Horváth, I. (2015). Experimental and economical evaluation of bioconversion of forest residues to biogas using organosolv pretreatment. *Bioresource Technology, 178,* 201–208.

Karthikeyan, O. P., Trably, E., Mehariya, S., Bernet, N., Wong, J. W. C., & Carrere, H. (2018). Pretreatment of food waste for methane and hydrogen recovery: A review. *Bioresource Technology, 249,* 1025–1039.

Moscoviz, R., Trably, E., Bernet, N., & Carrère, H. (2018). The environmental biorefinery: State-of-the-art on the production of hydrogen and value-added biomolecules in mixed-culture fermentation. *Green Chemistry, 20,* 3159–3179.

Sindhu, R., Binod, P., Satyanagalakshmi, K., Janu, K. U., Sajna, K. V., Kurien, N., et al. (2010). Formic acid as a potential pretreatment agent for the conversion of sugarcane bagasse to bioethanol. *Applied Biochemistry and Biotechnology, 162,* 2313–2323.

Sulfate Ion Removal from Reverse Osmosis Concentrate Using Electrodialysis and Nano-Filtration in Combination with Ettringite Precipitation

Yongxun Jin, Kangwoo Cho, Chong Min Chung, and Seokwon Hong

Abstract

NF membranes reject divalent ions (SO_4^{2-}) at much higher rate than monovalent ions (Cl^-); Electrodialysis showed higher removal efficiency of SO_4^{2-} and Cl^-; Sulfate coexists with calcium- and aluminum-enhanced ettringite precipitation.

Keywords

Nano-filtration (NF) • Reverse osmosis (RO) • Electrodialysis (ED) • Sulfate • Ettringite • Brine concentrate

1 Introduction

In recent years, hitherto unregulated pollutants are of a serious concern in more stringent water regulation, including micro-pollutants and ionic species such as sulfate ions (SO_4^{2-}). It was corroborated that highly concentrated sulfate ions from industrial wastewater and reverse osmosis (RO) brine water result in osmotic inhibition and witheredness of crops. Anaerobic reduction of sulfate can also generate H_2S to bring about odor and sewer corrosion. Therefore, environmental agencies in many countries have controlled the concentrations of SO_4^{2-} for industrial effluents to prevent water pollution (Runtti et al. 2016). Generally, the sulfate removal can be achieved by chemical precipitation, membrane filtration, and ion exchange process (Kijjanapanich et al. 2013; Qian et al. 2015). A chemical precipitation based on $CaSO_4$ requires a high dosage of calcium and, due to slight solubility of gypsum, the effluent would carry dissolved sulfate and calcium. Although RO is a viable option for further volume reduction and SO_4^{2-} separation, nano-filtration (NF) and electrodialysis (ED) could be more energy efficient in selected composition of target water (total dissolved solids concentration and valency of primary ions among others). On the other hand, the above separation processes inevitably produce (secondary) brine water with highly concentrated sulfate ions. Distillation-based processes have been deployed for so-called zero liquid discharge, but they are energy intensive. In the presence of monovalent ions such as Cl^-, an increase in boiling point would further elevate the energy consumption. The ettringite precipitation is a modification of high pH lime precipitation (Tolonen et al. 2016), and judging from the lower solubility of ettringite, we postulated that the ettringite precipitation can be a promising tool for handling the brine water from either NF or ED process.

In this research, our goal was to optimize the sulfate removal from model industrial wastewater (RO concentrate) by combination of NF or ED with the ettringite formation. The necessary conditions for an optimal deionization system include (i) minimum dosage of chemicals which increase the level of counter ions (SO_4^{2-} and Cl^-), (ii) selective separation of SO_4^{2-}, and (iii) minimum usage of energy.

Y. Jin · S. Hong
Center for Water Resource Cycle Research, Korea Institute of Science and Technology, P.O. Box 131 Cheongryang, Seoul, 130-650, Korea
e-mail: jin0808@kist.re.kr

S. Hong
e-mail: swhong@kist.re.kr

K. Cho (✉)
Division of Environmental Science and Engineering, Pohang University of Science and Technology (POSTECH), Pohang, 790-784, Korea
e-mail: kwcho1982@postech.ac.kr

C. M. Chung
Facility Team, Samsung Electronics Co., Ltd, Giheung Hwaseong Complex, Hwaseong, Giheung, Korea
e-mail: cm78.chung@samsung.com

2 Materials and Methods

2.1 Laboratory-Scale Experiments for Volume Reduction of RO Brine Water

A commercial thin film composite NF membrane (HL 4040 FM, GE) with an average salt rejection of 98% (determined at an applied pressure of 10 bar and 2000 mg/L $MgSO_4$ concentration) was used for the fouling experiments. All the membranes were stored in deionized (DI) water at 4–7 °C and rinsed regularly prior to use. The configuration of a plate-and-frame type membrane cell was $146 \times 95 \times 1.85$ mm, and the effective membrane area was 0.0139 m^2. During the cross-flow filtration, the permeate was collected in a reservoir (300 mL) and returned to the feed tank (4 L) automatically after monitoring the flow rate through the electronic balance. The cross-flow velocity and operating pressure were controlled by a back-pressure regular and pump frequency as well as by a bypass valve. The cross-flow velocity in the NF cell was maintained in all experiments at 20 cm/s, and the operating pressure was kept at 10 ± 0.5 bar. The feed water temperature was controlled at 20 ± 1 °C through a cooling coil submerged in the feed tank.

2.2 Specification of Commercial ED Module

ED lab-scale tests were performed to evaluate the removal efficiency of SO_4^{2-} and Cl^- using Electrodialysis Laboratory Unit P DER-Z (Mega). The ED system consisted of a stack and electrode compartments. The stack contained 10 pairs of cation and anion exchange membranes (Ralex) with an effective area of 1344 cm^2. The platinum and titanium were used as an anode and cathode, respectively. The batch tests were carried out under varying applied voltages (16, 24 V) and flow rate (45, 65 L/h) at room temperature.

2.3 Volume Reduction and Ettringite Precipitation Experiments for Synthetic/Real RO Brine Water

The synthetic wastewater was prepared by dissolving Na_2SO_4 and $NaCl$ at three different concentrations (high: SO_4^{2-}:6000 mg/L, Cl^-: 2000 mg/L; medium: SO_4^{2-}:4500 mg/L, Cl^-: 1500 mg/L; low: SO_4^{2-}:3000 mg/L, Cl^-: 1000 mg/L). The conductivity, current, and pH in the dilute and concentrate solution were measured at 5 min intervals. The concentration of SO_4^{2-} and Cl^- in the dilute was analyzed by IC (Thermo, USA). An industrial wastewater was obtained whose main concentration of SO_4^{2-} was averaged to be 1970 ppm. Both NF and ED experiments were performed for secondary handling of the RO brine water. The pH was adjusted to the optimized value of 12.00–12.50 using 0.2 mol/L $Ca(OH)_2$ solution. All runs were stirred at 250 rmp for 30 min and settled for 30 min. The $NaAlO_2$ was, then, added in above four samples because the presence of Al^{3+} enhances the efficacy of ettringite precipitation.

2.4 Analysis

To characterize of ettringite, the collected precipitates were evaluated by field-emission scanning electron microscope (SEM, Nova) and X-ray diffraction (XRD, Dmax2500/PC). In SEM analysis, a special attention was paid to the surface of the crystal to illustrate the details of the precipitates microstructure. In addition, the main peaks obtained from XRD analysis were further compared to verify the conformance with a model ettringite.

3 Results and Discussion

In this study, the volume from RO brine concentrate was further reduced for cost and energy effectiveness. The ED and NF membrane process was employed to minimize the concentration of separated ions and optimize the sulfate removal during the subsequent ettringite precipitation. The ettringite precipitation was tested to remove SO_4^{2-} ion from the secondary concentrate and verified by the XRD and SEM analysis.

3.1 Electrodialysis

The applicability of the ED process for the removal of SO_4^{2-} and Cl^- was investigated by employing synthetic and real wastewater. Water quality analysis and solution chemistry under various operating conditions were conducted in this research. In case of synthetic wastewater, the applied voltage is a dominant factor since the conductivity was decreased significantly as the applied voltage increased. Since the concentration of real wastewater was similar to the low concentration of synthetic wastewater, the activity of ED process for the removal of SO_4^{2-} and Cl^- in the real wastewater was further examined under the optimized conditions (voltage of 24 V and flow rate of 65 L/h). The results demonstrated that the removal efficiency of SO_4^{2-} and Cl^- was over 99% in 60 min, which was similar to the previous synthetic conditions. Although the ED process showed a high efficacy, a large energy consumption and scaling problem should be addressed before its real application for wastewater treatment.

Fig. 1 Comparison of the **a** SO_4^{2-} and **b** Cl^- concentration after ettringite precipitation as concentrate ratio decreased in NF membrane filtration process
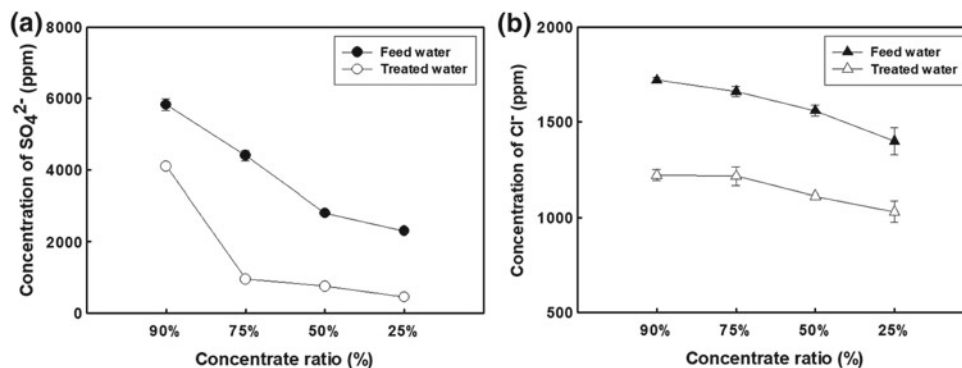
3.2 Nano-Filtration

Prior to the brine water volume reduction experiments by NF, the permeability and selectivity (solute rejection) of the NF membrane were evaluated. The SO_4^{2-} in raw brine water ranged from 1000 to 1200 ppm. During the filtration period, the water flux gradually reached a steady-state value even though there was approximately 6% decline in the flux within the first few hours. The measured steady-state product water flux was 63 LMH under an applied pressure of 10 bar at 20 °C. The results showed that the rejection rate of SO_4^{2-} and Cl^- was 98.0 and 90.6%, respectively. Additionally, the brine water from CDI was further concentrated at the concentrate ratio of 25, 50, 75, and 90% to reduce the brine volume; the concentration of SO_4^{2-} increased significantly as the concentrate ratio increased.

Fig. 2 XRD and SEM analysis of ettringite formed on the membrane surface

3.3 Optimization of Sulfate Removal in Ettringite Precipitation

In sulfate removal process, the hydrated lime ($Ca(OH)_2$) is widely used by raising the pH of the solution, which provides a source of calcium ions (Ca^{2+}) to precipitate and remove the dissolved sulfate ions as gypsum ($CaSO_4 \cdot 2H_2O$). In this study, the pH was firstly adjusted approximately 12.5 with the hydrated lime. Under this condition, the concentration of SO_4^{2-} was reduced from 3000 to 1500 ppm after gypsum precipitation treatment. However, the gypsum precipitation by itself would not be sufficient to meet the target concentration of 200 ppm of SO_4^{2-}, because the gypsum is slightly soluble in water.

Another precipitation process, the formation of ettringite was investigated in this research. Because the ettringite is much more insoluble in water compared to gypsum, the removal of sulfate by precipitating ettringite significantly is more expected. In this experiment, the $NaAlO_2$ was more added to concentrated brine water because the Al^{3+} alternates with groups of Ca^{2+} arranged around a symmetry axis

to form the columns of ettringites. The result of SO_4^{2-} concentration was reduced lower than 300 ppm in the concentrate ratio of 50%. Moreover, the collected precipitates were characterized by X-ray diffraction (XRD) and field-emission scanning electron microscope (SEM) to evaluate their composition and morphology of ettringite on the membrane surface. The morphology and composition analysis of the precipitates revealed that XRD spectra obtained well proved that an ettringite peak was observed in XRD spectrum with an addition of $NaAlO_2$, demonstrating a further decrease in sulfate concentration was due to ettringite formation (Figs. 1 and 2).

4 Conclusion

This study explored an optimal solution to reduce the sulfate ion in reverse osmosis concentrate. Research and evaluation on electrodialysis and NF membrane unit process optimization both with synthetic and real brine water. When compared to commercial technologies, our novel approach

was found to decrease the energy consumption and investment by combining novel deionization system, NF treatment, and ettringite precipitation, respectively.

References

Runtti, H., Luukkonen, T., Niskanen, M., Tuomikoski, S., Kangas, T., Tynjälä, P., et al. (2016). Sulphate removal over barium-modified blast-furnace-slag geopolymer. *Journal of Hazardous Materials, 317,* 373–384.

Kijjanapanich, P., Annachhatre, A. P., Esposito, G., van Hullebusch, E. D., & Lens, P. N. L. (2013). Biological sulfate removal from gypsum contaminated construction and demolition debris. *Journal of Environmental Management, 131,* 82–91.

Qian, J., Lu, H., Jiang, F., Ekama, G. A., & Chen, G.-H. (2015). Beneficial co-treatment of simple wet flue gas desulphurization wastes with freshwater sewage through development of mixed denitrification–SANI process. *Chemical Engineering Journal, 262,* 109–118.

Tolonen, E.-T., Hu, T., Rämö, J., & Lassi, U. (2016). The removal of sulphate from mine water by precipitation as ettringite and the utilisation of the precipitate as a sorbent for arsenate removal. *Journal of Environmental Management, 181,* 856–862.

Increasing Sustainability on the Metallurgical Industry by Integration of Membrane NF Processes: Acid Recovery

J. López, M. Reig, X. Vecino, C. Valderrama, O. Gibert, and J. L. Cortina

Abstract

Treatment of hydrometallurgical effluents by nanofiltration membranes for acid recovery. Application of Solution-Electro-Diffusion Model to determine membrane permeances.

1 Introduction

Hydrometallurgical industries generate effluents characterised by a great acidity and a high content of metallic (e.g. Fe, Zn, Cu) and non-metallic ions (e.g. As, Se, Sb). These streams are usually generated in the leaching process, pickling baths or gas cleaning (Agrawal and Sahu 2009). These kinds of acidic waters are usually treated to regenerate the acids. Different techniques such as electrodialysis (Boucher et al. 1997; Chekioua and Delimi 2015), diffusion dialysis (Li et al. 2016) and ion-exchange resins (Nenov et al. 1997) are used to recover acids. Among these techniques, nanofiltration (NF) exhibits high rejection of multivalent ions, while the transport of monovalent ions (e.g. H^+) is favoured. Studies conducted with polyamide-based membranes at high sulphuric acid concentrations (pH < 2)

showed high metal ion rejection (> 90%) and low acid rejections (Visser et al. 2001; Mullett et al. 2014).

Ion transport across the membrane depends on the membrane active layer and aqueous compositions (acidity and ion concentrations). However, there is still a lack of modelling tools to scale up NF for its applications to treat acidic waters. Among the different models to describe ion transport, solution-diffusion (SD) model is widely used (Yaroshchuk et al. 2009; Yaroshchuk et al. 2011; Pages et al. 2013). This model is based on: (i) separation is achieved by the differences on ion diffusivities inside the membrane, and (ii) the membrane does not present fixed pores, but it contains a free volume. Yaroschuck et al. (Yaroshchuk et al. 2009) coupled the SD model with the film model theory for single salts and later extended it to electrolytes mixtures (Yaroshchuk et al. 2011; Pages et al. 2013) to develop the so-called Solution-Electro-Diffusion (SED) model. At certain conditions, for instance in the case of weak electrolytes, ions can be presented forming complexes between them. Certain studies involved the transport of ions described by SED model considering the chemical equilibrium among them (Niewersch et al. 2014; López et al. 2018).

The main objective of this work is to study the performance of a NF membrane (NF270) with an effluent from hydrometallurgical industry, containing a mixture of H_2SO_4/H_3AsO_4 and metallic species (Fe, Cu, Zn, Ni, Co, Cd). Results were modelled according to SED model coupled with reactive transport to determine the membrane permeances to ions.

J. López · M. Reig · X. Vecino · C. Valderrama · O. Gibert · J. L. Cortina (✉)
Chemical Engineering Department and Barcelona Research Center for Multiscale Science and Engineering, UPC-BarcelonaTECH, C/Eduard Maristany, 10-14 (Campus Diagonal-Besòs), 08930 Barcelona, Spain
e-mail: jose.luis.cortina@upc.edu

J. L. Cortina
Water Technology Center CETaqua, Carretera D'Esplugues 75, 08940 Cornellà de Llobregat, Spain

2 Materials and Methods

NF270 (from Dow Chemical), with an active layer based on a semi-aromatic poly(piperazine amide), was tested. The membranes have thus ionogenic amine (R–NH₂) and carboxylic (R–COOH) groups, which are responsible for the membrane charge. The isoelectric point (IEP) for these

Table 1 Composition of the hydrometallurgical effluents

pH	Concentration, g/L								
	SO$_4$	As	Zn	Fe	Cu	Cd	Pb	Ni	Cl
0.60	19.02	0.33	0.062	0.015	0.009	0.011	0.005	0.001	3.02

membranes is 2.5 (Kallioinen et al. 2016). Experiments were performed with an effluent from hydrometallurgical industry (Table 1).

Experiments were carried out with a flat-sheet membrane (active membrane area of 0.014 m^2), which was placed in a test cell (GE SEPA^{TM} CF II) with a spacer-filled feed channel. The experimental set-up allowed the possibility to vary the cross-flow velocity (cfv) and transmembrane pressure (TMP). Experiments were carried out at a pre-fixed cfv (0.7 m/s), and the TMP was varied from 4 to 16 bar. Once the experiment was finished, the set-up was cleaned with deionised water to remove any impurity that may be left inside the cell. Samples were analysed using inductively coupled plasma (ICP) by an external laboratory.

2.1 Ion Transport Modelling Through NF Membranes Coupled with Reactive Transport

Ion transport across the membrane was described with the basis of SED model taking into account the reactive transport to include the chemical equilibrium between the different species in solution. This model does not consider convective flow (no coupling between ions and solvent), and ions transport is due to a combination of diffusive forces and electromigration. The model uses "virtual" concentrations, defined as those that are in thermodynamic equilibrium with an infinitely small volume inside the membrane. The use of these concentrations satisfies the chemical equilibrium conditions inside the membrane with the bulk association constant (Niewersch et al. 2014). Equation (1) describes the ion flux through the membrane.

$$j_i = -P_i \cdot \left(\frac{dc_i}{dx} + c_i \cdot \frac{d(\ln \gamma_i)}{dx} + z_i \cdot c_i \cdot \frac{d\varphi}{dx} \right) \quad (1)$$

where j_i is the flux of component i through the membrane (µm·mol/L·s), x is the dimensionless position in the membrane, P_i is the membrane permeance to ion i (µm/s), c_i is the concentration of component i (mol/L), γ_i is the activity coefficient of component i, z_i is the valence charge of component i and φ is the dimensionless virtual electrostatic potential in the membrane.

Mass balance equations were solved using MATLAB$^{®}$ software, where the membrane permeances to ions were varied to minimise the error between the rejection obtained experimentally and the one from the model.

3 Results and Discussion

Figure 1 shows the rejection curves for the ions in solution. NF270 showed high metal rejection (> 70%) and lower H$^+$ (< 30%) and S (< 50%) rejections. At pH < 1.92, the main sulphate specie in solution is a monovalent anion (HSO$_4^-$), which is less affected by dielectric exclusion and then responsible for low sulphate rejections. Moreover, its transport is also favoured by the presence of a positively charged membrane surface. According to the IEP (2.5), at pH 1 free carboxylic groups are fully protonated (R–COOH) and amine groups are partially protonated (R$_2$NH$_2^+$). Cations are rejected, which leads to H$^+$, which is the more mobile ion and the one with the highest concentration in solution, to permeate easily.

Calculated membrane permeance values were in agreement with dielectric exclusion. For instance, membrane permeance to HSO$_4^-$ was higher than the one to SO$_4^{2-}$ (25.7 and 0.13 µm/s, respectively). The fact that metals were highly rejected by the membrane implied lower membrane permeance values than for H$^+$, being membrane permeance to H$^+$ 116.04 µm/s, while the one for Zn^{2+} was 0.001 µm/s.
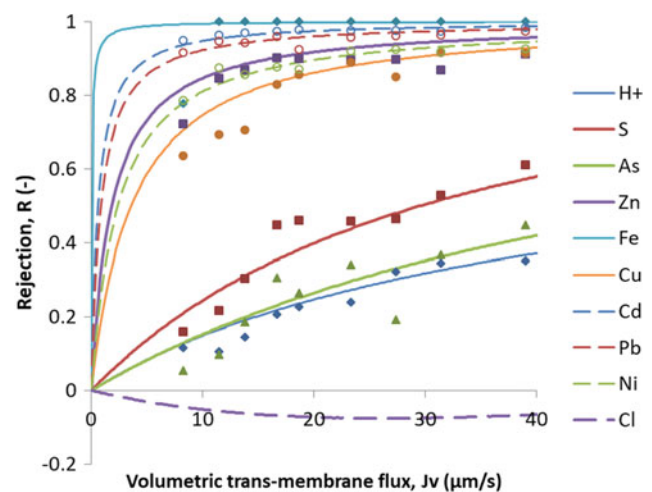
Fig. 1 Rejection curves for the ions in solution referred to the total concentration of the element as a function of permeate flux. Symbols: experimental data; lines: model fitting

4 Conclusion

The experimental data showed that it was possible to recover H^+ from hydrometallurgical industries while, at the same time, metallic impurities were rejected by the NF270 membrane. The positive charge of the membrane leaded to a better passage of H^+ than metals. Moreover, SED model was able to fit properly the experimental data, and membrane permeance values were calculated.

References

Agrawal, A., & Sahu, K. K. (2009). An overview of the recovery of acid from spent acidic solutions from steel and electroplating industries. *Journal of Hazardous Materials, 171,* 61–75. https://doi.org/10.1016/j.jhazmat.2009.06.099.

Boucher, M., Turcotte, N., Guillemette, V., Lantagne, G., Chapotot, A., Pourcelly, G., et al. (1997). Recovery of spent acid by electrodialysis in the zinc hydrometallurgy industry: Performance study of different cation-exchange membranes. *Hydrometallurgy, 45,* 137–160.

Chekioua, A., & Delimi, R. (2015). Purification of H_2SO_4 of pickling bath contaminated by Fe(II) ions using electrodialysis process. *Energy Procedia, 74,* 1418–1433. https://doi.org/10.1016/j.egypro.2015.07.789.

Kallioinen, M., Sainio, T., Lahti, J., Pihlajamäki, A., Koivikko, H., Mattila, J., et al. (2016). Effect of extended exposure to alkaline cleaning chemicals on performance of polyamide (PA) nanofiltration membranes. *Separation and Purification Technology, 158,* 115–123. https://doi.org/10.1016/j.seppur.2015.12.015.

Li, W., Zhang, Y., Jing, H., Zhu, X., & Wang, Y. (2016). Separation and recovery of sulfuric acid from acidic vanadium leaching solution by diffusion dialysis. *Journal of Environmental Chemical Engineering, 4,* 1399–1405. https://doi.org/10.1016/j.jece.2015.11.038.

López, J., Reig, M., Gibert, O., Torres, E., Ayora, C., & Cortina, J. L. L. (2018). Application of nanofiltration for acidic waters containing rare earth elements: Influence of transition elements, acidity and membrane stability. *Desalination, 430,* 33–44. https://doi.org/10.1016/j.desal.2017.12.033.

Mullett, M., Fornarelli, R., & Ralph, D. (2014). Nanofiltration of mine water: Impact of feed pH and membrane charge on resource recovery and water discharge. *Membranes (Basel)., 4,* 163–180. https://doi.org/10.3390/membranes4020163.

Nenov, V., Dimitrova, N., & Dobrevsky, I. (1997). Recovery of sulphuric acid from waste aqueous solutions containing arsenic by ion exchange. *Hydrometallurgy, 44,* 43–52. https://doi.org/10.1016/S0304-386X(96)00029-1.

Niewersch, C., Bloch, A. L. B., Yüce, S., Melin, T., & Wessling, M. (2014). Nanofiltration for the recovery of phosphorus—Development of a mass transport model. *Desalination, 346,* 70–78. https://doi.org/10.1016/j.desal.2014.05.011.

Pages, N., Yaroshchuk, A., Gibert, O., & Cortina, J. L. (2013). Rejection of trace ionic solutes in nanofiltration: Influence of aqueous phase composition. *Chemical Engineering Science, 104,* 1107–1115. https://doi.org/10.1016/j.ces.2013.09.042.

Visser, T. J. K., Modise, S. J., Krieg, H. M., & Keizer, K. (2001). The removal of acid sulphate pollution by nanofiltration. *Desalination, 140,* 79–86.

Yaroshchuk, A., Martínez-Lladó, X., Llenas, L., Rovira, M., de Pablo, J., Flores, J., et al. (2009). Mechanisms of transfer of ionic solutes through composite polymer nano-filtration membranes in view of their high sulfate/chloride selectivities. *Desalination and Water Treatment, 6,* 48–53.

Yaroshchuk, A., Martínez-Lladó, X., Llenas, L., Rovira, M., & de Pablo, J. (2011). Solution-diffusion-film model for the description of pressure-driven trans-membrane transfer of electrolyte mixtures: One dominant salt and trace ions. *Journal of Membrane Science, 368,* 192–201. https://doi.org/10.1016/j.memsci.2010.11.037.

Energy Saving Technologies and Future Clean Energy Solutions Under Water Constraints

Overview of the Water Requirements for Energy Production in Africa

Rocio Gonzalez and Nicolae Scarlat

Abstract

86% of the total water consumed for fuel production in Africa corresponds to oil. 74% of the water consumption for power plant operations is for coal power plants and 60% of the water withdrawals is for natural gas power plants. Renewable energies represent 2% of water consumption and 0.06% of water withdrawals in electricity production in Africa.

Keywords

Water–energy nexus • Water footprint • Energy Africa

1 Introduction

Water scarcity is affecting many regions in the world. In Africa, where two-thirds of the continent is arid or semi-arid, more than 300 million people living in sub-Saharan countries are affected by water shortages (NEPAD 2006). The energy sector is one of the largest consumers of water after agriculture. In 2014, 10% of total water abstractions worldwide were used for energy production and power generation (IEA 2014). This study aims to provide an overview of the water footprint of the energy sector in Africa including fuel extraction, conversion, refining, transport, power plants construction and electricity generation. Water requirements vary considerably among the different cooling systems, fuel extraction methods, location or climatic conditions (Meldrum et al. 2013). When analyzing the water footprint, it is important to make a distinction between withdrawals and consumption. Water withdrawals represent the water removed from the water source, while water consumption is the part of water withdrawn that is not returned to the water source, mainly water incorporated to crops or lost by evaporation. These two water terms differ significantly in many cases depending on the technology used.

2 Materials and Methods

Water withdrawals and water consumption have been estimated for the main stages of energy production in Africa, including fuel production, power plant construction and electricity generation. Fuel production country-level data for coal, crude oil, natural gas, charcoal and fuelwood were collected from AFREC statistics (2017) and IEA (2015). Data on uranium production were obtained from the World Nuclear Association (2015). To estimate the water use for the production of each fuel type, water factors in m^3/MWh have been gathered from Macknick et al. (2011), Meldrum et al. (2013), and Wu et al. (2011). Water used for fuel production is mainly related to extraction and processing; however, both do not necessarily take place in the same country. This fact and the water used in processing imported fuels extracted abroad have been considered in the calculations of the present research (IEA 2015). For the estimation of the water use for electricity generation, data on electricity production from PLATTS (WEPP 2016) have been combined with the water factors from Macknick et al. (2011) and Meldrum et al. (2013). The WEPP database is fairly comprehensive; however, some plants in the database do not include information of the cooling system used. In these cases, a number of assumptions have been considered to assign a cooling system type to each of them.

The capacity factors for the calculation of the electricity production in MWh for each plant have been estimated using UN (2017) and IRENA (2018) data of installed capacity and electricity generation by fuel type at a country level.

R. Gonzalez (✉) · N. Scarlat
European Commission, Joint Research Centre (JRC), Directorate for Energy, Transport and Climate, Energy Efficiency and Renewables, Ispra, Italy
e-mail: Rocio.GONZALEZ-SANCHEZ@ec.europa.eu

N. Scarlat
e-mail: Nicolae.SCARLAT@ec.europa.eu

The water use in renewable energies is also included in the study showing a wide variation across technologies. Macknick et al. (2011) and Meldrum et al. (2013) provide water factors for solar (PV and CSP), wind, biofuel, geothermal, and hydroelectricity. Operational water requirements for PV and wind are mainly for cleaning purposes, making these two technologies the ones with the lowest water footprint of electricity generation. Gerbens-Leenes et al. (2009) provide a comparison of the water footprints for different primary energy carriers, showing that the water footprint of hydroelectricity is the highest aside from biomass production. Evaporation from the reservoirs is the main water loss in hydroelectric plants; however, it is difficult to estimate accurately due to lack of data, having the highest range of variation among the water factors (Macknick et al. 2011; Meldrum et al. 2013). It is important to consider the water consumption of hydropower production due to the fact that it represents 15% of the total installed capacity in Africa (WEPP 2016) and 80% of all renewables (IRENA 2018). A preliminary analysis of the water footprint of hydroelectricity based on data from 139 African dams has been performed, and some results will be presented. A more in-depth analysis is underway with the results to be presented in the authors' future work.

A point to take into account is that water consumption and withdrawals depend not only on the fuel type, technology used, and cooling system but also on the location and climate. The water factors provided by the literature do not display these differences, and therefore, climate and location

differences are not considered for the water estimations at this stage of the present study.

3 Results and Discussion

In the year 2016, electricity in Africa was generated mainly from natural gas (39%), coal (23%), oil (18%), hydroelectricity (15%), and the remaining from solar, wind, biomass, geothermal, nuclear, and waste heat (5.3%). Renewable energies accounted for a total of 20%. Water consumption for fuel production and water consumption and withdrawals for power plant operation are depicted in Figs. 1, 2, and 3, showing the top 25 and 20 countries, respectively, in terms of water use. The total water consumed for fuel production (oil, natural gas, coal, and uranium) in Africa was 1292 million m^3. Leading countries include Algeria, Nigeria, Angola, Egypt, and Libya with economies based on oil and South Africa based on coal. The highest water consumption for fuel production corresponds to oil with 91% of the total water consumed, including extraction and refining.

Total water consumption and withdrawals for electricity generation account for 503 and 23,461 million m^3, respectively. A total of 95 and 90% share of the water consumption and withdrawals, respectively, are covered by fossil fuels, mainly by coal (64% of the consumption, driven by South Africa) and natural gas (60% of the withdrawals, lead by northern African countries). This appears to be a consequence of the generalized use of wet cooling towers in coal

Fig. 1 Water consumption for fuel production in 2015
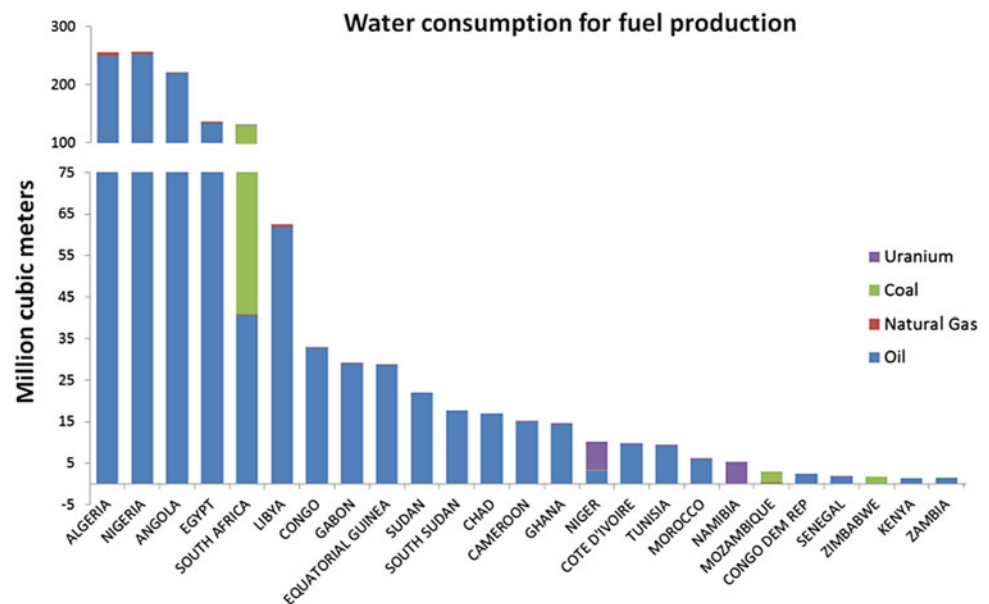
Fig. 2 Water withdrawals for electricity generation in 2016
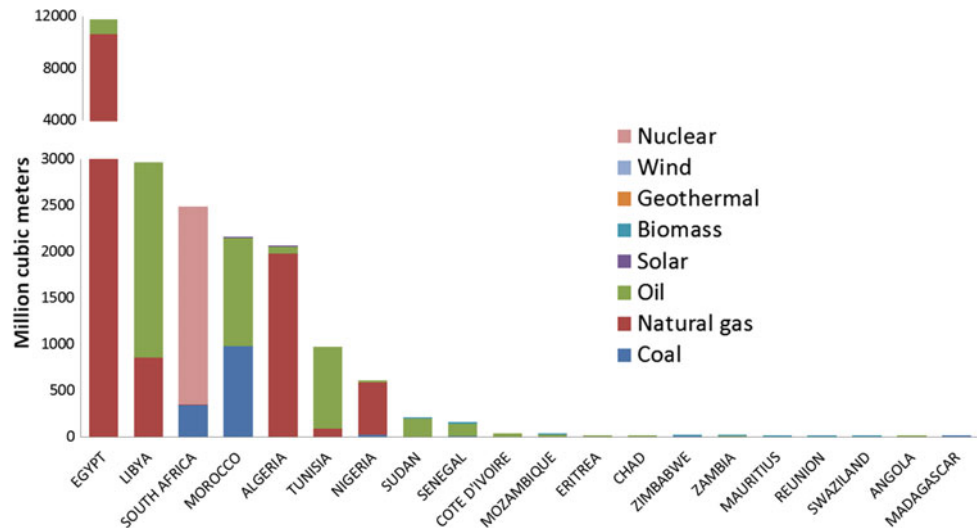
Fig. 3 Water consumption for electricity generation in 2016
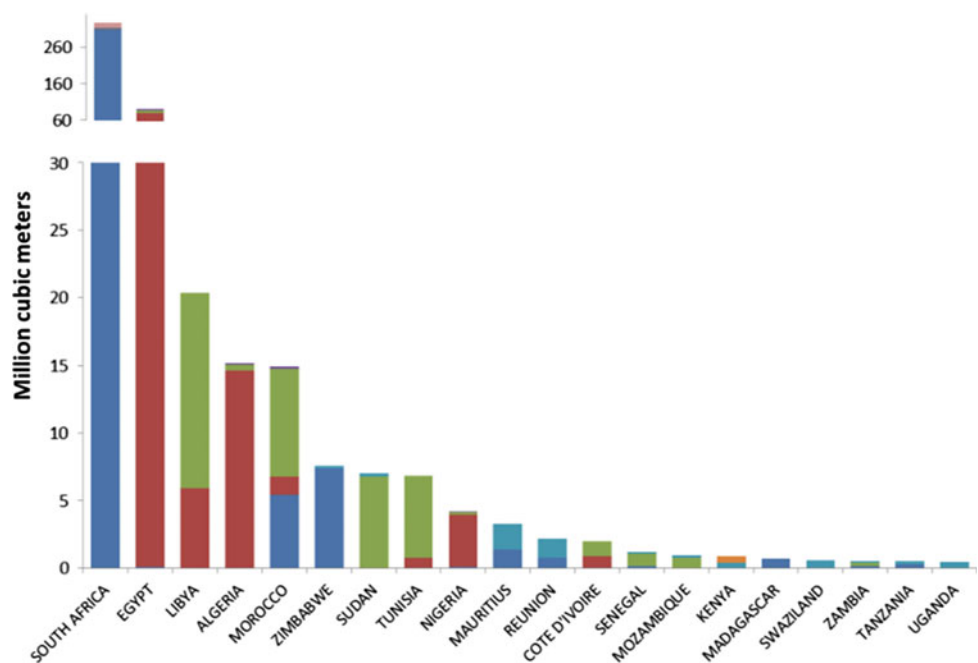
power plants and once-through cooling systems in natural gas power plants throughout Africa. Renewable energies (not including hydroelectricity) cover 2% of water consumption and 0.06% of water withdrawals.

It is important to note that hydroelectric plants have not been included in this comparison. A preliminary analysis of 139 hydroelectrical plants in Africa for which data were available shows a water consumption (water loss by evaporation) of around 9066 million cubic meters. These plants represent only 75% of the total hydroelectric installed capacity in Africa and 12% of the total installed capacity of the continent. The magnitude of the results indicates that water use for hydroelectricity production should be carefully looked at.

4 Conclusion

A preliminary analysis of the water use (consumption and withdrawals) for energy production in Africa has been performed (hydropower not included), showing a clear dominance of fossil fuels. Future work should be focused on several points such as refining the data on cooling systems, a better and more complete estimation of water use for hydroelectricity, and the inclusion of water use for biofuel production, taking into account also fuelwood as an important source of energy for cooking in Africa. These estimations could be further refined considering also different climatic conditions and geographical locations.

References

AFREC. (2017). *Africa energy database*.

Gerbens-Leenes, P. W., Hoekstra, A. Y., & van der Meer, T. (2009). The water footprint of energy from biomass: A quantitative assessment and consequences of an increasing share of bio-energy in energy supply. *Ecological Economics, 68*(4), 1052–1060.

IEA. (2014). Water Energy Nexus (World Energy Outlook 2016).

IEA. (2015). Retrieved May 2018, from https://www.iea.org/statistics/statisticssearch/report/?country=ETHIOPIA&product=balances&year=2015.

IRENA. (2018). *Renewable electricity capacity and generation statistics*. Retrieved April, 2018, from http://resourceirena.irena.org/gateway/dashboard/?topic=4&subTopic=54.

Macknick, J., Newmark, R., Heath, G., & Hallett, K. (2011). *A review of operational water consumption and withdrawal factors for electricity generating technologies*. National Renewable Energy Laboratory.

Meldrum, J., Nettles-Anderson, S., Heath, G., & Macknick, J. (2013). Life cycle water use for electricity generation: A review and harmonization of literature estimates. *Environmental Research Letters, 8*(1), 015031.

NEPAD (New Partnership for Africa's Development). (2006). *Water in Africa: Management options to enhance survival and growth*. Addis Ababa, United Nations Economic Commission for Africa (UNECA).

PLATTS. (2016). WEPP.

UN Data. (2017). *Energy statistics database*.

World Nuclear Association. (2015). Retrieved May, 2018, from http://www.world-nuclear.org/information-library/nuclear-fuel-cycle/mining-of-uranium/world-uranium-mining-production.aspx.

Wu, M., & Chiu, Y. (2011). *Consumptive water use in the production of ethanol and petroleum gasoline-2011 update*. Center for Transportation Research.

Evaluation of Water–Energy Nexus in Sakarya River Basin, Turkey

Zeynep Özcan, Merih Aydınalp Köksal, and Emre Alp

Abstract

Achieving sustainable water–energy relationship is especially important for semi-arid regions. Water consumption due to electricity generation can reach up to 8.4% of the total water potential in the study area. Between 659 and 2851 m^3 of water is found to be consumed per GWh of electricity generated at cooling systems.

1 Introduction

Water–energy systems have interconnected relationship. While water is needed to generate energy, energy is required for water extraction, treatment, and distribution. It is important to understand this relationship since a demand failure in one of the systems can cause a breakdown in the other one. Increase in water and energy demand, growing population, and climate change are significant threats to these systems. Achieving sustainable water–energy relationship is especially important for semi-arid regions where water availability is low. Water security is defined as access to safe drinking water and sanitation. While it is not part of most water security definitions yet, availability of and access to water for other human and ecosystem uses is also very important from a nexus perspective (Hoff 2011). Energy security, on the other hand, is defined as access to clean reliable and affordable energy services for cooking and heating, lighting, communications, and productive uses (WWAP 2014), and as uninterrupted physical availability of energy at a price which is affordable, while respecting environmental concerns. Gleick (1994) stated that energy and freshwater resources are intricately connected; that is, we use energy to help us clean and transport the fresh water we need, and we use water to help us produce the energy we need. This relationship between water and energy is called as water–energy nexus. Based on this description, ensuring energy security actually depends on ensuring water security and vice versa.

In light of this information, this study aims to evaluate the water–energy nexus in Sakarya River Basin (Fig. 1) which constitutes the 3.4% of total water potential of Turkey. Total surface water and groundwater potential of the basin are 5231 and 1806.7 hm^3/year, respectively. Sakarya River Basin is located in the northwest of Turkey and it has a semi-arid climate. It constitutes 7% of surface area of Turkey with a drainage area of 58,160 km^2. The population of the basin is 7.5 million and it represents 10% of Turkey's population. The total length of the Sakarya River along with its branches is 720 km. The majority of the watershed consists of agricultural lands with 52% of the total watershed area, and it is followed by forests and semi-natural area with 45%.

Sakarya River Basin has a high demand for electricity since it contains 20 active industrial zones. The total number of power plants within the basin is 98 with a total installed capacity of 5974 MW. Out of this 98 power plants, 46 of them are fossil fueled with a total installed capacity of 5220 MW (88% of the total). The installed capacities of these fossil-fueled plants range between 0.5 and 1540 MW, and the number of plants with installed capacities higher

Z. Özcan · E. Alp (✉)
Department of Environmental Engineering,
Middle East Technical University, Ankara, Turkey
e-mail: emrealp@metu.edu.tr

Z. Özcan
e-mail: zozcan@metu.edu.tr

M. A. Köksal
Department of Environmental Engineering,
Hacettepe University, Ankara, Turkey
e-mail: aydinalp@hacettepe.edu.tr

Fig. 1 Sakarya River Basin

than 30 MW is only 10. Among these fossil-fueled plants, the natural gas plants are dominant in terms of both number (23 plants) and installed capacity (3389 MW, 57% of the total), which is followed by coal/lignite power plants (1688 MW, 28 & of the total) (Table 1). Significant amount of water is lost through evaporation at hydroelectric power plants; hence, the water loss due to evaporation is also evaluated within the context of this study. There are 24 hydroelectric power plants in the Sakarya River Basin with a total installed capacity of 684 MW. The installed capacities of the hydroelectric power plants range between 0.18 and 278 MW.

Water–energy nexus can be dissected into two aspects: water for energy (WFE) and energy for water (EFW). In the context of this study, it is aimed to determine the amount of water consumed for electricity generation in the Sakarya River Basin. Significant amount of water is used for every step of electricity generation, i.e., fuel production, fuel

Table 1 The number of total capacity of thermal and non-thermal power plants

Fuel type		Number of power plants	Total installed capacity (MW)	Percentage (%)
Thermal power plants	Natural gas	23	3389	57
	Coal, lignite	8	1688	28
	Biomass	10	71	1.2
	Fuel oil	3	56	0.9
	Waste heat	1	6	0.1
	LPG	1	10	0.2
Non-thermal power plants	Solar	26	31	0.5
	Hydroelectric	24	684	11
	Wind	2	39	0.7
Total (Thermal + Non-thermal)		98	5974	

processing, and cooling systems in thermal power plants. In the scope of this study, the amount of water used in thermal power plants' cooling systems and the amount of water lost through evaporation in hydroelectric power plants are determined. By using these findings, it is aimed to determine what fraction of water potential of the basin is used for the cooling systems in the thermal power plants and lost with evaporation in hydroelectric power plants.

2 Materials and Methods

In the first stage of the study, the type of cooling systems, annual electricity generation, and water consumption of the plants are determined from companies' Web sites, from open literature or with plant visits. Using this information, the water consumption factors (WCF) of the power plants were calculated for each cooling system type as given in Eq. (1).

$$\text{WCF} = \frac{\text{Annual total water consumption } (\text{m}^3/\text{year})}{\text{Annual electricity generation } (\text{kWh/year})} \quad (1)$$

Similarly, the evaporation data of the hydroelectric power plants are obtained from the master plan prepared by State Water Works (SWW 2017).

3 Results and Discussion

When 46 thermal power plants are compared in terms of their cooling systems, it is seen there are 29 plants with dry cooling systems covering almost half of the total installed capacity of the basin (2668 MW). Out of 29 plants, 21 of them are natural gas power plants.

Within the context of the study, five natural gas and coal power plants installed capacities between 270 and 1540 MW are visited, and detailed information on their water use is obtained. Out of these five plants, two of them have dry cooling systems. The field data obtained through these plant visits show that the WCF of the plants with wet cooling system is determined between 659 and 2851 m^3 per GWh of electricity generated. The WCF of the plants with dry cooling systems is determined as 104 m^3/GWh. Similarly, the water withdrawal factors (WWF) of the plants are also determined. Based on these calculations, it is clearly seen that the plants with wet cooling system have higher water withdrawals and consumptions than the ones with dry cooling systems, which is also stated in the open literature (Macknick et al. 2012). Total water consumption of the thermal power plants is calculated as 27.72 hm^3/year. Hydroelectric power plant evaporation data are only available for the four major plants, which have installed capacities of 278, 160, 51, and 38 MW. The evaporation data are not available for the remaining 42 hydro power plants. The available data show that the total amount of water lost through evaporation is 58.13 hm^3/year.

Since Sakarya River has an average flow of 5231 hm^3/year; the amount of water consumed by thermal power plants and lost through evaporation in hydroelectric power plants make up 0.53 and 1.11% of the total water potential of the basin, respectively. The thermal power plants and hydroelectric power plants are mainly located in the middle region of the basin. There are six sub-basins in the basin; Orta Sakarya (Middle Sakarya) sub-basin (see Fig. 1) is the one where both industrial and agricultural activities are the most intense within the basin. Hence, the calculations are also performed on the basis of sub-basins. It is found that

water consumption can reach up to 8.4% of the total water potential in the Orta Sakarya sub-basin.

4 Conclusion

Sakarya River Basin is a semi-arid region with a high energy demand and production. There is considerable number of power plants, and hence, significant amount of water is used during electricity generation. In addition, there are several hydroelectric power plants with high installed capacities. Thus, the water loss through evaporation is also high. Increasing water and energy demand, growing population and climate change are putting more pressure on water and energy systems. These pressures will be more critical considering the fact that Sakarya River Basin has a semi-arid climate. Thus, it is important to understand the nexus thoroughly to be able to take precautions and to intervene when necessary. At this point, water conservation techniques in energy sector play a critical role. With these techniques, it is possible to save up to 30% of the water consumed. Considering all of these facts, this study aims to shed light on water–energy nexus in terms of water consumption in the power plant cooling systems and the hydroelectric power plants in the Sakarya River Basin.

References

Gleick, P. H. (1994). Water and energy. *Annual Review of Water and the Environment, 19,* 267–299.

Hoff, H. (2011). *Understanding the Nexus: Background paper for the Bonn 2011 nexus conference: The water, energy and food security nexus*. Stockholm Environment Institute: Stockholm, Sweden.

Macknick, J., Newmark, R., Heath, G., & Hallett, K. C. (2012). Operational water consumption and withdrawal factors for electricity generating technologies: A review of existing literature. *Environmental Research Letters, 7*(4), 45802.

SWW. (2017). Sakarya Havzası Master Plan Final Report, Ankara, Turkey.

WWAP (United Nations World Water Assessment Programme). 2014. *The United Nations World Water Development Report 2014: Water and Energy*. Paris: UNESCO.

Water-Energy Nexus in Shallow Geothermal Systems

Alessandro Casasso and Rajandrea Sethi

Abstract

Ground-source heat pumps (GSHPs) reduce CO_2 emissions compared to conventional heating and cooling systems. The thermally altered zone (thermal plume) is a key aspect for land management of GSHPs.

Keywords

Ground-source heat pump • Heat transport • Greenhouse gases • Thermal plume

1 Introduction

Shallow geothermal energy is a widely available renewable energy source, which can be used to cover the heating and/or cooling demand of buildings through ground-source heat pumps (GSHPs). Closed-loop systems, also known as ground-coupled heat pumps (GCHPs), exchange heat with the shallow ground through pipes buried at different depths and in different modes: shallow heat collectors (pipes buried horizontally at 1–3 m of depth), thermo-active structures (pipes installed into other foundation elements such as foundation piles or diaphragms), and borehole heat exchangers (pipes installed into a small diameter borehole, drilled on purpose). Open-loop systems, or groundwater heat pumps (GWHPs), exchange heat directly with groundwater through abstraction and reinjection well(s). GSHPs can reduce up to 90% of CO_2 emissions compared to gas boilers, depending on the carbon intensity of the electrical grid (Rivoire et al. 2018). Also, heat pumps have no air pollutant emissions on site, which is a great strength compared to wood biomass in view of increasing renewable heat

production, especially in urban areas. However, shallow geothermal energy is a limited resource which should be managed to avoid its overexploitation. The propagation of thermal alteration (plumes) is therefore a key aspect to be assessed in the design phase. In this paper, we provide figures on the avoided greenhouse gas (GHG) emissions and indications on the thermal footprint assessment for shallow geothermal systems.

2 Climate Change Mitigation

About 40% of the energy consumption, and about 30% of the total GHG emissions in the world, can be attributed to buildings (Nejat et al. 2015). For this reason, reducing the use of fossil fuels in this field is essential to mitigate the global warming trend. Shallow geothermal systems can reduce the carbon intensity of both heating and cooling of buildings, and this reduction can be assessed by comparing CO_2 emission factors of different technologies, i.e. the CO_2 equivalent, per unit of heat conveyed or removed from the building. Heating with fossil fuels produces GHG ranging between 240 g CO_2/kWh (methane) and 306 g CO_2/kWh (heating oil) (Koffi et al. 2017). The emission factor of a heat pump is the ratio between the emission factor of the electricity supply and the seasonal performance factor (SPF) of the heat pump. The SPF is the ratio between the heat delivered to (or removed from) the building and the electricity consumed in a heating or cooling season. An estimation of CO_2 emission factors of different types of heat pump in heating mode is reported in Table 1 for some European countries, along with a comparison with a gas boiler. GWHPs are the most efficient among heat pump systems and hence also the least carbon-intensive, but they require the presence of a productive aquifer, while GCHPs can be installed almost everywhere (Casasso and Sethi 2017). With the average energy mix adopted for electricity production in European Union (EU-28), heat pumps reduce 38% to 63% of GHG emissions compared to gas boilers,

A. Casasso (✉) · R. Sethi
Politecnico di Torino—DIATI, Corso Duca Degli Abruzzi 24, 10129 Turin, Italy
e-mail: alessandro.casasso@polito.it

R. Sethi
e-mail: rajandrea.sethi@polito.it

Table 1 Comparison of the CO_2 emission factors (EFs) for electricity (*Source* Ref. Koffi et al. (2017)) and for heating with air-source, closed-loop and open-loop geothermal heat pumps. The variation of CO_2 emissions compared to gas boiler is reported (negative=reduction, positive=increase)

Country	Electricity EF (gCO_2/kWh)	Air source (SPF = 3)		Closed-loop geothermal (SPF = 4)		Open-loop geothermal (SPF = 5)	
		EF	CO_2 red. (%)	EF	CO_2 red. (%)	EF	CO_2 red. (%)
Sweden	38	13	−94.7	10	−96.0	8	−96.8
France	93	31	−87.1	23	−90.3	19	−92.3
Italy	424	141	−41.1	106	−55.8	85	−64.7
EU-28	444	148	−38.3	111	−53.8	89	−63.0
Germany	658	219	−8.6	165	−31.5	132	−45.2
Poland	1090	363	+51.4	273	+13.5	218	−9.2
Estonia	2017	672	+180.1	504	+110.1	403	+68.1

a margin likely to increase with time since electricity is reducing its carbon intensity (−14.1% in EU-28 from 2004 to 2013 (Koffi et al. 2017)). On the other hand, heat pumps are still more carbon-intensive than fossil fuels in countries such as Poland and Estonia, where most of the electricity is produced with coal (Table 1). Geothermal heat pumps reduce CO_2 emissions also in cooling mode: since most chillers are driven with electricity, the emissions depend on the electricity consumed and hence on the SPF. For example, a GWHP with SPF = 5 emits 40% GHG less than an air-source chiller with SPF = 3, regardless of the carbon intensity of the electrical production.

Since buildings may have both a heating and a cooling demand, the climate change mitigation effect may vary depending on the building type and on the climate, which determines the usage profile. According to Rivoire et al. (2018), the highest benefits are achieved in heating-dominated buildings if the electricity CO_2 emission factor is not higher than the EU-28 average (444 g CO_2/kWh), while GSHPs driven with carbon-intensive electricity (800 g CO_2/kWh or higher) are beneficial only for cooling-dominated buildings.

3 Thermal Impact on the Subsurface

The use of the ground as a heat source or sink results in the propagation of a subsurface thermal plume, which should be assessed to support the land management of geothermal installations. The extent of the plume depends on (i) the type of heat exchanger (closed or open loop), (ii) the thermal power and the usage profile, (iii) the thermal properties of the ground (thermal conductivity and, to a lesser extent, capacity), and (iv) the hydrodynamic properties (hydraulic conductivity and gradient, saturated thickness) of the aquifer. Closed-loop systems are based on a mainly conductive heat exchange with the ground, and generally, the thermal footprint of these systems does not largely exceed the surface occupied, while open-loop systems exchange large thermal power across the relatively small depth of the

aquifer, thus propagating their impact at relatively large distances outside the cadastral plot of the building. An example of land planning issues of open-loop geothermal systems is shown in Fig. 1, and it is drawn from a feasibility study for the use of GWHPs to cover the heating needs of a small-town historical centre in NW Italy (Becchio et al. 2017). Two different configurations were hypothesized: 17 GWHPs, each one connected to a few buildings (Fig. 1a), and a district heating network with a large power GWHP composed of three abstraction and three injection wells (Fig. 1b). The district heating configuration proves to be more efficient compared to the installation of individual systems, since the abstracted water temperature is not negatively impacted by the plumes propagated from upstream installations, and the thermal impact of the district heating power station propagates towards an uninhabited area.

The effect of thermal and hydrogeological subsurface properties on the propagation of thermal plumes from GWHPs has been recently addressed by Piga et al. (2017). They identified the thermal plume with the ±1 °C temperature alteration isotherms: for example, if the undisturbed aquifer temperature is equal to 12 °C, the isotherm of 11 °C or 13 °C is the boundary of the thermal plume, depending on the prevailing mode (heating or cooling). Two timescales of thermal plume propagation affect the management of open-loop systems. In the short term, i.e. within a year, GWHPs alternatively inject cold water during heating seasons and warm water during cooling seasons, which may affect the closest neighbouring and downstream installations. At larger distances, water temperature oscillations are dampened and an average long-term (and long-range) temperature alteration is observed, which depends on the prevailing use between heating and cooling. The long-term effect of GWHPs is cumulated from upstream to downstream and may therefore mitigate (or exacerbate) the underground heat island, i.e. the anthropogenic heat anomaly of aquifers in urban areas (Menberg et al. 2013). The main source of uncertainty in the simulation of thermal plumes is the groundwater flow velocity: as the plume area diminishes at higher flow velocities, this means that a higher spatial

Fig. 1 Comparison of the thermal plumes propagated from multiple GWHPs (**a**) and a single GWHP for district heating (**b**). Processed from Becchio et al. (2017)
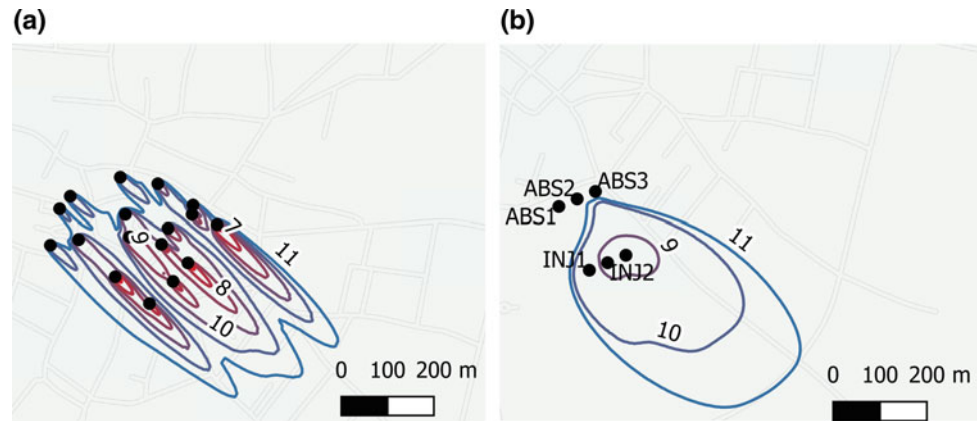
density of geothermal systems is sustainable. However, the hydraulic conductivity is hardly known with precision, and it is a highly heterogeneous parameter. The propagation of thermal plumes should be performed in 3D to take into account the thermal exchange of the aquifer with overlying and underlying strata; however, using a 2D geometry (thus neglecting these heat exchanges) is a conservative approach since the plume size is overestimated. Finally, the unbalance between heat abstracted (heating) and injected (cooling) into the aquifer is a key parameter, and this means that heating and cooling thermal loads should be evaluated with care, since overestimating them could be not on the safe side.

A share of the injected flow rate can also return to the abstraction well, thus inducing a thermal drift of abstracted groundwater called thermal recycling. Thermal recycling can impair the performance of the heat pump or even lead to the failure of the geothermal system. Recently, Casasso and Sethi developed a numerical code for its quick assessment (Casasso and Sethi 2015).

4 Conclusions

GSHPs could dramatically reduce the CO_2 emissions due to the heating and cooling of buildings, thus contributing to the mitigation of climate change. The carbon intensity of GSHPs depends on its efficiency (SPF) and on the energy mix adopted to produce electricity but, with the average EU-28 energy mix, heat pumps reduce the GHG emissions of 38 to 63%. The subsurface thermal impact of GSHPs is a crucial aspect to be addressed through numerical simulations based on a thorough characterization of the aquifer and of the heating/cooling demand.

References

Becchio, C., Bottero, M. C., Casasso, A., et al. (2017). Energy, economic and environmental modelling for supporting strategic local planning. *Procedia Engineering, 205,* 35–42. https://doi.org/10.1016/j.proeng.2017.09.931.

Casasso, A., & Sethi, R. (2015). Modelling thermal recycling occurring in groundwater heat pumps (GWHPs). *Renewable Energy, 77,* 86–93. https://doi.org/10.1016/j.renene.2014.12.003.

Casasso, A., & Sethi, R. (2017). Assessment and mapping of the shallow geothermal potential in the province of Cuneo (Piedmont, NW Italy). *Renewable Energy, 102*(Part B), 306–315. http://dx.doi.org/10.1016/j.renene.2016.10.045.

Koffi, B., Cerutti, A., Duerr, M., et al. (2017). *CoM default emission factors for the member states of the European Union—Version 2017.* European Commission, Joint Research Centre (JRC).

Menberg, K., Blum, P., Schaffitel, A., & Bayer, P. (2013). Long-term evolution of anthropogenic heat fluxes into a Subsurface Urban Heat Island. *Environmental Science and Technology, 47,* 9747–9755. https://doi.org/10.1021/es401546u.

Nejat, P., Jomehzadeh, F., Taheri, M. M., et al. (2015). A global review of energy consumption, CO_2 emissions and policy in the residential sector (with an overview of the top ten CO_2 emitting countries). *Renewable and Sustainable Energy Reviews, 43,* 843–862. https://doi.org/10.1016/j.rser.2014.11.066.

Piga, B., Casasso, A., Pace, F., et al. (2017). Thermal impact assessment of groundwater heat pumps (GWHPs): Rigorous vs. simplified models. *Energies, 10.* https://doi.org/10.3390/en10091385.

Rivoire, M., Casasso, A., Piga, B., & Sethi, R. (2018). Assessment of energetic, economic and environmental performance of ground-coupled heat pumps. *Energies, 11.* https://doi.org/10.3390/en11081941.

Singular Applications of Capacitive Deionization: Reduction of the Brine Volume from Brackish Water Reverse Osmosis Plants

Julio J. Lado, Cleis Santos, Enrique García Quismondo,
Marc A. Anderson, Belén Gutiérrez, Fernando Huertas,
Antonio Ordóñez, and Ángel de Miguel

Abstract

Current desalination technologies present certain limitations associated with brine management. CDI operational conditions similar to EDL capacitors might become a solution for brine volume reduction. Innovative operating procedure utilizes a concentrated brine stream as a washing solution during the salt desorption phase. A high energy efficiency in the adsorption–desorption cycle was obtained using the electrolyte replacement procedure. A coupled RO-CDI system integration was proposed as a method to reduce the volumetric flow of brine.

Keywords

Capacitive deionization • Electrochemical supercapacitor • Electrochemical water treatment • Brine concentration

1 Introduction

Due to the increasing worldwide water scarcity associated with the climate change, desalination technologies have been positioned as one of the solutions with the greatest potential for generating drinking water from brackish water sources. Reverse osmosis (RO) is the fastest-growing method of desalination but its implementation has still to confront the problems derived from the management of brines produced in the rejection streams. The effluent generated presents a relatively high salinity that is necessary to get rid of, either by effluent discharge, rising treatment costs, or by deep well injection, with the consequent potential risk to the environment. Capacitive Deionization (CDI) represents a promising technology that offers the opportunity to purify saline water by removing ionic species while storing energy simultaneously, using a straightforward, non-energy intensive and low environmental impact fashion (Anderson et al. 2010; Suss et al. 2015). CDI mechanism is based on the adsorption of charged particles (ions) in the electrical double layer of an electrode upon polarization by a direct current power source. This is essentially the same work principle as charging a supercapacitor. During deionization (or charging), a feed solution is circulated through polarized electrodes, usually based on activated carbon, resulting in a less concentrated output. In the regeneration step (or discharge), a wash solution is circulated while the electrodes are depolarized, so that ions are desorbed from the electrodes and pass into the bulk of the solution, resulting in a stream of higher concentration (final effluent solution). Here, the coupling of RO with CDI is proposed as a potential way for reducing the volume of effluent mitigating the environmental impacts of the brine on the environment.

2 Materials and Methods

Carbon electrodes were prepared by mixing activated carbon (Picactif BP 10) with polyvinylidene fluoride (PVDF), Vulcan XC-72R in a 8:1:1 mass proportion and adding N-methyl pyrrolidone (NMP) in order to form the slurry that was employed to coat a titanium foil. Then, the electrode was heated up 140 °C (2 °C/min ramp) for 4 h. In this fashion, electrodes with 50 µm carbon thickness and

J. J. Lado (✉) · C. Santos · E. G. Quismondo · M. A. Anderson
Electrochemical Processes Unit, IMDEA Energy Institute, Ave. Ramón de la Sagra 3, Mostoles Technology Park, E28935 Mostoles (Madrid), Spain
e-mail: julio.lado@imdea.org

C. Santos
Advanced Materials for Multifunctional Application Group, IMDEA Materials Institute, Eric Kandel 2, E28005 Getafe (Madrid), Spain

B. Gutiérrez · F. Huertas · A. Ordóñez
GS INIMA Environment, Calle Quintanavides 17, 28050 Madrid, Spain

Á. de Miguel
Proingesa, Calle Acero, 5, 47012 Valladolid, Spain

2 mg cm^{-2} were obtained. The cell consisted of a pair of carbon electrodes separated by non-conductive mesh. The cell was hydraulically sealed with Viton gaskets. The inter-electrode gap was controlled by a polypropylene electrolyte flow compartment 30 mm × 80 mm. The cell design utilizes two identical polypropylene plates (95 mm 45 mm × 10 mm). Two holes toward the top and bottom of the plates act as entries and exits for the electrolyte. The cells in the was held using two stainless steel plates and six screws and bolts. More details related to the cell configuration could be found in our previous work (Santos et al. 2018; Garcia-Quismondo et al. 2013). The flow circuit consisted of the cell and a Masterflex Model 77521-47 pump fitted with a Masterflex pump head, Type 7518-00, interconnected with Viton tubing. The tubing was connected to the cell entries and exits with polytetrafluoroethylene (PTFE) connectors. NaCl aqueous solutions were used as the electrolyte. Experiments were performed at a temperature of 298 K and employed 70 mL of electrolyte. Electrolyte was pumped through the CDI system at a constant flow rate of 1 mL s^{-1}. Constant current experiments were performed using an electrochemical workstation (Biologic VMP3 multichannel potentiostat–galvanostat coupled with EC-Lab v10.18 software). Consecutive charge-discharge cycles were performed using current densities ranging from 2.5 to 50 A m^{-2} and setting a maximum potential difference of 1.5 V. During testing, conductivity, pH and temperatures were measured periodically (Hanna Instruments HI 2550 pH/ORP & EC/TDS/NaCl Meter). A detailed explanation about the CDI experiments and the energy components calculations can be found in a previous work (Santos et al. 2018; Garcia-Quismondo et al. 2013, 2016).

3 Results and Discussion

Electrosorption experiments were performed using the high-efficient operating procedure (HEOP-CDI) described previously (Santos et al. 2018; Garcia-Quismondo et al. 2013, 2016). This procedure allowed us to test the CDI system performance using two different concentration solutions in each one of the CDI steps (removal and regeneration). This means that the CDI system is fed in the ion adsorption step with a brine solution (3–20 g L^{-1} NaCl) emerging from the RO system. Once the ion adsorption phase is finished, the water-treated solution is replaced by a concentrated brine stream (200 g L^{-1} NaCl) and the electrode regeneration step is conducted. This strategy has different purposes: (i) operate the CDI system maximizing the charge efficiency in each one of the cycles, (ii) concentrate the rejection solution in the discharge phase while increasing the water recovery of the whole system by treating the brine emerging from the RO system.

Figure 1 shows the Power–time plots recorded for a conventional mode using the same brackish solution in the deionization and regeneration steps, and for the HEOP-CDI using brine for regeneration. For both cases, one can see a linear response in voltage, with a positive slope during charge applying current when the anions and cations are adsorbed in the electrodes with opposite charge, and linear with a negative slope during discharge provoking the ion desorption. As expected for an electrochemical supercapacitor, the greater the area under the curve, the larger the energy stored or recovered in Watts hour (Wh). This is a typical characteristic of double-layer capacitors that allows to calculate relevant parameters such as the round-trip efficiency.

The round-trip efficiency is an important indicator of the electrochemical behavior of the CDI system. It can be calculated as the ratio between the energy retrieved during the discharge and the energy applied for charging, expressed as a percentage (%):

$$\eta_{\text{round-trip}} = \eta_{\text{charge}} \cdot \eta_{\text{discharge}} \tag{1}$$

Generally, the loss of efficiency in terms of energy in CDI comes from either ohmic losses or side reactions in the charge-discharge cycles. When medium-high currents are applied parasitic losses are minimized while keeping moderate ohmic losses. A conventional electrochemical capacitor can reach round-trip efficiencies over 95%. Results shown in Fig. 1 indicated that employing a brine solution in regeneration, the area under the curve in the regeneration step is enlarged increasing the discharge efficiency from 65 to 74%, and this has a positive impact on the round-trip efficiency that improves from 53 to 71%. The increase of the discharge efficiency observed during the ion desorption phase performed using the concentrated stream (200 g L^{-1} NaCl) indicated also that a larger amount of ions (previously adsorbed in the ion removal step) were desorbed from the electrodes to the brine effluent, increasing in this fashion the concentration of the brine. This result points out the potential of the HEOP-CDI for increasing the concentration of the rejection brines reducing consequently the brine disposal volume and thus improving the water recovery. The brine reduction volume would lead to an important decrease of the global desalination costs. Furthermore, the higher discharge efficiency of the ions previously adsorbed in the regeneration step means that more adsorption sites will be available for the next ion removal cycle improving, therefore, the salt adsorption capacity of the following cycles. This observation can be also appreciated in Fig. 1 in which an increase from 82 to 97% of the charge efficiency was observed during the ion removal step.

Extended laboratory experiments confirmed that it is possible to operate the CDI system using a range of

Conventional Mode

$\eta_{round\ trip} = \eta_{charge} \cdot \eta_{discharge} = 53\%$

Optimized Mode (HEOP)

$\eta_{round\ trip} = \eta_{charge} \cdot \eta_{discharge} = 71\%$
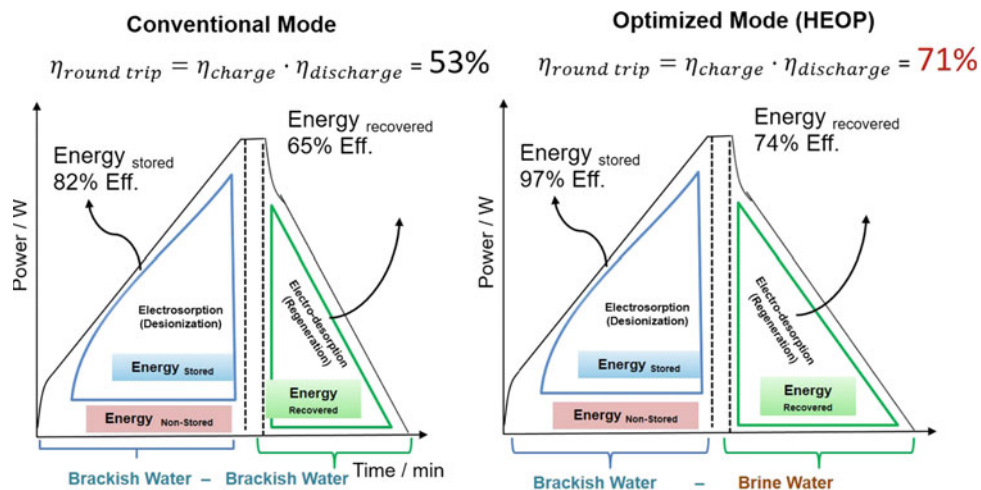
Fig. 1 Charge–discharge responses according to conventional (left) and optimized (right) procedures. Graphical results of charge, discharge and round-trip efficiencies for a 20 g L^{-1} NaCl solution was employed in the salt removal step (Charge) and a brackish water solution (200 g L^{-1}) was used in the salt desorption step. Currents applied were charge at 10 A m^{-2} and discharge at 10 A m^{-2} using the regular CDI system mode, charge at 10 A m^{-2} and discharge at 20 A m^{-2} using the optimized mode (HEOP) in order to compare both operational modes performance

concentrations between 3 and 20 g L^{-1} in the salt adsorption stage combined with salt concentrations of 200 g L^{-1} in the desorption step, confirming the charging/discharging behavior of a supercapacitor, and improving extensively the salt desorption step (electrode discharge) of the CDI system retrieving up to 70–80% of energy employed in the salt removal stage (electrode charge). Therefore, operating the CDI cell using the HEOP-CDI operational mode the system was able to increase the salt adsorption capacity (amount of ions removed by mass of electrode) in the charging step and increase the concentration of the rejection stream allowing the volume reduction of the brine that should be disposed.

4 Conclusion

Current desalination technologies present certain limitations associated to brine management. In this research, the role of a CDI system as a technique to treat the outgoing rejection from RO was evaluated. The evaluation of the CDI operational conditions allowed the authors to demonstrate an innovative operating procedure that utilizes a concentrated brine stream as a washing solution during the salt desorption phase (electrode regeneration). This operational mode provided a relatively high energy efficiency in the adsorption–desorption cycle rate which remarkably increases the water recovery possibilities. Based on the reported results, a coupled RO-CDI system integration was proposed as a method to reduce the volumetric flow of brine, and therefore, the brine disposal cost of the desalination plant.

References

Anderson, M. A., Cudero, A. L., & Palma, J. (2010). Capacitive deionization as an electrochemical means of saving energy and delivering clean water. Comparison to present desalination practices: Will it compete?, *Electrochimica Acta, 55*, 3845–3856.

Garcia-Quismondo, E., Santos, C., Lado, J., Palma, J., & Anderson, M. A. (2013). Optimizing the energy efficiency of capacitive deionization reactors working under real-world conditions. *Environmental Science and Technology, 47*, 11866–11872.

García-Quismondo, E., Santos, C., Soria, J., Palma, J., & Anderson, M. A. (2016). New operational modes to increase energy efficiency in capacitive deionization systems. *Environmental Science and Technology, 50*, 6053–6060.

Santos, C., Lado, J. J., García-Quismondo, E., Soria, J., Palma, J., & Anderson, M. A. (2018). Maximizing Volumetric removal capacity in capacitive deionization by adjusting electrode thickness and charging mode. *Journal of The Electrochemical Society, 165*(7), 294–302.

Suss, M. E., Porada, S., Sun, X., Biesheuvel, P. M., Yoon, J., & Presser, V. (2015). Water desalination via capacitive deionization: What is it and what can we expect from it? *Energy & Environmental Science, 8*, 2296–2319.

An Unprecedented Thousandfold Enhancement of Antimicrobial Activity of Metal Ions by Selective Anion Treatment

Jakka Ravindran Swathy, Ligy Philip, and Thalappil Pradeep

Abstract

The synergy between anions and cations is understood for their enhanced antimicrobial activity. Up to thousandfold enhancement of antibacterial and antiviral activity in drinking water by this technique. Enhancement makes disinfection of water affordable, compact and adaptable to multiple purification systems. A decrease in consumption of inorganic ions reduces health risks caused by disinfection by-products (DBPs). Thus DBPs and bioaccumulation related issues can be handled efficiently. This understanding of synergy helps to speed up the disinfection process.

1 Introduction

Complexity of contaminants, growth of population, emergence of resistive pathogens and their impact on the environment have led to the demand for advanced technologies for clean and safe drinking water. Such technologies to reach the masses should be efficient and affordable and thus several ion-based commercial water purification units (e.g., Silver-based treatments) are evolving. But several such technologies have been reported for the production of disinfection by-products (DBPs) which are toxic than the pollutant itself.

Antimicrobial activity of various transition metals is well-reported in the literature. Silver, copper, gold, iron and zinc have been of special interest, largely because they have no known long-term health effect on humans at the concentrations of use as well as their large disinfection potential. With high degree of certainty, it can be stated that biocidal property of silver is the highest researched subject of water purification. There are several mechanisms associated with the biocidal property of silver and copper and are covered in several recent articles (Pradeep 2009; Feng 2000). However, other transition metals are comparitively less effective disinfectants, especially with regard to enteric microorganisms (Xiu 2012). Anti-bacterial effect of transition metals is usually named as oligodynamic effect, as they are most effective at low concentrations (because of solubility limits imposed by various anions, they cannot exist as ions at higher concentrations in real water). It is suggested that toxicity of metal ions for fungi goes in the following order: Ag > Hg > Cu > Cd > Cr > Ni > Pb > Co > Au > Zn > Fe > Mn > Mo > and Sn (Berger et al. 1976). The presence of natural organic matter reduces the toxicity of biocides (Day et al. 1997). Similarly, silver ion is known to form complexes with organic species present in water. It is therefore understood that silver ion as an antimicrobial agent is severely affected by the presence of other ions and species in drinking water. Similarly, other transition metals also suffer from similar difficulties imposed by various species present in water. It is therefore important to develop new antimicrobial compositions containing transition metal ions like silver, copper, zinc ion, which can provide disinfection ability in diverse conditions of water quality.

Availability of appropriate sites for adsorption is important for effective antibacterial activity. A study has shown

J. R. Swathy (✉) · T. Pradeep
DST Unit of Nanoscience (DST UNS) and Thematic Unit of Excellence (TUE), Department of Chemistry, Indian Institute of Technology Madras, Chennai 600036, India
e-mail: mailmeswathy@gmail.com

T. Pradeep
e-mail: pradeep@iitm.ac.in

L. Philip
EWRE Division, Department of Civil Engineering, Indian Institute of Technology Madras, Chennai 600036, India
e-mail: ligy@iitm.ac.in

the relevance of lipopolysaccharide (LPS)-cation interaction with bacteria to demonstrate how the resistance to microorganisms originates (Schneck 2010). LPS is a major polysaccharide present in the outer membrane of gram-negative bacteria and therefore interacts with the external environment. It is suggested that Ca^{2+} forces the replacement of K^+ ion from the negatively charged LPS and leads to the aggregation of O-side chain in LPS. With reduced surface energy, sites become inaccessible for biocidal species to enforce bactericidal action. It is important to note that concentration of biocides is significantly low (in ppb level) which limits their availability to microorganisms (Herrmann 2015). To nullify the effect of interfering species so as to retain the antibacterial activity, still remains a concern. It is learnt from prior art that the presence of various interfering species in water is a serious problem affecting the disinfection potential of wide range of biocides. It is an important need to identify a composition based on transition metal ions which provide robust antimicrobial activity even in the presence of various species present in water. It is important to note that such a composition should be permitted for use in water, especially drinking water.

Therefore, the objective of this work is to provide an effective, simple and cost-effective composition based on transition metal ions and more particularly silver, iron, zinc and copper ions for obtaining a resilient antimicrobial activity even in the presence of interfering species usually found in water. The activity if enhancement was tested on the transition metal ion M^{n+} releasing compound (like Ag^+, Cu^{2+}, Fe^{3+}, Zn^{2+}) along with either a CO_3^{2-}-releasing compound, HCO_3^- or a SiO_3^{2-}-releasing compound. The 5–100 ppm HCO_3^- / CO_3^{2-}-releasing compound is selected from $NaHCO_3$, $KHCO_3$, Na_2CO_3 or K_2CO_3, and the SiO_3^{2-}-releasing compound is selected from Na_2SiO_3 or K_2SiO_3. We have demonstrated that the killing efficiency of the combination is significantly improved compared to the killing efficiency obtained with transition metal ions alone (more particularly silver and copper ion). We initially focused on experiments to optimize the concentrations of anions below the drinking water norms (Secondary standard, US Environmental Protection Agency) and to decrease active-metal to minimum limits.

2 Materials and Methods

Testing protocol for antibacterial and antiviral efficacy: Synthetic challenge water was used for all the testing. Flasks containing 100 mL of water were spiked separately with 10–50 ppb of selected metal ions (Ag^+, Cu^{2+}, Fe^{3+}, Zn^{2+}) respectively and to the duplicates 10–50 ppm anions namely HCO_3^-, SiO_4^{2-} and CO_3^{2-} were spiked. A bacterial load

of $\sim 1 \times 10^5$ CFU/mL of *Escherichia coli* (ATCC 10536) was introduced into it. In the case of antiviral testing, $\sim 1 \times 10^3$ F-specific bacteriophage MS2 (ATCC 15597-B1) was used. Thereafter, the water was shaken gently and left for a contact time of 1 h, and subsequently, the viable microbial count was measured by conventional pour plate technique (for bacteria) and double layer plaque assay (for virus using *Escherichia coli host* C-3000 (ATCC 15597). Viable microbial counts were evaluated after an incubation period of 20–24 h at 37 °C. Corresponding control and blank experiments were maintained for each trial.

Concentration of Ag^+ present in both cells/viruses, and the filtrate were digested and measured using Perkin Elmer NexION 300X ICP MS.

3 Results and Discussion

In this work, we demonstrate the effectiveness of a synergetic combination of transition metal ions commonly used in water purification with the anions (SiO_4^{2-}, HCO_3^- and CO_3^{2-}) which enhances the antimicrobial activity. In order to explain the anion's promotional activity, a metal (25 ppb of Ag^+/Cu^{2+}/Fe^{3+}, Zn^{2+}) release device was prepared, using nanoparticle-loaded biopolymer composite (Sankar et al. 2013). To the output water various anions, namely NO_3^-, SO_4^{2-}, SiO_4^2, PO_4^3, I^-, Br^- and CO_3^{2-} (or species derived from them, at prevalent conditions), as many of them can also be present in natural waters, were added at varying amounts to achieve a cent percent potential system. Among these, SiO_4^{2-}, HCO_3^- and CO_3^{2-} were promising compared to other anions, and the latter was more significant in this property. Therefore, the experiments were designed to reduce the Ag^+ concentration to a minimum at acceptable metal ion levels, sufficient to kill bacterial and viral cells in the synthetic challenge water. It is important to note that antimicrobial activity due to bicarbonate, carbonate or silicate alone was insignificant even at 100 mM (10,000 ppm). However, we found that in presence of these anions, 50% lower concentration of silver, i.e., 25 ppb Ag^+, or 100 ppb Cu^{2+} was enough to obtain a complete 5-log reduction in the input bacterial load (up to 99%), in synthetic challenge water.

In the case of antiviral property, we observed that while 50 ppb Ag^+ alone (even after 1–2 h contact time) was unable to affect the phage, the combination of 50 ppb Ag^+ and 20 ppm CO_3^{2-} was found to achieve effective antiviral property within a contact time of 15 min. Moreover, by this study, we proved that this combination can handle virus at concentrations likely in groundwater (10^3 PFU/mL) but can also efficiently control comparatively higher concentrations ($\sim 10^6$ PFU/mL) that can prevail in non-portable water.
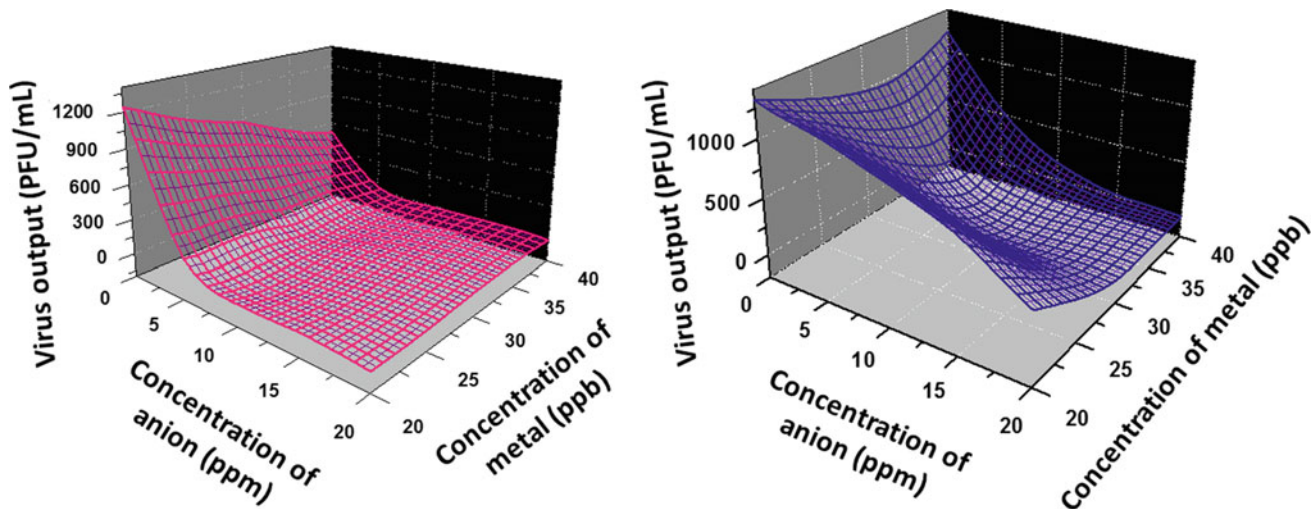
Fig. 1 Antibacterial activity of metal ions with anion at varying combinations. (In this case, metal used was Ag^+ and anion used was CO_3^{2-}). Bacteria tested: *E.coli*. Virus tested: MS2 bacteriophage grown on *E. coli*

4 Conclusion

In conclusion, the proposed combination of metal ions with selective anions like bicarbonates, carbonates and silicates yielded more than 5-log reduction in the case of bacteria and 3-log reduction in the case of virus at concentrations as low as 25 ppb. In the absence of anions, even double the concentration of efficient metals like silver (50 ppb) resulted in only 2-log reduction in the case of bacteria and negligible reduction in the case of virus. The mechanism behind the enhancement was found to be the disturbance caused to the cell by anions in water which target the peripheral membrane proteins. Thus, exposed cells were disturbed, and a lower concentration of transition metals was sufficient to cause complete cell damage. By reducing the metal concentration for antimicrobial activity, the unrecoverable release of metal ions into the environment is halved (Eckelman and Graedel 2007). This work leads to a new paradigm in the field of affordable water purification by reducing the cost of antimicrobial treatment, particularly in the developing world, without disinfection by-products.

A defective outer membrane/capsid is suspected as the reason for enhanced activity of the combination. Membrane permeabilization is seen in all the bacteria upon treatment with $Ag^+ + CO_3^{2-}$ (Fig. 1). We note that this happens for both *E. coli* and *Staphylococcus aureus*, showing the effectiveness of the composition for gram-negative and gram-positive bacteria. These peripheral proteins are associated with the membrane lipids and other proteins via electrostatic forces or hydrophobic interactions. Thus, conditions like high salt concentrations or an alkaline environment disrupt the interactions leading to the detachment of peripheral proteins (Hausman and Cooper 2000).

References

Berger, T. J., et al. (1976). Antifungal properties of electrically generated metallic ions. *Antimicrobial Agents and Chemotherapy, 10*(5), 856–860.

Day, G. M., et al. (1997). Influence of natural organic matter on the sorption of biocides onto goethite, II. Glyphosate. *Environmental Technology, 18*(8), 781–794.

Eckelman, M. J., & Graedel, T. E. (2007). Silver emissions and their environmental impacts: A multilevel assessment. *Environmental Science and Technology, 41*, 6283.

Feng, Q. L., et al. (2000). A mechanistic study of the antibacterial effect of silver ions on *Escherichia coli* and *Staphylococcus aureus*. *Journal of Biomedical Materials Research, 52*(4), 662–668.

Hausman, R. E. C., & Cooper, G. M. (2000).*The Cell: A molecular approach* (2ⁿᵈ ed., Chap. 2, pp. 29–34). Washington, D.C.: ASM Press.

Herrmann, M., et al. (2015). Bacterial lipopolysaccharides form physically cross-linked, two-dimensional gels in the presence of divalent cations. *Soft Matter, 11*(30), 6037–6044.

Pradeep, T. (2009). Noble metal nanoparticles for water purification: A critical review. *Thin Solid Films, 517*(24), 6441–6478.

Sankar, M. U., et al. (2013). Biopolymer-reinforced synthetic granular nanocomposites for affordable point-of-use water purification. *Proceedings of the National Academy of Sciences of the United States of America, 110*, 8459.

Schneck, E., et al. (2010). Quantitative determination of ion distributions in bacterial lipopolysaccharide membranes by grazing-incidence X-ray fluorescence. *Proceedings of the National Academy of Sciences, 107*(20), 9147–9151.

Xiu, Z.-m., et al. (2012). Negligible particle-specific antibacterial activity of silver nanoparticles. *Nano Letters, 12*(8), 4271–4275.

Harnessing Water Chemistry to Address Complex Water Challenges for a Thirsty World

Haizhou Liu

Abstract

Harnessing the photochemistry of chloramines can provide a promising approach for water reuse and treatment.

Keywords

Water chemistry • Photochemistry • Water reuse • Chloramines • Trace organic contaminants

1 Introduction

Water scarcity has become a global crisis. This situation is exacerbated—and will continue to be so—by the global shrinkage of surface water sources. Meanwhile, large populations have grown in these warm and arid regions. This shift in population and associated water demand make it extremely challenging and expensive to find high-quality natural water sources. Wastewater reuse offers the potential to significantly increase the global total available water resources. The major challenge to recycling is the development of efficient and cost-effective purification processes. In particular, our existing water treatment systems are poorly equipped to deal with trace organic chemicals including pharmaceuticals and personal care products, petroleum hydrocarbons and industrial solvents that are often present in the effluent.

Meanwhile, ultraviolet-driven advanced oxidation processes (UV/AOP) are becoming increasingly important for potable water reuse to remove trace chemical contaminants from wastewater effluent. The unique aqueous photochemistry of the overlooked but important chloramines can provide a novel approach for water reuse. Membrane treatment processes including microfiltration (MF) and reverse osmosis (RO) are employed prior to any UV/AOP in water reuse facilities. Chloramines are deliberately generated in the feed water to minimize membrane biological fouling. Because of their small molecular size and neutral charge, chloramines easily diffuse through RO membranes and subsequently will undergo photolysis in the UV/AOP. The objective of this paper is to investigate the photochemistry of chloramines for water reuse applications.

2 Materials and Methods

All chemicals used were of ACS or equivalent grade. Experiments were performed in deionized water (18.2 MΩ cm, Millipore). A 50 mM NH_2Cl solution was prepared by titrating a 30 mM solution of ammonium sulfate with a solution of 50 mM sodium hypochlorite. The ammonium sulfate was buffered to pH 8.8 with 4 mM of borate buffer. The solution was equilibrated for at least 1-h prior to use. For dichloramine, the pH of a ~ 50 mM NH_2Cl solution was lowered below 5.5 using perchloric acid. The dichloramine was equilibrated 10 min prior to use. The concentration of all chloramine and free chlorine concentrations in stock solutions were confirmed by standard DPD method prior to use (Rice et al. 2012).

Each experiment was carried out in an air-cooled photochemical reaction chamber (Ace Glass Inc.), using a low-pressure Hg lamp (254 nm) with a maximum energy fluence (UV dose) of 3500 mJ/cm^2 at 20 °C. The experimental solutions were dispensed into sealed 8-mL quartz reaction tubes and placed in the photoreaction chamber. Samples were removed at 5-min intervals and quenched with 5.5 mM thiosulfate to prevent further reaction of reactive species with 1,4-D. A competition kinetics approach was adopted for the calculation of steady-state radical concentrations (Zhang et al. 2015) in each experiment using nitrobenzene and benzoic acid as probes for reactive species formed in UV/chloramine systems. The pseudo-first-order degradation of nitrobenzene, 1,4-D, and benzoic acid were

H. Liu (✉)
Department of Chemical and Environmental Engineering,
University of California, Riverside, CA 92521, USA
e-mail: haizhou@engr.ucr.edu

used in combination with the second-order rate constants reported in the literature to calculate radical steady-states.

3   Results and Discussion

The photolysis of monochloramine and dichloramine was first characterized in a lab-scale investigation, and the transformation of 1,4-D was studied in single oxidant (monochloramine or dichloramine only), mixed chloramine (monochloramine and dichloramine), and mixed oxidant (monochloramine and dichloramine with H_2O_2) systems. For both monochloramine and dichloramine systems, amine-radical did not contribute to the degradation of 1,4-D; hydroxyl radical and chlorine dimer were responsible for 1,4-D transformation. The rate of 1,4-D removal increased with an increase in chloramine dosage in the single oxidant systems, until log removal peaked at a dose of 2 mM monochloramine and 4 mM for dichloramine in monochloramine and dichloramine system, respectively. With a further increase in chloramine concentration, log removal decreased due to scavenging of reactive species by chloramine oxidants. In a mixed chloramine system, the log removal of 1,4-D decreased with a decrease in monochloramine and an increase in dichloramine, although the relative contribution of hydroxyl radicals and chlorine dimer remained unchanged. These findings suggested that in a real system consisting of a mixture of chloramines, monochloramine would be the preferred oxidant.

4   Conclusion

The photolysis of chloramines produced amine and halide radicals, which further transformed into a series of reactive radical species that assist the contaminant degradation. These novel findings show that the presence of chloramines in UV/AOP as carry-over chemical residuals from membrane treatment processes can also be harnessed as an oxidant beneficial to water reuse.

References

Rice, E. W., Bridgewater, L., Association, A. P. H., Association, A. W. W., & Federation, W. E. (2012). *Standard methods for the examination of water and wastewater*. American Public Health Association.

Zhang, R., Sun, P., Boyer, T. H., Zhao, L., & Huang, C.-H. (2015). Degradation of pharmaceuticals and metabolite in synthetic human urine by UV, UV/H_2O_2, and UV/PDS. *Environmental Science and Technology, 49*(5), 3056–3066.

Photo(cata)lytic Membrane Bioreactors for Bacterial Disinfection and Antifouling Enhancement in Advanced Wastewater Treatment

Xiaolei Zhang and Kwang-Ho Choo

Abstract

Photo(cata)lytic membrane bioreactors (pMBR) were investigated for bacterial disinfection and fouling control. The pMBR achieved >2.5 log removal in total bacterial count under optimum condition. The signal molecules were significantly inactivated by the photo(cata)lytic treatment. Biofouling was well inhibited during continuous pMBR operation.

Keywords

Disinfection • Membrane fouling • Membrane bioreactor • Photocatalysis • Titania

1 Introduction

Photocatalytic disinfection with UV illumination onto TiO_2 particles is notable because it generates hydroxyl radicals on the surface of the catalyst (Cho et al. 2004; Foster et al. 2011). Photocatalytic degradation of toxic and refractory micropollutants under UV and/or visible light is additional merit of this method (Andriantsiferana et al. 2015). It has been demonstrated that the membrane photoreactor was able to degrade a variety of micropollutants and refractory organic matter in water, while managing the effective confinement of photocatalysts inside the reactor (Choo et al. 2008). In addition, significant virus removal (bacteriophage f2) was achieved by photocatalysis, showing the role of OH radicals and electrons generated (Zheng et al. 2015).

Viral inactivation was found to occur mainly by photocatalysis (as opposed to membrane filtration and TiO_2 adsorption). However, the bacterial disinfection of water and wastewater samples by the photocatalytic membrane reactor has not been well investigated.

In order to inhibit the biofilm formation on the membrane in membrane bioreactors (MBRs), quorum quenching (QQ) has been developed and widely studied as a new biofouling control strategy (Oh and Lee 2018). QQ approaches applied for MBR biofouling control mainly include: (1) inactivation of signal molecules using QQ enzyme, bacteria, and fungi (Kyungmin et al. 2009; Lee et al. 2016; Weerasekara et al. 2014); (2) biostimulation of QQ bacteria (Yu et al. 2016); (3) inhibition of quorum sensing receptors using signal molecule analogs (Ponnusamy et al. 2009). However, most of these approaches have their own limitations. The QQ enzyme, bacteria, or fungi are usually vulnerable or instable in real wastewater environments, which requires firm immobilization using specially designed media. This could increase the complexity of the operation in field applications. Signal molecule analogs and biostimulants seem costly for use in wastewater treatment.

It is thus interesting to investigate whether the degradation of signal molecules secreted by the microorganisms in MBRs can be inactivated by the photo(cata)lysis. Hence, a photo(cata)lytic MBR (pMBR) was tested as another strategy (targeting on different signal molecules) for biofouling control, compared to the microbial QQ strategy. Therefore, the focus of this study was to investigate the potential of photo(cata)lysis for degrading the signal molecules for quorum quenching and bacterial inactivation in batch and continuous reactor modes.

2 Materials and Methods

For bacterial inactivation tests, a pMBR was constructed and operated in continuously stirred tank reactor mode, while the secondary effluent was fed at the same flow rate as the

X. Zhang · K.-H. Choo (✉)
Advanced Institute of Water Industry, Kyungpook National University, 80 Daehak-ro, Buk-gu, Daegu 41566
Republic of Korea
e-mail: chookh@knu.ac.kr

K.-H. Choo
Department of Environmental Engineering, Kyungpook National University, 80 Daehak-ro, Buk-gu, Daegu 41566
Republic of Korea

permeate was discharged during the continuous runs. Initially, the feed and TiO_2 powders were mixed in the reactor (which was defined as −60 min in the time scale) and agitated for 60 min for equilibration before membrane filtration. There was no direct wastage or discharge of liquid from the reactor other than the membrane permeate. The reactor volume was maintained at a constant level (700 mL) throughout the experiments, with the use of a level sensor. The membrane was operated at a constant flux between 50 and 100 L/m² h (corresponding to a flow rate of 5–10 mL/min), so that the hydraulic residence time in the reactor varied between 140 and 70 min. Continuous experiments were run for 8 h evaluating the reactor performance (e.g., bacterial removal). The transmembrane pressure was also monitored continuously using a pressure sensor, which was recorded on a personal computer. An 8-W black light blue UV lamp (Sankyo, Japan) was used for the activation of TiO_2 photocatalyst. The UV lamp had a maximum wavelength of 360 nm, with a photon flux of 4 mW/cm².

For quorum quenching tests, batch reactors containing *N*-acyl homoserine lactone (C8-HSL) signal molecules ($\sim$200 nM) were run for 8 h. Continuous aeration (1 L/min) was provided to simulate the real reactor condition, and the degradation of the signal molecules was examined. Following the batch tests, continuous pMBR operations were carried out to find out the effect of photo(cata)lysis on biofouling control.

3 Results and Discussion

The efficacy of a pMBR for the removal of bacteria from secondary effluent was first investigated. The effects of pMBR components, such as catalyst doses, physical cleaning, and membrane permeability, on bacterial removal were evaluated during continuous reactor operations. It was found that the pMBR achieved disinfection through several mechanisms: rejection by a membrane, inactivation by direct UV radiation, adsorption onto photocatalysts, and oxidation by reactive oxygen species. Bacterial removal by the pMBR reached a maximum at a TiO_2 dose of 1.0 g/L, with the TiO_2 dose ranging between 0 and 5 g/L. The optimal TiO_2 dose for bacterial removal resulted from the trade-off between accelerated catalytic reactions and the light obstruction by surplus catalysts. Continuous aeration required for membrane fouling control had a negative impact on bacterial removal. Although intermittent backpulsing reduced bacterial removal, its impact was not as significant as that of continuous aeration. Backpulsing frequencies and durations did not play a significant
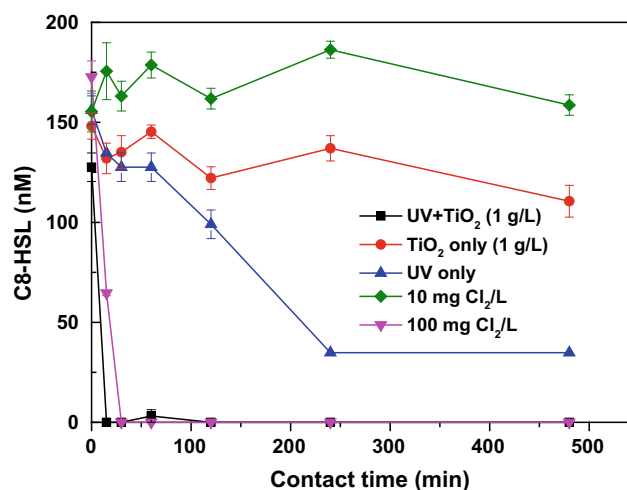
Fig. 1 Variations in C8-HSL concentration during the treatments using UV/TiO_2 (1 g/L) and chlorine (10 and 100 mg Cl_2/L)

role, but the dynamic cake layer formed on the membrane was responsible for the bactericidal behavior. An increase in membrane flux deteriorated the bacterial removal performance because it resulted in shorter reaction times, even though the formation of a thicker cake layer was possible at higher fluxes. The process can guarantee >2.5 log removal in total bacterial count, given that the optimal conditions are maintained. This is significantly larger than the removal achieved by microfiltration alone (ca. 0.5 log removal).

The effects of UV/TiO_2 (1 g/L), chlorine (10 and 100 mg Cl_2/L) on the C8-HSL degradation are shown in Fig. 1. The signal molecule C8-HSL was rapidly degraded by UV/TiO_2 (1 g/L) and consequently, the C8-HSL concentration reached almost 0 mM within 5 min of UV irradiation. The C8-HSL was also degraded quickly when high chlorine (100 mg Cl_2/L) was dosed. However, only 10% C8-HSL reduction was achieved by the low dose of chlorine treatment (10 mg Cl_2/L). The UV radiation alone already gave a significant reduction of C8-HSL (>85%) during the 480-min test, although the degradation rate was much slower than that of the UV/TiO_2 and 100 mg Cl_2/L of chlorine treatment. Almost no C8-HSL removal was observed by TiO_2 particles only, indicating that adsorption of signal molecules onto TiO_2 was negligible.

In addition to the batch test results, the pMBR inhibited the biofouling development on the membrane. Membrane fouling in the MBR was mitigated with photo(cata)lysis compared to that of conventional MBR. Fouling mitigation is possibly due to the inactivation of bacteria or degradation of organics, which may otherwise attach to the membrane

surface. However, further studies on specific mechanisms on antifouling efficacy by UV photolysis are needed.

4 Conclusion

Potential of photo(cataly)sis on membrane bioreactor treatment was investigated. The pMBR treatment achieved >2.5 log removal in total bacterial count under the optimal operating condition, which was significantly greater than the removal achieved by microfiltration alone. The C8-HSL could be rapidly degraded by UV/TiO$_2$ (1 g/L) and slightly inactivated by the UV irradiation alone. Significant biofouling delay was accomplished by the pMBR compared to the conventional MBR.

References

Andriantsiferana, C., Mohamed, E. F., & Delmas, H. (2015). Sequential adsorption-photocatalytic oxidation process for wastewater treatment using a composite material TiO$_2$/activated carbon. *Environmental Engineering Research, 20*(2), 181–189.

Cho, M., Chung, H., Choi, W., & Yoon, J. (2004). Linear correlation between inactivation of *E. coli* and OH radical concentration in TiO$_2$ photocatalytic disinfection. *Water Research, 38*(4), 1069–1077.

Choo, K.-H., Tao, R., & Kim, M.-J. (2008). Use of a photocatalytic membrane reactor for the removal of natural organic matter in water: Effect of photoinduced desorption and ferrihydrite adsorption. *Journal of Membrane Science, 322*(2), 368–374.

Foster, H., Ditta, I., Varghese, S., & Steele, A. (2011). Photocatalytic disinfection using titanium dioxide: Spectrum and mechanism of antimicrobial activity. *Applied Microbiology and Biotechnology, 90*(6), 1847–1868.

Kyungmin, Y., Wonseok, C., Hyunsuk, O., Woonyoung, L., Byung-kook, H., Chunghak, L., et al. (2009). Quorum sensing: A new biofouling control paradigm in a membrane bioreactor for advanced wastewater treatment. *Environmental Science and Technology, 43*(2), 380–385.

Lee, K., Lee, S., Lee, S. H., Kim, S.-R., Oh, H.-S., Park, P.-K., et al. (2016). Fungal quorum quenching: A paradigm shift for energy savings in membrane bioreactor (MBR) for wastewater treatment. *Environmental Science and Technology, 50*(20), 10914–10922.

Oh, H.-S., & Lee, C.-H. (2018). Origin and evolution of quorum quenching technology for biofouling control in MBRs for wastewater treatment. *Journal of Membrane Science, 554*, 331–345.

Ponnusamy, K., Paul, D., & Kweon, J. H. (2009). Inhibition of quorum sensing mechanism and aeromonas hydrophila biofilm formation by vanillin. *Environmental Engineering Science, 26*(8), 1359–1363.

Weerasekara, N. A., Choo, K.-H., & Lee, C.-H. (2014). Hybridization of physical cleaning and quorum quenching to minimize membrane biofouling and energy consumption in a membrane bioreactor. *Water Research, 67*, 1–10.

Yu, H., Liang, H., Qu, F., He, J., Xu, G., Hu, H., et al. (2016). Biofouling control by biostimulation of quorum-quenching bacteria in a membrane bioreactor for wastewater treatment. *Biotechnology and Bioengineering, 113*(12), 2624–2632.

Zheng, X., Wang, Q., Chen, L., Wang, J., & Cheng, R. (2015). Photocatalytic membrane reactor (PMR) for virus removal in water: Performance and mechanisms. *Chemical Engineering Journal, 277*, 124–129.

Water Networks as Flexible Loads to Power Systems

Mahdi Rouholamini, Carol Miller, Caisheng Wang,
Mohsen Mohammadian, and Mohammadamin Moghbeli

Abstract

Water facilities consume a large amount of electrical power. The components of water networks (mostly pumps and tanks) represent an incomparable opportunity for joint operation of water networks and power systems. These components are well suited for being responsive loads to power systems because water is storable

Keywords

Demand response • Power systems • Water-energy nexus • Water networks

1 Introduction

Water distribution systems, water treatment plants, and wastewater treatment plants consume nearly 3–4% of the total electricity used in the USA (Appelbaum 2002) of which about 80% is for pumping and distributing purposes and the remaining 20% accounts for water treatment (Leiby and Burke 2011). Drinking and wastewater utilities consume 30–40% of the total electricity used in a municipal area, which can be considered as the largest energy consumer (Copeland 2014). Indeed, water distribution systems are energy intensive infrastructures that mostly rely on water pumps and tanks.

Water networks are well suited for improving the operational flexibility of power systems. This is mostly due to the fact that there is a bunch of flexible components in water networks. Therefore, co-optimization of power systems and water/wastewater facilities may provide a great opportunity to reduce peak electricity demand and increase the energy efficiency of both the networks (House 2006; Oikonomou et al. 2017). Nowadays, we know that water and power networks are inextricably linked commonly known as energy-water nexus (Rouholamini et al. 2018). This paper aims to briefly introduce one important co-optimization opportunity of this nexus from the perspective of power system operation. The discussions in this paper may serve as foundations for new approaches to joint operation of water and electricity networks.

2 Water Networks as Responsive Loads

In renewable energy sources, smart allocation of power and time-of-use pricing, as well as increasing generation efficiency and network stability are the key features of a modern power system. As time goes on, these features are more observable in water systems as well (Lubega and Farid 2013). The potential capability of a water system for energy storage probably is a unique advantage to power system operators. Pumped hydraulic systems (elevated reservoirs) still serve as storage systems for both water supply and power transmission and are one of the most efficient large-scale energy storage technologies available (Diaz et al. 2017).

On the other hand, although the worldwide power demand has been growing over the past few decades concomitantly with the generation capacity, there are always times during which generators cannot meet the power

M. Rouholamini (✉) · C. Wang
Electrical and Computer Engineering Department, Wayne State University, Detroit, MI, USA
e-mail: gj9598@wayne.edu

C. Wang
e-mail: cwang@wayne.edu

C. Miller
Department of Civil and Environmental Engineering, Wayne State University, Detroit, MI, USA
e-mail: ab1421@wayne.edu

M. Mohammadian
Notashan Sanat Co., Tehran, Iran
e-mail: mohammadian@notashan.com

M. Moghbeli
University of Politecnico di Milano, Milan, Italy
e-mail: m.moqbeli@gmail.com

demand. That is why the power industry requires new criteria to ensure that production is adequate to meet the power demand. Indeed, a transformation from generation response to load response is needed to alleviate the risk of failure. In load response, customers manually or automatically reduce their consumption. These actions are possible in the form of demand response (DR) plans (Boutin and Bergerand 2013). DR deals with a compromise between comfort and reliability. In fact, in DR an electricity consumer reduces or shifts its power consumption (Fig. 1) when requested to do so in exchange for compensation. Responsive loads can be classified into two categories: adjustable and deferrable loads. An adjustable load is flexible during all time service while a deferrable load has a fixed energy requirement at the end of the service.

To implement DR, a virtual energy market is necessary. Participants in this market may take opportunities to reduce energy demand for short periods of time at peak hours, or at the opposite to absorb energy surplus in case of high production levels (from renewable sources in particular) at low demand hours. Considering the large volume of water storage and the pumping capabilities, the water networks offer unique opportunities for this DR business. Therefore, DR in water networks may be considered by modeling water networks as flexible loads. DR from water systems can offer financial benefits to water utility operators while providing response energy to the grid with less greenhouse gas emissions than that of energy storage technologies. Electricity storage schemes and grid management methods are becoming ever more important as the landscape of the power grid moves toward more decentralized renewable production.
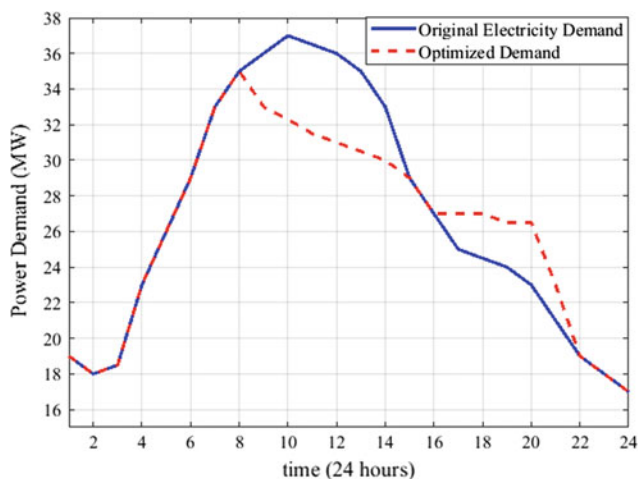
A typical example of water network as responsive load to power systems is the pump stations. It is clear that the water industry wants to achieve cost-effective and energy-efficient operations of water pumps. A pump scheduling optimization seeks cost reduction, moves energy use into cheaper tariff periods, reduces peak demand charges by limiting the maximum number of pumps, and also reduces the energy required to deliver water by running a group of pumps closer to their optimal efficiency. One of the major operating costs for water utilities is the energy needed to overcome geographical differences in head pressure and head losses due to pipe friction. Electric utilities sometimes use dynamic electricity pricing to reflect the varying cost of electricity production. In such energy markets, water utilities can significantly reduce operational costs by optimizing their pump schedules based on the forecasted electricity prices. Optimal pump scheduling can be considered as a small-scale form of DR except that in pump scheduling the problem is formulated mostly from the viewpoint of water utility operators rather than the perspective of both the water and power networks (Alighalehbabakhani et al. 2013).

Therefore, generally it can be claimed that water distribution systems represent suitable candidates for enhancing the flexibility of power systems through optimizing the operation of flexible components (mostly pumps and tanks) while respecting the hydraulic integrity of the water network. Figure 2 shows a very basic integration of a water and a power network coupled via a pump station. As seen, the pump is capable of meeting the water demand as well as maintaining the tank level. During the contribution of the pump to a DR program, i.e., when the pump power consumption reduces, the direction of Q1 changes and the tank helps with satisfying the water demand.

3 Discussion and Conclusions

In the traditional framework of analyzing water and power networks, latent opportunities such as simultaneous scheduling of power units and water components had been neglected. Nowadays, thanks to moving toward smart operation of power/water networks and the presence of highly advanced sensors, power converters, data aggregators, etc. simultaneous scheduling of these two systems is no longer out of reach. It is demonstrated in literature that a simultaneous scheduling is always superior to the sequential one and results in the enhancement of the social welfare. By employing the co-management approach presented in the paper, water utilities will be capable of giving power utilities new degrees of demand response to help them improve their performance and flexibility.

Fig. 1 An electric demand profile with/without DR

Fig. 2 A simple water network coupled with a power grid via a pump station

References

Alighalehbabakhani, F., McElmurry, S., Miller, C. J. & Abkenar, S. M. S. (2013). A case study of energy cost optimization in Monroe water distribution system. In *2013 International Green Computing Conference Proceedings* (pp. 1–5), Arlington, VA.

Appelbaum, B. (2002). *Water & sustainability (Vol. 4): Us electricity consumption for water supply & treatment the next half century* (Technical Report).

Boutin, V., & Bergerand, J. L. (2013). Water networks contribution to demand response. In *2013 IEEE Grenoble Conference* (pp. 1–4), Grenoble.

Copeland, C. (2014). *Energy-water nexus: The water sectors energy use* (Vol. 3). Congressional Research Service.

Diaz, C., Ruiz, F., & Patino, D. (2017). Modeling and control of water booster pressure systems as flexible loads for demand response. *Applied Energy, 204,* 106–116.

House, L. (2006). *Water supply related electricity demand in California* (p. 026). Contract No. 500-03.

Leiby, V. M., & Burke, M. E. (2011). *Energy efficiency best practices for North American drinking water utilities*. Water Research Foundation.

Lubega, W. N., & Farid, A. M. (2013). A meta-system architecture for the energy-water nexus. In *8th International Conference on System of Systems Engineering* (pp. 76–81), Maui, HI.

Oikonomou, K., Parvania, M., & Burian, S. (2017). Integrating water distribution energy flexibility in power systems operation. In *IEEE Power & Energy Society General Meeting* (pp. 1–5), Chicago, IL. https://doi.org/10.1109/pesgm.2017.8274374.

Rouholamini, M., Miller, C. J., Wang, C., & Mohammadian, M. (2018). A review of water/energy co-management opportunities. In *IEEE Power & Energy Society General Meeting*, Portland, USA (in press).

Preparation of PES/GO/APTES-SiO$_2$ Mixed Matrix Membrane for the Treatment of Oily Wastewater

Maryam B. Alkindy, Munirasu Selvaraj, Fawzi Banat, and Shadi Wajih Hasan

Abstract

PES/GO mixed matrix membranes were fabricated and characterized. Water permeability tests, hydrophilicity, and surface morphology characterizations were conducted. A max of 2870 L/m^2 h water flux and contact angle of 64.5° were achieved.

Keywords

Mixed matrix membrane • Graphene oxide • Silica • APTES • Oily wastewater • Phase inversion

1 Introduction

The selection of materials for the fabrication of mixed matrix membranes is still a concern among the research community. Nanomaterials such as graphene oxide (GO) and silica (SiO$_2$) which are favorable for wastewater treatment-related applications due to their significant impact on water permeability and contaminant rejection have been investigated. Hydrophilicity, high surface area, mechanical robustness, and thermal stability are among the properties of excellent membranes. Therefore, the main objective of this paper was to fabricate a novel polyethersulfone (PES)/GO/3-aminopropyl triethoxy silane (APTES)-SiO$_2$ mixed matrix membrane for the treatment of oily wastewater.

2 Materials and Methods

2.1 Synthesis of Amine-Functionalized SiO$_2$ (APTES)

Amine-functionalized SiO$_2$ nanoparticles were prepared according to the literature (Lu 2013). Firstly, 0.5 mL of APTES was added to a solution of 2 g of SiO$_2$ nanoparticles (having average diameter of 20 nm and were supplied from EPRUI Nanoparticles & Microspheres Co. Ltd.) in 150 mL ethanol (99.8% purity). Secondly, the solution was ultrasonicated using Branson 1510 Ultrasonic Cleaner at 40 kHz frequency in a water bath for 30 min and then stirred at 60 °C for 18 h. Thirdly, the solution was centrifuged (using HERMLE Labortechnik Z 326 K centrifuge) with ethanol and water several times to ensure excess APTES is washed off. Finally, the obtained product was dried in the oven at 50 °C and designated as ATS and crushed to obtain a powder form.

2.2 Preparation of PES/GO Mixed Matrix Membranes

PES/GO membranes were prepared via phase inversion method. Different concentrations of GO was prepared according to Hummers' method (Hummers and Offeman 1958). Precise amounts of GO in wt% of PES (0.01, 0.05, 0.1, 0.5 and 1%) were dispersed in dimethylacetamide (DMAC) and ultrasonicated in a water bath for 30 min. Polyvinylpyrrolidone (PVP) was dissolved in the above solutions followed by the addition of PES (average Mw. 75,000 and was bought from Prakash Chemicals Pvt. Limited, India) and stirred for

M. B. Alkindy (✉) · M. Selvaraj · F. Banat · S. W. Hasan
Department of Chemical Engineering, Center for Membrane and Advanced Water Technology, Khalifa University of Science and Technology, Masdar City Campus,
P.O. Box 127788 Abu Dhabi, UAE
e-mail: maryam.alkindy@ku.ac.ae

M. Selvaraj
e-mail: munirasu.selvaraj@ku.ac.ae

F. Banat
e-mail: fawzi.banat@ku.ac.ae

S. W. Hasan
e-mail: shadi.hasan@ku.ac.ae
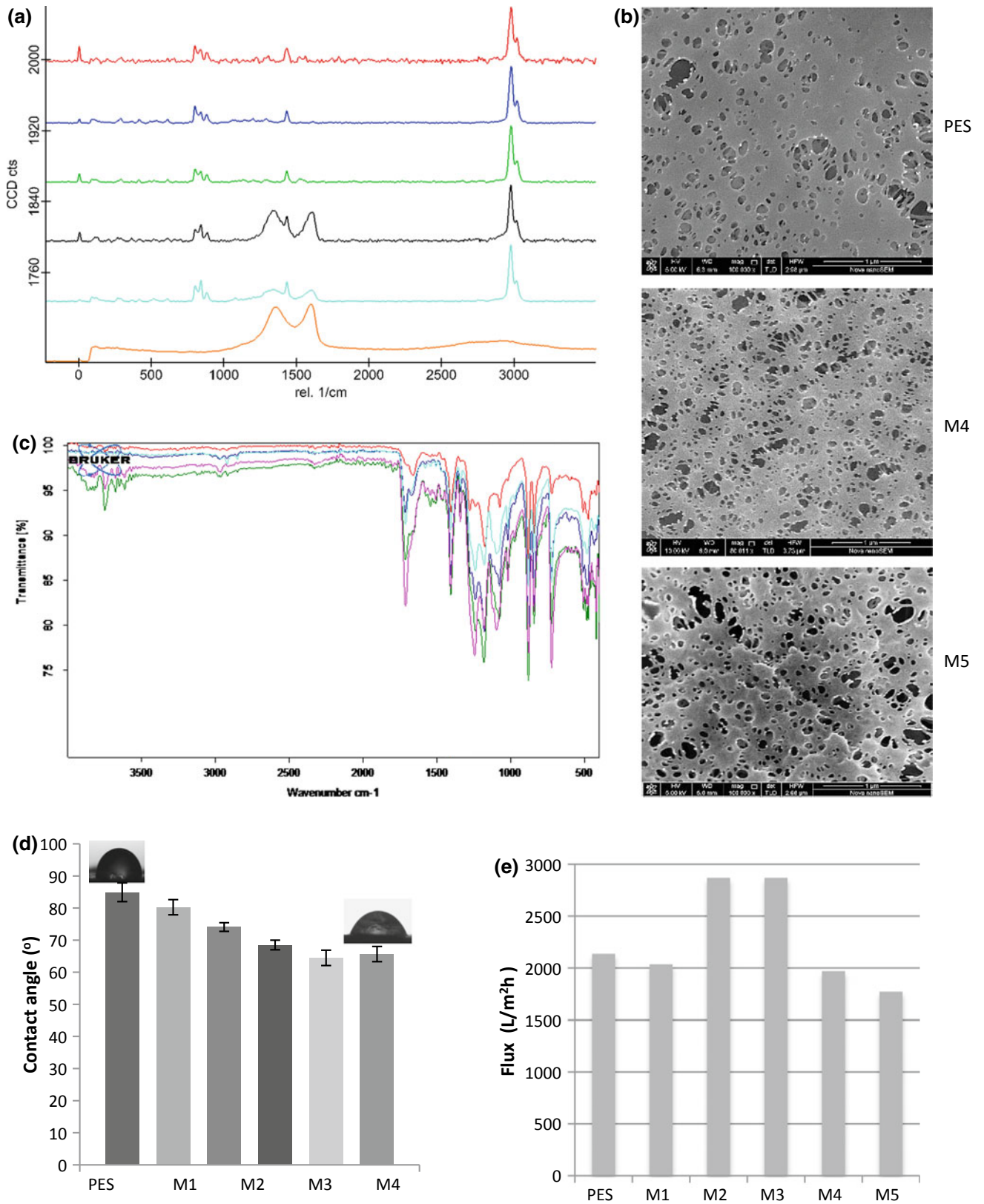
Fig. 1 **a** Raman spectra. Red: PES, Blue: M2, Green: M3, Black: M5, Blue: M6, Orange: GO sample; **b** SEM images of PES, M4 and M5 membranes; **c** FTIR spectra of all membranes; **d** water contact angle indicating hydrophilic membranes; and **e** water flux data

24 h at 60 °C. The dope solution was cast aside for 24–48 h to remove entrapped air bubbles (i.e., membrane degassing). The solution was subsequently cast on a polyester membrane support on clean glass at a thickness of 200 μm. The glass plate was horizontally immersed into deionized water (with a resistivity of 15 MΩ cm) at a temperature of 25 °C for 48 h. Finally, the membranes were washed with deionized water and stored for use. A bare (control) PES membrane was also prepared using the same method for comparison.

2.3 Characterization of PES/GO Mixed Matrix Membranes

Zeta potential measurements using NanoBrook ZetaPALS Potential Analyzer with a scattering angle of 15° was used for a quick confirmation of functionalized SiO₂ nanoparticles with amino groups. Fourier-transform infrared spectroscopy (Bruker Vertex 80 FTIR) was carried out to observe the chemical structure of the membranes and their functionalities. IR-attenuated total reflectance (ATR) spectra analysis was performed in the wavelength range of 4000–400 cm⁻¹ and at a resolution of 4 cm⁻¹ via Bruker Vertex 80 FTIR spectrometer. The vibrational characteristics of the bonds in the fibers were further confirmed through Raman spectroscopy. WITec's Alpha 300R confocal micro-Raman imaging spectrometer was used to obtain the Raman signals with visible laser excitation source at the wavelength of 532 nm. FEI Nova Nano-SEM 650 scanning electron microscope (SEM) with monopole magnetic immersion final lens and 60° objective lens geometry at an electron beam energy of 5 kV, 4.0 spot size, emission current of 100 μA, and chamber vacuum <10 mPa was used. The hydrophilicity of the membrane was determined using Krüss GmbH Drop Shape Analyzer using the sessile drop technique. Finally, a permeation test was carried out using vacuum filtration to determine the pure water permeability. The test was carried out at room temperature under 0.07 MPa and the flux was calculated using the below equation:

$$J = \frac{V}{A\Delta t}$$

where J is the pure water permeability (L/m² h), V is the volume of the permeate (L), A is the effective membrane area (m²) and Δt is the sampling time (h).

3 Results and Discussion

The surface charge of particles increased as SiO₂ nanoparticles was modified with amine groups (Soto-Cantu et al. 2012). This was witnessed with the synthesized particles which showed a significant increase in the surface charge (i.e., zeta potential) from −130 to −5 mV. GO peaks were observed in membranes with a higher concentration of GO (i.e., M4 and M5) as shown in Fig. 1a. The GO peaks in the other membranes (M2–M3) were not detected by Raman possibly due to their very low concentration. SEM images (Fig. 1b) confirm the formation of pores in GO-modified membranes. FTIR spectra shown in Fig. 1c confirm the chemical structure of the PES in all of the fabricated mixed matrix membranes. The hydrophilicity of the membranes has improved with the addition of GO. It was observed that a small amount of GO (i.e., 0.01 wt%) was enough to witness an instant reduction in contact angle from 84.9 to 80.5° (Fig. 1d). The initial water flux (Fig. 1e) was improved significantly upon the addition of GO, reaching its highest at a concentration of 0.1 wt%. The flux began to slightly decrease possibly due to the agglomeration of GO particles.

4 Conclusion

PES/GO membranes were developed as a precursor to ongoing work for the preparation of a novel PES/GO/APTES-SiO₂ membrane. The effect of GO incorporation on PES in terms of hydrophilicity and permeability was studied. It was shown that even a slight amount of GO introduced into the PES membrane can improve hydrophilicity. Similarly, water permeability was also shown to improve with the addition of GO. Amine-functionalized SiO₂ nanoparticles were also successfully prepared. Several investigations will be carried out to develop the novel (PES)/GO/APTES-SiO₂ mixed matrix membrane for the treatment of oily wastewater.

References

Hummers, W. S., Jr., & Offeman, R. E. (1958). Preparation of graphitic oxide. *Journal of the American Chemical Society, 80,* 1339.

Lu, H. (2013). Synthesis and characterization of amino-functionalized silica nanoparticles. *Colloid Journal, 75*(3), 311–318.

Soto-Cantu, E., Cueto, R., Koch, J., & Russo, P. (2012). Synthesis and rapid characterization of amine-functionalized silica. *Langmuir, 28* (13), 5562–5569.

Ayun Mousa Springs: Integrated Hydrological, Environmental and Geophysical Studies

Ahmed M. H. Shaban, Bassem S. Nabawy, Ali Abbas, and Mohamed M. Kassab

Abstract

Ayun Mousa springs area is the most important religious and historical sites in Sinai. The water quality of the exposed springs (seven springs) indicates brackish water suitable for medical purposes. Air quality indicates some pollution next to the highway.

1 Introduction

Sinai Peninsula is considered as a unique region in the world due to its geographical location, tectonic and thermal activities. It has a great number of springs, the most famous of which are Ayun Mousa and Hammam Fara'aun springs. Most of these springs produce water through active fault plains affecting the tertiary rocks lying unconformable on the Lower Cretaceous Nubian Sandstones Basin. Based on their chemical properties as well as their historical and medical values, the water of these springs could be used in recreation, touristic purposes, and urbanization of the area. Ayun Mousa oasis (Fig. 1) is believed to be based on 12 springs, but today only seven of the original 12 springs still exist. Some past oil activities close to Ayun Mousa springs caused a flow of saline connate to the area which may contaminate the groundwater of the springs and change its properties into brackish and highly saline water causing death of the present palm trees in the Ayun Mousa Oasis. Due to its historical and touristic values, more attention has to be paid for Ayun Mousa which has been neglected for many decades causing burying and disappearing of some wells and great contamination of the sole well which has some stagnant water (Fig. 2a–c). Therefore, the present study aims to study the dynamic relationships between environmental and hydrological systems to develop the Ayun Mousa area, to rediscover the seven buried wells and to supply it with the ground subsurface water supplies for the environmental and agricultural sustainability in Ayun Mousa area to get back its location on the touristic map of Egypt. Ecological, hydrological and geophysical assessment for Ayun Mousa area was carried out using different techniques. The present study concerns mostly with the water quality assessment of Ayun Mousa springs. It is a part of this integrated study that included: (1) geophysical exploration for the subsurface strata to determine the main water-bearing layers using VES and 2D electric tomography and self-potential (SP) as well, (2) physicochemical analyses for the surface and groundwaters, and (3) evaluation of the air quality in the studied area.

A. M. H. Shaban (✉)
National Research Centre, Cairo, Egypt
e-mail: ashaba12311@gmail.com

B. S. Nabawy
Geophysical Sciences Department, National Research Centre, Cairo, Egypt
e-mail: bsnabawy@yahoo.co.uk

A. Abbas
Geological and Geophysical Engineering Department, Faculty of Petroleum Engineering, Suez University, Suez, Egypt
e-mail: dr_alyabbas@hotmail.co.uk

M. M. Kassab
Exploration Department, Egyptian Petroleum Research Institute, Cairo, Egypt
e-mail: mkassab68@yahoo.com

2 Materials and Methods

A total number of 10 water samples were collected and analyzed according to (APHA 2012) from the different springs (seven samples) and the water pipes (three samples) to compare the chemical composition of these springs with the pipes in the area of study. The air quality was measured
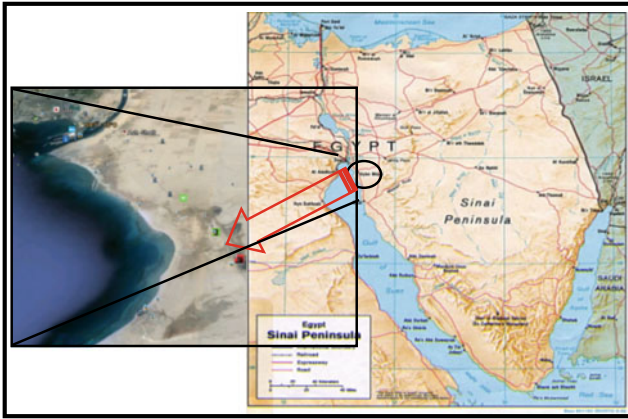
Fig. 1 Location map of Ayun Mousa along the Gulf of Suez coast, Sinai Peninsula, Egypt
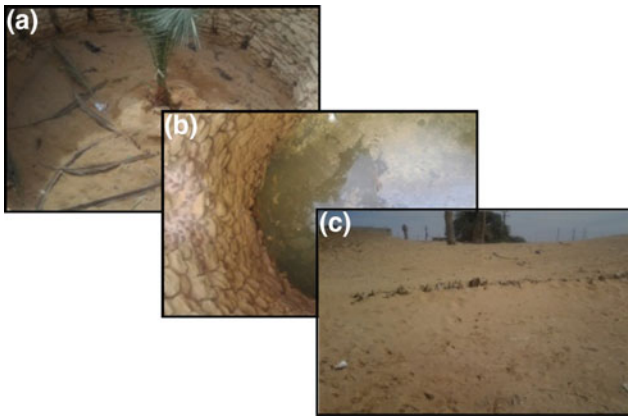
Fig. 2 Some buried and contaminated wells from Ayun Mousa springs

throughout in the atmosphere in some three selected sites during the year 2016 including (particulate matter (PM10), ozone, sulfur dioxide, nitrogen dioxide, carbon monoxide, lead, heavy metals, nitrates, sulfates, volatile organic compounds, and toxic compounds). A total of six vertical electrical sounding (VES) using Syscal R2 were conducted to check the depth of the water carrier bed. In addition, self-potential (SP) and two-dimensional resistivity tomography (ERT) are applied to explore the already known springs (seven) and to prospect the hidden five springs.

3 Results and Discussion

The chemical composition of the studied water samples is shown in Table 1. This study was undertaken to assess the physical and chemical water quality of

Ayun Mousa springs as well as other wells in the same area. The results showed that there were considerable variations among the examined samples with respect to their physical and chemical parameters. The groundwater had no color and odor while turbidity revealed clear variation between different springs. Also, the samples were analyzed for conductivity, pH, major cations (Ca^{2+} and Mg^{2+}), major anions (Cl^-, NO_3^-, HCO_3^-, SO_4^{2-}, F^-) and important trace elements (Fe^{2+}, Mn^{2+}). Water quality for Ayun Mousa springs and available springs in the study area showed high salinity due to longer period of contact with rocks. The chemical composition of the springs' water samples refer to alkalinity with prevailing bicarbonate and chloride. All springs showed pronounced fluctuation in sulfate contents. Moreover, the pH in all sampling sites was in the range of 6.5–8.9. The electrical conductivity (EC) of the spring water varied from 3760 μmohs/cm (sample no. 10) to 17,070 μmohs/cm (sample no. 4). However, the high conductivity of the water samples corresponds to the highest concentrations of dominant ions, which is resulted from ion exchange and solubility of rocks in aquifer. Chloride concentrations ranged from 900 mg/L in water pipe WS R 242 spring to 5600 mg/L in Bir El-Shaib spring. The chloride values in the water samples due to dissolution of rocks surrounded the aquifer. Chloride values which are higher than 200 mg/L are to be at risk for human health and may cause unpleasant taste of water. The nitrate concentrations showed slight variation and it ranged from 0.1 to 0.2 mg NO_3/L in all spring water samples, whereas ammonia concentration revealed a pronounced variation in different spring water samples and it is in the range of 0.0 mg NH_3/L in Bir Bigbaga and water pipe WS R 242 water samples to 2.3 mg NH_3/L in Bir El-Saqia water sample. Nitrate is the most common contamination in groundwater, due to its solubility and anionic form; nitrate is very mobile and can easily leach into the water table (Fetter 1988). In addition, the calcium concentration of the spring water varied from 216 mg/Lin Bir El-Saqia spring to 1200 mg/L in Bir El-Shaib spring. Bicarbonate values in the water samples ranged from 48.8 mg/L in Bir El-Shaib spring to 239.1 mg/L in water pipe WS R 242 spring. Clear variation was detected in the important trace element concentration (Fe and Mn) where iron concentration in the range of 0.3 mg/L (Bir El-Sheikh spring) to 2.5 mg/L (water pipe No. 2), while manganese concentration in the range of 0.01 mg/L (Bir Bigbaga, Bir El-Zahr and water pipe No 2) to 0.05 mg/L (water pipe WS R 242). It is declared that the Ayun Mousa springs are mostly brackish and not suitable for drinking purposes but may be used for medical and religious purposes. In brief, based on the air quality studies, it is achieved that the maximum mean concentration of TSPM in the atmosphere of the investigated three sites is 385 μg/m^3 at May during Khamaseen storms. This concentration is more than five times the EPA air quality standard for TSP (75 μg/m^3) and higher than the WHO range (60–90 μg/m^3).

Table 1 Chemical composition of the collected water samples (sample nos. 1–7 from the flowing springs and 8–10 from some flowing water pipes)

Parameter	Unit	Results (sample nos.)										Egyptian Standards (2007)
		(1)	(2)	(3)	(4)	(5)	(6)	(7)	(8)	(9)	(10)	
pH		8.1	7.8	7.9	**8.9***	8.1	8	7.8	8.1	7.6	6.5	6.5–8.5
Turbidity	NTU	**1.1***	**4.8***	**2.0***	**2.6***	**2.8***	**2.1***	**2.1***	**1.2***	**7.2***	**6.1***	1.0
Odor		O less	O less	O less	O less	O less	O less	O less	O less	O less	O less	O less
Color	Co/Pt unit	C less	C less	C less	C less	C less	C less	C less	C less	C less	C less	C less
Electric conductivity	μmohs/cm	9500	4460	4860	17,070	15,450	4650	13,760	7160	3760	10,370	
TDS	mg/L	**6200***	**2500***	**2400***	**11,400***	**10,500***	**2700***	**9600***	**4600***	**2400***	**6200***	1000
Total alkalinity (CaCO₃)	mg/L	92	142	80	40	132	150	88	196	140	130	
Total hardness (CaCO₃)	mg/L	**2400***	**870***	**1200***	**3800***	**3600***	**970***	**3600***	**2500***	**850***	**2250***	500
Ca-Hardness (CaCO₃)	mg/L	**2050***	**540***	**1000***	**3000***	**3000***	**850***	**2500***	**2100***	**700***	**1750***	350
Mg-Hardness (CaCO₃)	mg/L	**350***	**330***	**200***	**800***	**600***	120	**1100***	**400***	150	**500***	150
Calcium (Ca)	mg/L	820	216	400	1200	1200	340	1000	840	280	700	
Magnesium (Mg)	mg/L	84	79.2	48	192	144	28.8	264	96	36	120	
Carbonate (CO₃)	mg/L	00	00	00	00	00	00	00	00	00	00	
Bicarbonate (HCO₃)	mg/L	112.2	173.2	97.6	48.8	161	183	107.4	239.1	170.8	158.6	
Chloride (Cl₂)	mg/L	**2600***	**1100***	**2000***	**5600***	**5000***	**1250***	**4800***	**900***	**1100***	**3400***	250
Sulfate (SO₄)	mg/L	**928***	**339***	**715***	**1516***	**2200***	**451***	**962***	**1162***	**385***	**498***	250
Dissolved silica (SiO₂)	mg/L	10.7	16.3	9.2	9.6	2.1	14.9	3.0	7.8	18.2	14.0	
Ammonia (NH₃)	mg/L	0.04	**2.3***	00	0.5	0.06	**1.2***	0.1	0.0	**1.0***	**2.4***	0.5
Nitrite (NO₂)	mg/L	0.19	00	00	0.19	0.02	0.01	00	00	00	00	0.2
Nitrate (NO₃)	mg/L	0.1	0.2	0.1	0.15	0.14	0.1	0.1	0.1	0.12	0.14	45.0
Iron (Fe)	mg/L	0.3	**1.2***	**0.7***	**0.4***	**0.44***	**1.2***	**0.8***	**0.56***	**2.5***	**1.0***	0.3
Manganese (Mn)	mg/L	0.03	0.02	0.01	0.03	0.02	0.01	0.04	0.05	0.01	0.02	0.4
Fluoride (F)	mg/L	**1.1***	**1.0***	**1.0***	**1.3***	**1.1***	**1.0***	**1.0***	**1.4***	**0.96***	**1.0***	0.8

Note Bold numbers with asterisks 0.0* are values outside the range of the Egyptian Standards (2007) for drinking water
Sample no. 1 represents Bir El-Sheikh; Sample no. 2 represents Bir El-Saqia; Sample no. 3 represents Bir Bigbaga; Sample no. 4 represents Bir El-Shaib; Sample no. 5 represents Bir El-Samaanah; Sample no. 6 represents Bir El-Zahr; Sample no. 7 represents the unnamed spring; Sample no. 8 represents water Pipe WS R 242; Sample no. 9 represents water pipe no. 2; Sample no. 10 represents water pipe no. 3; O less: odorless; C less: colorless

Geophysically, the study area was differentiated into four parts and the anomalies' each of the parts were traced. The anomalies are mostly related to the accumulation of water with diagnostic low or relatively high salinity, e.g., the SP in the first part (Fig. 3) (Abdullahi et al. 2011). A total of six ERT profiles were studied crossing these anomalies. The 2D sections introduced an explanation and tracing for the springs in the subsurface, e.g., profile 1 (Fig. 4). For the first profile, it passes through a positive SP anomaly which is located in the northeastern side and another strong positive
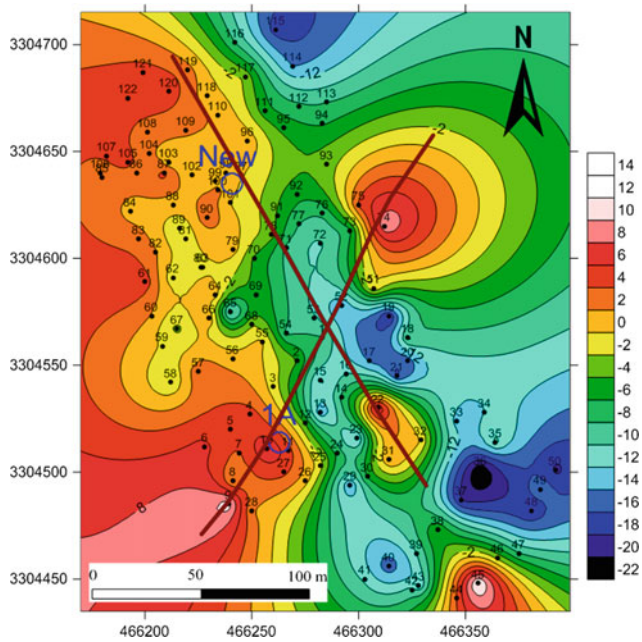
Fig. 3 Self-potential contour map of part (a) crossed by two intersecting ERT profiles

SP anomaly which is surrounded by the unnamed spring (1A) (El-Qady 2006; Mousa et al. 2009).

4 Conclusion

Hydrologically, the water quality of Ayun Mousa springs refers to brackish water quality with relatively high salinity which is not suitable for drinking purposes but may be applied for medical purposes and religious beliefs, but the water can be treated and used easily, if the water availability (quantity) is enough for different purposes. Environmentally, the air quality studies through the springs area indicated that the sources of pollution are more effective close to the highway (four times more than the limits of Air Quality Standard of the Egyptian Law), whereas less effective next to the Gulf of Suez and it is within the accepted limits. Geophysically and structurally, the configuration of Ayun Mousa springs is controlled by two major dip-slip faults trending NNW–SSE, parallel to the Gulf Suez and throwing westward, forming step-like pattern from the eastern highland.
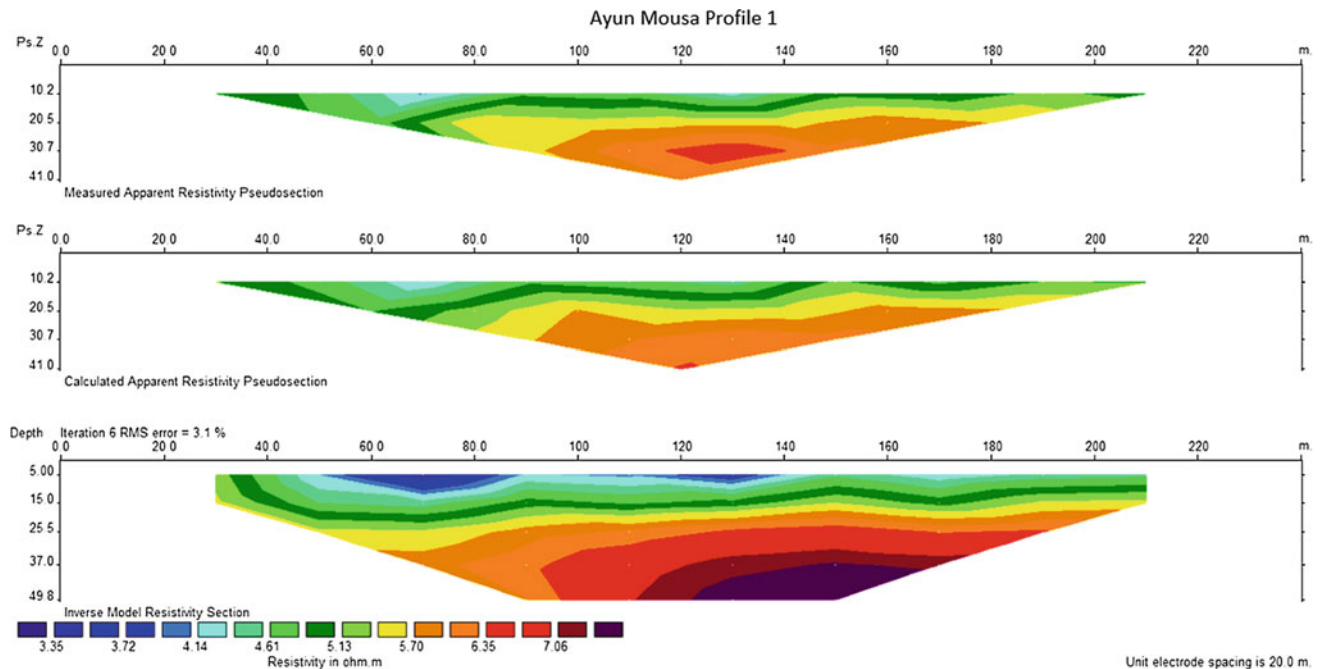
Fig. 4 The first two-dimensional electrical resistivity tomography

References

Abdullahi, N. K., Osazuwa, I. B., & Sule, P. O. (2011). Application of integrated geophysical technique in the investigation of groundwater contamination: A case study of municipal solid waste leachate. *Ozean Journal of Applied Sciences, 4,* 7–25.

APHA, American Public Health Association. (2012). *Standard methods for the examination of water and waste water* (22nd ed.). Washington, DC.

El-Qady, G. (2006). Exploration of a geothermal reservoir using geoelectrical resistivity inversion: Case study at Hammam Mousa, Sinai, Egypt. *Journal of Geophysics and Engineering, 3,* 114–121.

Fetter, C. W. (1988). *Applied hydrogeology* (2nd ed., p. 592). London: Merrill Publishing Company.

Mousa, S., Abbas, A. E., & Farag, K. (2009). Application of 2D resistivity imaging and VLS-EM techniques to detect the causes of saline nature of the subsurface layers in Ayun Mousa area, Sinai, Egypt. In *11th International Conference on Mining, Petroleum and Metal Engineering* (pp. 802–816). Sharm El-Sheikh: MPM.

Modelling Demand and Response in WWTPs: Extension of BSM1 with Aeration Tank Settling

Matteo Giberti, Recep Kaan Dereli, Damian Flynn, and Eoin Casey

Abstract

Demand shedding through aeration control can exploit the wastewater treatment plant (WWTP) flexibility to help maintain the power system grid balance and reduce operational costs. The reactions and settling process combination is not considered in traditional WWTP models, but it could play an important role in the modelling of demand response (DR) strategies and their effects on the plants.

1 Introduction

In Europe, the share of electrical energy generated from renewable sources has moved from around 8.5% in 2004 to 17% in 2016 (Renewable energy statistics—Eurostat 2018), and in Ireland, it has reached roughly 20% (EirGrid 2018). Energy systems are, hence, becoming more dependent on variable and uncertain generation. Since the operation of the electric grid requires a continuous balance between the production and consumption of energy, a higher share of wind and solar power poses a challenge to the maintenance of such an equilibrium. Addressing this issue requires

M. Giberti (✉) · R. K. Dereli · D. Flynn · E. Casey
University College Dublin, School of Chemical
and Bioprocess Engineering, Belfield, Dublin, Ireland
e-mail: matteo.giberti@ucdconnect.ie

R. K. Dereli
e-mail: recep.dereli@ucd.ie

D. Flynn
e-mail: damian.flynn@ucd.ie

E. Casey
e-mail: eoin.casey@ucd.ie

improving the flexibility of the entire energy system, for instance, increasing the available energy storage capacity or managing the end-users' behaviour (e.g. shifting or shedding their energy consumption) through demand response (DR) programmes (Bird et al. 2016).

Municipal wastewater treatment plants (WWTPs) have been found to be suitable candidates for the application of DR programmes, since they are quite energy-intensive and they tend to have high electrical load during utility peak demand periods (Goli et al. 2008). Mathematical modelling of WWTPs is a valuable tool for a preliminary assessment of the effects of such DR programmes without jeopardizing real plant operation. The Benchmark Simulation Model No. 1 (BSM1) (Alex et al. 2008; Rosen et al. 2004) provides a framework to compare different DR strategies in terms of energy consumption and effluent quality.

Among the potential flexibility elements seen in conventional activated sludge WWTPs, aeration is generally the largest energy consumer (Rosso et al. 2008). Demand shedding through aeration control, subject to maintaining plant operational limits, could therefore have a large impact on the DR potential of the plant. In many cases, aeration is also responsible for the mixing of the tank, so that decreasing the aeration intensity not only affects dissolved oxygen (DO) concentration but also promotes the settling of the biomass flocs and particulate matter present in the reactor liquid phase. Once aeration is restarted, the settled solids are resuspended, and their concentration in the stream exiting the tank is increased. That may exceed the capacity of the secondary clarifier, leading to sludge washout and to the increase in the effluent turbidity occasionally reported in the literature (Lekov et al. 2010). This phenomenon is not taken into account in current benchmark simulation models. The inclusion of sludge settling in aerated tanks within the simulation model may therefore allow to investigate under which conditions the effluent total suspended solids (TSS) concentration increases following demand shedding events, adding more realism to simulation results.

2 Materials and Methods

Activated sludge settling models for final clarifiers based on the discretization of settling tanks into layers are well established in the literature (Takács et al. 1991; Gernaey et al. 2004; Bechmann et al. 2002). There are also several approaches to combine sludge settling and biological processes in secondary clarifier tanks (Gernaey et al. 2006). However, these methods were deemed impractical for the present case, as they were meant to include biochemical reactions in a settling model rather than vice versa. This would have led to issues related to the lack of a real underflow stream in the aerated tank, which has an important role in the clarifier settling process. For practical simplicity, the dual-layer aeration tank settling model proposed by Bechmann et al. (2002) may be a suitable approach to combine reaction and settling in activated sludge models and to describe the aerated tank behaviour when aeration and mixing are off. The layer above the sludge blanket level is assumed to be clear water (no suspended solids) zone, whereas the layer at the bottom of the tank contains all the suspended solids and is fully mixed. The depth of the sludge blanket is then calculated as a function of the settling velocity of the sludge. Activated Sludge Model No. 1 (ASM1) (Henze et al. 2015) is used as kinetic model, but in our study the mass balance for the components contained in the wastewater is modified to include the effect of changing volumes. For the soluble components,

$$\frac{dS_i}{dt} = \frac{Q}{V_{\text{tot}}} \cdot \left(S_i^{\text{in}} - S_i\right) + R_i \cdot \frac{V^B}{V_{\text{tot}}}$$

$$\frac{dS_{\text{oxygen}}}{dt} = \frac{Q}{V_{\text{tot}}} \cdot \left(S_o^{\text{in}} - S_o\right) + k_L a \cdot \left(S_o^{\text{sat}} - S_o\right) + R_o \cdot V^B / V_{\text{tot}}$$

whereas for the particulate components,

$$\frac{dX_i}{dt} = \left(Q \cdot \left(X_i^{\text{in}} - X_i^{\text{out}}\right) + R_i \cdot V^B + A \cdot X_i^B \cdot \frac{dd_{\text{sb}}}{dt}\right) \cdot \frac{1}{V_B}.$$

The settling velocity is modelled with the same expression and parameters used in the BSM1 secondary clarifier (Takács et al. 1991).

$$V_S = \max\left(0, \min\left(v_0', v_0 \cdot \left(\exp\left(-r_{\text{h}} \cdot \text{TSS}^B\right) - \exp\left(-r_{\text{p}} \cdot \text{TSS}^B\right)\right)\right)\right)$$

The sludge blanket depth is then calculated from the settling velocity

$$\frac{dd_{\text{sb}}}{dt} = \text{mix} \cdot \left(-\frac{1}{\tau_{\text{mix}}}\right) \cdot d_{\text{sb}} + (1 - \text{mix}) \cdot V_S$$

The parameters used are listed in Table 1. This set of equations was coded into a BSM1 open-loop Simulink implementation. Constant influent conditions were assumed to assess the response of the system to an aeration switch off period of 1 hour in the third aerated tank. The mixing and the suspension of activated sludge flocs are provided by the aeration system.

3 Results and Discussion

Figure 1 shows the total suspended solids concentration profiles in the clarifier underflow, in the effluent and in the aerated tank where the settling process was incorporated to the biochemical reactions. It can be seen that turning the blower off for 1 h results into an increase of the TSS concentration in the tank, and into a concurrent decrease in both the clarifier underflow and the plant effluent. As expected, there is peak in the TSS concentration leaving the aerated tank due to the resuspension of solids when the aeration is restarted. This affects the suspended solids concentration in the clarifier effluent, which also increases in accordance with the literature (Lekov et al. 2010).

Figure 2 illustrates the behaviour of the ammonia concentration as an example of one of the biochemical reactions described by the ASM1 model. The concentration in the tank increases when the aeration stops as a result of the lack of oxygen that is required for the nitrification reactions. Once the aeration is restored, the concentration returns to the pre-event level. The ammonia concentration in the clarifier effluent exhibits a similar trend, but the peak is lower and there is a delay due to the hydraulic retention time in the secondary settler. Further simulations of the WWTP behaviour over a longer time period with dynamic influent load may then be used to determine the DR capabilities of the plant (e.g. energy

Table 1 List of terms

S_i	Concentration of soluble ASM1 components	r_{h}	Hindered zone settling parameter
X_i	Concentration of particulate ASM1 components	r_{p}	Flocculant zone settling parameter
V^B, V_{tot}	Volume of the sludge layer and of the whole tank	d_{sb}	Sludge blanket depth
R_i	Rate expression for the ith ASM1 component	TSS^B	TSS concentration in the sludge layer
v_0'	Maximum settling velocity	mix	Mixing signal (ON/OFF)
v_0	Maximum Vesilind settling velocity	τ_{mix}	Mixing time constant

Fig. 1 Total suspended solids profiles in the plant
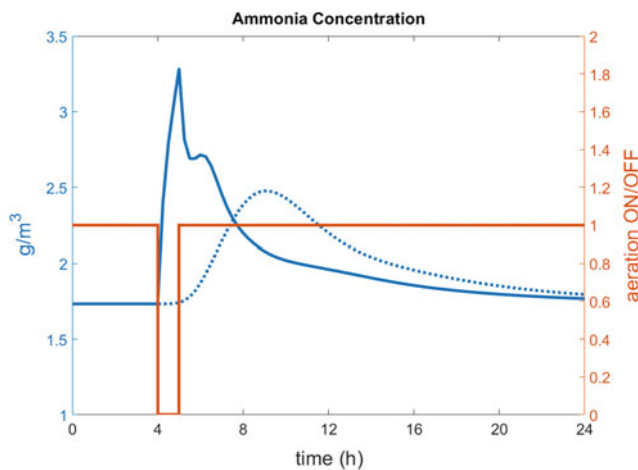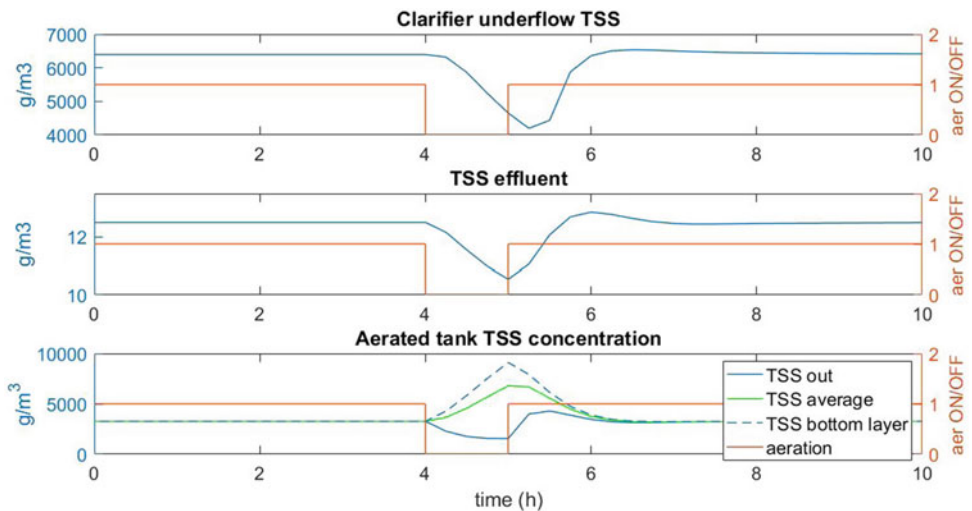
Fig. 2 Blue solid line represents the ammonia concentration in the aerated tank and the blue dotted line is the clarifier effluent ammonia concentration. The orange line is the aeration signal (1: ON, 0: OFF)

consumption that can be shifted, DR frequency, DR duration, etc.) with the discharge permits as constraints.

4 Conclusion

The preliminary simulations conducted with the modified set of equations proposed in the present study show reasonable trends for the TSS concentration in the aeration tank and in the secondary clarifier. Results in line with the expectations are also obtained for the biological process kinetics. Calibration and validation of the model against real data are, however, still required, but the use of this dual-layer approach to combine reaction and settling in BSM1 may extend its capabilities, so that it can provide an improved understanding of various DR strategies impact on the WWTP's operation.

References

Alex, J., et al. (2008). *Benchmark simulation model no. 1 (BSM1)*.

Bechmann, H., Nielsen, M. K., Poulsen, N. K., & Madsen, H. (2002). Grey-box modelling of aeration tank settling. *Water Research, 36* (7), 1887–1895.

Bird, L., et al. (2016). Wind and solar energy curtailment: A review of international experience. *Renewable and Sustainable Energy Reviews, 65*, 577–586.

EirGrid. (2018). Available: http://www.eirgridgroup.com/ (Online). Accessed April 26, 2018.

Gernaey, K. V., Jeppsson, U., Batstone, D. J., & Ingildsen, P. (2006). Impact of reactive settler models on simulated WWTP performance. *Water Science and Technology, 53*(1), 159–167.

Gernaey, K. V., et al. (2004). Conservation principles suspended solids distribution modelling to support ATS introduction on a recirculating WWTP. *Water Science and Technology, 50*(11), 179–188.

Goli, S., Olsen, D., McKane, A., & Piette, M. A. (2013). *2008–2010 research summary: Analysis of demand response opportunities in California industry*.

Henze, M., Gujer, W., Mino, T., & van Loosedrecht, M. (2000). *Activated sludge models ASM1, ASM2, ASM2d and ASM3*. London UK: IWA Publishing.

Lekov, A., Thompson, L., McKane, A., Song, K., & Piette, M. A. (2010). *Opportunities for energy efficiency and open automated demand response in wastewater treatment facilities in California—Phase I report*.

Renewable energy statistics—Eurostat. (2018). Available: http://ec.europa.eu/eurostat/statistics-explained/index.php/Renewable_energy_statistics (Online). Accessed April 22, 2018.

Rosen, C., Jeppsson, U., & Vanrolleghem, P. A. (2004). Towards a common benchmark for long-term process control and monitoring performance evaluation. *Water Science and Technology, 50*(11), 41–49.

Rosso, D., Larson, L. E., & Stenstrom, M. K. (2008). Aeration of large-scale municipal wastewater treatment plants: State of the art. *Water Science and Technology, 57*(7), 973–978.

Takács, I., Patry, G. G., & Nolasco, D. (1991). A dynamic model of the clarification-thickening process. *Water Research, 25*(10), 1263–1271.

Miscanthus as Energy Crop and Means of Mitigating Flood

Jason Kam, Daniel Traynor, John C. Clifton-Brown, Sarah J. Purdy,
and Jon P. McCalmont

Abstract

Miscanthus is a suitable alternative for energy biomass.
Particularly, in cultivation area that is prone to flooding.
Current commercial Miscanthus can survive in the
winter-flooded environment. There is no significant
difference in yield and other physiological development.
Observed height and tiller number have no differences
between winter flooded and non-flooded ground.

Keywords

Miscanthus • Flood • Yield • Survival

1 Introduction

Anaerobic digestion (AD) has been in the public limelight
recently. In particular, the use of feedstock become an
interesting topic for many different parties both for and
against this technology. Particularly, the use of crop plant as
substrate is in much debate. Fodder maize is the most
commonly used crop for biogas production. However,
environmental concerns and possible future conflict with
land for food production may limit its long-term use
(European Environmental Agency 2006; Palmer and Smith
2013; European Commission 2014). Particularly in South
England where it is prone to flooding during winter. Such

results in soil erosion and sedimentary runoff into the water
system. With the current practice of growing maize in these
areas, the rate of land degradation would certainly be
hastened.

To mitigate such environmental complication, there is a
rising interest in using the Miscanthus because of the asso-
ciated environmental benefits. The bioenergy grass, Mis-
canthus, is a high-yielding perennial that can grow on
marginal land and, with "greener" environmental credentials,
may offer an alternative. Because of Miscanthus' perennial
nature, annual plantation process is not required and there-
fore reduces soil disturbance to minimal particularly in the
critical time of autumn. The physiology structure of Mis-
canthus includes extra underground structure such as the
rhizome in addition to root that contribute to stabilizing soil
structure making it more resilient against flood-caused soil
erosion. Current Miscanthus cultivation practice is to harvest
the plant in late winter or early spring allowing the above
ground material to remain standing in the flooded area. This
will prevent soil losses, flood depths, and velocity of over-
land flow (Palmer and Smith 2013; Rose and Rosolova
2015). Furthermore, Miscanthus will yield highly on mar-
ginal land, such as flood zones, offering a sustainable energy
source that does not compete with food production or
compromise the landscape through soil erosion. The current
commercial cultivar M x giganteus (Mxg) may struggle to
keep up with the gas production potential with maize.
However, one has to also account for the energy use and
CO_2 emission during cultivation. There is a possibility, taken
from currently available publications, to believe that Mis-
canthus produces little CO_2 emission and is energy efficient
in cultivation (Felten et al. 2013; Hastings et al. 2017).

While observations indicate that Miscanthus can survive
under winter flood condition (Summerset and Swindon),
empirical evidence and yield data are lacking. To establish
the evidence of Miscanthus survival as well as yield
potential under flooding environment, a plot trial has been
established.

J. Kam (✉) · D. Traynor · J. C. Clifton-Brown
The Institute of Biological, Environmental and Rural Sciences,
Aberystwyth University, Aberystwyth, UK
e-mail: jak42@aber.ac.uk

S. J. Purdy
The University of Sydney, I.A Watson Grains Research Institute,
12656 Newell Hwy, 2390 Narrabri, Australia

J. P. McCalmont
University of Exeter, Streatham Campus, Rennes Drive, Exeter,
UK

2 Materials and Methods

The trial is currently underway in Aberystwyth where a winter waterlogged (flooded) patch is only 3 m away from the dry patch. It is not waterlogged during late spring to early winter.

Miscanthus x giganteus (Mxg) were planted in 2.5 × 2.5 m replicated plots in randomized block design with 16 plants per plot. 3 plots were planted in the dry patch while 3 plots in the wet patch. The Mxg harvest yield data, height, tiller number, number of flowering tiller per plant as well as survival rate from the second growing season have been recorded in late winter.

To detect the soil moisture differences, regular moisture measurement were made. Each plot soil moisture content was detected using a Delta-T Theta probe ML3 attached to a HH2 moisture metre. Three measurements were made across each plot.

3 Results and Discussion

There was distinct moisture difference between the dry and the wet plot throughout 2017. Dry and wet patches both seems to be highest in winter while lowest in summer with the wet patch constantly having higher moisture content, which matched quite well with the pattern of dryer soil in summer and higher chance to flood in winter. The soil moisture can possibly be explained by the plants transpiring over the summer while such activities stopped over winter.

The result showed no significant difference in terms of yield or survival. In addition, there were no significant differences between other physiological characteristics that may influence biomass production such as height and tiller number. It appeared to agree with many observations that Miscanthus can grow well even in winter flood condition.

4 Conclusion

This study has shown that the currently commercial Miscanthus can be cultivated in winter flood zone while retaining yield comparable with the non-flooded area. This will be an important empirical evidence to support using Miscanthus as an alternative feedstock for bioenergy.

References

European Commission. (2014). *State of play on the sustainability of solid and gaseous biomass used for electricity heating and cooling in the EU*. Brussels.

European Environmental Agency. (2006). *How much bioenergy can Europe produce without harming the environment?*

Felten, D., Fröba, N., Fries, J., & Emmerling, C. (2013). Energy balances and greenhouse gas-mitigation potentials of bioenergy cropping systems (Miscanthus, rapeseed, and maize) based on farming conditions in Western Germany. *Renewable Energy, 55*, 160–174.

Hastings, A., Mos, M., Yesufu, J. A., McCalmont, J., Schwarz, K., Shafei, R., et al. (2017). Economic and environmental assessment of seed and rhizome propagated Miscanthus in the UK. *Frontiers in Plant Science 8*(1058).

Palmer, R. C., & Smith, R. P. (2013). Soil structural degradation in SW England and its impact on surface-water runoff generation. *Soil Use and Management, 29*(4), 567–575.

Rose, S., & Rosolova, Z. (2015). *Energy crops and floodplain flows*. Bristol: Environmental Agency.

Technical-Economic Comparison of Chemical Precipitation and Ion Exchange Processes for the Removal of Phosphorus from Wastewater

Chiavola Agostina, Bongirolami Simona, and Di Francesco Giorgia

Abstract

Superior performance of phosphorous removal was achieved by ion exchange process with respect to chemical precipitation. The ion exchange resins required a lower dosage to ensure compliance with the effluent limit. The ion exchange process was less costly due to the lower energy consumption and sludge production.

Keywords

Chemical precipitation • Ion exchange • Phosphorus • Wastewater treatment plants

1 Introduction

Increasing nutrient content, such as nitrogen (N) and phosphorus (P), in water bodies through untreated discharges is the main responsible of the eutrophication process, that is a fast growth of algae and other forms of plants which produce adverse effects on the balance of organisms and water quality (Beccari et al. 1997). Therefore, it is mandatory to reduce P load in the wastewater before its release into the receiving water body. In a wastewater treatment plant (WWTP), P removal occurs through mechanical (e.g., in the primary sedimentation tank) and biological (due to bacterial synthesis) processes. However, these systems are usually unable to comply with the more stringent limits on P in the effluent. Then, an additional treatment unit, specifically designed to enhance P removal, must be operated. The most commonly adopted process to this purpose is the chemical precipitation through the addition of ferric chloride: In this way, orthophosphates react with iron to form iron phosphate, which is slightly soluble and can be removed by sedimentation (Caravelli et al. 2010; Metcalf & Eddy 2013). Although widely diffused, several are the drawbacks of this process: the presence of competing reactions between PO_4^{3-} and HCO_3^- can increase chemical requirements; pH value must be carefully controlled in order to optimize process efficiency; a significant production of chemical sludge is generated, which must be disposed of. Due to these issues, alternative solutions for reducing P content are strongly fostered (Nur et al. 2014; Acelas et al. 2015). Furthermore, due to the decreasing availability of natural resources worldwide, phosphorus recovery from wastewater is receiving increasing attention for its reuse as in the fertilizer production (Sengupta and Pandit 2011; Egle et al. 2015).

The present study aimed at obtaining a technical and economic comparison between anion exchange process using a specifically designed resin and chemical precipitation with the addition of ferric chloride, for the removal of P from wastewater. The experimental work was carried out in two wastewater treatment plants (WWTP1 and WWTP2, respectively) at full scale, located in Central Italy, and managed by Acqualatina S.p.A. They both have to respect the limit of 2 mg/L P_{tot} posed on the final effluent and receive domestic wastewater with a similar P content. A polymeric anion exchange resin impregnated with aluminum ions was used in the study to accomplish selective orthophosphate ions' removal, exploiting the high affinity between these ions and polyvalent metals. The comparison was carried out taking into account removal efficiency as well as sludge production and costs of process operation.

C. Agostina (✉) · D. F. Giorgia
Department of Civil, Constructional and Environmental Engineering (DICEA), Faculty of Civil and Industrial Engineering, Sapienza University of Rome, Via Eudossiana 18, 00184 Rome, Italy
e-mail: agostina.chiavola@uniroma1.it

D. F. Giorgia
e-mail: giorgy89@msn.com

B. Simona
Acqualatina S.p.A, Viale P. L. Nervi snc—C.Com, Latinafiori—Torre 10 Mimose, 04100 Latina, Italy
e-mail: simona.bongirolami@acqualatina.it

2 Materials and Methods

The anion exchange resin (named CATFLOC 441), provided by CATRA S.r.l., is made by insoluble organic polyamines containing the functional group $Al(OH)_3$ and aluminum polychloride (PAC) as coagulant. Three different dosages of CATFLOC 441 were tested, equal to 1, 3, and 6 L/h, respectively. They were applied in WWTP1 to the effluent of the aerobic biological tank prior to the secondary sedimentation tank. The resin operates through two steps: (1) PAC allows destabilization of the surface charges, hydrolysis of the aluminum salts, and formation of the functional group $Al(OH)_3$; and (2) polyamines act as aggregation nucleus for particles, thus improving sludge sedimentation. Ferric chloride was added in the pre-denitrification tank of WWTP2; it was used in an aqueous solution at 40% $FeCl_3$ and it was dosed at a flow rate of 6 L/h.

Removals at WWTP1 and WWTP2 were calculated based on P concentrations measured on samples collected from the influent (instantaneous sample) and the effluent (24-h composite sample) over a four-month experimental period. The following parameters were determined on these samples: total phosphorus (P_{tot}), dissolved phosphorus ($P_{dissolved}$) and particulate phosphorus ($P_{particulate}$), COD, ammonia nitrogen (NH_3–N), nitrate nitrogen (NO_3–N), nitrous nitrogen (NO_2–N), and total suspended solids (TSS).

3 Results and Discussion

3.1 Anion Exchange Process Efficiency

Figure 1 shows the average P removal at the different dosages in comparison with the average value measured during the operation of WWTP1 without the anion exchange process.
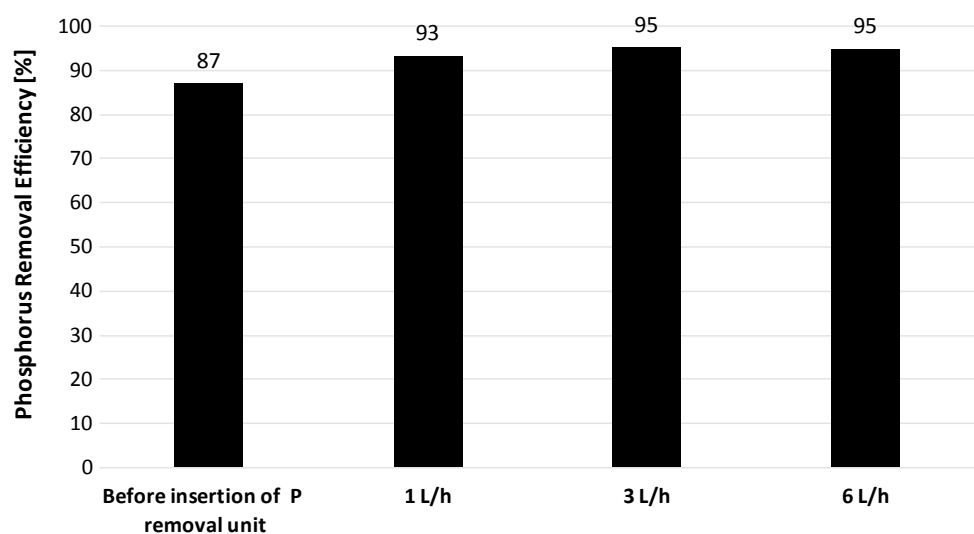
The figure highlights that the addition of the anion exchange process enhanced P removal with respect to the previous period when it was due only to the removal by the bacterial synthesis process carried out in the biological reactor; besides, by increasing the dosage, the efficiency improved further, passing from 93 to 95%. It is worth noting that during the experimental period, COD and ammonia nitrogen removal efficiency showed a decrease with respect to the average values measured in the past, due to lower influent concentrations; consequently, P removal occurring in the pre-treatment stages through mechanical processes and in the biological reactor due to the bacterial synthesis process. Therefore, the real incremental improvement of P removal due to CATFLOC 441 addition accounted for 25%. It was also observed that a decrease of TSS removal efficiency caused a reduction of dissolved phosphorous removal, because the presence of solids hindered the contact between the orthophosphate ions and the ion exchange sites on the resin. The Imhoff cone tests conducted in WWTP1 showed that the resin addition produced an improvement of the sludge sedimentation characteristics; in particular, increasing CATFLOC 441 dosage caused a lowering of the sludge volume after 30-min settlement.

Regarding sludge production in the biological process carries out only a transfer of ions, it can be assumed that it was approximately equal to the applied resin weight. Therefore, considering the CATFLOC 441 consumption, it was estimated a sludge production of approximately 25 kg/d.

3.2 Chemical Precipitation Efficiency

Different dosages of ferric chloride solution were tested in WWTP2 with the aim to find out the value that allowed to

Fig. 1 Average P removal efficiency prior and after the addition of the anion exchange process

Fig. 2 Incidence of cost items [%] for the two technologies of P removal

always comply with the limit set on the effluent of the plant (equal to 2 mg/L P_{tot}). The addition of 6 L/h (as the resin dosage in WWTP1) resulted in a total P removal efficiency of 78% (by means of primary sedime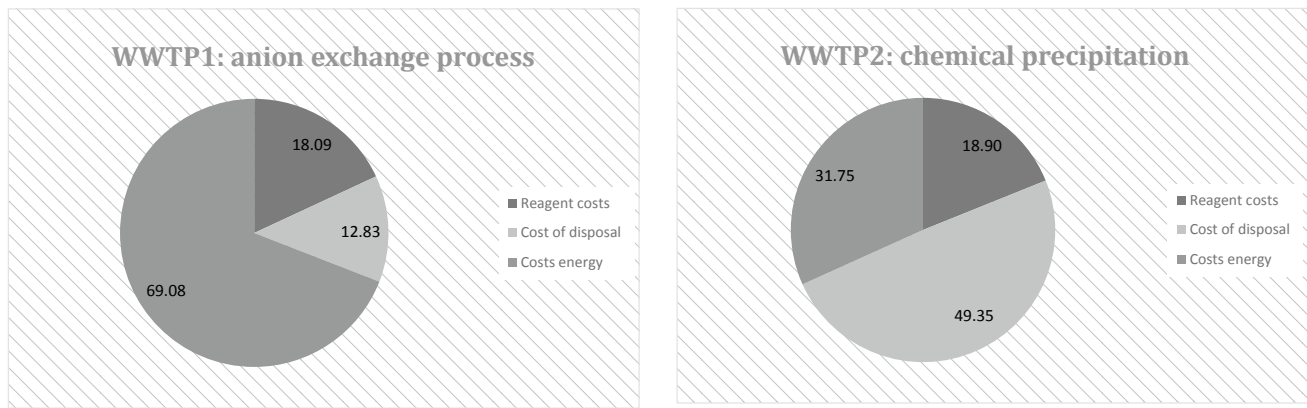ntation, biological processes, and chemical precipitation), which was not enough to achieve the goal. Therefore, it was required to increase the chemical dosage up to at least 12 L/h.

To estimate sludge production, it was used the stoichiometric relationship of the following equation:

$$Fe^{3+} + H_nPO_4^{3-n} \leftrightarrow FePO_4 + nH^+ \qquad (1)$$

Therefore, at the optimal dosage equal to 12 L/h, the quantity of sludge produced was estimated to be approximately 105 kg/d.

3.3 Operating Cost Evaluation

The comparison of operating costs of anion exchange and chemical precipitation processes showed a significant difference in the unit cost of reagents: 0.75 and 0.19 €/kg, for the resin and ferric chloride solution, respectively. By contrast, the cost of sludge disposal associated with chemical precipitation was higher because of the greater sludge production as well as energy consumption. Therefore, the overall operating costs of the P removal unit of WWTP1 resulted accounted to be 16% of the total costs of P removal unit in WWTP2. Figure 2 shows the percentage incidence of each cost item for the two systems.

4 Conclusion

At the same dosage of 6 L/h and influent P concentration (about 6 mg/L), the addition of the anion exchange process and of the chemical precipitation determined a total P removal efficiency (including also that occurring in the mechanical and biological processes) of 95 and 78%, respectively. In the latter case, this dosage was unable to ensure consistent compliance with the limit of 2 mg/L P_{tot} set on the effluent; to achieve this goal, ferric chloride dosage must be risen up to 12 L/h, thus increasing the related costs. Considering sludge production, about 25 and 105 kg/d were generated using the anion exchange process and chemical precipitation (at the required dosage), respectively.

These results show that the removal of phosphorus from wastewater by means of anion exchange resins is more efficient and convenient than chemical precipitation with the addition of ferric chloride. Furthermore, the ion exchange process offers also the opportunity to recover P from the exhausted resin.

References

Acelas, N. Y., Martin, B. D., López, D., & Jefferson, B. (2015). Selective removal of phosphate from wastewater using hydrated metal oxides dispersed within anionic exchange media. *Chemosphere, 119,* 1353–1360.

Beccari, M., Passino, R., Ramadori, R., & Vismara, R. (1997). *Rimozione di azoto e fosforo dai liquami.* Italy: Hoepli.

Caravelli, A. H., Contreras, E. M., & Zaritzky, N. E. (2010). Phosphorous removal in batch systems using ferric chloride in the presence of activated sludges. *Journal of Hazardous Materials, 177* (1–3), 199–208.

Egle, L., Rechberger, H., & Zessner, M. (2015). Overview and description of technologies for recovering phosphorus from municipal wastewater. *Resources, Conservation and Recycling, 105*(Part B), 325–346.

Metcalf & Eddy, Tchobanoglous, G., Stensel, H. D., Tsuchihashi, R., & Burton, F. L. (2013). *Wastewater engineering: Treatment and resource recovery.* USA: Mc Graw-Hill Education.

Nur, T., Johir, M. A. H., Loganathan, P., Nguyen, T., Vigneswaran, S., & Kandasamy, J. (2014). Phosphate removal from water using an iron oxide impregnated strong base anion exchange resin. *Journal of Industrial and Engineering Chemistry, 20*(4), 1301–1307.

Sengupta, S., & Pandit, A. (2011). Selective removal of phosphorus from wastewater combined with its recovery as a solid-phase fertilizer. *Water Research, 45,* 3318–3330.

Implementation and Best Practices

Advancements of Electrically Enhanced Membrane Bioreactor (eMBR) for Wastewater Treatment via Coupling with Novel Inorganic and Polymeric Mixed Matrix Membranes

Shadi Wajih Hasan

Abstract

eMBR is recently developed technology for wastewater treatment. Nanoporous hollow fiber PES membranes were fabricated and tested for eMBR post-treatment. α-MnO$_2$/TiO$_2$ inorganic membranes were fabricated, characterized, and tested for eMBR post-treatment. PES-fβCD mixed matrix membranes were fabricated, characterized, and tested for eMBR post-treatment.

1 Introduction

Many countries in the world are still facing water problems, not only for drinking purposes but also for other applications like agriculture and industrial process heating/cooling that require near-to-potable water quality. According to the World Bank data of 2015, about 84.6% of people living in the rural area now have access to water. Therefore, the reuse of water for sustainable development is indispensable. Notable wastewater treatment approaches, such as activated sludge processes (ASPs), membrane bioreactors (MBRs), and enhanced biological nutrients removal (EBNR), have been conducted to generate reusable and safely dischargeable effluents. However, with the increasing need for a higher quality effluent, the development of new and improved wastewater treatment units is necessary.

Recent advances have demonstrated that the application of an electric field to membrane bioreactors (i.e., electrically enhanced membrane bioreactors, eMBR) can effectively enhance water quality (Hasan et al. 2014). eMBR is a recently developed technology for wastewater treatment through which biodegradation of organic matters, electrokinetics, and membrane filtration exists in a hybrid reactor. eMBR has been tested by many researchers where water quality was significantly improved when compared to conventional MBR or ASP treatment processes. However, reaching a near potable water quality using eMBR has driven several research studies in this field. Therefore, the main objective of this review was to briefly highlight the recent advancements of eMBR for wastewater post-treatment via coupling with novel inorganic and polymeric mixed matrix membranes as demonstrated in Fig. 1.

2 Selectivity of Nanoporous MnO$_2$ and TiO$_2$ Membranes for Residual Contaminants in Treated Wastewater

In this study, MnO$_2$ or TiO$_2$ nanoporous membranes were used as eMBR post-treatment filters for the removal of biological oxygen demand (BOD), bacteria, and residual heavy metals (Fig. 2). The fresh and spent membranes were characterized via thermogravimetric analysis (TGA), zeta potential, and energy-dispersive X-ray spectroscopy (EDAX). Water quality analyses were obtained via UV/Vis Hach spectrophotometry. The results revealed that eMBR-TiO$_2$ performed better than eMBR-MnO$_2$ for most contaminants, i.e., 97.8% BOD, 96.9% Zn, and 100% bacteria removal when as compared to 97.6% BOD, 80% Zn, and 97.5% bacteria removal obtained from eMBR-MnO$_2$ membrane. However, eMBR-MnO$_2$ showed higher removal efficiency for Fe reporting 97.9% as compared to 81.1% by eMBR-TiO$_2$.

S. W. Hasan (✉)
Department of Chemical Engineering, Center for Membrane and Advanced Water Technology, Khalifa University of Science and Technology, Masdar City Campus, P.O. Box 127788
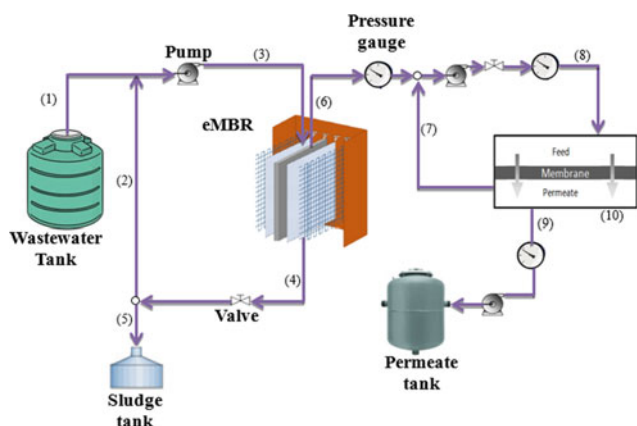Abu Dhabi, UAE
e-mail: shadi.hasan@ku.ac.ae

Fig. 1 Schematic diagram of mixed matrix membrane filtration set-up with eMBR pre-treatment, flows, and materials, numbered as: (1) raw municipal wastewater; (2) recycled (conditioned) sludge from eMBR; (3) influent to eMBR; (4) conditioned sludge released from the drain valve of eMBR; (5) sludge passed to the sludge tank for storage and end use; (6) treated effluent from eMBR; (7) concentrate of the treated effluent after mixed matrix membrane filtration, recycled back to module inlet; (8) mixed matrix membrane feed; (9) final product water; (10) cross-flow mixed matrix membrane filtration module

3 Nanoporous Hollow Fiber Polyethersulfone Membranes for the Removal of Residual Contaminants from Treated Wastewater Effluent: Functional and Molecular Implications

In this research study, the performance of hollow fiber membranes consisting of polyethersulfone (PES) reformed with high proportions of –OH, aryl-N, and alkyl-F groups in nonsolvent additives (Fig. 3) was investigated for the removal of residual Cr (VI), COD, and bacteria from treated wastewater effluent. Functional and molecular interactions during dope preparation and phase separation were also studied in the context of dope and membrane characteristics such as membrane morphology, dope viscosity, water contact angle, functionalities in the fabricated membranes, pure water permeability, and rejection of residual solute. The membranes were characterized via Fourier transform infrared (FT-IR), Raman, and scanning electron microscopy (SEM).

Results showed that molecular weights and dope viscosity of nonsolvent additives with –OH group had more impact on phase separation while phase separation was affected by thermodynamic instability for those with aryl-N and alkyl-F groups. Functional interactions also influenced the lumen shapes and membrane thickness. Additives containing –OH group reported the highest rejection of contaminants and the least water flux while additives containing aryl amide and fluoroalkyl groups improved water permeability yet reported low rejection of contaminants. The PES membrane modified with –OH group reported residual contaminant concentrations from 36.9 ppm COD, 14 ppb Cr (VI), and 18,300 ppm total bacterial counts (TBC) to 20.3 ppm COD, 8.3 ppb Cr(VI), and 8601 ppm TBC with an intrinsic water permeability of 22.9 LMH/bar.

4 Nucleophilic-Functionalized β-Cyclodextrin-Polyethersulfone Structures from Facile Lamination Process as Nanoporous Membrane Active Layers for Wastewater Post-treatment: Molecular Implications

Nanocomposite membranes made of functionalized β-cyclodextrin (fβ-CD) and polyethersulfone (PES) were fabricated, characterized, and tested for wastewater post-treatment. The effect of nucleophilic functionalization of β-CD was investigated via three substitution routes: crosslinking with nucleophilic dicarboxyl groups (M1) in maleic acid; co-polymerization with excess amino group (M2) in hyperbranched polyethyleneimine (HPEI); and nucleophilic modification with amino and hydroxyl groups (M3) in chitosan. Results revealed that all fβ-CD-incorporated membranes were hydrophilic. Water permeability of M1, M2, and M3 membranes were 61, 239, and

Fig. 2 Proposed eMBR post-treatment using MnO_2 and TiO_2 nanoporous membranes (Giwa et al. 2018)
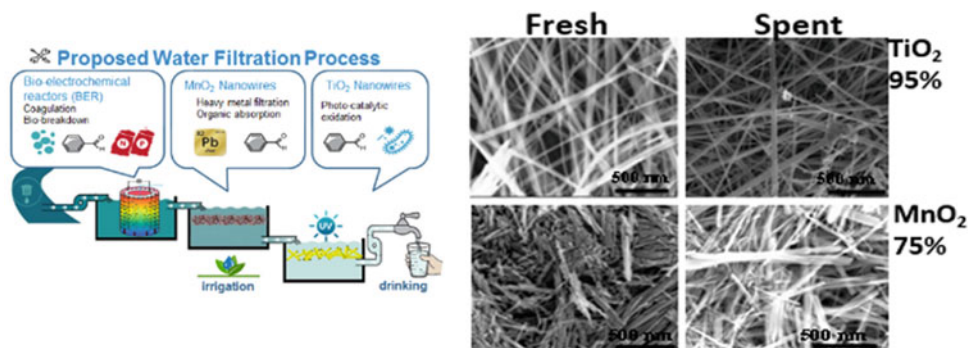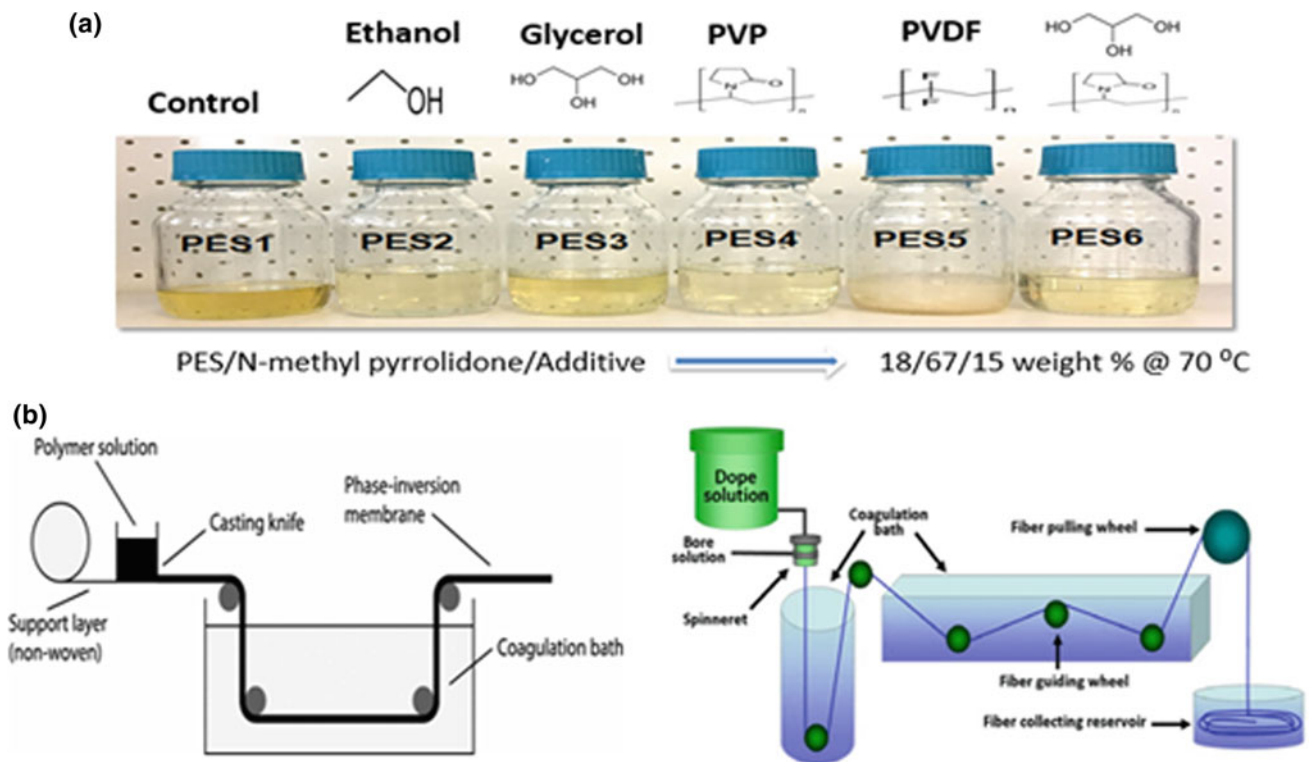
Fig. 3 **a** Dope solutions containing nonsolvent additives and **b** hollow fiber fabrication line (Giwa et al. 2017)
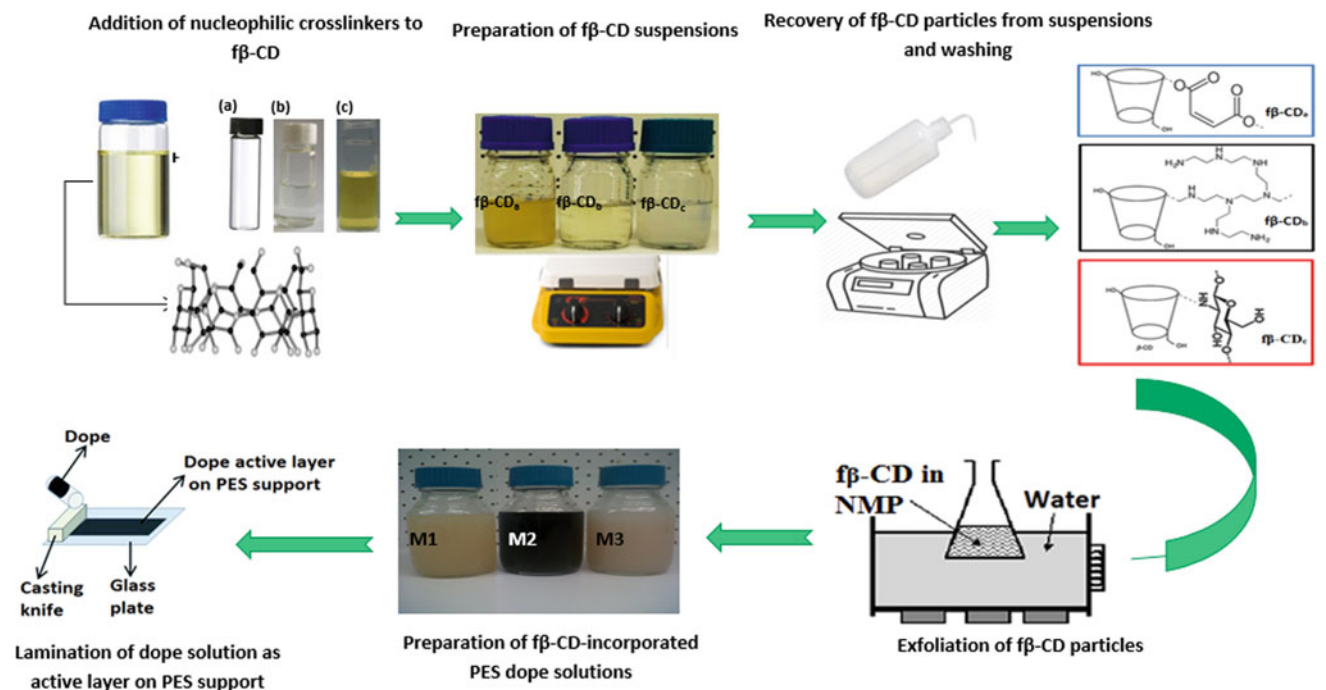
Fig. 4 Fabrication procedure for M1, M2, and M3 membranes containing nucleophilic-substituted β-CD. fβ-CDa, fβ-CDb, and fβ-CDc are β-CD functionalized with maleic acid, HPEI, and chitosan, respectively (Giwa and Hasan 2018)

167 LMH/bar, respectively. M3 membrane reported 92, 90, 82, and 87% removal of Cr^{6+}, Zn^{2+}, Fe^{2+}, and Cd^{2+}, respectively. However, M2 membrane displayed the highest removal efficiencies for residual organics, i.e., 67% chemical oxygen demand (COD) and 84% bacteria due to the hydrophobic interior of its dense fβ-CD (Fig. 4).

5 Conclusions

– MnO$_2$ and TiO$_2$ membranes were inefficient for Cd^{2+} removal.
– Functionalized PES membranes showed lower performance than the inorganic membranes.
– The fβ-CD mixed matrix membranes showed better performance than inorganic and polymeric membranes.

References

Giwa, A., & Hasan, S. W. (2018). Nucleophilic-functionalized β-cyclodextrin-polyethersulfone structures from facile lamination process as nanoporous membrane active layers for wastewater post-treatment: Molecular implications. *Journal of Membrane Science, 563,* 914–925.

Giwa, A., Chakraborty, S., Mavukkandy, M. O., Arafat, H. A., & Hasan, S. W. (2017). Nanoporous hollow fiber polyethersulfone membranes for the removal of residual contaminants from treated wastewater effluent: Functional and molecular implications. *Separation and Purification Technology, 189,* 20–31.

Giwa, A., Jung, S. M., Ahmed, M. A., Fang, W., Kong, J., & Hasan, S. W. (2018). Selectivity of nanoporous inorganic membranes for residual contaminants in treated wastewater effluent: The comparative effects of MnO$_2$ and TiO$_2$. *Chemical Engineering and Technology, 41,* 413–420.

Hasan, S. W., Elektorowicz, M., & Oleszkiewicz, J. A. (2014). Start-up period investigation of pilot-scale submerged membrane electro-bioreactor (SMEBR) treating raw municipal wastewater. *Chemosphere, 97,* 71–77.

Cost-Effective Removal of COD in the Pre-treatment of Wastewater from Paper Industry

Boguniewicz-Zablocka Joanna, Klosok-Bazan Iwona, Vincenzo Naddeo, and Mozejko Clara

Abstract

Different pre-treatment processes were applied to investigate the removal of chemical oxygen demand (COD) from paper mill effluent. The objective of this paper is to find the optimal operating conditions for coagulation process. The effect of key operational parameters, including the type of coagulant, initial pH, temperature, and coagulant dose, on the percent removal of COD was investigated. Under the optimal operational conditions, the treatment of wastewater from paper industries by coagulation has led to a reduction of fee paid for wastewater discharged.

Keywords

Wastewater treatment • Paper industry • COD • TSS • Coagulation

1 Introduction

Chemical oxygen demand (COD) is parameter that describes amount of oxygen taken from the oxidant for chemical oxidation of organic matter and some inorganic compounds (e.g., nitrites, nitrates, sulfates). It is an important indicator of the quality of an industrial wastewater system effluent as it covers the BOD (Biochemical Oxygen Demand) ratio, and informs about substances that microorganisms are unable to break down. High concentration of slowly biodegradable COD fraction can disturb the biological processes at the treatment plant.

In order to reduce parameters such as COD, heavy metals or colors physicochemical processes are used in industrial wastewater. In practice, ozonation and adsorption in combination with coagulation in the pre-treatment are frequently used. The coagulation process ensures a high degree of removal of colloids, TSS, and micro-pollutants (Oeller et al. 1997). The wastewaters from paper industries are one of the most polluting as indicated by many researchers (Lin and Peng 1996; Chen and Horan 1998; Clesceri 2005). COD can range from 1000 to 10,000 mg/l. There are significant differences in the wastewater from different paper industries that depends from diversity of raw products and technology used in industry.

If sewage from the factory is only pre-treated and the recipient is a municipal sewage treatment plant, the value of the COD parameter is strictly determined by the municipal wastewater treatment plants (WWTP) council. For the bigger pollution loads, the company will pay the bigger fees. While reducing COD, reduction of fees for using the environment is expected. In addition, with limited water resources, the opportunity to return some of the water used to circulation is very valuable.

This paper evaluates the pre-treatment processes of paper industry wastewater and examines the effects which they could have on COD and TSS removal efficiency in order to reuse it in processes during paper pulp preparing. The study compared effectiveness of different coagulants that were tester for different paper mill effluent. The coagulation is mainly used to meet the requirements of the recipient's water license pre-treated sewage and to avoid increased charges or penalties for overruns permissible concentrations of pollutants in sewage.

B.-Z. Joanna · K.-B. Iwona
Department of Thermal Engineering and Industrial Facilities, Faculty of Mechanical Engineering, Opole University of Technology, Opole, Poland

V. Naddeo (✉) · M. Clara
Sanitary Environmental Engineering Division (SEED), Department of Civil Engineering, University of Salerno, Fisciano, Italy
e-mail: vnaddeo@unisa.it

473

2 Materials and Methods

The wastewater samples were taken from two different paper mills in the Opolskie Voivodship (Opole Province) in Poland. Wastewater samples were taken from industries, and tests were done in laboratory conditions. From each industry, few series was taken for raw wastewater and after screen bar treatment in industrial plant. COD was measured by standard dichromate method; TSS was analyzed; pH value was measured.

Before starting the coagulation test, the wastewater was analyzed, for determining parameters such as pH, temperature, COD, and total suspended solids (TSS) in the raw wastewater. The dichromate reflux method has been selected for the COD determination because it has advantages over other oxidants in oxidizability, applicability to a wide variety of samples, and easy manipulation. Temperature was measured using electronic thermometer. Electronic pH meter with temperature compensation adjustment for pH value measurement was used.

The commonly used metal coagulants fall into two general categories: those based on aluminum and those based on iron. The first ones include aluminum sulfate, aluminum chloride, and sodium aluminate. The second ones include ferric sulfate, ferrous sulfate, ferric chloride, and ferric chloride sulfate.

In the last years, pre-hydrolyzed coagulants products has been developed; that are able to function efficiently over wide ranges of pH and low temperatures. Also they turn to be more economic, because lower dosages are required to achieve water treatment goals and less chemical residues are produced. During this study, four coagulants were used: FLOKOR DM 17 H; FLOKOR 1,2 A; PAX XL 19H; PIX FeCl3.

The FLOKOR coagulant can be also known as poly aluminum chloride (PAC), and it is a high-efficient coagulant with low generation of waste sludge in a wide pH range, even at low temperatures. This one is known for being highly efficient with low generation of waste sludge. They consist of an aqueous solution of aluminum hydroxy-chloride.

The PAX coagulant belongs to the aluminum group of coagulants that contains Al^{3+} as active component with a rage of concentration between 4.5 and 12%. They are known for their high effectiveness in fighting filamentous bacteria.

The PIX belongs to the ferric coagulants that comprise iron sulphates, chlorides and iron chlorosulphates. They are particularly recommended for removal of phosphorus content from wastewater, for binding of hydrogen sulfide, and for wastewater sludge conditioning purposes.

In the first stage, four coagulants were chosen for COD coagulation. Coagulation was carried using each coagulant in 4 different pH values. Velocity of the mixing was the same for each sample.

3 Results and Discussion

Based on the conducted experiments, the effects of wastewater treatment were compared using different coagulants. The tests were carried out under the same laboratory conditions. In the coagulation process, the coagulant was added to the treated wastewater. In the method of volume coagulation with aluminum sulfate, a decrease of individual parameters characterizing sewage was noted along with the increase of the coagulant dose. It was noted that the turbidity was reduced by about 50%. The highest efficiency of COD removal (about 60%) was obtained using the coagulant dose, 200 g/m^3 in pH value 6.9. For the remaining doses of coagulant, the removal of COD was about 50%. It can be seen that the largest loss of COD occurs with a coagulant dose of 100 g/m^3, when the pH Value is 7.12. Efficiency of pollutants removal, described by selected parameters, during the coagulation process is presented in Figs. 1 and 2. Similar results were obtained by other researchers for coagulation pre-treatment (Konieczny 2011).

Fig. 1 Industry 1. Dependence of effectiveness on the dose of coagulant and type A—FLOKOR, B—PAX
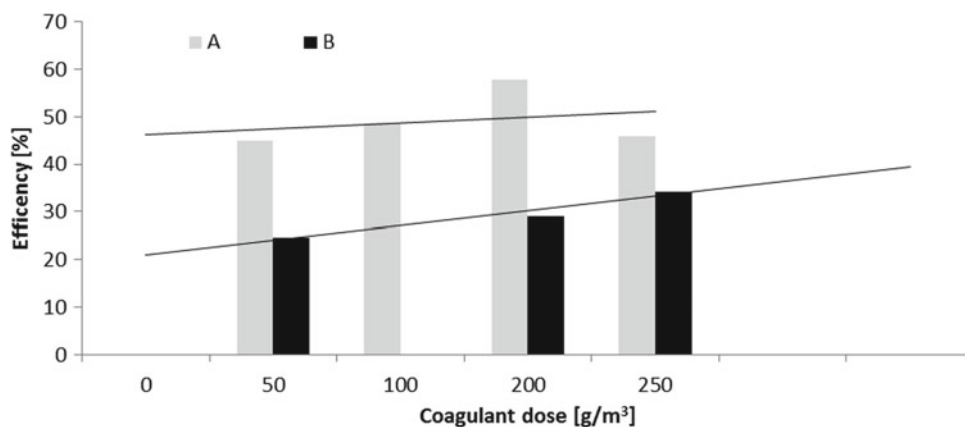
Fig. 2 Industry 2. Dependence of effectiveness on the dose of coagulant and type A—FLOKOR, B—PAX
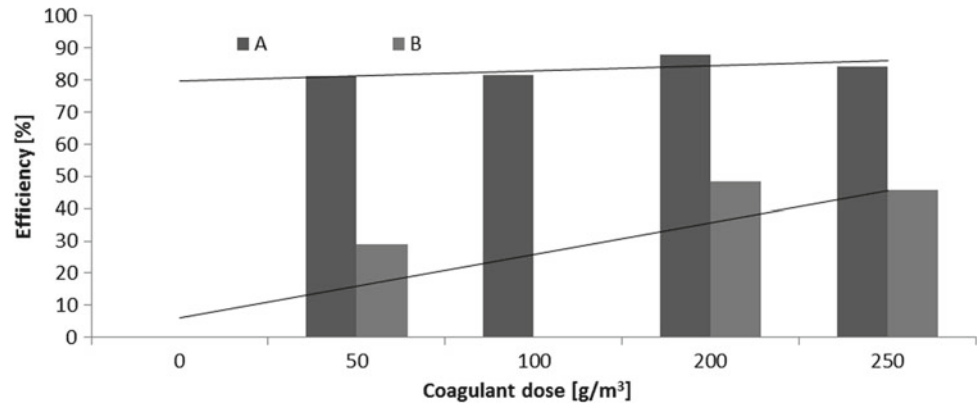
It was evaluated that reduction of COD in wastewater discharged allow to reduce fee paid about 40%. Cost estimation based on available cost data of chemicals and fee paid for discharged loads.

4 Conclusion

Wastewater from analyzed industries is discharged into municipal sewerage network. Therefore, their parameters do not have to fulfill rigorous standard for wastewater discharged directly to the river or ground. Municipal wastewater treatment plant that receive wastewater from analyzed industry is quite small unit (P.E. 44,000), and may be sensitive to irregular discharges of high COD polluted sewage. Nevertheless, care for the natural environment and the agreement defining the permissible values of sewage discharged to the municipal sewage system require the industry to use pre-treatment technology for wastewater.

The analysis is to be used to create a multi-module system for the treatment of industrial wastewater, with recycling of parts of process waters and recovery of heat from waste and parts of chemicals. The project of sewage pre-treatment and water circuit closing is carried out on the basis of BAT (Best Available Technique) guidelines. Thanks to it, a 60% decrease in the value of COD is expected, a 95% reduction in the total suspended solids content and a 60% reduction in color.

In the majority of analyzed cases, sewage from industrial paper mills met the applicable legal norms. However, these standards do not currently cover all parameters that may affect the microorganisms of activated sludge or biological deposits, such as the content of heavy metals or sewage toxicity. In large wastewater treatment plants, industrial wastewater is diluted to a large extent by domestic and rainwater wastewater, but in the case of small biological wastewater treatment plants, discharge of paper mill wastewater can disturb their work.

References

Chen, W., & Horan, N. J. (1998). The treatment of high strength pulp and paper mill effluent for wastewater re-use III) Tertiary treatment options for pulp and paper mill wastewater to achieve recycle. *Environmental Technology, 19,* 173–182.

Clesceri, L. S. (2005). Standard methods fort the examination of water and wastewater (Vol. 21). American Public Health Association.

Konieczny, P. (2011). Strącanie bezpośrednie i wstępne jako efektywne i przyjazne środowisku metody oczyszczania ścieków komunalnych i przemysłowych, *Forum Eksploatatora*, 3, 82–85.

Lin, S. H., & Peng, C. F. (1996). Continuous treatment of textile wastewater by combined coagulation, electrochemical oxidation and activated sludge. *Water Research*, *30*(2), 587–592.

Oeller, H. J., Demel, I., & Weinberger, G. (1997). Reduction in residual COD in biologically treated paper mill effluents by means of combined ozone and ozone/UV reactor stages. *Water Science and Technology, 35,* 269–276.

Sensors for Water Purification Using the Example of Wastewater Treatment Plant Gabrovo, Bulgaria

S. Kartunov and B. Kosev

Abstract

The article analyzes water purification and methods for the purpose. Types of sensors and appliances used for wastewater treatment are considered. The scheme and the principle of operation of a sewage treatment plant in Gabrovo, Bulgaria are presented.

Keywords

Sensors for water purification • Scheme and the principle of operation of a sewage treatment plant in Gabrovo

1 Introduction

Nowadays when the world population has reached 7.6 billion people, the necessity of drinkable water is significant. This on the other hand leads to enormous amount of wasted water. In order to save the society from contagious diseases, this water has to be treated. There are various methods for wastewater treatment. Each one of them is very specific and is used in different cases. This is due to the fact that every factory, working shop or production plant pollute the water with different types of hazardous substances. The analysis of wastewater is an essential part of whole water treatment process. According to the results from analysis, the most appropriate methods are chosen. In order to monitor all machines and values, a large number of sensors are engaged. This is absolutely necessary in order to control the process accurately and to have full automation. In addition, this article is also shown how all methods and machines work together. As an example is given The Water Treatment Plant of Gabrovo, Bulgaria.

2 Materials and Methods

2.1 Analysis of Wastewater

The analysis of wastewater is the first step on the road to the construction of the treatment plants. A detailed analysis is needed to in order to build the most efficient equipment possible. Drinkable water used in household and other purposes is polluted with different substances and changes its natural physical properties and chemical composition. There are different classifications of the polluted water and its substances according to several factors (Цачев Цачо 2001).

2.1.1 Categorization of the Water by Origin and Its Characteristics

Household, industrial, rain water

2.1.2 Categorization of Pollutants in Wastewater by Physical State

Insoluble substances with particle diameter $d > 10^{-4}$ mm. They are in a rough dispersed state. Larger ones, with dimensions from 1 to 1.10^{-2} mm, are deposited. Another part of them with a diameter of 1.10^{-2} to 10^{-4} mm is in the form of a suspension, an emulsion and foam.

Substances in colloidal state—with particle diameter $d = (1.10^{-4}$ to 1.10^{-6} mm). They do not pass through a simple paper filter. An example of such a substance is the soap. Colloidal systems are resistant. The particles in these systems are continuously floating in random motion (Brownian motion).

Substances in dissolved form. They are in the form of molecularly dispersed particles with a diameter $d < 10^{-6}$ mm and cannot be deposit. They do not form a single phase, the system becomes one-phase and represents a real solution. They include various types of gases such as

S. Kartunov (✉) · B. Kosev
TU of Sofia, Sofia, Bulgaria
e-mail: skartunov@abv.bg

B. Kosev
e-mail: bogi895@abv.bg

hydrogen sulfide and carbon dioxide. The amount of dissolved substances depends to a large extent on the salt composition of drinking water as well as the polluting substances used by the population and industry.

2.1.3 Categorization by Origin and Chemical Composition of Pollutants

– mineral (particles of sand, glass, particles containing the elements calcium, magnesium, silicon, tin etc.);
– organic (substances that have plant or animal origin);
– bacterial and biological (bacteriological and biological contaminations are caused by the presence of various microorganisms (up to 100 million in 1 cm^3 of water) in the water, such as yeast and mold fungi, algae and bacteria, as well as pathogenic bacterial infections caused by typhoid, paratyphi, diphtheria, dysentery, cholera, tuberculosis and others.)

2.2 Different Methods for Water Treatment

In recent years, as a result of increasing pollution, needs of purification are constantly growing. As a result, many methods are invented (Kartunov 2014).

2.2.1 Physical Purification

(mechanical, primary) Applied to coarse substances released by precipitation and filtration. The most popular appliances used are mechanized screens and grit chambers.

2.2.2 Physical and Chemical Purification

In this group are the following processes: coagulation, flocculation flotation, sorption, ion exchange, hyperfiltration, reverse osmosis, extraction, evaporation, crystallization.

2.2.3 Chemical Purification

The chemical treatment is applied for the pH correction and removal of some dissolved substances from industrial wastewater. Main processes are chemical oxidation electrochemical oxidation/recovery; neutralization.

2.2.4 Biological (Secondary) Purification

The main process is the conversion of biological substances from wastewater into living mass (active sediment). This is achieved by the concentration of microorganisms in a basin.

2.2.5 Decontamination

It is used to remove pathogenic bacteria. The main processes are: chemical oxidation, radiation exposure and thermal treatment.

2.2.6 Sludge Treatment

Sludge is usually sent to drying beds or after dehydration to methane tanks where biogas is produced.

In most cases for better efficiency, not only one method is used but two or three together. Thus, the wastewater is cleaned.

2.3 Sensors in Water Plant

In all modern water plants, nowadays sensors are used to control the quality of the water and to automate the process. Due to the fact that specific technological processes occur many types of sensors take part in it. The most important of them is given as well as their measured parameter and working principle in the following Table 1.[1,2,3,4]

This is a classification of the most common sensors used in water treatment. They provide nonstop online information for all parameters. Finally, water is released crystal clear.

3 Results and Discussion

Water treatment plant Gabrovo (WTPG) Purification plants are very complicated facilities. In order to be easily understandable how all processes and equipment are engaged is given simplified scheme and description of the processes in (Fig. 1). In the beginning of the treatment, plant water passes through the physical purification methods. After the overflows, which are 3, each with a capacity of over 30,000 inhabitants, water reaches a large waste grid.

Ultrasonic level meters are also installed to monitor the water level and to ensure the automatic operations of the system. For each overflow corresponds a large mechanized bar screen. Behind it, in the technological scheme, the screen for fine waste takes space. The fine screen stops 5 mm waste. It is driven by a hydraulic piston. Then comes the screw screen that is equipped with a screw which pushes the waste to a larger one. From there, it goes to the gathering basket. In the room, there is also a tangential flow grit chamber. To control subsequent processes, water needs to be measured and this happens in the Venturi flume. Further, the purified water from the largest waste goes to the grit chamber. There is air coming in the chamber, and the water

---

[1] https://kansai-automation.co.jp/en/catalog_pdf/ZZ-167-1501E.pdf.
[2] http://www.processinstruments.co.uk/products/chlorineanalyser/?gclid= EAIaIQobChMItbLcjvX22wIVBz8bCh1mBA5lEAAYASAAEgIaAPD_ BwE.
[3] https://catalog.nova-gas.com/item/inuous-methane-analyzers-continu ous-ch4-analyzers-/thane-gas-analyzer-by-infrared-detector-470-series/ series-470n4?&origin=keyword&by=prod&filter=0.
[4] https://en.wikipedia.org/wiki/Venturi_flume.

Table 1 Sensors used in water treatment plant

Measured parameter	Sensor or way of measurement	Working principle
The amount of incoming sedimentary and biologically purified water	Venturi flume Parshall flume	Measurement of discharge with Venturi flumes requires two measurements, one upstream and one at the throat (narrowest cross-section), if the flow passes in a subcritical state through the flume. If the flumes are designed so as to pass the flow from subcritical to supercritical state while passing through the flume, a single measurement at the throat (which in this case becomes a critical section) is sufficient for computation of discharge. The Parshall flume accelerates flow through a contraction of both the parallel sidewalls and a drop in the floor at the flume throat. Under free-flow conditions, the depth of water at specified location upstream of the flume throat can be converted to a rate of flow
Amount of raw and compacted sludge	Parshall flume, Venturi flume, Overflow	
Amount of air	Diaphragm or Venturi tube	Fluid flows through a length of pipe of varying diameter
Density of the raw, compacted or composed sludge	Photoelectric sensor	Ultrasonic sensor which measures the amplitude of received signals and observes the shape of signal. It takes all energy as envelope and then converts it into density
Dissolved oxygen	Electrochemical sensor	A membrane-isolated electrochemical cell contains cathode, anode and electrolyte solution. A gas-permeable membrane allows dissolved oxygen from the sample to the electrodes. There, the electrochemical reaction generates an electrical current proportional to the dissolved oxygen concentration
Concentration of carbon dioxide, methane	Gas analyzer	The detector pulses an infrared beam of light through the sample tube, without the need for a mechanical chopper. In operation, the internal sample pump draws the sample gas through the filter/condensate trap, secondary filter, flow meter, and then on to the infrared detector. The detector output is digitally linearized and then displayed as percent or PPM CH_4 on
pH of water or sludge	pH meter	Potentiometric pH meters measure the voltage between two electrodes and display the result converted into the corresponding pH value
Sludge temperature in the methane tank	Resistance thermometer	Platinum wire wrapped around a ceramic. The wire has accurate resistance/temperature relationship which is used to provide an indication of temperature
Residual chlorine in the purified water	Electrochemical sensor	The sensors work by separating the electrodes that perform the measurement from the sample, by a membrane. This membrane allows the free residual chlorine (HOCl and OCl–) or the total residual chlorine (HOCl and OCl– plus chloramines) through the membrane. Inside the sensor the dissolved chlorine meets the electrolyte which is at a low pH. This converts the majority of the OCl– to HOCl. The HOCl is reduced at the gold working electrode and the current generated is proportional to the chlorine present, and the instrument gives a reading in ppm or mg/l
Level of wastewater or sludge	Level meter	Ultrasonic float
Pressure of air, water, methane	Manometer, explosion-proof manometer	Bourdon tube

becomes lighter. As a result, the sand falls to the bottom. There it is collected by a pump. The water then flows through the primary settling tanks. The sludge, which is pushed to the center of the plant, is separated there. There it is sucked out. The water is sent to a large activated sludge basin. The basin is divided into two parts. In the first one, it is mixed with large mixers. In the second part, the water stays motionless. But underneath, there is a network of pipes on the bottom. At the outlets of these pipes, there are membranes. Thus, the air is provided for aerobic digestion. For this purpose, there is a pumping station, which delivers a low pressure of about 0.5 bar. Secondary settling tanks follow. A level sensor system is used to control the gear and to actuate the pumps. If the water is not sufficiently purified, it can still be sent to the primary settling tanks and cleaned better. After that are placed the fields where the sludge is stored and then dumped. Previously, however, the process continues in chlorine contact tank. Three pumps from chlorine building deliver previously dissolved lime. Pumped sludge from settling tanks is centrifuged to drain and is sent to methane tanks. There biogas is produced. It is stored in a gas holder and is used for the production of
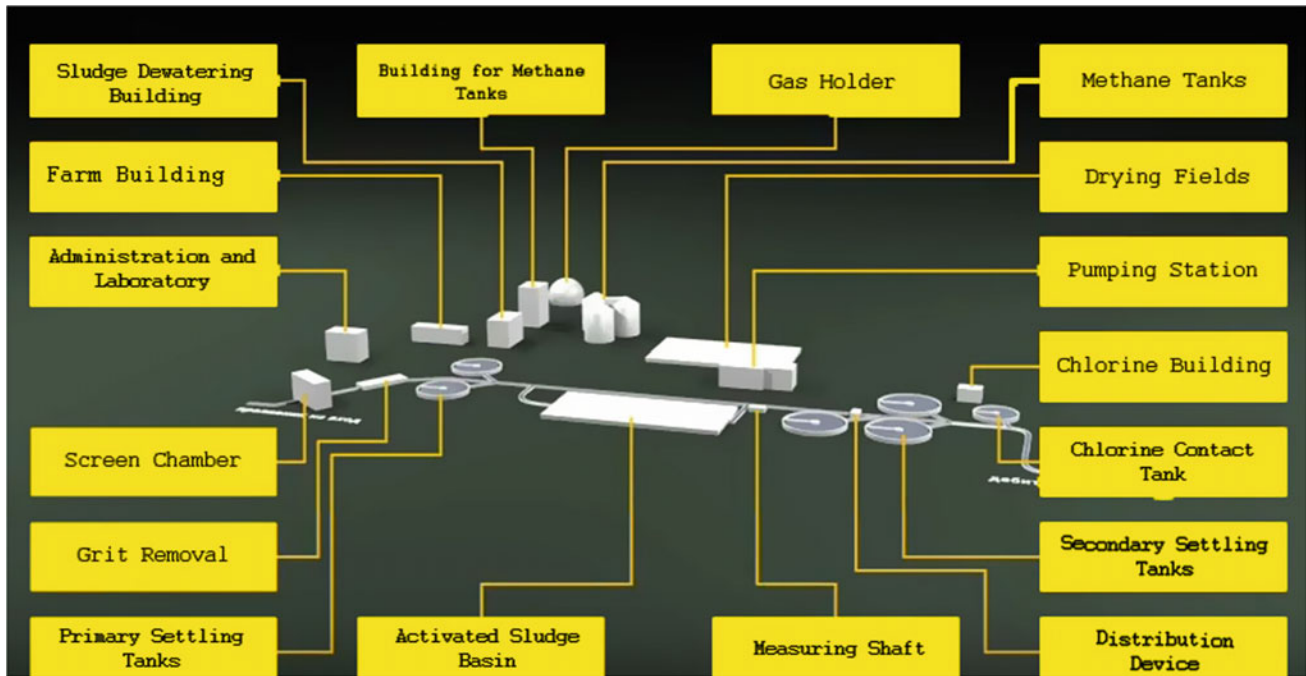
Fig. 1 Scheme of water treatment plant Gabrovo, Bulgaria

Fig. 2 Methane tanks, biobased area with aerobic and anaerobic digestion zone, secondary settler

electricity. The ecological solution is able to some extent to satisfy the energy needs of the water treatment plant (Fig. 2).

4 Conclusion

In this article were shown some short classifications of wastewater, main methods for treatment and the most important sensors that are used to monitor these processes. A short description of WTPG was made in order to give an idea how technology and machines are working together.

Undoubtedly, the problem of water recycling has become fundamental and vital to the whole planet. From finding the right solution, to some extent, also depends on the quality of life of future generations.

References

Цачев Цачо, Пречистване на битови отпадъчни води, София, Техника, 2001, (in Bulgarian).

Kartunov, S. (2014) Waste Processing Technique and Technologies, Gabrovo, W. Aprilov. ISBN 978-954-683-512-3.

Design an Integration Platform Between Water Energy Nexus and Business Model Applied for Sustainable Development

Heba Ahmed Mosalam and Mohamed El-Barad

Abstract

Sustainable Development Calculator Application—Innovating tool for Sustainable Development WEN—A Platform for applying WEN Concepts—Integration Between Business Model and WEN—Mobile Application for Water Energy Nexus.

1 Introduction

The rapid population and global economic development will add a pressure on the limited resources in our planet, including water, energy, food, land, and ecosystems. It needs not to know the interlinkage between all resources, but also it has to create a qualified generation of WEN academicians and establishing a tools help the community with WEN concepts (Trinex platform 2017). Many WEN studies developed or applied a specific method and tried to adapt it to the characteristics of their case studies. For example, different models were developed on the Foreseer online tool platform to meet the nexus research demands of

different countries, including China and the UK (Hamiche et al. 2016). In believing that water crisis is a present and future risk, with a growing demand for local resources, this paper proposed comprehensively an integrated platform or an application between business model, water, energy, and food nexus. It is considering as a Web-based knowledge-sharing system to facilitate the cooperation between the investors and researchers. A cross-application is proposing to apply Trinex concepts merged with business model in new projects. It is expected that this can assist policymakers and resource managers in water and energy conservation and sustainability due to the effective management of interdependent water and energy systems and of course food which is provided through a new application (Healy et al. 2015). There are many existing methods and tools for water and energy system analysis (Schnoor 2011), but what makes this research unique is the combination between WE and WEF and Business model. In addition to functions providing to the investors starting from data providing, analytics and statics and even access to determine the budget for each element used in the project related to WEF nexus. Water and energy resources, land use, land cover, and many other criteria loaded in geo-database to provide an obvious view for the investor and a key person to take a decision in new projects or develop a static plans, especially when the data linked to the business model or cost analysis to execute a project. A financial data related to each location and country all the calculation will be done in the background without involving the user into WEF Nexus deeply. If the user needs to invest in water, energy, or agricultural project in a certain area, the system proposed a comprehensive study related to WEF perspective which makes the development more ease.

2 Materials and Methods

The main methodological frameworks will be applied and developed by consultant groups of experts in different fields such as water resource management and energy in addition

H. A. Mosalam (✉)
Energy Program, Electromechanics Department, Heliopolis University for Sustainable Development, Belbes-Cario Desert Road, Cairo, Egypt
e-mail: heba.mosalam@hu.edu.eg

M. El-Barad (✉)
Public works Section, Construction Department, Egyptian Russian University, Cario-Suez road, Badr City, Egypt
e-mail: mohamed.fahmy@eru.edu.eg

to expert developers understanding WEF concepts. Creating a platform needs two main tasks. The first one is a backend which including a spatial database like environmental data needed for project study, water resource, solar density, wind direction, humidity, land cover, and land use then merged with business model like solar panel cost, pumping, batteries, windmills cost, and other material costs. The second one is a frontend which represents an impressive screen design for interacting with the data like screens "User Login, Dashboard, and other interaction screens." It can be applied in any area to calculate project cost study. The study has to include WEF or WE nexus concepts. It has to convert all international stand art and sustainable development objectives from formal context to programming or coding. Data will be updated periodically by new amounts of data sets related to freshly acquired and accurate data, considering the integration between different data sets and international standers.

In a digital world, our plan can be represented as layers, and each layer represents specific phenomena "solar density, land use, and other criteria" can be named as a "Thematic Layer" reflect the geo-database. A layer consists of many pixels. Each pixel has only one value, so when the user selects in a certain location in the system. System will show its value. The system have various thematic layers of natural resources which help researchers and potential users to gain a clearer vision for their projects and development target.
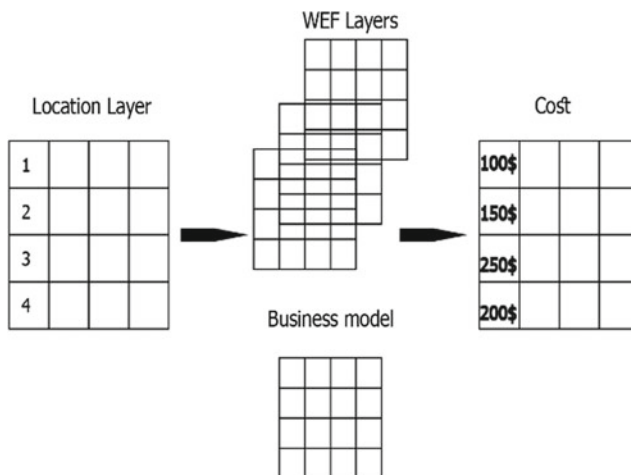
The combination between business model and resource information will create a system taking into consideration both technical and financial issues respecting the sustainable development concepts and WEF nexus approach. Figure 1 clarifies the idea of merged layers in the system.

For creating layers, there are many methods like field data gathering, trusted Web sites, and governmental cooperation, and it can use automated approaches like interpolation to determine missing data, also using expert system could be predicting the cost for any project will be executed in the future depending on previous calculations for different projects in the past. The system will be covered by international standards for water energy and food, which will help for creating a WEF stander in the future.

Data gathering is considered as main challenges; also, cooperation with government agencies and civil society organizations will be essential to ensure the effectiveness of the application in the wider range. It is expected that there will be various functionalities in the system, but when the investor presses at the calculator button, the world map will be appearing to select the area for investment. After he selects the area he will choose the field of investment "Water–Energy–Food", then he has to fill the application form depending on the field of the investment. Figure 2 represents the application workflow. The expected cost will be calculated, and the user will find a report and recommendation according to the database created.

The system will be available in both desktop and mobile devices using enterprise geo-database, with impressive and effective design for client comfortable. Figure 3 represents the proposed—draft design—screen, and this shows the login interface for tablet, mobile, and desktop machine. After the user logins, there are many options like getting a specific data or statistical data for certain area or project; also, user can navigate with specific criteria. The first function is to calculate the cost for its project considering WEF nexus and sustainable development. Figure 4 proposes dashboard screen.

The first step is to select a certain area by select location on map or using GPS, write adders or even by location coordinates. Figure 5 shows site selection screen. After selecting the project location, the system will open an application form, and the user will fill the form related to the project.

According to the investor interest, he will select the field he wants like "Water–Energy–Food" and the form depending on the type of the project illustrated into Fig. 6, and the user has to fill the data needed like;

Fig. 1 Idea of merged layers system

Fig. 2 Application workflow
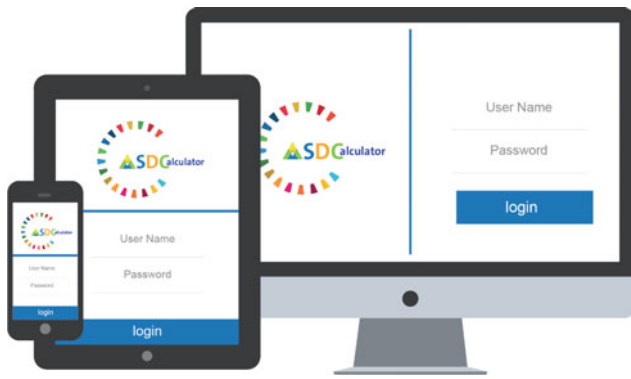
Fig. 3 Proposed screens
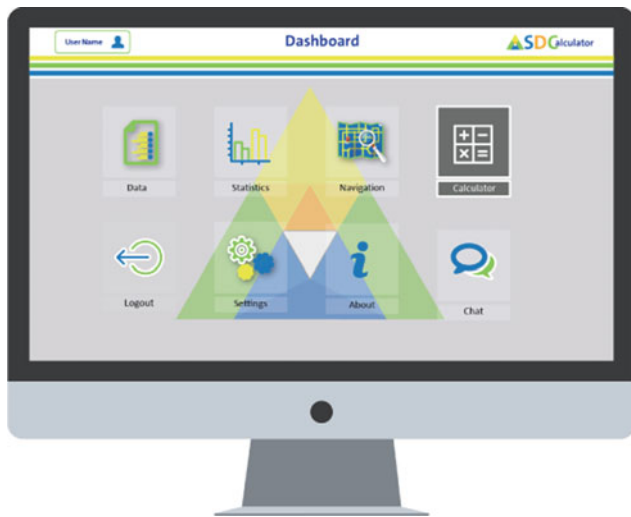
Fig. 4 Dashboard screen

Fig. 5 Site selection screen

Fig. 6 The form screen

Fig. 7 Report template screen

- Discharge needed for water project
- Capita needed to cover
- Total megawatt needed for electricity project.

Finally, the report will process according to WEF perspective considering international standers, by integrated sustainable development WEF nexus with its cost. Figure 7 represents the proposed report template screen.

- Report will be per element to provide user obvious view for budget needed.
- Reports will be validated and verified in beta version.

3 Results and Discussion

Effective management of interdependent water and energy systems is critical to sustainable development at all scales: for cities, countries, regions, and the entire planet. Analysis of the nexus between water and energy flows can improve the understanding on the quantitative relationship between the two resources and finally to guide actions and policy-making toward optimized outcomes and minimized risk (Dai et al. 2018). Sustainable Development or SD Calculator Application is pivotal to sustaining and improving the quality of life. For example, Discover a new area for investment in solar energy or crop production. These discoveries lead to the development of the projects that increase incomes and build new development communities based on the best use of water resources and using a renewable energy to produce food. SD Calculator will be a unique idea putting the platform in a leading position in WEF nexus approach, and it combining three different fields criteria together in an automated system integrated with business needs for budget calculations. For example, the investor needs to build his own project in the west desert, the system can provide the best location in this area and the irrigation methods with respect to the power needed and water resources according to databases and its experts not only that but also with a budget for this project all of this in one report respecting the sustainability and WEF nexus concepts. And after a while, it can be an expert system to calculate any area automatically and precise. There are many objectives for the application: (1) providing separated data for the investors or users; (2) providing statistical data for investors; (3) send mail or chat with consultants; (4) specific system will be calculating the cost to invest in a certain area considering WEF nexus and sustainable development aspects.

4 Conclusion

Sustainable Development Calculator Platform, convert the vision to numbers can be measuring and evaluating with considering the water, energy and food WEF aspects. It will be one of the automated systems applying Trinex concepts on the ground. Supporting from the groups of experts and consultants in different fields believing in WEF nexus and financial issues system will be implemented. Platform reduces time and effort consuming by the investor to know the cost needed for the project or know the best area suitable for a certain project not only that this result respecting WEF nexus concepts and sustainable development to be applied in the project. An application will be implemented with international standers in the three main fields, water, energy, and food, by the combination between experts in different scientific fields and specialized developers.

References

Dai, J., Wu, S., Han, G., Weinberg, J., Xie, X., Wu, X., et al. (2018). Water-energy nexus: A review of methods and tools for macro-assessment. *Applied Energy, 210,* 393–408. https://doi.org/10.1016/J.APENERGY.2017.08.243.

Hamiche, A. M., Stambouli, A. B., & Flazi, S. (2016). A review of the water-energy nexus. *Renewable and Sustainable Energy Reviews, 65,* 319–331. https://doi.org/10.1016/J.RSER.2016.07.020.

Healy, R. W., Alley, W. M., Engle, M. A., McMahon, P. B., & Bales, J. D. (2015). *The water-energy nexus: An earth science perspective.* U.S. Geological Survey Circular.

Schnoor, J. L. (2011). Water-energy nexus. *Environmental Science and Technology, 45,* 5065. https://doi.org/10.1021/es2016632.

Trinex platform. (2017). E. plus project. *The national water energy food nexus strategy of Egypt executive summary.*

New Tools and Approaches for Soil and Water Bioengineering in the Mediterranean to Enhance Water Quality

George N. Zaimes, Guillermo Tardio, Valasia Iakovoglou, Martin Gimenez, Jose Luis Garcia-Rodriguez, and Paola Sangalli

Abstract

Soil and water bioengineering works can improve water quality. Soil and water bioengineering works are nature-based methods. Stakeholder inputs can improve soil and water bioengineering works. Case studies in soil and water bioengineering from the Mediterranean. New protocols and a template for soil and water bioengineering work for the Mediterranean.

G. N. Zaimes (✉)
Dept. of Forestry and NEM, UNESCO Chair Con-E-Ect on the Conservation and Ecotourism of Riparian and Deltaic Ecosystems & Eastern Macedonia and Thrace Institute of Technology, Drama, 66100, Greece
e-mail: zaimesg@teiemt.gr

G. Tardio
Spanish Association of Landscape Engineering, Technical University of Madrid, Getafe, 28905, Spain
e-mail: gtarcer@gmail.com

V. Iakovoglou
Dept. of Forestry and NEM, Eastern Macedonia and Thrace Institute of Technology, Drama, 66100, Greece
e-mail: viakovoglou@yahoo.com

M. Gimenez · J. L. Garcia-Rodriguez
School of Forestry, Technical University of Madrid, Avda de las Moreras, Madrid, 28040, Spain
e-mail: martin.gimenez@upm.es

J. L. Garcia-Rodriguez
e-mail: josel.garcia@upm.es

P. Sangalli
Sangalli Coronel y Asociados SL. and EFIB (European Federation of Soil and Water Bioengineering), San Sebastian Gipuzkoa, Spain
e-mail: sangalli@sangallipaisaje.com

1 Introduction

Anthropogenic activities, such as agriculture, deforestation and urbanization, have significantly accelerated soil erosion and loss in the last centuries (Montgomery 2007; Bakker et al. 2008). This has scientists considering accelerated soil erosion and loss major threats to human societies with potential impacts equivalent to those of climate change (Zaimes et al. 2016). Soil erosion and loss have major impacts on humans, their society and the environment such as decreasing land productivity, degrading ecosystem's dynamics including aquatic habitats, reducing water quality and increasing flooding that can lead to loss of life and property (Yang et al. 2003; Pinter and Heine 2005; Owens et al. 2005). Accelerated soil erosion increases nonpoint source pollutants that are a major problem worldwide (Zaimes and Emmanouloudis 2012). Excessive sediment and nutrient loading in stream waters (a) pose health risks to humans, (b) lead to increased costs due to water purification, (c) kill livestock and wildlife and (d) cause eutrophication that can kill aquatic species (Kotak et al. 1994; Pierzynski et al. 2000; Midgley et al. 2012).

Improving water quality is a necessity for EU member states based on the Water Directive 2000 (Kalampouka et al. 2011), and it can be achieved with the increased adoption of soil and water bioengineering works. This was the main aim of the ECOMED project that focuses on the Mediterranean region. The ECOMED project generated sector-specific, new, theoretical and practical tools and approaches to help specialize the process and enhance soil and water bioengineering in the Mediterranean. The project consortium has 13 partners with a mix of academic institutes and companies and is led by the Technical University of Madrid. The partners are from eight countries (Spain, Portugal, France, Italy, Greece, UK, Turkey and FYROM), with seven from the Mediterranean.

2 Materials and Methods

The Mediterranean region should be a priority in the implementation of soil erosion mitigation efforts (Cerdan et al. 2011). The region has been inhabited by humans for thousands of years, and their negative impacts are evident with the many unsustainable agricultural lands and the few remaining patches of natural ecosystems (Tal 2010). The natural and frequent wildfires of its ecosystems lead to burnt bare areas with very high erosion rates (Pausas et al. 2007; Ranis et al. 2015). The socioeconomic changes of the past century in the region have led to the frequent abandonment of agricultural fields that have also increased soil loss susceptibility (Ries 2009). Finally, the forecasted climate change impacts for the region should lead to higher surface runoff volumes and peaks thus increased sediment transport capacity (Giupponi and Shechter 2003).

Soil and water bioengineering is a natured-based method that can decrease soil erosion (Giupponi et al. 2017). It involves the use of living plants or cut plant material, either alone or in combination with inert structures, to control soil erosion and the mass movement (Bischetti et al. 2014). They are widely used in soil and fluvial works to improve resilience against soil loss by stabilizing stream bank and slopes. The lack of specialized training and shortage of specialized staff in soil and water bioengineering in most of the Mediterranean countries makes it a necessity to develop training tools and approaches on their implementation, specific to its environment. For these tools and approaches to be successful, the interaction and feedback of the stakeholders of the sector are needed.

Three major activities have taken place. Firstly, an online questionnaire that addressed the needs and existing gaps in the soil bioengineering sector was developed for the stakeholders. The questionnaire had five different sections: (a) design, (b) construction, (c) maintenance/monitoring, (d) training and (e) enterprise/company. Each section had 25–35 questions. Secondly, protocols and templates for soil and water bioengineering in the region that address the design, time and elements durability throughout life of the work to achieve an effective assessment were developed specialized for the Mediterranean (Tardio and Mickovski 2016). Thirdly, with most experiences, examples and methodologies originating from the Atlantic and Continental, examples from the Mediterranean are necessary. Specifically, existing soil and water bioengineering works (case studies) from the entire Euro-Mediterranean region were selected and analyzed that included slope, fluvial and coastal scenarios.

3 Results and Discussion

More than 110 professionals in soil and water bioengineering from 11 different countries answered the questionnaires. The participants answered all or some of the five sections of the questionnaire. In the design section, most participants answered that there is a need for specialization in this stage, new design tools need to be generated and that the awareness of existing tools is low. In the construction section based on the participants' answers, it was encouraging that many different scientific disciplines were involved in soil and water bioengineering works and that native material was preferred. The greatest concern was that quality control of the work did not occur in many cases during their construction. The rewriting of the maintenance/monitoring guidelines, the need for monitoring because of the semi-empirical nature of soil and water bioengineering works and the need for workshops/seminars in regard to regulations were the main findings in the maintenance/monitoring section. The participants of the training section, stated that there is a lack of soil and water bioengineering professionals in the Mediterranean and that the development of new training courses and even an M.Sc. is a main necessity in the region. In addition, participants stated that the existing professional would also attend these courses. Finally, in the enterprise/company section, participants said that soil and water bioengineering has and will continue to grow, that they have been experiencing an increased demand for soil and water bioengineering works and that training courses need to be established.

Currently, 15 existing works from Italy, France, Greece, FYROM, Portugal, Spain and Turkey have been selected. The case studies deal with slope, fluvial and coastal stabilization that decrease soil erosion and nonpoint source pollutants that reach water bodies. In Greece, currently two case studies were analyzed. Specifically, the first is the use of log barriers after a wildfire, a common practice utilized by the Greek Forest Service. Greece has frequent wildfires every summer and faces flood and erosion problems in these burned areas with the first rainfall events in the fall (Ranis et al. 2015). The other includes the rehabilitation of a marble quarry. Marble is utilized heavily by the construction industry in Greece. In this specific case study, hydro-seeding along with plant seedlings was utilized.

Protocols and templates are necessary for the effective and efficient field monitoring of soil and water bioengineering works. Three protocols and a template applicable and adopted for the entire Mediterranean region were developed by the ECOMED project. Protocol 1—*Soil Bioengineering Work Selection Criteria*, provides the criteria to

be followed to ensure the selection of the proper soil and water bioengineering works for the specific site. Protocol 2—*Soil Bioengineering Work Analysis Definition*, describes the structure and stages that need to be followed when analyzing each selected soil and water bioengineering work. It provides guidelines on information required and the management plans that need to be developed before starting the work analyses for the different stages (such as design, construction, maintenance and monitoring stages). Protocol 3—*Field Work Protocol*, defines all the procedures and methodologies for analyzing fieldwork parameters and variables. Template 1—*Case Study Report*, showcases and shares the main information and conclusions of the soil bioengineering work analysis.

4 Conclusion

This ECOMED consortium developed sound and practical tools and approaches based on the accumulated experience that exists in the Mediterranean region for the soil and water bioengineering professionals that should further promote its adoption and proper utilization. This was accomplished by mining the experiences of the soil and water bioengineering sector of the region by the analysis of the professionals' answers in the questionnaire and case studies. Finally, new tools, three protocols and a template, to better monitor and assess soil and water bioengineering works were developed. These activities will be the basis for the long-term promotion and improvement of the specialization of the Mediterranean soil and water bioengineering sector. The adoption of soil and water bioengineering techniques should improve water quality with nature-based solutions.

References

Bakker, M. M., Govers, G., van Doorn, A., Quetier, F., Chouvardas, D., & Rounsevell, M. (2008). The response of soil erosion and sediment export to land-use change in four areas of Europe: The importance of landscape pattern. *Geomorphology, 98,* 213–226.

Bischetti, G. B., Di Fi Dio, M., & Florineth, F. (2014). On the origin of soil bioengineering. *Landscape Research, 39,* 583–595.

Cerdan, O., Desprats, J.-F., Fouché, J., Le Bissonnais, Y., Cheviron, B., Simonneaux, V., et al. (2011). Impact of global changes on soil vulnerability in the Mediterranean Basin. In *Proceedings of the International Symposium on Erosion and Landscape Evolution.* ASABE Anchorage, Alaska, pp. 495–503.

Giupponi, C., & Shechter, M. (Eds.). (2003). *Climate change in the Mediterranean: Socio-economic perspectives of impacts, vulnerability and adaptation.* Glos, UK: Edward Elgar Publications.

Giupponi, C., & Gain, A. K. (2017). Integrated spatial assessment of the water, energy and food dimensions of the sustainable development goals. *Regional Environmental Change, 17,* 1881–1893.

Kalampouka, K., Zaimes, G. N., & Emmanouloudis, D. (2011). Harmonizing member state water policies to the EU Water Directive 2000/60/EU: The Case of Greece. *International Journal of Geology, 2,* 29–33.

Kotak, B. G., Prepas, E. E., & Hrudey, S. E. (1994). Blue green algal toxins in drinking water supplies: research in Alberta. *Lake Line, 14,* 37–40.

Midgley, T. L., Fox, G. A., Derek, M., & Heeren, D. M. (2012). Evaluation of the bank stability and toe erosion model (BSTEM) for predicting lateral retreat on composite streambanks. *Geomorphology, 145–146,* 107–144.

Montgomery, D. R. (2007). Soil erosion and agriculture sustainability. *Proceedings of the National Academy of Science USA, 104,* 13268–13272.

Owens, P. N., Batalla, R. J., Collins, A. J., Gomez, B., Hicks, D. M., Horowitz, A. J., et al. (2005). Fine-grained sediment in river systems: Environmental significance and management issues. *River Research and Applications, 21,* 693–717.

Pausas, J. G., Llovet, J., Rodrigo, A., & Vallejo, R. (2007). Are wildfires a disaster in the Mediterranean basin?—A review. *International Journal of Wildland Fire, 17,* 713–723.

Pierzynski, G. M., Sims, J. T., & Vance, G. F. (2000). *Soils and environmental quality.* Boca Raton, FL: CRC Press.

Pinter, N., & Heine, R. A. (2005). Hydrodynamic and morphodynamic response to river engineering documented by fixed-discharge analysis, Lower Missouri River, USA. *Journal of Hydrology, 302,* 70–91.

Ranis, G. D., Iakovoglou, V., & Zaimes, G. N. (2015). Ecosystem post-wildfire effects of Thasos island. *International Journal of Environmental, Chemical, Ecological, Geological and Geophysical Engineering, 9,* 1242–1245.

Ries, J. B. (2009). Methodologies for soil erosion and land degradation assessment in Mediterranean-type ecosystems. *Land Degradation and Development, 21,* 171–187.

Tal, A. (2010). Desertification. In F. Uekötter (Ed.), *The turning points of environmental history* (pp. 146–161). Pittsburgh, USA: University of Pittsburgh Press.

Tardio, G., & Mickovski, S. B. (2016). Implementation of eco-engineering design into existing slope stability design practices. *Ecological Engineering, 92,* 138–147.

Tardio, G., Mickovski, S. B., Stokes, A., & Devkota, S. (2017). Bamboo structures as a resilient erosion control measure. *Proceedings of the Institution of Civil Engineers—Forensic Engineering, 170,* 72–83.

Yang, D., Kanae, S., Oki, T., Koike, T., & Musiake, K. (2003). Global potential soil erosion with reference to land use and climate changes. *Hydrological Processes, 17,* 2913–2928.

Zaimes, G. N., & Emmanouloudis, D. (2012). Sustainable management of the freshwater resources of Greece. *Journal of Engineering Science and Technology Review, 5,* 77–82.

Zaimes, G. N., Ioannou, K., Iakovoglou, V., Kosmadakis, I., Koutalakis, P., Ranis, G., et al. (2016). Improving soil erosion prevention in Greece with new tools. *Journal of Engineering Science and Technology Review, 9,* 66–71.

Multi-Criteria Decision Making for the Selection of Best Practice Seawater Desalination Technologies

Dunia AbdulBaki, Fatima Mansour, Ali Yassine, Mahmoud Al-Hindi, and Majdi Abou Najm

Abstract

Choice of optimum desalination technology is posited as a multi-criteria decision-making (MCDM) problem. Formulation considers technical, economic, environmental and social criteria. MCDM is an effective tool for selecting the best practice technology. Seawater reverse osmosis was found to consistently outperform thermal desalination technologies.

Keywords

Decision support system • Multi-criteria decision making • Desalination • Water technologies

1 Introduction

Multi-criteria decision-making (MCDM) methods efficiently deal with problems in water and energy resource management because they provide a tool through which multiple criteria can be considered and used to reach an optimal solution. Due to the fact that technologies have their own set of advantages and disadvantages and that different water applications have different sets of constraints, selecting the optimal technique of choice is a complicated task involving multiple criteria and conditions that need to be considered and met satisfactorily at the same time (Ghassemi and Danesh 2013; Sadr et al. 2015; Sudhakaran et al. 2013). This paper proposes a MCDM model for the allocation of water resources when subjected to specific constraints, prominent among which are energy and environmental concerns; a case study featuring seawater illustrates the workings of this model.

2 Materials and Methods

The overall methodology consists of: technology selection, criteria selection, database compilation, and simulation. Consequently, based on an extensive literature review and the results of a questionnaire sent to academic experts, a set of criteria for MCDM is adopted. There were six technical criteria (water recovery, treated water quality, pretreatment requirement, operating temperature, and reliability/robustness), two economic criteria (capital cost and operating/maintenance costs), three environmental criteria (greenhouse gas emissions, energy consumption, and land requirement), and two social criteria (acceptability and ease of integration).

Matching data values and their respective weights are inputted into the decision-making software, which uses the specified criteria as measures against the suggested alternatives (water technologies) to reach a decision based on criteria weighting and their respective values [obtained from different literature references (Abdulbaki et al. 2017)]. Different runs are simulated with different weighting schemes. A base run is conducted at equal weighting for all criteria categories so as to provide a point of reference for comparison. Expert-derived weights are obtained from a survey in which experts are asked to rank and prioritize the criteria categories. The experts' averaged score allocated a score of 0.3 to the technical criterion, 0.36 to the economic criterion, 0.16 to the

D. AbdulBaki · A. Yassine
Industrial Engineering and Management Department, American University of Beirut, P.O. Box 11-0236 Riyad El-Solh, Beirut, Lebanon
e-mail: afd05@mail.aub.edu

A. Yassine
e-mail: ay11@aub.edu.lb

F. Mansour · M. Al-Hindi (✉) · M. Abou Najm
Chemical and Petroleum Engineering Department, American University of Beirut, P.O. Box 11-0236 Riyad El-Solh, Beirut, Lebanon
e-mail: ma211@aub.edu.lb

F. Mansour
e-mail: fam16@mail.aub.edu

M. Abou Najm
e-mail: majdian@aub.edu.lb

environmental criterion, and 0.18 to the social criterion. Two further weighting schemes were considered as these represented the extremes of the experts' opinions where the first scheme allocated 0.4, 0.25, 0.25 and 0.1 and the second allocated 0.2, 0.3, 0.1 and 0.34 to the technical, economic, environmental, and social criteria, respectively.

The optimization problem at hand aims to minimize the technical, economic, environmental, and social requirements and impacts of water technologies. The mathematical formulation of the proposed MCDM methodology falls under the general form of utility calculation for each alternative (i.e., technology). The utility for a particular technology is calculated by summing the products of each category weight (w_i) with the respective utility generated for that category (u_i), as shown in the equation below.

$$U_{\text{tech}} = \sum_{i}^{n} w_i u_i \tag{1}$$

The utilities are then compared to determine which technology is best. The utilities for the individual categories within a particular technology are calculated using the criteria data points and the respective weight assigned to each criterion based on the weighting schemes discussed above. The overall weight assigned to a category (technical, economic, environmental, or social) is split equally across the criteria, regardless of the number of criteria within that category. The software used is Logical Decisions for Microsoft Excel 2010, on a laptop with Intel® Core™ i7-2620M, 2.7 GHz, 8.00 GB RAM, 64-bit operating system. For accurate comparison of the criteria data points, all quantitative values are normalized accordingly to fit the range of values for each criterion, such that the minimum and maximum values for any criterion are 0 and 1, respectively. Furthermore, the software requires specification of the most and least preferred values for each criterion, thus providing direction for the ranking of one alternative against another. In this problem, all of the qualitative criteria have a least preferred value of 1 with the exception of water recovery. This can be explained by the fact that increased costs (capital and operating), higher emissions, more energy consumption, greater land use, and higher operating temperature render a technology less advantageous; higher values for these criteria would make the respective technology less preferred. The only technical criteria where the most preferred value is 1 (i.e., highest assigned value) are water recovery, as the more water the technology can produce, the more suitable it is. As for qualitative criteria, they are assigned labels of high, medium, or low, as befits each alternative; these criteria are: acceptability, ease of integration, reliability/robustness, improvement potential, and pretreatment requirement. With the exception of the last

criterion, a label of high indicates a better technology; this is because high pretreatment requirement makes the technology less favorable. As such, the values for this criterion were inverted for accurate assessment. The weights are then assigned based on the weighting schemes discussed above. The weights are then multiplied by values corresponding to the specific criteria and summed to yield an overall utility value. Based on the set up described above, the problem is such that the maximum utility indicates the most suitable technology.

3 Results and Discussion

The MCDM methodology proposed above is applied in a case study with seawater as a water resource. Thus, the alternatives in this case study are the technologies that seawater can be subjected to: multi-effect distillation (MED), multi-stage flash (MSF), mechanical vapor compression (MVC), and seawater reverse osmosis (SWRO). To illustrate how different technologies have different capacity limits, two scenarios will be played out. The first consists of a large-scale system, and the second of a small-scale system. Both systems will produce potable water from seawater. The major difference between the two scenarios is that while the first will include all the aforementioned desalination technologies, the second will omit one, MVC, because it is not suitable for large-scale water production.

Table 1 presents the resulting utilities obtained for each alternative (technology) throughout the two scenarios within each weighting scheme. The ranking of the technologies did not change between the large- and small-scale production scenarios for any weighting scheme; in fact, the ranking of technologies remains the same for all scenarios, but the resulting utilities differ slightly between the different weighting schemes. For a particular weighting scheme, the utilities' values remain the same for both the large-scale and small-scale production scenarios (even though the latter contains an additional technology alternative). In terms of the most favorable technology, SWRO consistently wins in all the schemes for both the small-scale and large-scale production scenario. On the other hand, the least favorable technology is MSF in all scenarios. Between the most and least favorable technologies, MVC comes in as second most favorable and MED as third most favorable. The results are expected and support the already existing notion that membrane technologies are more favorable across a wide spectrum of criteria. It is noteworthy that the consistency of the results, even with different emphasis on different criteria categories, reinforces the conclusiveness of preferring membrane technologies to thermal technologies. In order to observe how SWRO and MSF perform on an individual

Table 1 Case study results

Technology	Equal		Expert avg.		Expert 2		Expert 3	
Capacity	Large	Small	Large	Small	Large	Small	Large	Small
MVC	–	0.704	–	0.668	–	0.706	–	0.678
MED	0.538	0.538	0.568	0.568	0.555	0.555	0.554	0.554
SWRO	**0.781**	**0.781**	**0.796**	**0.796**	**0.756**	**0.756**	**0.796**	**0.796**
MSF	*0.249*	*0.249*	*0.240*	*0.240*	*0.249*	*0.249*	*0.300*	*0.300*

Indicates that the most favoured configuration was the SWRO (bold) while the least favoured is the MSF (italic)

Fig. 1 Comparison of technologies: **a** MSF and SWRO and **b** MVC and SWRO
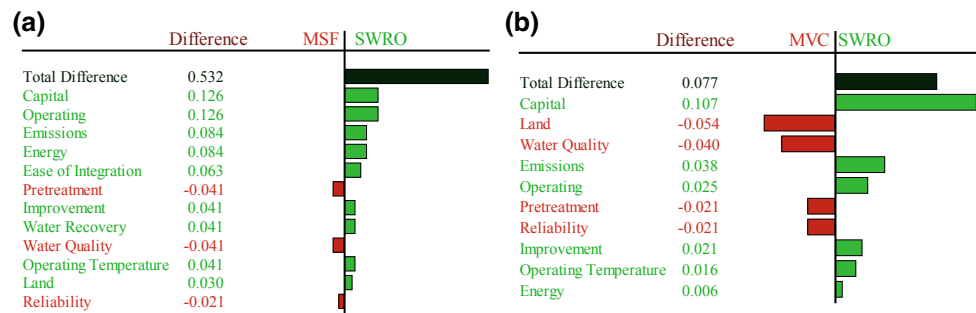
criteria basis, Fig. 1 compares the utilities for the two technologies; the figure applies to the Equal Categories weighting scheme and presents the criteria, which have values that differ between the technologies (i.e., criteria with the same values for both technologies are not included).

MSF outperforms SWRO on three criteria (shown in red in Fig. 1a). MSF requires less pretreatment (SWRO feed water requires treatment to prevent membrane fouling) and produces water with less total dissolved solids count (10 ppm compared to SWRO distillate of 425 ppm). Furthermore, thermal technologies are more deeply established than membrane technologies; this, combined with membrane sensitivity to feed quality and operating conditions, renders MSF more reliable than SWRO. The remaining criteria included in the figure have values that favor SWRO, and because these criteria number 9, as compared to 3 in favor of MSF, the total utility difference between the SWRO and MSF is 0.532, in favor of the former.

Moreover, as MVC consistently comes in second place, with only a minor difference in utility between it and SWRO, it is worthwhile to assess how this difference comes about. Figure 1b provides a criterion-by-criterion comparison (for all criteria that have different values) between the two technologies. It is worth noting that the utility difference between the two technologies is quite minor at a value of 0.077. Of the ten criteria with different values between the technologies, four favor MVC (shown in red) while the other six favor of SWRO (shown in green). In addition to the criteria discussed above, the land requirement criterion favors MVC (2 m^2/MLD for MVC compared to 5 m^2/MLD for SWRO).

4 Conclusion

This case study illustrates how MCDM can be used to select the best water treatment technology, given a certain set of specified conditions. However, application of such MCDM-based solutions remains limited due to: (i) the varying degrees of uncertainty associated with different parameters (Chung and Kim 2014), (ii) a lack of data to accurately represent the chosen criteria, especially for qualitative criteria (Ghassemi and Danesh 2013), (iii) not all factors can be specified and some factors vary geographically, (iv) the use of expert opinion renders a subjective touch, and (v) distributing category weight equally among the criteria within that category can overinflate the weighting assigned to a criterion in another category with less number of criteria. It is observed that the results arising from this case study cannot be overly generalized without specifying a set of base assumptions. Despite these limitations, MCDM allows for a preliminary and often accurate screening of the various available technologies and the selection of the most appropriate technology given the multitude of technical, economic, environmental, and social considerations.

References

Abdulbaki, D., Al-Hindi, M., Yassine, A., & Abou Najm, M. (2017). An optimization model for the allocation of water resources. *Journal of Cleaner Production, 164,* 994–1006.

Chung, E. S., & Kim, Y. (2014). Development of fuzzy multi-criteria approach to prioritize locations of treated wastewater use

considering climate change scenarios. *Journal of Environmental Management, 146,* 505–516.

Ghassemi, S. A., & Danesh, S. (2013). A hybrid fuzzy multi-criteria decision making approach for desalination process selection. *Desalination, 313,* 44–50.

Sadr, S. M., Saroj, D. P., Kouchaki, S., Ilemobade, A. A., & Ouki, S. K. (2015). A group decision-making tool for the application of

membrane technologies in different water reuse scenarios. *Journal of Environmental Management, 156,* 97–108.

Sudhakaran, S., Lattemann, S., & Amy, G. L. (2013). Appropriate drinking water treatment processes for organic micropollutants removal based on experimental and model studies—A multi-criteria analysis study. *The Science of the Total Environment, 442,* 478–488.

Modeling Co-treatment of Leachate in Municipal Wastewater Treatment Plants in the Context of Dynamic Loads and Energy Prices

Recep Kaan Dereli, Matteo Giberti, Qipeng Liu, and Eoin Casey

Abstract

Different leachate feeding strategies were tested and compared based on BSM1 framework. Leachate co-treatment adversely effected nitrogen removal efficiency and increased aeration energy costs. Shock loading at noon resulted in the worst treatment performance by overloading the plant. Drip feeding based on ammonia control ensures a higher degree of flexibility by adjusting the leachate flow.

Keywords

Co-treatment • Energy • Leachate • Model • Nitrogen • Wastewater treatment plant

1 Introduction

The management of municipal solid waste is still a major environmental concern as waste volume is growing faster than the world's population (Renou et al. 2008). Landfilling is globally the most commonly applied method for the final disposal of municipal solid waste (Hoornweg and Bahada-Tata 2012). The most important disadvantages of landfilling as a solid waste management method are inevitable greenhouse gas emissions and leachate production, which continues for several decades extending to the post-closure period of a landfill site. Rain seeping through the waste pile and water present in the waste slowly leaches from the landfill body generating a heavily contaminated wastewater with organic and inorganic pollutants. Landfill leachate is a very complex wastewater containing various types of organic matter ranging from simple volatile fatty acids to high molecular weight compounds such as hydrocarbons, phenols, chlorinated aliphatics, fulvic and humic substances and inorganics (nitrogen, phosphorus, trace elements, heavy metals) (Zhang et al. 2013). The biodegradability of leachate tends to decrease as the landfill ages due to the stabilization of organic matter within landfill body.

Leachate can be treated on-site and off-site by using several biological, physco-chemical, advanced oxidation and membrane processes (Wiszniowski et al. 2006; Renou et al. 2008). Co-treatment of leachate in publicly owned wastewater treatment plants (WWTPs) is traditionally the most commonly applied method due to several reasons, such as less capital investment by using already existing plants and dilution of pollutants with municipal wastewater, which may improve leachate treatability by biological processes. Leachate can be co-treated with municipal wastewater up to a volumetric mixing ratio of 10% without affecting the efficiency of WWTPs (Renou et al. 2008). However, this is mainly dependent on leachate characteristics, treatment plant capacity, process and operation. It was reported that 51% (0.56 million m^3 in 2013) of leachate was discharged to sewer systems and the rest was hauled to WWTPs in Republic of Ireland (EPA 2017; Brennan et al. 2016). The ratio of co-treatment was reported as 21% in France (Renou et al. 2008). High concentrations of nitrogen, inert organic matter and toxic substances present in leachate may increase the complexity and operational costs (i.e., aeration energy costs) of municipal WWTPs, adversely affect treatment efficiency and make it difficult to comply with discharge standards (Brennan et al. 2016).

Mathematical modeling of the co-treatment of leachate and wastewater is of high importance in order to understand the impact of leachate on municipal wastewater treatment plants and to develop reliable and better management strategies for co-treatment. This study was undertaken to

R. K. Dereli (✉) · M. Giberti · Q. Liu · E. Casey
University College Dublin, School of Chemical and Bioprocess Engineering, Belfield, Dublin 4, Ireland
e-mail: recep.dereli@ucd.ie

M. Giberti
e-mail: matteo.giberti@ucdconnect.ie

Q. Liu
e-mail: qipeng.liu@ucdconnect.ie

E. Casey
e-mail: eoin.casey@ucd.ie

evaluate the impact of different leachate feeding strategies in WWTPs in the context of dynamic pollutant loads and energy prices by using mathematical modeling.

2 Materials and Methods

Several leachate feeding scenarios were tested by using Benchmark Simulation Model 1 (BSM1) framework which is a commonly accepted modeling platform for testing different control and operation strategies in WWTPs (Gernaey et al. 2014). It defines a conventional activated sludge plant in Modified Ludzack-Ettinger (MLE) configuration for organic matter and nitrogen removal (Fig. 1). The BSM1 was implemented in GPS-X 6.5 software (Hydromantis, Canada) with some modifications such as addition of a leachate storage tank and a sludge dewatering unit to account for returned nitrogen load from centrate stream. The WWTP defined in BSM1 is significantly overloaded with nitrogen and struggles in complying with NH_4^+–N and total nitrogen (TN) discharge standards (4 and 18 mg/L, respectively) (Dealman et al. 2014). In order to achieve discharge limits, BSM1 default closed-loop scenario (active dissolved oxygen (DO) control in Aer3 tank and nitrate (NO) control in Anox2 tank) was optimized by decreasing sludge wastage flow from 385 to 250 m^3/d. The simulations

were run with dynamic wastewater flow and pollutant loads in dry weather conditions for 28 days.

The average flow and pollutant concentrations of wastewater and leachate are given in Table 1. Leachate pollutant characterization compatible with Activated Sludge Model No. 1 (ASM1) was taken from Galleguillos and Vasel (2011), who conducted a detailed experimental study for a mature landfill leachate. As can be seen from Table 1, leachate contains significantly higher concentrations of chemical oxygen demand (COD) and TN than municipal wastewater. Its biodegradability, indicated by biochemical oxygen demand (BOD) to COD ratio, is also very low. During simulations, constant leachate composition was assumed in order to make an objective comparison of different loading scenarios. Leachate co-treatment increased the volumetric and TN load of the plant by 1.4 and 7.3%, respectively. The performance of the plant was evaluated under five different leachate feeding strategies, namely shock loading at noon or midnight, drip feeding for the whole day, drip feeding at night and drip feeding based on effluent ammonia concentrations, by comparing effluent NH_4^+–N and TN concentrations (50 and 95 percentiles), net environmental quality index (Hydromantis 2016), cumulative aeration energy consumption and cost. A day/night electricity tariff was used such as 0.156 €/kWh between 7 a.m. and 11 p.m. and 0.084 €/kWh for the rest of the day.
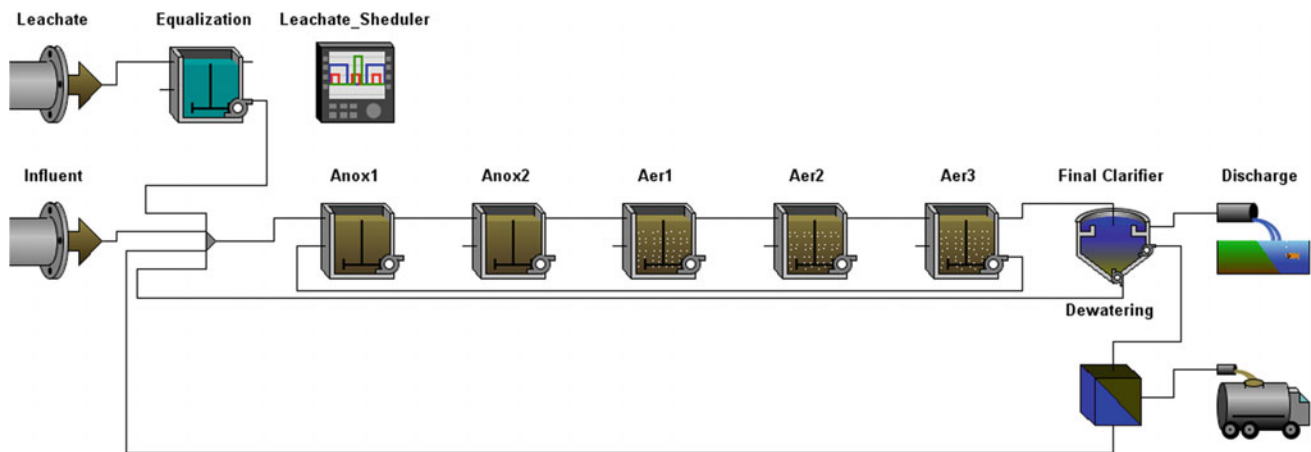

Fig. 1 Process flow diagram of modified BSM1

Table 1 Average flow and pollutant concentrations of wastewater and leachate

Parameter	Unit	Municipal WW	Leachate
Flow	m^3/d	18,466	250
COD	mg/L	381	1549
BOD	mg/L	198	110
TN	mg/L	54	293
NH_4^+–N	mg/L	32	261

Table 2 Comparison of different leachate co-treatment scenarios

Scenario	50 and 95% NH_4^+–N concentration (mg/L)	50 and 95% TN concentration (mg/L)	Net environmental quality index (kg)	Cumulative (28 days) aeration energy (kWh)	Cumulative (28 days) aeration energy cost (€)
Default (no leachate)	0.9–3.1	15.7–17.4	100	104,670	13,885
Shock loading at 12 p.m. for 2 h	1.4–6.5	18.0–21.4	579	107,180	14,275
Shock loading at 12 a.m. for 2 h	1.2–3.0	18.6–20.0	492	107,630	14,130
Drip feeding (for the whole day)	1.0–3.4	18.0–19.7	514	107,310	14,231
Drip feeding (between 11 p.m. and 7 a.m.)	0.8–2.6	18.0–20.1	518	107,130	14,102
Drip feeding based on effluent NH_4^+–N concentrations	0.9–3.0	17.7–20.3	495	107,030	14,187

3 Results and Discussion

All leachate co-treatment scenarios adversely effected the nitrogen removal efficiency and energy consumption of the treatment plant (Table 2). This is expected since the BSM1 plant is quite overloaded with nitrogen, especially during the day time, and barely meeting TN discharge limit. The simulations highlighted that shock loading at noon (12 p.m.) guarantees the worst performance by significantly overloading the plant. On the other hand, shock loading at midnight (12 a.m.) resulted in a better effluent quality indicating that the plant is underloaded during the night. Although all drip feeding scenarios provided quite similar results, drip feeding based on effluent ammonium measurements provided a better net effluent quality index, which is an indication of compliance with discharge limits. It should be noted that the leachate pollutant composition was assumed constant in this study. In fact, the main advantage of drip feeding based on effluent ammonium concentrations is the dynamic adjustment of the leachate flow in line with the changing leachate composition. This would utilize plant capacity in an optimum way by considering both the effluent quality and costs. The control strategy can even be more sophisticated by applying a cascade ammonium controller to adjust the DO set points in the aerated tanks, which may further improve both treatment performance and energy consumption.

Leachate co-treatment also increased the aeration energy demand of the plant about 2.5% due to oxygen requirement for nitrification of the additional nitrogen load. Treating leachate during the off-peak hours provides an advantage on both complying discharge limits and reducing energy costs. The simulation results also highlighted that when the leachate was co-treated at night, the aeration energy cost is lower (Table 2).

This would become more important for large WWTPs treating leachate at higher volumetric mixing ratios.

4 Conclusion

Leachate co-treatment was investigated in the BSM1 modeling framework by testing different leachate feeding strategies in the context of dynamic municipal wastewater loads and electricity prices. Co-treatment of leachate at a volumetric mixing ratio of 1.4% deteriorated treatment efficiency and increased the energy consumption. Shock loading at noon resulted in the worst treatment performance, whereas drip feeding based on effluent ammonium concentration offered the best performance with a reasonable aeration energy cost increase. Therefore, establishing an effluent ammonium concentration based leachate strategy may allow the utilization of plant capacity in an optimum way by considering both the effluent quality and energy costs.

References

Brennan, R. B., Healy, M. G., Morrison, L., Hynes, S., Norton, D., & Clifford, E. (2016). Management of landfill leachate: The legacy of European Union directives. *Waste Management, 55,* 355–363.

Daelman, M. R. J., Van Eynde, T., van Loosdrecht, M. C. M., & Volcke, E. I. P. (2014). Effect of process design and operating parameters on aerobic methane oxidation in municipal WWTPs. *Water Research, 66,* 308–319.

EPA. (2017). *Suitability of municipal wastewater treatment plants for the treatment of landfill leachate*. Wexford, Ireland: Environmental Protection Agency.

Galleguillos, M., & Vasel, J.-L. (2011). Landfill leachate characterization for simulation of biological treatment with activated sludge model no. 1 and activated sludge model no. 3. *Environmental Technology, 32*(11), 1259–1267.

Gernaey, K. V., Jepson, U., Vanrolleghem, P. A., & Copp, J. B. (2014). *Benchmarking of control strategies for wastewater treatment plants* (Scientific and Technical Report No. 23). London, UK: IWA Publishing.

Hoornweg, D., & Bhada-Tata, P. (2012). *What a waste: A global review of solid waste management*. Washington, USA: World Bank.

Hydromantis. (2016). *GPS-X Technical Reference Version 6.5*. Ontario, Canada.

Renou, S., Givaudan, J. G., Poulain, S., Dirassouyan, F., & Moulin, P. (2008). Landfill leachate treatment: Review and opportunity. *Journal of Hazardous Materials, 150,* 468–493.

Wiszniowski, J., Robert, D., Surmacz-Gorska, J., Miksch, K., & Weber, J. V. (2006). Landfill leachate treatment methods: A review. *Environmental Chemistry Letters, 4,* 51–61.

Zhang, Q. Q., Tian, B. H., Zhang, X., Ghulam, A., Fang, C. R., & He, R. (2013). Investigation on characteristics of leachate and concentrated leachate in three landfill leachate treatment plants. *Waste Management, 33,* 2277–2286.

Microfiltered Digestate to Fertigation: A Best Practice to Improve Water and Energy Efficiency in the Context of Biogasdoneright™

Paolo Mantovi, Giuseppe Moscatelli, Sergio Piccinini, Stefano Bozzetto, and Lorella Rossi

Abstract

Biogasdoneright™ is an innovative agricultural model aimed at achieving a sustainable agricultural intensification. The microfiltration of the by-product from biogas production, the digestate, is among technology innovations supporting the implementation of best practices in the Biogasdoneright™ system. Digestate microfiltration tests were carried out under different operating conditions, to fine tune the best working conditions of the equipment. Then it was possible to distribute the microfiltered digestate in fertigation on growing maize through drip lines without causing blockage. Microfiltered digestate to fertigation has proven to be a best practice to improve nutrients, water and energy efficiency in the context of Biogasdoneright™.

Keywords

Anaerobic digestion • Water use efficiency • Renewable energy • Digestate • Microfiltration • Fertigation

1 Introduction

Anaerobic digestion at farm level, producing renewable energy and leaving a by-product known as digestate, potentially addresses several aspects of agricultural sustainability (Möller 2015).

The Italian Biogas Consortium (CIB), assisted by an international panel of experts, developed an innovative agricultural model, with a platform of technologies aimed at achieving a sustainable agricultural intensification: the

P. Mantovi (✉) · G. Moscatelli · S. Piccinini
Centro Ricerche Produzioni Animali—CRPA, Reggio Emilia, Italy
e-mail: p.mantovi@crpa.it

S. Bozzetto · L. Rossi
Consorzio Italiano Biogas e Gassificazione—CIB, Lodi, Italy

Biogasdoneright™. It produces renewable energy with positive environmental externalities, such as increased agricultural productions, carbon content of soils, soil fertility and lower input of chemical fertilizers (ECOFYS 2016; Mantovi et al. 2018).

The Biogasdoneright™ system is an example of multifunctional and sustainable agriculture according to "The Roadmap to a Resource Efficient Europe" (COM(2011) 571), and it is based on three main pillars: year-long cultivated soil, efficient recycling of organic matter/nutrients/water through the digestate and conservation tillage practices. Biogasdoneright™ has already been defined as a bioenergy with carbon capture and storage (BECCS) system (Valli et al. 2017).

Among technology innovations supporting the implementation of best practices in the Biogasdoneright™ system is the solid/liquid separation of the digestate followed by the microfiltration of the clarified fraction. The obtained microfiltered digestate should be used to fertigate growing crops, mixed with irrigation water.

2 Materials and Methods

An innovative integrated system for the efficient agronomical use of digestate was set up and validated, made of "screw press separation + microfiltration + fertigation" (Fig. 1), to be applied to the digestate obtained from livestock manure and energy crops. The possibility of using digestate on growing crops, in place of mineral fertilizers, was evaluated in the frame of circular economy (Buckwell and Nadeu 2016).

Digestate microfiltration tests were carried out at Maiero Energia farm in northern Italy (Portomaggiore, Ferrara), which manages a 1 MWe biogas plant, to evaluate the performance of a new microfilter developed by Saveco™ (member of Wamgroup), under different operating conditions, characterizing incoming digestate and output fractions, to fine tune the best working conditions of the machinery.

Fig. 1 Scheme of the treatment and mass balance (as a percentage of the total raw digestate)
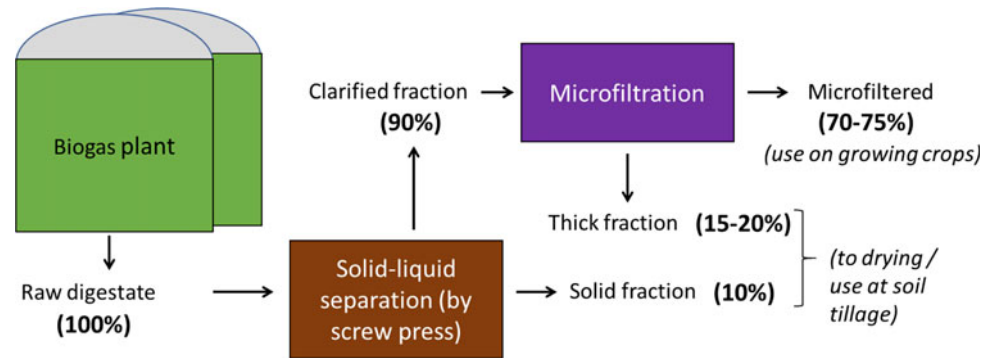

Table 1 Main characteristics of the raw digestate and the fractions obtained from screw press + microfiltration

Type of digestate	Total solids (%)	Total Kieldahl nitrogen (kg/t)	Ammonia nitrogen (%TKN)
Raw digestate	7.7–8.0	4.8–5.0	58–60
Solid fraction (from screw press)	22–26	6.1–6.2	42–46
Clarified fraction (from screw press)	5.6–6.5	4.7–4.9	60–62
Dense fraction (from microfilter)	7.0–8.1	5.0–5.1	57–62
Microfiltered digestate	5.0–5.6	4.5–4.8	62–63

Microfiltration tests were carried out using a 50 μm spacing sieve. This configuration proved to be the most performing by analysing the concentration of dry matter in the microfiltered material in relation to the working capacity.

Maize fertigation trials were set up using the microfiltered digestate mixed with irrigation water through drip lines, on 2.5 ha, compared with maize with the same type of drip lines and only irrigation water but with urea distributed in two periods (at sowing and stem extension), on another 2.5 ha. The feasibility of the digestate injection in the fertigation plant was evaluated, together with the performance of the safety filters, of the various types of Netafim™ drip lines and of the maize crop.

3 Results and Discussion

The daily production of digestate from the Maiero Energia biogas plant is around 60 tons which results in 22,000 t/year containing more than 100,000 kg N/year.

The microfilter was able to treat digestate from energy crops and livestock manure, despite the high residual dry matter content (6%) of the clarified fraction coming from the screw press separator. Under the tested conditions, with a 50 μm filter, the equipment produced up to over 6 m^3 per hour of microfiltered digestate. It is possible to treat all the digestate produced every day. The main characteristics of the raw digestate and of the fractions obtained, including the microfiltrate, are reported in Table 1. The mass balance is shown in Fig. 1.

During the fertigation trials, the ratio of microfiltered digestate to irrigation water varied from 1:30 to 1:10. At 1:10 dilution, the solution had a pH of 8 and about 450 mg/l total nitrogen, of which more than 60% was in the ammoniacal form (the rest organic). The conductivity was 4 mS/cm, medium-high but acceptable if we consider that during irrigation with water alone it was 10 times less (0.4 mS/cm).

More than 50 m^3/ha of microfiltered digestate were distributed by fertigation to the maize during almost two months in 13 fertigation operations. Irrigation supplied a total of 2800 m^3/ha of water over 150 h.

Maize yield was measured both for the production of silage and at grain harvesting. In both cases, there were no significant differences between the two treatments compared (digestate vs. urea): silage yield varied between 65 and 70 t/ha (33% dry matter), grain around at an average value of 11 t/ha (15.5% commercial moisture).

The cost of separation and microfiltration, taking into account the total volume of digestate that is produced by the biogas plant, was estimated at 0.80 €/m^3. This cost can be compensated by the savings of water and fertilizers due to the microfiltered digestate use in fertigation.

4   Conclusion

If the digestate is not subjected to solid/liquid separation and microfiltration, its agronomic use as a raw by-product in most cases does not occur on growing crops and therefore the use efficiency of nutrients and water may result rather low. In fact, the digestate is usually distributed on the soil before ploughing and the fertilization of the crops must be integrated with mineral fertilizers.

The trials demonstrated that it is possible to distribute the digestate in fertigation during the growing season of crops and through drip lines, without causing blockage: the keystone is the new digestate microfiltration equipment. The overall system (screw press separation + microfiltration + fertigation) allows high nutrients/water/energy use efficiency and therefore can lead to significant savings of resources.

In practical terms, however, it is important to highlight the need for an underground network of pipes for transport the microfiltrate or temporary storages at the field. Otherwise, the alternative is to leave some hours the slurry tanks at the field, for filling the fertigation plant with microfiltrate.

The integrated system fully fits into the Biogasdoneright™ model proposed by Italian Biogas Consortium (ECOFYS 2016; Valli et al. 2017). Indeed, it is a technically feasible solution that optimizes the use of clarified digestate, which is generally more difficult to use because of its high water content compared to other components. Biogasdoneright™ is a work in progress model based on real farm experience like the one described in this paper. More studies are needed in order to improve knowledge for a sustainable application in different geographical areas and type of farms.

References

Buckwell, A., & Nadeu, E. (2016). *Nutrient Recovery and Reuse (NRR) in European agriculture. A review of the issues, opportunities, and actions*. Brussels: RISE Foundation. http://www.risefoundation.eu.

ECOFYS. (2016). *Assessing the case for sequential cropping to produce low ILUC risk biomethane*. Final report. In D. Peters, M. Zabeti, A.-K. Kühner, M. Spöttle (Ecofys), W. van der Werf, & T. Jan Stomph (WUR). https://www.consorziobiogas.it/wp-content/uploads/2017/02/Ecofys_Assessing-the-benefits-of-sequential-cropping-for-CIB_Final-report.pdf.

Mantovi, P., Fabbri, C., Valli, L., Rossi, L., Bozzetto, S., Folli, E., et al. (2018). Enhance soil organic carbon stocks by means of the Biogasdoneright system. In *International Symposium on Soil Organic Matter Management in Agriculture—Assessing the Potential of the 4per1000 Initiative*. Book of abstracts. https://www.som-management.org/fileadmin/som-management/Book_of_abstracts/Book_of_abstracts_NEW.pdf.

Möller, K. (2015). Effects of anaerobic digestion on soil carbon and nitrogen turnover, N emissions, and soil biological activity. A review. *Agronomy for Sustainable Development, 35,* 1021–1041. https://doi.org/10.1007/s13593-015-0284-3.

Valli, L., Rossi, L., Fabbri, C., Sibilla, F., Gattoni, P., Dale, B. E., et al. (2017). Greenhouse gas emissions of electricity and biomethane produced using the BiogasdonerightTM system: Four case studies from Italy. Biofuels, Bioproducts and Biorefining. https://doi.org/10.1002/bbb.1789.

Optimal Design of Water Distribution Networks Incorporating Reliability Criteria

Alireza Moghaddam, Ali Naghi Ziaei, Carol Miller, Zahra Fahim,
Hossein Ansari, Fatemeh Attarzadeh, Mahdi Rouholamini,
and Mohammadamin Moghbeli

Abstract

To achieve a robust and optimal design of water distribution networks, both hydraulic constraints and reliability concerns must be met. This paper aims at employing multi-objective particle swarm optimization (MOPSO) algorithm for reliability-oriented design of a water distribution network. We use Pareto-front analysis to make a compromise between cost and reliability satisfaction. Two criteria, referred to as Todini's resilience index (I_r) and network resilience index (I_n), are used to evaluate the resilience of the network under study. The simulation results clearly show that MOPSO is capable of being used in optimal design of water distribution networks and I_n is an effective criterion for water networks' reliability evaluation.

A. Moghaddam
Department of Water Engineering, Urmia University, Urmia, Iran
e-mail: Alireza.moghaddam@yahoo.com

A. N. Ziaei · Z. Fahim · H. Ansari · F. Attarzadeh
Department of Water Engineering, Ferdowsi University
of Mashhad, Mashhad, Iran
e-mail: an-ziaei@um.ac.ir

C. Miller
Department of Civil and Environmental Engineering,
Wayne State University, Detroit, MI, USA
e-mail: ab1421@wayne.edu

M. Rouholamini (✉)
Department of Electrical and Computer Engineering,
Wayne State University, Detroit, MI, USA
e-mail: gj9598@wayne.edu

M. Moghbeli
University of Politecnico di Milano, Milan, Italy
e-mail: m.moqbeli@gmail.com

1 Introduction

Nowadays, it is commonly accepted that the optimal and sustainable design of water distribution networks involves taking into account the reliability of network as well as investment costs. Recently, the use of alternative reliability indices has become more prevalent as these indices are more convenient and rapider than direct methods (Todini 2000). Among all, the one introduced by Todini (2000) is the most common and well-known index which represents the capability of the system when facing pipe failures and indirectly relates to network reliability. Researchers have lately improved these reliability indices and pointed out their applications (Liu et al. 2016; Jayaram and Srinivasan 2008; Prasad and Park 2004). In multi-objective optimization, a trade-off has to be made to reach a relatively acceptable balance among different optimization purposes. In this paper, we apply MOPSO to a benchmark network to not only minimize the investment costs but also maximize the reliability. Accordingly, the solution method is first coded in MATLAB. This M-file code, as the optimizer tool, is then interfaced with EPANET, which is used as the hydraulic simulator. Finally, the paper in a systematic way provides water system operators with a set of candidate solutions in the form of a Pareto-front.

2 Materials and Methods

In this section, the optimization problem formulation, including the objective functions and constraints, is presented. The formulation aims to optimally re-size a water distribution network considering the costs and reliability of the system. Equations (1–3) define the three different objective functions that we are to optimize:

$$\text{Minimize} f_1 = \sum_{i=1}^{np} C_i(L, D) \qquad (1)$$

$$\text{Maximize} f_2 = I_r \qquad (2)$$

$$\text{Maximize} f_3 = I_n \qquad (3)$$

where np denotes the number of pipes, $C_i(L, D)$ is the cost of the ith pipe with a length of L and a diameter of D. I_r is the resilience index that Todini has suggested and is calculated by using Eq. (4):

$$I_r = \frac{\sum_{j=1}^{nn} Q_j \left(H_j - H_j^{\min}\right)}{\left(\sum_{k=1}^{nr} Q_k H_k + \sum_{i=1}^{npu} P_i H_j\right) - \sum_{j=1}^{nn} Q_j H_j^{\min}} \qquad (4)$$

I_n is the network resilience index that considers the impact of excessive power and reliable loops existing in the network (Prasad and Park 2004):

$$I_n = \frac{\sum_{j=1}^{nn} C_j Q_j \left(H_j - H_j^{\min}\right)}{\left(\sum_{k=1}^{nr} Q_k H_k + \sum_{i=1}^{npu} P_i H_j\right) - \sum_{j=1}^{nn} Q_j H_j^{\min}} \qquad (5)$$

In Eq. (5), Q_k and H_k are the flow rate and head of reservoir k, respectively, and nr represents the number of reservoirs. P_i and npu are the energy produced by pump i and the number of pumps, respectively. Q_j, H_j and $H_j^{\min}$, respectively, are representatives of flow rate, head, and minimum allowed head at node j. C_j denotes the uniformity of node j and is calculated as defined by Eq. (6).

$$C_j = \frac{\sum_{i=1}^{np} D_{ij}}{np \times \max\left(D_{ij}\right)} \qquad (6)$$

D_{1j}, D_{2j}, …, D_{nj} denote the diameters of the pipes connected to node j. The value of $C = 1$, if pipes connected to a node have the same diameter; and $C < 1$, if pipes connected to a node have different diameters. For nodes connected with only one pipe, the value of C is taken to be one.

The constraints of the optimization problem are as below:

$$H_j^{\min} \leq H_j \quad j = 1, \ldots nn \qquad (7)$$

$$D_k \in \{D\}, \quad \forall k \in np \qquad (8)$$

Equation (7) is responsible for minimum allowed nodal heads, and (8) defines the set of commercially available diameters. D_k is the diameter of pipe k, and D is the set of commercially available diameters. The mass and energy continuity theorem are also the major constraints of the optimization problem. These constraints automatically realize as we use EPANET for hydraulic analysis (Moghaddam et al. 2018). In the following, MOPSO is used to solve the
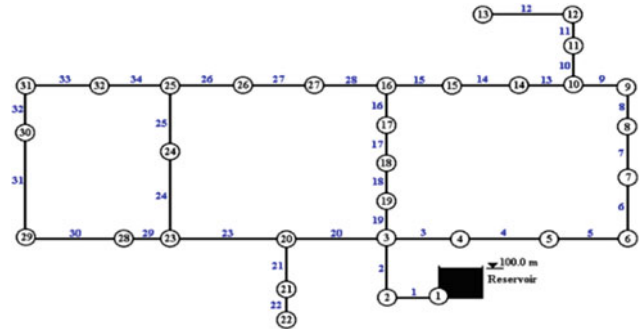

Fig. 1 Layout of Hanoi network

aforementioned constraints and objective functions. MOPSO was first introduced by Coello and Lamont (2004) and is applied to solve multi-objective optimization problems (Coello and Lamont 2004). MOPSO is inspired from Pareto-envelope-based selection algorithm (PESA) except that in MOPSO the optimizer, which is genetic algorithm (GA), is replaced with PSO. Detailed description about MOPSO has been given in Coello and Lamont (2004).

3　Results and Discussions

Hanoi network consists of 32 nodes and 34 links arranged in three loops, fed from a single fixed head source providing a head of 100 m (Fig. 1) (Fujiwara and Khang 1990). The lower allowed pressure limit is 30 m. The Hazen–Williams coefficient of all the pipes is 130. Other input data remain the same as used in Fujiwara and Khang (1990). There are six different diameters available for each of the pipes. Therefore, the search space includes $6^{34} = 2.865 \times 10^{26}$ distinguishable configurations. Table 1 presents the per-length costs of the different commercially available diameters.

Table 2 shows the solutions obtained for different objectives including least cost, maximizing I_r as well as maximizing I_n. As seen, the maximum I_r and I_n are 0.339 and 0.345, and their costs are 10.84 and 10.70 million USD, respectively. Therefore, the I_n-based solution is achieved at a lower cost and gives a better reliability. The Pareto-analysis of costs versus I_r and I_n indices is shown in Figs. 2 and 3, respectively.

As it is seen from Fig. 4, when the demand is increased by 20% in the $I_r(I_n)$-maximizing solutions, still there are 22 (21) nodes whose pressure is within permissible band. However, the situation is quite different for the solutions of minimum cost, which leads to serious pressure drop at 22 nodes. Therefore, the more $I_r(I_n)$ is, the greater the network would be reliable against demand increase.

Table 1 Diameters and per-length costs

Pipe number	Diameter (mm)	Cost ($/m)
1	304.8	45.726
2	406.4	70.400
3	508	98.378
4	609.6	129.333
5	762	18.748
6	1016	278.280

Table 2 Solutions with least cost and maximum reliability criteria

| *Solution: least cost*											*Cost $\times 10^6$ ($)*	
Pipe number	1–4	5	6	7–9	10	11–12	13	14–20	21	22	6.83	
Diameter (mm)	1016	609.6	1016	304.8	1016	609.6	762	1016	609.6	304.8		
Pipe number	23	24-25	26-27	28	29	30-31	32	33-34				
Diameter (mm)	1016	609.6	304.8	609.6	508	304.8	406.4	508				
Solution: maximum I_r											*Cost $\times 10^6$ ($)*	I_r
Pipe number	1–14	15	16–24	25	26–34						10.84	0.339
Diameter (mm)	1016	304.8	1016	304.8	1016							
Solution: maximum I_n											*Cost $\times 10^6$ ($)*	I_n
Pipe number	1–14	15	16–25	26–27	28–34						10.70	0.345
Diameter (mm)	1016	304.8	1016	304.8	1016							
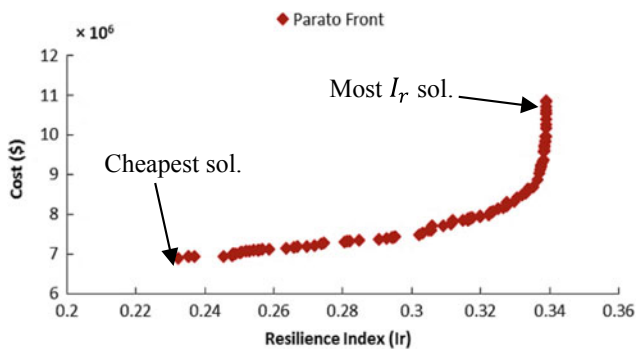
Fig. 2 Pareto-front in cost-I_r space
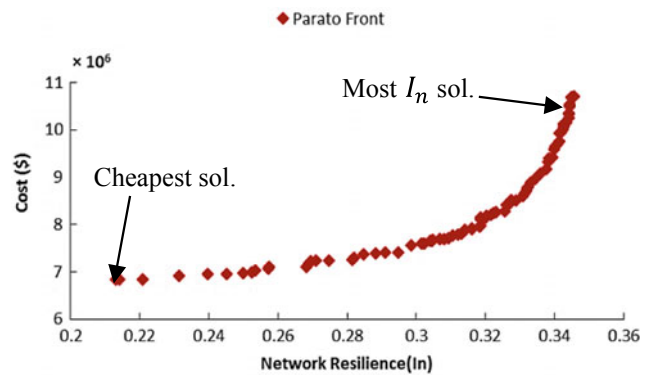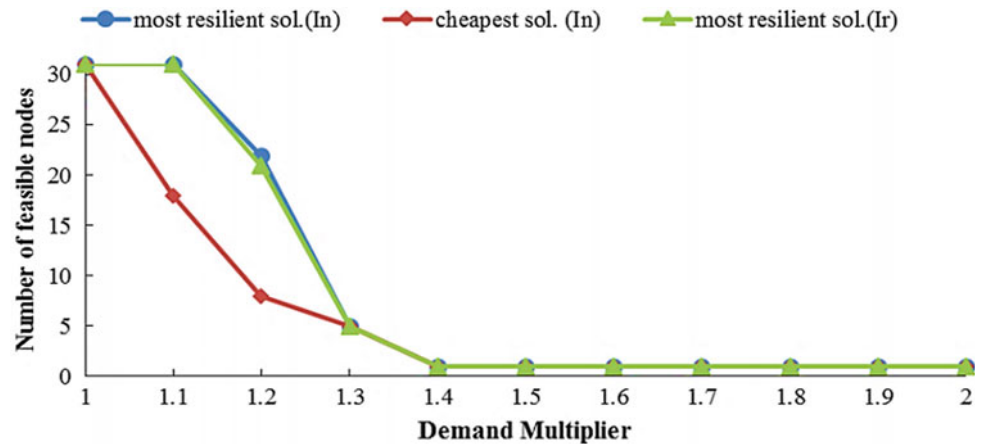

Fig. 3 Pareto-front in cost-I_n space

Fig. 4 Number of nodes with acceptable pressure-versus-demand increment

4 Conclusions

The findings of this paper clearly shows that I_n index out-performs I_r when it comes to designing a robust water distribution network because I_n gives more excessive potential energy at each node and through optimal size selection of pipes and maintaining reliable loops in the network improves the system performance in responding to demand increase and pipe failures. In addition, it was demonstrated that multi-objective optimal designing of a water network based on reliability criteria provides a set of feasible solutions in a Pareto-front of a cost-vs-reliability space for system operators, which is a state-of-the-art decision-making tool.

References

Coello, C. A. C., & Lamont, G. B. (2004). *Applications of multi-objective evolutionary algorithms*. London: World Scientific.

Fujiwara, O., & Khang, D. B. (1990). A two-phase decomposition method for optimal design of looped water distribution networks. *Water Resources Research, 26*(4), 539–549.

Jayaram, N., & Srinivasan, K. (2008). Performance-based optimal design and rehabilitation of water distribution networks using life cycle costing. *Water Resources Research, 44,* W01417.

Liu, H., Savić, D. A., Kapelan, Z., Creaco, E., & Yuan, Y. (2016). Reliability surrogate measures for water distribution system design: A comparative analysis. *Journal of Water Resources Planning and Management, 143*(2), 04016072.

Moghaddam, A., Alizadeh, A., Faridhosseini, A., Ziaei, A. N., & Heravi, D. F. (2018). Optimal design of water distribution networks using simple modifed particle swarm optimization approach. *Desalination and Water Treatment, 104,* 99–110.

Prasad, T. D., & Park, N.-S. (2004). Multiobjective genetic algorithmsfor design of water distribution networks. *Journal of Water Resources Planning and Management, 1*(73), 73–82.

Todini, E. (2000). Looped water distribution networks design using a resilience index based heuristic approach. *Urban Water, 2*(2), 115–122.

Creating Abundance: Nexus Stress as a Driver for Innovation in Solving Energy and Water Stress

William Sarni and Joshua Sperling

Abstract

Energy and water nexus stress drives innovation in technology, financing models, business models, and partnerships. There are new platforms to accelerate nexus innovation that leverage the skills and experience of successful entrepreneurs from outside the energy and water sectors. New business and financial models are needed to solve energy and water nexus stress challenges. New partnership models are emerging to foster cross-industry and entrepreneurial platform collaboration.

1 Introduction

While there is considerable discussion of the energy–water–food nexus and associated impacts, there is less of a focus on innovative solutions. Resource stress and scarcity foster innovation in technologies, financing, business models, and partnerships. We are also seeing innovation in public policy to address the nexus stress and scarcity. Public policy innovation is catching up to advances in technology, financing/funding, business models, and partnerships. Collectively, innovation will move the world from scarcity to abundance if managed effectively by the public sector, companies, non-governmental organizations, and civil society. This article explores innovative approaches to addressing the energy–water–food nexus and reframing solutions to *create abundance.*

2 Materials and Methods

The research and thinking for this article are based upon experience in working with XPRIZE (www.xprize.org), Imagine H$_2$O (www.imagineh20.org) and 101010 (www.101010.net) along with multinationals and non-governmental organizations (NGOs) on water risks to food and energy production. XPRIZE, Imagine H$_2$O, and 101010 exist to accelerate innovation to address complex problems—also known as wicked problems (Rittel and Webber 1973). The approaches range from prize competitions (XPRIZE and Imagine H$_2$O) to a unique program which brings 10 entrepreneurs together for 10 days to design commercial businesses to solve 10 wicked problems (www.101010.net). This article also builds upon "Beyond the Energy–Water–Food Nexus New Strategies for 21st-Century Growth" (Sarni 2015) and "Creating 21st Century Abundance through Public Policy Innovation: Moving Beyond Business as Usual" (Sarni and Koch 2018).

3 Results and Discussion

The projections of our ability to meet the water, food, and energy needs for a global population of 9 billion are not encouraging but also not a foregone conclusion.

Innovations in technology, financing, business models, partnerships, and even public policy have the potential to chart a better path forward. The potential is clear—what is required is the will to address these challenges together by recognizing that 9 billion people deserve access to energy, food, safe water, sanitation, and hygiene as part of fundamental quality life. In addition, we need to design and

W. Sarni (✉)
Denver Water, Denver, CO, USA
e-mail: will@waterfoundry.com

J. Sperling
National Renewable Energy Laboratory, Golden, CO, USA

scale innovative solutions and not just continue to rely upon current approaches which yield incremental progress.

Let us start with innovation in technology, partnerships, and financing/funding to illustrate how we can positively alter the business as usual trajectories. To do this, we need to view the energy–water–food nexus as a catalyst for innovation and an opportunity to scale solutions.

3.1 Technology

Integrated off-grid energy and water technologies.

Zero Mass Water (wwwzeromasswater.com) has built a residential solar air moisture capture system that can provide safe drinking water for a family of four. The system has been deployed in Ecuador, Jordan, Mexico, and the USA. Essentially, off-grid safe drinking water powered by solar energy.

3.2 Digital Solutions

John Deere is now using sensors in several of its products to increase farm productivity (http://www.bigdata-startups.com/BigData-startup/john-deere-revolutionizing-farming-big-data/). John Deere uses sensors added to its latest equipment lines to help farmers manage their fleets and to decrease tractor downtime while also saving on fuel. The information is combined with historical and real-time data on weather prediction, soil conditions, crop features, and many other data sets. These tools aim to increase the productivity and efficiency of the crops and which results in higher production and revenue.

3.3 Partnerships—Collective Action

Multinationals and Non-Governmental Organizations (NGOs). The 2030 Water Resources Group (www.2030wrg.org) released an online database of case studies to address water scarcity risks. It is designed to facilitate the adoption of leading practices to cover a wide range of common scarcity challenges, as well as proven solutions. The group offers for free download the full catalog of in-depth solutions (http://www.waterscarcitysolutions.org/).

WASH (access to safe drinking water, sanitation, and hygiene). The World Business Council on Sustainable Development (www.wbcsd.org) along with member companies developed WASH at the Workplace, a long-term vision and implementation plan to address access to safe water, sanitation, and hygiene in the workplace. Among the organizations that have signed the pledge to date are Greif,

Nestlé, Borealis AG, Roche Group, Hindustan Construction Company, and the Environmental Defense Fund.

3.4 Financing/Funding

Conservation Synergy and Blended Finance. In 2008, the investor-owned, California-based utility PG&E, along with several water agencies in California, offered a rebate program for high-efficient clothe washers. The rebate in 2013 ranged from $100 to $125—this includes a $50 rebate from PG&E and a variable rebate from $50 to $75 from the water utility. PG&E has seen a 63% increase in customer participation since the water utilities joined the program and the water utilities have seen a 30% increase in their customer participation. The program has since expanded to 41 municipal and private water agencies (municipal, regional, and private utilities).

We are also seeing a movement toward "blended finance" which as the name implies brings together diverse sources of capital to fund much-needed investment in infrastructure. One of the key actors in this movement is OECD and Alex Money (OECD 2017. Blended finance: Mobilizing resources for sustainable development and climate action in developing countries and OECD-WWC-Netherlands Roundtable on Financing Water Second meeting 13 September 2017, Tel Aviv Session 4. Background paper The potential for public, purposed, development and hybrid finance to bridge the water infrastructure gap (Money 2017).

3.5 Cross-Industry Sector Collaboration

The EDF Group is an integrated energy company, active in generation, transmission, distribution, energy supply, and trading. In order to optimize and balance water allocation for energy generation and water's many other uses in France's Durance Valle—including agriculture, tourism, flood control, and drinking water—as well as to prepare for future water demand from these and other uses, EDF implemented an innovative solution.

In 2000, the company signed a six-year Water Saving Convention along with the two main irrigation users in the valley, with a goal of saving 44 million cubic meters of water, with EDF offering financial incentives to reach the target. The saved water could then be used to generate additional energy during peak demand times (OECD 2015, Stakeholder Engagement for Inclusive Water Governance).

3.5.1 What Has to Change?

How did we get to accept business as usual and the scarcity trajectory and what has to change?

As with wicked problems, complex challenges with multiple distinguishing features, market failures occur when one or more of the following situations exist: No capital is being spent to address a problem; capital is being spent, but without the desired result; no capital is being spent because nobody knows it is a problem; the problem is known, but no one can imagine that it is not already being addressed; or no one is addressing because a solution is thought to be impossible.

An example of a platform to address market failure is 101010 (www.10101.net). The program identifies 110 wicked problems and the 10 prospective CEOs are challenged with developing market-based solutions to market failures. With four programs focused on healthcare and cities: infrastructure and water, they have launched several startups to address wicked problems.

Old ways of innovating are giving way to new thinking and tools to accelerate innovation. One only has to look at crowdsourcing and prize competitions for examples. We now have the tools to mobilize the best minds globally to address a wicked problem such as water scarcity, low carbon energy, and access to nutritious foods.

X-PRIZE is an excellent example of how to leverage prize competitions to develop innovative solutions to complex environmental and social issues. X-PRIZE is "an incentivized prize competition that pushes the limits of what's possible to change the world for the better. It captures the world's imagination and inspires others to reach for similar goals, spurring innovation and accelerating the rate of positive change." The following criteria define an X-Prize challenge: (http://www.xprize.org/about/what-is-an-xprize).

- Sets a bold and audacious goal
- Targets market failures
- Defines the problem versus the solution
- Is audacious but achievable
- Is winnable by a small team, in a reasonable time frame
- Is telegenic and easy to convey
- Drives investment
- Provides vision and hope

We are at a time where we can address the projections for water scarcity and provide sustainable energy and food for the current and projected global population. However, it will require accelerating the pace of adoption of *innovative technologies and partnerships and public policies*. It is within reach—even if it will not be easy. It also means abandoning our business as usual mindset and embracing a rethinking of how we have historically managed these resources. Abandoning the old way of thinking and moving to a twenty-first century mindset powered by new technologies, collaboration frameworks and public policies are possible.

What we need is a new framework for thinking and new rules to create energy water and food abundance.

4 Conclusion

Hope is not a strategy.

However, there is a reason to believe that we can deflect the scarcity trajectory framed by the business as usual scenarios. These scenarios reflect the energy–water–food nexus stress but do not acknowledge that this stress also creates opportunities for innovation. These innovation opportunities are coming to life through multi-sector initiatives, NGOs, and public-sector programs.

References

2030WRG. *A full catalog of in-depth solutions*.

Big Data Startups. *John Deere revolutionizing farming*. (http://www.bigdata-startups.com/BigData-startup/john-deere-revolutionizing-farming-big-data/).

Money, A. (2017). *Background paper. The potential for public, purposed, development and hybrid finance to bridge the water infrastructure gap*. University of Oxford.

OECD. (2015). *Stakeholder Engagement for Inclusive Water Governance*.

OECD. (2017). *Blended finance: Mobilising resources for sustainable development and climate action in developing countries and OECD-WWC-Netherlands Roundtable on Financing Water Second meeting 13 September 2017*, Tel Aviv Session 4.

Rittel, H., & Webber, M. (1973). Dilemmas in a general theory of planning. *Policy Sciences, 4*, 155–169. [Reprinted in Cross, N. (Ed.). (1984). *Developments in design methodology* (pp. 135–144.). Chichester: Wiley.

Sarni, W. (2015). *Beyond the energy–water–food nexus new strategies for 21st-century growth*. Greenleaf Publishing, June 2015.

Sarni, W., & Koch, G. (2018). *Creating 21st century abundance through public policy innovation: Moving beyond business as usual*. Greenleaf Publishing.

WBCSD. WASH in the workplace (WASH at the Workplace).

World Bank. *Water scarcity solutions: A catalogue of best practice solutions to addressing the growing water scarcity challenge*.

XPRIZE. *What is XPRIZE?* (http://www.xprize.org/about/what-is-an-xprize).

Using Fast Messy Genetic Algorithm to Optimally Schedule Pump Operation

Javad Karami, Alireza Moghaddam, Alireza Faridhosseini,
Ali Naghi Ziaei, Mahdi Rouholamini, and Mohammadamin Moghbeli

Abstract

Darwin Scheduler model based on fast messy genetic algorithm is utilized to best schedule the operation of the pump stations. Van Zyl, which is a well-known water network, is used to simulate the aforesaid model. FMGA reduces energy costs and the number of start/stop of the pumps. FMGA leads to the reduction of the maintenance costs.

Keywords

Darwin scheduler • Genetic algorithm • Optimization • Pump station • Water distribution networks

1 Introduction

The ever-growing urban population has made the use of complex and large water distribution systems (WDSs) inevitable today. The huge operation costs of the system cause water utility operators to seek ways to improve the

J. Karami · A. Faridhosseini · A. N. Ziaei
Department of Water Engineering, Ferdowsi University of Mashhad, Mashhad, Iran
e-mail: jkkormanje@gmail.com

A. Faridhosseini
e-mail: farid-h@um.ac.ir

A. N. Ziaei
e-mail: an-ziaei@um.ac.ir

A. Moghaddam (✉)
Department of Water Engineering, University of Urmia, Urmia, Iran
e-mail: Alireza.moghaddam@yahoo.com

M. Rouholamini
Department of Electrical and Computer Engineering, Wayne State University, Detroit, MI, USA
e-mail: gj9598@wayne.edu

M. Moghbeli
University of Politecnico di Milano, Milan, Italy
e-mail: m.moqbeli@gmail.com

facilities and efficacy involved. Since nearly 65% of energy usage in a water system is associated with pump operation, focusing on the optimal operation of pumps is worth investigating (Rouholamini et al. 2018). Having performed a survey, Electric Power Research Institute (EPRI) has determined how much water will be needed in 2050. On the one hand, the population growth will definitely result in the increase in safe drinking water demand. On the other hand, soon enough freshwater resources will be shrinking and less available due to the more strict requirements of drinking water treatment. Therefore, we will have to reach to those alternative water resources that are located in a farther distance, meaning that the energy costs of water supply will increase dramatically. According to this survey, energy usage to meet future water demand in commercial, public, and hospitalization sectors is going to grow by 50%. The growth will be thrice as big as the current energy consumption for industrial water treatment. Thus, even a small improvement in energy consumption may be counted as a considerable amount. This is not the only advantage. Any optimizations in energy consumption will lead to carbon emission reduction as well (Giacomello et al. 2012). The fluid in water systems is time-variant. Accordingly, dynamic models are involved to best evaluate and analyze the behavior of the fluid in a water pipeline network. By optimizing this model, it is possible to perform effective measures for operation cost reduction in a way that both the design requirements and water demand are softly satisfied though the objective function may vary depending on the design purposes. It should be mentioned that most of the optimization techniques are capable of being customized to be compatible with a specific objective function. In some water distribution networks, the desired flow and pressure are maintained using pump stations. Most of these devices are fed by a power grid in which the electricity bill is calculated based on daily or time-of-use tariffs. These conditions necessitate carrying out a research study to optimally schedule these pumps.

2 Materials and Methods

2.1 Fast Messy Genetic Algorithm (FMGA)

Genetic algorithm (GA) is one of the meta-heuristic methods that can find the optimal solution through considering a random initial population in which the length of all the strings is the same. This is while in a fast messy genetic algorithm (FMGA) the length of the strings is different and may vary over the generations. The search procedure is positively influenced by this mess (Goldberg 1989; Goldberg et al. 1993). This paper applied FMGA method in Darwin Scheduler optimizer in WaterGEMS (Bentley Systems 2009a).

2.2 Optimization Model of Pumping Station

$$\text{Min(EC)} = \rho g \sum_{j=1}^{m} \sum_{i=1}^{n} C_E \frac{Q_{j,i} H_{j,i}}{\eta_{j,i}(Q_{j,i})} \Delta t_j + \rho g \sum_{j=1}^{m} \sum_{i=1}^{n} C_D \frac{Q_{j,i} H_{j,i}}{\eta_{j,i}(Q_{j,i})} \tag{1}$$

$$\eta_{j,i}(Q_{j,i}) = a_{j,i} Q_{j,i}^2 + b_{j,i} Q_{j,i} + c_{j,i} \quad i = 1, 2, 3, \ldots, n \tag{2}$$

where i and j are the pump and time interval indices, respectively. $Q_{j,i}$, $H_{j,i}$, and $\eta_{j,i}$ are the outlet flow rate, head and efficiency of the i-th pump in j-th time interval. C_E is the hourly electricity tariff, and C_D is the price of power demand. Here, the outlet flow rate of the pump is the decision variable.

The constraints include providing the water demand, maximum permissible velocity in pipes, lower and upper bounds of the nodal pressures, minimum and maximum allowable water levels in the reservoir, and the maximum number of start/stop of the pumps.

3 Results and Discussion

In this study, the test network is Van Zyl which was first introduced in Van Zyl et al. (2004). It contains three pumps and two tanks. The layout of the network is shown in Fig. 1. Pumps 1A and 2B are identical pumps connected in parallel. When neither of these pumps is active, a booster pump 3B transfers the water from Tank A to Tank B. In case one or
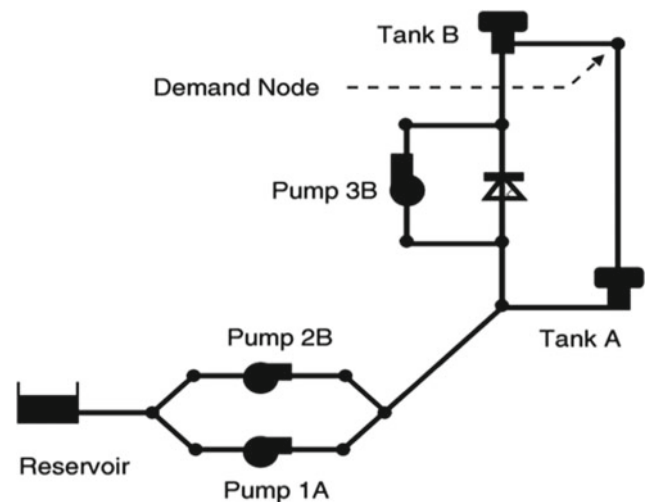

Fig. 1 Water distribution network under study

both, the pumps 1A and 2B are active, and pump 3B boosts the flow toward Tank B. Tank B is of higher elevation than Tank A, and thus water may flow by gravity from Tank B to Tank A through the pipes connected to the load node. It should be mentioned that scheduling time horizon (T) is 24 h that is divided into one-hour intervals.

This network has been optimized in research studies using various evolutionary algorithms such as GA, ant colony optimization (ACO), and non-dominated sorting genetic algorithm (NSGA). Table 1 presents the results obtained in this paper in comparison with the findings of the previous research works. As it is seen from Table 1, the cost obtained with the proposed method (Darwin Scheduler optimizer in WaterGEMS) is $355.51 for 24-h time period. It should be mentioned that the results proposed by NSGA-II and Hybrid GA are slightly lower than the one suggested by FMGA; however, the number of times that the pumps turn off/on, respectively, is 2 and 3 times. This is while it occurs only once in the scheduling scenario proposed by FMGA, which consequently leads to the reduction of maintenance costs and the increase of pumps' life cycle.

As seen in Figs. 2 and 3, the water levels in both tank A and B remain within these predetermined bounds in case FMGA is used.

In this network, the outlet flow rates of the pumps are determined as stated by the hourly profile shown in Fig. 4.

The values of the parameters of the utilized FMGA are given in Table 2. It is worth noting that the stopping criterion was reaching a certain number of iterations.

Table 1 Results obtained for Van Zyl network

Model	Cost ($/24 h)	Number of start/stop of pumps (in 24 h)	Year	Researcher(s)
GA	352.5	3	2004	Van Zyl et al.
Hybrid GA	350.81	3	2004	Van Zyl et al.
ACO	357.6	9	2008	López-Ibáñez et al.
ACO	388.04	6	2014	Hashemi et al.
NSGA-II	354.24	2	2017	Makaremi et al.
FMGA	355.51	1	2017	This paper

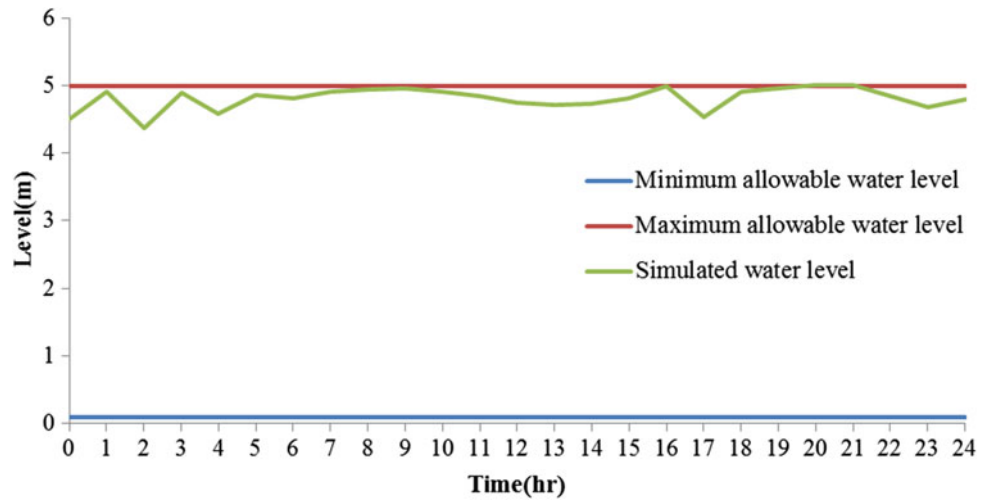**Fig. 2** Water level in tank A

Fig. 3 Water level in tank B

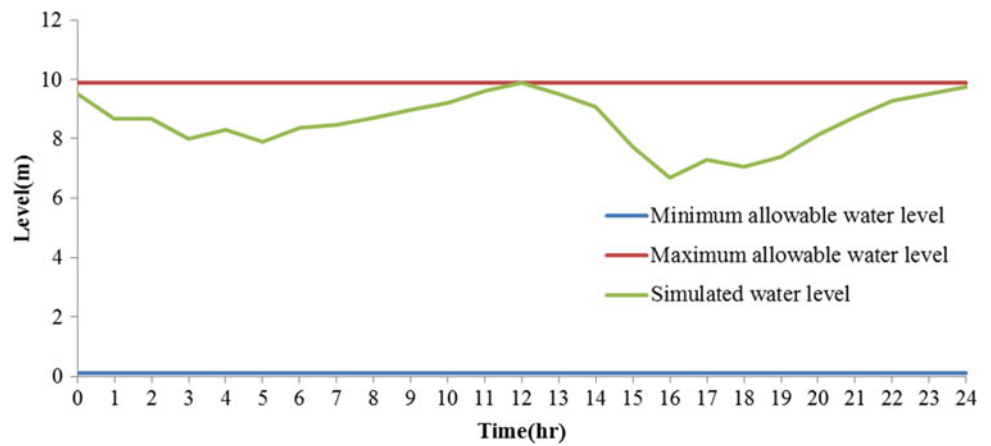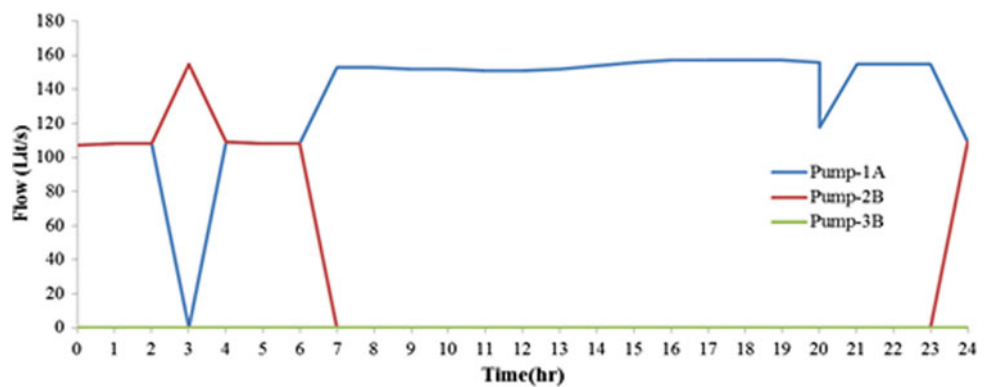**Fig. 4** Hourly profile of the output flow rates of the pumps

Table 2 Values of the parameters of the utilized FMGA

FMGA		
	Population size	100
	Number of crossover point	4
	Probability of crossover	95
	Probability of mutation	1.5
	Maximum trials	100,000

4 Conclusion

In this paper, fast messy genetic algorithm (FMGA) was used to optimally schedule the hourly operation of pump stations. The obtained results clearly showed that the proposed method not only meets the hydraulic constraints of the network, but also reduces the electricity bill. More importantly, the number of start/stop of pumps in the operation strategy suggested by FMGA is lower than the ones proposed by the previous research studies.

References

Bentley Systems. (2009a). *WaterGEMS v8i User Manual*. Haestad Solution Center, 27 Siemon Company Drive, Suite200 W, Watertown CT, USA.

Giacomello, C., Kapelan, Z., & Nicolini, M. (2012). Fast hybrid optimization method for effective pump scheduling. *Journal of Water Resources Planning and Management, 139*(2), 175–183.

Goldberg, D.E. (1989). *Genetic algorithm in search optimization and machine learning*. Addison-Wesley Pub; Hashemi, S. S., Tabesh, M., Ataeekia, B. (2014). Ant colony optimization of pumping schedule to minimize the energy cost using variable speed pump in water distribution networks. *Urloan Water Journal, 11*, 334–347.

Goldberg, E., Deb, K., Kargupta, H., Harik, G. (1993). *Rapid, accurate optimisation of difficult problems using fast messy genetic algorithms* (Illigal Report 93004). University of Illinois.

López-Ibáñez, M., Prasad, T. D., & Peachter, B. (2008). Ant clony optimization for optimal control of pumps in water distribution network. *Journal of Water Resource planning and Management, 134*, 337–346.

Rouholamini, M., Miller, C. J., Wang, C., Mohammadian, M.(2018). *A review of water/energy co-management opportunities*. In IEEE Power & Energy Society General Meeting, Portland, USA, In press.

Van Zyl, J. E., Savic, D. A., & Walters, G. A. (2004). Operational optimization of water distribution systems using a hybrid genetic algorithm. *Journal of Water Resources Planning and Management, 130*, 160–170.

Membrane Aerated Biofilm Reactor (MABR)—Distributed Treatment of Wastewater at Low Energy Consumption

Udi Tirosh and Ronen Shechter

Abstract

Membrane-aerated biofilm reactor (MABR) is an energy efficient biological wastewater treatment process, based on passive aeration: by diffusion of oxygen through membranes, which also support an aerobic biofilm. The theoretical energy savings of MABR over that of conventional activated sludge (CAS) process were calculated to 86.8%. The paper analyzes two case studies of MABR implementation: one treating 25,000 GPD (95 m^3/day) of municipal wastewater at US Virgin Islands and the second treating 125 m^3/day of concentrated wastewater at Ha-Yogev WWTP in Israel. Energy consumption was measured and averaged over 2 months of operation. The results show the energy consumption for operation of the secondary treatment with MABR amounts to 0.212 kWh/m^3 at the first case, while removing 98.9% BOD, 94.8% of NH4, and 96.8% of TSS. In the second case, the energy consumption for operation of the secondary treatment was below 0.4 kWh/m^3 for the biological treatment achieving the required removal rates. By consuming very low energy at small treatment capacities, MABR supports the most important principles in water and energy efficiency: reduced energy for treatment and local water reuse.

Keywords

MABR • Wastewater • Low energy • Energy efficient

1 Introduction

Membrane-aerated biofilm reactor (MABR) is an especially-energy efficient biological wastewater treatment process, based on passive aeration: by diffusion of oxygen through membranes, which also support an aerobic biofilm. The effluent of MABR is suitable for reuse in irrigation as well as for discharge to the environment.

Table 1 compares the theoretical energy consumption of MABR with that of conventional activated sludge (CAS) process.

With very low energy consumption even at small treatment capacity, MABR supports the most important principles in water and energy efficiency: reduced energy for treatment and local water reuse. Local water reuse also minimizes resources for handling wastewater and water and saves pumping water back and forth.

Two case studies will be presented.

2 Materials and Methods

Case Study #1—US Virgin Islands

Dealing with water scarcity has been a challenge in the US Virgin Islands for many years. Much of the water shortage influences irrigation for local farmers, domestic demand, and tourism.

The primary criterion for qualifying an economical wastewater treatment process is the final effluent quality and further impact on the environment. Another major consideration is operating cost, much influenced by the high cost of electricity in USVI, of about US$0.30 per kWh.

MABR technology was selected due to its promise to enable nitrogen removal with simple operation and low energy consumption.

The Fluence MABR modules installed in the Bordeaux plant comprise a large surface area of a spirally wound oxygen permeable membrane. The modules are designed to hold MLSS in suspension between the wraps of the spiral. Low-pressure air from a fan is continuously blown through the membrane. The module content is mixed by aerating the water for 20–30 seconds, 4–5 times per hour, and in total about 2–3% of the time.

U. Tirosh (✉) · R. Shechter
Fluence Products and Innovations Ltd., Caesarea, Israel
e-mail: utirosh@fluencecorp.com

Table 1 MABR energy consumptions as a percent of CAS textbook figures

	Pressure (%)	Flowrate (%)	Duty (%)	Power (%)
Mixing	60	400	2.5	6.0
Aeration	9.1	80	100	7.2
Total				13.2

Case Study #2—Ha-Yogev WWTP, Israel

Ha-Yogev is a Kibbutz located at the middle of the Jezreel Valley near the historical site of Armageddon.

Ha-Yogev Wastewater Treatment Plant was re-commissioned on May 2017 after being upgraded with a 125 m³/day sidestream MABR process. It was then transferred to operation and maintenance by the water utility (Yuvaley Ha-Emek).

Wastewater is combined sewage and dairy farms. There is an existing primary anaerobic lagoon, and the MABR process was set up to treat part of the flow in order to help maintain ammonia below allowed limit; MABR effluent returns to the lagoons. The combined effluent is then locally reused by Ha-Yogev Kibbutz for irrigation. The configuration installed at Ha-Yogev is similar to that of USVI and double in size—18 MABR modules vs. 9 MABR modules at USVI.

Note that in Ha-Yogev, the effluent returns to the lagoon treatment process, so the excess nitrate is not an issue—it actually provides some oxidative capacity there.

3 Results and Discussion

3.1 Effluent Quality Results

The most important parameter of concern is nitrogen. The chart below shows the average wastewater concentration of 90 mg/l with up to 120 mg/l at times. The effluent average concentration is 35 total nitrogen including nitrate. However, since water
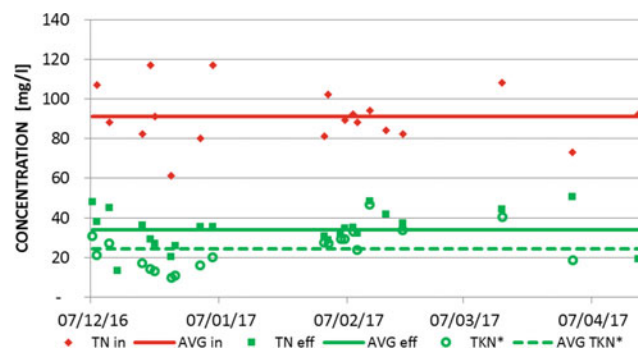

Fig. 1 TN and TKN concentration over time—influent and effluent. TKN* is a calculated value for total nitrogen analysis without the nitrate. It is a more relevant performance indicator for the MABR influence on the poorly aerated non-nitrifying pond to which it returns the treated wastewater.
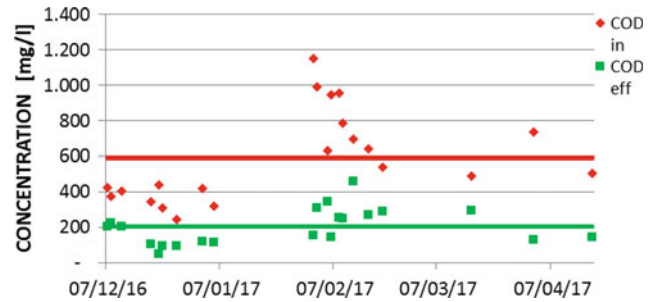

Fig. 2 COD influent and effluent over time

is returned to a poorly aerated lagoon, nitrate is a resource providing oxidation of organic matter (BOD). The remaining nitrogen is similar to TKN, and its concentration is in average 25 mg/l. This means that lagoon effluent can be mixed 1:1 with MABR effluent to obtain less than 50 mg/l as required (Fig. 1).

The chart below presents wastewater and MABR plant effluent COD concentrations (Fig. 2).

Influent is highly variable having time periods when the typical concentrations are around 400 mg/l, and others when it is around 1000 mg/l. These variations indicate unauthorized dairy waste dumping into the sewer.

Bottom line is that Ha-Yogev plant can be operated at below 0.4 kWh/m³ for the biological treatment or less than 0.45 kWh/m³ for the entire MABR plant.

3.2 USVI Bordeax Plant Results

3.2.1 Plant Description

The Bordeaux plant is a localized municipal WWTP located in Saint Thomas, designed to serve a population of approximately 200 houses. The plant started operation in

Table 2 Design data

Parameter	Wastewater	Effluent requirements
BOD mg/l	140	10
TSS mg/l	205	10
TN mg/l	46	10
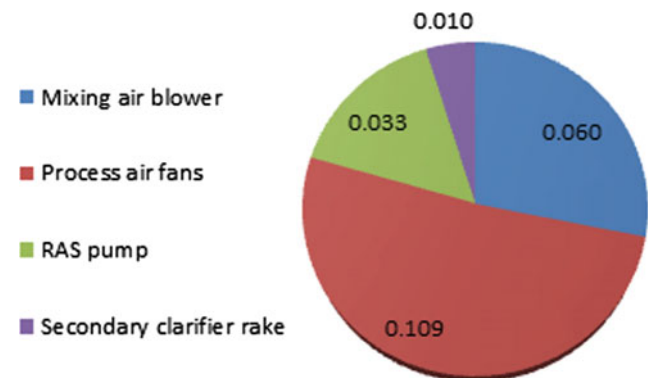
Fig. 3 Energy consumption distribution in kWh/m³

Table 3 Bordeaux plant results

Date	BOD inf	BOD eff	% Removal	NH$_4$-N inf	NH$_4$-N eff	% Removal	TSS inf	TSS eff	% Removal
8/3/2017	463.7	8.2	98.2%	310.0	17	94.5%	120	5.1	95.8%
7/25/2017	357.4	4.7	98.7%	220.0	10	95.5%	90	2.5	97.2%
7/11/2017	517.7	5.2	99.0%	133.3	3	97.7%	75	3.1	95.9%
6/28/2017	518.3	6.1	98.8%	90.0	10	88.9%	170	3	98.2%
6/14/2017	452.6	8.6	98.1%	99.0	8	91.9%	110	3	97.3%
5/24/2017	276.2	0.7	99.7%	160.0	0	100.0%	140	5	96.4%
		Average	98.8%		Average	94.8%		Average	96.8%

November 2016, and the commissioning is planned in December 2016.

The plant is based on the innovative MABR described above. It has a nominal design capacity of 25,000 GPD (95 m^3/day) and will be able to expand in the future up to double the initial capacity, by adding MABR modules. The plant also includes fine screens and equalization as pretreatment and tertiary treatment based on media filters and disinfection unit.

The MABR modules are arranged in two stages and use a secondary clarifier similar to the activated sludge process.

3.2.2 Process and Energy Performance Results

The plant has been operating since November 2016. The process performance exceeds effluent requirements of TSS/BOD/TN/TP of 10/10/10/1 mg/l as shown in Table 2.

The results show that the energy requirements for the operation of the secondary treatment with MABR amount to 0.212 kWh/m^3. The distribution by source is presented in a pie diagram in Fig. 3, where it can be seen that total energy consumption is approximately split three ways between pumping, process air supply, and mixing by intermittent aeration (Table 3).

4   Conclusion

Both Boudreaux and Ha-Yogev plants maintained excellent effluent quality while demonstrating very low energy consumption. By this, both MABR-based WWTPs enable very efficient local wastewater treatment and reuse for local agricultural needs. By considering piping and pumping capital and operational expenses, the savings of such local treatment go way beyond the energy savings.

Method to Assess Wastewater Pumps in the Nexus of Functionality and Energy Efficiency

Michael Pöhler and Paul Uwe Thamsen

Abstract

To date, there is no standardised test available, which assesses the actual performance of a pump for wastewater (especially its clog resistance) as well as providing references about its efficiency. The developed testing procedure presented in this paper can display the different levels of performance for different pumps. The functionality of the pump, together with its efficiency is aggregated to the Function Efficiency Index (FEI). The FEI is thus a holistic parameter to describe a wastewater pump and enables a revaluation of the technologies available on the market.

1 Introduction

In the light of upcoming EU energy efficiency regulations, it is necessary to design a new method for evaluating wastewater pumps. Efficiency should of course be included as an important criterion. It has to be considered, however, subordinated to the functional performance of the technology used. This has become especially clear in the last years, with an increasing amount of pump blockages caused by nonwoven wet wipes. These clogging events cause either an instantaneous drop in pump performance or a continuous degradation over a short period of time. Often, clog-resistant and robust impeller technologies have low energy efficiencies, while efficient impellers are more prone to clogging. While there are standards to assess the clear water efficiency of a pump (ISO 2012), to date there is no such standard for

the assessment of the functional performance of a wastewater pump. Therefore, we suggest the introduction of a Functional Efficiency Index, which combines the functional performance (or "clog resistance") of available impeller technologies for different types of wastewater with the respective achievable efficiencies. Only in this way can it be ensured that the application of energy-efficient technologies actually leads to a system improvement and not to a shift of energy costs to operational costs due to increased maintenance—while at the same time reducing the operational stability of the infrastructure.

As the assessment of the performance of pumps for wastewater is inherently more complicated than assessing their performance for clear water (due to the complex medium), the universal validity and the comparability of the results of the assessment have to be ensured. Therefore, a standard medium (wastewater) is needed, as well as specific parameters for the pump performance and an evaluation scale, which combines hydraulic performance and resilience. In this way, a more holistic assessment of the actual performance of the critical asset "wastewater pump" can be achieved.

2 Materials and Methods

According to (DWA 2016) and operators of wastewater networks, wet wipes are the most common causes for pump clogging and have therefore been used in this study as the ingredient for the designed standard artificial wastewater. A standard nonwoven textile wipe was chosen (sold commercially as a duster), with which it was possible to reproduce the clogging behaviour of wastewater pumps in the laboratory.

The degree of contamination of the wastewater with textiles and fibrous material is an important parameter for the pump performance. In order to create a measurable degradation in the pump performance, three classes of artificial wastewater were defined (see Table 1). The respective

M. Pöhler (✉) · P. U. Thamsen
Technische Universität Berlin, Berlin, Germany
e-mail: michael.poehler@tu-berlin.de

amount of wipes for each defined specific fibre content was added to clear water and then presented to the pump. The detailed testing parameters as well as the test rig, testing procedures and the different classes of artificial wastewater are described in detail in (Pöhler and Thamsen 2016).

In this study, nineteen impellers/pumps from different manufacturers were tested. The impellers presented in the results are listed in Table 2. Two types of functional performances were tested (Pöhler and Thamsen 2016): The degree of functional performance D_F describes the pumps ability to pump a certain amount of contaminated wastewater once. It is calculated using the ratio of the pumped textiles to the total amount of textiles added to the system.

The degree of long-term functional performance D_{LTF} expresses the functionality of a pump for continuous pump operation, when clogging and blocking can occur due to slow accumulation of fibrous material. To assess both, the resilience against accumulative clogging as well as the functional performance, the D_{LTF} is composed of two equal parts. Part one is the ratio of the mean efficiency during the whole test to the respective clear water efficiency at the operating point tested. The second part is the D_F.

D_F, D_{LTF} and the clear water efficiency make up the holistic assessment of the hydraulic and functional performances of the wastewater pump (for the tested operating point) named Functional Efficiency Index (FEI) (see Eq. 1).

$$\text{FEI} = (\alpha \times D_F + \beta \times D_{LTF}) \times (\rho \times g \times H \times Q)/P_{el} \quad (1)$$

where alpha and beta are scaling factors, ρ is the density, g is the gravitational constant, H is the delivered head, Q is the flow and P_{el} is the electric power consumption.

The Functional Efficiency Index (FEI) is an extension of the pump efficiency. It is designed to award pumps that are highly functional for contaminated wastewater with a subordinate clear water efficiency. With the help of scaling factors (α, β, here 0.5, respectively) in Eq. (1), the various wastewater-specific test parameters should be set in relation to the pump efficiency. This allows the comprehensive comparison of different pumps, by considering not only their energy efficiency but also their respective capability to pump highly contaminated wastewater. As a result, energy-efficient pumps applicable for slightly contaminated wastewater and less efficient pumps used for the transportation of wastewater with a high amount of solids can be directly compared to one another.

3 Results and Discussion

In Fig. 1, the clear water efficiencies can be identified (the highlighted areas in Figs. 1, 2 and 3 describe the respective ranges of all tested impeller types). As to be expected, the clear water efficiency of the vortex impellers lies in the lower section of the efficiency of all impellers tested, while the single-channel and two-vane impellers have higher clear water efficiencies. With increasing contamination, the efficiency decreases for all tested impellers, except for the *single-d* impeller, which remains nearly constant. However, the degree of decrease in efficiency differs greatly among the impellers. While most impellers show a slight decrease, the two-vane impeller *two a* (with the highest clear water efficiency) decreases most strongly. The spread of the impeller efficiencies with decreasing contamination can be seen more clearly in Fig. 2, which shows the change in relative efficiency with the increasing contamination. It is clear that the efficiency cannot be differentiated according to impeller type. Two groups can be distinguished in the diagram: While the impellers *vortex e* and *two a* lose 60 and 90% of their efficiency, respectively, the other impellers only lose between 5 and 20% of efficiency.

Table 1 Classes of artificial wastewater

Wastewater class	Specific fibre content in g/m³	Wipes/m³	Degree of contamination D_C
Clear water	0	0	0
Low contamination	95	25	0.125
Medium contamination	190	50	0.25
High contamination	380	100	0.5

Table 2 Impellers presented in the results

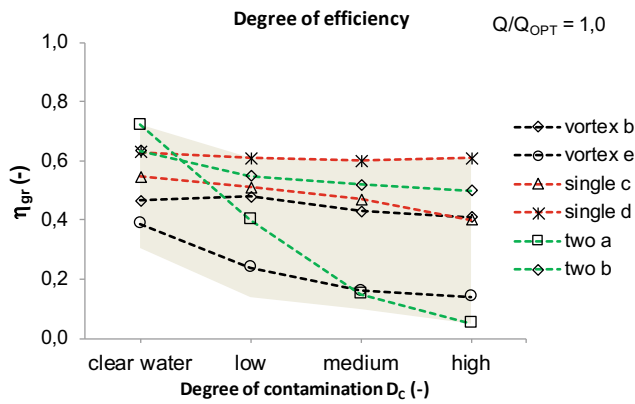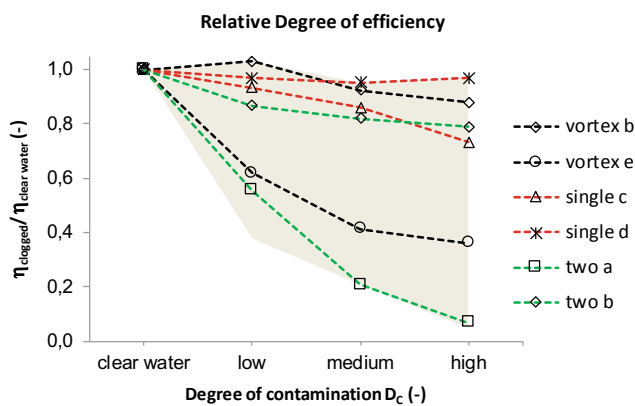| Impeller type	Specific design	Nomenclature in results
Vortex	–	Vortex *b*, *e*
Single-vane	Open	Single *d*
	Closed	Single *c*
Two-channel impeller	Open	Two *b*
	Closed	Two *a*

Fig. 1 Degree of efficiency

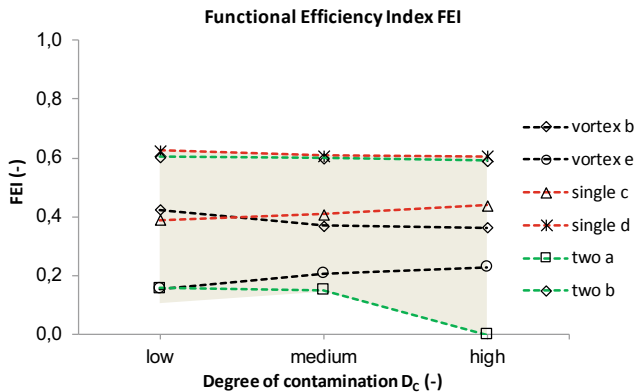**Fig. 2** Relative degree of efficiency

Fig. 3 Functional efficiency index (FEI)

Figure 3 shows the combination of efficiency and functionality (how much can the pump pump at the given degree of contamination with the respective degree of efficiency). When comparing the FEI with the clear water efficiencies

(Fig. 1), it can be seen that the general tendencies remain similar, though the picture becomes clearer. The two impellers with the highest clear water efficiency (*two a* and *single d*) also show superior performance pumping the contaminated wastewater and thus have the best FEI, which hardly decreases with increasing wastewater contamination. The vortex impellers have a lower hydraulic and specific clogging resistance than very good single-channel and two-vane impellers and are thus to be found in the centre and lower part of the FEI values. Nevertheless, a well-designed vortex impeller can compete with a single-vane impeller in terms of functional and hydraulic performances. For example, the *vortex b* impeller is close to the *single-vane c* impeller in functional performance. Most interestingly, the two-vane impeller *two a* shows the lowest FEI. Again, this underlines the fact that wastewater pumps should not be assessed only according to their clear water efficiency: The *two-a* impeller, with the highest clear water efficiency of all tested impellers, could not cope with contaminated wastewater and thus showed one of the lowest FEIs of all tested impellers.

4 Conclusion

Failure-free operation of wastewater pumps is a crucial criterion for operators of wastewater networks. Highly resilient wastewater pumps can prolong the mean time between failures and reduce energy consumption as well as the expenses for maintenance or emergency services. To date, there is no standardised test available, which assesses the actual performance of a pump for contaminated water (especially its clog resistance) as well as providing references about its efficiency. There are pumps available with minor clear water efficiencies, but with high capabilities of transporting fluids with a high contamination of clogging material and vice versa. Pump users and developers have to rely on their experience or a "trial and error" process to choose the correct pump. This not only costs a lot of money but can seriously endanger the operational stability of the critical wastewater infrastructure.

The developed testing procedure and assessment of wastewater pumps presented in this paper can display the different levels of performance for different pumps: their capability to deal with one-time contamination (D_F) as well as long-term contamination (D_{LTF}). The functionality of the pump, together with its efficiency, is aggregated to the Function Efficiency Index (FEI). This FEI is thus a holistic parameter to describe a wastewater pump and enables a revaluation of the technologies available on the market.

References

DWA. (2016). *Feuchttücher*, KA Betriebsinfo, issue 01.2016 (pp 2428–2434), DE.

ISO 9906. (2012). *Rotodynamic pumps—Hydraulic performance acceptance tests—Grades 1, 2 and 3*. Geneva, CH: International Organisation for Standardisation.

Pöhler, M., Thamsen, P.U. (2016). Functional performance of wastewater pumps. In *3rd International Rotating Equipment Conference (IREC) Pumps, Compressors and Vacuum Technology in Düsseldorf* (pp. 1–12), September 2016, ISBN 978 3 8163 0697-9, DE.

Role of Pretreatment in Adsorption of Cobalt, Mercury and Nickel by Native Algae

Muhammad Rizwan, Alia Naz, Abdullah Khan, Wisal Shah, Ghulam Mujtaba, Mona Syed, Qadeer Ahmed, and Noor Fatima

Abstract

Native macroalgae were used as an inexpensive and efficient biosorbent. Mercury (Hg), nickel (Ni) and cobalt (Co) were removed from synthetic wastewater. The algal biomass was pretreated with 0.1 HCl, 0.2 HCl, $CaCl_2$ NaOH Na_2CO_3 and hot water. NaOH pretreatment was most suitable for the removal of Hg. Na_2CO_3 pretreatment was the best technique for the removal of Ni and Co.

1 Introduction

Environmental pollution is usually caused by heavy metals or metal-like elements, or those compounds which cannot be degraded by biological means, and as a result they are bioaccumulated (Herrera-Estrella and Guevara-Garcia 2009). Several heavy metals are released into the environment because of various technological activities by humans; these heavy metals either prevail for an indefinite time or are transformed, circulate and ultimately gather all over the food chain, as a result they become a serious environmental issue (Volesky and Holan 1995). Therefore, they have an enormous impact on environment, economic and public health (Brower et al. 1997). The health impacts associated with nickel include dermatitis, eczema and lichenification. Discharge of heavy metals into water bodies in the form of wastewater will have an irredeemable effect on the marine life and will terminate the self-purification capability of a water body (Khan et al. 2008). Currently, the techniques which are used for heavy metal recovery from wastewater include: chemical precipitation, electrodialysis, ultrafiltration, reverse osmosis, phytoremediation and ion-exchange, etc. However, these methods have several drawbacks like partial metal removal, not cost-effective, generate toxic sludge or other waste products for which careful disposal is required (Ahalya et al. 2003). Macroalgae not only possess greater heavy metals remediation efficacy; the recovery of heavy metals requires few simple desorption chemicals. Living macroalgae require minimal nutrients and other environmental factors; however, dead microalgal biomass does not need oxygen or nutrients additionally, they can remove heavy metals from wastewater containing several heavy metals (Rajamani et al. 2007).

M. Rizwan (✉)
U.S-Pakistan Centers for Advanced Studies in Water (USPCASW), Mehran University of Engineering and Technology, Jamshoro, 76062, Pakistan
e-mail: drmrizwan.uspcasw@faculty.muet.edu.pk

M. Rizwan · A. Naz · A. Khan · W. Shah · M. Syed · Q. Ahmed · N. Fatima
Department of Environmental Sciences, University of Haripur, Haripur, 22620, Pakistan
e-mail: aliaawkum@gmail.com

G. Mujtaba
Department of Energy and Environment Engineering, Dawood University of Engineering and Technology, Karachi, Pakistan
e-mail: gmujtabaawan@gmail.com

2 Materials and Methods

a. *Collection and Washing*

Algae samples were collected from Kot Najibullah and Shah Maqsood. It was washed with tap water to remove sand and other cretaceous material. The algae were then soaked in deionized water for one hour to ensure the cleanliness of the samples. Algae were re-washed until their pH reached 7.0. Then it was dried in oven 104 °C for four–six hours and grinded into a fine powder using mortar and pestle. Grounded algae were sieved and stored in plastic tubes.

b. *Preparation of stock and working solutions*

100 ml solution of heavy metals was prepared such as of Cd, Ni, Pb, etc. Seven working solutions were made from each stock solution by adding 2 ml from the stock solution to each flask of working solution.

Experiments Undertaken

c. *Pretreatment of algae*

The required solutions for pretreatment methods were made by adding required moles or grams in deionized water (0.1 N HCl, 0.1 N NaOH, 0.1 M NaOH, 0.2 M $CaCl_2$, 0.2 M Na_2Co_3, 0.2 HCl 37%, Hot Water). 1 g of algae was added into each pretreatment solution then centrifuged for about 2 h. Then water was strained from it and washed with deionized water. Algae were dried in the oven in petri dishes at 50 °C and weighed and stored in plastic tubes.

d. *Effect of pretreatment on heavy metal*

Each working solution pH was maintained b/w 5 and 5.5 by NaOH and HCl solutions. 0.1 g of algae was added in each working solution then placed in shaking incubator for about 2 h. A 10 ml sample was taken from each solution and centrifuged for 5 min. 10 ml of water was then collected from each solution for atomic absorption analysis.

3   Results and Discussion

Cobalt (Co)

Native macroalgae were used for biosorption of cobalt from wastewater. Macroalgal biomass without pretreatment was compared with six different pretreatment methods namely 0.1 HCl, 0.2 HCl, $CaCl_2$, NaOH, Na_2CO_3 and hot water. As shown in Fig. 1, algae treated with 0.1 N HCl remove 15% metal contamination. Similarly, algae treated with 0.2 N HCl absorb 0.185 and give 13% removal, $CaCl_2$ gives absorbance 0.150 by removing 42% metal, Na_2CO_3 removes 53% by absorbing 0.135, algae treated with 0.1 N NaOH remove 39% by absorbing 0.154 metal, hot water gives results like removal of 29% metal by absorbing 0.167 and untreated algae means without any pretreatment with chemicals, solutions give 0.165 absorbance and remove 31% metal contaminant. Best results were found when algae were pretreated with Na_2CO_3 that is maximum removal of 53% by absorbing 0.135.

Many other scientists conduct the same experiments with same and by applying different conditions like according to Romera et al. (2007) at pH 5.5 when algae type with cell wall, used that gives 0.89 mg/g metal uptake but at same pH when he used biomass type without cell wall got 1.3 mg/g metal uptake. Another study of Macfie and Welbourn (2000)
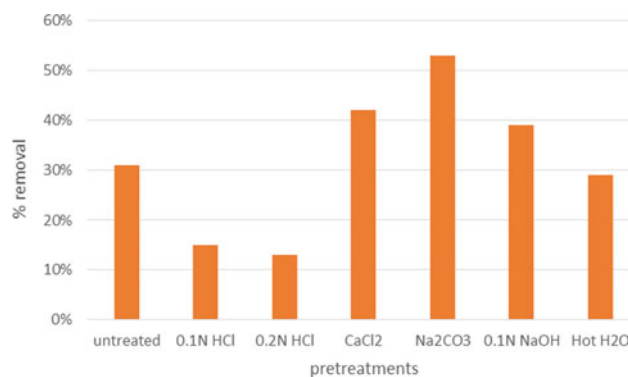

Fig. 1 Percentage removal of cobalt with and without pretreatments

shows 15.32 mg/g metal uptake at pH 4 by using non-living type of biomass, according to Mehta and Gaur (2005) metal uptake was 12.82 mg/g while using non-living type of biomass, similarly according to Kumar and Oommen (2012) when non-living type of biomass used at pH 7.5 that gives 0.01 mg/g metal uptake.

Mercury (Hg)

The biomass of algae was used to remove Hg from wastewater. Maximum sorption capacity for each pretreatment algal biomass was 49, 39, 37, 37, 31, 31 and 18% for 0.1 N NaOH, hot water, Na_2CO_3, $CaCl_2$, 0.2 N HCl, 0.1 N HCl and untreated, respectively, as shown in Fig. 2. From our experimental studies, it was suggested that 0.1 N NaOH are the best methods for the removal of mercury from wastewater.

In Thailand, according to Inthorn et al. (2002), the uptake of Hg^{2+} by using non-living biomass *Calothrix parietina* TISTR 8093 showed that biosorption of Hg^{2+} at pH in 7. The maximum absorption is 19 mg/g (Chojnacka et al. 2004). Tüzün et al. (2005) by using non-living biomass *Chlamydomonas reinhardtii*, the uptake of metal Hg^{2+} maximum absorption is 72.2 mg/g, at pH 6 [20]. Similar research by Inthorna et al. (2002) investigated Hg^{2+} using
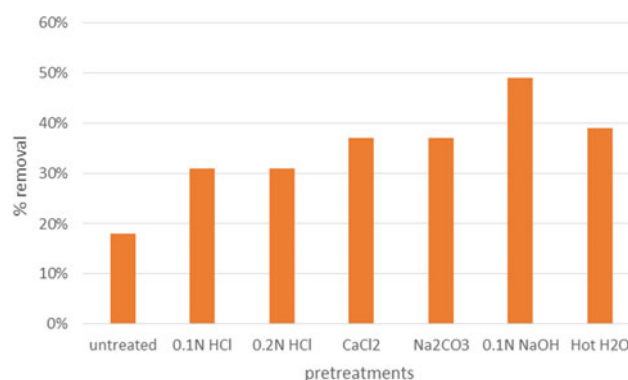

Fig. 2 Percentage removal of mercury with and without pretreatments

non-living algae biomass *Chlorella vulgaris* BCC 15 is the most metal uptake at pH 7. Treatment maximum sorption is 18 mg/g (Inthorn et al. 2002). Another scientist Schmitt et al. 2001 reported that biomass *Cyclotella cryptica* has ability to remove mercury at pH 4 resulting in maximum sorption 11.92 mg/g (Tüzün et al. 2005). Similarly, Schmitt et al. 2001 showed in his study, maximum biosorption capacity is 0.51 mg/g by using biomass of *Phaeodactylum tricornutum* and *Porphyridium purpureum* at 4 pH (Schmitt et al. 2001). Similar research by Kumar and Oommen (2012) was on the uptake of Hg^{2+} by *Spirogyra hyaline biomass*. Maximum number of absorbed ions being 35.71 mg/g (Kumar and Oommen 2012).

Nickel (Ni)

In the current study, native algae were used for removal of nickel from synthetic wastewater. Figure 3 shows maximum removal efficiency for nickel was 36, 29, 27, 21, 20, 17 and 17% for Na_2CO_3, NaOH, untreated, $CaCl_2$, 0.2 N HCl hot water and 0.1 N HCl, respectively. From the current study, it was concluded that Na_2CO_3 pretreatment was most suitable for the removal of nickel from synthetic wastewater.

Ferreira reported that the metal uptake was 20.78, and he used algae *Arthrospira* in pH ranging 5–5.5. And another scientist named Chojnacka et al. (2004) reported that the Chlorella Vulgaris algae were used for the removal of nickel from wastewater pH ranging 5. Another scientist used the biomass of algae named *Chlorella Vulgaris* in the pH ranging 4.7 for the removal of nickel from synthetic wastewater and the metal uptake was 24.06 mg/g (Ferreira et al. 2011). Similarly, another scientist that uses the non-living algal biomass having pH range 5 and the metal uptake was 15.4 mg/g for the removal of Nickel from wastewater (Dönmez et al. 1999).
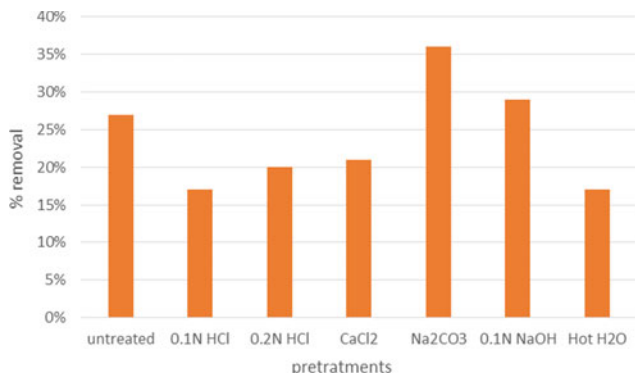

Fig. 3 Percentage removal of nickel with and without pretreatments

4 Conclusion

In this study, native macroalgae were used for biosorption of cobalt from wastewater. Macroalgal biomass without pretreatment was compared with six different pretreatment methods namely, 0.1 HCl, 0.2 HCl, $CaCl_2$, NaOH, Na_2CO_3 and hot water. From our current study, it was concluded that Na_2CO_3 pretreatment was most suitable for the removal of cobalt from synthetic wastewater. NaOH pretreatment was most appropriate for the removal of mercury from synthetic wastewater. Na_2CO_3 pretreatment was most suitable for the removal of nickel from synthetic wastewater.

References

Ahalya, N., Ramachandra, T. V., & Kanamadi, R. D. (2003). Biosorption of heavy metals. *Research Journal of Chemistry and Environment, 7*(4), 71–79.

Brower, J. B., Ryan, R. L., & Pazirandeh, M. (1997). Comparison of ion-exchange resins and biosorbents for the removal of heavy metals from plating factory wastewater. *Environmental Science and Technology, 31,* 2910–2914.

Chojnacka, K., Chojnacki, A., & Górecka, H. (2004). Trace element removal by Spirulinasp. From copper smelter and refinery effluents. *Hydrometallurgy, 73,* 147–153.

Dönmez, G. Ç., et al. (1999). A comparative study on heavy metal biosorption characteristics of some algae. *Process Biochemistry, 34* (9), 885–892.

Ferreira, L. S., et al. (2011). Adsorption of Ni^{2+}, Zn^{2+} and Pb^{2+} onto dry biomass of Arthrospira (Spirulina) platensis and *Chlorella vulgaris*. I. Single metal systems. *Chemical Engineering Journal, 173*(2), 326–333.

Herrera-Estrella, L. R., Guevara-Garcia, A. A. (2009). *Heavy metal adaptation. Encyclopedia of life sciences* (pp. 1–9). Chichester: Wiley. http://dx.doi.org/10.1002/9780470015902.a0001318.pub2 (Published Online: 15 Mar 2009).

Inthorn, D., Sidtitoon, N., Silapanuntakul, S., & Incharoensakdi, A. (2002). Sorption of mercury, cadmium and lead by microalgae. *ScienceAsia, 28,* 253–261.

Khan, M. A., Rao, R. A. K., & Ajmal, M. (2008). Heavy metal pollution and its control through non-conventional adsorbents (1998–2007): A review. *Journal of International Environmental Application & Science, 3*(2), 101–141.

Kumar, J. I. N., & Oommen, C. (2012). Removal of heavy metals by biosorption using freshwater alga Spirogyra hyaline. *Journal of Environmental Biology, 33,* 27–31.

Macfie, S. M., & Welbourn, P. M. (2000). The cell wall as a barrier to uptake of metal ions in the unicellular green alga *Chlamydomonas reinhardtii* (Chlorophyceae). *Archives of Environmental Contamination and Toxicology, 39,* 413–419.

Mehta, S. K., & Gaur, J. P. (2005). Use of algae for removing heavy metal ions from: Progress and prospects. *Critical Reviews in Biotechnology, 25,* 113–152.

Rajamani, S., Siripornadulsil, S., Falcao, V., Torres, M.A., Colepicolo, P., & Sayre, R. (2007). Phycoremediation of heavy metals using transgenic microalgae. *Advances in Experimental Medicine and Biology, 616,* 99–109.

Romera, E., Gonzalez, F., Ballester, A., Blazquez, M. L., Munoz, J. A. (2007). Comparative study of biosorption of heavy metals using different types of algae. *Bioresource Technology, 98*(17), 3344–3353.

Schmitt, D., Müller, A., Csögör, Z., Frimmel, F. H., & Posten, C. (2001). The adsorption kinetics of metal ions onto different microalgae and siliceous earth. *Water Research, 35*(3), 779–785.

Tüzün, İ., Bayramoğlu, G., Yalçın, E., Başaran, G., Çelik, G., & Arıca, M. Y. (2005). Equilibrium and kinetic studies on biosorption of Hg (II), Cd(II) and Pb(II) ions onto microalgae *Chlamydomonas reinhardtii*. *Journal of Environmental Management, 77,* 85–92.

Volesky, B., & Holan, Z. R. (1995). Biosorption of heavy metals. *Biotechnology Progress, 11*(3), 235–250.

A Model-Based Approach for Energy Optimization of Real Wastewater Pumping Station

Manuel De Chiara, Roberto De Rosa, Anna Giuliani, Salvatore Guadagnuolo, Angelo Leopardi, Luca Pucci, and Dario Torregrossa

Abstract

Wastewater pumping plants represent important energy consumers. A real case study in Italy is analyzed. A model-based approach is proposed. Optimization of pumps start/stop number is performed. The approach can be easily extended to different case studies.

1 Introduction

Climate change and growing demands are straining our energy and water supplies (Di Fraia et al. 2018). The water sector is a very important energy consumer. In the Campania Region (Italy), it represents 3% of the total energy consumption, and it is the 30–40% of the total public energy bill. The energy consumption of wastewater treatment plants (WWTPs) is often high and relevant energy saving potential estimates are available in the literature (Castellet and Molinos-Senante 2016). Furthermore, the adoption of higher water treatment standards is expected to increase the energy consumption of water and wastewater treatments (Di Fraia et al. 2018). Consequently, many authors developed strategies and tools to increase the understanding of plant processes and support the energy efficiency of the plants (Castellet-Viciano et al. 2018; Torregrossa and Hansen 2018). In WWTPs, pumping stations represent one of the most important energy consumer (Torregrossa 2017), and consequently their optimization can contribute to improve the energy balance performance of WWTPs. The aim of this manuscript is to propose a model-based approach to optimize the operation of a real WWTP pumping station.

In the paper, a specific case study is analyzed: the South Pumping plant of the Nocera WWTP. Such a system uses about 20% of the energy consumed by the plant, and consequently, its operational and energy optimization is mandatory for an efficient management. Using the real data provided by the SCADA, a model for the simulation of the pumping plant behavior (and in particular for the computation of start/stop number of the pumps) is built. This model is then used to find optimal management strategies and minimize the start/stop number in the plant.

The proposed model-based approach can be easily extended to other case studies, and then it can be considered of general applicability. Considerations on possible structural modification of the system are also made.

2 The Case Study

Nocera wastewater treatment plant serves five municipalities in the Campania Region, treating domestic wastewater of 105,000 inhabitants. Moreover, industrial wastewater (mainly tomato industry) is also treated reaching a total seasonal load of 300,000 PE during summer. Water comes in the plant through two main pumping systems namely, the Northern and the Southern Pumping systems. In present work, the Southern Pumping plant is analyzed, since it represents about 20% of the total energy consumption of the plant (Pucci et al. 2016). This system has a nominal discharge of 1656 m^3/h, while the peak discharge is 6516 m^3/h.

M. De Chiara · A. Leopardi
DICeM, Università di Cassino e del Lazio Meridionale, Cassino, Italy
e-mail: angelo.leopardi@unicas.it

R. De Rosa · A. Giuliani · S. Guadagnuolo · L. Pucci (✉)
Consorzio Nocera Ambiente, Via S. Maria delle Grazie 562, 84015 Nocera Superiore, SA, Italy
e-mail: pucci@noceraambiente.it

D. Torregrossa
Eco Data Hub, 117 Mulenweg, 2155 Luxembourg Ville, Luxembourg

The inlet discharge can be very variable, both for rain events and during the summer, in which the food industries concentrate their most important activities. Operations of the Southern Pumping station were analyzed in dry weather conditions first. Wastewater passes through two rectangular concrete channels, after the coarse and fine screening. The difference in height between the bottom of the channels and the bottom of the loading tank is 2.5 m. The loading tank total surface is 100 m^2; the pumping is equipped with ten submersible pumps, six pumps (P05/P10) with nominal power equal to 80 kW and unit capacity of 375 l/s and four overflow pumps (E01/E04) of nominal power equal to 30 kW and unit capacity of 200 l/s.

The operation of the pumps is governed by ON/OFF control with cyclical rotation work sequence. The start/stop of the individual units is regulated by the signal transmitted by the level gauge of the tie rod in the suction tank. Specifically, up to a maximum of three pumps operating in parallel with the six pumps of 80 kW ensure the lifting of the flow inlet in normal operating conditions (dry weather, rains of modest extent), i.e., until the rod in the tank load does not reach the level of 2.7 m. Southern station wastewater is pumped, via the DN1200 pressure pipe 300 m long, to the inlet of grit and oil removal section joining northern station wastewater. Once the level of 2.7 m is exceeded, E01/E04 pumps progressively start to work, as the level increases, overflow is discharged into Casarzano Canal, which is the receiving body of Nocera WWTP (Fig. 1).

It is important to remark that, in this case, the volume of the receiving tank is undersized. Consequently, the water level in the tank rapidly varies during operations. Following,

raw data were extracted from the SCADA system: water level in the suction chamber, pumps working status, total pumped flow; these data were used in the model (Fig. 2).

3 The Model-Based Approach

First of all, a numerical model of the pumping system was built. The model can reproduce water level time history under an assigned inlet discharge. It was calibrated using one week of collected data. This dataset represents a dry weather week. The results are very sensitive to the time step used in the simulation: large errors can appear if a too large time step is assumed in the computation. This is due to the fast variations of water level during the pumping (see Sect. 2). After intensive tests, the time step of 10 s was found as a good compromise between accuracy and computation time need.

The model is fully developed in Excel that is extended with a function for the research of constrained optimum. The cell to be minimized reports the number of the pump starts over a week. This value needs to be minimized in order to: (1) enlarge the life of pump components, (2) reduce the energy consumption, since it is known that the pump switch on is energy expensive.

The algorithm tries to optimize the activation heights of the pumps in order to reduce the daily activation number of the pumps. The following constraints need to be taken into consideration:

1. minimum sump height $h_{MIN} = 1.8$ m, to avoid cavitation;

Fig. 1 Picture of the pumping system and the actual start/stop setting
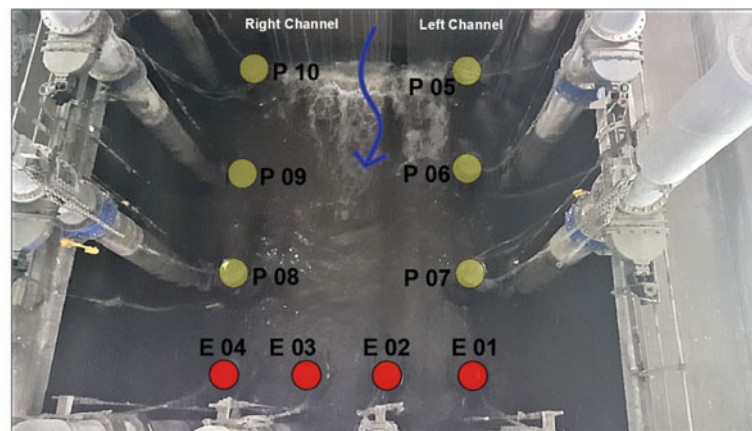
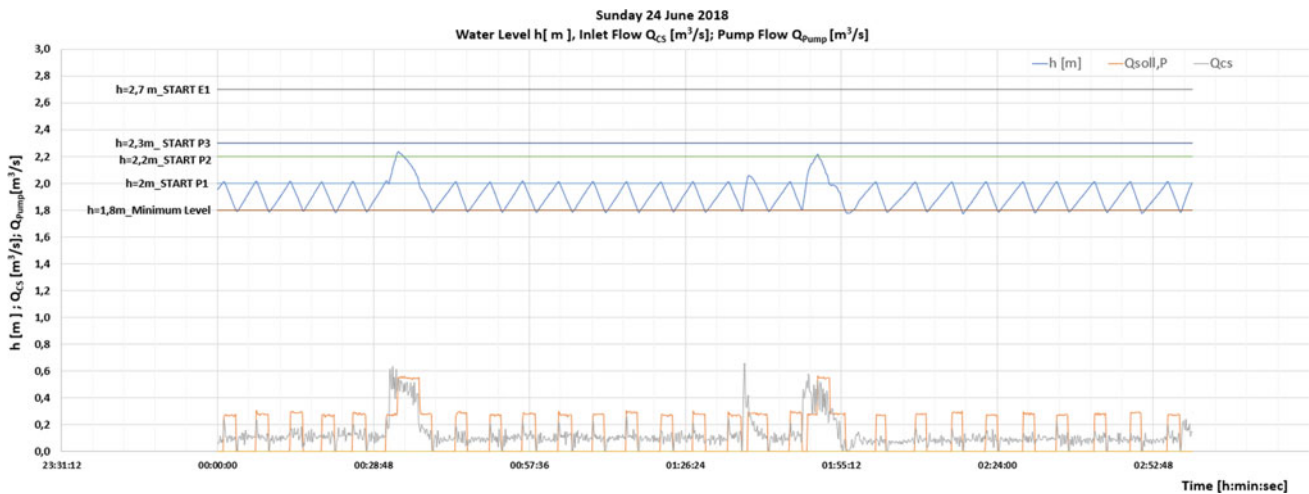| Start Level				Stop Level		
Level No	Setting [m]	Pump "P"		Level No	Setting [m]	Pump "P"
1	2	P1		1	2.2	P1
2	2,2	P2		2	2	P2
3	2,3	P3		3	1.8	P3

Fig. 2 Tank level time history

2. Emergency pumps are switched off because the investigation takes into account only dry periods. The emergency level must be avoided, i.e., the water level is below the starting height of emergency pumps.

As an example, in Fig. 3 it is drawn the water level time history in a day (Sunday) using the original setting (a) and the optimized one (b). As can be observed, the start/stop number can be reduced of about 50%.

4 Results, Discussion and Conclusions

The analysis of activation height shows that it is possible to reduce the number of activations by 50% or more. This reduction has a direct impact on the operational life of pump components and an effect on energy consumption. The model is validated by comparison of model output and real value. The coefficient of determination, $R^2 = 0.92$ can be
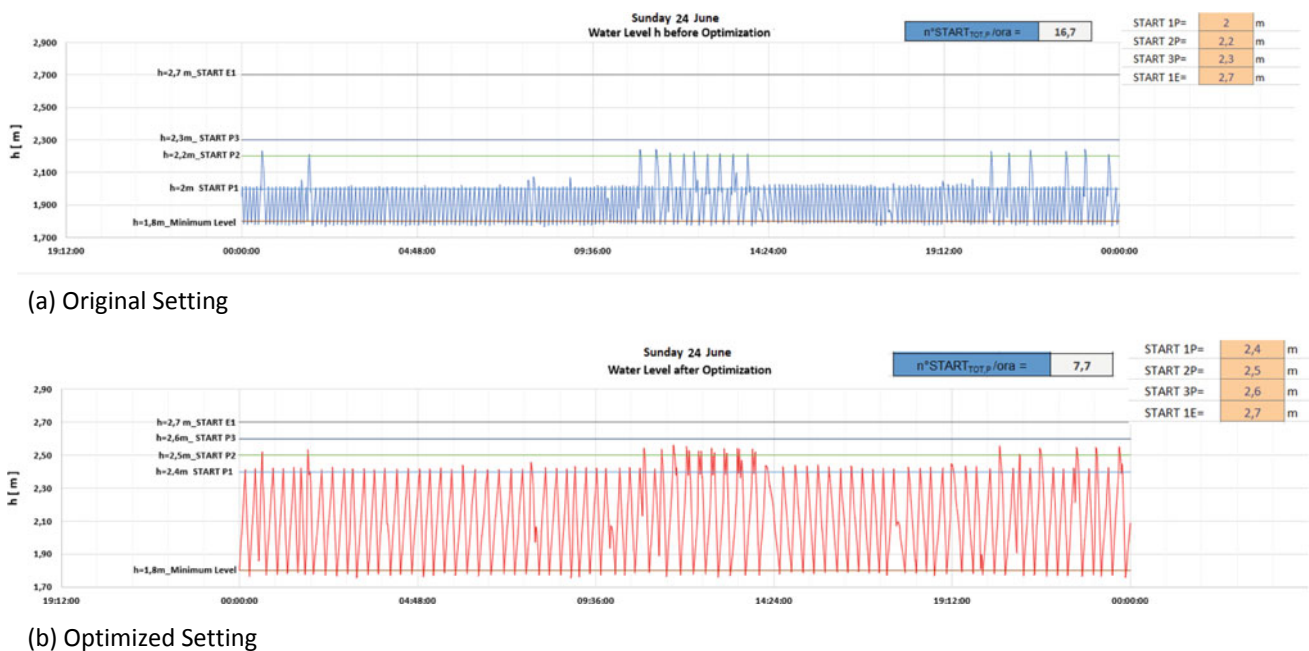

(a) Original Setting

(b) Optimized Setting

Fig. 3 Water level time history before and after the optimization (Sunday)

considered adequate enough to support the analysis. Currently, direct measurements of energy are not available. Future works will take into consideration an extended set of variables. Moreover, additional investigations will be carried out for the rain periods and for the use of variable speed drivers. After these more detailed analyzes of the pump performance, a real implementation will be performed. In conclusion, the present paper proposes the first development of a model-based approach for pump optimization in WWTPs applied to a real case study.

References

Castellet, Lledó, & Molinos-Senante, María. (2016). Efficiency assessment of wastewater treatment plants: A data envelopment analysis approach integrating technical, economic, and environmental issues. *Journal of Environmental Management, 167,* 160–166. https://doi.org/10.1016/j.jenvman.2015.11.037.

Castellet-Viciano, L., et al. (2018). The relevance of the design characteristics to the optimal operation of wastewater treatment plants: Energy cost assessment. *Journal of Environmental Management, 222,* 275–283. https://doi.org/10.1016/j.jenvman.2018.05.049.

Di Fraia, S., et al. (2018). A novel energy assessment of urban wastewater treatment plants. *Energy Conversion and Management, 163,* 304–313. https://doi.org/10.1016/j.enconman.2018.02.058.

Pucci, L., et al. (2016). Optimization-based methodology for improving energy efficiency in wastewater treatment plants. In *Proceedings Ecostp IWA Conference*—Cambridge, June 2016.

Torregrossa, D. et al. (2017). Pump efficiency analysis of waste water treatment plants: A data mining approach using signal decomposition for decision making. In *Computational Science and Its Applications—ICCSA 2017 Lecture Notes in Computer Science* (pp. 744–752). https://doi.org/10.1007/978-3-319-62407-5_56.

Torregrossa, D., Hansen, J. (2018). SK-DSSy: how to integrate the YouTube platform in a cooperative decision support? *Decision Support Systems VIII: Sustainable Data-Driven and Evidence-Based Decision Support Lecture Notes in Business Information Processing* (pp. 145–156). https://doi.org/10.1007/978-3-319-90315-6_12.